forests

Special Issue Reprint

Improvement of Forest Ecosystem Functions in Karst Desertification Control

Edited by
Kangning Xiong, Mingsheng Zhang and Junbing Pu

mdpi.com/journal/forests

MDPI

Improvement of Forest Ecosystem Functions in Karst Desertification Control

Improvement of Forest Ecosystem Functions in Karst Desertification Control

Editors

Kangning Xiong
Mingsheng Zhang
Junbing Pu

MDPI

Basel • Beijing • Wuhan • Barcelona • Belgrade • Novi Sad • Cluj • Manchester

Editors

Kangning Xiong
Guizhou Normal University
Guiyang, China

Mingsheng Zhang
Guizhou University
Guiyang, China

Junbing Pu
Chongqing Normal University
Chongqing, China

Editorial Office
MDPI
St. Alban-Anlage 66
4052 Basel, Switzerland

This is a reprint of articles from the Special Issue published online in the open access journal *Forests* (ISSN 1999-4907) (available at: https://www.mdpi.com/journal/forests/special_issues/5ZRIUJ27T4).

For citation purposes, cite each article independently as indicated on the article page online and as indicated below:

Lastname, A.A.; Lastname, B.B. Article Title. *Journal Name* **Year**, *Volume Number*, Page Range.

ISBN 978-3-0365-9186-5 (Hbk)
ISBN 978-3-0365-9187-2 (PDF)
doi.org/10.3390/books978-3-0365-9187-2

Cover image courtesy of Kangning Xiong

Contents

About the Editors

Kangning Xiong

Kangning Xiong, male, born in April 1958, is a professor holding a doctoral supervisor position at the School of Karst Science, State Engineering Technology Institute for Karst Desertification Control / Guizhou Normal University, with honorary titles of State Council Government Special Allowance Expert, National Outstanding Professional and Technical Talent, National Outstanding Teacher, and Guizhou Provincial Core Expert.

Professor Xiong, with research interests in fields of world heritage conservation and karst desertification control, ecosystem function and service, holds part-time academic posts as a Director of the Council of the Chinese Geographical Society, a member of the Teaching Steering Committee for Nature Conservation and Environmental Ecology Majors in Universities of the Ministry of Education, a Vice Chairman of the National Innovation Alliance Council for Karst Desertification Control, a member of the World Heritage Expert Committee of the State Forestry and Grass Administration of China, an Associated Editor in the Chief of Editorial Board for *Caisologica Sinica*, a Guest Editor for the *Forests* Special Issue, and a peer reviewer for *Catena, Science of the Total Environment, Plants, Ecological Indicators, and Land Degradation & Development.*

Prof. Xiong has successively led and completed 17 China national projects, 5 China-UNESCO projects, 118 national ministry key projects, 6 provincial key projects and 38 others, 78 projects entrusted by central and local enterprises and institutions, with 6 books, 562 papers including 152 SCI-index, 156 patents including 34 invention, and 44 computer software copyrights. As a result, he has received 27 educational and scientific awards at the international, national, and provincial levels.

Mingsheng Zhang

Mingsheng Zhang, male, born in October 1963, holds a PhD, professor with doctoral supervisor position, USDA-ARS visiting scholar. He is currently a deputy director of the School of Life Sciences / the Key Laboratory on Plant Resources Conservation and Germplasm Innovation in Mountainous Region (Ministry of Education) in China of Guizhou University. And with honorary titles of Guizhou Provincial Management Expert, Guizhou Province "Hundred" Level Innovative Talent, and Guizhou Province Outstanding Young Scientific and Technological Talent.

Prof. Zhang with research interests in fields of the plant stress physio-biochemistry and molecular biology, medicinal plant biotechnology and sustainable resource utilization, and medicinal plant secondary metabolism bioengineering and biopharmaceutical. He holds part-time the Chief Scientist of the Modern Industrial Technology System of Traditional Chinese Medicine in Guizhou Province, the Leader of the Sci-technology Innovation Talent Team for Characteristic Resource Plant Stress Resistant Germplasm Breeding in Guizhou Province, the vice Chairman of the Guizhou Society for Plant Physiology and Plant Molecular Biology, the Executive Director of the China Agri-Biotechnology Society, and also is an associate editor in Chief of Editorial Board for *Journal of Medicinal Plants Research*, a editorial board member for *Research in Pharmaceutical Biotechnology*, a guest editor for *Forests* Special Issue, peer reviewers for *Scientia Horticulturae, Journal of Plant Research, Postharvest Biology and Technology*, etc.

Prof. Zhang has successfully led and completed 6 China national projects, more than 30 provincial-ministerial projects, and 29 others, with 5 books, 219 papers including 52 SCI-index, and 25 patents including 16 inventions.

Junbing Pu

Junbing Pu, male, born in 1982, is a professor of the karst research team of Chongqing Key Laboratory of Carbon Cycling and Carbon Regulating of Mountain Ecosystem, School of Geography and Tourism, Chongqing Normal University. He is a vice-chair of the Karst Commission, International Geographical Union, a full member of the Karst Commission, International Association of Hydrogeologists, and an associate editor of the *Journal of Hydrology*.

His research interests mainly focus on the physical and chemical hydrogeology of karst aquifers, karst hydrology, biogeochemistry in the hydrological cycle, isotope hydrology, carbon cycle in groundwater-surface water continuum, and carbonate weathering dynamics. He led and completed more than 15 projects on karst sciences, and has published more than 100 papers at some international journals, including *Water Research*, *Journal of Hydrology*, *Science of the Total Environment*, and so on.

Preface

The South China karst is one of the three most ecologically fragile and desertification-affected areas in the world. In recent years, with the advancement of the national desertification control project, the large-scale return of farmland to forests has made the South China karst a global greening hotspot. The combination of regional vulnerability and seasonal superposition has led to soil fragmentation, water and soil erosion. There are high-incidence phenomena of regional ecosystem degradation, biodiversity decline and high densities of people in poverty. Therefore, focusing on the research of forest ecosystem function improvement in karst desertification control serves the purpose of providing countermeasures to afforestation in karst areas and contributing to the sustainable development of the regional economy. The theme of this Special Issue includes the improvement mechanism of ecosystem structure, function, and services, the mechanism of ecosystem service tradeoff/synergy and function optimization. An optimization model of ecosystem function and an improvement path for eco-product supply are introduced. The role of functional traits in the maintenance of ecological function and services is determined. Social-ecological responses to afforestation in karst desertification control are also discussed.

This Special Issue consists of 16 articles, and in order to facilitate quick and systematic reading, we have organized the content into four major landmark achievements: (i) ecosystem evaluation (chapters 7, 8, and 14), (ii) structure optimization configuration (chapters 2, 6, and 11), (ii) water and fertilizer regulation technology (chapters 5, 9, 12, 13, and 15), and (iv) function improvement strategies (chapters 4, 10, and 16) and the formation of corresponding four major key scientific questions to be addressed. This Special Issue brings together, to some extent, the latest progress, cutting-edge theories and technical achievements in the research of forest ecosystem function enhancement for karst desertification management.

This Special Issue has been written and published with the full support of the *Forests* Editorial Office, the concern of the leadership of School of Geography & Environmental Science (School of Karst Science), Guizhou Normal University, and the help and support of Professor Mingsheng Zhang and Junbing Pu. In addition, numerous colleagues and scholars have submitted articles and made other contributions to this Special Issue.

Due to the limited space in this Special Issue, there are some deficiencies in the endeavor to condense the major landmark achievements and key scientific issues to be solved, and there are some limitations in the research on the improvement of the function of karst desertification control forest ecosystems, so I would like to invite readers and friends to contribute their critical readings and any potential corrections.

Kangning Xiong, Mingsheng Zhang, and Junbing Pu
Editors

forests

MDPI

Review

A Commented Review of Eco-Product Value Realization and Ecological Industry and Its Enlightenment for Agroforestry Ecosystem Services in the Karst Ecological Restoration

Ying Yang [1,2], Kangning Xiong [1,2,*], Huiqiong Huang [1,2,3], Jie Xiao [1,2], Biliang Yang [1,2] and Yu Zhang [4]

[1] School of Karst Science, Guizhou Normal University, Guiyang 550001, China
[2] State Engineering Technology Institute for Karst Desertification Control, Guiyang 550001, China
[3] College of Public Management, Guizhou University of Finance and Economics, Guiyang 550025, China
[4] Department of Resource Management, Tangshan Normal University, Tangshan 063000, China
* Correspondence: xiongkn@gznu.edu.cn

Abstract: The achievement of eco-product value and the growth of eco-industry can boost the economic advancement of karst areas. The findings of a statistical analysis of 520 relevant studies reveal the following: (1) From a time series perspective, the amount of papers increase with each wave of research; (2) contents mainly concentrate on four aspects, namely, ecosystem services supply (8.46%), value accounting (10.58%), value realization (37.88%), and eco-industry (30.38%); (3) the study areas are primarily concentrated in Asia (85.96%), Europe (7.12%), and North America (4.04%), most of which are located in China's karst areas with vulnerable ecological environments and regions that are aware of eco-product values; and (4) research frontiers are reflected through four aspects of the ecosystem, namely, services supply, value accounting, value realization, and the eco-industry. Based on the analysis in this paper, it can be concluded that paths, mechanisms, and models for eco-product value realization are still slow. Therefore, to support the growth of karst agroforestry ecosystem services, it is imperative to further research the capacity of agroforestry ecosystem services supply, value accounting systems, ecological compensation mechanisms, the value realization models of eco-products, and the formation mechanism of eco-industries.

Keywords: ecosystem service supply; value accounting; eco-industry

Citation: Yang, Y.; Xiong, K.; Huang, H.; Xiao, J.; Yang, B.; Zhang, Y. A Commented Review of Eco-Product Value Realization and Ecological Industry and Its Enlightenment for Agroforestry Ecosystem Services in the Karst Ecological Restoration. *Forests* **2023**, *14*, 448. https://doi.org/10.3390/f14030448

Academic Editor: Peter Elsasser

Received: 18 December 2022
Revised: 16 February 2023
Accepted: 17 February 2023
Published: 22 February 2023

1. Introduction

Eco-environmental issues are some of the most heated researched topics in the world today [1]. Ecological restoration plays an important role in restoring degraded, damaged, and crumbled ecosystems to a long-term and stable state of health [2,3]. Ecological restoration is not only an essential step in improving the ecological environment in China [4], but also plays a crucial role in moving toward a more ecological society [5]. It is pertinent to the nation's ecological security [6] and is crucial to pushing forward green development [7] and fostering a more harmonious relationship between human beings and nature [8]. In recent years, ecological restoration research has developed rapidly around the world, and it is being actively promoted in China [9]. The global proportion of relevant Chinese scientific research achievements has increased exponentially, but its global influence still needs to be strengthened [10]. This research helps in propeling the advancement of karst ecological restoration.

Global karst regions account for about 10% to 15% of continental land areas and are inhabited by a quarter of the world's population, forming a special ecological environment system with strong regionality, integrity, and comprehensiveness [11,12]. They are mostly distributed on the Mediterranean coast, in the eastern United States, and the karst mountains of southwestern China [13]. Old, hard carbonate rocks with inadequate water-holding ability can be found in the Mediterranean and on the Asian continent [14]. Carbonate

rock formations in China are wide and strong, and the karst types are widespread, with numerous types and styles [15]. However, in the southeastern United States, carbonates are less troublesome than those in southern China and tertiary macroporosity is common [14]. Yunnan, Guizhou, and other regions in southwestern China are the most concentrated areas of karst distribution in the country, with a total area of 1.7608 million km^2, of which the distribution zones of exposed and semi-exposed carbonate rocks account for 41.3% of the total area [15]. In karst areas of southwest China, due to the fragility of the environment and the influence of human factors, a large degree of damage to the environment has occurred, leading to the emergence of many environmental problems including karst desertification [15,16].

Ecosystem services are widely described as the benefits that people obtain from natural ecological processes [17,18]. Ecosystem services are classified by the MA as provision, support, and regulation, as well as cultural services. The products obtained from ecosystems are called provision services. The benefits derived from the regulation of ecosystem processes are called stewardship services. Cultural services refer to the nonmaterial benefits, usually spiritual enrichment, intellectual abilities, perception, entertainment, and aesthetic enjoyment, gained from ecosystems. Support services comprise those processes necessary to support the above services, such as the production of oxygen in the atmosphere, soil structure, and soil retainment [19]. However, one of the most debatable facets of ecosystem services is the question of the valuation of services [20].

Agroforestry is the deliberate integration of shrubs and trees into crop and animal farming systems, which can strengthen agricultural output and provide ecosystem services [21–26]. In ancient Mayan cultures, agroforestry was used for crop output and forest management in environmentally sensitive karst areas [27] and continues to play a role in numerous places of the agrarian systems. After years of government benefits, it can be seen that the development of agroforestry in karst areas of southwest China, focused on the Guizhou Plateau, has not merely optimized the ecological benefits of both agroforestry and ground and water conservation efforts [28], but has also controlled the effects of soil erosion, improved the productivity of karst desertified karst land, and protected soil animal diversity [29,30]. Since the current research on agroforestry ecosystem services in karst areas has not been able to uncover the internal development mechanisms, the agroforestry ecosystem services explored are relatively isolated (as can be seen in soil and water preservation, production application, and land degradation restoration, etc.), and often lag behind regional studies. The improvement of ecosystem services has even become a constraint on the coordinated development of human-land relations [31]. There are few studies on the value realization of agroforestry eco-industries and eco-products. Therefore, by studying the research progress on the worth achievement of the eco-industry and eco-products, the development of these karst agroforestry factors can be promoted.

For the first time, "eco-product" was proposed in China, and the eco-products were primary products in the ecosystem, such as leaves, twigs, etc. [32]. At present, there is no common agreement on the definition. Scholars have interpreted the concept of eco-products from different perspectives. There are three main understandings of what an eco-product is. The first perspective relates eco-products to ecosystem services, since they are healthy natural ecosystems that benefit people [33,34]. The second view considers the co-products of man and nature to be eco-products [35]. The third view posits that eco-products can also be described by other names, such as eco-labeled goods, green-labeled goods, eco-design products, eco-friendly products, and non-polluting products [36]. Some scholars considered eco-products to be ecosystem services, arguing that agroforestry products are associated with human beings providing ecosystem provision services [37]. In summary, scholars have yet to reach an agreement regarding the concept and categorization of eco-products. Moreover, the worth of eco-products is difficult to account for and there is little in-depth discussion on the topic. Therefore, this paper presents key scientific issues that can help in advancing the study of the realization of eco-product value.

The eco-industry is an emerging industry that follows the precepts of industrial ecology as well as circular economy, is predicated on ecosystem carrying capacity, and collaborates with natural, economic, technological, social, environmental, and other systems [38]. In karst areas, due to their special geographical environment, to achieve environmental enhancement and economic growth, the derivative industries of karst desertification control must be put in place first and must be organically integrated along with agricultural economic development [39]. It can be seen that eco-industries in the field of karst ecological restoration can contribute to regional economic progress by clarifying the link between the realization of the value of eco-products and eco-industries, which can further have an illuminating effect on the development of the agroforestry industry.

Research on eco-industries and eco-product values in karst regions has been ongoing for the past 40 years. This report investigates that research and reviews its major developments and major accomplishments in four areas, namely, the ecosystem service supply, value accounting, value realization and eco-industry, and recommends key scientific and technological issues. It can not only offer a scientific basis for the study of agroforestry ecosystem services in karst regions, but can also maintain the integrity and sustainability of the ecosystem, and ultimately lead to the coexistence of humans and environment.

2. Materials and Methods

To locate relevant studies, a search was conducted using the databases Web of Science (WOS) (https://www.webofscience.com, accessed on 30 June 2022) and China National Knowledge Infrastructure (CNKI) (https://www.cnki.net, accessed on 30 June 2022). This study used the following search terms: "Eco-industry" and "eco-product" together and "eco-industry", "ecosystem services", "eco-product", and "value realization", as well as "ecosystem services" in combination with "value realization". The removal of irrelevant papers was performed via artificial selection. The search had a 30 June 2022 deadline. The search retrieved 520 relevant Chinese and English language studies, of which 158 were in English, including 127 theses, 27 review papers, 3 proceeding papers, and 1 study that was published online; however, there were no editorials or book chapters. In the English-language journals, 78 articles were written by Chinese scholars. Of the remaining 362 articles from Chinese periodicals, 208 were from core Chinese journals, 64 were Master's theses, 13 were Doctoral dissertations, 16 were conferences papers, 58 were articles from newspapers, 1 was a book, and 2 were achievements. No yearbooks, patents or standards were found. The procedure for the literature screening and search is depicted in Figure 1.

We ultimately obtained 362 Chinese publications and 158 English articles after deduplication. The top 10 contributors with numerous papers on the topic were Yihong Zhou (7 papers), Xiahui Wang (5 papers), Leshan Jin (5 papers), Xiaolong Gao (5 papers), Linbo Zhang (4 papers), Shuilin Qiu (4 papers), Huiyi Yu (4 papers), Jinnan Wang (3 papers), Zhiyun Ouyang (3 papers), and Bowen Sun (3 papers). Regardless of the author's placement within the study, all authors were taken into account when determining the number of research papers by each author.

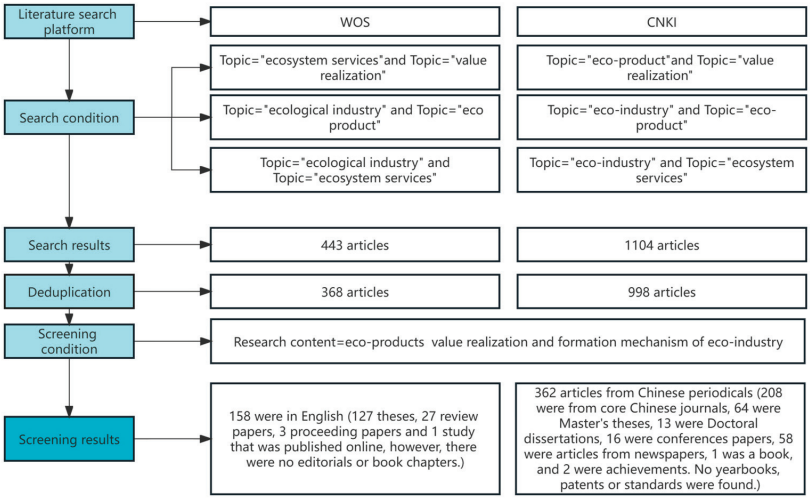

Figure 1. The research process illustrated from the initial search to the thorough screening using the study's systematic mapping process (identification, screening, qualification, and inclusion). Database searches were used to find documents during the identification stage. Then, the papers that had been selected underwent the screening and eligibility phases for ecosystem service supply, value accounting, value realization, and eco-industry (by title, keywords, abstract, and full text articles). Ultimately, the study included articles that satisfied the eligibility requirements.

3. Results

3.1. Annual Distribution of Articles

There are roughly three stages regarding research on the realization of eco-product value and the eco-industry both domestically and abroad (Figure 2). In the first stage (1985–2009), there were only about 55 total studies and not many articles published yearly—the topic was still in its early phases. In the second stage (2010–2020), there were some significant fluctuations in the number of articles; however, it was still in a stage of slow growth—only 101 articles were published during that period. In the third stage (2021–30 June 2022), there was a trend was toward rapid growth, and there were currently many articles published during this period.

3.2. Content Distribution of Documents

Of the studied categories, ecosystem service supply papers comprise 8.46% of the total number, value accounting comprise 10.58%, value realization comprise 37.88%, eco-industry comprise 30.38%, and other categories comprise 12.69% of the total papers published (Figure 3). The ratios of these articles show that eco-products are worth attaining and the state of eco-industries is improving. However, current research in this area still focuses on how eco-product value is realized, and how the eco-industry is established, while ecosystem service supply and value accounting is still in the exploratory and development stages.

3.3. Distribution of Study Areas of Literature

The development of eco-products is unbalanced due to the variations in regional natural, economic, and social conditions and exhibits powerful regional characteristics (Figure 4). As the graph illustrates, the areas under research are primarily in coastal countries in Asia, Europe, North America, and Australia. However, the majority of these are in China. Asian studies account for 85.96% of publications, which is related to government policy assistance, research group focus, and possibly the use of CNKI databases. Relevant articles in Asia have been primarily published in China in Asia. Global problems including

rapid population growth, food insecurity, resource shortages, and ecological pollution, have necessitated that eco-products and sustainable development must be significant aspects of the 21st century society. As a result, publications that emphasize the value of eco-product realization and the overall advantages of eco-industries have gradually expanded. Relevant European studies account for 7.12% and North America accounts for 4.04%, which is more advanced than the research output of other continents. As a result, numerous European nations and research institutes have begun to pay attention to eco-product worth realization and eco-industries, and thus the number of publications is increasing steadily.

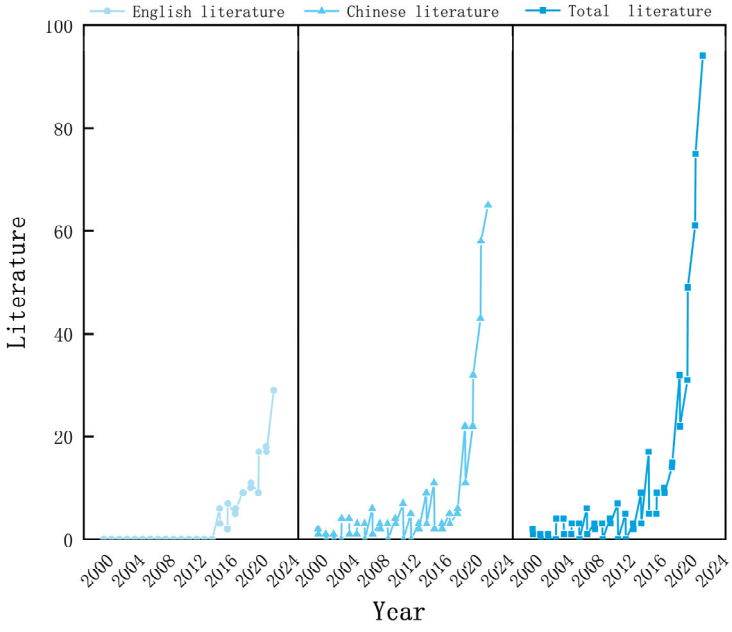

Figure 2. The pattern in the yearly distribution of the study of the realization of eco-product value and the eco-industry.

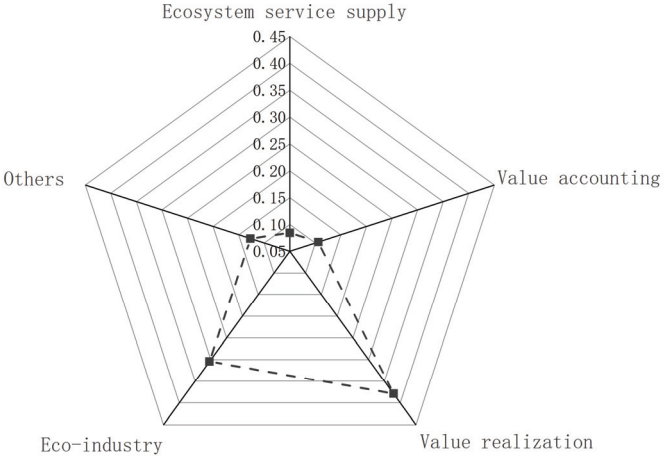

Figure 3. The literature classified by ecosystem service supply, value accounting, value realization, eco-industry, etc.

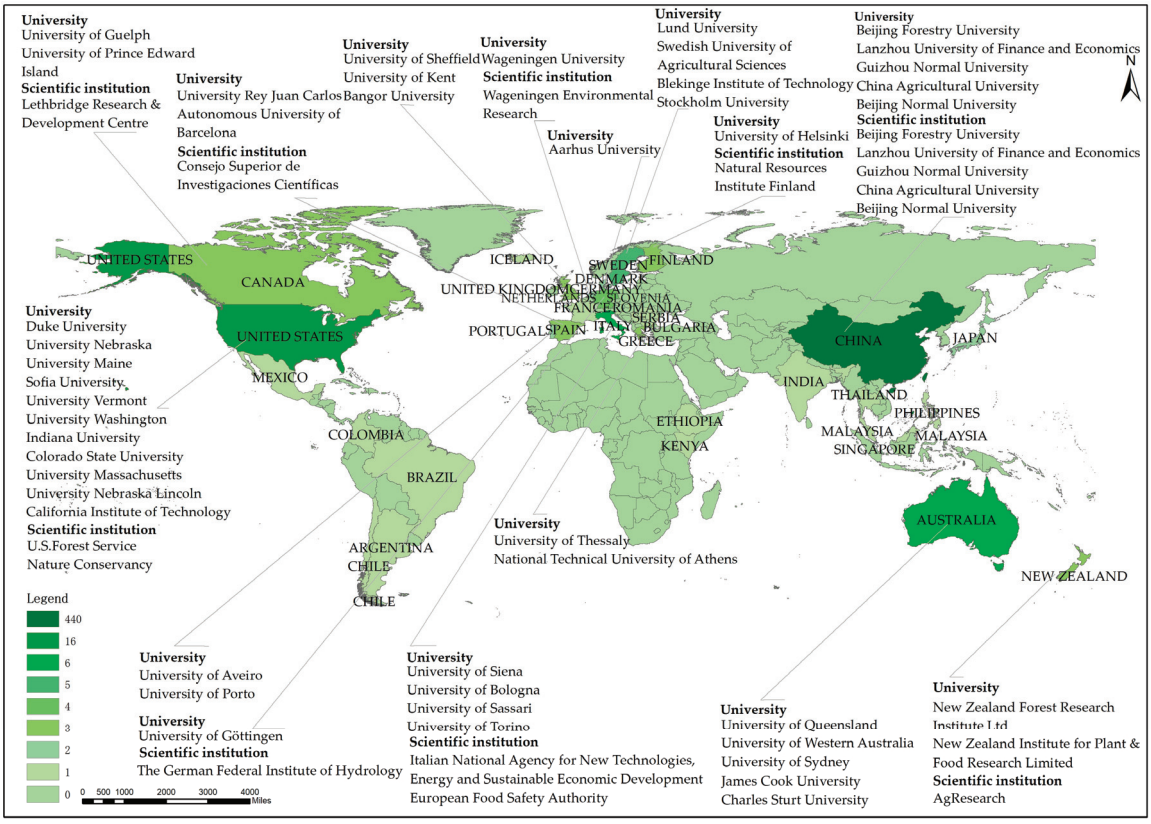

Figure 4. The breakdown of the institutions and nations described in the study (due to space limitations, only countries with more than two publications are marked). The number of publications is indicated by the bottom digits and bands of different colors; the greener the color, the more publications are cited.

3.4. Institution Distribution of the Literature

The distribution of eco-industry-related organizations and eco-product value realization was interpreted and analyzed. This paper utilizes the employer institution of the primary authors of the available literature as units, since there are multiple institutions with relevant publications and only a limited amount of graph space. Only those units with more than four published papers were considered in the selected Chinese literature and only institutions with one paper in foreign studies, totaling 10 units (Figure 5). The top Chinese institutions (Figure 5a) in terms of the number of studies comprise the Research Center for Eco-Environmental Sciences, the Chinese Academy of Sciences (10), the Beijing Forestry University (10), the Beijing Normal University (9), the Environmental Planning Institute of the Ministry of Ecology and Environment (8), the China University Of Geosciences and China Agricultural University and Finance and Economics University Of Lanzhou (7), and the Zhejiang University and Guizhou Normal University (5). The top English-language institutions that have published two relevant articles include Aarhus University, the National Technical University of Athens, Bangor University, the Swedish University of Agricultural Sciences, and the University of Helsinki (Figure 5b). Among all research units, there are more domestic than foreign research units. Almost all of the top research units are agricultural and forestry institutions of higher education, which are located in both forested and highly developed regions.

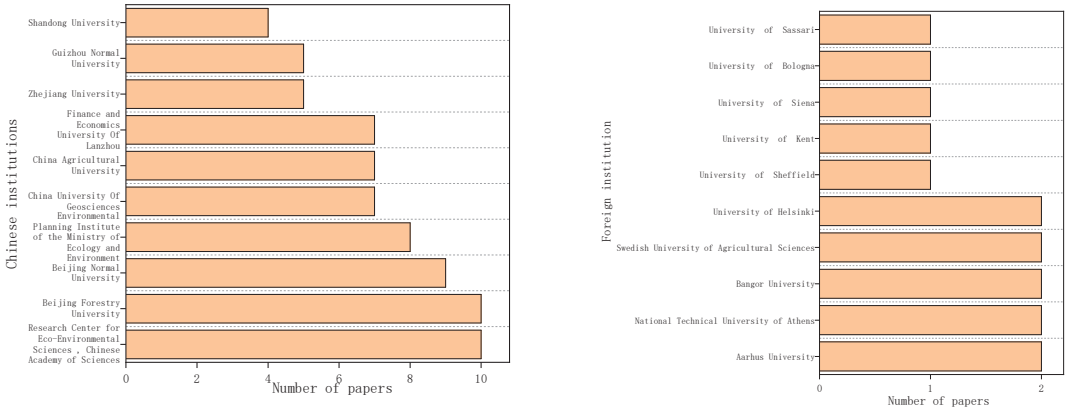

(**a**) (**b**)

Figure 5. (**a**) Ranking of Chinese institutions in terms of the number of articles published; (**b**) ranking of foreign institutions in terms of the number of articles issued.

3.5. Research Stages

According to the literature's annual allocation chart, in 1985, the first studies on eco-product worth achievement and eco-industries were conducted, thus giving the field an approximately 40-year history. Three stages of research have been identified regarding the value of eco-products and eco-industries, namely, the beginning stage, the sluggish growth stage, and the rapid growth stage (Table 1), which is in line with the research background and main features of this period.

Table 1. Division of the stages of the research.

Research Stage	Main Characteristics	Background
Beginning stage (1985–2009)	Concepts and theories are discussed, and there are few practical studies on the realization of eco-product value.	The publication of the "Preliminary Account on Ecological Products" [40].
Sluggish growth stage (2010–2020)	Most of the retrieved content focuses on the eco-product supply capacity and the framework of eco-industries, and most of these are descriptive theoretical research and practical experience summaries.	The "National Main Function Area Planning (Guo Fa (2010) No. 46)" was published in 2010.
Rapid growth stage (2021–30 June 2022)	The realization paths, mechanisms, and modes of eco-product value are the focus of current research. Quantitative research and exploration of gross ecosystem product (GEP) and eco-product value accounting are beginning to appear.	In 2021, the General Office of the Central Committee of the Communist Party of China and the General Office of the State Council issued the "Opinions on Establishing and Improving the Value Realization Mechanism of Eco-product", which proposed the establishment and improvement of the value realization mechanism of eco-products.

4. Research Progress and Landmark Results

4.1. Ecosystem Service Supply

4.1.1. To Study the Environmental Costs and Advantages of Ecosystem Service Supply Capacity, the Environment's Mechanism Should Be Understood

The capacity of the ecosystem to provide services is closely connected to the environment. In the karst environment, the energy conversion pathway of the ecosystem is fragile and sensitive. For instance, once a forest is destroyed, the material and energy

exchange of the ecosystem will be temporarily interrupted, and the ecological balance will be abruptly changed. If the forest is destroyed, the exchange of materials and energy in the ecosystem will be temporarily disrupted, and the ecological balance will be abruptly changed, even to the extent that the ecological environment may not be conducive to human survival [11]. This shows that the ecological environment has a certain influence on eco-product supply capacity. Due to the variability of each active component's demand for various nutrients in the soil, some scholars analyzed the nutrient demand of *Lonicera japonica Thunb.* and showed that different components of honeysuckle showed different accumulation and change patterns in different grades of stone desertification [41], further illustrating the impact of different grades of rock desertification on eco-products. Broadly increased crop yields, reduced soil erosion, the preservation of biodiversity, improved soil fertility, carbon sequestration, and lower greenhouse gas emissions are only a few of the many advantages of agroforestry systems [42–44]. Additionally, some researchers have demonstrated that vineyards can offer a variety of ecosystem services, including weed and pest control, water supply and purification, field accessibility, soil species diversity, carbon sequestration, poverty alleviation, and the reduction in land degradation [45–48]. Therefore, the karst agroforestry ecosystem services are closely related to the surrounding environment. Government initiatives to enhance environmental protection will help in increasing the provision of agroforestry ecosystem services in karst zones. Various enterprise departments should also strengthen their awareness regarding environmental protection. This will help in maintaining the ecosystem service role and ensuring the supply capacity at the source.

4.1.2. Study of the Crop Composition and Configuration Relationship of Ecosystem Services to Develop a Theoretical Foundation for Their Supply Capacity

On the issue of eco-product supply capacity and enhancement, some scholars summarized the research content as mainly involving two aspects of ecosystem services and public goods supply capacity in foreign countries [49]. Ecosystem service supply refers to the services produced by the regional ecosystem over a specific time frame [50]. Some characteristics, such as those pertaining to the growth form, composition, and configuration of woody plants and crops [51] affect the system function and ecosystem service supply. Numerous studies have demonstrated that preserving ecosystem stability can help in boosting biodiversity [52,53]. Therefore, to advance the study of agroforestry ecosystems, discussions on the existence of a link between ecosystem structure and stability are necessary [54]. In summary, it is important to explore an agroforestry model in karst areas that can protect the environment and reap economic benefits at the same time. Scholars have also continued to explore the composition and configuration of different agroforestry methods. Table 2 summarizes the characteristics of different agroforestry patterns in karst areas.

In addition, humans can protect the ecosystem through social means to improve supply capacity [50]. The supply of public eco-products mainly concerns how to combine market mechanisms to improve supply capacity [55]. Chinese scholars have elucidated the supply capacity of eco-product from various aspects. For example, Li and Rong used the PPP model to strengthen the eco-product supply capacity in a new way. The PPP (Public–Private Partnership) model is a public–private partnership. The PPP model is a means for government departments and the private sector to entrust enterprises or other social organizations with the building of public facilities or the provision of public services to the public through the signing of long-term agreements. By appropriately cooperating with producers, the government can further promote the adoption of ecological production methods in the industry, compensate for the effects of the long production cycle and slow cost recovery in the industry, encourage and stabilize the development of industrial production, and increase the production of eco-products in a broader context [56].

Table 2. The characteristics of different agroforestry patterns in karst areas.

Agroforestry Pattern	Scalable Pattern	Feature	Distribution	Source
Rosa rugosa Thunb. + *Glycine max (Linn.) Merr.*, *Rosa rugosa Thunb.* + *Malus pumila Mill.* + *Glycine max (Linn.) Merr.*, *Rosa rugosa Thunb.* + *Zea mays* L.	*Rosa rugosa Thunb.* + *Glycine max (Linn.) Merr.*	The *Rosa rugosa Thunb.* + *Glycine max (Linn.) Merr.* mode was beneficial for the improvement of soil mite diversity.	China	Yang et al., 2021 [57]
Forest Chinese herbal medicine, Forest + Grain, Forest + Grass	Forest Chinese herbal medicine	The agroforestry of forest Chinese herbal medicine appeared to provide the greatest impact on soil infiltration, followed by forest + grass.	China	He et al., 2020 [58]
Zea mays L. Pattern, *Malus pumila Mill.* Pattern, *Malus pumila Mill.* + *Glycine max (Linn.) Merr.* Pattern, *Pyrus* spp. Pattern, *Pyrus* spp. + *Cucurbita moschata Duch.* Pattern, *Punica granatum* L. Pattern, *Punica granatum* L. + Grass + Sheep Pattern (PGSP)	*Malus pumila Mill.* Pattern, *Pyrus* spp. Pattern, *Punica granatum* L. + Grass + Sheep Pattern (PGSP)	The multilevel agroforestry growing and boosting methods used in PGSP were able to optimize the interaction between tree–grass–sheep, and enhance both the environmental and financial benefits.	China	Zou et al., 2019 [59]
Forest + *Lanxangia tsao-ko (Crevost and Lemarié) M.F.Newman and Škorničk.*, Artificial forest + *Lanxangia tsao-ko (Crevost and Lemarié) M.F.Newman and Škorničk.*, *Zea mays* L. + *Lanxangia tsao-ko (Crevost and Lemarié) M.F.Newman and Škorničk.*	Forest + *Lanxangia tsao-ko (Crevost and Lemarié) M.F.Newman and Škorničk.*	Of these three types of agroforestry system, the most productive model was forest + *Lanxangia tsao-ko (Crevost and Lemarié) M.F.Newman and Škorničk.*, the production of which was remarkably greater than the other systems ($p < 0.05$).	China	Jin et al., 2016 [60]
Shellac + *Zea mays* L.	*Shellac* + *Zea mays* L.	The *Shellac* + *Zea mays* L. agroforest ecosystem had positive effects on the protection of ground-dwelling ants.	China	Lu et al., 2016 [61]
Hornbeam + Oak + Beech	Hornbeam + Oak + Beech	The overall stock of soil organic carbon is high, regardless of land use history.	Slovakia	Ahmed et al., 2012 [62]
Alstonia scholaris (L.) *R. Br.* + *Camellia sinensis*, *Alstonia scholaris* (L.) *R. Br.* + Coffee	*Alstonia scholaris* (L.) *R. Br.* + *Camellia sinensis*	In terms of total biomass per plant, the *Alstonia scholaris* (L.) *R. Br.* + *Camellia sinensis* model is slightly better than the *Alstonia scholaris* (L.) *R. Br.* + coffee model.	China	Liu et al., 2008 [63]
Eucommia ulmoides + *Atractylodes macrocephala Koidz.*, *Eucommia ulmoides* + *Perilla frutescens*, *Eucommia ulmoides* + *Capsicum annuum* L.	*Eucommia ulmoides* + *Atractylodes macrocephala Koidz.*	In economic output, the order is: *Eucommia ulmoides* + *Atractylodes macrocephala Koidz.*'s model > *Eucommia ulmoides* + *Capsicum annuum* L.'s model > *Eucommia ulmoides* + *Perilla frutescens*'s model.	China	An et al., 2001 [64]

4.1.3. From the Potential Supply Capacity and Actual Supply Capacity of Ecosystem Services, We Designed and Built the Ecological Connection Chain of Eco-Industries, and Thus Consolidated the Theoretical Foundation for Ecosystem Services Supply Capacity

Supply is split into potential supply and actual supply based on the ecosystem carrying capacity and the extent of the human use of ecosystem services. Of the two, potential supply is the capacity of ecosystems to deliver services over time in a sustainable way, and actual supply is the product or ecological process that is consumed or used by people [65]. Some scholars pointed out that water filtered from the karst topography areas (service supply unit) is provided as drinking water to the residents of the cities (service use unit) through long-

distance underground transport (service connection area) [66]. It can be seen that increasing the supply capacity of karst regions can further boost the availability of eco-products in these regions. The potential supply capacity of eco-products is related to the economy; for instance, the availability of eco-products from the forest depends on its ability to continue growing sustainably. Farmers will often turn to illegal practices or stop producing forest eco-products if government subsidies to landowners are provided at only a very low level. Therefore, providing farmers with adequate and timely compensation is an efficient incentive to increase their motivation to supply forest eco-products [67]. However, the supply of eco-products is often insufficient. The main reasons are the complete value return and intergenerational value return [68], the lack of quality standards for eco-products [69], the government supply model, and the lack of cooperation between governments [70,71] and other reasons.

The development of eco-industries is closely related to the supply of eco-products. According to research from certain foreign academics, storage time has the greatest impact on fruit quality, followed by output, storage temperature, humidity, and harvesting time [72]. Other scholars have shown that respiration and transpiration processes are the primary causes of post-harvest plant loss and poor quality [73]. Therefore, to keep the fruit fresh and promote the development of industry, the best solution is to shorten the travel time between the production areas and the demand areas. Moreover, processing plants can be set up near the origin of the eco-product in question, in order that the products can be directly purchased by manufacturers and processed into various types of food. On the one hand, this can promote the employment of farmers in karst areas and, on the other hand, it can promote the development of the local industrial chain.

4.2. Value Accounting

4.2.1. From the Perspective of Accounting Methods, Value Accounting and Evaluation of Eco-Product Area Provide a Good Theoretical Basis

It is challenging to evaluate eco-product value accurately. In 2013, the concept of gross ecosystem product (GEP) was first proposed by Ouyang et al., which was defined as "the final product that the ecosystem can provide for human life and social development and the sum of service value", and the corresponding theoretical basis, accounting framework, and accounting method of GEP were proposed [74], which have been subsequently researched and applied by scholars and used for practical applications by governments at all levels. To date, many provinces [75–78] and regions have carried out GEP accounting. However, the improvement of the market mechanism is related to the transaction price. Therefore, fully calculating the eco-product supply is the key to the good marketization of an eco-product. Currently, there are three main ways to implement eco-product value accounting: (a) The functional price method [77]; (b) the equivalent factor method [79]; and (c) the ecological element method (based on the energy method) [80,81]. Based on the research results of Costanza, Xie et al. proposed the equivalent factor method [79].

Along with value-based approaches to financial assessment [82–84], in recent years, scholars have concentrated on quantitative assessment methods for spatial mapping and ecological modeling, in addition to value-based economic assessment methods. For instance, the AFES assessment tool, which was created using an empirical methodology, evaluates regulatory services [85]. The identification and mapping of cultural ecosystem services have been performed primarily using data from preference surveys and social value models of ecosystem services [86]. However, the majority of ecosystem services are not only undervalued, but also excluded from routine decision making. The sustainable use of ecosystem services and the alleviation of poverty both strongly depend on the value of ecosystem goods and services. Furthermore, people can indeed utilize the value of ecosystem services, assisting in the global integration of natural resources into daily decision-making processes [87]. Therefore, a full accounting of the value of agroforestry eco-products in karst regions can contribute to better decision-making and management.

4.2.2. From the Perspective of the Accounting Index System, Scholars Have Extensively Explored the Index System to Reasonably Calculate and Evaluate the Eco-Product Values

Provinces and regions across the country tend to build eco-product value accounting index systems. For example, in recent years, Zhang and Zou have established a GEP accounting index system that conforms to the features and main functions of the Yarlung Zangbo river basin based on reviewing the research progress of GEP accounting [88]. Liang et al. used the Pearl River Delta region as the research area and used the green GDP accounting theory to carry out the calculation of the gross economic and ecological production (GEEP), which showed that the effectiveness, as well as the quality of economic growth, in the Pearl River Delta region, continued to improve and that the regional economic environment displayed a trend toward coordinated development [89]. In addition, after the establishment of the indicator system, some scholars tend to study the policy formulation related to the value accounting of eco-products. For example, the paper by Yu et al., who, from the perspectives of standardization of ecological value accounting methods, parameter localization, the application of policy decision making, and eco-product transactions, put forward suggestions for promoting the transformation of Chinese ecological value accounting from academic research to practical management [90]. In karst regions, the value accounting system of agroforestry eco-products has not yet been developed, and should be further developed in the future.

4.3. Value Realization

4.3.1. The Analysis of Eco-Compensation Lays a Theoretical Foundation for Eco-Product Value Realization

Eco-compensation is an important form of eco-product value realization. International research on eco-compensation began in the 1970s, and while there were earlier related practices, these practices were not marked as eco-compensation. Terms related to ecological compensation are used internationally including payment for ecosystem services, compensation for ecosystem services, the market for environmental services, etc. Of these, "payment for ecosystem services" (PES for short) is widely used, reflecting the fact that countries have begun to achieve the valuation of ecosystem services and incorporate them into their economic decision-making processes [91]. PES is specifically defined as "resource transfers between social actors to establish incentives to harmonize individual and/or cooperative land utilization choices with social interests in natural resource management" [92]. Its primary aim is to obtain a consistent supply of ecosystem services [93]. However, since the social benefits of ecosystem services are intricate and varied, it is impossible to determine when payment is appropriate [94].

We focus especially on the interactions between institutional and ecological problems, which are currently underrepresented in the PES literature [94]. However, a number of scholars are studying it. For example, according to the spatial scale of benefit, the value realization of global eco-product should be transferred from the ecological beneficiaries to the eco-protectors, such as the eco-compensation of the German-Czech Elbe river basin and the eco-compensation of the US-Canadian Columbia river basin, etc.; the value realization of national eco-product should be transferred from the central to the local. For example, transfer payments for key ecological function areas and the project of returning farmland to forestland and grassland in China, the fallow land protection program in the United States and the protection program for environmentally sensitive areas in the United Kingdom. Moreover, the realization of the value of territorial eco-products should establish a horizontal transfer payment system between ecological protection areas and beneficiary areas, such as horizontal ecological compensation upstream and downstream of watersheds in China, the interstate fiscal balance fund in Germany, and the equalization transfer payment system in Australia [95]. However, in karst areas, ecological compensation systems for agroforestry eco-products are less common and research could be strengthened in the future.

4.3.2. The Analysis of the Mode of Eco-Product Value Realization Provides a Practical Basis for the Diversification of Eco-Products' Worth Achievement Patterns

Promoting the realization of the value of eco-products is conducive to economic development. The existing research on this topic mainly focuses on the analysis of value realization models and specific cases [96]. At present, international and domestic studies are different, and scholars have analyzed the model of eco-product value realization from different angles. From the perspective of the leading initiator, eco-product value realization models can be categorized as government-led models, market-led models, social-led models, etc. The government-led model is still the main model for eco-product value realization under the current national conditions [95]. Wang et al. analyzed the value realization mode of eco-product from three perspectives: Material products, cultural service products, and regulatory services and goods. First, by relying on rich ecological resources and environmental quality, people can promote ecological material supply products' value realization. Second, by developing ecological tourism and cultural industry features, people can deepen the cultural service class eco-product value realization. Finally, by exploring resource rights transfer and ecological compensation, they can promote the ecological regulating service of product value realization [97]. Liu asserts that there are three main approaches to appraising the worth of eco-products. These are the basic development type, the extended development type, and the supportive development type. On this basis, they can be further subdivided into seven specific models: Industrial ecological type, eco-industry type, property rights transaction type, eco-premium type, eco-compensation type, eco-initiative type, and green finance type [98]. In karst areas, different models for realizing the value of agroforestry eco-products should be explored under different grades of karst desertification and the best model should be identified.

4.4. Eco-Industry

The eco-industrial chain is the fundamental unit of an eco-industrial system [99], which improves the utilization of industrial resources by imitating the use of materials and power in a natural ecosystem [100]. The eco-chain structure pattern is comprised of four connections associated with the input viewpoint of eco-products: Eco-product chains, derivative chains, product requirement markets, and assisting industry chains [101]. Regarding the unique characteristics of eco-products, some scholars put forward a feasible eco-industry chain in this region. For example, Su et al. believed that the agricultural industry chain is able to systematically reduce negative services and convert certain by-products or waste types in the industry chain into inputs for another production process, thereby effectively reducing purchasing inputs and increasing the output of other associated products, such as fish or duck meat, etc., which increases the economic benefits of rice fields from 132% to 135% [102]. In some protected areas, according to the uniqueness of different eco-products, constructing corresponding eco-industry chains can better promote local economic development. For example, Wei and Zhao based on the analysis of the product background and the industrial uniqueness of the industrial development of nature reserves and through the construction and analysis of the eco-industry chain system model of nature reserves, attempted to solve the difficulty of supplying eco-products and protecting the nature reserve market. Effective development ideas are provided by the balanced, environmental sustainability of nature reserves [101].

In certain karst areas with a special geographical environment, combined with the surrounding environment, according to the characteristics of different eco-products, are suitable eco-industries models that can be developed to upgrade the growth of the eco-industry chain in the region. In the low-yielding rice paddies in the karst mountains of Guangxi, for instance, the experiment and demonstration of the "rice (*Oryza sativa* L.) + sugarcane (*Saccharum officinarum* L.) + fish + mushroom (*Agaricus campestris*) + vegetable" mixed ecological agriculture model revealed that it was 8.4 times greater than in the comparison group (planting only two times the amount of the cropping rice) and the net earnings were 10.1 times more, which developed local economic and ecological benefits

under this model [103]. On arable land at a slope of about 15 degrees in Bijie, Guizhou Province, a comparative technology demonstration trial of a potato (*Solanum tuberosum* L.) and maize (*Zea mays* L.) cross-slope cluster monopoly and potato (*Solanum tuberosum* L.) and maize (*Zea mays* L.) down-slope cluster monopoly was conducted. According to the findings, the potato (*Solanum tuberosum* L.) yield increased by 10.94%, maize (*Zea mays* L.) yield grew by 8.29%, compound yield increased by 10.17%, and compound production value improved by 9.36% when compared to the potato (*Solanum tuberosum* L.) and maize (*Zea mays* L.) down-slope cluster planting treatment [104]. Researchers have demonstrated that industrial restructuring, which boosted the percentage of industry and services while decreasing the proportion of agriculture, also served to save soil [105]. Therefore, in the special karst environment, the region can choose to implement a developable agroforestry eco-product chain based on the features of the agroforestry eco-products.

The agroforestry ecosystem services provide the basis for the revitalization of agroforestry [31]. There is a growing demand for the growth of ecological mountain agriculture based on agroforestry in karst areas [106,107], which has gained the support and adoption of many scholars in succession [108,109]. However, the current agroforestry industry is characterized by a homogeneous stand structure, interspecies relationships, and a disconnect between industries and other problems [110–112]. The characteristics of agroforestry should be taken advantage of, such as its high efficiency, the capacity of intrinsically powered eco-products, and the ecological transformation of externally powered industries that can be used to promote eco-industrialization, environmental perception enhancement, and a higher demand for eco-products [113]. It is a comprehensive approach to optimizing and upgrading the various resources and crop groupings within the agroforestry ecosystem services, in order to achieve a multi-level and efficient use of energy and material cycles. The possibility of boosting the local economy and advancing the evolution of agroforestry ecosystem services in karst areas is presented by raising the worth of agroforestry ecosystem services.

5. Key Scientific Issues to Be Addressed

5.1. Creating a Framework for Calculating the Value of Agroforestry Ecosystem Services

The agroforestry ecosystem structure not only improves the ecological environment, but also increases its durability and restoration power since the rotation of crops in the specific structure minimizes pest problems, lessens contests and sickness, and boosts the soil's fertility and crop yield [114]. At present, the karst desertification agroforestry governance model with comprehensive soil and water improvement as its core has developed into agroforestry ecological governance derivative industries, such as forest-fruit, forest-medicine, and forest-grass. One of its positive aspects resolves the paradox between humanity and the land by playing a win-win role in time and place for ecological, social, and economic benefits [115,116]. However, agroforestry's contribution to the development of the eco-industry is based on the ecosystem services it offers. Therefore, clarifying the systems to realize the worth of agroforestry ecosystem services can better improve the economic development of karst areas and can also play a certain demonstration role. Many academics use the gross ecosystem product (GEP) to assess the value of eco-products directly, including items from agriculture, forestry, livestock, and fishing [117,118]. GEP indicators may be inflated and overlap with those for eco-products and traditional goods [113]. Since the realization of agroforestry ecosystem service value is an extremely complex process, various theories and viewpoints on agroforestry ecosystem service value accounting are constantly being debated and no one viewpoint dominates. Therefore, the discussion on the agroforestry ecosystem service value accounting of agroforestry is still a relatively large scientific question for the future.

5.2. In-Depth Study of Ecological Compensation Mechanisms for Agroforestry Ecosystem Services

China has investigated several ecological compensation models, primarily the compensation scheme for financial transfers from the government, the environmental resource tax

and compensation system, the ecological resource producer payment compensation model, and the ecological damage compensation model [119]. For ecological compensation, the regional ecological compensation objects need to be determined and a regional ecological compensation framework must be built. In karst regions, agroforestry ecosystem services lack the establishment of a system of ecological compensation. The implementation of the compensation objects should be strengthened, and the framework should be used to make reasonable compensation, in order that it offers a certain theoretical foundation for the ecological compensation mechanism of agroforestry ecosystem services in karst ecological restoration.

5.3. Exploring the Pathways, Mechanisms, and Models for Realizing the Value of the Agroforestry Eco-Products

In regard to the existing research, due to the diversity and complexity of agroforestry ecosystem services, the current research focus is mainly on the worth realization mechanism of agroforestry ecosystem services; however, few scholars emphasize the worth realization of karst agroforestry ecosystem services. Appropriate agroforestry ecological services should be rationally designed for the environment, and the market's crucial role in determining how to distribute agroforestry ecosystem services should be activated. At present, agroforestry ecosystem services in karst areas have a selective preference under the guidance of human values, and they focus a large amount of attention on regulating services while ignoring the importance of supply services and cultural services [31]. Focusing on the effectiveness and level of karst ecological restoration, we can focus on research on the supply services and cultural services of agroforestry ecosystem services. This can be achieved by comparing the varieties of agroforestry ecosystem services in different areas and exploring the worth realization paths, mechanisms, and modes of karst agroforestry ecosystem services through questionnaires, farmer interviews, etc.

5.4. In-Depth Study of the Formation Mechanisms of the Eco-Industry

Industrial colocalization, as well as ecological industrialization, are both theoretical and policy-based issues, and they have not yet been completely "solved". In-depth research is also needed in theory, especially the dynamic, incentive, restraint, price, and investment mechanisms, as well as industrial regulation, industrial organization, market organization, and market regulation theories [120]. In addition, the coupling connection between ecological governance and industrial growth in ecologically fragile regions should be researched and a coupling collaboration extent prototype between ecological governance, as well as sourced ecological businesses in ecologically fragile places should be formed. The goal of these studies and models is to assist in methodically comprehending and properly assessing the coordination condition of environmental governance and the industrial economy in ecologically vulnerable places [121]. In the future, to explore the coupling relationship between karst agroforestry ecosystem services and eco-industries and the formation mechanism of the industry, research theory should be improved, contributing to the sustainable and coordinated development of agroforestry products and agroforestry industries in karst areas. Therefore, the best agroforestry models should be studied in karst ecological restoration areas to promote local development. Figure 6 depicts the ecological processes, by which different agroforestries form eco-industries.

5.5. Strengthen the Supply Ability of Agroforestry Ecosystem Services

Agroforestry ecosystem services are tangible products, as well as services provided by agroforestry ecosystems, that satiate the needs of both individuals and the environment through the synergistic impacts of biological and human production [122]. This demonstrates that the highlight of boosting the supply ability of agroforestry ecosystem services is regulating the productive agents of ecosystem services [123,124]. The market is significantly impacted by the agroforestry ecosystem services supply capacity. Agroforestry ecosystem services with a strong supply capacity and strong market demand will have

better development and are generally able to form a certain scale of eco-industries, which will promote local development. In the future, on the basis of previous research, we will investigate and evaluate how to increase the supply of agroforestry ecosystem services, in order to provide more information for the achievement of the worth of agroforestry ecosystem services and the formation of eco-industries. Good products can help the local economy grow as well as help karst agroforestry ecosystem services and evaluation systems to flourish.

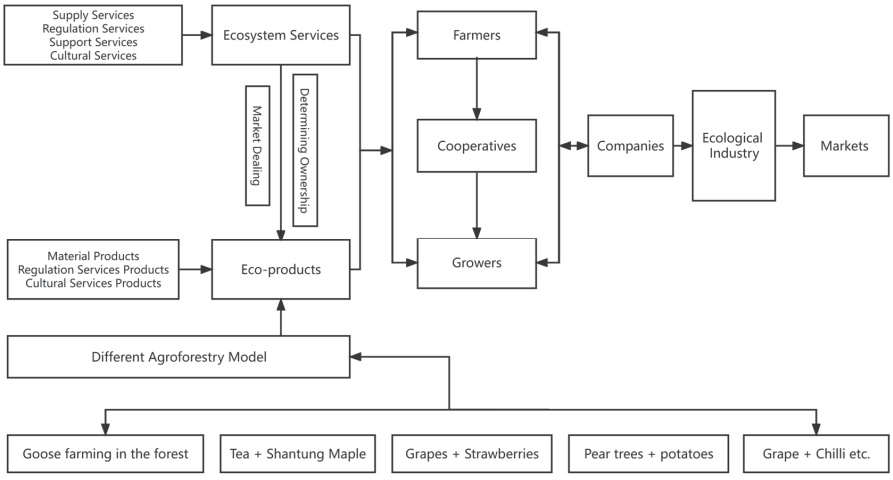

Figure 6. Ecological processes in the formation of eco-industries in different agroforestries.

5.6. In-Depth Study of the Property Rights System of Agroforestry Ecosystem Services

Under normal circumstances, the ecosystem's material supply function, which includes the provision of water resources, agricultural products, forest products, energy resources, etc., can be traded directly on the market. Cultural services, such as ecotourism and natural landscapes, can also be attached to related eco-industries, transforming them into clear property rights [97]. Therefore, the property rights of ecological material products and cultural service products are more clear than ecological regulation products. According to Zhou et al., there are currently several issues, such as unclear agroforestry ecosystem services property rights, a lack of an adequate system for accounting for the value of agroforestry ecosystem services, and limitations on the growth of the mechanism for realizing the worth of agroforestry ecosystem services. By enhancing the property rights system for natural resources and agroforestry ecosystem services, financial investment and ecological compensation mechanisms, market systems and price mechanisms, steps should be taken to establish a production product accounting mechanism and a financial support mechanism [125]. Therefore, the property rights of agroforestry ecosystem services in karst areas are clear, which is helpful for the growth of eco-industries and the comprehension of the value of karst agroforestry ecosystem services.

6. Conclusions

6.1. Conclusions

Studies in karst areas have been primarily concentrated in Asia, Europe, and North America, with the majority being dispersed in karst regions in China with a vulnerable ecological environment as well as eco-product worth accomplishment areas. The present value realization of eco-products and the eco-industries are still lacking a fully developed theoretical system, according to the research literature currently available. There is a need for more in-depth and expanded theoretical research. This study's findings are presented as follows: (1) The ecosystem services supply capacity mainly focuses on the research on the

environment where ecosystem services are located, the interaction of supply and demand, potential supply and actual supply capacity, and the findings of the low supply capacity of ecosystem services. (2) Ecosystem services value accounting and evaluation are mainly studied from two perspectives: The accounting method and the accounting system. At present, the agroforestry ecosystem services accounting method has not been unified. In the future, we might further deepen our research on ecosystem services value accounting and establish a unified scientific and reasonable agroforestry ecosystem services accounting research framework. (3) The main topics of this study comprise the paths, mechanisms, and models, among which eco-compensation is an important way for eco-product value realization. (4) The goal of eco-industry is to find suitable eco-industry models that will encourage the growth of the regional eco-industry chain.

6.2. Enlightenment

This paper outlines the six major scientific and technological issues that should be resolved, in order to determine the future direction of karst agroforestry ecosystem services. The following factors can be used to determine the future of agroforestry ecosystem services: (1) Accounting approaches and system standards for the value of agroforestry ecosystem services; (2) the in-depth study of ecological compensation mechanisms for agroforestry ecosystem services; (3) paths, mechanisms, and models for realizing the value of the agroforestry eco-products; (4) the formation mechanism of eco-industries; (5) the strengthening of the supply ability of agroforestry ecosystem services; (6) the in-depth study of the property rights system of agroforestry ecosystem services. These areas, which are rich in agroforestry ecosystem services and require a better accounting system for the regulation of agroforestry ecosystem services, are particularly suited as future research topics.

Author Contributions: All authors are contributed to the manuscript. Conceptualization, Y.Y. and K.X.; methodology, Y.Y.; validation, Y.Y. and H.H.; formal analysis, Y.Y. and J.X.; data curation, Y.Y. and H.H.; writing—original draft preparation, Y.Y.; writing—review and editing, Y.Y., K.X. and H.H.; visualization, Y.Y., B.Y. and Y.Z.; project administration, K.X.; funding acquisition, K.X. All authors have read and agreed to the published version of the manuscript.

Funding: This research was supported by the Key Science and Technology Program of GuizhouProvence: Poverty Alleviation Model and Technology demonstration for Ecoindustries Derivated from the karst desertification control (No. 5411 2017 Qiankehe Pingtai Rencai), the Science and Technology Research Project of Higher Education Institutions in Hebei Province: Comparative study of model and technology for characteristic high efficiency forestry from the karst desertification control in North and South China Karst (No. QN2021412), and the China Overseas Expertise Introduction Program for Discipline Innovation: Overseas Expertise Introduction Center for South China Karst Eco-environment Discipline Innovation (D17016).

Institutional Review Board Statement: Not applicable.

Informed Consent Statement: Not applicable.

Data Availability Statement: The data presented in this study are openly available in (China National Knowledge Infrastructure (CNKI)) at (https://www.cnki.net, accessed on 30 June 2022), and (Web of Science (WOS)) at (https://www.webofscience.com, accessed on 30 June 2022).

Acknowledgments: We are grateful for Shilian Jiang for her help in the presentation of Figure 4.

Conflicts of Interest: The authors declare no conflict of interest. The funders had no role in the design of the study; in the collection, analyses, or interpretation of data; in the writing of the manuscript, or in the decision to publish the results.

References

1. He, H.S.; Zhao, Y.H.; Wu, J.S. Simulation of urban landscape pattern under the Influence of Low Carbon: A Case Study of Shenzhen. *Acta Ecol. Sin.* **2021**, *41*, 8352–8363.
2. Jackson, S.T.; Hobbs, R.J. Ecological restoration in the light of ecological history. *Science* **2009**, *325*, 567–569. [CrossRef] [PubMed]

3. Martin, D.M. Ecological restoration should be redefined for the twenty-first century. *Restor. Ecol.* **2017**, *25*, 668–673. [CrossRef] [PubMed]
4. Wang, C.; Wu, X.; Fu, B.J.; Han, X.G.; Chen, Y.N.; Wang, K.l.; Zhou, H.K.; Feng, X.M.; Li, Z.S. Ecological restoration in the key ecologically vulnerable regions: Current situation and development direction. *Acta Ecol. Sin.* **2019**, *39*, 7333–7343.
5. Han, Y.; Zhao, W.W.; Zheng, B.F. Promoting the construction of ecological civilization and promoting regional sustainable development: A review of the 2020 academic forum on ecological civilization and sustainable development in China. *Acta Ecol. Sin.* **2021**, *41*, 1259–1265.
6. Gao, J.X.; Zhang, X.H.; Zou, C.X.; Li, G.Y.; Zhang, K.; Ye, X. Build a strong ecological barrier and build a beautiful China. *Environ. Prot.* **2021**, *49*, 17–20.
7. Li, B.L.; Wu, Y.G. On the ecological relationship between ecological protection and green development during the 14th Five-Year Plan. *Sci. Technol. Rev.* **2021**, *39*, 88–101.
8. Gong, Q.H.; Zhang, H.G.; Ye, Y.Y.; Yuan, S.X. Planning strategy of land and space ecological restoration under the framework of man-land system coupling: Take the Guangdong-Hong Kong-Macao Greater Bay Area as an example. *Geogr. Res.* **2020**, *39*, 2176–2188.
9. Guan, Y.; Kang, R.; Liu, J. Evolution of the field of ecological restoration over the last three decades:a bibliometric analysis. *Restor. Ecol.* **2019**, *27*, 647–660. [CrossRef]
10. Guan, Y.J.; Liu, J.G.; Cui, W.H.; Jia, J.L. Progress and future direction of ecological restoration research in China. *Acta Ecol. Sin.* **2022**, *42*, 1–11.
11. Yang, M.D. On the fragility of karst environment. *Yunnan Geogr. Environ. Res.* **1990**, *2*, 21–29.
12. Ford, D.; Williams, P. *Karst Hydrogeology and Geomorphology*; John Wiley & Sons: Hoboken, NJ, USA, 2007; pp. 1–8.
13. Ouyang, Z.Y. On the comprehensive management, development and breaking away from poorness of the ecologically fragile karst area in south-west China. *World Sci.-Tech R D* **1998**, *20*, 53–56.
14. Yuan, D.X. World correlation of karst ecosystem: Objectives and implementation plan. *Adv. Earth Sci.* **2001**, *16*, 461–466.
15. Lu, Y.R. *Geo-Ecology and Sustainable Development—Developing Ways for Karst Regions in Southwest and Abjacent Karst Regions of China*; Hohai University Press: Nanjing, China, 2003; pp. 1–10.
16. Xiong, K.N.; Bai, L.N.; Peng, X.W.; Li, Y.B. Research on changes of land-use in different scale in karst mountain. *Carsologica Sin.* **2005**, *1*, 43–49.
17. Costanza, R.; Darge, R.; Degroot, R.; Farber, S.; Grasso, M.; Hannon, B.; Limburg, K.; Naeem, S.; Oneill, R.V.; Paruelo, J.; et al. The values of the world's ecosystem services and natural capital. *Nature* **1997**, *387*, 253–260. [CrossRef]
18. Millenium Ecosystem Assessment. *Ecosystems and Human Well-Being: Biodiversity Synthesis*; World Resources Institute: Washington, DC, USA, 2005.
19. Holdren, J.P.; Ehrlich, P.R. Human Population and the Global Environment: Population growth, rising per capita material consumption, and disruptive technologies have made civilization a global ecological force. *Am. Sci.* **1974**, *62*, 282–292.
20. Dempsey, J.; Robertson, M.M. Ecosystem services: Tensions, impurities, and points of engagement within neoliberalism. *Prog. Hum. Geogr.* **2012**, *36*, 758–779. [CrossRef]
21. Smith, J.; Pearce, B.D.; Wolfe, M.S. Reconciling productivity with protection of the environment: Is temperate agroforestry the answer? *Renew. Agr. Food Syst.* **2013**, *28*, 80–92. [CrossRef]
22. Lehmann, L.M.; Smith, J.; Westaway, S.; Pisanelli, A.; Russo, G.; Borek, R.; Sandor, M.; Gliga, A.; Smith, L.; Ghaley, B.B. Productivity and Economic Evaluation of Agroforestry Systems for Sustainable Production of Food and Non-Food Products. *Sustainability* **2020**, *12*, 5429. [CrossRef]
23. Zhu, X.A.; Liu, W.J.; Chen, J.; Bruijnzeel, L.A.; Mao, Z.; Yang, X.D.; Cardinael, R.; Meng, F.R.; Sidle, R.C.; Seitz, S.; et al. Reductions in water, soil and nutrient losses and pesticide pollution in agroforestry practices: A review of evidence and processes. *Plant Soil* **2020**, *453*, 45–86. [CrossRef]
24. Bentrup, G.; Hopwood, J.; Adamson, N.L.; Vaughan, M. Temperate Agroforestry Systems and Insect Pollinators: A Review. *Forests* **2019**, *10*, 981. [CrossRef]
25. Schoeneberger, M.M.; Bentrup, G.; Patel-Weynand, T. *Agroforestry: Enhancing Resiliency in U.S. Agricultural Landscapes under Changing Conditions*; WO-96; United States Department of Agriculture, Forest Service: Washington, DC, USA, 2017; p. 213.
26. Beillouin, D.; Ben-Ari, T.; Malezieux, E.; Seufert, V.; Makowski, D. Positive but variable effects of crop diversification on biodiversity and ecosystem services. *Glob. Chang. Biol.* **2021**, *27*, 4697–4710. [CrossRef] [PubMed]
27. McNeil, C.L. Deforestation, agroforestry, and sustainable land management practices among the Classic period Maya. *Quatern. Int.* **2012**, *249*, 19–30. [CrossRef]
28. Wu, Q.L.; Liang, H.; Xiong, K.N.; Li, R. Eco-benefits coupling of agroforestry and soil and water conservation under KRD environment:frontier theories and outlook. *Agroforest. Syst.* **2019**, *93*, 1927–1938. [CrossRef]
29. Chen, H.; Zhu, D.Y.; Chen, H.; Wen, Y.Q. Effect of Agroforestry on Soil Environment in Rocky Desertification Area and Its Application Prospect. *World For. Res.* **2019**, *32*, 13–18.
30. Liu, Q.S.; Chen, H.; Li, L.Z.; Wang, C.L.; Chen, J.; Yang, Y.W.; Zhang, H.M. Edge effect of a soil mite community in a controlled agroforestry area. *Chin. J. Appl. Environ. Biol.* **2020**, *26*, 370–377.
31. Xiong, K.N.; Xiao, J.; Zhu, D.Y. Research progress of agroforestry ecosystem services and its implications for industrial revitalization in karst regions. *Acta Ecol. Sin.* **2022**, *42*, 851–861.

32. Hong, Z.Y.; Yang, Z. Discussion on the transformation of planting grass, planting trees and ecological products from the historical changes of the Loess Plateau. *J. Henan Univ. Sci. Technol. (Agr. Sci.)* **1985**, *1*, 70–76.
33. Wang, J.J.; Rong, D.M. Study on Evaluation and Realization Mechanism of Ecosystem Services Value of the UK Government. *Nat. Resour. Inform.* **2021**, *2*, 9–14.
34. Li, Y.L.; Chen, K.L. An analysis on the formation process and various realization approaches of ecological product value. *Ecol. Econ.* **2021**, *37*, 152–162.
35. Zhang, L.B.; Yu, H.Y.; Li, D.Q.; Jia, Z.Y.; Wu, F.C.; Liu, X. Connotation and value implementation mechanism of ecological products. *T. Chin. Soc. Agr. Mach.* **2019**, *50*, 173–183.
36. Liu, J.Y.; Mou, D.G. Research Progress of Ecological Product Value and Its Realization Mechanism. *Ecol. Econ.* **2020**, *36*, 207–212.
37. Zhou, J.Y.; Xiong, K.N.; Wang, Q.; Tang, J.H.; Lin, L. A Review of Ecological Assets and Ecological Products Supply: Implications for the Karst Rocky Desertification Control. *Int. J. Env. Res. Pub. He.* **2022**, *19*, 10168. [CrossRef] [PubMed]
38. Fang, Y.P.; Zeng, Y.; Li, S.M. Basic Connotation of Ecological Transforming of Industrial System and Support Mechanism in China. *J. Univ. Electron. Sci. Technol. China (Soc. Sci. Edit.)* **2010**, *12*, 1–5.
39. Wu, Q.; Xiao, H.; Chen, H.; Zhou, G.F. Research on derivative industries and targeted poverty alleviation in the vulnerable ecological karst area of southern china. *Fresen. Environ. Bull.* **2021**, *30*, 2069–2076.
40. Ren, Y.W.; Yuan, G.B. Preliminary Account on "Ecological Products". *Chin. J. Ecol.* **1992**, *6*, 50–52.
41. Xiong, K.N.; Lai, J.L.; Zhang, Y.; Ji, C.Z.; Ma, X.W.; Xiao, S.Z. Study on the effective components of honeysuckle bud and flower in different grades of rocky desertification in karst area and their relationship with soil nutrients. *China J. Tradit. Chin. Med. Pharm.* **2021**, *36*, 3142–3146.
42. Jose, S.; Gold, M.A.; Garrett, H.E. The future of temperate agroforestry in the United States. In *Agroforestry: The Future of Global Land Use*; Springer: Dordrecht, The Netherlands, 2012; pp. 217–245.
43. Kim, D.G.; Kirschbaum, M.U.F.; Beedy, T.L. Carbon sequestration and net emissions of CH4 and N2O under agroforestry: Synthesizing available data and suggestions for future studies. *Agr. Ecosyst. Environ.* **2016**, *226*, 65–78. [CrossRef]
44. Muchane, M.N.; Sileshi, G.W.; Gripenberg, S.; Jonsson, M.; Pumarino, L.; Barrios, E. Agroforestry boosts soil health in the humid andsub-humid tropics: A meta-analysis. *Agr. Ecosyst. Environ.* **2020**, *295*, 106899. [CrossRef]
45. Zhang, L.; Wang, Z.L.; Xue, T.T.; Gao, F.F.; Wei, R.T.; Wang, Y.; Han, X.; Li, H.; Wang, H. Combating Desertification through the WineIndustry in Hongsibu, Ningxia. *Sustainability* **2021**, *13*, 5654. [CrossRef]
46. Garcia, L.; Celette, F.; Gary, C.; Ripoche, A.; Valdes-Gomez, H.; Metay, A. Management of service crops for the provision ofecosystem services in vineyards: A review. *Agr. Ecosyst. Environ.* **2018**, *251*, 158–170. [CrossRef]
47. Paiola, A.; Assandri, G.; Brambilla, M.; Zottini, M.; Pedrini, P.; Nascimbene, J. Exploring the potential of vineyards for biodiversityconservation and delivery of biodiversity-mediated ecosystem services: A global-scale systematic review. *Sci. Total Environ.* **2020**, *7*, 150.
48. Han, X.; Xue, T.T.; Liu, X.; Wang, Z.L.; Zhang, L.; Wang, Y.; Yao, F.; Wang, H.; Li, H. A Sustainable Viticulture Method Adapted to the Cold Climate Zone in China. *Horticulturae* **2021**, *7*, 150. [CrossRef]
49. Peng, W.Y.; Yuchi, X.J. The Supply Capacity Improvement and Value Realization Path of Ecological Products in Beijing-Tianjin-Hebei. *China Bus. Market* **2021**, *35*, 49–60.
50. Boyd, J.; Banzhaf, S. What are ecosystem services? The need for standardized environmental accounting units. *Ecol. Econ.* **2007**, *63*, 616–626. [CrossRef]
51. Marais, Z.E.; Baker, T.P.; O'Grady, A.P.; England, J.R.; Tinch, D.; Hunt, M.A. A natural capital approach to agroforestry decision-making at the farm scale. *Forests* **2019**, *10*, 980. [CrossRef]
52. Varah, A.; Jones, H.; Smith, J.; Potts, S.G. Temperate Agroforestry systems provide greater pollination service than monoculture. *Agric. Ecosyst. Environ.* **2020**, *301*, 107031. [CrossRef]
53. Jiang, L.; Pu, Z. Different effects of species diversity on temporal stability in single-trophic and multitrophic communities. *Am. Nat.* **2009**, *174*, 651–659. [CrossRef]
54. Jiang, S.L.; Xiong, K.N.; Xiao, J. Structure and Stability of Agroforestry Ecosystems: Insights into the Improvement of Service Supply Capacity of Agroforestry Ecosystems under the Karst Rocky Desertification Control. *Forests* **2022**, *13*, 878. [CrossRef]
55. Tambouratzis, T.; Karalekas, D.; Moustakas, N. A methodological study for optimizing material selection in sustainable product design. *J. Ind. Ecol.* **2014**, *18*, 508–516. [CrossRef]
56. Li, F.R.; Rong, A.P. The research of PPP mode in ecological products supply. *Econ. Probl.* **2016**, *12*, 11–16.
57. Yang, Y.M.; Xiao, H.; Chen, H.; Xiao, N.J.; Guo, C. Structural characteristics of soil mite communities under different modes of rose-based agroforestry in Karst area. *Acta Agr. Zhejiangensis* **2021**, *33*, 112–121.
58. He, F.Y.; Xiong, K.N.; Zhu, D.Y.; Zhang, S.H.; Zhang, J.J.; Fu, Y.Y. Characteristics and Simulations of Soil Infiltration in Agroforestry on Karst Mountains. *Fujian J. Agr. Sci.* **2020**, *35*, 200–209.
59. Zou, Z.G.; Zeng, F.P.; Wang, K.L.; Zeng, Z.X.; Zhao, L.L.; Du, H.; Zhang, F.; Zhang, H. Emergy and Economic Evaluation of Seven Typical Agroforestry Planting Patterns in the Karst Region of Southwest China. *Forests* **2019**, *10*, 138. [CrossRef]
60. Jin, M.; Cai, C.T.; Liu, G.Z.; Ma, C.N. Response of Amomum tsao-ko's Productions and Benefits to Different Environmental Factors and Cultural Measures in the Canyon Region of Nujiang. *Chin. J. Trop. Crops* **2016**, *37*, 446–455.
61. Lu, Z.X.; Li, K.L.; Zhang, N.N.; Chen, Y.Q. Effects of lac-corn agroforest ecosystem on ground-dwelling ant diversity and functional groups. *Chin. J. Eco-Agr. Jan.* **2016**, *24*, 81–89.

62. Ahmed, Y.A.R.; Pichler, V.; Homolak, M.; Goemoeryova, E.; Nagy, D.; Pichlerova, M.; Gregor, J. High organic carbon stock in a karstic soil of the Middle-European Forest Province persists after centuries-long agroforestry management. *Eur. J. Forest Res.* **2012**, *131*, 1669–1680. [CrossRef]
63. Liu, G.Z.; Cai, C.T.; Luo, Y.; Liu, B.; Sun, C.X. Biomass and growth law of alstonia scholar is under different patterns of agroforestry. *Chinese. J. Eco-Agr.* **2008**, *16*, 150–154.
64. An, H.P.; Zhou, J.W.; Xu, L.Y. Effects of Different Agroforestry Management Model on the Soil of Eucommia ulmoides and Evaluation. *Guizhou For. Sci. Technol.* **2001**, *29*, 41–45.
65. Ma, L.; Liu, H.; Peng, J.; Wu, J.S. A review of ecosystem services supply and demand. *Acta Geogr. Sin.* **2017**, *72*, 1277–1289.
66. Xiao, Y.; Xie, G.D.; Lu, C.X.; Xu, J. Involvement of ecosystem service flows in human wellbeing based on the relationship between supply and demand. *Acta Geogr. Sin.* **2016**, *36*, 3096–3102.
67. Dai, F.; Feng, X.M.; Song, X.F. Game Game Analysis on Forest Eco-products Supply. *World For. Res.* **2013**, *26*, 93–96.
68. Jin, B.H.; Huang, R.; Feng, J.M.; Ma, X.L. Analysis on Internal Driving Mechanism of Eco-label Product Supply: From the Perspectives of Complete Value and Intergenerational Value. *China Land Sci.* **2021**, *35*, 81–88.
69. Ke, W.; Zhang, J.S. Quality Quantification: Structural Dilemma and Reform of Ecological Supply Side. *Trib. Study* **2017**, *33*, 47–52.
70. Qin, Y.; Zeng, X.G.; Xu, Z.H. Promoting the supply side reform of ecological products based on PPP model. *J. Arid Land Resour. Environ.* **2018**, *32*, 7–12.
71. Wang, M.A.; Dong, S.J. The Necessity, Reality and Transformation of Local Government Cooperation on the Supply of Regional Ecological Public Goods. *Ecol. Econ.* **2019**, *35*, 165–169.
72. Owoyemi, A.; Porat, R.; Lichter, A.; Doron-Faigenboim, A.; Jovani, O.; Koenigstein, N.; Salzer, Y. Evaluation of the Storage Performance of 'Valencia'Oranges and Generation of Shelf-Life Prediction Models. *Horticulturae* **2022**, *8*, 570. [CrossRef]
73. Flores-Lopez, M.L.; Cerqueira, M.A.; de Rodriguez, D.; Vicente, A.A. Perspectives on utilization of edible coatings and nano-laminate coatings for extension of postharvest storage of fruits and vegetables. *Food Eng. Rev.* **2016**, *8*, 292–305. [CrossRef]
74. Ouyang, Z.Y.; Zhu, C.Q.; Yang, G.B.; Xu, W.H.; Zheng, H.; Zhang, Y.; Xiao, Y. Gross ecosystem product: Concept, accounting framework and case study. *Acta Ecol. Sin.* **2013**, *33*, 6747–6761. [CrossRef]
75. Yang, M.; Xiao, Y.; Ouyang, Z.Y.; Ye, H.; Deng, M.T.; Ai, L. Ecosystem regulation services accounting of gross ecosystem product (GEP) in Sichuan province. *J. Southwest Minzu Univ. (Nat. Sci. Edit.)* **2019**, *45*, 221–232.
76. Song, C.S.; Ouyang, Z.Y. Gross Ecosystem Product accounting for ecological benefits assessment: A case study of Qinghai Province. *Acta Ecol. Sin.* **2020**, *40*, 3207–3217.
77. Ouyang, Z.Y.; Lin, Y.Q.; Song, C.S. Research on Gross Ecosystem Product(GEP): Case study of Lishui City, Zhejiang Province. *Environ. Sustain. Dev.* **2020**, *45*, 80–85.
78. Qiu, S.L. Realization of the Value of Diversified Ecological Products: Government Role Positioning and Behavioral Boundaries: A Typical Analysis Based on the "Lishui Model". *Theory Mon.* **2021**, *8*, 77–85.
79. Xie, G.D.; Zhang, C.X.; Zhang, L.M.; Chen, W.H.; Li, S.M. Improvement of the Evaluation Method for Ecosystem Service Value Based on Per Unit Area. *J. Nat. Resour.* **2015**, *30*, 1243–1254.
80. Liu, S.J. The Multiplication of Middle-Income Group and Construction of High-Standard Market Economy. *J. Lanzhou Univ. (Soc. Sci. Edit.)* **2019**, *47*, 1–10.
81. Song, F.; Su, F.L.; Mi, C.X.; Sun, D. Analysis of driving forces on wetland ecosystem services value change: A case in Northeast China. *Sci. Total Environ.* **2020**, *751*, 141778. [CrossRef]
82. Alam, M.; Olivier, A.; Paquette, A.; Dupras, J.; Revéret, J.P.; Messier, C. A general framework for the quantification and valuation of ecosystem services of tree-based intercropping systems. *Agroforest. Syst.* **2014**, *88*, 679–691. [CrossRef]
83. Kay, S.; Graves, A.; Palma, J.H.N.; Moreno, G.; Roces-Diaz, J.V.; Aviron, S.; Chouvardas, D.; Crous-Duran, J.; Ferreiro-Dominguez, N.; Garcia de Jalon, S.; et al. Agroforestry is paying off–Economic evaluation of ecosystem services in European landscapes with and without agroforestry systems. *Ecosyst. Serv.* **2019**, *36*, 100896. [CrossRef]
84. Doddabasawa; Chittapur, B.M. Quantification of ecoservices in traditional agroforestry systems in semi arid tropics. *Bangl. J. Bot.* **2021**, *50*, 427–432. [CrossRef]
85. Tsonkova, P.; Quinkenstein, A.; Böhm, C.; Freese, D.; Schaller, E. Ecosystem services assessment tool for agroforestry (ESAT-A): An approach to assess selected ecosystem services provided by alley cropping systems. *Ecol. Indic.* **2014**, *45*, 285–299. [CrossRef]
86. Zhou, L.L.; Guan, D.J.; Huang, X.Y.; Yuan, X.Z.; Zhang, M.J. Evaluation of the cultural ecosystem services of wetland park. *Ecol. Indic.* **2020**, *114*, 106286. [CrossRef]
87. Daily, G.C.; Polasky, S.; Goldstein, J.; Kareiva, P.M.; Mooney, H.A.; Pejchar, L.; Ricketts, T.H.; Salzman, J.; Shallenberger, R. Ecosystem services in decision making: Time to deliver. *Front. Ecol. Environ.* **2009**, *7*, 21–28. [CrossRef]
88. Zhang, J.; Zou, Z.Y. Research on calculation and application of GEP in Brahmaputra River Basin. *Ecol. Econ.* **2022**, *38*, 167–172, +227.
89. Liang, L.N.; Wang, M.X.; Li, Z.H.; Wang, G. Calculation of gross economic-ecological product in Pearl River Delta region and the discussion on the transformation path from "lucid waters and lush mountains" to "invaluable assets". *Environ. Pollut. Control* **2021**, *43*, 121–125.
90. Yu, F.; Yang, W.S.; Ma, G.X.; Zhou, Y. The Latest Development and Prospect of Ecological Value Accounting at Home and Abroad. *Environ. Prot.* **2020**, *48*, 18–24.
91. "Realizing values of ecological products: Pathways, mechanisms and patterns" research group. In *Realizing Values of Ecological Products: Pathways, Mechanisms and Patterns*; China Development Press: Beijing, China, 2019; pp. 16–116.

92. Muradian, R.; Corbera, E.; Pascual, U.; Kosoy, N.; May, P.H. Reconciling theory and practice: An alternative conceptual framework for understanding payments for environmental services. *Ecol. Econ.* **2010**, *69*, 1202–1208. [CrossRef]
93. Xiao, J.; Xiong, K.N. A review of agroforestry ecosystem services and its enlightenment on the ecosystem improvement of rocky desertification control. *Sci. Total Environ.* **2022**, *852*, 158538. [CrossRef]
94. Cook, D.C.; Kristensen, N.P.; Liu, S. Coordinated service provision in payment for ecosystem service schemes through adaptive governance. *Ecosyst. Serv.* **2016**, *19*, 103–108. [CrossRef]
95. Qiu, S.L.; Jin, L.S. Realization of Ecological Product Value: Theoretical Basis, Basic Logic and Main Model. *Agr. Econ.* **2021**, *4*, 106–108.
96. Gao, X.L.; Lin, Y.Q.; Xu, W.H.; Ouyang, Z.Y. Research progress on the value realization of ecological products. *Acta Ecol. Sin.* **2020**, *40*, 24–33.
97. Wang, X.H.; Zhu, Y.Y.; Wen, Y.H.; Xie, J.; Liu, G.H. The Basic Patterns and Innovation Path of Realizing the Value of Ecological Products. *Environ. Prot.* **2020**, *48*, 14–17.
98. Liu, B.N. The Connotation, Classification and Institutional Framework of Value Realization Mechanism of Ecological Products. *Environ. Prot.* **2020**, *48*, 49–52.
99. Roberts, B.H. The application of industrial ecology principles and planning guidelines for the development of eco-industrial parks: An Australian case study. *J. Clean. Prod.* **2004**, *12*, 997–1010. [CrossRef]
100. Liu, J.; Tan, H.; Zhang, Z.H.; Li, Y.R. Ecological Development of Chemical Industry Park: A Review. *China Popul. Resour. Environ.* **2016**, *26*, 172–175.
101. Wei, H.L.; Zhao, S.S. Construction on the system model of the ecological industry chain in the nature reserves. *Ecol. Econ.* **2014**, *30*, 38–41.
102. Su, Y.; He, S.; Wang, K.; Shahtahmassebi, A.R.; Zhang, L.P.; Zhang, J.; Zhang, M.; Gan, M.Y. Quantifying the sustainability of three types of agricultural production in China: An emergy analysis with the integration of environmental pollution. *J. Clean. Prod.* **2020**, *252*, 119650. [CrossRef]
103. Liang, Q.B.; Lin, D.J.; Luo, H.F. A Preliminary Report on a Complex Eco-agro-model in Low Output Peddy Field in Southern Karst Region. *Eco-Agr. Res.* **1995**, *3*, 54–59.
104. Wang, X.H.; Ruan, P.J.; Mei, Y.; Yang, Y.P.; Gu, S.J.; Zheng, Y.Z.; Zhao, M.Y. Research on planting methods of light rocky desertification slope farmland in karst ecological zone. *Cultiv. Cultiv.* **2008**, *1*, 40–41.
105. Rao, E.M.; Xiao, Y.; Ouyang, Z.Y. Changes in ecosystem service of soil conservation between 2000 and 2010 and its driving factors in southwestern China. *Chin. Geogr. Sci.* **2016**, *26*, 165–173. [CrossRef]
106. Su, W.C.; Zhu, W.K. A study on the models and countermeasures of eco-agriculture development in Guizhou karst region. *Syst. Sci. Compr. Stud. Agr.* **2000**, *16*, 40–44.
107. Mei, Z.M.; Xiong, K.N. A study on the fundamental models and environmental beneficial results of ecological rehabilitation in Guizhou karst mountain areas. *J. Guizhou Norm. Univ. (Nat. Sci.)* **2000**, *18*, 9–17.
108. Zhou, J.W.; An, H.P. Study on classification of agroforestry systems in karst section of Guizhou. *Guizhou For. Sci. Technol.* **2002**, *30*, 31–34, +51.
109. Wang, K.L.; Zhang, C.H.; Chen, H.S.; Yue, Y.M.; Zhang, W.; Zhang, M.Y.; Qi, X.K.; Fu, Z.Y. Karst landscapes of China: Patterns, ecosystem processes and services. *Landsc. Ecol.* **2019**, *34*, 2743–2763. [CrossRef]
110. Yang, S.M.; Xiong, K.N.; Yu, Y.H.; Liu, X.Y.; Dong, X.C. Identification and Modification of Vegetation Recovery Model at China's Karst Rockified Areas. *World For. Res.* **2017**, *30*, 91–96.
111. Saj, S.; Jagoret, P.; Etoa, L.E.; Fonkeng, E.E.; Tarla, J.N.; Nieboukaho, J.D.E.; Sakouma, K.M. Lessons learned from the long-term analysis of cacao yield and stand structure in central Cameroonian agroforestry systems. *Agr. Syst.* **2017**, *156*, 95–104. [CrossRef]
112. Sun, Y.; Liang, Z.Y.; Wang, G.B.; Jia, W.G.; Zheng, W.J.; Lu, X.A.; Guo, Q.R.; Cao, F.L. Research hotspots and frontier analyses for agroforestry management. *J. Nanjing For. Univ. (Nat. Sci. Edit.)* **2020**, *44*, 228–235.
113. Zhang, Z.Z.; Xiong, K.N.; Chang, H.H.; Zhang, W.X.; Huang, D.H. A Review of Eco-Product Value Realization and Ecological Civilization and Its Enlightenment to Karst Protected Areas. *Int. J. Env. Res. Pub. He.* **2022**, *19*, 5892. [CrossRef]
114. Ripoche, A.; Autfray, P.; Rabary, B.; Randriamanantsoa, R.; Blanchart, E.; Trap, J.; Sauvadet, M.; Becquer, T.; Letourmy, P. Increasingplant diversity promotes ecosystem functions in rainfed rice-based short rotations in Malagasy highlands. *Agric. Ecosyst. Environ.* **2021**, *320*, 107576. [CrossRef]
115. Xiong, K.N.; Li, P.; Zhou, Z.F.; An, Y.L.; Lǔ, T.; Lan, A.J. *A Typical Study on Remote Sensing-GIS of Karst Rocky Desertification—Taking Guizhou Province as an Example*, 1st ed.; Geology Press: Beijing, China, 2002; pp. 144–145.
116. Wu, Q.L.; Liang, H.; Xiong, K.N.; Li, R. Frontier theories and countermeasures for integrated regulation of soil and water loss and mountainous agroforestry in rocky desertification environment. *J. Soil Water Conserv.* **2018**, *32*, 11–18.
117. Schlüter, M.; Haider, L.J.; Lade, S.J.; Lindkvist, E.; Martin, R.; Orach, K.; Wijermans, N.; Folke, C. Capturing emergent phenomena in social-ecological systems: An analytical framework. *Ecol. Soc.* **2019**, *24*, 62–87. [CrossRef]
118. Li, F.; Zhang, L.B.; Shu, J.M.; Meng, W. Accounting system for products in the ecosystem of the Three-River Headwater Area. *Sci. Technol. Rev.* **2017**, *35*, 120–124.
119. Liu, C.L.; Liu, W.D.; Lu, D.D.; Chen, M.X.; Dunford, M.; Xu, M. Eco-compensation and harmonious regional development in China. *Chinese Geogr. Sci.* **2016**, *26*, 283–294. [CrossRef]

120. Gu, S.Z. Theoretical analyses on industrial green transformation and ecological industrialization. *Chin. J. Agr. Resour. Region. Plan.* **2020**, *41*, 8–14.
121. Li, L.; Fan, Z.H.; Xiong, K.N.; Shen, H.T.; Guo, Q.Q.; Dan, W.H.; Li, R. Current Situation and Prospects of the Studies of Ecological Industries and Ecological Products in Eco-fragile Areas. *Environ. Res.* **2021**, *201*, 111613. [CrossRef]
122. Jose, S. Agroforestry for ecosystem services and environmental benefits: An overview. *Agroforest. Syst.* **2009**, *76*, 1–10. [CrossRef]
123. Deheuvels, O.; Avelino, J.; Somarriba, E.; Malezieux, E. Vegetation structure and productivity in cocoa-based agroforestry systems in Talamanca, Costa Rica. *Agr. Ecosyst. Environ.* **2012**, *149*, 181–188. [CrossRef]
124. Saj, S.; Durot, C.; Sakouma, K.M.; Gamo, K.T.; Avana-Tientcheu, M.L. Contribution of associated trees to long-term species conservation, carbon storage and sustainability: A functional analysis of tree communities in cacao plantations of Central Cameroon. *Int. J. Agr. Sustain.* **2017**, *15*, 282–302. [CrossRef]
125. Zhou, B.; Chen, X.M. Research on the value realization mechanism of China's ecological products in the new era. *Prices Mon.* **2022**, *5*, 28–33.

forests

MDPI

Review

Review on Driving Factors of Ecosystem Services: Its Enlightenment for the Improvement of Forest Ecosystem Functions in Karst Desertification Control

Lingwei Kong [1,2], Kangning Xiong [1,2,*], Shihao Zhang [1,2], Yu Zhang [3] and Xuehua Deng [1,2]

[1] School of Karst Science, Guizhou Normal University, Guiyang 550001, China; konglw@gznu.edu.cn (L.K.)
[2] State Engineering Technology Institute for Karst Desertification Control, Guiyang 550001, China
[3] Department of Resource Management, Tangshan Normal University, Tangshan 063000, China
* Correspondence: xiongkn@gznu.edu.cn

Abstract: Understanding the multi-scale and multi-factor driving mechanisms of ecosystem services (ES) change is crucial for combating the severe degradation of the ecosystem. We reviewed 408 publications on ecosystem structure, biodiversity, and plant functional traits related to ES in forest ecosystems. Strategies were proposed and key scientific issues were pointed out to improve the forest ecosystem in the karst desertification area. The results showed that the total number of publications has increased rapidly since 2014, of which biodiversity studies contributed the majority. China, the USA, and Germany were the top three countries, accounting for 41%, 9%, and 6% of the research, respectively. Further review found that structure, species diversity, and functional traits have an apparent effect on ES at different (macro, meso, and micro) scales. The optimization of tree structure contributes to the improvement in ES provision and the regulation capacity. Species diversity plays an important role in provision services, while functional diversity is equally important in regulation services. Plant root functional traits can not only help regulation services but also determine the species and structure of rhizosphere microbial communities. The response of ES to a certain factor has been extensively reviewed, but the interaction of multiple driving factors needs to be further studied, especially in how to drive the supply capacity of ES in multi-factor and multi-scale ways. Clarifying the driving mechanism of ES at different scales will help to improve the supply capacity of the ecosystem and achieve the goal of sustainable development.

Keywords: biodiversity; ecosystem services; forests; karst desertification; plant functional traits; structure

Citation: Kong, L.; Xiong, K.; Zhang, S.; Zhang, Y.; Deng, X. Review on Driving Factors of Ecosystem Services: Its Enlightenment for the Improvement of Forest Ecosystem Functions in Karst Desertification Control. *Forests* **2023**, *14*, 582. https://doi.org/10.3390/f14030582

Academic Editor: Mykola Gusti

Received: 26 January 2023
Revised: 2 March 2023
Accepted: 14 March 2023
Published: 15 March 2023

1. Introduction

Ecosystem service (ES) has been defined as the benefits for human populations derived directly or indirectly from ecosystem functions [1], which provide essential material and non-material conditions for human existence and development. However, ES and biodiversity have been severely degraded in recent years [2,3]. The Millennium Ecosystem Assessment (MA) evaluated 24 ESs globally and suggested that 60% were degrading. In addition, according to the report of the Intergovernmental Science-Policy Platform on Biodiversity and Ecosystem Services (IPBES), the average abundance of species in most important terrestrial communities has declined by at least 20%; 14 of the 18 services assessed were declining; and the global species extinction rate was tens or even hundreds of times faster than the average for the past 10 million years [4]. These conclusions indicated that biodiversity loss might lead to a severely negative impact on ES supply [5,6]. Climate change, ecosystem structure, and land use change were the main driving factors of ES change at the macro scale [7–9], with plant functional traits, species invasion, and microbial diversity acting at the micro and meso scales [10,11]. The impact of global climate change and disturbance mechanisms on mountain areas is greater than that of other biogeographic regions [12] and is expected to intensify further [13]. Human activities are the main factors

affecting the significant decline in ecosystem service value and ecological problems, and land use change is the most obvious manifestation of human activities [14]. Climate and land use change will cause changes in the structure and process of different ecosystems and ultimately affect the supply capacity of ES. The functional diversity of plant traits is linked to ecosystem function and biodiversity [15]. Plant communities composed of functionally divergent species or traits contain species combinations that enhance productivity through complementary resource use [16]. The impacts of climate change [17] and land use/cover [18] on ES have been summarized well. This study focuses on the role of ecosystem structure, biodiversity, and plant functional traits, which is of great significance to optimizing ecosystem function.

Many researchers have studied the impacts of climate change [19–23], land use [24–27], and landscape structure [28–32] on ES in different ecosystems. The results showed that all these drivers have a direct and significant effect on ES. However, climate change, land use, and landscape structure change do not affect ES directly but by controlling community structure, plant functional traits, and species diversity in the forest ecosystem. Studies have found that both negative and positive climatic impacts have only small effects on forest dynamics compared to silvicultural measures. Only for very few water-limited stands did climate change affect forest growth negatively due to pronounced drought stress and mortality [33]. On the contrary, forests can regulate the climate through their own attributes. Forests efficiently recycle water using several plant traits, such as deep rooting systems, high leaf area, and surface roughness that facilitates upward water vapor transport. These conditions, strongly related to the forest structure, increase rainfall over tropical forests compared to grass in grazing lands or soy crops [34]. In addition to carbon sinks and carbon storage services (biogeochemical processes of climate regulation), forests also provide climate regulation ES through biogeophysical processes [35]. Forests are responsible for an atmospheric cooling effect through transpiration, and surface winds can transmit the cold air beyond the forest boundary [36], which plays a role in regulating the regional microclimate. Furthermore, biodiversity has been considered to be either the basis for ecosystem services provisioning or a service in itself [2,37]. As the terrestrial ecosystem with the highest biodiversity, the forest has been widely recognized for its role in biodiversity conservation and ecosystem multifunctionality maintenance [38–40]. However, many precious studies paid more attention to species diversity and ignored the role of functional diversity. Lyashevska and Farnsworth [41] pointed out that plant diversity consists of multiple dimensions of diversity, including classification (such as species richness), function (such as diversity of wood density), and structure (such as the average height of the community). Different plant diversity indicators can show different relationships with different ecosystem services [42]. For example, forest functional diversity is positively correlated with hydrological regulation services. The increase in land use intensity led to a reduction in niche differentiation of interspecific functional traits, resulting in the degradation of hydrological services in the forest ecosystem [43]. Although some studies have shown the role of functional traits [44], species diversity [45,46], and functional diversity [47] in forest ES, the relationship among them needs further study, and the key scientific issues need to be clarified.

In the carbonate region, especially in the karst desertification area, the soil layer is shallow and forms slowly because of the binary (aboveground and underground) hydrological structure and process. Serious soil erosion limits vegetation growth, and strong human disturbance leads to the occurrence of karst desertification eventually [48,49]. Further, karst desertification intensifies the frequency of droughts, floods, and other disasters, which seriously damage ecological functions and restrict regional sustainability [50]. For example, water and wind can erode the topsoil easily after vegetation degradation, which reduces the water conservation and nutrient supply capacity [51]. Moreover, the decline in plant coverage also degrades regulation services such as carbon sequestration, oxygen release, and hydrological regulation [52]. Water flow takes nutrients into underground spaces, which limits the growth of ground flora and reduces product provision services [51].

Restoring damaged ecosystems rapidly and effectively and improving ES supply capacity are the primary tasks of the eco-degradation area. According to a study by Duarte et al. [53], landscape composition and configuration significantly affect ES. Hodder et al. [54] believed that conservation, management, and interventions at the landscape scale might enhance the supply of a series of ESs (carbon storage, fiber and food, etc.). Laughlin [55] proposed a quantitative model for ES recovery using trait values (e.g., selecting species with high wood density and low specific leaf area to improve community resistance to drought). Biodiversity and ES loss not only directly affect the livelihood of poor populations but may also further exacerbate a decline in human well-being [2]. The ecosystem structure and landscape pattern lend support to this theory at the macro scale, while tree structure, functional trait, species diversity, and functional diversity at the meso and micro scale can provide specific community construction and species configuration schemes. Although the combination of the two scales can effectively optimize the functions of degraded forest ecosystems, there are few existing studies that have been reported.

The purpose of this study is to provide a theoretical basis for the optimization of forest ecosystem function by summarizing the relationship between structure, functional traits, and biodiversity and ES. A systematic review of 408 publications related to ES driving was conducted. We analyzed the annual, institution, and country distribution of publications and created a co-occurrence network analysis for keywords. The research progress on the driving effect of structure, biodiversity, and plant functional traits on ES change was emphatically summarized, and the findings for improving forest ecosystem function in karst desertification areas were put forward. Specifically, we (i) identify the development trend of ES drivers research, (ii) discuss the enlightenment of ES driving factors for forest ecosystem improvement in karst desertification areas, and (iii) explore some scientific issues and opportunities for future work.

2. Materials and Methods

2.1. Publications Acquisition Source

The web of Science (WoS) is an important database for obtaining global academic information. The three major citation indexes (SCIE + SSCI + A&HCI) of WoS include more than 12,400 authoritative and high-impact international academic journals worldwide, covering natural science, engineering technology, social sciences, and arts and humanities. China National Knowledge Infrastructure (CNKI) is the largest academic resource data platform in China, which includes academic resources in multiple research fields and disciplines. These two databases can provide a large amount of research data for this study, so we chose WoS and CNKI as the literature acquisition sources. On 12 October 2022, "Structure (ST) + Ecosystem services (ES)", "Biodiversity (BD) + Ecosystem services (ES)", "Plant functional trait (PFT) + Ecosystem services (ES)" were used as the search terms, and a document search was carried out in WoS and CNKI databases (Figure 1). To ensure that the retrieved publications were highly relevant to this research topic, the search criteria were set as "title". A total of 521 publications were obtained, and screening and statistics of publications were conducted. It should be emphasized that due to the restrictions of access rights and language barriers, we only accessed the WoS and CNKI databases and read the articles that written in English and Chinese, which makes many publications in other languages unavailable.

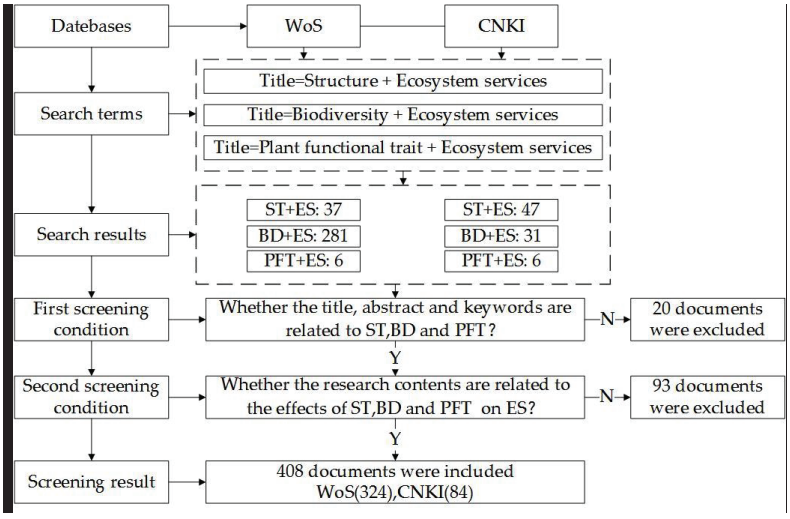

Figure 1. Process of publications' acquisition and screening. This study's systematic mapping process illustrates articles from the initial search to screening for synthesis (identification, screening, eligibility, and inclusion). Publications were found through a database search in the identification stage. Then, the articles captured were screened based on ecosystem services drivers (through titles, keywords, abstracts, and full-text articles) at the screening and eligibility stages. Finally, the publications satisfying the eligibility criteria were included in the study.

2.2. Publications Screening and Statistic

After searching, we selected and exported all publications to excel sheets. Then, publications were preliminarily screened by reading titles, abstracts, and keywords. The title, abstract and keywords that did not contain "ecosystem services" or did contain but had nothing to do with "ecosystem services" were not considered. A total of 20 articles were excluded that were not relevant to the research topic. After that, 501 remaining full-text publications were read. Excluded publications included those in which there were "ecosystem services", "structure", "biodiversity", "plant functional traits" in the text, but the text did not involve research on the driving force of ecosystem services. A total of 93 articles which were uncorrelated to the purpose of this study were excluded. Eventually, 408 publications were retained, including 84 (21%) for structure, 312 (76%) for biodiversity, and 12 (3%) for plant functional traits. The included 408 publications (84 in Chinese and 324 in English) were read entirety to extract useful information. MS Office excel 2016 was used for statistical analysis and drawing. We graphed the number of publications in each year from 2005 to 2022 to identify the specific year in which there was the co-occurrence of ES and drivers and development trends in ES drivers research. We then used ArcMap 10.5 to map the publications' distribution in countries and institutions to analyze major ES research countries and organizations. Finally, the keywords of all articles were exported as "ris" files in WoS and CNKI and imported into VOSviewer 1.6.16 software to create a co-occurrence network of keywords.

3. Results and Discussion

3.1. Distribution of Documents

The annual distribution of literature (Figure 2) shows that the research on biodiversity and plant functional traits occurred later than that on structure. In terms of quantity, the research on biodiversity has increased significantly, while the research on structure and plant functional traits has increased slowly. From 2005 to 2014, the total amount fluctuated, but the growth rate was slow. Therefore, we divided the period from 2005 to

2014 into the initial stage of ES research. In 2015, the total amount of literature increased significantly, so we named the period after 2014 the mature stage, mainly due to the outstanding contributions of biodiversity research.

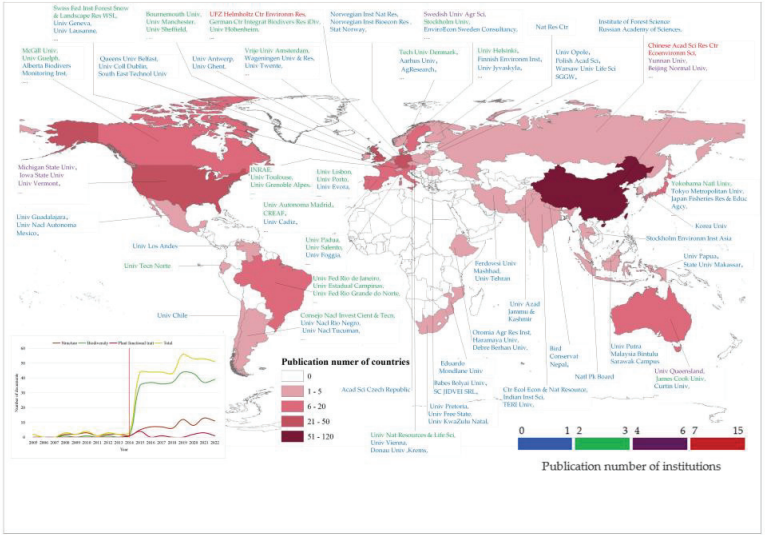

Figure 2. Distribution of documents.

The global distribution of literature was analyzed based on the country where the first author's organization was located. The area distribution is shown in the red map in Figure 2 (after sorting out 408 publications). China has the largest number (112), accounting for 27% of the total number of publications, followed by the United States with 47 (12%), and Germany tied for third with 32 (8%). The reason for the large differences in the international distribution of publications may be that there are few databases, and many publications cannot be obtained. It may also be that there are differences in expressions at home and abroad, so some publications are missed.

Based on the organization of the first authors, the organization distribution analysis was carried out. There was a wide range of research institutions (303 in total), but the chart space was limited. Therefore, only the top three organizations of each country were listed here. Among them, the top 10 institutions are Chinese Acad Sci Res Ctr Ecoenvironm Sci, UFZ Helmholtz Ctr Environm Res, Yunnan Univ, Michigan State Univ, Beijing Normal Univ, Iowa State Univ, Swedish Univ Agr Sci, Univ Queensland, Univ Vermont, and Henan Univ. Universities occupied most of the research institutions, indicating that the education organizations paid more attention to ES drivers. Judging from the individual author, the top 10 contributors to the number of publications on the topic are Ricketts Taylor H (5), Sonter Laura J (5), Polasky Stephen (4), Watson Keri B (4), Woodward Guy (4), Ding Shengyan (3), Xue Fengzhi (3), Fu Bojie (3), Wen Zhi (3), Yu Dandan.

3.2. Co-Occurrence Network of Keywords

Keywords are the condensed key information of a paper, and we can determine the research focuses of each field by analyzing the keywords. A co-occurrence network clustering analysis was performed using the keywords of 408 publications (Figure 3). Each keyword must appear in at least 5 publications or will not be counted; a total of 162 keywords were extracted. The larger the label and shape in the figure, the higher the frequency of the keyword, and the thickness of the connecting line is proportional to the co-occurrence frequency of the keyword. The most frequently used keywords were ecosystem services (150), conservation (125), biodiversity (97), management (81), diversity

(62), climate change (49). It can be seen in the figure that cluster 1 (green) is centered on ES, with conservation, biodiversity, patterns, etc., as auxiliary research; cluster 2 (blue) focuses on diversity and land use; cluster 3 (red) pays close attention to management and values. In addition, keywords such as climate change, natural capital, and agriculture were widely used.

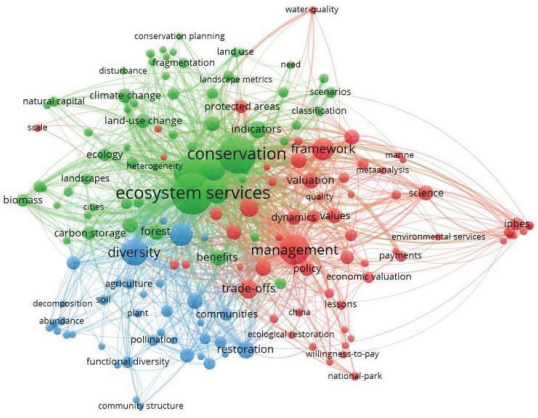

Figure 3. Co-occurrence network of keywords.

3.3. Main Developments and Landmark Achievement

(1) Ecosystem structure determines ecosystem processes and functions

Landscape structure not only affects the biodiversity [56] and vertical structure [57] of urban plants but also has a significant impact on the diversity of plant communities, the structure of agroecosystems [58], and pollination [59]. The composition and configuration of the landscape are considered key factors when explaining the changes in plant species diversity at different spatial scales [60]. Habitat loss and fragmentation, such as the reduction in patch size and loss of connectivity, have adverse effects on plant species diversity [61,62]. Habitat fragmentation leads to patch area reduction, connectivity loss, and edge effect increase, which may lead to a loss of ecosystem functions related to carbon and nitrogen conservation, ecosystem productivity, and pollination [63]. Fragmentation of the watershed landscape leads to a decline in soil conservation services [64]; a reduction in forest area and an increase in impervious surfaces are the main reasons for the decline in regional ecosystem service value [65]; landscape heterogeneity directly affects various attributes of the ecosystem, such as seed propagation, animal movement, population maintenance, the interaction between species, and dynamics and basic functions of the ecosystem [66]. In other words, landscape structure, including composition (quantity of each land use/cover type) and configuration (spatial arrangement of land use/cover type), can affect the supply of ES [67].

(2) Forest spatial structure influences water regulation and species diversity

Forest spatial structure refers to the spatial relationship of trees in the forest (such as size and distribution), which reflects the spatial relationship among species in the forest communities [68]. It also determines the competition between trees, the spatial niches, and the stability of the stand structure. In forest ecosystems, the density, spatial arrangement and canopy structure of vegetation exert strong control over many ecosystem functions that depend on the scale of the ecosystem [69]. The forest structure plays an important role in regulating water and air circulation. Canopy coverage, leaf characteristics (area, biomass, morphology), and branching characteristics (density, quantity, length) are considered key factors affecting the canopy water storage capacity [70,71]. Tree height not only affects canopy fluctuation and energy exchange with the atmosphere [72] but also affects soil splash

erosion by water. In addition, the stand density can regulate the species diversity under the forest. The species diversity of the shrub and herb layer under the high-density *Eucalyptus robusta* Smith forest is significantly less than in low-density forests [73]. The shrub layer diversity of the *Cupressus funebris* Endl. plantation in Yunding Mountain showed a single peak change of first increasing and then decreasing with the decrease in stand density, while the herb layer diversity showed a double peak change [74]. Tending and cutting can effectively regulate the spatial structure of the forest, but the cutting intensity should be different according to different forest types [75]. The more reasonable the structure of the stand is, the higher its stability will be and the more functions it will play [76].

(3) Biodiversity is a crucial driver of the nutrient cycle

Some researchers believe that losing plant diversity will reduce soil microbial diversity [77]. High plant diversity will increase the carbon input from the rhizosphere to the microbial community, thereby increasing microbial activity and carbon storage [78]. Increasing plant diversity can increase the accumulation and use efficiency of soil total nitrogen [79,80], improve plant productivity and pollination media, and inhibit weeds and pests [81]. Some researchers believe that the impact of plant diversity on dryland ecosystem functions and services (i.e., multi-functionality) is indirect but is the result of the positive impact of plant diversity on microbial diversity [11,82]. Most microbial species are heterotrophs, which can produce specific extracellular enzymes to decompose fauna, plant, microbial residues, and various complex organic substances into inorganic substances (such as CO_2, H_2O, NH_3, $SO^{2-}{}_4$, and $PO^{3-}{}_4$). These inorganic substances can be used by primary producers to participate in the material cycle again [83,84]. The increase in soil biodiversity from a very low level to a medium level may also accelerate nutrient cycling [85]. In addition, microbial species are also involved in the mineralization of organic matter, biological control of pathogens, and remediation of ecological environmental pollution [86,87]. Therefore, some researchers claimed that microbial diversity determines the productivity of ecosystems (especially in nutrient-poor ecosystems) and plant diversity. On the other hand, when soil microbial species compete for nutrients with plants as pathogens or convert nutrients into forms unavailable to plants, they may also harm plant productivity [88]. However, the driving mechanisms of plant diversity and microbial diversity on ecosystem functions and services lack sufficient empirical evidence and need further study.

(4) Functional diversity promotes the maintenance of ecosystem multi-functionality

Species require different conditions for seed production, propagation, and germination [89]. They can promote species coexistence by adjusting lifestyle or phenology habits (such as the growth rate, shade tolerance, crown retention time, and reproductive capacity), thus forming different ecosystem functions [90]. As the foundation, changing ecosystem functions directly affects ES and human well-being [91]. Ecosystem multi-functionality (EMF) was first proposed in 2004 [92]; since then, the maintenance of EMF has gradually become one of the focuses of researchers, and substantial progress has been made. Gamfeldt et al. [93] put forward a conceptual model to explore the impact of species loss on the comprehensive functions of the ecosystem (i.e., EMF). They found that the overall function is more vulnerable to the impact of species loss than a single function due to the complementarity between the multiple functions. Xu et al. [94] emphasized that maintaining multiple functions requires not only higher species richness but also diversified community types. Because different functional traits of coexisting species can increase the overall utilization efficiency of resources and thus promote ecosystem functions. The functional traits of dominant species strongly affect the ecosystem functions of communities. Therefore, functional diversity is considered the key driver of ecosystem versatility [95,96]. Though species diversity is also considered an important influencing factor of EMF, the positive correlation between species diversity (especially species richness) and ecosystem function may be due to the increase in species number leading to the increase in trait diversity [97]. Functional traits are related to the resource utilization (including selection effect and complementary effect) of species [98]; it may be a better predictor of ecosystem

functions [99]. Therefore, functional diversity may be more conducive to maintaining EMF than species diversity [100,101].

(5) Plant functional traits of both aboveground and underground parts affect ESs simultaneously

Functional traits reflect the adaptation of organisms to physical and biological environment change and the trade-offs among different functions [102], which is a core concept of functional ecology [103]. Many studies have shown that plant functional traits play an important role in ES. For example, high leaf nitrogen content can promote soil organic carbon storage [104]. Plant canopy density and fine root percentage have an important impact on ecosystem hydrological regulation services [43]. Different traits affect services differently. Root traits are mainly related to erosion control, climate regulation, and biomass production; flower traits are concerned with aesthetic attraction and pollination; and stem and whole plant traits are associated with biomass production [105]. Dennis et al. [106] believed that the type and quantity of root exudates determine the type and quantity of rhizosphere microbial species, as well as affect the structure of the rhizosphere microbial community and carbon utilization. As a key aspect supporting plants' ability to stand and nutrient absorption, the root system continuously secretes various substances to promote the absorption of mineral elements by plants and provides carbohydrates, sugar alcohols, amino acids, and phenols for rhizosphere microbial species as nutrients and energy supply [107]. At the same time, root-related microbial species can directly affect plant growth and population dynamics and indirectly affect nutrient cycling by controlling plant litter input and root nutrient absorption [88,108], forming a mutual feedback mechanism among plants soil microbial species. The plant root system also has an important effect in promoting material circulation and hydrological regulation [109]. Under specific conditions, plant roots can transfer soil moisture in the deep layer to the dry surface soil through conduction tissues, thereby completing water redistribution [110]. The interlacement of underground roots can effectively improve the soil shear strength and soil permeability, which can reduce soil erosion [111]. Plant functional traits are important driving forces for ES changes, both aboveground and underground.

3.4. A Systematic Review of ES Drivers for Forest Ecosystem Improvement in Karst Desertification

(1) The optimization of stand spatial structure helps improve the quality of the ecosystem

The regulation of forest spatial structure and distribution pattern by manual measures is conducive to promoting interspecific interaction and improving ecosystem functions. Pruning significantly increases the light intensity, temperature, understory biomass, and Shannon Weiner index of species [112]. The intercropping of forest and grass can promote the regulation of soil quality and microclimate and increase forest products [113]. This shows that reasonable management measures can not only improve the forest structure and productivity but improve the carbon fixation capacity of vegetation. Thinning and replanting can significantly improve the forest layer index and mixing degree. The increase in individual differences between trees can expand the growth space of young and middle-aged forests, which reduces the competitive pressure between trees and significantly improves the stand structure (Figure 4) [114,115]. There are more problems in the spatial structure of the karst desertification forest ecosystem compared with non-karst desertification. Common situations include sparse understory vegetation and incomplete hierarchical structure of arbor, shrub, and grass; broken patches and a lack of a large, connected forest landscape; and a single species disposition, which is not conducive to resisting diseases and pests. Therefore, implementing artificial management in this area to optimize the forest spatial structure is conducive to improving the forest ecosystem function and service supply capacity. According to the characteristics of karst desertification forest, the optimization of stand spatial structure can be carried out horizontally and vertically. In the horizontal space, natural forests can be thinned, replanted, and renewed manually. Intercropping of trees and cereal/grass and mixed plantation can be implemented to regulate

the composition and the proportion in the artificial forest. In the vertical space, trees can be pruned and reshaped to control their height and crown width [116] so that the lower trees can fully absorb solar energy and improve the community' productivity. In short, during planting and ecological restoration, the layers of trees, shrubs and herbs should be intact to improve the self-regulation ability of the ecosystem in terms of nutrient decomposition and circulation [117].

(**a**) (**b**)

Figure 4. Comparison of different stand structures: (**a**) Worse stand structure with Tectona grandis L.F. only. (**b**) Better stand structure with Quercus fabri Hance, Lindera glauca (Sieb. et Zucc.) Bl, Arthraxon hispidus (Trin.) Makino, etc. (Source of the pictures: Photoed by Lingwei Kong.).

(2) Building plant functional groups based on functional characteristics and environmental conditions is conducive to improving ecological functions

Plant functional types combine a series of plants with certain plant functional traits, which are the basic units for studying the dynamic changes of vegetation along with the environment [118,119]. They link plant morphology, community science, and ecological processes, and are a very useful tool for studying the dynamic changes between climate and vegetation. Environmental heterogeneity (such as soil, light, and terrain) shapes the characteristics of individual plants to a certain extent, it also affects the interactions between species and their proportions in different spatial ranges. The aim of community structure optimization can be achieved by making full use of the adaptability of species characteristics to the environment to dispose of species [120,121]. In karst desertification areas, due to exposed bedrock and a lack of surface water, adaptive plants are usually drought resistant, lithophytic, and calciphilous [122]. The existing research found that the soil enzyme activity, soil nutrients, and microbial community diversity index of forest grass intercropping in karst mountain areas were significantly higher than in wasteland and farmland returning to grassland [123]. Therefore, since few species are included in afforestation for karst desertification control (Figure 5a), multi-species interplanting can play an important role in promoting ecological restoration. In addition, in forest gaps with enough sunlight, short-lived and shade-intolerant species have higher growth rates than long-lived and shade-tolerant species [124]. In forests with high canopy density and insufficient light, shade tolerant species can be selected for planting, which can enhance the integrity of the stand structure (Figure 5b). The characteristics of herbaceous plants are mostly similar—weaker than most trees and shrubs, but they can also be appropriately added to enhance the overall stability of the community.

(**a**) (**b**)

Figure 5. Comparison of communities comprising different species in Guizhou, China: (**a**) Single species with *Zanthoxylum bungeanum* Maxim. only. (**b**) Multiple species with *Pinus massoniana* Lamb, *Quercus fabri* Hance, *Populus alba* L., etc. (Source of the pictures: Photoed by Lingwei Kong.).

(3) Biodiversity conservation is the foundation for maintaining EMF

Biodiversity determines ecosystem functions and processes [125,126]. Higher biodiversity can produce higher levels of ecosystem functions [127,128]. The plants are more abundant in karst habitats than in non-karst habitats in South China karst (accounting for 30%–40% of the total local species). Many species are rare, endangered, protected groups, and endemic species (10% are endemic karst species, and 20%–30% are characteristic karst species) [129]. However, the change and degradation in the ecological environment in karst desertification have led to the fragile karst ecosystem becoming more unstable and biodiversity declining [130]. The degradation of plant communities led to reduced biomass and soil organic matter, which affected microbial diversity. The evolution of habitat toward drought accelerated the decomposition rate of soil organic matter [131]. As a result, the content of soil organic matter and water permeability decreased, and finally, a fragile ecosystem with poor ecological structure and functions was formed. The assessment and protection of biodiversity loss should be one of the core tasks in this area. Unfortunately, few researchers have carried out assessments and proposed feasible protection plans so far. Under the threat of climate change, Hylander et al. [132] proposed two forest biodiversity conservation tools (Resistance and Transformation) at the landscape scale, including eight specific implementation measures. In addition, Lindenmayer [133] also proposed four general principles from the perspective of natural forest restoration. We believe that these are of great significance for biodiversity conservation in karst desertification areas. However, due to the differences in natural conditions, it is better to seek local protection schemes based on others' measures. Here, we proposed some suggestions, hoping to help the biodiversity conservation of karst desertification forest ecosystems. (1) In response to the loss of biodiversity caused by climate change, the endemic species in this region can be transplanted to other regions with suitable conditions, or the characteristics of species can be improved to adapt to climate change. At the same time, it is important introduce new species from other regions that do not exist in this region, but the scale should be controlled to prevent the occurrence of biological invasion. (2) To address the loss of biodiversity caused by human activities, supervision should be strengthened, and arbitrary logging, mining, and hunting should be prohibited. In addition, people ought to be encouraged to carry out relevant protection work, such as artificial afforestation, breeding instead of killing wild animals, and anthropic management of natural forests (Figure 6). (3) In the face of the loss of biodiversity caused by niche change, manual intervention can be carried out (cultivate endangered species and appropriately remove excessive species) to prevent the food chain from breaking. In a word, biodiversity conservation of karst desertification ecosystems is a long-term job, and there is still a long way to go.

(**a**) (**b**)

Figure 6. Biodiversity conservation measures in Guizhou, China: (**a**) Close hillsides to facilitate afforestation. The dominant species include *Toona sinensis* (A. Juss.) Roem., *Pyracantha fortuneana* (Maxim.) Li, *Cladrastis platycarpa* (Maxim.) Makino, etc. (**b**) Artificial afforestation. The dominant species include *Zanthoxylum bungeanum* Maxim., *Juglans regia* L., *Prunus salicina* Lindl., etc. (Source of the pictures: Photoed by Kangning Xiong.).

(4) The combination of macro-scale landscape structure optimization and micro-scale biodiversity improvement can effectively increase the supply of ES

As a result of ecological degradation, the landscape in karst desertification areas shows high heterogeneity and fragmentation (Figure 7a) [134]. Meanwhile, the loss of plant and microbial diversity has also caused great damage to the EMF at the micro scale [81,85]. However, the relationships of services have obvious spatial scale dependence [135]. Research on a single scale may miss or even distort the interaction rules between ESs, which is not conducive to a comprehensive and objective understanding of ESs [136]. The fragmentation of landscape in karst desertification areas not only leads to a loss of biodiversity but also reduces the sustainability of land use [137]. Research showed that after implementing a series of afforestation and forest cultivation measures, the landscape diversity increased by 8%, and fragmentation decreased by 25% [138]. Therefore, it is necessary to adjust the type, number, and spatial distribution pattern of landscape components and patches at the macro scale (Figure 7b) so as to make each component harmonious and orderly, ultimately restoring the damaged ecosystem and achieving regional sustainable development [139]. For example, according to the ecological vulnerability characteristics of karst desertification areas, steep slopes and gentle slopes can be planned as forests/grasslands and farmland, which can improve soil and water conservation capacity and make full use of soil nutrients [140,141]. The configuration of patches (such as forest land, grassland, and water) around farmland can help to increase landscape diversity and biodiversity, improving the EMF [142]. The coupling of water and fertilizer in poor soil regions can help to increase the content of soil organic matter and the number of microorganisms, improving plant productivity [143]. Therefore, at the micro scale, plant and microbial diversity can be increased by artificial afforestation [144] and organic matter addition.

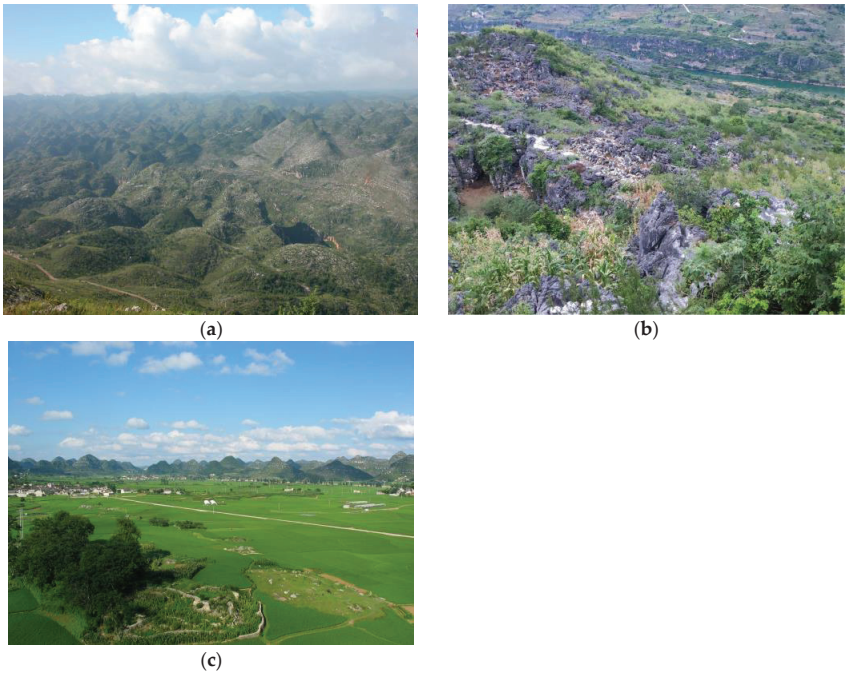

Figure 7. Comparison of landscapes configured by different patches in Guizhou, China: (**a**) Single patch configuration landscape with karst desertification. (**b**) Small vegetation patches and large stone patches in the process of ecological restoration. (**c**) Multiple patch configuration landscape without desertification. (Source of the pictures: Photoed by Kangning Xiong.).

3.5. Key Scientific Issues to Be Solved and Prospects

(1) How do ecosystem functions respond to structural changes? Research on interspecific relationships and functional differences in ecosystems with different structures can be carried out.

Understanding the response of ES and functions to the change in ecosystem structure is crucial for the efficient allocation of environmental resources and rational formulation of environmental policies [145]. An unreasonable landscape structure will lead to an overall decline in ESs and functions [146]. In the stand structure, interspecific interactions not only directly affect the flow and circulation of matter and energy among different components of the ecosystem but also affect the process of community construction, making the network structure closely related to ecosystem functions and community stability [147]. Mixed forests and multi-storied forest have stronger disease and pest resistance than monoculture forests and single-storied forests; natural forest have a better stand structure and biodiversity than artificial forests, as well as stronger overall ecological function [148,149]. Although more and more evidence show that landscape structure and stand structure are crucial to the supply of services, there are still some important questions to answer about the mechanism and process behind this role, including the key question about how to configure them to improve the ecosystem function. There are detailed results on the impact of a certain ecosystem structure on services, but few researchers have focused on the interspecific relationships and ecosystem functions driven by different ecosystem structures. In the future, research on biodiversity and ecosystem function differences within different structures should be strengthened, and the role of structures in ecological processes, functions, and services should be revealed.

(2) Species diversity or functional diversity contributing more to ESs; comparative studies on species and functional traits of different communities are needed.

Functional traits determine ecosystem functions, and species are considered a collection of functional traits [150]. Species provide many material products for human beings, and functional traits can affect regulating services such as the water cycle. They are indispensable carriers of ES. However, it is unclear who contributes more to ES supply between species and functional diversity. At present, research on the driving mechanism of biodiversity to ES is mostly focused on a single scale or dimension, and different conclusions will be drawn in different ecosystems [151,152]. Thus, the impact of species diversity and functional diversity on ES change needs to be further studied. In addition, aboveground and underground biodiversity, as well as their comprehensive impact in different scales or dimensions, can effectively explain more variations in EMF [153,154]. Researchers should pay more attention to the synergistic effect of above- and below-ground biodiversity in the future, extending the field observation period, enriching the community survey content, and selecting representative functional indicators to construct a long-term, multi-spatial, and multi-dimensional biodiversity-EMF database [155].

(3) The application of relationships between biodiversity and ecosystem service is insufficient. The practical application of existing research results should be strengthened.

Although some studies have paid attention to the interaction between biodiversity and ES, most focused on the impact of biodiversity on ESs. Few studies have talked about how to apply the relationship between biodiversity and ES at the practical level, and there is a lack of effective ways to realize relevant cognition. An important research direction is thus to explore ways to improve ESs according to the relevant knowledge of biodiversity and ESs, as well as diminishing the leap from theory to the application of the biodiversity ES relationship. In the face of the continuous impact of human interference and environmental change on ES, maintaining and improving ESs of oceans, forests, grasslands, and agriculture has become a practical problem that many regions must address [156]. Theoretically, it is possible to formulate management measures to improve and restore ES from the perspective of biodiversity, and the implementation of ecosystem management measures can, in turn, improve biodiversity and ESs. For example, forest restoration can increase species diversity and ecosystem productivity at the same time [157]. In practice, some studies have explored and verified the feasibility of applying the knowledge of biodiversity-ES relationships to policy-making and natural reserve management, forest ecosystem management, degraded ecosystem restoration, and agricultural ecosystem improvement, but the application of existing research results still needs to be strengthened in future studies.

(4) Few pieces of research integrate multiple driving factors of ES change; the research on the co-influence of natural and human factors should be strengthened.

In addition to climate change and human activities, ES changes are also affected by various drivers, such as ecosystem structure, biodiversity, and landscape. There are complex interactions between these driving factors [158]. Most existing research mainly focuses on the role of a single driver, while research on the synergy of multiple factors and their contribution rate is scarce. In the future, we should not only continue to deeply explore the mechanism of impact of climate change and land use on services but also strengthen the driving force of population, economy, policy, culture, and other social factors, as well as natural factors, such as ecosystem structure, biodiversity, landscape pattern, regional differentiation, and the interaction of multiple factors on service change. Meanwhile, it is necessary to reveal the contribution rate of different driving factors on the service change to manage the environment in the development, utilization, and protection of ecological resources. This will provide scientific guidance for ecological restoration in ecologically vulnerable areas and promote the realization of sustainable development goals.

(5) There is no case study on improving ES through landscape pattern optimization. Long time-series sample plot monitoring should be carried out to explore the optimal landscape pattern.

The landscape composition and configuration affect the ecological process. Understanding how landscape composition and configuration affect the supply of ES is the key to improving landscape management [67]. Most researchers have focused on the response of ESs to landscape structure changes, there are few reports on how to improve ES via landscape composition and configuration. Thus, effectively configuring the landscape to promote ESs and function is a difficult problem for landscape ecology, especially in areas with high spatial heterogeneity and changing land cover. Core area and grid size are important determinants of ecosystem service trade-offs and synergies, which affect ES interactions [159]. Future research needs to include a long-term dynamic observation of the field landscape configuration to determine an optimal landscape composition and configuration scheme and provide scientific basis for improving regional ecosystem functions and services.

4. Conclusions

A total of 408 publications were reviewed, and the annual distribution of publications showed a significant growth trend, in which biodiversity research accounted for the majority. The driving factors of ESs mainly focused on biodiversity, ecological protection and management, land use, and climate change. The role of structure, species/functional diversity, and functional traits is still unclear. Further review found a progressive synergy among structure, biodiversity, ecosystem function, and ES. A complete ecosystem structure has higher biodiversity and ecosystem stability. The increase in biodiversity can accelerate the material cycle and improve the ecosystem's productivity. Multifunctionality of the system helps to improve the supply capacity of ES. The combination of macro-scale ecosystem structure optimization and micro-/medium-scale species disposition is helpful for the ecological restoration and management in karst desertification areas. Specifically, land use types and landscape structures can be planned according to actual conditions, such as soil erosion, rock exposure rate, and soil quality, which is conducive to vegetation restoration and biodiversity protection. Management measures (such as plantation) can optimize the forest structure and promote the improvement of ecosystem functions. In addition, constructing forest communities according to plant characteristics can help to retard water and soil loss, accelerating nutrient cycling and improving the EMF.

Author Contributions: Conceptualization, L.K.; methodology, L.K. and S.Z.; software, L.K. and S.Z.; validation, L.K., Y.Z. and X.D.; formal analysis, L.K.; investigation, L.K.; resources, S.Z. and Y.Z.; data curation, L.K.; writing—original draft preparation, L.K.; writing—review and editing, L.K. and S.Z.; visualization, L.K., Y.Z. and X.D.; supervision, K.X.; project administration, K.X.; funding acquisition, K.X. All authors have read and agreed to the published version of the manuscript.

Funding: This research was supported by the Key Science and Technology Program of Guizhou Provence: Poverty alleviation model and technology demonstration for eco-industries derivated from the karst desertification control (No. 5411 2017 Qiankehe Pingtai Rencai); the Science and Technology Research Project of Higher Education Institutions in Hebei Province: Comparative study of model and technology for characteristic high efficiency forestry from the karst desertification control in North and South China Karst (No. QN2021412) and the project of Guizhou Geographical Society: Research on characteristic high efficiency forestry from vegetation restoration of the karst desertification control (No. 2020HX05).

Institutional Review Board Statement: Not applicable.

Informed Consent Statement: Not applicable.

Data Availability Statement: Not applicable.

Acknowledgments: We would like to thank all the editors for their contributions to this paper and the anonymous reviewers for their thoughtful comments, which enriched the paper.

Conflicts of Interest: The authors declare no conflict of interest.

References

1. Costanza, R.; Arge, R.D.; Groot, R.D.; Farberk, S.; Grasso, M.; Hannon, B.; Limburg, K.; Naeem, S.; Paruelo, J.; Raskin, R.G.; et al. The value of the world's ecosystem services and natural capital. *Nature* **1997**, *25*, 3–15. [CrossRef]
2. Millennium Ecosystem Assessment (MEA). *Ecosystems and Human Well Being: Synthesis*; Island Press: Washington, DC, USA, 2005.
3. Steffen, W.; Crutzen, P.J.; McNeill, J.R. The Anthropocene: Are humans now overwhelming the great forces of nature? *AMBIO* **2007**, *36*, 614–621. [CrossRef] [PubMed]
4. IPBESs. *Summary for Policymakers of the Global Assessment Report on Biodiversity and Ecosystem Services of the Intergovernmental Science-Policy Platform on Biodiversity and Ecosystem Services*; IPBESs Secretariat: Bonn, Germany, 2009; p. 56.
5. Díaz, S.; Fargione, J.E.; Chapin, F.S.; Tilman, D. Biodiversity Loss Threatens Human Well-Being. *PLoS Biol.* **2006**, *4*, e277. [CrossRef]
6. Cardinale, B.J.; Duffy, J.E.; Gonzalez, A.; Hooper, D.U.; Perrings, C.; Venail, P.; Narwani, A.; Mace, G.M.; Tilman, D.A.; Wardle, D.; et al. Corrigendum: Biodiversity loss and its impact on humanity. *Nature* **2012**, *489*, 326. [CrossRef]
7. Scholes, R.J. Climate change and ecosystem services. *Wires Clim Change* **2016**, *7*, 537–550. [CrossRef]
8. Song, W.; Deng, X.Z. Land-use/land-cover change and ecosystem service provision in China. *Sci. Total Environ.* **2017**, *576*, 705–719. [CrossRef]
9. Teixeira, D.G.; Marques, S.P.; Garabini, C.T.; Cezar, R.M.; Pereira, P.A. The effects of landscape patterns on ecosystem services: Meta-analyses of landscape services. *Landsc. Ecol.* **2018**, *33*, 1247–1257.
10. Brown, L.M.; Anand, M. Plant functional traits as measures of ecosystem service provision. *Ecosphere* **2022**, *13*, e3930.
11. Delgado-Baquerizo, M.; Maestre, F.T.; Reich, P.B.; Jeffries, T.C.; Gaitan, J.J.; Encinar, D.; Berdugo, M.; Campbell, C.D.; Singh, B.K. Microbial diversity drives multifunctionality in terrestrial ecosystems. *Nat. Commun.* **2016**, *7*, 10541. [CrossRef]
12. Price, M.F.; Gratzer, G.; Duguma, L.A.; Kohler, T.; Maselli, D.; Romeo, R. *Mountain Forests in a Changing World-Realizing Values, Addressing Challenges*; Food and Agriculture Organization of the United Nations: Rome, Italy, 2011.
13. Seidl, R.; Thom, D.; Kautz, M.; Martin-Benito, D.; Peltoniemi, M.; Vacchiano, G.; Wild, J.; Ascoli, D.; Petr, M.; Honkaniemi, J.; et al. Forest disturbances under climate change. *Nat. Clim. Chang.* **2017**, *7*, 395–402. [CrossRef]
14. Chen, Y.; Liu, Y.; Yang, S.; Liu, C. Impact of Land-Use Change on Ecosystem Services in the Wuling Mountains from a Transport Development Perspective. *Int. J. Environ. Res. Public Health* **2023**, *20*, 1323. [CrossRef] [PubMed]
15. Helfenstein, I.S.; Schneider, F.D.; Schaepman, M.E.; Morsdorf, F. Assessing biodiversity from space: Impact of spatial and spectral resolution on trait-based functional diversity. *Remote Sens. Environ.* **2022**, *275*, 113024. [CrossRef]
16. Winfrey, B.K.; Hatt, B.E.; Ambrose, R.F. Biodiversity and functional diversity of Australian stormwater biofilter plant communities. *Landsc. Urban Plan.* **2018**, *170*, 112–137. [CrossRef]
17. Runting, R.K.; Bryan, B.A.; Dee, L.E.; Maseyk, F.J.F.; Mandle, L.; Hamel, P.; Wilson, K.A.; Yetka, K.; Possingham, H.P.; Rhodes, J.R. Incorporating climate change into ecosystem service assessments and decisions: A review. *Glob. Chang. Biol.* **2018**, *32*, 28–41. [CrossRef]
18. Hasan, S.S.; Zhen, L.; Miah, M.G.; Ahamed, T.; Samie, A. Impact of land use change on ecosystem services: A review. *Environ. Dev.* **2020**, *34*, 100527. [CrossRef]
19. Bünemann, E.; Oberson, A.; Frossard, E. Phosphorus in action-Biological processes in soil phosphorus cycling. *Soil Biol.* **2011**, *26*, 371–406.
20. Liu, J.J.; Huang, G.L. A review of grassland ecosystem service and human well-being in Xilingol League and Xilinhot City. *Pratac. Sci.* **2019**, *36*, 573–593.
21. Li, Q.; Gao, Y.; Wang, H.B.; Wang, X.P.; Yang, Y.P. Changes in Water and Carbon in Farmland Ecosystems Due to the Combined Impact of Temperature Rise and Drought: A Review. *J. Irrig. Drain.* **2021**, *40*, 110–118.
22. Moreno, J.L.; Bastida, F.; Díaz-López, M.; Li, Y.; Plaza, C. Response of soil chemical properties, enzyme activities and microbial communities to biochar application and climate change in a Mediterranean agroecosystem. *Geoderma* **2022**, *407*, 115536. [CrossRef]
23. Li, C.Y.; He, M.Z.; Tang, L. Advances on phosphorus cycle and their driving mechanisms in desert ecosystems: A review. *Acta Ecol. Sin.* **2022**, *12*, 1–10.
24. Liang, M.W.; Bai, X.; Wang, Y.S.; Miao, B.L.; Bao, G.R.; Wang, H.; Liang, C.Z. The Effect of Moderate Grazing on Carbon Cycle of the Typical Steppe in Inner Mongolia. *J. Inn. Mon. Univ.* **2016**, *47*, 278–284.
25. Alonso-Sarría, F.; Martínez-Hernández, C.; Romero-Díaz, A.; Cánovas-García, F.; Gomariz-Castillo, F. Main Environmental Features Leading to Recent Land Abandonment in Murcia Region (Southeast Spain). *Land Degrad. Dev.* **2016**, *27*, 654–670. [CrossRef]
26. Ma, M.; Zhang, S.W.; Wei, B.C. Temporal and Spatial Pattern of Grassland Degradation and Its Determinants for Recent 30 Years in Xilingol. *Chin. J. Grassl.* **2017**, *39*, 86–93.
27. Anwar, M.; Yang, Y.H.; Guo, Z.D.; Fang, J.Y. Grassland Aboveground Biomass in Xinjiang. *Acta Sci. Nat. Univ. Pekin.* **2006**, *4*, 521–526.
28. Kremen, C.; Williams, N.M.; Aizen, M.A.; Gemmill-Herren, B.; LeBuhn, G.; Minckley, R.; Packer, L.; Potts, S.G.; Roulston, T.; Steffan-Dewenter, I.; et al. Pollination and other ecosystem services produced by mobile organisms: A conceptual framework forthe effects of land-use change. *Ecol. Lett.* **2007**, *10*, 299–314. [CrossRef] [PubMed]

29. Lvzeng, Z.Z.; Huang, X.X.; Sun, X.N.; Wang, X.Y.; He, K.J.; Zhang, Y. Effects of disturbance on landscape pattern and meadow ecosystem services, in the Yak Park of Mt. Jade Dragon, Yunnan. *Ecol. Environ. Sci.* **2020**, *29*, 725–732.
30. Wang, X.H.; Wu, Y.; Manevski, K.; Fu, M.Q.; Yin, X.G.; Chen, F. A Framework for the Heterogeneity and Ecosystem Services of Farmland Landscapes: An Integrative Review. *Sustainability* **2021**, *13*, 12463. [CrossRef]
31. Kazemi, H.; Klug, H.; Kamkar, B. New services and roles of biodiversity in modern agroecosystems: A review. *Ecol. Indic.* **2018**, *93*, 1126–1135. [CrossRef]
32. Guo, S.S.; Wu, C.Y.; Wang, Y.H.; Qiu, G.Q.; Zhu, D.; Niu, Q.; Qin, L. Threshold effect of ecosystem services in response to climate change, human activity and landscape pattern in the upper and middle Yellow River of China. *Ecol. Indic.* **2022**, *136*, 108603. [CrossRef]
33. Martin, G.; Lasch-Born, P.; Kollas, C.; Suckow, F.; Reyer, C.P.O. Balancing trade-offs between ecosystem services in Germany's forests under climate change. *Environ. Res. Lett.* **2018**, *12*, 045012.
34. Costa, M.H.; Yanagi, S.N.M.; Souza, P.J.O.P.; Ribeiro, A.; Rocha, E.J.P. Climate change in Amazonia caused by soybean cropland expansion, as compared to caused by pastureland expansion. *Geophys. Res. Lett.* **2007**, *34*, L07706. [CrossRef]
35. Borma, L.S.; Costa, M.H.; da Rocha, H.R.; Arieira, J.; Nascimento, N.C.C.; Jaramillo-Giraldo, C.; Ambrosio, G.; Carneiro, R.G.; Venzon, M.; Neto, A.F.; et al. Beyond Carbon: The Contributions of South American Tropical Humid and Subhumid Forests to Ecosystem Services. *Rev. Geophys.* **2022**, *60*, e2021RG000766. [CrossRef]
36. Coe, M.T.; Brando, P.M.; Deegan, L.A.; Macedo, M.N.; Neill, C.; Silvério, D.V. The forests of the Amazon and Cerrado moderate regional climate and are the key to the future. *Trop. Conserv. Sci.* **2017**, *10*, 671. [CrossRef]
37. Mace, G.M.; Norris, K.; Fitter, A.H. Biodiversity and ecosystem services: A multilayered relationship. *Trends Ecol. Evol.* **2012**, *27*, 19–25. [CrossRef]
38. Ge, Y.; Chen, H.; Zhang, M.; Li, X. Area Threshold Interval of Urban Forest Patches Required to Maintain the Synergy between Biodiversity Conservation and Recreational Services: Case Study in Beijing, China. *Forests* **2022**, *13*, 1848. [CrossRef]
39. Takala, T.; Brockhaus, M.; Hujala, T.; Tanskanen, M.; Lehtinen, A.; Tikkanen, J.; Toppinen, A. Discursive barriers to voluntary biodiversity conservation: The case of Finnish forest owners. *For. Policy Econ.* **2022**, *136*, 102681. [CrossRef]
40. Perez-Verdin, G.; Monarrez-Gonzalez, J.C.; Tecle, A.; Pompa-Garcia, M. Evaluating the Multi-Functionality of Forest Ecosystems in Northern Mexico. *Forests* **2018**, *9*, 178. [CrossRef]
41. Lyashevska, O.; Farnsworth, K.D. How many dimensions of biodiversity do we need? *Ecol. Indic.* **2012**, *18*, 485–492. [CrossRef]
42. Steur, G.; Verburg, R.W.; Wassen, M.J.; Verweij, P.A. Shedding light on relationships between plant diversity and tropical forest ecosystem services across spatial scales and plot sizes. *Ecosyst. Serv.* **2020**, *43*, 101107. [CrossRef]
43. Wen, Z.; Zheng, H.; Smith, J.R.; Zhao, H.; Liu, L.; Ouyang, Z.Y. Functional diversity overrides community-weighted mean traits in linking land-use intensity to hydrological ecosystem services. *Sci. Total Environ.* **2019**, *682*, 583–590. [CrossRef]
44. Zheng, H.; Pan, Q.; Wen, Z.; Yang, Y.Z. Relationships between plant functional traits and ecosystem services in forests: A review. *Acta Ecol. Sin.* **2021**, *41*, 7901–7912.
45. Schuler, L.J.; Bugmann, H.; Snell, R.S. From monocultures to mixed-species forests: Is tree diversity key for providing ecosystem services at the landscape scale? *Landsc. Ecol.* **2017**, *32*, 1499–1516. [CrossRef]
46. Benneter, A.; Forrester, D.I.; Bouriaud, O.; Dormann, C.F.; Bauhus, J. Tree species diversity does not compromise stem quality in major European forest types. *For. Ecol. Manag.* **2018**, *422*, 323–337. [CrossRef]
47. Esquivel, J.; Echeverria, C.; Saldaa, A.; Fuentes, R. High functional diversity of forest ecosystems is linked to high provision of water flow regulation ecosystem service. *Ecol. Indic.* **2020**, *115*, 106433. [CrossRef]
48. Xiong, K.N.; Li, J.; Long, M.Z. Features of Soil and Water Loss and Key Issues in Demonstration Areas for Combating Karst Rocky Desertification. *Acta Geogr. Sin.* **2012**, *67*, 878–888.
49. Xiong, K.N.; Zhu, D.Y.; Peng, T.; Yu, L.F.; Xue, J.H.; Li, P. Study on Ecological industry technology and demonstration for Karst rocky desertification control of the Karst Plateau-Gorge. *Acta Ecol. Sin.* **2016**, *36*, 7109–7113.
50. Xiong, K.N.; Li, P.; Zhou, Z.F.; An, Y.L.; Lü, T.; Lan, A.J. *Remote Sensing and GIS Typical Study of Karst Rocky Desertification: Taking Guizhou Province as an Example*; Geology Press: Beijing, China, 2002.
51. Green, S.M.; Dungait, J.A.J.; Tu, C.L.; Buss, H.L.; Sanderson, N.; Hawkes, S.J.; Xing, K.; Yue, F.; Hussey, V.L.; Peng, J.; et al. Soil functions and ecosystem services research in the Chinese karst Critical Zone. *Chem. Geol.* **2019**, *527*, 119107. [CrossRef]
52. Zhang, S.H.; Xiong, K.N.; Qin, Y.; Min, X.Y.; Xiao, J. Evolution and determinants of ecosystem services: Insights from South China karst. *Ecol. Indic.* **2021**, *133*, 108437. [CrossRef]
53. Duarte, G.T.; Santos, P.M.; Cornelissen, T.G.; Ribeiro, M.C.; Paglia, A.P. Does landscape-scale conservation management enhance the provision of ecosystem services? *Int. J. Biodivers. Sci. Ecosyst. Serv. Manag.* **2014**, *10*, 71–83.
54. Hodder, K.H.; Newton, A.C.; Cantarello, E.; Perrella, L. Cost–benefit analysis of ecological networks assessed through spatial analysis of ecosystem services. *J. Appl. Ecol.* **2012**, *49*, 571–580.
55. Laughlin, D.C. Applying trait-based models to achieve functional targets for theory-driven ecological restoration. *Ecol. Lett.* **2014**, *17*, 771–784. [CrossRef]
56. Ribeiro, M.P.; de Mello, K.; Valente, R.A. Landscape structure aiming at the biodiversity conservation of urbanized landscape. *Cienc. Florest.* **2020**, *30*, 819–834. [CrossRef]
57. Mitchell, M.G.E.; Wu, D.; Johansen, K.; Maron, M.; McAlpine, C.; Rhodes, J.R. Landscape structure influences urban vegetation vertical structure. *J. Appl. Ecol.* **2016**, *53*, 1477–1488. [CrossRef]

58. Silveira, D.S.J.; Silva-Neto, C.M.; Castro Silva, T.; Nascimento, S.K.; Ribeiro, M.C.; Garcia, C.R. Landscape structure and local variables affect plant community diversity and structure in a Brazilian agricultural landscape. *Biotropica* **2022**, *54*, 239–250. [CrossRef]
59. Rahimi, E.; Barghjelveh, S.; Dong, P.L. Estimating landscape structure effects on pollination for management of agricultural landscapes. *Ecol. Process* **2021**, *10*, 59. [CrossRef]
60. Rocha-Santos, L.; Benchimol, M.; Mayfield, M.M.; Faria, D.; Pessoa, M.S.; Talora, D.C.; Mariano-Neto, E.; Cazetta, E. Functional decay in tree community within tropical fragmented landscapes: Effects of landscape-scale forest cover. *PLoS ONE* **2017**, *12*, e0175545. [CrossRef]
61. Jacquemyn, H.; Butaye, J.; Hermy, M. Impacts of restored patch density and distance from natural forests on colonization success. *Restor. Ecol.* **2003**, *11*, 417–423. [CrossRef]
62. Uroy, L.; Ernoult, A.; Mony, C. Effect of landscape connectivity on plant communities: A review of response patterns. *Landsc. Ecol.* **2019**, *34*, 203–225. [CrossRef]
63. Haddad, N.M.; Brudvig, L.A.; Clobert, J.; Davies, K.F.; Gonzalez, A.; Holt, R.D.; Lovejoy, T.E.; Sexton, J.O.; Austin, M.P.; Collins, C.D.; et al. Habitat fragmentation and its lasting impact on Earth's ecosystems. *Sci. Adv.* **2015**, *1*, e150052. [CrossRef]
64. Zhang, J.X.; Liu, D.Q.; Gong, J.; Ma, X.C.; Cao, E.J. Impact of landscape fragmentation on watershed soil conservation service—A case study on Bailongjiang Watershed of Gansu. *Resour. Sci.* **2018**, *40*, 1866–1877.
65. Zheng, B.F.; Huang, Q.Y.; Tao, L.; Xie, Z.Y.; Ai, B.; Zhu, Y.H.; Zhu, J.Q. Landscape pattern change and its impacts on the ecosystem services value in southern Jiangxi Province. *Acta Ecol. Sin.* **2021**, *41*, 5940–5949.
66. Lu, X.L.; Liu, J.L.; Ding, S.Y. Impact of agricultural landscape heterogeneity on biodiversity and ecosystem services. *Acta Ecol. Sin.* **2019**, *39*, 4602–4614.
67. Lamy, T.; Liss, K.N.; Gonzalez, A.; Bennett, E.M. Landscape structure affects the provision of multiple ecosystem services. *Environ. Res. Lett.* **2016**, *11*, 124017. [CrossRef]
68. Hui, G.Y.; Hu, Y.B. Measuring Species Spatial Isolation in Mixed Forests. *For. Res.* **2001**, *1*, 23–27.
69. Hardiman, B.S.; LaRue, E.A.; Atkins, J.W.; Fahey, R.T.; Wagner, F.W.; Gough, C.M. Spatial variation in canopy structure across forest landscapes. *Forests* **2019**, *9*, 474. [CrossRef]
70. Li, X.; Niu, J.; Zhang, L.; Xiao, Q.; McPherson, G.E.; Van Doorn, N.; Yu, X.; Xie, B.; Dymond, S.; Li, J.; et al. A study on crown interception with four dominant tree species: A direct measurement. *Hydrol. Res.* **2016**, *47*, 857–868. [CrossRef]
71. Atkins, J.W.; Fahey, R.T.; Hardiman, B.H.; Gough, C.M. Forest Canopy Structural Complexity and Light Absorption Relationships at the Subcontinental Scale. *J. Geophys. Res. Biogeosci.* **2017**, *123*, 1387–1405. [CrossRef]
72. Dietz, J.; Hölscher, D.; Leuschner, C. Rainfall partitioning in relation to forest structure in differently managed montane forest stands in Central Sulawesi, Indonesia. *For. Ecol. Manag.* **2006**, *237*, 170–178. [CrossRef]
73. Liu, Y.J.; Zhang, S.Y.; Li, J.; Zhang, X.Y.; Qiu, Q. Effect of Slope Position and Density on the Species Diversity of Understory Vegetation and Productivity of Eucalyptus Plantation. *For. Environ. Sci.* **2019**, *35*, 48–55.
74. Wang, M.Z.; Bi, H.J.; Jin, S.; Liu, J.; Liu, Y.H.; Wang, Y.; Qi, J.Q.; Hao, J.T. Effects of stand density on understory species diversity and soil physicochemical properties of a *Cupressus funebris* plantation in Yunding Mountain. *Acta Ecol. Sin.* **2019**, *39*, 981–988.
75. Wei, H.Y.; Dong, L.B.; Liu, Z.G. Spatial structure optimization simulation of main forest types in Great Xing'an Mountains, Northeast China. *J. Appl. Ecol.* **2019**, *30*, 3824–3832.
76. Xiang, B.W.; Zeng, S.Q.; Gan, S.S.; Long, S.S.; Liu, X. Spatial structure optimization of Quercus in Hunan. *J. Cent. South Univ. For. Technol.* **2019**, *39*, 33–40.
77. Zhang, X.; Johnston, E.R.; Barberán, A.; Ren, Y.; Lü, X.; Han, X. Decreased plant productivity resulting from plant group removal experiment constrains soil microbial functional diversity. *Glob. Chang. Biol.* **2017**, *23*, 4318–4332. [CrossRef] [PubMed]
78. Lange, M.; Eisenhauer, N.; Sierra, C.A.; Bessler, H.; Engels, C.; Griffiths, R.I.; Mellado-Vázquez, P.G.; Malik, A.A.; Roy, J.; Scheu, S.; et al. Plant diversity increases soil microbial activity and soil carbon storage. *Nat. Commun.* **2015**, *6*, 6707. [CrossRef] [PubMed]
79. Fornara, D.A.; Tilman, D. Plant functional composition influences rates of soil carbon and nitrogen accumulation. *J. Ecol.* **2008**, *96*, 314–322. [CrossRef]
80. van Ruijven, J.; Berendse, F. Diversity-productivity relationships: Initial effects, long-term patterns, and underlying mechanisms. *Proc. Natl. Acad. Sci. USA* **2005**, *102*, 695–700. [CrossRef]
81. Isbell, F.; Adler, P.R.; Eisenhauer, N.; Fornara, D.; Kimmel, K.; Kremen, C.; Letourneau, D.K.; Liebman, M.; Polley, H.W.; Quijas, S.; et al. Benefits of increasing plant diversity in sustainable agroecosystems. *J. Ecol.* **2017**, *105*, 871–879. [CrossRef]
82. Maestre, F.T.; Quero, J.L.; Gotelli, N.J.; Escudero, A.; Ochoa, V. Plant species richness and ecosystem multifunctionality in global drylands. *Science* **2012**, *335*, 214–218. [CrossRef]
83. Lin, X.G.; Hu, J.L. Scientific connotation and ecological service function of soil microbial diversity. *Acta Pedol. Sin.* **2008**, *5*, 892–900.
84. Waring, B.G. Exploring relationships between enzyme activities and leaf litter decomposition in a wet tropical forest. *Soil Biol. Biochem.* **2013**, *64*, 89–95. [CrossRef]
85. Bardgett, R.D.; van der Putten, W.H. Belowground biodiversity and ecosystem functioning. *Nature* **2014**, *515*, 505–511. [CrossRef] [PubMed]
86. Vitorino, L.C.; Bessa, L.A. Microbial Diversity: The Gap between the Estimated and the Known. *Diversity* **2018**, *10*, 46. [CrossRef]

87. Li, M.; Chen, L.D.; Yang, X.R.; Zhao, F.K.; Sun, L.; Xu, S.L.; Yang, L. Community Characteristic and Functional Variability of Soil Microbes in Urban-rural Complex Ecosystem. *Acta Pedol. Sin.* **2021**, *58*, 1368–1380.
88. van der, H.M.; Ba Rdgett, R.D.; Straalen, N. The unseen majority: Soil microbes as drivers of plant diversity and productivity in terrestrial ecosystems. *Ecol. Lett.* **2008**, *11*, 296–310. [CrossRef]
89. Hou, J.H.; Ma, K.P. On mechanisms of species coexistence in plant communities. *Chin. J. Plant Ecol.* **2002**, *26*, 1–8.
90. Lusk, C.H.; Smith, B. Life history difference and species coexistence in an old growth New Zealand rain forest. *Ecology* **1998**, *79*, 795–806. [CrossRef]
91. Feng, S.Y.; Zhao, W.W.; Han, Y. Biodiversity conservation in a changing environment—Review of the fourth One Planet Summit. *Acta Ecol. Sin.* **2022**, *42*, 2050–2058.
92. Sanderson, M.A.; Skinner, R.H.; Barker, D.J.; Edwards, G.R.; Tracy, B.F.; Wedin, D.A. Plant Species Diversity and Management of Temperate Forage and Grazing Land Ecosystems. *Crop. Sci.* **2004**, *44*, 1132–1144. [CrossRef]
93. Gamfeldt, L.; Hillebrand, H.; Jonsson, P.R. Multiple functions increase the importance of biodiversity for overall ecosystem functioning. *Ecology* **2008**, *89*, 1223–1231. [CrossRef]
94. Xu, W.; Ma, Z.Y.; Jing, X.; He, J.S. Biodiversity and ecosystem multifunctionality: Advances and perspectives. *Biodivers. Sci.* **2016**, *24*, 55–71. [CrossRef]
95. Naeem, S.; Thompson, L.J.; Lawler, S.P.; Lawton, J.H.; Woodfin, R.M. Declining biodiversity can alter the performance of ecosystems. *Nature* **1994**, *368*, 734–737. [CrossRef]
96. Bagousse-Pinguet, Y.L.; Soliveres, S.; Gross, N.; Torices, R.; Berdugo, M.; Maestre, F.T. Phylogenetic, functional, and taxonomic richness have both positive and negative effects on ecosystem multifunctionality. *Proc. Natl. Acad. Sci. USA* **2019**, *116*, 8419–8424. [CrossRef] [PubMed]
97. Huang, X.B.; Lang, X.D.; Li, S.F.; Liu, W.D.; Su, J.R. Indicator selection and driving factors of ecosystem multifunctionality: Research status and perspectives. *Biodivers. Sci.* **2021**, *29*, 1673–1686. [CrossRef]
98. Díaz, S.; Marcelo, C. Vive la différence: Plant functional diversity matters to ecosystem processes. *Trends Ecol. Evol.* **2001**, *16*, 646–655. [CrossRef]
99. Zirbel, C.R.; Grman, E.; Bassett, T.; Brudvig, L.A. Landscape context explains ecosystem multifunctionality in restored grasslands better than plant diversity. *Ecology* **2019**, *100*, e02634. [CrossRef]
100. Steudel, B.; Hallmann, C.; Lorenz, M.; Abrahamczyk, S.; Prinz, K.; Herrfurth, C.; Feussner, I.; Martini, J.W.R.; Kessler, M. Contrasting biodiversity-ecosystem functioning relationships in phylogenetic and functional diversity. *New Phytol.* **2016**, *212*, 409–420. [CrossRef]
101. Zhang, Y.; Cheng, J.; Su, J.S.; Cheng, J.M. Diversity-productivity relationship of plant communities in typical grassland during the longterm grazing exclusion succession. *Chin. J. Plant Ecol.* **2022**, *46*, 176–187. [CrossRef]
102. Xiao, Y.; Xie, G.D.; An, K.; Lu, C.X. A research framework of ecosystem services based on functional traits. *Chin. J. Plant Ecol.* **2012**, *36*, 353–362. [CrossRef]
103. Shipley, B. Comparative plant ecology as a tool for integrating across scales. *Ann. Bot.* **2007**, *99*, 965–966. [CrossRef]
104. Garcia-Palacios, P.; Gattinger, A.; Bracht-Jorgensen, H.; Brussaard, L.; Carvalho, F.; Castro, H.; Clément, J.C.; De Deyn, G.; d'Hertefeldt, T.; Foulquier, A.; et al. Crop traits drive soil carbon sequestration under organic farming. *J. Appl. Ecol.* **2018**, *55*, 2496–2505. [CrossRef]
105. Hanisch, M.; Schweiger, O.; Cord, A.; Volk, M.; Knapp, S. Plant functional traits shape multiple ecosystem services, their trade-offs and synergies in grasslands. *J. Appl. Ecol.* **2020**, *57*, 1535–1550. [CrossRef]
106. Dennis, P.G.; Miller, A.J.; Hirsch, P.R. Are root exudates more important than other sources of rhizodeposits in structuring rhizosphere bacterial communities? *FEMS Microbiol. Ecol.* **2010**, *72*, 313–327. [CrossRef] [PubMed]
107. Chaparro, J.M.; Badri, D.V.; Bakker, M.G.; Sugiyama, A.; Manter, D.K.; Vivanco, J.M. Root exudation of phytochemicals in Arabidopsis follows specific patterns that are developmentally programmed and correlate with soil microbial functions. *PLoS ONE* **2013**, *8*, e55731. [CrossRef]
108. Mitchell, C.E. Trophic control of grassland production and biomass by pathogens. *Ecol. Lett.* **2010**, *6*, 147–155. [CrossRef]
109. Lin, F.R.; Gu, D.X.; Huang, Y.Q.; He, C.X.; Wei, Q.S. Research advances in hydraulic redistribution of plant roots. *Chin. J. Ecol.* **2021**, *40*, 2978–2986.
110. Richards, J.H.; Caldwell, M.M. Hydraulic lift: Substantial nocturnal water transport between soil layers by *Artemisia tridentata* roots. *Oecologia* **1987**, *73*, 486–489. [CrossRef] [PubMed]
111. Wang, J.; Zhao, W.W.; Liu, Y.; Jia, L.Z. Effects of plant functional traits on soil conservation: A review. *Acta Ecol. Sin.* **2019**, *39*, 3355–3364.
112. Zhang, K.; Huang, K.D.; Zhao, X.J.; She, J.W.; Zheng, X.; Tang, L.Z. Effects of Pruning on Microclimate and Understory Vegetation in A Poplar Plantation. *Ecol. Environ.* **2019**, *28*, 1548–1556.
113. Chen, L.; Xiong, K.N.; Tang, X.P. A Review of Forest-Grass Intercropping System. *World For. Res.* **2019**, *32*, 25–30.
114. Cao, X.Y.; Li, J.P.; Feng, Y.; Hu, Y.J.; Zhang, C.C.; Fang, X.N.; Deng, C. Analysis and Evaluation of the Stand Spatial Structure of *Cunninghamia lanceolata* Ecological Forest. *Sci. Silvae Sin.* **2015**, *51*, 37–48.
115. Yao, J.B.; Zeng, P.S.; Yuan, X.P.; Wu, J.G.; Chu, X.L.; Zhou, Z.C. Impacts of Thinning Intensities on Growth and Stand Structure of *Schima superba*-Sprouting *Cuninghamia lanceolata* Mixed Plantation. *For. Res.* **2017**, *30*, 511–517.

116. Kong, L.W.; Yu, Y.H.; Xiong, K.N.; Wei, C.S.; Zhang, S.H. Leaf functional traits of *Zanthoxylum planispinum* var. *dintanensis and their response to management measures. J. For. Environ.* **2022**, *42*, 364–373.
117. Yu, Y.H.; Zhong, X.P.; Zheng, W.; Chen, Z.X.; Wang, J.X. Species diversity, functional traits, stoichiometry and correlation of plant community in different succession stages of karst forest. *Acta Ecol. Sin.* **2021**, *41*, 2408–2417.
118. Smith, T.M.; Woodward, F.I.; Shugart, H.H. *Plant Function Types*; Cambridge University Press: Cambridge, UK, 1996.
119. Woodward, F.I.; Cramer, W. Plant functional types and climatic change: Introduction. *J. Veg. Sci.* **1996**, *7*, 306–308. [CrossRef]
120. Zang, R.G.; Zhang, Z.D. Plant functional groups and their dynamics in tropical forests: A review. *Acta Ecol. Sin.* **2010**, *30*, 3289–3296.
121. Jiang, S.L.; Xiong, K.N.; Xiao, J. Structure and Stability of Agroforestry Ecosystems: Insights into the Improvement of Service Supply Capacity of Agroforestry Ecosystems under the Karst Rocky Desertification Control. *Forests* **2022**, *13*, 878. [CrossRef]
122. Xiong, K.N.; Chi, Y.K. The Problems in Southern China Karst Ecosystem in Southern of China and Its Countermeasures. *Ecol. Econ.* **2015**, *31*, 23–30.
123. Huang, Y.F.; Shu, Y.G.; Xiao, S.Y.; Chen, M.J. Quantification of soil nutrient levels and enzyme activities in different grassl and categories in karst mountains. *Acta Prataculturae Sin.* **2020**, *29*, 93–104.
124. Baker, T.R.; Swaine, M.D.; Burslem, D.F. Variation in tropical forest growth rates: Combined effects of functional group composition and resource availability. *Perspect. Plant Ecol.* **2003**, *6*, 21–36. [CrossRef]
125. Tilman, D.; Reich, P.B.; Knops, J.; Wedin, D.; Mielke, T.; Lehman, C. Diversity and productivity in a long-term grassland experiment. *Science* **2001**, *294*, 843–845. [CrossRef]
126. Hooper, D.U.; Adair, E.C.; Cardinale, B.J.; Byrnes, J.; Hungate, B.A.; Matulich, K.L.; Gonzalez, A.; Duffy, J.E.; Gamfeldt, L.; O'Connor, M.I. A global synthesis reveals biodiversity loss as a major driver of ecosystem change. *Nature* **2012**, *486*, 105–108. [CrossRef] [PubMed]
127. Bai, Y.; Wu, J.; Clark, C.M.; Naeem, S.; Pan, Q.; Huang, J.; Zhang, L.; Han, X. Tradeoffs and thresholds in the effects of nitrogen addition on biodiversity and ecosystem functioning: Evidence from Inner Mongolia grasslands. *Global Chang. Biol.* **2010**, *16*, 358–372. [CrossRef]
128. de Deyn, G.B.; van der, P.W.H. Linking aboveground and belowground diversity. *Trends Ecol. Evol.* **2005**, *20*, 625–633. [CrossRef] [PubMed]
129. Zhu, H. The kasrt ecosystem of southern China and its biodiversity. *Trop. For.* **2007**, *35*, 44–47.
130. Yuan, C.J.; Xiong, K.N.; Rong, L.; Weng, Y.F. Research Progress on the Biodiversity during the Ecological Restoration of Karst Rocky Desertification. *Earth Environ.* **2021**, *49*, 336–345.
131. Liu, F.; Wang, S.J.; Liu, Y.S.; He, T.B.; Luo, H.B.; Long, J. Changes of soil quality in the process of karst rocky desertification and evaluation of impact on ecological environment. *Acta Ecol. Sin.* **2005**, *3*, 639–644.
132. Hylander, K.; Greiser, C.; Christiansen, D.M.; Irena, A.; Koelemeijer, I.A. Climate adaptation of biodiversity conservation in managed forest landscapes. *Conserv. Biol.* **2021**, *36*, e13847. [CrossRef]
133. Lindenmayer, D.B. Integrating forest biodiversity conservation and restoration ecology principles to recover natural forest ecosystems. *New For.* **2018**, *50*, 169–181. [CrossRef]
134. Wang, K.L.; Zhang, C.H.; Chen, H.S.; Yue, Y.M.; Zhang, W.; Zhang, M.Y.; Qi, X.K.; Fu, Z.Y. Karst landscapes of China: Patterns, ecosystem processes and services. *Landsc. Ecol.* **2019**, *34*, 2743–2763. [CrossRef]
135. Su, C.; Dong, M.; Fu, B.; Liu, G. Scale effects of sediment retention, water yield, and net primary production: A case study of the Chinese Loess Plateau. *Land Degrad Dev.* **2020**, *31*, 1408–1421. [CrossRef]
136. Zhang, C.; Li, Z.J.; Zeng, H. Scale effects on ecosystem service trade-off and its influencing factors based on wavelet transform: A case study in the Pearl River Delta, China. *Geogr. Res.* **2022**, *41*, 1279–1297.
137. Lu, Y.; Hua, C.; Zhou, X. A Study of Landscape Patterns in the Karst Mountainous Area Using RS and GIS. *Mt. Res.* **2002**, *6*, 727–731.
138. Wang, Y.Y.; Zhou, Z.F.; Wei, X.D. Rocky Desertification Landscape Pattern on Spatio-temporal Evolution of Land Use the Response. *Mt. Res.* **2013**, *31*, 307–313.
139. Han, W.Q.; Chang, Y.; Hu, Y.M.; Li, X.Z.; Bu, R.C. Research advance in landscape pattern optimization. *Chin. J. Ecol.* **2005**, *12*, 1487–1492.
140. Wu, X.Q.; Cai, Y.L.; Meng, J.J. Impacts of Land Use on Soil Erosion in Karst Mountainous Area —A Case Study in Shibanqiao Catchment in Guanling county, Guizhou Province. *Res. Soil Water Conserv.* **2005**, *4*, 46–48+77.
141. Wang, H.; Gao, J.B.; Hou, W.J. Quantitative attribution analysis of soil erosion in different morphological types of geomorphology in karst areas: Based on the geographical detector method. *Acta Geogr. Sin.* **2018**, *73*, 1674–1686.
142. Lemessa, D.; Hamback, P.A.; Hylander, K. The effect of local and landscape level land-use composition on predatory arthropods in a tropical agricultural landscape. *Landsc. Ecol.* **2015**, *30*, 167–180. [CrossRef]
143. Hu, T.H.; Li, K.P.; Xiong, K.N.; Wang, J.; Yang, S.; Wang, Z.F.; Gao, A.; Yu, X. Research Progress on Water–Fertilizer Coupling and Crop Quality Improvement and Its Implication for the Karst Rock Desertification Control. *Agronomy* **2022**, *12*, 903. [CrossRef]
144. Lautenbach, S.; Jungandreas, A.; Blanke, J.; Lehsten, V.; Mühlner, S.; Kühn, I.; Volk, M. Trade-offs between plant species richness and carbon storage in the context of afforestation—Examples from afforestation scenarios in the Mulde Basin, Germany. *Ecol. Indic.* **2017**, *73*, 139–155. [CrossRef]

145. Chen, M.Y.; Liu, S.H.; Yu, L.H.; Feng, J.Z.; Yu, P.X.; Gao, B.J. Response of Ecosystem Service Value to Ecosystem Structure Change in Fuping Basin of the Daqinghe River. *J. Nat. Resour.* **2018**, *33*, 1376–1389.
146. Zhang, Y.R.; Meng, J.J.; Zhou, T. Dynamic analysis of landscape structure and function in Erdos during 1988–2000. *J. Arid. Land. Resour. Environ.* **2009**, *23*, 49–55.
147. Li, H.D.; Wu, X.W.; Xiao, Z.S. Assembly, ecosystem functions, and stability in species interaction networks. *Chin. J. Plant Ecol.* **2021**, *45*, 1049–1063. [CrossRef]
148. Chen, J.H.; Gong, G.T.; Zhu, Z.F.; Mu, C.L. Landscape structure and ecological function of protection forests in Guansi river watershed. *Ecol. Environ.* **2010**, *19*, 712–717.
149. Wang, J.M.; Liu, J.; Chen, X.M.; Wen, Q.Z.; Duan, Z.Y.; Lai, X.H. Comparison of Community Structures and Species Diversity in Natural Forests and Forest Plantation of *Pinus yunnanensis*. *For. Res.* **2010**, *23*, 515–522.
150. Mc Gill, B.J.; Enquist, B.J.; Weiher, E.; Westoby, M. Rebuilding community ecology from functional traits. *Trend Ecol. Evolut.* **2006**, *21*, 178–185. [CrossRef]
151. Hertzog, L.R.; Boonyarittichaikij, R.; Dekeukeleire, D.; de Groote, S.R.E.; van Schrojenstein, L.I.; Sercu, B.K.; Smith, H.K.; de la Peña, E.; Vandegehuchte, M.L.; Bonte, D.; et al. Forest fragmentation modulates effects of tree species richness and composition on ecosystem multifunctionality. *Ecology* **2019**, *100*, e02653. [CrossRef]
152. Sylvanus, M.; Kolawolé, V.S.; Achille, A.; Romain, G.K.; Brice, S.; Seifert, T. Functional trait diversity is a stronger predictor of multifunctionality than dominance: Evidence from an Afromontane forest in South Africa. *Ecol. Indic.* **2020**, *115*, 106415.
153. Yan, Y.Z.; Zhang, Q.; Alexander, B.; Liu, Q.F.; Niu, J.M. Plant functional β diversity is an important mediator of effects of aridity on soil multifunctionality. *Sci. Total Environ.* **2020**, *726*, 138529. [CrossRef]
154. Yuan, Z.Q.; Arshad, A.; Paloma, R.B.; Tommaso, J.; Akira, S.M.; Wang, S.P.; Zhang, X.K.; Li, H.; Hao, Z.Q.; Wang, X.G.; et al. Above and below-ground biodiversity jointly regulate temperate forest multifunctionality along a local-scale environmental gradient. *J. Ecol.* **2020**, *108*, 2012–2024. [CrossRef]
155. Wang, K.; Wang, C.; Feng, X.M.; Wu, X.; Fu, B.J. Research progress on the relationship between biodiversity and ecosystem multifunctionality. *Acta Ecol. Sin.* **2022**, *42*, 11–23.
156. Chillo, V.; Vázquez, D.P.; Amoroso, M.M.; Bennett, E.M. Land-use intensity indirectly affects ecosystem services mainly through plant functional identity in a temperate forest. *Funct. Ecol.* **2018**, *32*, 1390–1399. [CrossRef]
157. Mori, A.S. Biodiversity and ecosystem services in forests: Management and restoration founded on ecological theory. *J. Appl. Ecol.* **2017**, *54*, 7–11. [CrossRef]
158. Zhang, B.; Shi, Y.T.; Wang, S. A Review on the Driving Mechanisms of Ecosystem Services Change. *J. Resour. Ecol.* **2022**, *13*, 68–79.
159. Karimi, J.D.; Corstanje, R.; Harris, J.A. Understanding the importance of landscape configuration on ecosystem service bundles at a high resolution in urban landscapes in the UK. *Landsc. Ecol.* **2021**, *36*, 2007–2024. [CrossRef]

forests

MDPI

Review

A Review of Eco-Product Value Realization and Eco-Industry with Enlightenment toward the Forest Ecosystem Services in Karst Ecological Restoration

Biliang Yang [1,2], Yu Zhang [3], Kangning Xiong [1,2,*], Huiqiong Huang [1,2,4] and Ying Yang [1,2]

[1] School of Karst Science, Guizhou Normal University, Guiyang 550001, China; yangbl97@163.com (B.Y.); yingyang1220@163.com (Y.Y.)
[2] State Engineering Technology Institute for Karst Desertification Control, Guiyang 550001, China
[3] Department of Resource Management, Tangshan Normal University, Tangshan 063000, China; hxcandzy@163.com
[4] College of Public Management, Guizhou University of Finance and Economics, Guiyang 550025, China
* Correspondence: xiongkn@gznu.edu.cn

Abstract: Eco-product value realization and eco-industry are in a rapid development stage, but the eco-product value realization mechanism is still unclear. Strengthening research on eco-industry and eco-product value realization not only helps to coordinate the relationship between regional ecologies and the economy but also contributes to regional sustainable development. This study conducted a systematic literature review based on related articles retrieved from the Web of Science database and China National Knowledge Infrastructure database. The results showed the following: (1) Regarding time series, the average annual number of published works in the literature from 2000 to 2017 is less than 4, while the average annual number of published works in the literature from 2018 to 2022 is more than 97. The overall study on eco-product value realization and eco-industry has shown a year-on-year growth trend. (2) The research content primarily involves five aspects, including the connotation and extension of eco-products, eco-product supply, eco-product value accounting, eco-product value realization, and eco-industry. (3) It is essential to deepen the study on the improvement mechanism of the eco-product supply capacity, eco-products property rights, evaluation system for eco-product value realization, ecological compensation mechanism, driving mechanism for eco-products to eco-industry, and coupled development of ecological restoration and eco-industry. Based on the above research, this paper presents an enlightment of the forest ecosystem services in the karst ecological restoration area from three aspects: enhancing the supply ability of eco-products, improving the compensation mechanism of forest ecological services, and coordinating the development of ecosystem services and eco-industries.

Keywords: ecological products; value realization; ecological industry; value accounting

Citation: Yang, B.; Zhang, Y.; Xiong, K.; Huang, H.; Yang, Y. A Review of Eco-Product Value Realization and Eco-Industry with Enlightenment toward the Forest Ecosystem Services in Karst Ecological Restoration. *Forests* **2023**, *14*, 729. https://doi.org/10.3390/f14040729

Academic Editor: Peter Elsasser

Received: 19 February 2023
Revised: 30 March 2023
Accepted: 31 March 2023
Published: 3 April 2023

1. Introduction

The extensive mode of economic development has seriously damaged the ecological environment; thus, changing the course of economic development and promoting ecological environmental protection is necessary [1]. A good ecological environment can provide more eco-products and services for people [2]. A hot topic is how to promote the transformation of ecological value by adding value to the ecological environment and natural resources and reflecting that in high prices, so that protecting the ecological environment can be rewarded and, thus, promote improving the ecological environment and coordinating economic development and environmental protection.

The concept of ecosystem services was first proposed by Holdre and Ehrlich in 1974 [3]. In 1997, Costanza [4] defined ecosystem services as representing the benefits human populations derive, directly or indirectly, from ecosystem functions. Since the definition was

proposed, it has attracted widespread academic attention and ecosystem services have been classified. The classification of ecosystem services defined by the Millennium Ecosystem Assessment [5]—provision, regulation, support, and cultural services—is generally accepted. The proposed definition and classification of ecosystem services provides the basis for valuing ecosystem services and quantifying the services that natural ecosystems provide to humans. Introducing ecosystem services has led to a focus on ecological conservation [6,7]. Researching ecosystem services encourages people to give more attention to protecting the ecological environment.

With environmental awareness being enhanced, "ecological products" appeared in the mid-1980s in China [8]. Ren and Yuan defined eco-products in 1992 [9]. In China's National Plan for Main Functional Zones in 2010, natural elements such as air, water, and the climate were each attributed as a "product" for the first time and classified into the category of eco-products [10]. The plan proposed that eco-products are the natural elements that maintain ecological safety, guarantee ecological regulation, and provide good living environments [10]. This definition is similar to that of ecosystem services [11]. At present, the definition of eco-products proposed by Zhang et al. is generally recognized and accepted by scholars [12]. They suppose that eco-products are terminal products or services which are provided for the use and consumption of human society by the interaction between the biological production within the ecosystem and the production of human society. The initial purpose of eco-products is to use them as a standard to measure ecological environmental protection when developing key ecological functional areas. With human demand for quality eco-products, local governments and academics have gradually carried out research on realizing the value of eco-products and other aspects. Most studies focus on the concept of eco-products [12,13], eco-product value accounting [14,15], and value realization paths and models [16,17]. The research on how to improve the supply capacity of eco-products and how to build an assessment system for the realization of eco-product value is rarely mentioned. Research in these aspects is necessary to improve the eco-product value realization mechanism.

Eco-industry is a network-evolved industry organized according to the principles of ecological economy and the laws of knowledge economy, with efficient economic processes and harmonious ecological functions based on the carrying capacity of the ecosystem [18]. The idea emerged in the 1970s and grew rapidly in the late 1990s [19]. The idea of eco-industry is widely used in product design and new product development for raw materials, energy, and other industries [18]. In addition, based on Jinping Xi's proposal that "lucid waters and lush mountains are invaluable assets", eco-industry can also depend on the ecological resources of ecosystems. To elaborate, ecological resources require ecological innovation; thus, through the ecological value realization mechanism, ecological resources are converted into products, with ecological industrialization enabling ecological resource protection and adding value to them [20]. This is a new industry that belongs to the coordinated development of ecological resource utilization, ecology, and economy. As a specific form of sustainable development, eco-industry harmonizes the unbalanced relationship between ecological protection and economic development [21], which is consistent with the goal of realizing the value of eco-products. On the basis of realizing the value of eco-products, how to drive the formation of eco-industry and establish the formation mechanism of eco-industry are the problems that need to be explored [22].

The global karst landscape covers about 15% of the world's total area, in which a quarter of the world's population lives [23]. China's karst area accounts for about one-third of the national land area, and it is one of the countries with the largest area of karst landscapes [24]. China's karst area is widely distributed with many types, mainly in its southern region. However, the karst ecosystem has been degraded due to unreasonable human activities, with a dramatic reduction in biodiversity and a gradual intensification of soil erosion, thus resulting in severe rocky desertification and causing the karst region to be vulnerable [25]. Rocky desertification has become an essential ecological problem restricting the development of regional economies and societies in South China's karst areas [26]. To reduce land degradation and promote ecological and economic development, scholars

have identified forests as the preferred target for ecological restoration in the region [27,28]. Management results have shown that forests are beneficial in stopping land degradation and provide products and services such as carbon sequestration, oxygen release, soil and water conservation, and timber in the control process [29,30]. Karst forest ecosystems contain enormous ecological service values, and their own values are conducive to human wellbeing [31]. At present, research on forest ecosystem services in karst restoration mainly focuses on assessing ecosystem services [32–34] and the tradeoff synergy between ecosystem services, and certain research results have been achieved [35–37]. However, owing to the high elasticity of karst desertification management, how to maintain a sustainable supply of forest ecosystem services requires continuous attention. Researching eco-product value realization and eco-industry can help promote the sustainable supply of forest ecosystem services for karst ecological restoration.

Agroforestry refers to a sustainable land use system formed by artificially combining multiple components such as woody plants, crops, and livestock breeding in the same land unit [38], which is a production mode designed to promote sustainable development of forestry [39]. It is included in the scope of forestry. As a type of forestry, agroforestry provides less biodiversity and ecosystem services than old-growth forests [40]. Based on the value realization of eco-products and eco-industry research, some researchers have proposed the enlightenment of agroforestry ecosystem services for karst ecological restoration [41], but they only focused on agroforestry. Therefore, based on the value realization of eco-products and eco-industry research, this study proposes that the supply capacity of forest eco-products can be improved by realizing forest ecosystem service function optimization through karst ecological restoration. The long-term dynamic observations and ecological protection of forest ecosystem service value in karst ecological restoration is established as the basis for formulating an ecological compensation standard, to improve the forest ecological compensation mechanism. The synergistic development of forest ecosystem services and eco-industry is proposed, for it aims to balance the development of ecological benefits and economic benefits.

Understanding eco-product value realization and eco-industry helps to coordinate ecological protection with economic development and promote ecological environment improvement. The study of eco-product value realization and eco-industry is in a rapid growth stage. Extensive studies have been conducted on eco-product value accounting, the value realization mode, and the value realization path. However, the value realization mechanism of ecological products still needs to be explored in depth, and the mechanism of how eco-products drive the formation of eco-industries is unclear. Therefore, based on a systematic review of the literature, this paper aims to (1) clarify the development trend of studies on eco-product value realization and eco-industry; (2) summarize the landmark achievements in eco-product value realization and eco-industry; and (3) condense the key scientific issues that need addressing in the study on eco-product value realization and eco-industry. This will help provide theoretical references for eco-product value realization and scientific support for transforming forest ecosystem service values in karst areas.

2. Materials and Methods

To identify relevant studies, a literature search was conducted based on the China National Knowledge Infrastructure (CNKI) and Web of Science (WOS) databases. To ensure the timeliness of the number of publications, the search date was on 31 December 2022. Figure 1 shows the process of the literature search and screening.

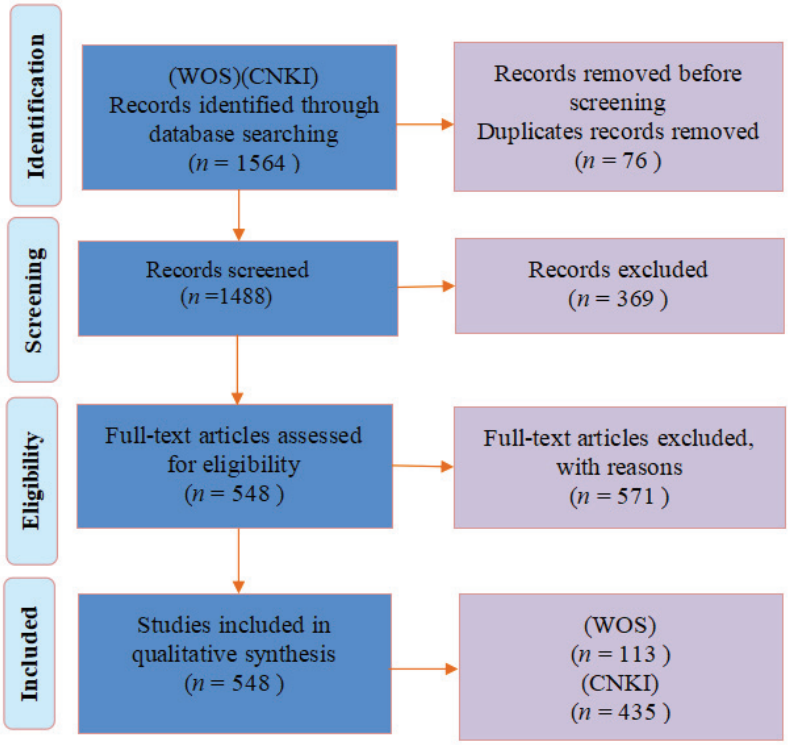

Figure 1. The process of the literature search and screening.

Above all, Chinese literature was obtained from CNKI. For CNKI, "item" was the search item, "eco-product value realization" was the search term for the first search, "eco-product" and "eco-industry" were entered into the subject for the second search, and finally, "ecosystem services" and "eco-industry" were the subjects for the third search. Next, English literature was obtained from the WOS database. For WOS, "theme" was the search item, "eco-product value realization" was the search term for the first search, "eco-product" and "eco-industry" were entered into the subject for the second search, and, finally, "ecosystem services" and "eco-industry" were the subjects for the third search. By removing any duplicate items from the literature, 1048 Chinese articles and 440 English articles were obtained. The statistical analysis was conducted on the retrieved articles. First, according to the realization of the eco-product value and the research content of eco-industry, the articles that were inconsistent with this research were screened out through article titles, keywords, and abstracts. Second, the full text was read to filter out the articles that were not relevant to this study. Lastly, 435 Chinese articles and 113 foreign articles were obtained, with a total of 548 Chinese and English articles.

3. Results

3.1. Annual Distribution of Reports

As shown in Figure 2, studies on eco-product value realization and eco-industry began to germinate in 2000 and has expanded swiftly since 2018. The studies can be roughly divided into two phases. The first phase has a total of 61 articles from 2000 to 2017. The related study started late, with an average annual publication volume of less than four articles, representing the embryonic phase. The second stage is from 2018 to 2022, which had a rapid growth phase, with a total of 487 papers, suggesting that this field of study has a broad future.

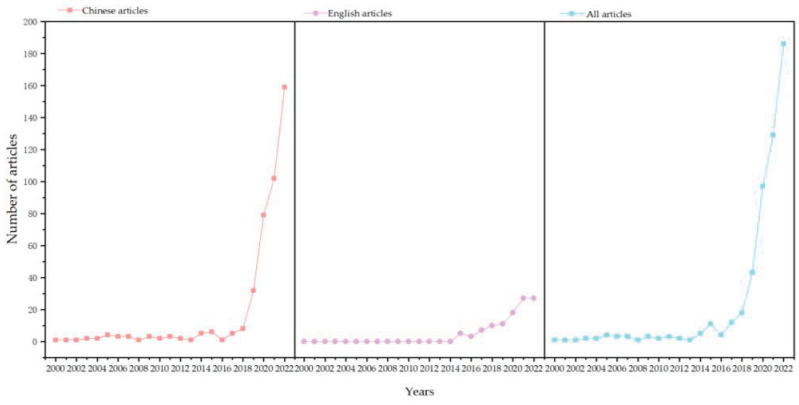

Figure 2. Annual distribution of articles.

3.2. Distribution of Research Areas in the Literature

As shown in Figure 3, the study institutions of eco-product value realization and eco-industry formation were counted. Regarding the regional distribution, the study units were mainly distributed in Asia (94.53%), followed by Europe (4.20%) and North America (0.73%), with less distribution in Africa (0.18%) and Oceania (0.18%). Asia is mainly distributed in China, India, Japan, and other regions; North America is mainly distributed in the United States and Canada; and Europe is mainly distributed in Sweden, the United Kingdom, and other regions. The largest number of articles was issued by Chinese institutions, followed by India, the UK, Sweden, and the US. This is inseparable from the concern of local governments and people for ecological protection and sustainable economic development.

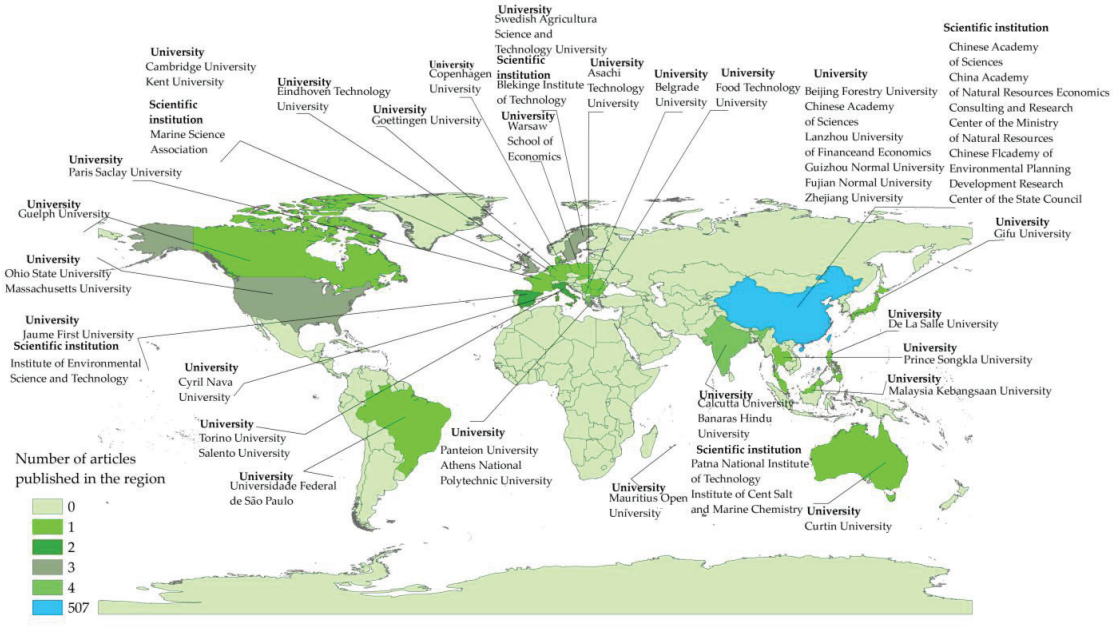

Figure 3. The breakdown of the institutions and nations described in the study (owing to space limitations, only institutions in China with more than seven publications are marked).

3.3. Institution Distribution of the Literature

Owing to the large number of issuing institutions, the number of institutions with more than seven articles was counted(Figure 4). Results of the statistical analysis show that the institutions with more than seven articles are all from China and that the top units in the number of publications in China are mainly divided into three categories: first, the scientific research units that have been engaged in ecological environmental protection and sustainable development for a long time include: the Environmental Planning Institute of the Ministry of Ecology and Environment (seven articles), the China Institute of Natural Resources Economics (eight articles), Development Research Center of the State Council (seven articles), and the Consulting and Research Center of the Ministry of Natural Resources (nine articles); second, the units in the regions where the national eco-product value realization mechanism points are located include: Zhejiang University (seven articles), Fujian Normal University (seven articles), Guizhou Normal University (nine articles); and, third, the unit whose research objects are mainly finance and resources, such as: Lanzhou University of Finance and Economics (eight articles). In addition, the colleges and universities related to forestry and agriculture are also the main publishing units, such as Beijing Forestry University (twelve articles), Eco-Environmental Research Center, Chinese Academy of Sciences (twelve articles), etc. In general, the article distribution for the research institutions is affected by factors such as research foundation and experience, geographical advantages, and majors.

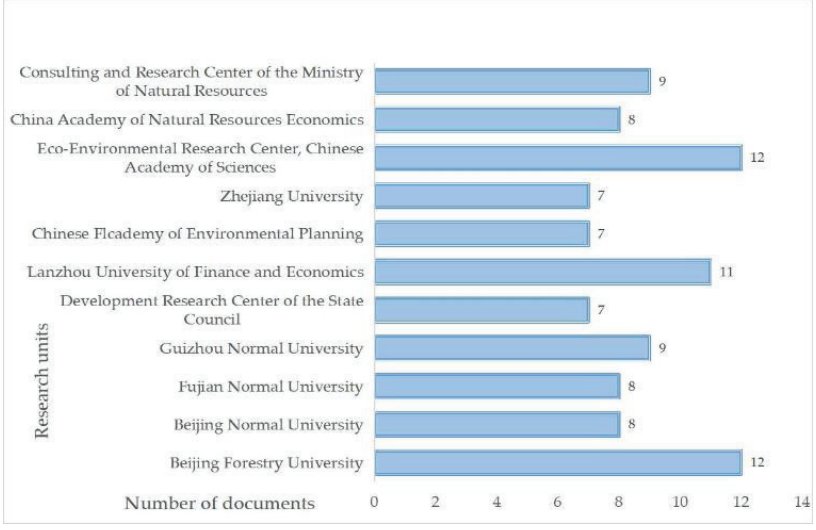

Figure 4. Literature by unit.

3.4. Content Distribution in the Literature

All of the identified literature is classified and summarized from the aspects of connotation and expansion, supply of eco-products, value accounting of eco-products, value realization of eco-products, and eco-industry (Figure 5). The literature on eco-product value realization accounts for 49.42%, mainly including eco-product value realization paths, models, and mechanisms. Eco-industry literature accounts for 21.82%, and mainly concerns technology research and development, industrial model construction, and experimental demonstration in eco-industry. The connotation and extension, and the value-accounting literature account for 12.28% and 11.27%, respectively. These are mainly about the concept and connotation of eco-products, value composition of eco-products, value-accounting indexes and methods, etc. The literature on the supply of eco-products accounts for 5.20% and mainly concerns the innovation of supplying the main body model, landscape planning,

and so on. These proportions in the literature indicate that research on the value realization of ecological products and eco-industries is becoming more mature, while the supply and value accounting of eco-products are still in the exploratory and developmental stages.

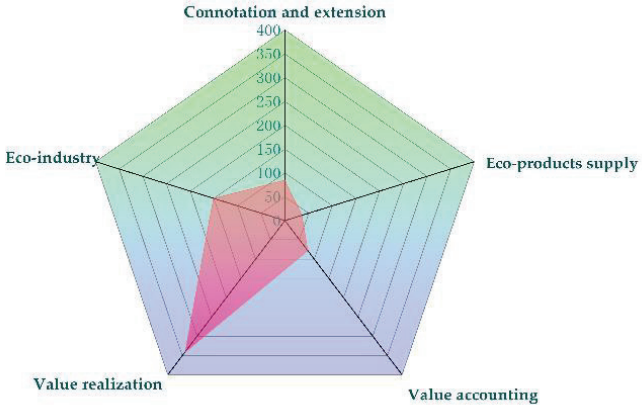

Figure 5. Research content division.

3.5. Division of the Main Study Stages

As can be seen from Table 1, the related studies started in 2000. According to changes in the research background, the studies about eco-product value realization and eco-industry are divided into two stages, namely, the sprouting stage and rapid growth stage.

Table 1. Division of the research stages.

Research Stage	Development Background	Main Features
Budding stage (2000–2017)	In 2010, China's national main functional area plan proposed the concept of "eco-products" for the first time, but there was no clear and unified concept. Some scholars have studied and discussed the concept and theory of eco-products.	There were less than four relevant articles per year, and mostly focused on the concept and theory of eco-products. For eco-industry development, it mainly focused on the transformation of traditional industries and the design and planning of ecological technology.
Period of rapid growth (2018–2022)	China has issued several documents and policies on the realization of eco-product value and carried out pilot projects sequentially, realizing the value of eco-products in several cities. Quality eco-products have become a scarce resource, and the coordinated development between ecologies and the economy is attracting increasing attention.	More than six relevant articles are published every year, and the average annual publication volume is more than 97. It is mainly about eco-product value accounting, realization path, mode, and mechanism research. A new industrial form has emerged around eco-products, and some scholars define it as the fourth industry of eco-products.

3.6. Major Progress and Landmark Achievements

3.6.1. Connotation and Extension

(1) Eco-product concept

As research has deepened, the academic community has maintained different views on defining eco-products. From the perspective of the natural environment, eco-products, as important components of the ecosystem, are natural elements that can maintain ecological security, safeguard ecological functions, and provide a good living environment [42]. From the perspective of social development, eco-products also include products that humans dedicate a certain amount of labor to and use in production, such as eco-agricultural

products and eco-industrial products produced through clean production, recycling, energy conservation, and emission reduction [12].

(2) Eco-products classification

Classifying eco-products is a prerequisite for studying their supply patterns and operational mechanisms [43]. Currently, there are several approaches to classifying eco-products. First, eco-products are classified into public eco-products, quasi-public eco-products, and commercial eco-products, according to different paths and modes for realizing their values [12]. Second, based on the theory of public goods, eco-products are divided into national public eco-products, regional or regional public eco-products, community public eco-products, and "private" eco-products [43]. Third, eco-products are divided into natural-factor eco-products, natural-attribute eco-products, eco-derived eco-products, and eco-label products, according to supply attributes [44]. Fourth, eco-products can be divided into ecological material products, ecological regulatory services, and ecological cultural services according to their manifestations and functions [45]. This is similar to the classification of ecosystem services into support, supply, regulation, and cultural services proposed by the Millennium Ecosystem Assessment [5].

(3) Composition of eco-product value

The types of eco-products are diverse and their value compositions are diverse. An eco-product's value is mainly manifested through its ecological, social, and economic value [46]. Its value permeates in human life and production, cultural needs, economic development, and other aspects [47]. Among them, the economic value of eco-products is realized by directly participating in market transactions, which is also the embodiment of direct-use value. The ecological value of eco-products is reflected in the natural value of eco-products, which shows the function of eco-products in the process of conservation, restoration, and regeneration of the whole ecosystem. It is also the embodiment of the value of indirect use [48]. Social value refers to the value of eco-products embodied in the process of enriching human spirit and culture and satisfying human needs for a better living environment [49]. It is a concrete expression of nonuse value.

3.6.2. Eco-Product Supply

Several studies have improved eco-product supply capacity from the perspective of supply-agent model innovation and spatial planning [42,50]. The single mode of supplying eco-products is not conducive to efficiently supplying eco-products. Some scholars use game theory to analyze the relationship between eco-product supply subjects by building a multicentered supply mechanism with the government as the main body and the market and society working together to enhance the effective supply of eco-products [51]. Moreover, from the perspective of the relationship between macro- and microsuppliers of eco-products, Zhang et al. [52] proposed multiple supply models such as a government-led supply model, government-participatory market model, government-service-oriented guarantee model, and government-cooperative promotion model. Supply-mode innovation not only realizes the diversification and individuation of supply content but also guarantees the supply efficiency and quality of eco-products. From the perspective of spatial planning, the normal play of ecosystem service functions depends on effective protection, restoration, and expansion [53]. Therefore, some scholars start with regional landscape planning to promote restoring damaged ecosystems by assigning various landscape types, quantities, and spatial patterns, thus improving the quality of the regional ecological environment and enhancing the supply capacity of high-quality eco-products [54].

3.6.3. Eco-Product Value Accounting

Quantifying the value of eco-products is fundamental to incorporate the welfare and conservation effects of ecosystem services on humans into all decisions and is a prerequisite to realizing the value of eco-products [55,56]. Currently, there is no unified method to account for the value of eco-products, and the main approach is assessing the value of ecosystem

services. There are three main methods. The first is the equivalence factor method [57]. This is based on different types of ecosystem service functions, using quantifiable criteria to construct the equivalent value of different types of ecosystem service functions [58,59]. Wang et al. [60] quantitatively analyzed the spatial and temporal distribution characteristics of land use changes and ecosystem service values in Xinjiang from 1990 to 2020 using equivalent factors combined with spatial autocorrelation and sensitivity. The second is the functional value method [61]. The service types are divided based on clear ecosystem types. Based on various monitoring and statistical data, the number of products and services provided by the ecosystem is calculated and multiplied by the price to obtain the total value [62,63]. Different types of eco-products require different functional value methods (Table 2). Mou et al. [64] used the functional value approach to estimate the value of ecosystem product supply, regulation service, and cultural service in the Yanqing district. The third is the emergy analysis method [65]. Based on the solar energy value required by each type of ecological resource to provide ecological services as a link, the service value for different types of ecological resources is calculated, and finally expressed in emergy units [66–68]. On account of the emergy analysis, Liu et al. [69] constructed the service accounting method system provided by the agroecosystem and calculated the typical agricultural ecosystem services per unit area in China.

Table 2. Classification of functional value method.

Type	Methods	Advantages	Disadvantages
Functional value method	Market value method [4]	It can directly evaluate some of the value of ecological service function and is widely recognized by the public.	Products and services that can be traded through the market are evaluated, their indirect benefits are ignored, and they are easily influenced by market institutions and policies.
	Alternative cost method [70–72]	The alternative approach solves the problem of estimating the value of ecosystem services in terms of the willingness to pay.	The method's effectiveness depends on the public's grasp of the information and the calculation of the cost produces errors.
	Shadow engineering [73,74]	The value of the ecological service function, which is difficult to estimate directly, can be calculated and processed using alternative engineering methods.	The replacement project is not unique, and the replacement project has great differences in time and space.
	Cost of protection method [75]	No detailed information or materials are required.	The value is affected by many factors, cost being only one of them, and it is easy to underestimate.
	Usage-of-travel fee [76]	Established based on the market, recognized by the public, and has a high degree of recognition.	The assessment results are influenced by local economic conditions.
	Hedonic price method [77,78]	Based on the market, it reflects the actual preference of consumers and has high credibility.	The statistical models are complex.

3.6.4. Eco-Product Value Realization

Through some studies, local governments and scholars have produced explorations and summaries on the mode of eco-product value realization. Its main models can be summarized as the ecological resource index and property rights trading model [79], ecological protection compensation model [80], ecological industrialization management mode [81], green finance model [82], and ecological protection and restoration, maintenance and appreciation model [83]. For example, the "Chongqing Land Stamp Model" [84] and "Fujian Forest Ecological Bank" [85] realize the value of eco-products through the capitalization of ecological resources by implementing the flow of ecological resources. For regulating service products, we mainly adopt the ecological protection compensation method to achieve the goal of protecting the environment and social benefits through governmental and market-based paths of ecological compensation [86,87]. Costa Rica has

been able to achieve a win–win situation in terms of forest conservation and economic development through market-based operations, relying on diversified funding channels and a differential compensation standard [88]. Material products and cultural service products need to rely on the organic combination of natural, constructed, and human capital to transform ecological advantages into economic advantages through management and development [89]. Zhou et al. [90] analyzed that the value realization of the Zhangye Danxia landform in the original ecological mode relies on government policies, government actions, scientific research institutions and researchers, local enterprises, farmers, and other forces to realize its value through developing ecological tourism. The green finance model is used to effectively reduce polluting projects and improve the investment return and financing availability of green projects [82]. Green finance provides products such as green credit, environment and climate fund, ecological trust, ecological insurance and ecological benefit bonds to realize resource and capital complementarity [81]. The normal operation of green finance requires a mature legal system, sustainable market conditions, and a sound infrastructure construction system [91]. For areas with damaged ecological environments, the mode of ecological protection and restoration and value preservation and appreciation should be adopted to restore the natural ecosystem's structure and function, enhance eco-product supply capacities, and improve eco-product value by repairing the damaged ecosystem [92]. Concerning China, some experiences in eco-product value realization have been summarized for river basin management [93], mine ecological restoration [94], and marine ecological restoration [95].

3.6.5. Eco-Industry

In the industrial age, humans have neglected the environment's importance, thus resulting in the increasing contradiction between resources, environment, and economic development. Therefore, eco-environmentally friendly industry, circular economy, and the design and optimization of eco-industrial parks have become the research focus [96,97]. Their purpose is to harmonize the relationship between the ecological environment and economic development and achieve regional sustainable development. The speed of knowledge flow and technology flow in the eco-industrial park ecosystem is fast, which drives the speed of material, energy, information, and value flows in the system, strengthening its ecological function [98]. Therefore, eco-industrial parks are an important vehicle to promote environmentally friendly industries and develop a circular economy. In eco-industrial parks, existing resources can be fully utilized to minimize waste emissions and environmental pollution by connecting clean production and eco-industrial chains [99]. In addition, the ecological carrying capacity and industrial ecological suitability also need to receive focus [100]. Industrial ecological suitability is an assessment of the suitability and limitations of industrial development and resource exploitation based on regional natural environment characteristics, resource endowments, environmental capacity, social and economic development needs, and the planned industrial structure, industrial layout, and development scale [101]. The ecological carrying capacity determines the type and spatial layout of regional industry. The ecological carrying capacity has become an important constraint on regional industry development [101]. Therefore, the ecological carrying capacity factor is considered when assessing the industrial ecological suitability, which facilitates optimizing the industrial structure.

Entering the age of ecological civilization, the traditional division of labor among the three industries cannot meet the needs of industrial development. Ye et al. [102] proposed defining waste recycling as the fourth industry, thus expressing the worth of environmental production. However, it is too incomprehensive to define ecological environmental production only as waste recycling. Subsequently, Wang et al. [103] proposed the concept of the fourth industrial product from the viewpoint of eco-products, further analyzed its formation mechanism and constituent elements, and constructed a system of evaluation indicators for developing the fourth industrial product. With a continuously improving eco-product value realization mechanism, the fourth industry of eco-products is being

formed around eco-product supply and value realization. Nonetheless, the fourth industry of eco-products is in the early stage of formation, and the theory and practice still need to be expanded. Further clarifying the boundary of the fourth industry of eco-products, standardizing the industrial classification system, strengthening the development index system, and aligning with the economic accounting system to promote the sustainable development of the fourth industry of eco-products are all recommended [104].

With the concepts of eco-industrialization and industrial ecologization being promoted, the eco-industry has been developing. Eco-products are the basis of ecological industrialization and industrial ecologization [105]. Eco-industrialization refers to the process of forming various industries through market-oriented means relying on existing natural environment resources and finally realizing the value-added process [106]. Eco-industrialization emphasizes transforming and applying ecological resources in the industrialization process. It is necessary to consider the ecological effects. The sustainable use of ecological resources can only be achieved through protection during development. Industrial ecologization refers to the process of using resource-saving and environmentally friendly new technologies to transform and upgrade various industries to achieve green production [107]. Industrial ecologization is an inevitable requirement of sustainable development and an effective integration of economic and social development and ecological protection. Therefore, eco-industrialization is mostly appropriate for areas with better ecological resources. Producing eco-products facilitates ecological industrialization, which is one of the intrinsic drivers of value realization; industrial ecological transformation promotes the improvement of ecological concepts and enhances the demand for eco-products, which is the external driving force to realize the value of eco-products [22].

4. Discussion

4.1. Differences in the Value Realization of Eco-Products and the Annual Volume of Eco-Industry Publications

The number of articles related to eco-product value realization and eco-industry is rapidly increasing (Figure 2). Therefore, discussing eco-product value realization and eco-industry is a valuable research topic. Since the emergence of eco-product value realization and eco-industry research, the number of articles has been increasing in the rapid growth phase, accounting for 88.86% of the overall number of papers. In the early stage, eco-product value realization and eco-industry research mainly focused on the concept and theory of eco-products. As the research progressed, the literature on the path, mode, and mechanism of eco-product value realization gradually increased. Local governments also began carrying out pilot projects on eco-product value realization in different regions and summarizing different value realization models. Relevant research on eco-product value realization and eco-industry is mainly in key ecological function areas, national parks, and agricultural products, and there are also some relevant studies on forest eco-product value realization. However, there are few studies on the value realization of forest eco-products in karst ecological restoration. There is a lack of research on how eco-products drive eco-industries' formation mechanisms.

4.2. Differences in the Distribution of Research Areas

The differences in natural economic conditions and social situations among regions contribute to the uneven development of eco-product value realization and eco-industry research (Figure 3). Regarding the number of publications, Asia has the largest number of publications, accounting for 94.53%, while Europe, North America, Oceania, and Africa are less distributed, and account for 4.2%, 0.73%, 0.18%, and 0.18%, respectively. Among them, China has the highest number of publications, with a total of 92.51% of publications. This may be because the concept of eco-products was presented by Chinese scholars, and international academics use the concept of ecosystem services more than eco-products. Additionally, it may be related to the use of the CNKI database. Pilot projects on ecosystem goods value realization have been carried out in various parts of China, and these pilot

projects have developed models worthy of emulation. As a result, the number of articles that describe studies of eco-product value realization and eco-industries is increasing.

4.3. Key Scientific Problems and Prospects to Be Solved at Home and Abroad

Based on the research status of eco-product value realization and eco-industry, this study summarizes the problems of eco-products shortage, unclear quantity and ownership boundary of natural resource assets, insufficient subsequent guarantee for eco-product value realization, single ecological compensation models, insignificant implementation effects, and insufficient internal driving force of eco-product to eco-industry. There are also some problems, such as the deterioration of the ecological environment caused by the unreasonable industrial structure. Among them, the remaining challenges in this field are how to clarify the number and ownership boundary of natural resource assets, and how eco-products drive the formation mechanism of eco-industry.

4.3.1. Mechanism of Improving Eco-Products' Supply Capacity

In response to the current shortage of eco-products, improving the supply capacity of eco-products is necessary [108]. Currently, research on the supply capacity of eco-products has focused on improvement paths and strategies, such as innovating supply motifs, ecological space optimization [109], certifying eco-products [110,111], and landscape planning [112,113]. However, less research has been conducted on enhancing eco-product supply capacities by optimizing ecosystem service functions [114]. By optimizing the ecosystem structure, the ecosystem's stability is enhanced, the ecosystem's integrity is ensured, the ecosystem's service function optimization is realized, and the ecosystem's quality is improved to provide more eco-products.

4.3.2. Building an Open and Shared Eco-Product Information "Cloud Platform"

Given the problems of unclear natural resource asset basis and ownership boundaries, we combine digital technology applications to build an open and shared eco-product information database. Eco-products require clear property rights before they can be transformed into manageable production factors. However, in natural public resources with characteristics of dispersion, mobility, and cross-region, such as rivers, forests, climate, and other ecosystems, there are problems such as the unclear property rights ownership of eco-products. Therefore, establishing a multisource monitoring mechanism for eco-products and a unified system of natural resource classification standards is necessary [115]. By fully utilizing the latest digital technologies such as big data, we organize and carry out a nationwide "pre-investigation" of natural resource assets. At the same time, we must also dynamically adjust and optimize the classification standards according to the actual situation in different regions, build an open and shared "cloud platform" for eco-product information, and establish an eco-product catalogue information system to facilitate the timely tracking and grasping of information on eco-product quality grades, ownership, quantity distribution, etc. [116].

4.3.3. Establishing an Evaluation System for Realizing the Value of Eco-Products

Regarding the insufficient follow-up guarantee for realizing eco-product value, an assessment and evaluation system for realizing eco-product value should be constructed. Some studies have shown that why excellent eco-products become scarce is inseparable from the neglect of including ecological protection in environmental consciousness. This stems from adopting the extensive development mode in the past. Therefore, scholars and local governments should give attention to research assessing eco-product value realization to guarantee the sustainable development of eco-product value realization. The evaluation system of eco-product value realization should be constructed according to local conditions, and the accounting results of natural resource asset quality and eco-product value should be regarded as an important reference for evaluation. For the key ecological functional areas mainly providing eco-products, we should focus on assessing the eco-product supply capacity, environmental quality improvement, ecological protection effectiveness, and other

indicators [117]. Most assessments of social and economic development only considered gross domestic product (GDP) unilaterally. In the future, it will be necessary to consider applying gross ecological product (GEP) indicators when evaluating relevant local government performance. The assessment results of GDP and GEP will be implemented in property rights transactions, ecological compensation, and ecological and environmental damage compensation.

4.3.4. Improving the Ecological Compensation Mechanism

In response to the problems of single ecological compensation models and insignificant implementation effects, a corresponding benefit evaluation and monitoring system should be established, and a corresponding response should be proposed to improve the ecological compensation mechanism. Most studies on ecological compensation standards and ecological compensation pathways are more extensive, but there are relatively few studies on ecological compensation that affect monitoring and environmental dynamics after ecological compensation implementation. Dynamic monitoring using GIS and RS technologies can meet the objectives and needs for large-scale, efficient, and accurate monitoring and understanding of ecological environment conditions and change factors such as soil cover, vegetation conditions, and soil erosion across study areas. In addition, ecological protection costs together with regional ecological and environmental management investment and effectiveness are included when evaluating ecological compensation benefits, and long-term dynamic observation is used as the basis for ecological compensation standard development to improve the ecological compensation standard system [118].

4.3.5. Driving Mechanism of Eco-Products in Eco-Industry

Eco-products contain strong ecological and economic value. With the development of the social economy, the social demand for eco-products has been gradually increasing. Eco-products are the basis for forming eco-industries, but there is still a lack of an internal driving force for forming them. In the future, research must focus on integrating eco-products, socializing the re-operation of eco-products, cultivating eco-product market agents, and constructing eco-product market circulation systems. By investigating the spatial distribution, quantity, and size of eco-products and being guided by the product size and spatial concentration, product distribution and distribution centers are developed to provide a basic platform for market transactions. We will strengthen the processing of material products and brand building and promote integrating primary, secondary, and tertiary industries. According to the spatial distribution in the main body supply, the supply capacity, cost revenue, and market supply main body need to be cultivated. According to the spatial distribution, consumption potential, demand size, and willingness to pay for consumer agents, the market consumer agents are cultivated. Integrating product distribution, market circulation, trading platform construction, and product trading paths will build the eco-industry market circulation system to realize eco-product values.

4.3.6. Research on the Coupled Development of Ecological Protection and Restoration and Eco-Industry

The problem of unreasonable industrial structures deteriorating the ecological environment has affected regional sustainable development. It is necessary to accelerate the research on the coupled development of ecological protection and restoration and eco-industry. The organic coupling and coordination of industry and ecological restoration is conducive to the coordinated development of economic, social, and ecological benefits. Combining ecological protection and eco-industry in ecological restoration areas has attracted increasing academic attention. Eco-industry is the most suitable industry to realize the coordinated development of ecological protection and economy in ecological restoration areas. By establishing the coupling mechanism of the ecosystem carrying capacity and eco-industry in ecological restoration zones, we clarify their relationship and explore the optimization of the industrial layout. To clarify the stability between inputting ecological

protection and restoration and developing eco-industry, a coupled coordination model of ecological protection and restoration and eco-industry is constructed based on the theory of the coupling coordination degree, and the coordination degree between them is clarified. However, the coupling mechanism between ecological restoration and industrial models is still in the exploratory phase, and there are few studies on integrating key technologies and processes in coupled systems. In the future, the process characteristics, coupling purpose, and overall benefits of coupled systems should be fully considered, and the degree of coupling coordination should be used as a theoretical approach to evaluate the coordination between the two systems.

4.4. Enlightenment toward Forest Ecosystem Services in Karst Ecological Restoration

Under the background of large-scale karst forest ecological restoration, the area of rocky desertification has gradually decreased in China [119]. The ecological restoration of karst forests involves not only restoring forest vegetation, but also restoring and reconstructing the structure and function of the whole ecosystem, the above- and belowground biodiversity, the ecological value and economic value, etc. [20]. The karst rocky desert ecosystem can be improved by artificial afforestation and closed mountain afforestation (Figure 6). The results show that forest ecosystem services are beneficial to controlling degraded land and play an essential role in local agricultural and forestry production, improving people's living conditions, and maintaining the ecological environment. Controlling the desertification of karst involves acknowledging that it is prone to recurrence. How to promote the sustainability of forest ecosystem services in karst ecological restoration is worth considering.

(**a**) (**b**)

Figure 6. Measures to control rocky desertification: (**a**) artificial afforestation; (**b**) closed mountain afforestation.

4.4.1. Increasing Supply Capacity

Southwest China's karst area is the country's largest contiguous poverty-stricken area. In recent years, in the rocky desertification control process, poverty alleviation and economic improvement, the development of characteristic industries, and the large-scale planting of economic forests and fruit forests, fast-growing timber forests, and other artificial forests, have all occurred in the karst areas [119]. The area of plantation forests significantly accelerated the increase in vegetation coverage and biomass in karst areas and increased the regional wood stock [120]. However, plantation tree species are relatively monophyletic, have low biodiversity conservation functions, and have increased the incidence of pests and diseases. It is also limited by the shallow soil layers, insufficient total soil, and lack of mineral nutrients in the karst region [120]. These factors also lead to the poor stability of ecologically restored forest ecosystems. Karst ecological restoration cannot just blindly pursue the "greening" of vegetation coverage, but must turn to improving the quality of karst ecological restoration forest ecosystem services and regional development. Forest species allocation involves optimizing the forest ecosystem structure, enhancing the forest ecosystem structure's stability, maintaining the forest ecosystem integrity, realizing

the forest ecosystem service function optimization, promoting the overall improvement of karst forest ecosystem quality, and enhancing the supply capacity of forest eco-products.

4.4.2. Improving Mechanism Compensation for Forest Ecological Services

Ecological compensation has been used to solve environmental problems and promote the sustainable provision of ecosystem services [121,122]. A reasonable forest ecological compensation scheme is conducive to protecting forest resources and sustainable ecological development. According to the ecological environment problem in karst areas and the need for a national security ecological barrier, the principle of "who protects, who benefits, who develops, who protects" should be highlighted in the artificial forest ecosystem and the closed forest ecosystem formed in the rocky desertification control process. In the future, long-term dynamic observations of forest ecosystem service value and ecological protection input for karst ecological restoration should be used as the basis for formulating ecological compensation standards and constructing long-term ecological compensation plans. To ensure the effective functioning of the ecological compensation program, it is necessary for the ecological compensation authority to track the whole compensation process and manage it. In addition, ecological compensation benefit assessment should be carried out.

4.4.3. Synergistic Development

Ecosystem services lay the foundation for eco-industries, which can consolidate and enhance the quality of ecosystem services [123]. Therefore, we should focus on the coordinated development of forest ecosystem services and forest ecological industries in karst regions. A karst ecology–restoration forest ecosystem service aims to provide high-quality materials and service products for the survival and development of local rural residents without compromising the ecosystem's stability and integrity. The forest eco-industry must promote local economic development under the premise of realizing the protection and sustainable utilization of forest resources. The former aims to promote ecological priority, through green and high-quality industrial development, while the latter aims to consolidate the results of economic development and focus on the ecosystem's stability and integrity. Different from other forest eco-industry development areas in the world, the previously fragile ecosystem patterns and functions are further degraded due to the karst's fragility and unreasonable human activities, with the spread of rocky desertification and other ecological problems being exacerbated. Therefore, it is necessary to assess the ecological and economic benefits of forest industrial structures in the karst regions. The forest industry structure can then be optimized to improve the service function of the ecological restoration forest ecosystem. Finally, with the actual situation of karst ecological restoration and its own advantages, we will actively explore ways to extend the forestry industry chain and promote developing the characteristic forest industry through cultivating and developing the characteristic forest products under the premise of ecological security (Figure 7).

(**a**) (**b**)

Figure 7. Rocky desertification control derivative industry in Guizhou: (**a**) prickly pear-planting industries; (**b**) under-forest chicken-raising (source: https://sck.gznu.edu.cn/erji.jsp?urltype=tree.TreeTempUrl&wbtreeid=1773 (accessed on 23 October 2022)).

5. Conclusions

In this study, we analyzed a systematic review by statistically analyzing 548 papers retrieved from the WOS and CNKI databases and concluded the following: (1) Regarding the number of publications, there has been a rapid growth trend since 2018, and the research process has experienced budding (2000–2017) and rapid development (2018–2022) stages. (2) The research region is mainly concentrated in Asia, which accounts for 94.53%, with China having the highest number of publications, with a total of 92.51% of publications. This is followed by Europe, with 4.2%. (3) Regarding research content, eco-product value realization research is the most abundant, accounting for 49.42% of the total, followed by eco-industry, accounting for 21.82% of the total; connotation and extension, and also value accounting, accounting for 12.28% and 11.27% of the total, respectively; and eco-product supply, which was relatively low, accounting for 5.20% of the total.

The following are ideas for future scientific problems and solutions that need attention: (1) For the shortage of eco-products, the eco-product supply capacities must be improved. This can be achieved by optimizing the ecosystem's structure, enhancing the ecosystem's stability, and realizing the ecosystem's service function optimization. (2) Regarding problems such as unclear boundaries in the quantity and ownership of natural resource assets, an open and shared eco-product information database should be built in conjunction with digital technology applications, and an eco-product catalogue information system should be established to keep track of information, such as the grade of eco-product quality, ownership of rights and interests, and quantity distribution, in a timely manner. (3) Because ecological environment quality can easily be ignored, an assessment and evaluation system for ecological product value realization should be constructed. The quality of natural resource assets and eco-product value-accounting results should be regarded as important references for assessment and evaluation. Additionally, the GEP index should be included when applying the relevant performance assessment of local governments. (4) Because the eco-protection compensation for eco-products is not obvious and the ecological compensation model is singular, it is necessary to establish a corresponding benefit evaluation and supervision system, and based on the benefit evaluation results and long-term dynamic monitoring, put forward applicable countermeasures to improve the ecological compensation mechanism. (5) To address the insufficient internal driving force of eco-products in eco-industry formation, research should be conducted on integrating eco-products, cultivating the main market of eco-product supply and of eco-product consumption, and constructing the eco-product market circulation system to drive eco-industry formation. (6) Because unreasonable industrial structures affect the sustainable development of regions and are deteriorating the ecological environment, accelerating research on the coupled development of ecological protection and restoration and eco-industry is necessary. Using the coupling coordination degree theory, a coupling coordination model of ecological protection and restoration and eco-industry can be constructed.

Author Contributions: Conceptualization, B.Y.; methodology, B.Y. and H.H.; software, B.Y. and Y.Y.; validation, B.Y.; formal analysis, B.Y. and H.H.; investigation, B.Y.; resources, B.Y.; data curation, B.Y.; writing—original draft preparation, B.Y.; writing—review and editing, B.Y. and Y.Z.; visualization, B.Y.; supervision, K.X.; project administration, K.X. and Y.Z.; funding acquisition, K.X. All authors have read and agreed to the published version of the manuscript.

Funding: This research was supported by the Oversea Expertise Introduction Program for Discipline Innovation of China: Overseas Expertise Introduction Center for South China Karst Eco-environment Discipline Innovation (No. D17016), the Science and Technology Research Project of Higher Education Institutions in Hebei Province: Comparative study of model and technology for characteristic high efficiency forestry from the karst desertification control in North and South China Karst (No. QN2021412) and the project of Guizhou Geographical Society: Research on characteristic high efficiency forestry from vegetation restoration of the karst desertification control (No. 2020HX05).

Data Availability Statement: The data presented in this study are openly available in [China NationalKnowledge Infrastructure (CNKI)] at [https://www.cnki.net, accessed on 30 June 2022 and 31

December 2022], and [Web of Science (WOS)] at [https://www.webofscience.com, accessed on 30 June 2022 and 31 December 2022].

Acknowledgments: We would like to thank all the editors for their contributions to this paper and the anonymous reviewers for their thoughtful comments, which enriched the paper.

Conflicts of Interest: The authors declare no conflict of interest.

References

1. Shi, T.; Yang, S.Y.; Zhang, W.; Zhou, Q. Coupling coordination degree measurement and spatiotemporal heterogeneity between economic development and ecological environment: Empirical evidence from tropical and subtropical regions of China. *J. Clean. Prod.* **2020**, 244. [CrossRef]
2. Wang, X.H.; Wang, J.J.; Xu, K.P.; Chi, Y.Y. Improve the Ecological and Environmental Space Management and ControlSystem, Enhance the Supply Capacity of Ecological Products. *Environ. Prot.* **2021**, *49*, 40–44.
3. Holdren, J.; Ehrlich, P. Human population and the global environment. *Am. Sci.* **1974**, *62*, 282–292.
4. Costanza, R.; d'Arge, R.; Groot, R.; Farber, S.; Grasso, M.; Hannon, B.; Limburg, K.; Naeem, S.; O'Neill, R.; Paruelo, J.; et al. The value of the world's ecosystem services and natural capital. *Nature* **1997**, *387*, 253–260. [CrossRef]
5. United Nations Environmental Program. *Millennium Ecosystem Assessment Ecosystems and Human Well-Being: Synthesis*; Island Press: Washington, DC, USA, 2005.
6. Cheng, H.; Hu, W.; Zhou, X.; Dong, R.; Liu, G.; Li, Q.; Zhang, X. Fruit Tree Legume Herb Intercropping Orchard System Is an Effective Method to Promote the Sustainability of Systems in a Karst Rocky Desertification Control Area. *Forests* **2022**, *13*, 1536. [CrossRef]
7. Promila, K.K.; Sharma, P. Assessment of ecosystem service value variation over the changing patterns of land degradation and land use/land cover. *Environ. Earth Sci.* **2023**, 82. [CrossRef]
8. Hong, Z.Y.; Yang, Z. Discussion on the transformation of planting grass, planting trees and ecological products from the historical changes of the Loess Plateau. *J. Yuxi Agric. Coll.* **1985**, *1*, 70–76.
9. Ren, Y.W.; Yuan, G.B. Preliminary account on "ecological products". *Chin. J. Ecol.* **1992**, *6*, 50–52.
10. Circular of the State Council on Printing and Distributing the National Main Function Zone Planning. Available online: http://www.gov.cn/zhengce/content/2011-06/08/content_1441.htm (accessed on 8 June 2011).
11. Zhang, L.B.; Yu, H.Y.; Li, D.Q.; Jia, Z.Y.; Wu, F.C.; Liu, X. Connotation and value implementation mechanism of ecological products. *J. Agric. Mach.* **2019**, *50*, 173–183.
12. Zhang, L.B.; Yu, H.Y.; Hao, C.Z.; Wang, H. Practice model and path of ecosystem product value realization. *Environ. Sci. Res.* **2021**, *34*, 1407–1416.
13. Shen, H.; Li, N. The Connotation Interpretation and Value Realization of Ecological Products. *Reform* **2021**, *331*, 145–155.
14. Ren, J.; Qian, F.J.; Li, S.S.; Hu, C.J.; Liu, P. Gross Ecosystem Product Accounting for Henan Province. *Environ. Sci. Manag.* **2022**, *47*, 159–164.
15. Du, A.; Shen, Y.Q.; Xiao, Y.; Ouyang, Z.Y. Research on accounting of ecological products value in National Parks. *Acta Ecol. Sin.* **2023**, *43*, 208–218.
16. Huang, D.; Li, S.S.; Wei, H.J.; Feng, M.T. Research on the Value Definition and Realization Mode of Ecological Products inTerritorial Space. *Urban Dev. Stud.* **2022**, *29*, 52–58.
17. Peng, Z.Y.; Huang, J.F.; Gao, H.B.; Liu, G.Q. Realizing approach of ecological product value regarding basin as a unit: A case study ofXishui River Basin in Huanggang Administive Area. *Express Water Resour. Hydropower Inf.* **2022**, *43*, 94–99.
18. Wang, R.S.; Yang, J.X. Industrial ecology and transition to eco-industry. *World Sci.-Tech. R D.* **2000**, *5*, 24–32.
19. Long, X.W. Construction of ecological industry and the developing strategy in Bashang Plateau. Master's Thesis, Capital Normal University, Beijing, China, 2004.
20. Wen, Y.G.; Zhou, X.G.; Wang, L.; Sun, D.J.; Zhu, H.G. Theory and technology of karst forest ecological protection and restoration in china. *Guangxi Sci.* **2022**, *29*, 61–70.
21. Yu, H.; Dong, S.; Li, F. A system dynamics approach to eco-industry system effects and trends. *Pol. J. Environ. Stud.* **2018**, *28*, 1469–1482. [CrossRef]
22. Zhang, Z.Z.; Xiong, K.N.; Chang, H.H.; Zhang, W.X.; Huang, D.H. A review of eco-product value realization and ecological civilization and its enlightenment to Karst protected areas. *Int. J. Environ. Res. Public Health* **2022**, *19*, 5892. [CrossRef]
23. Yang, M.D. On the fragility of karst environment. *Yunnan Geogr. Environ. Res.* **1990**, *1*, 21–29.
24. Yuan, D.X. On the Environmental and Geologic Problems of Karst Mountains and Rocks in the South-West China. *World Sci.-Tech. R D.* **1997**, *5*, 41–43.
25. Xiong, K.N.; Chen, Q.W. Discussion on karst rocky desert evolution trend based on ecologically comprehensive treatment. *Carsologica Sin.* **2010**, *29*, 267–273.
26. Xiong, K.N.; Chi, Y.K. The problems in southern china karst ecosystem in southern of china and its countermeasures. *Ecol. Econ.* **2015**, *31*, 23–30.
27. Pohjanmies, T.; Triviño, M.; Le, T.E.; Mazziotta, A.; Snäll, T.; Mönkkönen, M. Impacts of forestry on boreal forests: An ecosystem services perspective. *Ambio* **2017**, *46*, 743–755. [CrossRef]

28. Zhang, Y. Tree-Shrub-Grass Restoration Mechanism and Characteristic High-Efficiency Forestry Model in the Karst Rocky Desertification Control. Ph.D. Thesis, Guizhou Normal University, Guiyang, China, 2020.
29. Zhang, M.Y.; Wang, K.L.; Liu, H.Y.; Zhang, C.H.; Wang, J.; Yue, Y.M.; Qi, X.K. How ecological restoration alters ecosystem services: An analysis of vegetation carbon sequestration in the karst area of northwest Guangxi, China. *Environ. Earth Sci.* **2015**, *74*, 5307–5317. [CrossRef]
30. Matzek, V. Turning delivery of ecosystem services into a deliverable of ecosystem restoration: Measuring restoration's contribution to society. *Restor. Ecol.* **2018**, *26*, 1013–1016. [CrossRef]
31. Yue, Y.M.; Liao, C.J.; Tong, X.W.; Wu, Z.B.; Fensholt, R.; Prishchepov, A.; Jepsen, M.R.; Wang, K.; Brandt, M. Large scale reforestation of farmlands on sloping hills in South China karst. *Landsc. Ecol.* **2020**, *35*, 1445–1458. [CrossRef]
32. Li, W.J.; Wang, T.M.; Wang, G.P.; Chen, X. Value evaluation on the eco-services function of Zanthoxylum planispinum-var.dingtanensi woods in Huajiang Karst Valley. *Carsologica Sin.* **2010**, *29*, 152–161.
33. Wang, X.F.; Zhang, X.R.; Feng, X.M.; Liu, S.R.; Yin, L.C.; Chen, Y.Z. Trade-offs and synergies of ecosystem services in karst area of China driven by grain-for-green Program. *Chin. Geogr. Sci.* **2020**, *30*, 101–114. [CrossRef]
34. Chen, T.T.; Huang, Q.; Wang, Q. Differentiation characteristics and driving factors of ecosystem servicesrelationships in karst mountainous area based on geographic detectormodeling: A case study of Guizhou Province. *Acta Ecol. Sin.* **2022**, *42*, 6959–6972.
35. Qin, Y.; Xiong, K.N.; Chen, Q.W.; Zhang, S.H.; Yang, S.; Li, T.L. Ecosystem Service Changes and Trade-off Synergistic Relationships in Karst Areas. *Environ. Sci. Technol.* **2021**, *44*, 228–236.
36. Chen, X.B.; Ding, W.R. Spatial-temporal Evolution and Trade-off Synergy Relationships of Ecosystem Services in Karst Area of Shilin. *Res. Soil Water Conserv.* **2023**, *30*, 285–293.
37. Deng, X.H.; Xiong, K.N.; Yu, Y.H.; Zhang, S.H.; Kong, L.W.; Zhang, Y. A Review of Ecosystem Service Trade-Offs/Synergies: Enlightenment for the Optimization of Forest Ecosystem Functions in Karst Desertification Control. *Forests* **2023**, *14*, 88. [CrossRef]
38. Lundgren. What is agroforestry? *Agrofor. Syst.* **1982**, *1*, 7–12.
39. Xiong, W.Y.; Xue, J.H. Agroforestry-an effective way for forest development. *World For. Res.* **1991**, *2*, 27–31.
40. Pedro, Z.F.S.; Renato, C.; Jerônimo, B.B.S. Can agroforestry systems enhance biodiversity and ecosystem service provision in agricultural landscapes? A meta-analysis for the Brazilian Atlantic Forest. *For. Ecol. Manag.* **2019**, *433*, 140–145.
41. Yang, Y.; Xiong, K.N.; Huang, H.Q.; Xiao, J.; Yang, B.L.; Zhang, Y. A Commented Review of Eco-Product Value Realization and Ecological Industry and Its Enlightenment for Agroforestry Ecosystem Services in the Karst Ecological Restoration. *Forests* **2023**, *14*, 448. [CrossRef]
42. Zeng, X.G. The value realization mechanism of ecological products. *Environ. Sustain. Dev.* **2020**, *45*, 89–93.
43. Zeng, X.G.; Yu, H.Y.; Xie, F. Concept, classification and market supply mechanism of ecological products. *China Popul. Resour. Environ.* **2014**, *24*, 12–17.
44. Pan, J.H. On the attributes of ecological products and their value traceability. *Environ. Sustain. Dev.* **2020**, *45*, 72–74.
45. Liao, M.L.; Pan, J.H.; Sun, B.W. Analysis of the connotation and realization path of ecological products. *Reform Econ. Syst.* **2021**, *1*, 12–18.
46. Zhan, L.L.; Yang, J.Z. An economics analysis on the value and its implementation paths of eco-products. *Econ. Probl.* **2022**, 19–26.
47. Yue, D.P.; Yu, Q.; Zhang, Q.B.; Su, K.; Huang, Y.; Ma, H. Progress in research on regional ecological security pattern optimization. *Trans. Chin. Soc. Agric. Mach.* **2017**, *48*, 1–10.
48. Yu, G.R.; Yang, M. Ecological economics foundation research on ecological values, ecological asset management, and value realization: Scientific concepts, basic theories, and realization paths. *Chin. J. Appl. Ecol.* **2022**, *33*, 1153–1165.
49. Qin, G.W.; Dong, W.; Song, M.L. Theoretical implication, mechanism and path selection of ecological product value realization. *Chin. J. Environ. Manag.* **2022**, *14*, 70–75.
50. Zhao, Y.J. On the underlying infrastructure of the spatial planning. *City Plan Rev.* **2019**, *43*, 17–26.
51. Lin, L. Research on ecological products supplier in china: Based on polycentric governance. *Ecol. Econ.* **2016**, *32*, 96–99.
52. Zhang, H.R.; Liu, X. Game analysis of forestry ecological products supply in the state-owned forest regions of China. *World For. Res.* **2021**, *34*, 117–122.
53. Hong, C.C.; Zhang, Y.J.; Liu, M.C. A study on the construction of cooperative mechanism about ecological products supply in Beijing-Tianjin-Hebei area. *J. Hebei Univ. Econ. Trade* **2017**, *38*, 95–100.
54. Wang, X.H.; Zhu, Z.X.; Mou, X.J.; Zhang, X. Regional landscape planning: An important way to enhance the supply capacity of high quality ecological products. *Environ. Prot.* **2021**, *49*, 54–57.
55. Gretchen, C.D.; Ouyang, Z.Y.; Zheng, H.; Li, S.Z.; Wang, Y.K.; Marcus, F.; Peter, K.; Stephen, P.; Mary, R. Securing natural capital and human well-Being: Innovation and impact in China. *Acta Ecol. Sin.* **2013**, *33*, 669–685. [CrossRef]
56. Polasky, S.; Kling, C.L.; Levin, S.A.; Carpenter, S.R.; Daily, G.C.; Ehrlich, P.R.; Heal, G.M.; Lubchenco, J. Role of economics in analyzing the environment and sustainable development. *Proc. Natl. Acad. Sci. USA* **2019**, *116*, 5233–5238. [CrossRef] [PubMed]
57. Xie, G.D.; Lu, C.X.; Leng, Y.F.; Zheng, D.; Li, S.C. Ecological assets valuation of the Tibetan plateau. *J. Nat. Resour.* **2003**, *2*, 189–196.
58. Xie, G.D.; Zhang, C.X.; Zhang, L.M.; Chen, W.H.; Li, S.M. Improvement of the evaluation method for ecosystem service value based on per unit area. *J. Nat. Resour.* **2015**, *30*, 1243–1254.
59. Xie, G.D.; Zhang, C.A.; Zhen, L.; Zhang, L.M. Dynamic changes in the value of China's ecosystem services. *Ecosyst. Serv.* **2017**, *26*, 146–154. [CrossRef]

60. Wang, Y.; Shataer, R.; Zhang, Z.; Zhen, H.; Xia, T. Evaluation and analysis of influencing factors of ecosystem service value change in Xinjiang under different land use types. *Water* **2022**, *14*, 1424. [CrossRef]
61. Ouyang, Z.Y.; Zhu, C.Q.; Yang, G.B.; Xu, W.H.; Zheng, H.; Zhang, Y.; Xiao, Y. Gross ecosystem product: Concept, accounting framework and case study. *Acta Ecol. Sin.* **2013**, *33*, 6747–6761. [CrossRef]
62. Yan, S.G.; Zhang, H.; Li, H.D.; Tang, H.H. Ecosystem service values of the entire land area and ecological redlines in Jiangsu Province. *Acta Ecol. Sin.* **2017**, *37*, 4511–4518.
63. Shao, W.D.; Chen, M.; Liu, H.R. Comparison of functional value method and equivalent factor method in ecological value accounting. *Agric. Technol.* **2021**, *41*, 105–107.
64. Mou, X.J.; Wang, X.H.; Zhang, X.; Rao, S.; Zhu, Z.X. Accounting and mapping of gross ecosystem product in Yanqing District, Beijing. *Res. Soil Water Conserv.* **2020**, *27*, 265–282.
65. Liu, G.Y.; Yang, Z.F.; Chen, B.; Zhang, J.R.; Liu, X.Y.; Zhang, Y.; Su, M.R.; Ulgiati, S. Scenarios for sewage sludge reduction and reuse in clinker production towards regional eco-industrial development: A comparative emergy-based assessment. *J. Clean. Prod.* **2015**, *103*, 371–383. [CrossRef]
66. Li, L.; Wang, X.Y.; Luo, L.; Ji, X.Y.; Zhao, Y.; Zhao, Y.C.; Nabil, B.C.H. A systematic review on the methods of ecosystem services value assessment. *Chin. J. Ecol.* **2018**, *37*, 1233–1245.
67. Liu, G.Y.; Yang, Z.F. *Theory and Practice of Emergy Analysis–Ecological Economic Accounting and Urban Green Management*; Science Press: Beijing, China, 2018; pp. 272–284.
68. Yang, Q.; Liu, G.Y.; Giannetti, B.F.; Agostinho, F.; Almeida, C.V.B.; Casazza, M. Emergy-based ecosystem services valuation and classification management applied to China's grasslands. *Ecosyst. Serv.* **2020**, *42*, 101073. [CrossRef]
69. Liu, G.Y.; He, P.; Wang Y., Y. Agro-ecological products and its value realization pathway. *Chin. J. Appl. Ecol.* **2021**, *32*, 737–749.
70. Mitsch, W.J.; Gosselink, J.G. The value of wetlands: Importance of scale and landscape setting. *Ecol. Econ.* **2000**, *35*, 25–33. [CrossRef]
71. Mondal, B.; Dolui, G.; Pramanik, M.; Maity, S.; Biswas, S.S.; Pal, R. Urban expansion and wetland shrinkage estimation using a GIS-based model in the East Kolkata wetland. *Ecol. Indic.* **2017**, *83*, 62–73. [CrossRef]
72. Shi, F.; Weaver, D.; Zhao, Y.; Huang, M.; Tang, C.; Liu, Y. Toward an ecological civilization: Mass comprehensive ecotourism indications among domestic visitors to a Chinese wetland protected area. *Tour. Manag.* **2019**, *70*, 59–68. [CrossRef]
73. Wu, J.; Plantinga, A.J. The influence of public open space on urban spatial structure. *J. Environ. Econ. Manag.* **2003**, *46*, 288–309. [CrossRef]
74. Brown, G.; Schebella, M.F.; Weber, D. Using participatory GIS to measure physical activity and urban park benefits. *Landsc. Urban Plan.* **2014**, *121*, 34–44. [CrossRef]
75. Xiao, J.H.; Shi, G.Q.; Mao, C.M.; Xing, Z.X. Preliminary study on effects of hydraulic engineering on river ecosystem services. *J. Econ. Water Resour.* **2008**, *6*, 29–33.
76. Cheng, X.; Damme, S.V.; Li, L.Y.; Uyttenhove, P. Evaluation of cultural ecosystem services: A review of methods. *Ecosyst. Serv.* **2019**, *37*. [CrossRef]
77. Kim, H.N.; Boxall, P.C.; Adamowicz, W.L. The demonstration and capture of the value of an ecosystem service: A quasi-experimental hedonic property analysis. *Am. J. Agric. Econ.* **2016**, 37.
78. Cao, Y.; Swallow, B.; Qiu, F. Identifying the effects of a land-use policy on willingness to pay for open space using an endogenous switching regression model. *Land Use Policy* **2021**, *102*, 105183. [CrossRef]
79. Zhang, X.Y. A review of research on property rights transactions of ecological resources assets. *Mod. Econ. Inf.* **2019**, *6*, 1–6.
80. Wang, J.F.; Hou, C.B. Study on implementation framework and compensation pattern of basin ecological compensation mechanism in China: From the perspective of compensation funds source. *Chin. J. Popul. Resour. Environ.* **2013**, *23*, 23–29.
81. Ye, Y.H.; Lin, S.Y.; He, Y.L.; Wang, D.D.; Chen, X.Y.; Ni, G.Y. Restoration framework of coastal ecosystems in the Guangdong-Hong Kong-Macao Greater Bay Area. *Acta Ecol. Sin.* **2021**, *41*, 9186–9195.
82. Zhang, C.H. Green finance—A new entry point for regional financial cooperation. *Int. Financ.* **2016**, *1*, 13–15.
83. Peng, S.L.; Wu, K.K. Improving the ability of ecosystems to recover quickly: Restoring cities, villages and wilderness—A review of the 6th International Congress of Restoration Ecology (SER 2015). *Acta Ecol. Sin.* **2015**, *35*, 5570–5572.
84. Li, W.M.; Li, B.K. The exploration and practice on achieving the ecologic product values by expanding the ecologic function of Dipiao System in Chongqing. *J. Chongqing Univ. Technol. (Soc. Sci.)* **2020**, *34*, 1–5.
85. Huang, Y.; Wen, T.J.; Fan, S.S.; Luo, J.L. Economics of scale, multi-incentives and realization of ecological product value:Summary of experience of forest eco-bank in Nanping, Fujian. *Issues For. Econ.* **2020**, *40*, 499–509.
86. Zheng, H.X. Eco-compensation mechanism and mode for the river valley area. *J. Yunnan Norm. Univ. (Humanit. Soc. Sci. Ed.)* **2010**, *42*, 54–60.
87. Pan, D.; Yu, Y. Synergy between ecological product value realization and rural revitalization in the perspective of rural multifunctionality. *Environ. Prot.* **2022**, *50*, 12–17.
88. Wu, H.W.; Jia, W.H.; Xie, J. Practice and Enlightenment of Payments for Ecosystem Services in Costa Rica. *Environ. Prot.* **2022**, *50*, 75–80.
89. Shi, M.J.; Chen, L.N.; Lin, S.J. "Two mountains bank" and ecological industrialization. *J. Environ. Econ.* **2022**, *7*, 120–126.
90. Zhou, Y.H.; Zhang, M.J. Value realization of ecological products based on tourism services of Zhangye Danxia landform in Gansu Province. *Friends Account.* **2021**, *20*, 153–159.

91. Lan, H. Improving the mechanism for financial support to achieve carbon neutrality. *China Financ.* **2021**, *6*, 75–77.
92. Liu, T.; He, L.D.; Zhao, H.Y.; Zhang, W.L.; Cao, X.M. Discussion on the generalization path of regional ecological product value realization. *Ecol. Environ.* **2022**, *31*, 1059–1070.
93. Ji, F.X. Exploration of "quasi-market" governance of river basins and realization of ecological product value. *Gansu Soc. Sci.* **2022**, *5*, 206–216.
94. Gao, Y.N.; Wang, S.X.; Yang, C.Y.; Sun, Q.Y.; Liu, X.; Feng, C.Y. The main models and paths for realizing the value of ecological products based on mine ecosystem restoration. *Res. Environ. Sci.* **2022**, *35*, 1–10.
95. Xu, S.S.; Zhao, D.L.; Xie, J.Q.; Zhang, B.X. Enlightenment of ecological bank' on marine ecological restoration and value realization: Conception of establishing mangrove ecological bank. *Ocean Dev. Manag.* **2021**, *38*, 67–73.
96. Pan, M.; Sikorski, J.; Akroyd, J.; Mosbach, S.; Lau, R.; Kraft, M. Design technologies for eco-industrial parks: From unit operations to processes, plants and industrial networks. *Appl. Energy* **2016**, *175*, 305–323. [CrossRef]
97. Zhao, H.R.; Zhao, H.R.; Guo, S. Evaluating the comprehensive benefit of eco-industrial parks by employing multi-criteria decision making approach for circular economy. *J. Clean. Prod.* **2017**, *142*, 2262–2276. [CrossRef]
98. Wu, S.Y.; Wu, L.H. Research status and prospect of eco-industrial park theory. *Jianghai J.* **2005**, *3*, 225–229.
99. Zou, X.X.; Chen, H.X.; Fan, Y.L. Review on the carrier of domestic circular economy. *Recycl. Resour. Circ. Econ.* **2015**, *8*, 6–11.
100. Zhao, Q.; Huang, H.; Zhu, Y.; Cao, M.; Zhao, L.; Hong, X.; Chu, J. Analysing ecological carrying capacity of bivalve aquaculture within the Yellow River Estuary eco-region through mass-balance modelling. *Aquac. Environ. Interact.* **2022**, *14*, 147–161. [CrossRef]
101. Mou, X.J.; Rao, S.; Zhang, X.; Wang, X.H.; Jin, J. Preliminary study on the framework of early warning technology of the industrial development impact on ecological security. *Ecol. Econ.* **2022**, *38*, 186–192.
102. Ye, W.H.; Han, L. Study on the quaternary industry and the fostering of waste recycling industry. *Chin. J. Popul. Resour. Environ.* **2000**, *2*, 25–28.
103. Wang, J.N.; Wang, Z.K.; Liu, G.H.; Ma, G.X.; Wang, X.H.; Zhao, Y.H.; Cheng, L.; Wen, Y.H.; Yu, F.; Yang, W. A framework research of theory and its practice of the fourth industry of ecological products. *Chin. J. Environ. Manag.* **2021**, *13*, 5–13.
104. Wang, J.N.; Ma, G.X.; Wang, Z.K.; Wang, X.H.; Yu, F.; Liu, G.H.; Zhao, Y.H.; Yang, W.; Shi, M.J.; Deng, J.S.; et al. Development and application of indicator system about the quaternary industry of ecological products in China. *Chin. J. Popul. Resour. Environ.* **2021**, *31*, 1–8.
105. Li, M.R.; Zhang, H.R. Study continue to promote rural revitalization based on the concept of ecological industrialization and industrial ecologicalization. *Chin. J. Agric. Resour. Reg. Plan.* **2022**, *43*, 31–37.
106. Yu, H.Y.; Zhang, L.B.; Li, D.Q.; Yang, C.Y.; Gao, Y.N.; Song, T.; Wu, F.C. Domestic and foreign practical experience and enlightenment of ecological product value realization. *Environ. Sci. Res.* **2020**, *33*, 685–690.
107. Zhang, W.L. Research on the Coupled Development of Urbanization and Industrial Ecologicalization. Ph.D. Thesis, Jinan University, Guangzhou, China, 2009.
108. Yin, W.L. Improve the supply capacity of ecological products. *Outlook Wkly.* **2007**, *11*, 104.
109. Yan, S.Y.; Tang, J. Optimization of green space planning to improve ecosystem services efficiency: The case of Chongqing urban areas. *Int. J. Environ. Res. Public Health* **2021**, *18*, 8441. [CrossRef] [PubMed]
110. Zhao, J.; Gerasimova, K.; Peng, Y.; Sheng, J. Information asymmetry, third party certification and the integration of organic food value chain in China. *China Agric. Econ. Rev.* **2019**, *12*, 20–38. [CrossRef]
111. Batwara, A.; Sharma, V.; Makkar, M.; Giallanza, A. An empirical investigation of green product design and developmentstrategies for eco-industries using Kano model and fuzzy AHP. *Sustainability* **2022**, *14*, 8735. [CrossRef]
112. Ângelo, S.; Paula, R.A.; Cláudia, C.S.; Pedro, N.J.; João, H.; Joaquim, A.; Cristina, M.P.; João C, A. Trade-offs and synergies between provisioning and regulating ecosystem services in a mountain area in Portugal affected by landscape change. *Mt. Res. Dev.* **2016**, *36*, 452–464.
113. Xie, H.L.; Zhang, Y.W.; Choi, Y.; Li, F.Q. A scientometrics review on land ecosystem service research. *Sustainability* **2020**, *12*, 2959. [CrossRef]
114. Jiang, S.L.; Xiong, K.N.; Xiao, J. Structure and Stability of Agroforestry Ecosystems: Insights into the Improvement of Service Supply Capacity of Agroforestry Ecosystems under the Karst Rocky Desertification Control. *Forests* **2022**, *13*, 878. [CrossRef]
115. Dobre, A.C.; Pascu, I.S.; Leca, S.; Garcia-Duro, J.; Dobrota, C.E.; Tudoran, G.M.; Badea, O. Applications of TLS and ALS in evaluating forest ecosystem services: A southern carpathians case study. *Forests* **2021**, *12*, 1269. [CrossRef]
116. Sun, B.W. The bottleneck restriction and strategies of establishing and improving the value realization mechanism of ecological products. *Reform* **2022**, *5*, 34–51.
117. Zheng, Q.W.; Li, S.Y. Establishing assessment mechanism to promote efficient transformation of ecological product value. *China Econ. Trade Her.* **2021**, *11*, 46–48.
118. Peng, W.Y.; Wu, X.J. The supply capacity improvement and value realization path of ecological products in Beijing-Tianjin-Hebei. *China Bus. Mark.* **2021**, *35*, 49–60.
119. Wang, K.L.; Yue, Y.M.; Chen, H.S.; Wu, X.B.; Xiao, J.; Qi, X.K.; Zhang, W.; Du, H. The comprehensive treatment of karst rocky desertification and its regional restoration effects. *Acta Ecol. Sin.* **2019**, *39*, 7432–7440.
120. Zhang, X.B.; Wang, K.L. Ponderation on the shortage of mineral nutrients in the soil-vegetation ecosystem in carbonate rock-distributed mountain regions in southwest China. *Earth Environ.* **2009**, *37*, 337–341.

121. Wünscher, T.; Engel, S.; Wunder, S. Spatial targeting of payments for environmental services: A tool for boosting conservation benefits. *Sci. Direct* **2007**, *65*, 822–833. [CrossRef]
122. Engel, S.; Pagiola, S.; Wunder, S. Designing payments for environmental services in theory and practice: An overview of the issues. *Sci. Direct* **2008**, *65*, 663–674. [CrossRef]
123. Xiong, K.N.; Xiao, J.; Zhu, D.Y. Research progress of agroforestry ecosystem services and its implications for industrial revitalization in karst regions. *Acta Ecol. Sin.* **2022**, *42*, 851–861.

forests

MDPI

Article

Seedling Survival Strategies of *Zanthoxylum planispinum* 'Dintanensis' and *Zanthoxylum amatum* 'Novemfolius', Based on Functional Traits in Karst Desertification Control

Yanghua Yu *, Yanping Song and Yitong Li

School of Karst Science, State Engineering Technology Institute for Karst Decertification Control, Guizhou Normal University, Guiyang 550001, China
* Correspondence: yuyanghua2003@163.com; Tel./Fax: +86-851-86690199

Abstract: The exploration of the functional traits of *Zanthoxylum planispinum* 'dintanensis' and *Zanthoxylum amatum* 'novemfolius' at the seedling stage may provide a scientific basis for the zoning of germplasm resources and the introduction of plant varieties. The seedlings of the above mentioned two species with an age of about 8 months were selected as the study material, and the structure, nutrients, and physiological traits of leaves and roots were determined, respectively, to reveal their survival strategies. The results demonstrated the following four key elements. (1) The leaf thickness, specific leaf area, and leaf $\delta^{15}N$ value of *Z. planispinum* 'dintanensis' were significantly higher than those of Z. *amatum* 'novemfolius' ($p < 0.05$). However, the root diameter and Ca content showed the opposite results, and the other traits were not significantly different. (2) Leaf functional traits except Ca, as well as specific root length, and root P, Ca, and physiological traits had strong dominant effects on the functional trait system. (3) Among the main functional traits, leaf K and root P preferred environmental selection, leaf C, N, and P favored stable inheritance, and specific leaf area, leaf $\delta^{15}N$, and root Ca were affected by varieties. (4) There were significant synergies (promotion) and trade-offs (inhibition) between the functional traits, and the leaves and the root system were closely correlated. It is speculated that *Z. planispinum* 'dintanensis' may have a stronger defense system. Its leaves are mainly related to growth and defense functions, and its roots are mainly related to the regulation of functions.

Keywords: structural trait; element trait; physiological trait; leaf; root; karst

Citation: Yu, Y.; Song, Y.; Li, Y. Seedling Survival Strategies of *Zanthoxylum planispinum* 'Dintanensis' and *Zanthoxylum amatum* 'Novemfolius', Based on Functional Traits in Karst Desertification Control. *Forests* **2023**, *14*, 386. https://doi.org/10.3390/f14020386

Academic Editors: Claudia Cocozza and Cate Macinnis-Ng

Received: 3 December 2022
Revised: 2 February 2023
Accepted: 13 February 2023
Published: 14 February 2023

1. Introduction

Plant functional traits are characteristic attributes regarding their morphology, structure, physiology, and biochemistry. They characterize the strategies of plants to adapt to habitats [1], determine the level of productivity [2], and affect the elasticity of ecosystems [3]. So, the functional traits of plants are the core means for researchers to learn about the internal relationship between plants and the environment. The leaf is the specific site of photosynthesis and the valve of hydraulic safety, and its functional traits may reveal resource utilization and allocation strategies during plant growth and regulation [4], and the maintenance of photosynthetic capacity [5], and there are strong hydraulic, anatomical and economical traits [6]. The root system is an important organ for plants to absorb water and nutrients, and the fine roots are the main bearers of ecological metabolic functions. The functional traits of the root system were found to be closely related to plant phylogeny and could indicate resource utilization strategies [7], and they also had an impact on the content and stability of rhizosphere carbon [8]. Therefore, the study of the two main organs of the plant, i.e., the leaf and root system, will help to deepen an understanding of the changes in the patterns of plant nutrient and water balance [9], and to clarify the ecological strategies of plants to adapt to the environment.

The seedling stage is a vulnerable stage in the life cycle of a plant, and it is very sensitive to environmental changes [10]. Seedlings showed phenotypic plasticity in the process of adapting to changes in habitat factors [11]. Thus, the seedling stage is a key parameter during the growth period to inform about plant adaptation strategy in the habitat. Thus, elucidating the survival strategy of seedlings may lay a foundation for the planning and utilization of germplasm resources. Researchers have carried out various studies on the functional traits of seedlings, and they have achieved various results. The first one is the ecological implication of indicators. Studies have shown that functional traits could reveal the growth strategies of seedlings [12], indicating their great potential for drought resistance [13], and these traits may be different from those of adult plants [14]. The second one is the environmental factors that affect the variation of functional traits. It has been reported that the functional traits of the roots of *Cunninghamia lanceolata* (Lamb.) Hook. across various geographical provinces are more stable than those of the leaves [15]. It has also been revealed that the growth, biomass distribution, and morphologies of seedlings of different plants respond differently to their light environment, and thus, plant groups were categorized according to the finding [16]. Studies have also shown that the seedling traits of the same plant group are affected by environmental factors such as altitude [17], and these variations of traits have their own biological scales of effects [18], with clearly differentiated scaling patterns. The third is the regulation and application of traits. For example, brassinosteroids and gibberellins have control effects on the traits of maize seedlings [19], and they are closely related to the induction function of endogenous hormones. By regulating the functional traits of seedling roots, a foundation can be laid for germplasm improvement and quality optimization [20]. Different root traits also affect phosphorus utilization [21], establishing a theoretical basis for the screening of target traits. However, there is no research on the functional traits of the seedlings of *Z. planispinum* 'dintanensis' and *Zanthoxylum amatum* 'novemfolius' adapting to a drought environment. This knowledge gap has been limiting theoretical research on scientific introduction and germplasm resource zoning. Additionally, it is not conducive to the promotion and application of improved varieties, nor to the formulation of nursery stock standards.

Z. planispinum 'dintanensis' is a unique native plant in the karst dry-hot valley area of Guizhou, China. It has excellent properties, i.e., it can sustain a rocky habitat, it is calcium-preferred, and it is drought-resistant. The plant is famous for its 'pure fragrance, thick hemp flavor, excellent quality'. Additionally, it has been considered as a product-yielding species listed in the protected geographical areas, and as a preferred species for ecological industrial development. It has a planting area of more than 10,000 ha in China and has become a pillar industry for regional ecological construction and economic development. *Z. amatum* 'novemfolius' is the main variety of *Z. amatum* in the Sichuan and Chongqing regions. It has a large cultivation area in Jiangjin, Chongqing, which has won the title of "Hometown of *Zanthoxylum* in China". The species has also been introduced to the dry-hot valleys of Guizhou. As of now, the ages of the plants are mostly 3–5 years, and their growth and adaptability still need to be investigated. So, studying the functional traits of seedlings of these two varieties of *Zanthoxylum* can help us to explore the growth strategies of *Z. amatum* 'novemfolius' at the seedling stage in dry-hot valley areas. This provides a theoretical basis for introducing a fine variety, ecological restoration, and the utilization of germplasm resources. However, the research in this field is currently very limited, and there are no published literature reports. Therefore, this study selected the native plant *Z. planispinum* 'dintanensis', taking the introduced species *Z. amatum* 'novemfolius' as the control, to determine the functional traits of the leaf and root systems, mainly including the structural, nutrient, and physiological traits, which mainly reflect the resource acquisition and adaptive abilities of plants. These traits are the basis for selecting better traits in the future, and they can serve for trait regulation and germplasm creation. The purpose of elucidating their functional traits and growth strategies at the seedling stage is to answer the following two scientific questions: (1) to elucidate the differences in leaf and root

functional traits between *Z. planispinum* 'dintanensis' and *Z. amatum* 'novemfolius', and to reveal survival strategies at the seedling stage; (2) to screen the dominant functional traits, explore their sensitivities and selection tendencies, and to find out their internal correlation. In view of the above two scientific questions, this study made the following scientific hypotheses: (1) The resource acquisition and survival strategies of the local species of *Z. planispinum* 'dintanensis' and the exotic species of *Z. amatum* 'novemfolius' are different; (2) The dominance, selection tendency, and interaction of different plant functional traits were different. We hope to provide theoretical support for the introduction of *Zanthoxylum*, and to realize the scientific zoning and rational utilization of germplasm resources.

2. Materials and Methods

2.1. Study Site

The study area was located in Huajiang, Guanling, Anshun. The uniqueness of the habitat is indicated as a dry-hot climate, a deep valley, and with rocky desertification. The area has a dry and hot climate, mainly a subtropical humid monsoon climate, an annual average rainfall of approximately 1100 mm, with uneven seasonal distribution, severe drought in winter with spring and summer droughts, abundant heat resources, an annual average temperature of 18.4 °C with maximum and minimum temperatures of 32.4 and 6.6 °C, respectively, an annual total accumulated temperature of 6542.9 °C, a warm and dry winter and spring, and a hot and humid summer and autumn. The annual frost-free period is about 337 days, and the monthly mean meteorological data are shown in Table 1. The valley is 530–1473 m above sea level, with a 943 m elevation. The groundwater is deeply buried in the deep valley. Rocky desertification has developed in the Beipan River Basin of the upper reaches of the Pearl River. The exposed bedrock rate is between 50% and 80%, and carbonate rock accounts for 78.45%. The soil is mainly a calcareous soil of discontinuous soil mass. The vegetation is mainly natural secondary forest and *Z. planispinum* 'dintanensis' plantations. Although there is a lot of rainfall in this area, but the combination of geological and seasonal drought, as well as the tendency of plantation xerification, make the habitat tend to be arid.

Table 1. Meteorological data statistics (2019 data) [22].

Month	Rainfall/mm	Land Surface Evaporation/mm	Available Rainfall/mm	Temperature/°C	Radiation /(W·m^{-2})	Relative Humidity /%
January	17.00	16.49	0.51	12.17	227.26	80.02
February	10.40	10.32	0.08	14.79	320.71	70.44
March	12.60	12.51	0.09	19.15	373.30	67.19
April	33.50	32.84	0.66	26.40	572.70	64.11
May	31.20	30.65	0.55	26.20	465.80	67.24
June	253.00	125.07	127.93	27.41	582.78	78.13
July	156.60	112.47	44.13	27.40	585.91	78.62
August	75.60	70.09	5.51	28.70	761.22	73.05
September	296.40	105.78	190.62	25.30	587.69	73.80
October	101.00	80.77	20.23	23.80	332.78	70.10
November	57.60	45.43	12.17	14.30	282.56	68.47
December	43.50	36.05	7.45	12.00	247.72	72.34

2.2. Plot Setting and Sample Collection

During the higher seedling growth period of 11–12 June 2022, three standard quadrats of 10 × 10 m were set up for each of *Z. planispinum* 'dintanensis' and *Z. amatum* 'novemfolius' in their bases, with similar environments (Table 2). Then, a number of 20 seedlings with heights of 30–40 cm, with no visible signs of diseases or pests to the naked eye, were randomly selected. All seedlings were sown in the nursery site during October 2021. At the seedling stage, thinning and tending measures were adopted, and the seedling growth environment was consistent without transplanting. The seeds

of *Z. planispinum* 'dintanensis' were locally harvested, while the seeds of *Z. amatum* 'novemfolius' were from Jiangjin, Chongqing; all were collected from their respective adult mother trees. Select pure varieties, healthy growth, full fruits, stable yield, no pests and diseases as the seed trees. The picked seeds are dried in the sun, shelled, and sown in time to prevent damage due to heat.

Table 2. Basic situation of the seedling plots.

Variety	Altitude /m	Longitude	Latitude	Seedling Age/Month	Seedling Height/m	Insect Feed Rate
ZP	620	105°41′30.17″ E	35°39′49.35″ N	8	0.3–0.4	Less
AP	620	105°41′30.17″ E	35°39′49.35″ N	8	0.3–0.4	More

ZP: *Zanthoxylum planispinum* 'dintanensis'; AP: *Zanthoxylum armatum* 'novemfolius'. The same below.

All of the leaves and roots of 20 seedlings in each quadrat were collected. Only the primary roots were sampled, since the secondary roots had not fully grown by that time, and they were retained mostly on the primary roots. After collection, the samples were washed with tap water, and then rinsed 3 times with deionized water. In each quadrat, with the quadrate as the scale, 10 leaves and 10 roots were selected from all of the plants. After recording the number, the thickness, area, fresh biomass, saturated (in water for 12 h) fresh biomass of the leaf, as well as the diameter, length, and fresh biomass of the root were measured immediately, to prevent the impact of water loss on the test results. Among the measurements was each first-order branch root on the taproot; since plant root development in the karst area is greatly affected by underground cracks, the total root system could not be measured in this study. Then, all samples were dried in an oven at 65 °C to constant mass, and the biomass as dry wight was determined. The leaf thickness and root diameter were measured using a vernier caliper, the leaf area was measured using Delta-T Devices (Cambridge, UK), the root length was measured using a tape measure, and the mass was weighed using an analytical balance.

2.3. Sample Processing and Testing

All of the remaining fresh samples of leaves and roots were dried following the same procedure as that described before, being thoroughly mixed with the previously dried samples, and then ground and filtered through a 0.25 mm sieve for the analyses of chemical elements and stable isotopes. Plant carbon (C), nitrogen (N), and their stable isotopes were determined using elemental analyzer-stable isotope ratio mass spectrometry (Vario ISOTOPE Cube—IsoPrime IRMS, Elemental); a stable carbon isotope is denoted as $\delta^{13}C$, and a stable nitrogen isotope is denoted as $\delta^{15}N$. The contents of phosphorus (P), potassium (K), and calcium (Ca) were determined via perchloric acid–sulfuric acid digestion–molybdenum antimony anti-colorimetric–UV spectrophotometry, a flame spectrophotometer method, and inductively coupled plasma optical emission spectroscopy (ICP-OES) methods, respectively. Then, via calculation, the following parameters were obtained: the specific leaf area was the ratio of the leaf area to the dry mass, the leaf dry matter content was the ratio of the dry weight to saturated fresh mass, the specific root length was the ratio of the root length to dry weight, and the stoichiometric ratio was the element quality ratio.

2.4. Data Analysis

All data were organized and preprocessed using Microsoft Office Excel. In detail, firstly, Shapiro–Wilk function was used to test the normal distribution of the data, and lg transformation was performed if the data did not conform to the normal distribution. Then, a one-way analysis of variance (ANOVA) and least significant difference (LSD) methods were adopted to conduct multiple comparisons to test for the significant differences between the functional traits of the two *Zanthoxylum* varieties. Secondly, principal component analysis (PCA) was performed to screen out the main traits from all

of the functional trait indicators. Then, intraspecific and interspecific sensitivity indexes were calculated, respectively. Intraspecific refers to the internal species of *Zanthoxylum planispinum* 'dintanensis' or *Zanthoxylum armatum* 'novemfolius', and interspecific refers to between the two *Zanthoxylum* species. Intraspecific is to judge the changes within a single species, while interspecific is to judge the overall changes of two *Zanthoxylum* species. The calculation method was referred to the reference [23]. The intra-species and inter-species sensitivity indicators were calculated, respectively, by dividing the difference between the respective maximum and minimum values by the minimum value of a trait. The inter-species sensitivity was calculated using the maximum and minimum values of all values of a trait. The formula is $M_i = (I_{imax} - I_{imin})/I_{imin}$, where M is the sensitivity index and I is the functional trait. Finally, Pearson correlation analysis was used to reveal the correlation characteristics between the main characters, at a very significant and a significant level of $\alpha = 0.01$ and $\alpha = 0.05$, respectively. The data in the figures and the tables are the mean ± standard deviation. Origin 2021 (version 2021, Originlab Corporation, Hampton, NY, USA) was used to make the figures.

3. Results and Analysis

3.1. Leaf Functional Traits

3.1.1. Leaf Structural Traits

The leaf thickness and specific leaf area of *Z. planispinum* 'dintanensis' were significantly higher than those of *Z. amatum* 'novemfolius' ($p < 0.05$, same as following), suggesting that *Z. planispinum* 'dintanensis' had a stronger ability to utilize and to preserve resources and to resist diseases. The leaf dry matter content of *Z. amatum* 'novemfolius' was higher, but the difference was not significant (Figure 1a).

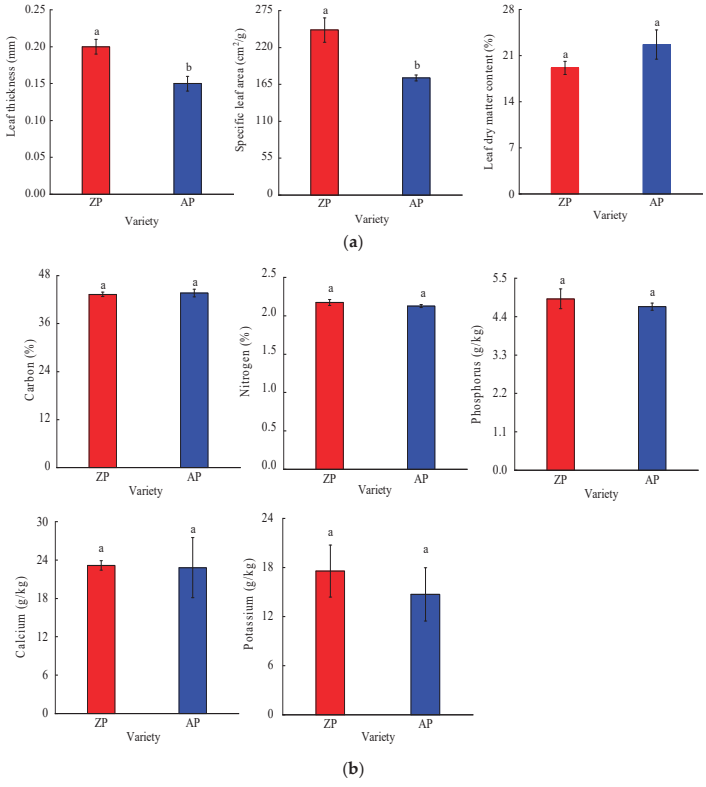

(**a**)

(**b**)

Figure 1. *Cont.*

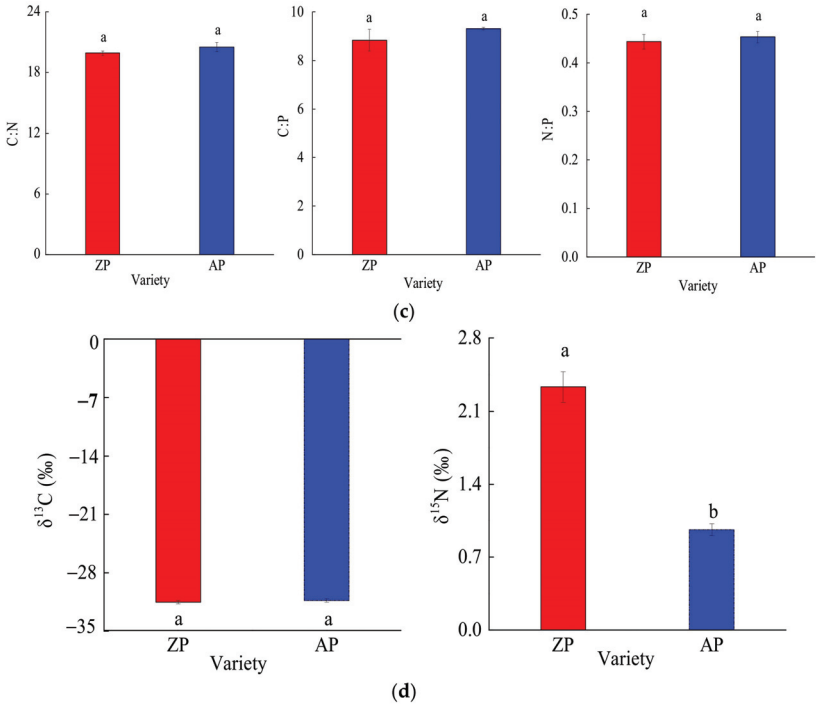

Figure 1. Leaf functional traits of *Zanthoxylum planispinum* 'dintanensis' and *Zanthoxylum armatum* 'novemfolius'. Different letters represent significant differences at the level of $p < 0.05$. (**a**) The comparison of the leaf structural traits between *Zanthoxylum planispinum* 'dintanensis' and *Zanthoxylum armatum* 'novemfolius'. (**b**) The comparison of the leaf element traits between *Zanthoxylum planispinum* 'dintanensis' and *Zanthoxylum armatum* 'novemfolius'. (**c**) The comparison of the leaf element stoichiometry between *Zanthoxylum planispinum* 'dintanensis' and *Zanthoxylum armatum* 'novemfolius'. (**d**) The comparison of the leaf physiological traits between *Zanthoxylum planispinum* 'dintanensis' and *Zanthoxylum armatum* 'novemfolius'.

3.1.2. Leaf Nutrient Traits and Stoichiometry

In general, the contents of C, N, P, K, and Ca in the leaves of *Z. amatum* 'novemfolius' were higher, but the differences were not significant. It thus indicates a similar ability of these two varieties to adjust and to store nutrients (Figure 1b). Neither were the ratios of C:N, C:P, or N:P significantly different (Figure 1c), supporting their consistency in regulating leaf nutrient balance.

3.1.3. Leaf Physiological Traits

The $\delta^{13}C$ values of *Z. planispinum* 'dintanensis' and *Z. amatum* 'novemfolius' were (-31.53 ± 0.22)‰ and (-31.33 ± 0.20)‰, respectively, with no significant differences. Additionally, both varieties had small variations, indicating no significantly different long-term water use efficiency between the two varieties. The $\delta^{15}N$ value was higher in *Z. planispinum* 'dintanensis', and 2.43 times that of *Z. amatum* 'novemfolius', suggesting that some volatile substances in *Z. planispinum* 'dintanensis' leaves were released, and that this resulted a strong fractionation effect (Figure 1d).

3.2. Root Functional Traits

3.2.1. Root Structural Traits

The root diameter of *Z. planispinum* 'dintanensis' was significantly smaller than that of *Z. amatum* 'novemfolius', and its variation was narrower as well. Additionally, the root length of *Z. planispinum* 'dintanensis' was also shorter than that of *Z. amatum* 'novemfolius', although the difference was not significant. The results suggested that *Z. planispinum* 'dintanensis' might absorb the available nutrients in niche spaces through a fine root strategy. There was no significant difference in the specific root length between the two varieties, but *Z. planispinum* 'dintanensis' exhibited less variation, indicating that the native species *Z. planispinum* 'dintanensis' may possess a more stable ability to withstand adversity (Figure 2a).

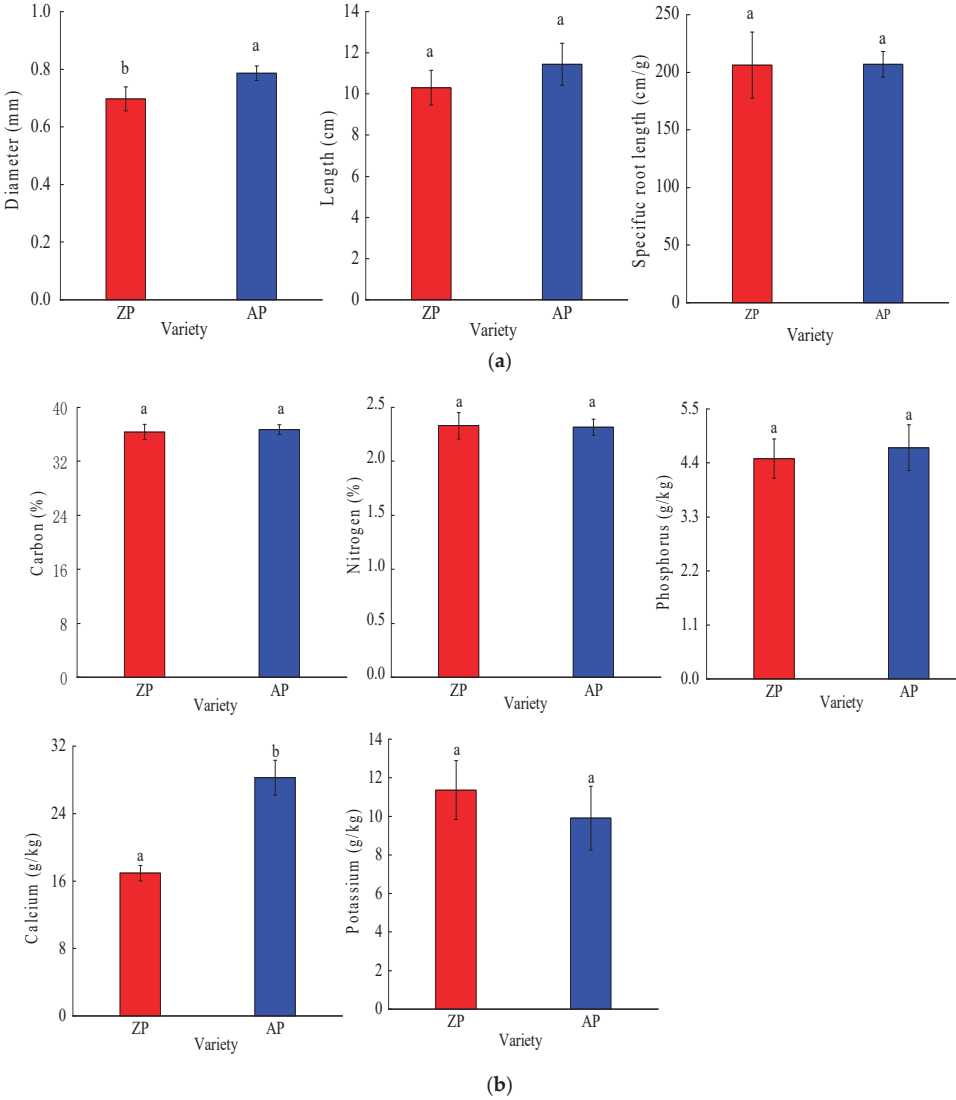

Figure 2. *Cont.*

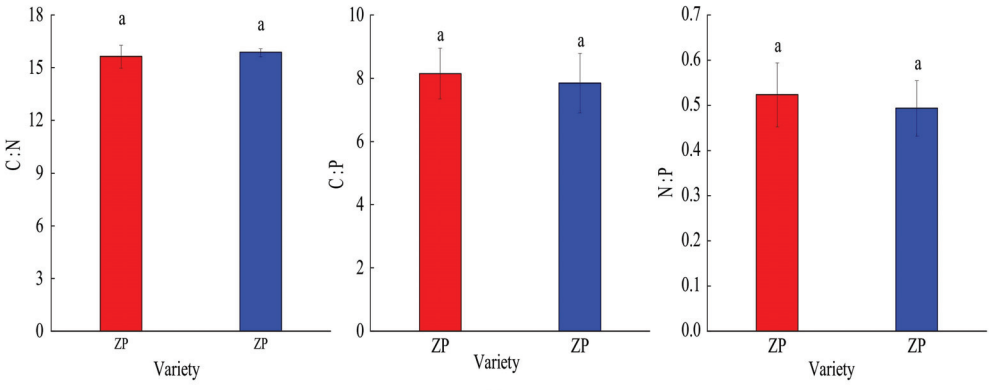

Figure 2. Root functional traits of *Zanthoxylum planispinum* 'dintanensis' and *Zanthoxylum armatum* 'novemfolius'. Different letters represent significant differences at the level of $p < 0.05$. (**a**) The comparison of the root structural traits between *Zanthoxylum planispinum* 'dintanensis' and *Zanthoxylum armatum* 'novemfolius'. (**b**) The comparison of the root element traits between *Zanthoxylum planispinum* 'dintanensis' and *Zanthoxylum armatum* 'novemfolius'. (**c**) The comparison of the root element stoichiometry between *Zanthoxylum planispinum* 'dintanensis' and *Zanthoxylum armatum* 'novemfolius'. (**d**) The comparison of the root physiological traits between *Zanthoxylum planispinum* 'dintanensis' and *Zanthoxylum armatum* 'novemfolius'.

3.2.2. Root Nutrient and Chemical Traits

There were no significant differences in root C, N, P, and their stoichiometric ratios, as well as the K content between the two varieties, indicating that *Z. planispinum* 'dintanensis' and *Z. amatum* 'novemfolius' had similar abilities to maintain a large number of elements and to regulate nutrient balance (Figure 2b,c). However, the Ca content was higher in *Z. planispinum* 'dintanensis' (Figure 2b), suggesting a possible regulatory mechanism of *Z. planispinum* 'dintanensis' for Ca uptake in a high Ca environment.

3.2.3. Root Physiological Traits

There was no significant difference in root $\delta^{13}C$ between the two varieties (Figure 2d). Combined with the results of root diameter and length, it indicated that *Z. amatum* 'novemfolius' might counteract the disadvantage of thick roots by increasing the root length to

obtain a larger specific surface area and physiological activity, thereby increasing the respiration rate. Similarly, there was no significant difference in $\delta^{15}N$, suggesting consistent volatilization patterns of the root secondary metabolites of the two varieties.

3.3. Screening for Major Functional Traits

According to the principal of an eigenvalue of >1 and a cumulative contribution rate of >90%, the functional traits were extracted into five principal components. Then, according to the loading cutoff of >0.80, 14 factors with a big influence were extracted. In detail, there were nine leaf functional traits, including specific leaf area. Those were leaf thickness, dry matter content, C, N, P, K, $\delta^{13}C$, and $\delta^{15}N$. Similarly, there were five root functional traits, including specific root length, P, Ca, $\delta^{13}C$, and $\delta^{15}N$. The results demonstrated that leaf functional traits play a dominant role, especially the leaf structural traits and physiological traits (Table 3).

Table 3. Principal component analysis of plant functional traits.

Factor	Principal Component (PC)				
	PC 1	PC 2	PC 3	PC 4	PC 5
Specific leaf area	−0.963	−0.018	−0.214	0.058	0.154
Leaf $\delta^{15}N$	−0.923	0.320	−0.077	−0.057	0.189
Leaf dry matter content	0.911	0.054	−0.016	0.302	0.274
Leaf thickness	−0.852	0.483	−0.200	0.007	0.021
Root diameter	0.766	−0.472	0.034	−0.430	0.057
Root length	0.694	0.042	0.414	0.376	0.452
Specific root length	0.250	0.965	0.039	0.025	−0.061
Root $\delta^{15}N$	0.151	−0.891	−0.388	−0.176	−0.048
Leaf K content	−0.288	0.867	−0.311	0.086	−0.248
Leaf N content	−0.463	0.860	−0.108	0.159	0.095
Leaf P content	−0.430	0.838	0.221	−0.181	−0.174
Root P content	0.243	0.182	0.941	−0.148	0.026
Leaf $\delta^{13}C$	0.364	−0.191	0.896	0.207	−0.118
Root Ca	0.398	−0.211	0.874	0.029	−0.178
Root K	−0.539	0.221	0.797	0.111	0.114
Root K	0.008	−0.304	−0.777	−0.342	0.432
Root C	0.431	0.391	−0.571	−0.507	0.278
Root $\delta^{13}C$	0.200	0.118	0.166	0.955	−0.085
Leaf C	0.141	0.307	0.188	0.194	−0.902
Leaf Ca	0.221	0.340	−0.506	0.477	0.594
Eigenvalue	5.909	5.086	4.910	2.149	1.946
Cumulative contribution rate/%	29.546	54.974	79.525	90.272	100

3.4. Sensitivity to Changes in Major Functional Traits

The sensitivity index can represent the sensitivity or dullness of different functional traits to a variable response. A high sensitivity means a low anti-interference ability. Among the 14 main functional traits, high intraspecific and interspecific sensitivity were leaf K and root P, indicating that they were more prone to environmental selection. The intraspecific and interspecific sensitivities of leaf C, N, and P all had small variations, suggesting their stable heritabilities and lagged responses to habitat changes. The intraspecific and interspecific sensitivities of leaf $\delta^{15}N$, specific leaf area, and root Ca had big variations, indicating that they were heavily affected by varieties (Table 4).

Table 4. Sensitivity analysis of changes in main functional traits.

No.	Functional Traits	ZP	AP	Interspecific
1	Leaf thickness	0.11	0.14	0.50
2	Specific leaf area	0.15	0.05	0.56
3	Leaf dry matter content	0.11	0.21	0.33
4	Leaf C content	0.03	0.04	0.04
5	Leaf N content	0.03	0.02	0.04
6	Leaf P content	0.12	0.05	0.13
7	Leaf K content	0.44	0.53	0.70
8	Leaf $\delta^{13}C$	0.01	0.01	0.01
9	Leaf $\delta^{15}N$	0.13	0.12	1.78
10	Specific root length	0.32	0.11	0.32
11	Root P	0.19	0.21	0.25
12	Root Ca	0.08	0.11	0.82
13	Root $\delta^{13}C$	0.02	0.01	0.02
14	Root $\delta^{15}N$	0.50	0.02	0.50

3.5. Correlations between Major Functional Traits

According to Table 5, there were highly significant positive correlations between leaf $\delta^{15}N$ with leaf thickness and specific leaf area, and between leaf $\delta^{13}C$ with root Ca. There were significant positive correlations of leaf N with leaf thickness, leaf P, and leaf K; of specific leaf area with leaf thickness; and of root P with leaf $\delta^{13}C$ and root Ca. In contrast, root $\delta^{15}N$ was significantly and negatively correlated with leaf N, and with P and specific root length.

Table 5. Correlation analysis of main functional traits.

Index	Leaf Thickness	Specific Leaf Area	Leaf N	Leaf P	Leaf $\delta^{13}C$	Specific Root Length	Root P
Specific leaf area	0.857 *	1					
Leaf dry matter content	−0.739	−0.850 *					
Leaf N	0.835 *	−0.332	1				
Leaf P	0.722	0.459	0.851 *	1			
Leaf K	0.721	0.335	0.903 *	0.809			
leaf $\delta^{13}C$	−0.534	0.285	−0.322	−0.052	1		
Leaf $\delta^{15}N$	0.961 **	0.932 **	0.720	0.626	−0.469		
Specific root length	0.244	−0.278	0.708	0.716	0.051	1	
Root P	−0.307	−0.426	−0.079	0.278	0.881 *	0.268	1
Root Ca	−0.619	−0.596	−0.472	−0.129	0.974 **	−0.058	0.872 *
Root $\delta^{15}N$	−0.484	−0.044	−0.827 *	−0.857 *	−0.242	−0.838 *	−0.466

There is no significant (*) or extremely significant (**) correlation between some indicators, and they are not written out.

4. Discussion

4.1. Characteristics of the Seedling Leaf Functional Traits of the Two Zanthoxylum Varieties

Traits such as leaf thickness and dry matter content affected the cellulose content and palatability of plants [24]; they also had an impact on the digestion of herbivores, and thus they are important defensive traits. According to an on-site investigation during sampling, the insect herbivory rate of *Z. amatum* 'novemfolius' leaves was ~60%, much higher than the ~30% insect herbivory rate of *Z. planispinum* 'dintanensis' leaves [25]. It is speculated that *Z. planispinum* 'dintanensis' may adopt thicker leaves and volatilize some metabolites that are harmful to herbivores, to defend against insect pests. The reason for this is that *Z. planispinum* 'dintanensis' is a native species and it has a dry-hot ecotype. It has already developed a relatively stable adaptive mechanism and a stronger defense against common diseases in the area. As a contrast, *Z. amatum* 'novemfolius' is

an exotic species and has a wet-hot ecotype. Its defense mechanism has not yet been fully developed, and the smaller leaves and higher nutritional contents make it preferred by animals. Studies have confirmed that the plant functional traits were closely correlated to the ability to resist pests and diseases [26]. In the future, the studies, including leaf texture, nutrient elements, and metabolites, to explore the plant's ability to resist pests, may provide a strong practical value.

Leaf $\delta^{13}C$ correlated positively with long-term water use efficiency [27,28]. No significant difference was seen in the seedling leaves of the two varieties, suggesting that their long-term water use efficiency was not significantly different. However, this was not consistent with the ecotype habits of these two *Zanthoxylum* varieties. The reasons might be that firstly, the precipitation in the first half of 2022 in the study area was relatively abundant, being higher than the historical period. There was less soil water deficit, and even drainage measures needed to be taken to prevent flooding in the nursery. Therefore, water was not a dominant or a limiting factor affecting the growth of seedlings. Secondly, both of the two varieties belong to the *Zanthoxylum* genus and share a common origin. During the later environmental selection process, although they evolved different traits, their water use capacity was controlled by their individual genetic characteristics and was highly stable, and this was also related to their climate-controlled ecotype. In the future, it is necessary to study the interpretation rates of genetics and habitat (soil moisture, light, etc.) on the water use capacities of different varieties of *Zanthoxylum*. In addition, there were no differences in leaf nutrient element traits between the two varieties of *Zanthoxylum*, indicating a similar nutrient retention capacity shared by them.

Plant secondary metabolites can represent environmental adaptability, including metabolic substances such as osmoregulation and antioxidants [29], have many functions such as allelopathic effects, drug components, signal transduction, and ecological adaptation [30,31], making their roles complicated in plant growth and physiology. The results of the present study suggested that more volatile substances were released from the leaves of *Z. amatum* 'novemfolius' seedlings [32], resulting in an effect in N isotope fractionation. The reason for this may be that chlorophyll was degraded, triggered a series of changes in physiological processes, and became a source of energy [33]. It may also be that *Z. planispinum* 'dintanensis' has evolved a special defense system and adaptive mechanism during its long-term adaptation to the environment [34]. In production practice, the main body of planting also employed the leaf flavor as a simple indicator for the screening of provenance. However, how leaf traits and quality traits are correlated and what is the underlying mechanism have not been elucidated yet, and these await further exploration.

4.2. Characteristics of Root Functional Traits of the Two Zanthoxylum Varieties

Plant root traits characterized the individual plant's strategy to cope with heterogeneous environments [35]. The thinner the roots, the better the ability to absorb nutrients. Previous studies have shown that root tips have evolved to be narrower and narrower from a nutrient-rich environment to a nutrient-deficient environment, in seeking to utilize nutrients efficiently [36]. It is speculated from our results that *Z. planispinum* 'dintanensis' prefers to obtain available nutrients in niche spaces through the fine root strategy and has evolved it into a stable trait during its long-term adaptation to the habitat. Compared with *Z. planispinum* 'dintanensis', *Z. amatum* 'novemfolius' might compensate for the deficiency of low surface area by increasing the root length to obtain nutrients and water. In the future, it is necessary to determine the morphology and diameter of root tip micro-domains to clarify the relationship between these root traits and nutrient utilization. Among the root structure traits, the specific root length of the two varieties did not vary significantly. Presumably, it is because the similar natural environment in the nursery caused the identical availability of soil resources, resulting in specific environmental selection pressure. Moreover, the nutrient-holding capacities of the root systems of these two varieties were also not

significantly different, and this was presumed to be related to the lower heterogeneities of nursery habitats.

Karst soil is rich in Ca due to its high inheritance of Ca in the parent rock, and accordingly, plants have developed a specific mechanism to adapt to the high Ca environment [37]. As an important biogenic element, Ca functions for both nutrient and signal transduction, and it is a key nutrient element and messenger substance [38]. As a Ca-loving plant, *Z. planispinum* 'dintanensis' possesses a specific Ca-dependent mechanism. The results of the present study demonstrated that the root Ca content of *Z. amatum* 'novemfolius' was significantly higher than that of *Z. planispinum* 'dintanensis'. The reason for this might be that *Z. planispinum* 'dintanensis' has a stronger buffer capacity to the fluctuation of Ca content, so as to maintain Ca^{2+} in a suitable range. In addition, the Ca content in the root system of *Z. planispinum* 'dintanensis' may also be limited by the type and quantity of soil Ca components, and it may also have a synergistic absorption relationship with elements such as C and N. It is speculated that *Z. planispinum* 'dintanensis' has a mechanism of affecting the distribution of other elements by regulating Ca. However, the related mechanism remains elusive. As an exotic species, the suitability of the introduction of *Z. amatum* 'novemfolius' needs to be further investigated.

Combined with the root $\delta^{13}C$ values of the two varieties, our results suggested small differences in root respiration rates and the activities between them [39]. It may be because of the weather that the root system was in water-saturated soil for a long time. Soil water content affected the root respiration intensity and rate. At the same time, the $\delta^{13}C$ values of roots were higher than those of leaves, consistent with the results reported by Diao [39]. This was related to the transport route of high $\delta^{13}C$ substances from leaves to roots [40], and it was also impacted by the fractionation of substances such as sucrose during their synthesis. In addition, from what was revealed by the $\delta^{15}N$ of the root system, the metabolites released by the root system and leaf behaved quite differently, indicating certain differences in the physiological functions of the underground and aerial parts of the two *Zanthoxylum* varieties. This may be due to the fact that the respective metabolites exert different effects, and it may also have practical value for a plant to construct its system of defense against external threats. In the future, isotopic methods may be adopted to study the functions of root respiration and vitality, and to explore the internal relationships between roots and leaves, branches, bark, soil, etc.

4.3. Trade-Offs and Synergies among Major Functional Traits

Leaf thickness and specific leaf area had highly significant positive correlations with leaf $\delta^{15}N$. Both of these two structural traits affect the ability of plants to capture light and to utilize nutrients, and to respond to element content and climate changes [41]. They also regulate heat and water [42], further affecting physiological processes in leaves such as photosynthesis and respiration, and they act on the utilization and fractionation of nitrogen. Thus, there are strong synergistic relationships between them. This indicated to a certain extent that easily observable phenotypic traits such as leaf thickness could serve as simple trait indicators to direct production practice. The results of this study also revealed a very significant enhancement effect between root Ca and leaf $\delta^{15}N$. The reason for this is that the abundant Ca element in the environmental background of the karst area mediates ecological function and resource utilization, and it restricts the stability and heterogeneity of the ecosystem. As the starting point of plant Ca transport, root Ca has nutrient and messenger functions for material synthesis, secondary metabolism, etc. [36], and further exerts a synergistic effect on the fractionation of nitrogen.

Leaf N had a significant enhancement effect on leaf P and K. N and P are the basic elements of biological proteins and genetic materials, and both of them are restrictive elements. They help each other and have a same-direction effect for growth and for physiological activities. K is an essential element in the regulation of photosynthesis and osmotic substances, and it has a synergistic gain with the nitrogen element of the synthetic organism. However, there is no significant correlation between P and K, and it may be

related to the trade-offs and synergies between the nutritional and messenger functions of the elements. Root P and Ca were synergistic. It might be due to the fact that Ca and P were converted into insoluble phosphorus in closed storage through precipitation, adsorption, immobilization, and microbial absorption [43]. Furthermore, the Ca content in karst areas was higher than those of Fe and Al and participated in the main chemical reaction. However, there was no similar pattern in the leaves. Presumably, this is related to nutrient reabsorption in the leaves, and a shorter distance between plants and the environment [44]. Moreover, it is also affected by the difference in the element transfer rate. Root $\delta^{15}N$ exhibited a significant negative effect on leaf N and leaf P. It may be that physiological activities such as root respiration and metabolism affected the microbe and extracellular enzyme activities involved in N and P cycles. Nevertheless, there was no significant effect on the contents of N and P in the root system itself. The reasons for this need to be further explored.

5. Conclusions

The local species of *Z. planispinum* 'dintanensis' has stronger ability to utilize and to preserve resources and to resist diseases, and builds stronger defense system by releasing volatile substances and forming fine roots. By increasing root length, *Z. amatum* 'novemfolius' can obtain a larger specific surface area and stronger physiological activity. Leaf functional traits (except Ca), specific root length, P, Ca, and physiological traits of the root had greater dominance on the trait system. Leaf K and root P tended to be selected by environment; leaf C, N, and P tended to be inherited stably, which was more greatly affected by variety than by specific leaf area, leaf $\delta^{15}N$, or root Ca. Leaf and root functional traits had strong interaction through synergistic and trade-off effects.

Author Contributions: Conceptualization, Y.L. and Y.S.; methodology, Y.Y.; software, Y.L.; validation, Y.S; formal analysis, Y.L.; investigation, Y.L. and Y.S.; resources, Y.Y.; data curation, Y.Y. and Y.S.; writing—original draft preparation, Y.Y.; writing—review and editing, Y.Y. and Y.S.; visualization, Y.L.; supervision, Y.Y.; project administration, Y.Y.; funding acquisition, Y.Y. All authors have read and agreed to the published version of the manuscript.

Funding: This work was funded by the Guizhou Province Science and Technology Support Plan Project (Qian-ke-he Zhicheng (2022) Yiban 103), and the Guizhou Province Science and Technology Support Plan Project (Qian-ke-he Zhicheng (2020) 1Y120).

Institutional Review Board Statement: Not applicable.

Informed Consent Statement: Not applicable.

Data Availability Statement: Data sharing is not applicable.

Conflicts of Interest: The authors declare no conflict of interest.

References

1. Li, X.; He, N.P.; Xu, L.; Li, S.G.; Li, M.X. Spatial variation in leaf potassium concentrations and its role in plant adaptation strategies. *Ecol. Indic.* **2021**, *130*, 108063. [CrossRef]
2. Zhang, Y.; He, N.P.; Li, M.X.; Yan, P.; Yu, G.R. Community cholorphyll quantity determines the spatial variation of grassland productivity. *Sci. Total Environ.* **2021**, *801*, 149567. [CrossRef] [PubMed]
3. Hu, Y.T.; Xiang, W.H.; Schafe, K.V.R.; Lei, P.F.; Deng, X.W.; Forrester, D.; Fang, X.; Zeng, Y.L.; Ouyang, S.; Chen, L.; et al. Photosynthetic and hydraulic traits influence forests resistance and resilience to drought stress across different biomes. *Sci. Total Environ.* **2022**, *828*, 154517. [CrossRef] [PubMed]
4. Ji, M.; Jin, G.Z.; Liu, Z.L. Effects of ontogenetic stage and leaf on leaf functional traits and the relationships between traits in *Pinus koraiensis*. *J. For. Res.* **2021**, *32*, 2459–2471. [CrossRef]
5. Khan, A.; Yan, L.; Wang, W.; Xu, K.; Zou, G.W.; Liu, X.D.; Fang, X.W. Leaf traits and leaf nitrogen shift photosynthesis adaptive strategies among functional groups and diverse biomes. *Ecol. Indic.* **2022**, *141*, 109098. [CrossRef]
6. Li, S.; Hamani, A.K.M.; Zhang, Y.Y.; Liang, Y.P.; Gao, Y.; Duan, A.W. Coordination of leaf hydraulic, anatomical, and economical traits in tomato seedlings acclimation to long-term drought. *BMC Plant Biol.* **2021**, *21*, 536. [CrossRef]
7. Wliiiams, A.; Langride, H.; Straathof, A.L.; Muhamadali, H.; Hollywood, K.A.; Goodacre, R.; de Varie, F.T. Root functional traits explain root exudation rate and composition across a range of grassland species. *J. Ecol.* **2021**, *110*, 21–33. [CrossRef]

8. Xu, H.D.; Zhu, B.; Wei, X.M.; Yu, M.K.; Cheng, X.R. Root functional traits mediate rhizosphere soil carbon stability in a subtropical forests. *Soil Biol. Biochem.* **2021**, *162*, 108431. [CrossRef]
9. Zadmorny, M.; Mucha, J.; BBagniewska-Zadworna, A.; Zytkowiak, R.; Maderek, E.; Danusevicius, D.; Oleksyn, J.; Wyka, T.P.; McCormack, M.L. Higher biomass partitioning to absorptive roots improves needle nutrition but also does not alleviate stomatal limitation of northern Scots pine. *Glob. Chang. Biol.* **2021**, *27*, 3859–3869. [CrossRef]
10. Wang, X.M.; Yan, B.G.; Shi, L.T.; Liu, G.C. Different responses of biomass allocation and leaf traits of *Dodonaea viscous* to concentrations of nitrogen and phosphorus. *Chin. J. Plant Ecol.* **2020**, *44*, 1247–1261. [CrossRef]
11. Elberse, I.A.M.; Van Damme, J.M.M.; Van Tienderen, P.H. Plasticity of growth characteristics in wild barley (*Hordeumspontaneum*) in response to nutrient limitation. *J. Ecol.* **2003**, *91*, 371–382. [CrossRef]
12. Qi, L.Y.; Chen, H.N.; Sairebieli, K.L.H.; Ji, T.Y.; Meng, G.D.; Qin, H.Y.; Wang, N.; Song, Y.X.; Liu, C.Y.; Du, N.; et al. Growth strategies of five shrub seedlings in warm temperate zone based on plant functional traits. *Chin. J. Plant Ecol.* **2022**, *46*, 1388–1399. [CrossRef]
13. Ahmed, M.; Kheir, A.M.S.; Mehmood, M.Z.; Ahmad, S.; Hasanuzzaman, M. Changes in germination and seedling traits of sesame under simulated drought. *Phyton-Int. J. Exp. Bot.* **2022**, *91*, 713–726.
14. Harrison, S.; Laforgia, M. Seedling traits predict drought-induced mortality linked to diversity loss. *Proc. Natl. Acad. Sci. USA* **2019**, *116*, 5576–5581. [CrossRef]
15. Xu, R.; Liu, J.; Wang, L.Y.; Yan, Y.; Ma, X.Q.; Li, M. Analysis of root and leaf functional traits and C, N, P stoichiometry of *Cunninghamia lanceolate* from different provenances. *Acta Ecol.* **2022**, *42*, 6311–6319.
16. Toledo-Aceves, T.; Lopez-Barrera, F.; Vasquez-Reyes, V. Preliminary analysis of functional traits in cloud forest tree seedlings. *Trees-Struct. Funct.* **2017**, *31*, 1253–1262. [CrossRef]
17. Alan, M.; Ezen, T. Magnitude of genetic variation in seedling traits of *Liquidambar orientalis* populations. *Fresenius Environ. Bull.* **2018**, *27*, 1522–1531.
18. Umana, M.N.; Zhang, C.C.; Cao, M.; Lin, L.; Swenson, N.G. Quantifying the role of intra-specific trait variation and organ-level traits in tropical seedling communities. *J. Veg. Sci.* **2018**, *29*, 276–284. [CrossRef]
19. Hu, S.L.; Sanchez, D.L.; Wang, C.L.; Lipka, A.E.; Yin, Y.H.; Gardner, C.A.C.; Lubberstedt, T. Brassinosteroid and gibberellina control of seedling traits in maize (*Zea mays* L.). *Plant Sci.* **2017**, *263*, 132–141. [CrossRef]
20. Ju, C.L.; Zhang, W.; Liu, Y.; Gao, Y.F.; Wang, X.F.; Yan, J.B.; Yang, X.H.; Li, J.S. Genetic analysis of seedling root traits reveals the association of root trait with other agronomic traits in maize. *BMC Plant Biol.* **2018**, *18*, 171. [CrossRef]
21. Nahar, K.; Bovill, W.; McDonald, G. Assessing the contribution of seedling root traits to phosphorus responsiveness in wheat. *J. Plant Nutr.* **2022**, *45*, 2170–2188. [CrossRef]
22. Ren, B.M. Research on the Driving Mechanism and Model Offarmers' Cooperatives Ecological Industry in Karst Rocky Desertification Treatment. Ph.D. Thesis, Guizhou Normal University, Guiyang, China, 2022. (In Chinese).
23. Bremer, E.; Janzen, H.H.; Johnston, A.M. Sensitivity of total, light fraction and mineralizable organic matter to management practices in a Lethbridge soil. *Can. J. Soil Sci.* **1994**, *74*, 131–138. [CrossRef]
24. Poorter, H.; Niinemets, U.; Poorter, L.; Wright, I.J.; Villar, R. Causes and consequences of variation in leaf mass per area (LMA): A meta-analysis. *New Phytol.* **2009**, *182*, 565–588. [CrossRef] [PubMed]
25. Wetzel, W.C.; Kharouba, H.M.; Robinson, M.; Holyoak, M.; Karban, R. Variability in plant nutrients reduces insect herbivore performance. *Nature* **2016**, *539*, 425–427. [CrossRef]
26. Luo, Q.Y.; Yu, M.S.; Yu, J.J.; Zheng, S.L.; Liu, J.J.; Yu, M.J. Effects of plant traits and the relative abundance of common woody species on seedling herbivory in the Thousand Island Lake region. *Chin. J. Plant Ecol.* **2017**, *41*, 1033–1040.
27. Farquhar, G.D.; OLeary, M.H.; Berry, J.A. On the relationship between carbon isotope discrimination and the intercellular carbon dioxide concentration in leaves. *Austrailan J. Plant Physiol.* **1982**, *9*, 121–137. [CrossRef]
28. Li, T.; Zhang, Z.H.; Sun, J.K.; Fu, Z.Y.; Zhao, Y.H.; Xu, W.J. Seasonal variation characteristics of C, N, and P stoichiometry and water use efficiency of *Messerschmidia sibirica* relationship with soil nutrients. *Front. Ecol. Evol.* **2022**, *10*, 948682. [CrossRef]
29. Mukarram, M.; Khan, M.M.A.; Zehra, A.; Petrik, P.; Kurjak, D. Suffer or survive: Decoding salt- sensitivity of lemongrass and its implication on essential oil productivity. *Front. Plant Sci.* **2022**, *13*, 903954. [CrossRef]
30. Shi, K.; Shao, H. Changes in the soil fungal community mediated by a *Peganum harmala* allelochemical. *Front. Microbiol.* **2022**, *13*, 911836. [CrossRef]
31. Mungan, M.D.; Harbig, T.A.; Perez, N.H.; Edenhart, S.; Stegmann, E.; Nieselt, K.; Ziemert, N. Secondarymetabolite transcriptomic pipeline (SeMa-Trap), an expression-based exploration tool for increased secondary metabolite production in bacteria. *Nucleic Acids Res.* **2022**, *50*, W682–W689. [CrossRef]
32. Wang, H.L.; Zhang, Y.; Xia, X.L.; Yin, W.L.; Guo, H.W.; Li, Z.H. Resaerch advances in leaf senescence of woody plants. *Sci. Sin. Vitae* **2020**, *50*, 196–206.
33. Keskitalo, J.; Bergquist, G.; Gardeström, P.; Jansson, S. A cellular timetable of autumn senescence. *Plant Physiol.* **2005**, *139*, 1635–1648. [CrossRef]
34. Hu, H.C.; Fei, X.T.; He, B.B.; Chen, X.; Ma, L.; Han, P.; Luo, Y.L.; Liu, Y.H.; Wei, A.Z. UPLC-MS/MS profile combined with RNA-Seq reveals the amino acid metabolism in *Zanthoxylum bungeanum* leaves under drought stress. *Front. Nutr.* **2022**, *9*, 921742. [CrossRef]

35. Carmona, C.P.; Bueno, C.G.; Toussaint, A.; Träger, S.; Díaz, S.; Moora, M.; Mouson, A.D.; Pärtel, M.; Zobel, M.; Tamme, R. Fine-root traits in the global spectrum of plant form and function. *Nature* **2021**, *597*, 683. [CrossRef]
36. Ma, Z.Q.; Guo, D.L.; Xu, X.L.; Lu, M.H.; Bardgett, R.D.; Eissenstat, D.M.; McCormack, M.L.; Hedin, L.O. Evolutionary history resolves global organization of root functional traits. *Nature* **2018**, *555*, 94. [CrossRef]
37. Meng, W.P.; Ren, Q.Q.; Tu, N.; Leng, T.J.; Dai, Q.H. Characteristics of the adaptations of Epilithic Mosses to high-calcium habitats in the karst region of southwest China. *Bot. Rev.* **2021**, *88*, 204–219. [CrossRef]
38. Poovaiah, H.W.; Reddy, A.S.N. Calcium and signal transduction in plants. *Crit. Rev. Plant Sci.* **1993**, *12*, 185–211. [CrossRef]
39. Diao, H.Y.; Wang, A.Z.; Yuan, F.H.; Guan, D.X.; Yin, H.; Wu, J.B. Stable carbon isotopic characteristics of plant-ltter-soil continuum along a successional gradient of broadleaved Korean pine forests in Changbai Mountain, China. *Chin. J. Appl. Ecol.* **2019**, *30*, 1435–1444.
40. Hobbic, E.A.; Werner, R.A. Intramolecular, compoundspecific, and bulk carbon isotope patterns in C3 and C4 plants: A review and synthesis. *New Phytol.* **2004**, *161*, 371–385. [CrossRef]
41. Huang, M.J.; Wang, S.P.; Liu, X.; Nie, M.; Zhou, S.R.; Hautier, Y. Intra- and interspecific variability of specific leaf area mitigate the reduction of community stability in response to warming and nitrogen addition. *Oikos* **2022**, *9*, e09207. [CrossRef]
42. Xu, X.N.; Sun, Y.X.; Liu, F.L. Modulating leaf thickness and calcium content impact on strawberry plant thermotolerance and water consumption. *Plant Growth Regul.* **2022**, *98*, 539–556. [CrossRef]
43. Lin, W.Q.; Cai, J.H.; Xue, L. Responses of *Cinnamomumcamphora* seedling growth and leaf traits to additions of nitrogen and phosphorous under different planting densities. *Acta Ecol.* **2019**, *39*, 6738–6744.
44. Zhang, J.H.; Tang, Y.Z.; Luo, Y.K.; Chi, X.L.; Chen, Y.H.; Fang, J.Y.; Shen, H.H. Resorption efficiency of leaf nutrients in woody plants on Mt. Dongling of Beijing, North China. *J. Plant Ecol.* **2014**, *8*, 530–538. [CrossRef]

forests

MDPI

Article

Farmland Hydrology Cycle and Agronomic Measures in Agroforestry for the Efficient Utilization of Water Resources under Karst Desertification Environments

Qinglin Wu, Kangning Xiong *, Rui Li and Jie Xiao

School of Karst, State Engineering Technology Institute for Karst Desertification Control, Guizhou Normal University, Guiyang 550001, China
* Correspondence: xiongkn@gznu.edu.cn

Abstract: Severe soil-water loss and unfertile soil frequently occur under karst desertification environments. The surface-underground dual structure in these areas allows the surface water to leak into the subsurface through cracks and sinkholes, as well as other conduits, causing a special "karst drought". Hence, water-resource shortage has become a challenge for local agricultural development. To realize efficient utilization of water resources, an urgent need is to clearly understand and study the law of farmland hydrological cycles under agroforestry practices, which is still understudied. Here, we focused on the hydrological cycle at the farmland scale and water-saving measures under agroforestry in three study areas representing different degrees of karst desertification. First, a significant positive correlation was found between total and available precipitations as well as land evapotranspiration (LET). Second, under agronomic measures, the soil water content in the three areas was all higher than that of the control group while soil evaporation was all lower. This indicates that agronomic measures can contribute to the efficient use of water resources by halting soil evaporation and increasing soil water content. Third, dwarf dense planting and pruning technologies were helpful in inhibiting crop transpiration and reducing vegetation interception. Fourth, in the farmland hydrological cycle of agroforestry, 77.45% of precipitation transformed into soil water storage, 24.81% into soil evaporation, 20.73% into plant transpiration, 17.40% into groundwater, and 5.18% into vegetation interception. However, their sum was greater than 100%, suggesting that the farmland-scale water cycle is an open system. The implication is that different agronomic practices under agroforestry bring certain water-saving benefits by constraining the conversion of ineffective water and promoting the storage of effective water, thus opening up promising opportunities for efficiently utilizing water resources in karst desertification areas. The finding is also significant to the control of karst desertification, soil and water conservation, and karst drought alleviation.

Keywords: karst desertification environment; farmland hydrological cycle; agroforestry; agronomic measures to water saving

Citation: Wu, Q.; Xiong, K.; Li, R.; Xiao, J. Farmland Hydrology Cycle and Agronomic Measures in Agroforestry for the Efficient Utilization of Water Resources under Karst Desertification Environments. *Forests* **2023**, *14*, 453. https://doi.org/10.3390/f14030453

Academic Editor: Massimiliano Schwarz

Received: 28 January 2023
Revised: 17 February 2023
Accepted: 20 February 2023
Published: 22 February 2023

1. Introduction

With carbonate rock exposure covering 10% of the world's land area [1], and providing water for 20%–25% of the world's population [2], karst regions are undoubtedly one of the most ecologically fragile areas in the world [3]. Karst desertification is a land degradation phenomenon caused by the interaction between unreasonable human activities and a fragile ecological environment in karst areas [4]. This is a serious ecological environment problem [5,6], and gives rise to a delicate ecological system [7,8]. It also constantly results in severe soil and water loss [9,10], and land degradation (a systemic global problem) [11]. In China, karst desertification has been recognized as one of the ecological disasters [12–15]. The focus of its control is on improving the environment and raising revenue through protecting and establishing vegetation, promoting sustainable land use, and implementing water conservation measures [16]. In Southwest China, afforestation and reforestation projects are important

ways of ecological restoration [17]. They have been adopted to combat desertification in the karst regions [18], which has an impact on the hydrologic process [19]. Karst regions are characterized by a discrete hydrological system [20]. Abundant precipitation fails to provide sufficient surface water [2] and unique "Karst Drought" appears. The reason is that rainfall tends to leak underground along rock fissures and pores [14,21]. A week with little rain will induce drought stress on many crops, and thus agronomic water-saving measures are necessary to alleviate this stress and improve crop productivity.

Currently, environmental degradation and loss of biodiversity are threatening the stability of our planet [22]. These problems are especially a focus of the UN Sustainable Development Goals (SDGs), which are trying to improve livelihoods while ensuring the conservation and sustainable use of terrestrial ecosystems [23]. In real practice, agroforestry is being widely implemented with the expectation that it can simultaneously meet each of these goals [24]. It is seen as a way of promoting sustainable dryland use [25], generating the ecological benefits of carbon storage rise [26], and land rehabilitation [27]. Agroforestry systems have so far proven to offer significant co-benefits to the healthy ecological system and crop yield growth and may be especially important for rural populations in low- and middle-income countries [28]. Correspondingly, in karst areas, they not only help to rein the rocky desertification process but also boost the ecological derived industry.

At the farmland scale, there has been some research involving the hydrological cycle of agroforestry in all aspects. One study reported that surface runoff declined by 1%–100% under agroforestry systems [29]. In another, it is said that agroforestry increased the soil water buffering capacity, which enhanced the drought tolerance of the system [30]. Reports on other aspects also appear from time to time. Ling et al. [31] suggested that agroforests generally improved water conditions in shallow soil layers compared to single-culture plantations. A study by Hombegowda et al. [32] showed that coffee plants drew water mainly from the topsoil (56% from 0 to 20 cm). In some extremely dry periods, agroforests are reported to be able to compete to absorb deeper soil water. One case showed that intercropping resulted in jujube trees absorbing deeper water (up to 3 m) in overlap layers below the main root [33]. According to research by Liu et al. [34], 27.83% (4.3%–58.0%) of precipitation recharged the groundwater of the agroforestry watershed in the Sichuan Basin. It was concluded in a study by Wu et al. [11] that agroforestry has the ecological benefit of reducing soil evaporation and crop transpiration. Zhang et al. [35] found that the actual evapotranspiration was 7.64 ± 5.75 mm day^{-1} in a karst silvopasture system, of which 4.24 ± 3.35 mm day^{-1} was for crops and 5.78 ± 3.53 mm day^{-1} was for grass ecosystems.

This line of research shows interest in different aspects like surface water, soil water content, soil water evaporation, plant transpiration, and groundwater. Nevertheless, investigations into hydrological processes are limited [29], and thus it is significant to examine the hydrological cycle at the farmland scale. This study selected the horizontal plots which generate little surface water from natural rainfall, and hence the focus was on rates of precipitation transforming into soil water, groundwater, soil evaporation, plant transpiration, and vegetation interception. This was to make clear the hydrological cycle law at the farmland scale under agroforestry systems, so as to provide a reference for the efficient utilization of water resources and promote the healthy and high-yield development of agroforestry.

2. Materials and Methods

2.1. Study Areas

Located in the northwest of Guizhou Province, Bijie Salaxi Research region (Bijie for short) (105°02′01″–105°08′09″ E, 27°11′36″–27°16′51″ N) covers an area of 86.27 km^2, of which 73.94% is karst. The altitude of the region is 1509–2180 m above sea level, and its average annual temperature is 12 °C, with 984.4 mm average annual precipitation. Mostly limestone, this region represents typically potential-mild level karst desertification on the karst plateau. The Guanling—Zhenfeng Huajiang Research Area (Huajiang in brief) (105°36′30″–105°46′30″ E, 25°39′13″–25°41′00″ N) is in the southwest of Guizhou Province.

It covers an area of 51.62 khm^2, of which 87.92% is karst, rising above sea level about 450–1450 m, with a mean annual temperature of 18.4°C and receiving 1100 mm average rainfall. It is dominated by dolomitic limestone, representing the typical medium-intensity karst desertification in karst plateau canyons. The Shibing Research Area (Shibing in brief) (108°01′36″–108°10′52″ E, 27°13′56″–27°04′51″ N) is in the eastern part of Guizhou Province. It has an area of 282.95 km^2, 89.11% of which belongs to karst. Its altitude is 600–1250 m, with a 16 °C annual average temperature and 1220 mm annual mean precipitation. It represents the no-potential karst desertification region in the dolomite plateau valleys (Figure 1).

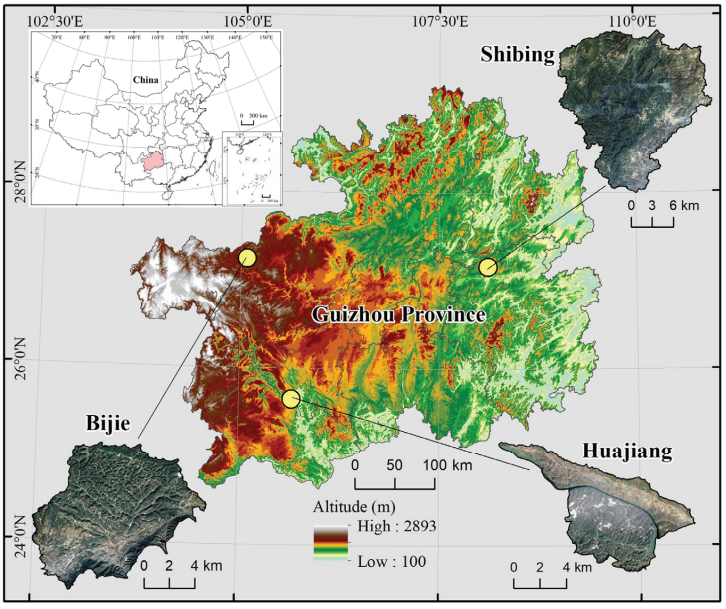

Figure 1. Topographic map of the study area.

2.2. Experimental Design and Data Processing

There were three study areas, each with two planting patterns and four treatments for each planting pattern, so a total of 24 plots were delineated (4 m × 5 m). The crop selection was based on natural conditions, economic growth needs, reasonable agroforestry configuration, and optimal use of water resources. In Bijie, we selected *Rosa roxburghii*, *Walnut*, *Potato,* and *Ryegrass*. *Rosa roxburghii* and *Walnut* are the dominating cash crop for the local people and *Potato* is one of the staple foods that is suitable for the natural conditions there. *Ryegrass* planting conforms to the requirements of controlling karst desertification and local livestock development. In Huajiang, we chose *Zanthoxylum planispinum var. Dintanensis*, *Chili,* and *Pitaya*, for they are drought-resisting and have become the local main cash crops. In Shibing, we selected *Osmanthus fragrans* and *Pseudostellariae Radix* because they are locally characteristic industrial crops. We planted these crops as: *Rosa roxburghii* + *Ryegrass* (Model A) and *Walnut* + *Potato* (Model B) in Bijie, *Pitaya* + *Zanthoxylum planispinum var. Dintanensis* (Model C) and *Zanthoxylum planispinum var. Dintanensis* + *Chili* (Model D) in Huajiang, and *Osmanthus fragrans* + *Pseudostellariae Radixo* (Model E) and *Pseudostellariae Radixo* monoculture (Model F) in Shibing. The agroforestry models realized the height configuration and avoided interspecific competition so that the species of the agroforestry system could maximize the use of soil water and nutrients and reasonably use rainfall and solar energy resources.

In April 2019, we applied four treatments (Table 1) to the plots according to the real conditions. The first one was straw + water retaining agent (SWR). We used a polyacrylamide water-retaining agent and the solution was prepared at 1% concentration. Later, this was evenly applied to the surface soil where the crop roots were distributed. We then covered the surface soil with 2 cm-long maize straw, to a thickness of 5 cm. The second was straw mulching (STR). We first used 2 cm-long maize straw to cover the surface soil to a thickness of 5 cm. We then dug 10 cm of soil in a vertical direction under the straw with a hoe and mixed them well. The third treatment was only water-retaining agent (WRA), and the same substance and concentration as that in the first treatment. After blending well in a plastic bucket, this was applied evenly into the soil layer where the crop roots were distributed. The fourth condition was the control plot (CON), with no agronomic treatment.

In the 2019 crop growing season (April–August), we monitored the soil's physical properties at the sample sites. The monitoring was conducted once a month with the cutting ring method, and three layers of soil were taken—0–10 cm, 10–20 cm, and 20–30 cm from the upper, middle, and lower layers (each layer was taken 3 times along an S-shape, and then averaged). Then it was taken back to the laboratory for test analysis to obtain soil properties such as soil water content, porosity, field water capacity, and saturated water content.

We monitored the surface water at the study sites by conducting artificial simulated rainfall tests in March 2019. When the rain intensity reached 140 mm h^{-1}, no surface runoff occurred. Data from the weather station (DAVIS-Vantage Pro), which we installed in the study sites, showed that in 2019 the maximum rain intensity was only 78 mm h^{-1} in Bijie, 60 mm h^{-1} in Huajiang, and 97 mm h^{-1} in Shibing, and the heaviest rainfall was 116 mm d^{-1}, 98 mm d^{-1}, 105 mm d^{-1}, respectively. Meanwhile, we built runoff plots (4 m $\times$ 5 m) around the sample plots with iron sheets of 3 mm thickness, 500 mm height, and 1900 mm length. These iron sheets were 200 mm high above the surface and 300 mm deep under the soil. Our monitoring did not find surface runoff. As a result, surface runoff was negligible and excluded from the hydrological cycle in this study.

We used self-made microlysimeters to monitor soil evaporation [36]. On days in the middle of every month from April to August 2019, 48 self-made microlysimeters were placed in the parts with and without vegetation cover in each of the 24 sample plots when there was no rain. Each microlysimeter consisted of inner and outer rings, made of Poly Vinyl Chloride (PVC). The inner ring was 300 mm long, 100 mm in diameter (cross-sectional area: 78.5 mm^2), and the wall thickness was 3 mm. The outer ring was 300 mm long, 150 mm in diameter, and 3 mm in wall thickness. At 8:00 on a given day, the inner ring was driven into the soil with a hammer, creating a column of soil in the inner ring. We used a hoe to dig out the inner ring along with the soil column (taking care not to damage the soil column in the inner ring and cleaning up the soil on its outer wall). After this, we wrapped the bottom with nylon netting to prevent soil from leaking. Third, the inner ring with the soil column was weighed with an electronic balance (a measuring range of 5 kg and an accuracy of 0.01 g). Fourth, the outer ring was installed vertically into the pit where the column was excavated so that the upper part was flush with the ground. A scrap newspaper was also placed inside the outer ring to stop the soil from sticking to the bottom of the inner ring. Finally, we placed the inner ring inside the outer ring. At the same time the next morning, the inner ring was taken out and weighed again. The difference between the two days of weighing was the 24-h soil evaporation (g). The average daily soil evaporation was measured for 3 consecutive days in each plot every month.

Table 1. Basic information of the sample plot in the study area.

Study Area	Land-Use Type (Model)	Agronomic Measure	Soil Type	Slope (°)	Plot Area (m^2)	Vegetation Coverage (%)	Row Space (m)	Planting Crops
Bijie	A	SWR	Yellow-brown earth	2°	4 m × 5 m	95	*Rosa roxburghii*: 2 m × 2 m, *Ryegrass*: sown	*Rosa roxburghii*: 6 years *Ryegrass*: planted in March 2019
		STR	Yellow-brown earth	2°	4 m × 5 m	87		
		WRA	Yellow-brown earth	2°	4 m × 5 m	85		
		CON	Yellow-brown earth	2°	4 m × 5 m	85		
	B	SWR	Yellow-brown earth	2°	4 m × 5 m	81	*Walnut*: 4 m × 4 m *Potato*: 0.25 m × 0.6 m	*Walnut*: 6 years *Potato*: planted in December 2018
		STR	Yellow-brown earth	2°	4 m × 5 m	79		
		WRA	Yellow-brown earth	2°	4 m × 5 m	80		
		CON	Yellow-brown earth	2°	4 m × 5 m	85		
Huajiang	C	SWR	Yellow earth	2°	4 m × 5 m	96	*Zanthoxylum planispinum var. Dintanensis*: 4 m × 4 m *Pitaya*: 2 m × 2 m	*Zanthoxylum planispinum var. Dintanensis*: 6 years *Pitaya*: 6 years
		STR	Yellow earth	2°	4 m × 5 m	96		
		WRA	Yellow earth	2°	4 m × 5 m	87		
		CON	Yellow earth	2°	4 m × 5 m	86		
	D	SWR	Yellow earth	0°	4 m × 5 m	86	*Zanthoxylum planispinum var. Dintanensis*: 4 m × 4 m *Chili*: 0.4 m × 0.6 m	*Zanthoxylum planispinum var. Dintanensis*: 6 years *Chili*: planted in March 2018
		STR	Yellow earth	0°	4 m × 5 m	87		
		WRA	Yellow earth	0°	4 m × 5 m	82		
		CON	Yellow earth	0°	4 m × 5 m	87		
Shibing	E	SWR	Yellow earth	2°	4 m × 5 m	75	*Osmanthus fragans*: 4 m × 4 m *Pseudostellariae Radixo*: sown between ridges with an inter-row space of 0.2 m	*Osmanthus fragrans*: 6 years *Pseudostellariae Radixo*: planted in December 2018
		STR	Yellow earth	2°	4 m × 5 m	73		
		WRA	Yellow earth	2°	4 m × 5 m	74		
		CON	Yellow earth	2°	4 m × 5 m	65		
	F	SWR	Yellow earth	2°	4 m × 5 m	75	*Pseudostellariae Radixo*: sown between ridges with an inter-row space of 0.2 m	*Pseudostellariae Radixo*: planted in December 2018
		STR	Yellow earth	2°	4 m × 5 m	71		
		WRA	Yellow earth	2°	4 m × 5 m	74		
		CON	Yellow earths	2°	4 m × 5 m	62		

We conducted real-time monitoring of precipitation and temperature with the installed small weather stations (DAVIS-Vantage Pro) in the three study sites. The Koichiro Takahashi formula (Equation (1)) [37–39] was applied to process the collected data to obtain land evapotranspiration and available precipitation. Land evapotranspiration (LET) refers to the loss of water from the land surface into the atmosphere through evaporation from ground and canopy rainfall interception and transpiration from vegetation; it is a key process in the climatic and biogeochemical cycles of terrestrial ecosystems and plays a vital role in the hydrological cycle, energy balance, and carbon cycle [40–42]. The two variables were then analyzed using SPSS to identify their relationship with precipitation in the corresponding period. Precipitation occurrence and transformation in the three study areas were analyzed according to temporal scale and spatial variation, hoping to provide a reference for studies on the storage and conversion of soil water, soil evaporation, plant transpiration, vegetation interception, and groundwater.

$$E = \frac{3100P}{3100 + 1.8P^2 \exp\left(-\frac{34.4t}{235+t}\right)} \quad (1)$$

where E is monthly LET (mm), P is monthly total rainfall (mm), and t is monthly average temperature (°C). Based on this formula, we obtained the following variables through linear equations: available precipitation F (mm) (Equation (2)), evapotranspiration coefficient α (Equation (3)), and available precipitation coefficient β (Equation (4)).

$$F = P - E \quad (2)$$

$$\alpha = E/P \quad (3)$$

$$\beta = (P - E)/P \quad (4)$$

We used the pruning and weighing method to assess the crop transpiration rates of agroforestry [43,44]. We conducted the measurements in the study sites from April to August 2019. First, we placed a wind-proof electronic balance with a precision of 0.001 in a relatively flat place, which was near the crops to be monitored in the field. We then cut off the standard branches (branches or leaves in the crown of a tree or crop, having an average diameter, length, and average leaf weight), and immediately put them on the balance to weigh. Third, we returned the weighed branches to their respective places and weighed them five minutes later. The difference between the two weights was the transpiration rate and amount (Equation (5)). We weighed the branches from 8:00 in the morning to 6:00 in the evening, once every 2 h, a total of 6 times a day.

$$Et = \frac{m_0 - m_1}{(m_0 - m_z) \times 5} \times 60 \quad (5)$$

where Et refers to the transpiration rate (g g^{-1} h^{-1}), m_0 to the initial weight of branches and leaves (g), m_1 to the final weight of branches and leaves (g), and m_z to the weight of branches (g).

Crop biomass and dry matter need monitoring when calculating transpiration and water use efficiency (WUE). Biomass is constantly changing and thus was obtained by the harvest method [45–47]. In order to ensure that continuous positioning monitoring can be carried out in the future, we applied an analogy for crop selection. We selected the crops with the same stand, species, average plant height, stand age, density, and planting method from adjacent plots (4 m × 5 m), which were 5 m apart and had similar altitudes, slope soil type, and agronomic measures. We harvested the aboveground parts of all the crops, weighing the fresh weight and taking them back to the laboratory for dry weight analysis.

We performed the immersion method (Equation (6)) to calculate vegetation interception. We immediately immersed the last-weighed branches and leaves in the water for 5 min and then removed them. After the branches and leaves stopped dripping (about 3

min later), we put them into a plastic bag to weigh. By removing the plastic bag weight, we assessed the difference between the left weight and that of the last-weighed branches and leaves, so as to obtain the weight of intercepted water; that is, the plant water capacity [48].

$$Iv = Pb \times Rw/S \times n \quad (6)$$

where Iv is the amount of vegetation interception (mm), Pb is crop biomass (g), Rw is plant water holding rate, S is the sample area (m^2), and n is the number of rainfall.

$$Wg = P - Wi - Wr - Ws \quad (7)$$

Equation (7) was used to calculate the groundwater of each planting mode. Where Wg represents groundwater (mm), P is rainfall (mm), Wi is the amount of vegetation interception (mm), Wr is surface water (mm), and Ws is soil water (mm).

3. Results

3.1. Characteristics of Precipitation Transformation

In the three research areas, summer (June to August) received the most rain yet spring suffered severe drought. During the 2019 crop-growing season (April to August), Shibing received the largest amount of rain (1003.00 mm), followed by Bijie (981.60 mm), with Huajiang at the bottom (549.90 mm) (Table 2). Spring drought is a meteorological disaster in karst areas. Of the three areas, Huajiang ranked the severest, where little rainfall events occurred in March and May; only 64.70 mm of rainfall was received from April to May. That was only 33.18% of Bijie's rainfall and 22.75% of Shibing's during the same period. Occasionally, sporadic light rain fell on the surface of the soil but quickly evaporated under the influence of the climate in the hot and dry valley (high temperature, strong sunshine, intense evaporation). Spring is when crops depend on a large amount of water to grow and is the time little soil water can be absorbed by plants. In Huajiang, severe spring drought was responsible for yellow or wilted crops, including the drought-resisting ones like *Zanthoxylum planispinum var. Dintanensis* and *Pitaya*.

Table 2. Precipitation, available precipitation and LET distribution in study areas.

Months	Precipitation (mm)			Available Precipitation (mm)			LET (mm)		
	Bijie	Huajian	Shibing	Bijie	Huajiang	Shibing	Bijie	Huajiang	Shibing
Apr.	88.00	33.50	112.80	28.41	0.66	52.24	59.59	32.84	60.56
May	107.00	31.20	171.60	39.39	0.55	107.56	67.61	30.65	64.04
Jun.	196.60	253.00	243.80	125.27	127.93	157.99	71.33	125.07	85.81
Jul.	304.00	156.60	216.60	243.73	44.13	119.01	60.27	112.47	97.59
Aug.	286.00	75.60	258.20	200.67	5.51	154.67	85.33	70.09	103.53
Total	981.60	549.90	1003.00	637.47	178.78	591.47	344.13	371.12	411.53

In the three areas, we monitored the precipitation from April to August. SPSS was employed to analyze the collected data to reveal the relationship among precipitation, available precipitation, and land evapotranspiration (LET). It was found that precipitation was positively correlated to the other two variables ($p < 0.01$). The highest correlation coefficient was found with available precipitation (Bijie r = 0.984, $p < 0.01$; Huajiang r = 0.965, $p < 0.01$; Shibing r = 0.994, $p < 0.01$), and the second with LET (Bijie r = 0.780, $p < 0.01$; Huajiang r = 0.889, $p < 0.01$; Shibing r = 0.975, $p < 0.01$). Based on the monitored temperature and precipitation, the Koichiro Takahashi formula was applied to generate the precipitation result; that is, precipitation was the sum of the available precipitation and LET. For instance, in Bijie, precipitation was 981.60 mm, the summation of the available precipitation (637.47 mm) and LET (344.13 mm). The same was true for the rest of the study areas. The implication here is that precipitation transforms into either available precipitation or LET. In other words, the sum of the two variables is precipitation and

there is a trade-off between them. For a certain amount of precipitation, the available precipitation is more if the LET is less, and vice versa.

3.2. Storage and Transformation of Soil Water and Efficient Utilization of Water Resources

Soil water consists of transformation amount, and soil water storage—an important index of soil water content. Agronomic treatments were implemented in April and analysis compared the soil water content for May and July. Under each treatment, it was higher in July than in May. While more rain in July did contribute to this, the agronomic measures certainly produced water conservation benefits, for there was higher soil water content under almost all treatments than that of the control plot (the soil water content of some individual treatments was lower than that of the control. A case was found in the model of *Rosa roxburghii* + *Ryegrass*. In May, the soil water content was 17.17% in the 0–10 cm soil layer under the water-retaining agent while it was 17.45% in the control plot. This may be because the surface soil was affected by the difference in terrain height, direction, and soil water absorption by plant roots. Analysis between groups produced the result that the average soil water content of the study areas in May and July was 23.17% in Shibing, higher than those for Bijie (18.60%) and Huajiang (17.63%). This was consistent with the distribution in the control group and the total rainfall distribution in the crop-growing season. Another finding was that straw mulching produced higher soil water content in the surface layer (Figure 2). The reason for this was that the straw on the surface of the soil became fertilizer after rotting and hence triggered the "coupling effect of water and fertilizer", which brought about the effect of "using fertilizer to increase and retain water". When comparing the soil water content between different measures, we found that the highest was from straw + water-retaining agent (21.83%), with the second from straw (20.42%), and the third from the water-retaining agent alone (19.73%). The lowest was found in the control (17.93%). Agronomic treatments presented obvious water-retaining effects.

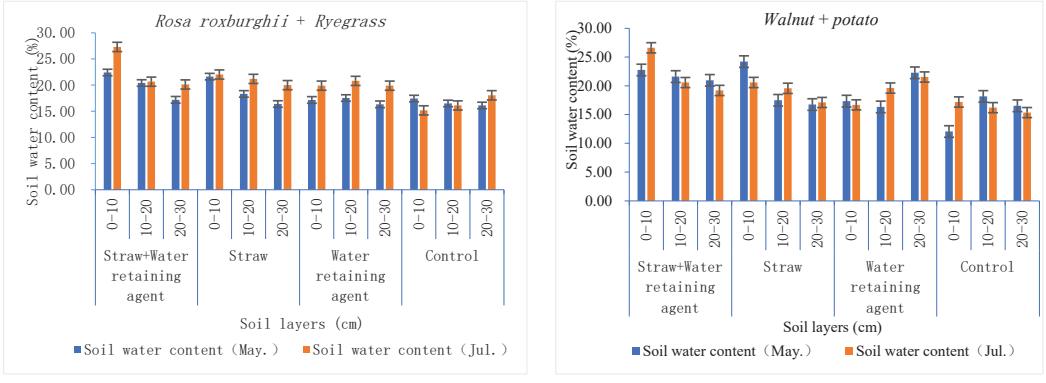

Figure 2. *Cont.*

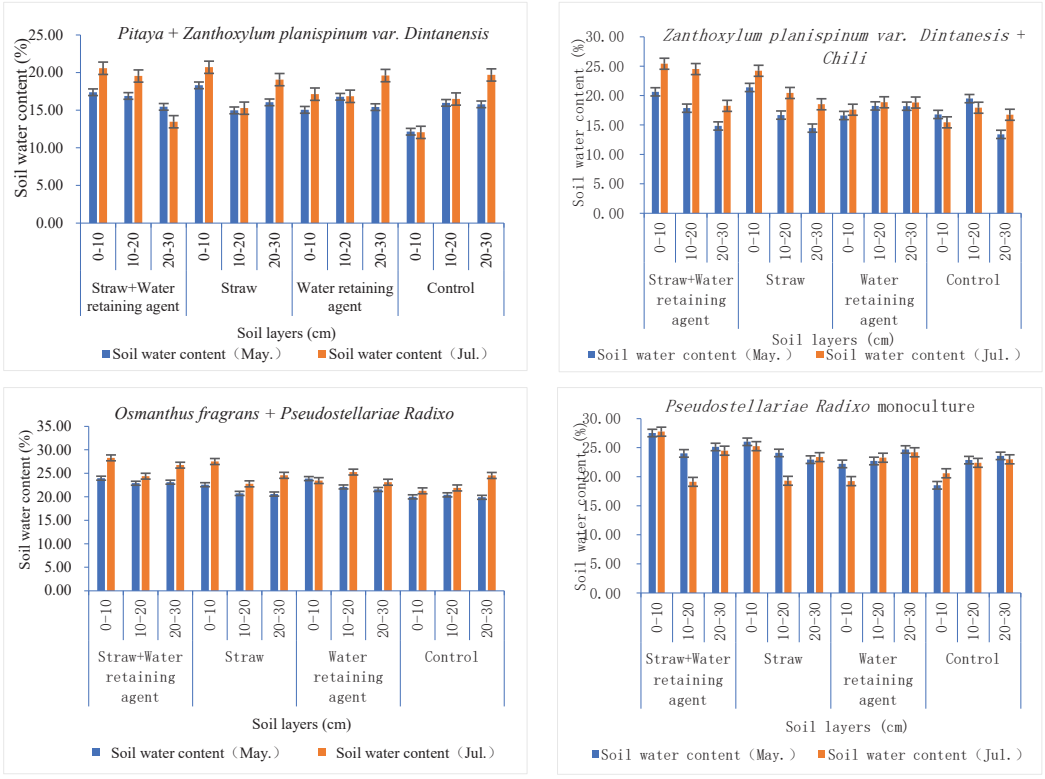

Figure 2. Soil water content under each treatment.

Soil water transformation is mainly manifested by soil evaporation. In the crop-growing season, soil evaporation occurred the most in Shibing (327.98 mm); Bijie (168.70 mm) followed and Huajiang (134.90 mm) evaporated the least. This conformed to the same law as the precipitation distribution in the three areas. Between the treatments, the lowest evaporation was found from straw + water-retaining agent (172.37 mm), and the highest from the control plot (253.57 mm), with the other two being in the middle (201.39 mm from the water-retaining agent and 214.78 mm from straw). The evaporation under each measure was lower than that of the control. Correlation analysis generated the following result: soil evaporation was positively related to soil water content ($r = 0.602$, $p < 0.01$) but negatively associated with vegetation coverage ($r = -0.943$, $p < 0.01$). To sum up, rich soil water content provided a water source for evaporation, which could be effectively slowed down by carrying out more vegetation covering, finally reaching the efficient use of water resources.

3.3. Characteristics of Plant Water Transformation and Efficient Use of Water Resources

Plant water transforms into transpiration and vegetation interception. The analyzed result was that the overall transpiration was greater under the agronomic treatments when compared to the control, and higher in the agroforestry treatments than monoculture. Of the agroforestry models, transpiration reached the maximum in the *Rosa roxburghii* + *Ryegrass* (344.98 mm) model and the minimum in *Pitaya* + *Zanthoxylum planispinum var. Dintanensis* (43.92 mm). Between the three regions, Bijie showed the highest average transpiration, with Shibing in the middle and Huajiang being the lowest. The results of the correlative analysis were: except for *Pitaya* + *Zanthoxylum planispinum var. Dintanensis*, the transpiration amounts and rates of the other planting models were significantly positively

correlated with biomass (r= 0.964–0.971, $p < 0.01$). This positive association was also found in the case of vegetation interception and biomass (r = 0.830, $p < 0.01$).

As presented in Figure 3, the *Pitaya + Zanthoxylum planispinum var. Dintanensis* model had the largest amount of vegetation interception (66.43 mm), resulting from the mass biomass of Pitaya. The least vegetation interception was *Pseudostellariae Radixo* (20.16 mm), which was strongly associated with vegetation transpiration (r = 0.993, $p < 0.01$). In contrast to the other models, *Pitaya + Zanthoxylum planispinum var. Dintanensis* produced a significant negative relationship between vegetation interception and transpiration (r = −0.993, $p < 0.01$). This could be attributed to the low evaporation rate of the *Pitaya*, which generated less transpiration and whose large biomass brought greater vegetation interception. Apparently, vegetation interception varied with transpiration (with the *Pitaya + ryegrass* model excluded) (Figure 3). Meanwhile, the regression coefficient of vegetation interception (−0.1122) was less than that of transpiration (0.87), indicating a smaller change in vegetation interception compared with transpiration.

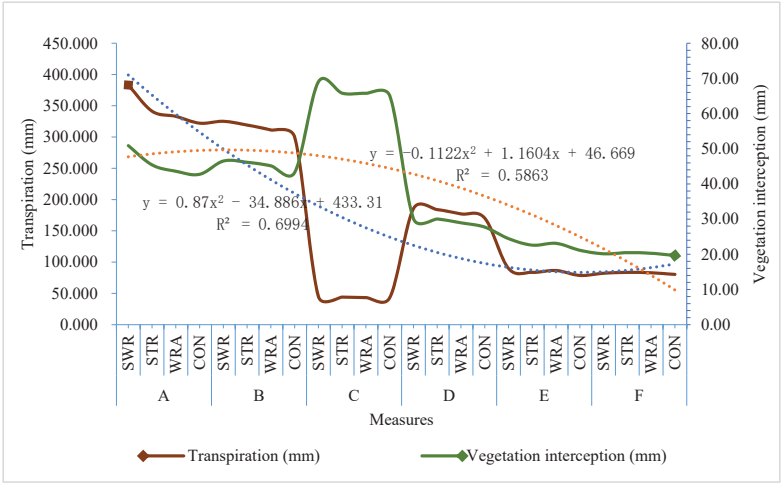

Figure 3. Plant water transpiration and vegetation interception under different measures.

Transpiration and vegetation interception are contradictory units, increasing or decreasing simultaneously. Transpiration is considered to be an effective water consumption while vegetation interception is ineffective because it all evaporates. Karst areas are dominated by rain-fed agriculture. In the same area, biomass increases along with flourishing crops, which further results in high transpiration and vegetation interception. To enhance the efficiency of water resource utilization, dwarf dense planting and pruning are suggested ways to reduce biomass and lower transpiration and vegetation interception.

3.4. Storage, Transformation and Efficient Utilization of Water Resources

Precipitation is the total water resource in karst areas, which further transforms into surface water, underground water, soil water, vegetation interception, plant transpiration, and soil evaporation (Table 3). Through situ monitoring, we found that soil water was positively correlated with the available precipitation and soil evaporation, yet negatively associated with vegetation interception ($p < 0.01$); groundwater was observed to have a positive relationship with the available precipitation ($p < 0.01$). Water consumption caused by plant transpiration is a form of conversion after plants take in soil water or groundwater. It is an effective water consumption for plants. We found a negative relationship between plant transpiration and soil evaporation ($p < 0.01$). Vegetation interception and soil evaporation, not absorbed by plants, were regarded as invalid water, and a negative association was revealed between them ($p < 0.01$).

Table 3. Storage and transformation of water resources.

Plant	Measure	Precipitation (mm)	Available Precipitation (mm)	Soil Water Storage (mm)	Underground Water (mm)	Transpiration (mm)	Vegetation Interception (mm)	Soil Evaporation (mm)
A	SWR	981.6	432.63	412.95	517.75	383.2	50.9	114.87
	STR	981.6	449.58	663.09	273.09	341.34	45.43	145.25
	WRA	981.6	467.58	866.33	71.64	333.14	43.62	137.26
	CON	981.6	471.34	823.73	115.11	322.26	42.75	145.25
B	SWR	981.6	423.74	493.78	441.29	325.21	46.53	186.12
	STR	981.6	415.52	677.3	258.13	319.23	46.17	200.68
	WRA	981.6	426.43	798.99	137.45	311.32	45.16	198.69
	CON	981.6	417.05	845.94	92.37	299.73	43.3	221.52
C	SWR	549.9	306.75	425.83	55	44.88	69.08	129.19
	STR	549.9	285.47	433.24	50.85	44.19	65.81	154.43
	WRA	549.9	305.91	462.57	21.56	43.32	65.78	134.89
	CON	549.9	264.78	419.9	64.94	43.3	65.06	176.76
D	SWR	549.9	231.27	512.63	7.18	185.81	30.09	102.73
	STR	549.9	214.02	514.4	5.46	184.02	30.04	121.82
	WRA	549.9	225.06	503.93	17.01	177.18	28.96	118.7
	CON	549.9	211.24	503.16	19	170.23	27.74	140.69
E	SWR	1003	660.1	706.69	271.84	89.85	24.47	228.58
	STR	1003	585.42	798.18	182.2	83.79	22.62	311.17
	WRA	1003	605.85	775.45	204.43	86.72	23.13	287.3
	CON	1003	506.52	799.49	182.35	78.82	21.16	396.5
F	SWR	1003	627.82	586.51	396.33	82.28	20.16	272.74
	STR	1003	543.51	677.45	305.07	83.66	20.49	355.34
	WRA	1003	568.13	858.7	123.98	83.06	20.31	331.5
	CON	1003	462.16	850.34	132.99	80.47	19.67	440.7

The conversion rates of rainfall to soil water, groundwater, transpiration, vegetation interception, and soil evaporation were 77.45% (42.07%–93.54%), 17.40% (0.99%–52.75%), 20.73% (7.86%–39.04%), 5.18% (1.96%–12.56%), and 24.81% (11.70%–43.94%). The highest conversion rate occurred in soil water and the lowest in vegetation interception. To realize the highly efficient use of water resources, we can perform agronomic measures to lower vegetation interception, control excessive plant transpiration, halt soil water evaporation, and increase soil water and groundwater storage. Thus, crops will have sufficient water to support their growth, alleviating spring drought and karst drought in the study areas and improving the *WUE* of crops.

4. Discussion

4.1. Available Precipitation and LET at Different Scales

It is still a worldwide challenge to study the water cycle in a water-air-land-plant system from a farmland scale to a watershed or regional scale, and even to a global scale [49]. In this study, Table 2 above presents the monitored temperature and precipitation at the watershed scale, and the LET and available precipitation calculated with the Koichiro Takahashi formula. These data represent the hydrological cycle at the watershed or regional scale. Precipitation at the watershed scale was equal to the sum of the available precipitation and LET, forming a closed system. Table 3 above presents the amount of precipitation transforming into soil water storage, groundwater, soil evaporation, plant transpiration, and vegetation interception, which reflects the hydrologic cycle at the farmland scale. At this scale, precipitation was not just the summation of surface water, soil water, groundwater, and plant water, thus forming an open system. Table 3 shows that by removing soil evaporation, plant transpiration, and vegetation interception, we obtained the average available precipitation at the farmland scale (Bijie 437.98 mm, Huajiang 255.56 mm, and Shibing 569.94 mm). Compared with Table 2, the available precipitation was relatively less, except for that in Huajiang which was a little larger.

The implication of these results is that data obtained by in-situ monitoring vary from model to model even in the same place and at the same time. LET is a way of water exchange between land and air [50], including water surface evaporation, soil evaporation, and plant

transpiration [51]. Vegetation interception is all evaporated and hence was also included in LET. Accordingly, precipitation at the farmland scale goes into two types: available precipitation and LET. The latter is the second largest component of the water cycle, accounting for 50.69% of precipitation in this study and 44.4% in another [52]. The Current global evapotranspiration products are derived from a variety of sources, including models, remote sensing, and in situ observations. However, existing approaches contain extensive uncertainties. The LET amount obtained varied when calculated by different methods at the same scale or with the same method at different scales. Nevertheless, in almost all studies, it is positively correlated with temperature and precipitation [53]. From the perspective of improving WUE, LET needs slowing down, and at the farmland scale, agroforestry contributes to increasing vegetation coverage and lowering forest temperature [13].

4.2. The Water-Saving Function of Agronomic Treatments in Agroforestry

Configurations of agroforestry are a biological measure to save water and belong to a water-saving value-added industry [13,54]. It is under the category of water-saving agriculture, being able to enhance water retention [55]. Compared to row crops, agroforestry practices help reduce runoff losses from the watershed and promote soil water infiltration, whereby it increases soil water storage [13,29,56,57]. Different agroforestry configurations have varying capacities for water retention. In Dehra Dun, India, researchers monitored the surface runoff of agroforestry at an erosion plot (90 × 15 m), finding that the runoff in a maize-wheat + leucaenad model (209.3 mm) was more than that in a maize-wheat + eucalyptus model (141.8 mm) [58]. This has also been confirmed in other studies: agroforest of eucalyptus has shown a superior water-retention capacity to the agroforestry of leucaenad; there are gaps between the soil moisture contents under different agroforestry systems [59].

Agronomic treatments also contribute to water saving. Compared to traditional tillage, agronomic tillage improved water productivity and increased soil organic carbon and total soil nitrogen [60]. In India, Manohar et al. [61] practiced four types of mulching tillage: Green gram (*Vigna radiatus*), Black gram (*Vigna mungo*), Sun hemp (*Crotalaria juncea*), and Daincha (*Sesbania aculeata*). When a comparison was made between these experimental models and the control group (without legume green mulching), they found that mulching tillage showed larger water-holding capacity and richer soil moisture (Figure 4). Summing up, different configurations of agroforestry produce varying water-saving functions. Agronomic measures do manifest water-retention capacity to varying degrees. Therefore, a combination of the two will significantly enhance the water-retaining function of agroforestry in karst areas.

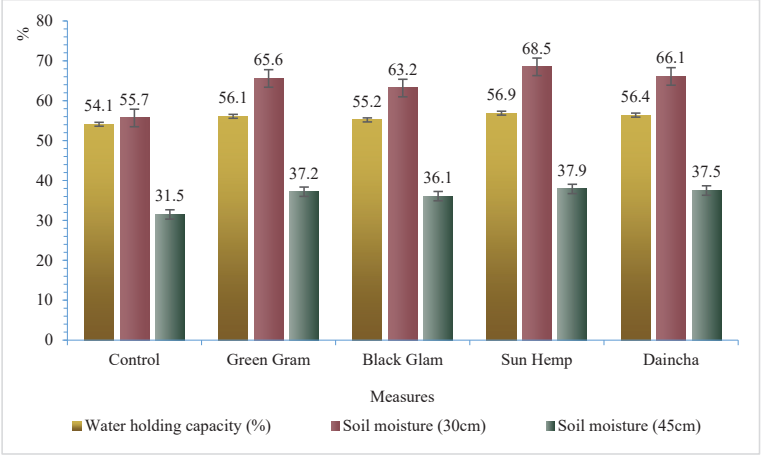

Figure 4. Water-holding capacity and soil moisture content under various agronomic measures.

4.3. Standard Selection for WUE and Improvement of Crop WUE by Agroforestry

WUE is the only effective index to evaluate the efficient water use of crops [62]. Improving WUE is essential for the advancement of agricultural production [63]. There are multiple standards for WUE, including leaf WUE, yield WUE, and community WUE [62,64]. Leaf WUE indicates the physiological characteristics of the crops and is of biological significance. Yield WUE manifests the average significance, yet fails to show the dynamic water consumption law of crops. While community WUE reflects the dynamic characteristics of crop water consumption, there is no consensus on whether crop water consumption refers to transpiration or evapotranspiration [65]. In view of such understandings, the suggestion is to combine WUE standard selection with the actual needs of the research. In the case of our study, since we aimed to identify the dynamic water consumption law of agroforestry in the three study areas, the pruning and weighing method was adopted to test the dynamic water consumption of leaves, which employed the leaf WUE stand.

Luxury transpiration refers to the extra part of water consumption that exceeds the necessary amount for the physiological and metabolic requirements of crops, the transfer and transportation of nutrients, the production of photosynthetic substances, and the formation of yield [65]. Luxury transpiration tends to lower the WUE. However, when drought stress occurs, it can be slowed down, so that the WUE is once again improved [49]. In all the planting models in Bijie, Huajiang, and Shibing, the highest water consumption through transpiration was found in the *Rosa roxburghii* + *Ryegrass* model, and lowered successively in the *Walnut* + *potato*, *Zanthoxylum planispinum var. Dintanensis* + *Chili*, *Osmanthus fragrans*, *Pseudostellariae Radixo*, *Pseudostellariae Radixo* monoculture, and *Pitaya* + *Zanthoxylum planispinum var. Dintanensis* models. Yet a different law was found in WUE, which reached the bottom in the *Rosa roxburghii* + *Ryegrass* model, and then rose successively in the *Walnut* + *Potato*, *Pseudostellariae Radixo* monoculture, *Zanthoxylum planispinum var. Dintanensis* + *Chili*, *Osmanthus fragrans* + *Pseudostellariae Radixo*, and *Pitaya* + *Zanthoxylum planispinum var. Dintanensis* models. Of these models, *Walnut* + *Potato*, with the lowest WUE (0.892 kg t^{-1}), transpired the most (342.070 mm). Conversely, *Pitaya* + *Zanthoxylum planispinum var. Dintanensis* transpired the least (44.021 mm) but reached the highest WUE (6.510 kg t^{-1}) (Figure 5). WUE was negatively correlated with transpiration ($p < 0.01$). The results suggest that crop WUE can be improved by reducing crop transpiration using effective ways such as drought stress, pruning, and dwarf dense planting. These measures will effectively decrease luxury transpiration and thus enhance the crop WUE.

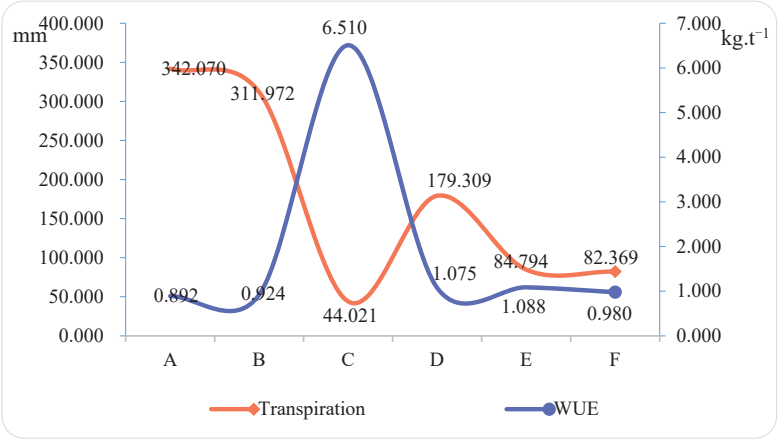

Figure 5. Transpiration and water use efficiency of crops under different planting models.

5. Conclusions

The unique hydrological cycle of the karst regions serves to be the basis for the efficient utilization of crop water resources. Agroforestry, a type of water-saving value-added industry, produces changing water-saving benefits with different configurations. Hence, varying configurations of agroforestry are in the agronomic water-saving category. To different degrees, agronomic treatments help to hold water, increase the conversion amount of effective water resources and weaken that of the ineffective ones. The combination of agroforestry and agronomic measures highlights the water-saving ability of crops. In this study, monitoring the farmland hydrological cycle generated the following results. (1) Precipitation was significantly positively related to the available precipitation and LET. The highest correlation coefficient was found with available precipitation, followed by evapotranspiration. (2) The soil water content under all agronomic measures was more than that of the control group while evaporation was less. This indicates that agronomic measures can halt soil evaporation, increase soil water content and promote efficient use of water resources. (3) Plant water consisted of transpiration consumption and vegetation interception. The latter fully evaporated and belonged to ineffective water consumption. When transpiration exceeded the minimum water consumption required for normal production, it was luxury transpiration. Transpiration, transpiration rate, and vegetation interception were positively associated with biomass. As a result, we can adopt dwarf-dense planting and pruning to reduce biomass to bring down luxury transpiration and improve the WUE. (4) In the cycle of precipitation transformation, most transformed into soil water; some transformed into groundwater, soil evaporation, and transpiration, and the least into vegetation interception. More water was transformed into soil water, which can satisfy the soil water absorption by crops and enhance water resource utilization. The conclusions of this study can provide a reference for other karst areas to develop water-saving value-added industries and improve the efficiency of water resource utilization.

Author Contributions: Conceptualization, Q.W. and J.X.; methodology, R.L.; software, J.X.; validation, K.X., R.L. and J.X.; formal analysis, Q.W.; investigation, Q.W.; resources, K.X.; data curation, Q.W.; writing—original draft preparation, Q.W.; writing—review and editing, Q.W.; visualization, J.X.; supervision, K.X.; project administration, K.X.; funding acquisition, K.X. All authors have read and agreed to the published version of the manuscript.

Funding: This study was supported by The China Overseas Expertise Introduction Program for Discipline Innovation (No. D17016), the Key Project of Science and Technology Program of Guizhou Province (No. 5411 2017 Qiankehe Pingtai Rencai), the Natural Science Foundation of Guizhou Province (No. 317 2022 QianKeHe JiChu -ZK), and the Science and Technology Support Plan of Guizhou Province (No. 462 2021 QianKeHe ZhiCheng).

Data Availability Statement: Data are contained within the article.

Conflicts of Interest: The authors declare no conflict of interest.

References

1. Ford, D.C.; Williams, P.W. *Karst Hydrogeology and Geomorphology*; Wiley: Chichester, UK, 2007; p. 9. [CrossRef]
2. Li, Y.; Liu, Z.; Liu, G.; Xiong, K.; Cai, L. Dynamic Variations in Soil Moisture in an Epikarst Fissure in the Karst Rocky Desertification Area. *J. Hydrol.* **2020**, *591*, 125587. [CrossRef]
3. Qi, X.; Zhang, C.; Wang, K. Comparing Remote Sensing Methods for Monitoring Karst Rocky Desertification at Sub-pixel Scales in a Highly Heterogeneous Karst Region. *Sci. Rep.* **2019**, *9*, 13368. [CrossRef]
4. Deng, X.; Xiong, K.; Yu, Y.; Zhang, S.; Kong, L.; Zhang, Y. A Review of Ecosystem Service Trade-Offs/Synergies: Enlightenment for the Optimization of Forest Ecosystem Functions in Karst Desertification Control. *Forests* **2023**, *14*, 88. [CrossRef]
5. Zhao, L.; Hou, R. Human causes of soil loss in rural karst environments: A case study of Guizhou, China. *Sci. Rep.* **2019**, *9*, 3225. [CrossRef]
6. Zhang, Y.; Tian, Y.; Li, Y.; Wang, D.; Tao, J.; Yang, Y.; Lin, J.; Zhang, Q.; Wu, L. Machine learning algorithm for estimating karst rocky desertification in a peak-cluster depression basin in southwest Guangxi, China. *Sci. Rep.* **2022**, *12*, 19121. [CrossRef]
7. Zhou, H.; Xu, X.; Jiang, X.; Ding, B.; Wu, P.; Ding, F. Plant Functional Trait Responses to Dolomite and Limestone Karst Forests in Southwest China. *Forests* **2022**, *13*, 2187. [CrossRef]

8. Qi, D.; Wieneke, X.; Xue, P.; DeSilva, W. Total nitrogen is the main soil property associated with soil fungal community in karst rocky desertification regions in southwest China. *Sci. Rep.* **2021**, *11*, 10809. [CrossRef]
9. Jiang, M.; Lin, Y.; Chan, T.O.; Yao, Y.; Zheng, G.; Luo, S.; Zhang, L.; Liu, D. Geologic factors leadingly drawing the macroecological pattern of rocky desertification in southwest China. *Sci. Rep.* **2020**, *10*, 1440. [CrossRef]
10. Wu, Z.; Zhu, D.; Xiong, K.; Wang, X. Dynamics of landscape ecological quality based on benefit evaluation coupled with the rocky desertification control in South China Karst. *Ecol. Indic.* **2022**, *138*, 108870. [CrossRef]
11. Burrell, A.L.; Evans, J.P.; De Kauwe, M.G. Anthropogenic climate change has driven over 5 million km^2 of drylands towards desertification. *Nat. Commun.* **2020**, *11*, 3853. [CrossRef]
12. Huang, X.; Zhou, Y.; Wang, S.; Zhang, Z. Occurrence mechanism and prediction of rocky land degradation in karst mountainous basins with the aid of GIS technology, a study case in Houzhai River Basin in southwestern China. *Environ. Earth Sci.* **2019**, *78*, 217. [CrossRef]
13. Wu, Q.; Liang, H.; Xiong, K.; Li, R. Eco-benefits coupling of agroforestry and soil and water conservation under KRD environment: Frontier theories and outlook. *Agroforest Syst.* **2019**, *93*, 1927–1938. [CrossRef]
14. Wu, Q.; Liang, H.; Xiong, K.; Li, R. Efectiveness of monitoring methods for soil leakage loss in karst regions. *Environ. Earth Sci.* **2021**, *80*, 278. [CrossRef]
15. Xiao, J.; Xiong, K. A review of agroforestry ecosystem services and its enlightenment on the ecosystem improvement of rocky desertification control. *Sci. Total Environ.* **2022**, *852*, 158538. [CrossRef]
16. Bryan, B.A.; Gao, L.; Ye, Y.; Sun, X.; Connor, J.D.; Crossman, N.D.; Stafford-Smith, M.; Wu, J.; He, C.; Yu, D.; et al. China's response to a national land-system sustainability emergency. *Nature* **2018**, *559*, 193–204. [CrossRef]
17. Li, C.; Fu, B.; Wang, S.; Stringer, L.C.; Wang, Y.; Li, Z.; Liu, Y.; Zhou, W. Drivers and impacts of changes in China's drylands. *Nat. Rev. Earth Environ.* **2021**, *2*, 858–873. [CrossRef]
18. Tong, X.; Brandt, M.; Yue, Y.; Horion, A.S.; Wang, K.; Keersmaecker, W.D.; Tian, F.; Schurgers, G.; Xiao, X.; Luo, Y.; et al. Increased vegetation growth and carbon stock in China karst via ecological engineering. *Nat. Sustain.* **2018**, *1*, 44–50. [CrossRef]
19. Zhao, M.; Zhang, J.; Velicogna, I.; Liang, C.; Li, Z. Ecological restoration impact on total terrestrial water storage. *Nat. Sustain.* **2021**, *4*, 56–62. [CrossRef]
20. Pitty, A. Calcium Carbonate Content of Karst Water in relation to Flow-through Time. *Nature* **1968**, *217*, 939–940. [CrossRef]
21. Jiang, Z.; Liu, H.; Wang, H.; Peng, J.; Meersmans, J.; Green, S.M.; Quine, T.A.; Wu, X.; Song, Z. Bedrock geochemistry influences vegetation growth by regulating the regolith water holding capacity. *Nat. Commun.* **2020**, *11*, 2392. [CrossRef]
22. Leakey, R.R.B. A re-boot of tropical agriculture benefits food production, rural economies, health, social justice and the environment. *Nat. Food* **2020**, *1*, 260–265. [CrossRef]
23. Grass, I.; Kubitza, C.; Krishna, V.V.; Corre, M.D.; Mußhoff, O.; Pütz, P.; Drescher, J.; Rembold, K.; Ariyanti, E.S.; Barnes, A.D.; et al. Trade-offs between multifunctionality and profit in tropical smallholder landscapes. *Nat. Commun.* **2020**, *11*, 1186. [CrossRef]
24. Blaser, W.J.; Oppong, J.; Hart, S.P.; Landolt, J.; Yeboah, E.; Six, J. Climate-smart sustainable agriculture in low-to-intermediate shade agroforests. *Nat. Sustain.* **2018**, *1*, 234–239. [CrossRef]
25. Syano, N.M.; Nyangito, M.M.; Wasonga, O.V.J.; Yeboah, L.E.; Six, J. Agroforestry practices and factors influencing their adoption by communities in the drylands of Eastern Kenya. *Agroforest. Sys.* **2022**, *96*, 1225–1235. [CrossRef]
26. Doelman, J.C.; Stehfest, E. The risks of overstating the climate benefits of ecosystem restoration. *Nature* **2022**, *609*, E1–E3. [CrossRef]
27. Wurz, A.; Tscharntke, T.; Martin, D.A.; Osen, K.; Rakotomalala, A.A.N.A.; Raveloaritiana, E.; Andrianisaina, F.; Dröge, S.; Fulgence, T.R. Win-win opportunities combining high yields with high multi-taxa biodiversity in tropical agroforestry. *Nat. Commun.* **2022**, *13*, 4127. [CrossRef]
28. Zeppetello, L.R.V.; Cook-Patton, S.C.; Parsons, L.A.; Wolff, N.H.; Kroeger, T.; Battisti, D.S.; Bettles, J.; Spector, J.T.; Balakumar, A.; Masuda, Y.J. Consistent cooling benefits of silvopasture in the tropics. *Nat. Commun.* **2022**, *13*, 708. [CrossRef]
29. Zhu, X.; Liu, W.; Chen, J.L.; Bruijnzeel, A.; Mao, Z.; Yang, X.; Cardinael, R.; Meng, F.R.; Sidle, R.; Seitz, S.; et al. Reductions in water, soil and nutrient losses and pesticide pollution in agroforestry practices: A review of evidence and processes. *Plant Soil* **2020**, *453*, 45–86. [CrossRef]
30. Sari, R.R.; Rozendaal, D.M.A.; Saputra, D.D.; Hairiah, K.; Roshetko, J.M.; Noordwijk, M. Balancing litterfall and decomposition in cacao agroforestry systems. *Plant Soil* **2022**, *473*, 251–271. [CrossRef]
31. Ling, Q.; Zhao, X.; Wu, P.; Gao, X.; Sun, W. Effect of the fodder species canola (*Brassica napus* L.) and daylily (*Hemerocallis fulva* L.) on soil physical properties and soil water content in a rainfed orchard on the semiarid Loess Plateau, China. *Plant Soil* **2020**, *453*, 209–228. [CrossRef]
32. Hombegowda, H.C.; Köhler, M.; Röll, A.; Hölscher, D. Tree species and size influence soil water partitioning in coffee agroforestry. *Agroforest. Syst.* **2020**, *94*, 137–149. [CrossRef]
33. Huo, G.; Zhao, X.; Gao, X.; Wang, S. Seasonal effects of intercropping on tree water use strategies in semiarid plantations: Evidence from natural and labelling stable isotopes. *Plant Soil* **2020**, *453*, 229–243. [CrossRef]
34. Liu, H.; Tang, J.; Zhang, X.; Wang, R.; Zhu, B.; Li, N.; Liang, C.; Zhao, P. Seasonal variations of groundwater recharge in a small subtropical agroforestry watershed with horizontal sedimentary bedrock. *J. Hydrol.* **2021**, *596*, 125703. [CrossRef]
35. Zhang, R.; Xu, X.; Liu, M.; Zhang, Y.; Xu, C.; Yi, R.; Luo, W. Comparing evapotranspiration characteristics and environmental controls for three agroforestry ecosystems in a subtropical humid karst area. *J. Hydrol.* **2018**, *563*, 1042–1050. [CrossRef]

36. Villalobos, F.J.; Fereres, E. Evaporation Measurements beneath Corn, Cotton, and Sunflower Canopies. *Agron. J.* **1990**, *82*, 1153–1159. [CrossRef]
37. Peng, J.; Li, G.; Wu, F. Analysis on the Changes of Utilizable Precipitation over Dongting Lake Region during the Past 100 Years. *Ecol. Environ. Sci.* **2017**, *26*, 104–110. (In Chinese) [CrossRef]
38. Sun, Z.; Wang, S.; Liu, J.; Gu, J.; Gong, W. Driving Force Analysis of Runoff Attenuation in Tuwei River Basin. *J. Nat. Resour.* **2017**, *32*, 310–320. (In Chinese) [CrossRef]
39. Wang, K.; Chen, H.; Zeng, F.; Yue, Y.; Zhang, W.; Fu, Z. Ecological Research Supports Eco-environmental Management and Poverty Alleviation in Karst Region of Southwest China. *Bull. Chin. Acad. Sci.* **2018**, *33*, 213–222. (In Chinese) [CrossRef]
40. Zhang, C.; Di, Z.; Duan, Q.; Wei, G. Improved land evapotranspiration simulation of the community land model using a surrogate-based automatic parameter optimization method. *Water* **2020**, *12*, 943. [CrossRef]
41. Liu, J.; Jia, B.; Xie, Z.; Shi, C. Ensemble Simulation of Land Evapotranspiration in China Based on a Multi-Forcing and Multi-Model Approach. *Adv. Atmos. Sci.* **2016**, *33*, 673–684. [CrossRef]
42. He, G.; Zhao, Y.; Wang, J.; Gao, X.; He, F.; Li, H.; Zhai, J.; Wang, Q.; Zhu, Y. Attribution analysis based on Budyko hypothesis for land evapotranspiration change in the Loess Plateau, China. *J. Arid Land* **2019**, *11*, 939–953. [CrossRef]
43. Lu, G.; Meng, P.; Ma, X. Study on the plant transpiration and system evapotranspiration within an agroforest system of forest belt-fruit tree crop. *J. China Agric. Univ.* **1996**, *1*, 103–109. (In Chinese)
44. Shi, L.; Sheng, H.; Man, X.; Cai, T. A review of the calculation method of water consumption by tree transpiration in different scales. *J. Nanjing For. Univ. (Nat. Sci. Ed.)* **2016**, *40*, 149–156. (In Chinese) [CrossRef]
45. Rong, R.; Sun, B.; Wu, Z.; Gao, Z.; Du, Z.; Teng, S. Study on above-ground biomass measurement of Caragana microphylla in shrub-encroached grassland. *Acta Prataculturae Sin.* **2023**, *32*, 36–47. (In Chinese) [CrossRef]
46. Tong, C.; Zhang, L.; Wang, W.; Gauci, V.; Marrs, R.; Liu, B.; Jia, R.; Zeng, C. Contrasting nutrient stocks and litter decomposition in stands of native and invasive species in a sub-tropical estuarine marsh. *Environ. Res.* **2011**, *111*, 909–916. [CrossRef]
47. Liu, B.G.; Tong, C.; Huang, J.F.; Tan, J.; Li, H. Estimation models of green and dead standing aboveground biomass of Cyperus malaccensis. *Chin. J. Ecol.* **2022**, *41*, 2163–2170. [CrossRef]
48. Yang, C.; Yao, W.; Xiao, P.; Qin, D. Effects of vegetation cover structure on runoff and sediment yield and its regulation mechanism. *J. Hydraul. Eng.* **2019**, *50*, 1078–1085. (In Chinese) [CrossRef]
49. Wu, Q. *Occurrence and Transformation of 'Five Water' and High Efficient Utilization Model of Agroforestry in the Karst Rocky Desertification Environment*; Guizhou Normal University: Guiyang, China, 2020.
50. Chen, Y.; Wen, J.; Liu, R.; Lu, X.; Chen, Y. Study on the spatial-temporal distribution pattern of land surface evapotranspiration over the source region of the Yellow River. *Plateau Mt. Meteorol. Res.* **2021**, *41*, 35–42. [CrossRef]
51. Yang, M.; Zhong, P.; Wang, M.; Shang, Y.; Cheng, C. Comparative study on the methods of estimating land surface evaporation in Dawenhe River basin. *South North Water Transf. Water Sci. Technol.* **2017**, *15*, 50–55. (In Chinese)
52. Zhao, M.; Liu, Y.; Konings, A.G. Evapotranspiration frequently increases during droughts. *Nat. Clim. Chang.* **2022**, *12*, 1024–1030. [CrossRef]
53. Pascolini-Campbell, M.; Reager, J.T.; Chandanpurkar, H.A.; Rodell, M. A 10 per cent increase in global land evapotranspiration from 2003 to 2019. *Nature* **2021**, *593*, 543–547. [CrossRef]
54. Wu, Q.; Liang, H.; Xiong, K.; Li, R. Frontier theories and countermeasures for Integrated regulation of soil and water loss and mountainous agroforestry in rocky desertification environment. *J. Soil Water Conserv.* **2018**, *32*, 11. [CrossRef]
55. Muthee, K.; Duguma, L.; Majale, C.; Mucheru-Muna, M.; Wainaina, P.; Minang, P. A quantitative appraisal of selected agroforestry studies in the Sub-Saharan Africa. *Heliyon* **2022**, *8*, e10670. [CrossRef]
56. Sahin, H.; Anderson, S.H.; Udawatta, R.P. Water infiltration and soil water content in claypan soils influenced by agroforestry and grass buffers compared to row crop management. *Agroforest. Syst.* **2016**, *90*, 839–860. [CrossRef]
57. Anderson, S.H.; Udawatta, R.P.; Seobi, T.; Garrett, H.E. Soil water content and infiltration in agroforestry buffer strips. *Agroforest. Syst.* **2009**, *75*, 5–16. [CrossRef]
58. Narain, P.; Singh, R.K.; Sindhwal, N.S.; Joshie, P. Agroforestry for soil and water conservation in the western Himalayan Valley Region of India 1. Runoff, soil and nutrient losses. *Agroforest. Syst.* **1997**, *39*, 175–189. [CrossRef]
59. Luo, D.; Xiong, K.; Wu, C.; Gu, X.; Wang, Z. Soil Moisture and Nutrient Changes of Agroforestry in Karst Plateau Mountain: A Monitoring Example. *Agronomy* **2023**, *13*, 94. [CrossRef]
60. Chaki, A.K.; Gaydon, D.S.; Dalal, R.C.; Bellotti, W.D.; Gathala, M.K.; Hossain, A.; Menzies, N.W. Achieving the win–win: Targeted agronomy can increase both productivity and sustainability of the rice–wheat system. *Agron. Sustain. Dev.* **2022**, *42*, 113. [CrossRef]
61. Manohar Reddy, R.; Ramkuma. Prospect and importance of green mulching on the soil status of tropical tasar plantation fields in India. *Nat. Preced.* **2011**, *6388*, 1–13. [CrossRef]
62. Dong, B.; Liu, H.; Wang, Y.; Qiao, Y.; Zhang, M.; Yang, H.; Jin, L.; Liu, M. Physio-ecological regulating mechanisms for highly efficient water use of crops. *Chin. J. Eco-Agric.* **2018**, *26*, 1465–1475. (In Chinese) [CrossRef]
63. Cui, Z.; Gao, Y.; Guo, L.; Wu, B.; Yan, B.; Wang, Y.; Liu, H.; Li, G.; Wang, Y.; Wang, H. Optimal Effects of Combined Application of Nitrate and Ammonium Nitrogen Fertilizers with a Ratio of 3:1 on Grain Yield and Water Use Efficiency of Maize Sowed in Ridge–Furrow Plastic Film Mulching in Northwest China. *Agronomy* **2022**, *12*, 2943. [CrossRef]

64. Fang, Q.; Chen, Y.; Li, Q.; Yu, S.; Luo, Y.; Yu, Q.; Ou, Y. Effect of irrigation on water use efficiency of winter wheat. *Trans. Chin. Soc. Agric. Eng.* **2004**, *20*, 34–39. (In Chinese)
65. Wang, Y.; Dong, B.; Qiao, Y.; Yang, H.; Jin, L.; Liu, J.; Liu, M. Experimental study on soil water threshold of luxury transpiration in winter wheat leaves during flowering and filling stage. *Chin. J. Eco-Agric.* **2019**, *27*, 1024–1032. [CrossRef]

forests

MDPI

Article

Leaf Functional Traits of *Zanthoxylum planispinum* 'Dintanensis' Plantations with Different Planting Combinations and Their Responses to Soil

Yitong Li, Yanghua Yu * and Yanping Song

School of Karst Science, State Engineering Technology Institute for Karst Decertification Control, Guizhou Normal University, Guiyang 550001, China
* Correspondence: yuyanghua2003@163.com

Abstract: Leaf structural and physiological traits, nutrients, and other functional properties reflect the ability of plants to self-regulate and adapt to the environment. Species diversity can positively affect plant growth by improving the habitat, and offers mutual interspecies benefits. Therefore, optimizing the types of plants grown in a specific area is conducive to achieving sustainable development goals for plant growth. In this study, companion planting of *Zanthoxylum planispinum* 'dintanensis' (hereafter *Z. planispinum*) with *Prunus salicina* Lindl., *Sophora tonkinensis* Gagnep., *Arachis hypogaea* L. and *Lonicera japonica* Thunb. was investigated, along with a monoculture *Z. planispinum* plantation. The effect of different planting combinations on the adaptive mechanisms of *Z. planispinum* and its response to the soil was explored. These results revealed that *Z. planispinum* preferred the slow growth strategy of small specific leaf area, high leaf water content, and high chlorophyll content after combination with *P. salicina*. Conversely, after combination with *S. tonkinensis*, *Z. planispinum* exhibited a fast growth strategy. Combination with *A. hypogaea* enabled *Z. planispinum* to adopt a transition from slow to fast growth. *Z. planispinum* regulated its economy of growth through multiple functional trait combinations, indicating that planting combinations impacted its adaptive strategies. The adaptability of *Z. planispinum* in combination with *P. salicina*, *L. japonica*, *A. hypogaea* and *S. tonkinensis* decreased in turn, with only the adaptability of *Z. planispinum* + *S. tonkinensis* lower than that of the pure forest. Leaf functional traits were jointly influenced by soil water content, microbial biomass carbon (MBC), MB nitrogen (N), MB phosphorus (P), available N, total P and available calcium (C:N:P). The main contributors were soil water content, the different component levels and stoichiometry of elements and the MB. The results demonstrated that companion planting can promote or inhibit the growth of *Z. planispinum* by adjusting its functional traits.

Keywords: planting combinations; investment strategy; plant adaptability; soil; response; karst

Citation: Li, Y.; Yu, Y.; Song, Y. Leaf Functional Traits of *Zanthoxylum planispinum* 'Dintanensis' Plantations with Different Planting Combinations and Their Responses to Soil. *Forests* **2023**, *14*, 468. https://doi.org/10.3390/f14030468

Academic Editor: Jason G. Vogel

Received: 22 December 2022
Revised: 18 February 2023
Accepted: 22 February 2023
Published: 24 February 2023

1. Introduction

Plant functional traits are stable properties formed by their interaction with the external environment during growth and development, which can both respond to environmental changes and influence ecosystem functions [1]. The leaf is the main site of photosynthesis and a key organ for maintaining hydrological balance, sensitive to environmental changes and highly plasticity [2]. Leaf functional and structural traits such as leaf thickness (LT), specific leaf area (SLA), leaf dry-matter content (LDMC); and leaf physiological traits such as chlorophyll (Chl) content and leaf nutrient levels, can sensitively indicate the adaptive strategy, ability to adjust, and response patterns to resource competition in plants [3].

Strategic combinations of plant species according to their physiological and ecological characteristics and their spatial locations form efficient artificial composite ecosystems that promote each other. Mixed forests can change the properties of soil [4]. Variable inputs and decomposition rates of litter from configured species, as well as different types and quantities of root secretions, drive changes in the quality of soil fertility [5]. Nutrient

reabsorption efficiency among the species present also changes the nutrient concentration of the soil [6]. In addition, plant type can indirectly affect the soil microbial community by changing the soil nutrient substrate [7]. Compared with pure forests, mixed forests can significantly improve the physical properties of soil, slow soil nutrient depletion and promote biomass recycling [8,9]. However, due to niche overlap between different species in mixed forest, water and nutrient competition and allelopathy can occur [10]. Therefore, clarifying the leaf functional traits and adaptability of *Zanthoxylum planispinum* 'dintanensis' (hereafter *Z. planispinum*) plantations in different planting combinations in the karst plateau canyon area in the middle of Guizhou Province, China, is beneficial for checking suitable planting patterns.

The response and adaptation strategies of plants to the environment have long been a central question in ecological research. At a small regional scale, soil is considered to be a key factor influencing leaf functional traits [11], due to its function in providing mechanical support and nutrient supply for plant growth [12]. In addition, the carbon (C): nitrogen (N): phosphorus (P) ratios can indicate the nutrient limitations of the ecosystem, reflecting the nutrient cycle and utilization efficiency within the plants [13]. It is, therefore, important to study the content and ratio of C, N, and P, as these nutrients affect the energy cycle and stability of ecosystems [14]. In recent years, many achievements have been made in exploring the synergy and trade-offs between leaf traits and soil factors on different latitudes [15], slopes [12], climates [16], community levels [17], etc. However, studies on the relationship between leaf functional traits and soil in different planting combinations are limited. Karst ecosystems are characterized by high habitat heterogeneity, fragile environment, low soil volume and weak nutrient supply capacity [18], but the adaptation mechanisms of native plants are still unclear [19]. Therefore, the study of the interactions between the karst plant *Z. planispinum* and soil is useful to conducting an in-depth analysis of its unique ecological strategies for adaptation to this habitat.

Z. planispinum is the oldest and most widely distributed pioneer tree species in the karst, dry hot valley of Guizhou Province, China [20]. During the process of long-term adaptation to the environment, the tree has formed excellent characteristics, such as calcium (Ca) preference, drought tolerance, and the ability to grow in stony areas. In recent years, the cultivation of pure forests on a large scale has led to the gradual degradation of soil fertility and productivity. The optimization of planting *Z. planispinum* in combination with other species is based on the biodiversity theory of restoring the terrestrial ecosystem. This is essential to prevent and control rocky desertification in karst areas and achieve sustainable development goals. However, the effect of planting combinations on the leaf functional traits of *Z. planispinum* and the relationship between the leaf functional traits and soil are unclear. Therefore, in this study, we selected four common planting combinations of *Z. planispinum* with *Prunus salicina* Lindl., *Sophora tonkinensis* Gagnep., *Arachis hypogaea* L. and *Lonicera japonica* Thunb., respectively, and compared them with pure forests. This study was conducted to explore the effects of planting combinations on the leaf functional traits of *Z. planispinum* and to analyze the response mechanisms of these traits to soil factors. We aimed to: (1) clarify the adaptation mechanism and resource utilization strategy of *Z. planispinum* in different planting combinations; (2) explore the adaptability of different planting combinations; and (3) extract the main factors from the soil that drive changes in the leaf functional traits of *Z. planispinum*. This study provides a scientific basis for diversity cultivation in plantations.

2. Materials and Methods

2.1. Study Sites

The research area was located in Zhenfeng County, Guizhou Province, China (105°38′35″E, 25°39′37″N), which has a mostly subtropical humid monsoon climate (Figure 1). The average annual rainfall is 1100 mm, with severe drought in winter, spring, and summer. The average annual temperature is 18.4 °C. It is a river valley terrain, with an elevation of 370~1,473 m [21]. The soil type is mainly lime soil, with limestone as the parent material.

Carbonate rock accounts for 78.45%, pH > 6.5, the soil layer is mostly <20 cm, and the soil cover is discontinuous. The soil is rich in Ca and Mg due to its high inheritance from the parent rock. The area exhibits rocky desertification, with low forest coverage and a bedrock exposure rate of 50~80% [21,22]. The types of microhabitats such as stone surfaces, stone ditches, stone cracks, stone grooves and stone caves are diverse, and the environmental heterogeneity is high. *Z. planispinum* has become a relatively stable ecological restoration tree species with the largest planting area in the study region. In addition, there are companion species such as *Zea mays*, *L. japonica*, *P. salicina*, *S. tonkinensis*, and *Arachis hypogaea*.

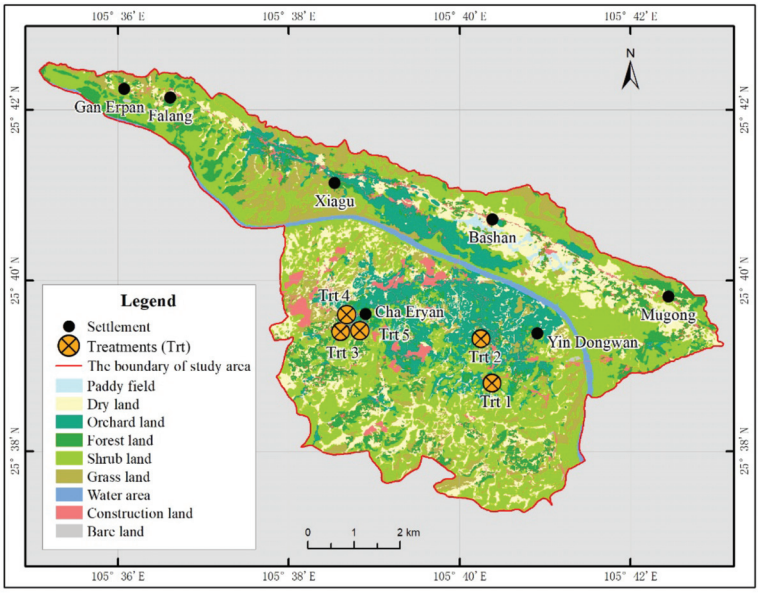

Figure 1. Distribution of treatments (Trt).

2.2. Treatment Setting

One treatment was set up for each of the five plantations (*Z. planispinum* + *P. salicina*, *Z. planispinum* + *S. tonkinensis*, *Z. planispinum* + *A. hypogaea*, *Z. planispinum* + *L. japonica*, and *Z. planispinum*) (Table 1). Before planting the experimental tree species, all treatments were planted mainly with *Z. mays*, with the same management measures and similar soil background values. In 2012, *Z. planispinum* was planted in five treatments. Since 2018, *P. salicina*, *S. tonkinensis*, *A. hypogaea*, and *L. japonica* have been planted around *Z. planispinum*. *A. hypogaea* has been planted continuously as an annual plant according to the phenology; other perennial plants are under community management. The age of the *Z. planispinum* individuals planted in the five treatments was 8 years, and the slope of all treatments was 10°. Detailed management practices for the five treatments can be found in the literature [23].

Table 1. Descriptions of plantation types.

Plantation Types	Species Combinations	Longitude	Latitude	Growing Area (ha)	Altitude (m asl)	Density (m)	Height (m)	Crown Width (m)	Coverage (%)
Trt 1	*Z. planispinum* + *P. salicina*	105°40′28.33″ E	25°37′57.41″ N	1.34	764	3 × 3	3.5	2 × 2.3	70
Trt 2	*Z. planispinum* + *S. tonkinensis*	105°40′19.79″ E	25°39′25.75″ N	0.67	728	2 × 2	2.0	1.2 × 1.8	60
Trt 3	*Z. planispinum* + *A. hypogaea*	105°38′36.32″ E	25°39′23.64″ N	0.67	791	2 × 2	2.5	2.5 × 2.8	85
Trt 4	*Z. planispinum* + *L. japonica*	105°38′36.35″ E	25°39′22.29″ N	6.67	814	3.5 × 3	2.5	1.5 × 2.5	70
Trt 5	*Z. planispinum*	105°38′35.64″ E	25°39′23.35″ N	33.35	788	3 × 4	2.2	2.5 × 2.3	65

The distance between plants was measured and expressed as "length × width", and the average value taken. Plant height was set as the distance from the root neck to the top of the main stem as measured by an altimeter. The width of the crown was measured with a tape measure, with the tree as the center. The measure was extended to the maximum value covered by the crown in the east-west and north-south directions, respectively. The average value of the two measurements was taken to obtain the width of the crown for each tree tested. For convenience in terms of operation and estimation, to measure coverage, a projected area approximately in the shape of a rectangle was measured using a tape measure. The maximum length and width of the lines corresponding to the upper part of the plant was used to estimate the projected rectangular area covered by the plant. All of the approximate projected areas of each plant in the area were added to calculate the total coverage. The calculation used to determine coverage was as follows:

$$\text{Coverage} = (S_1 + S_2 + \ldots + S_n)/S \times 100\% \quad (1)$$

2.3. Soil Sampling and Analysis

Between 19 and 21 November 2020, soil samples were collected, within a period of 15 or more consecutive sunny days. At this time, the soil material composition was relatively stable, and the degree of soil variability low. This ensured that fewer testing time-points could be used to characterize the component levels under long-term drought conditions, facilitating a better evaluation of the effect of the planting combinations on soil. Three sample squares (10 × 10 m) were set up in each treatment, with sufficient buffer strips left between the squares. Sampling points were laid along "S" lines in each sample square. We collected equal amounts of soil from the 0~10 and 10~20 cm soil layers (soil depth <20 cm) at each sample point. Samples from the same soil layer were fully mixed. The average value of the two soil layer values was taken for the final soil parameter calculation. Artificial fertilization areas (about 20 cm away from the tree trunks) were avoided as far as possible during sampling. The fresh soil samples were divided into two parts after removing gravel, root systems, and residues from animals and plants. One part was dried and passed through a 0.15 mm sieve to determine the soil nutrient contents. The other was sieved through a 2 mm sieve and stored at 4 °C to determine the microbial biomass as quickly as possible.

The soil water content (SWC) was measured with a TR-6 soil temperature and humidity meter. Soil pH was determined using the potentiometric method; soil organic carbon (SOC) with the potassium dichromate oxidation external heating method; total nitrogen (TN) through the Kjeldahl method; total phosphorus (TP) by using molybdenum antimony resistance colorimetry; total potassium (TK) with a sodium hydroxide melting flame photometer; and total calcium (TCa) by way of an atomic absorption spectrophotometer [24]. Available nitrogen (AN) was determined using the alkali hydrolysis diffusion method; available phosphorus (AP) using the HCl-H_2SO_4 extraction method; available potassium (AK) by flame photometry; and available calcium (ACa) content by atomic absorption spectrophotometry [25]. Soil microbial biomass carbon (MBC), nitrogen (MBN) and phosphorus (MBP) were determined with the chloroform fumigation K_2SO_4 extraction method [26]. Specific data are shown in Table 2. Relevant data have been previously analyzed [23]. This article uses existing data for in-depth analysis.

Table 2. Soil parameters in different planting combinations.

Soil Parameters	Trt 1	Trt 2	Trt 3	Trt 4	Trt 5
SWC	31.60 ± 6.29 ab	36.73 ± 2.65 a	25.05 ± 1.38 bc	28.69 ± 0.30 bc	21.15 ± 0.14 c
pH	6.70 ± 0.42 d	7.35 ± 0.33 bc	7.92 ± 0.05 ab	7.28 ± 0.05 cd	8.08 ± 0.05 a
SOC	37.73 ± 7.32 ab	29.40 ± 0.57 ab	28.68 ± 12.62 ab	50.83 ± 13.33 a	26.50 ± 2.19 b

Table 2. *Cont.*

Soil Parameters	Trt 1	Trt 2	Trt 3	Trt 4	Trt 5
TN	3.53 ± 0.46 ab	2.64 ± 0.07 b	2.78 ± 0.74 b	4.60 ± 0.44 a	2.76 ± 0.23 b
TP	1.37 ± 0.02 a	0.82 ± 0.03 b	1.10 ± 0.43 ab	1.52 ± 0.17 a	1.26 ± 0.04 ab
TK	6.95 ± 0.34 b	6.11 ± 1.51 b	12.33 ± 0.25 a	11.88 ± 0.53 a	10.88 ± 0.03 a
TCa	0.95 ± 0.28 b	1.48 ± 0.39 b	1.85 ± 0.71 b	1.88 ± 0.18 b	6.05 ± 0.21 a
AN	275.00 ± 74.25 ab	160.00 ± 5.66 b	161.75 ± 61.87 b	350.00 ± 55.15 a	153.75 ± 15.91 b
AP	45.80 ± 13.29 a	23.38 ± 11.63 a	26.55 ± 10.54 a	36.68 ± 10.01 a	20.08 ± 2.44 a
AK	393.00 ± 107.48 a	195.85 ± 32.03 b	172.75 ± 57.63 b	223.75 ± 98.64 ab	141.25 ± 2.47 b
ACa	317.50 ± 14.85 b	334.75 ± 0.35 b	347.75 ± 24.40 ab	371.00 ± 8.49 a	350.50 ± 7.07 ab
Soil C:N ratio	10.65 ± 0.70 a	11.13 ± 0.53 a	10.07 ± 1.85 a	10.97 ± 1.85 a	9.59 ± 0.00 a
Soil C:P ratio	27.68 ± 5.79 abc	35.83 ± 0.79 a	25.82 ± 1.33 bc	33.10 ± 4.99 ab	21.03 ± 2.38 c
Soil N:P ratio	2.59 ± 0.37 ab	3.22 ± 0.22 a	2.60 ± 0.34 ab	3.02 ± 0.05 a	2.19 ± 0.25 b
MBC	243.00 ± 4.95 a	254.75 ± 2.47 a	252.00 ± 2.83 a	262.75 ± 21.57 a	262.25 ± 26.52 a
MBN	12.40 ± 1.70 a	13.58 ± 1.31 a	14.38 ± 0.60 a	13.90 ± 1.06 a	14.08 ± 0.18 a
MBP	128.00 ± 23.33 a	144.50 ± 4.95 a	148.00 ± 8.49 a	154.50 ± 13.44 a	139.00 ± 3.54 a

Trts 1–5, five plantations, representing the research objectives of this article. SWC, soil water content; SOC, soil organic carbon; TN, total nitrogen; TP, total phosphorus; TK, total potassium; TCa, total calcium; AN, available nitrogen; AP, available phosphorus; AK, available potassium; ACa, available calcium; MBC, microbial biomass carbon; MBN, microbial biomass nitrogen; MBP, microbial biomass phosphorus. Means followed by the same lowercase letter are not significantly different ($p > 0.05$) among root types as determined by the least significance difference (LSD) test. Data are presented as mean ± standard deviation.

2.4. Leaf Sampling and Leaf Functional Trait Analysis

Z. planispinum leaves were collected in September 2021. At this time, the leaves had reached their full shape and were mature; new and old leaves could be distinguished easily. Because the treatments underwent the same nutrient management program in each growing season, the soil variations reflected the impact of the plants. In addition, as functional traits have a hysteresis effect on nutrient changes, soil and leaf samples were collected at different stages and selected at their most stable stages. Five *Z. planispinum* plants of good growth and uniform size were selected from each plot. We collected leaves of *Z. planispinum* from four directions (east, west, north, and south): 4–6 leaves from each direction. The collected leaves had good lighting conditions, were of similar size and shape, and were fully expanded and healthy. The collected leaves were wiped clean with gauze, numbered and marked, and then swiftly placed in a sealed bag for low temperature storage. Finally, they were taken back to the laboratory to determine their functional properties. In addition, about 200 g of leaves without disease and pests were collected from each plot. The samples were dried and crushed, and the contents of C, N, and P elements in the leaves were determined after passing through a 0.25 mm sieve.

On returning to the laboratory, we measured the leaf traits as soon as possible. The methods used to determine each trait specifically were as follows. Leaf fresh weight (LFW, g) of all numbered leaves was measured using a balance with an accuracy of ±0.0001 g. Leaf area (LA) was obtained by scanning the leaves using a Delta-T leaf area meter (Cambridge, UK). Electronic vernier calipers were used to measure the thickness at 0.25 cm on both sides of the main veins of the numbered leaves, and three points were selected uniformly for each leaf; the average value was taken as the leaf thickness of a single leaf. The Chl content (SPAD), as a typical physiological trait characterizing photosynthetic production capacity, was measured using a Minolta SPAD502 chlorophyll meter at three points on the main veins and leaf margins of the numbered leaves; the average value was taken to represent the Chl content of a single leaf. All numbered leaves were soaked in water for 12 h, and the water on the surface of the leaves was quickly dried with absorbent paper and weighed with an accuracy of ±0.0001 g on a balance to obtain the leaf saturated fresh weight (LSFW). After measuring the above functional trait indexes, the leaves were placed in an oven at 105 °C for 30 min and then baked at 70 °C until they achieved a constant weight to obtain

the leaf dry weight (LDW). Specific leaf area (SLA), leaf tissue density (LTD), LDMC, and leaf water content (LWC) were calculated as follows:

$$SLA = LA/LDW \quad (2)$$

$$LTD = LDW/(LA \times LT/10) \quad (3)$$

$$LDMC = LDW/LSFW \times 100\% \quad (4)$$

$$LWC = (LSFW - LDW)/LFW \times 100\% \quad (5)$$

The leaf nutrient traits included leaf carbon (LC), leaf nitrogen (LN), and leaf phosphorous (LP) contents and their stoichiometric ratios. LC, LN, and LP contents were determined with the potassium dichromate external heating method, Kjeldahl nitrogen determination, and molybdenum antimony resistance colorimetry, respectively. The stoichiometric ratios were calculated according to the element: mass ratio. The leaf functional traits selected and their ecological implications are shown in Table 3.

Table 3. Leaf functional traits and their ecological implications [27,28].

Trait	Unit	Ecological Connotation
LT	mm	LT is closely related to the rate of light energy utilization and photosynthetic efficiency, affecting the water supply and storage of leaves and the process of material and energy exchange in photosynthesis; the larger the value, the more suitable the plant for resource-deficient habitats.
SLA	cm^2	SLA reflects the carbon acquisition strategies, growth strategies, and adaptation characteristics of plants to different habitats and affects their relative growth rates; the higher the photosynthetic rate, the higher the transpiration.
LDMC	$mg \cdot g^{-1}$	LDMC reflects the ability of plants to acquire and maintain environmental resources and the tissue construction of leaves. Higher values indicate that the leaves are better able to lock up nutrients in the body and reduce losses.
LWC	%	Leaf water content is important in breeding for drought tolerance and water retention traits of plants; higher values indicate higher drought resistance.
Chl	-	The higher the Chl content, the more photosynthetically active and shade-tolerant the plant.
LTD	$g \cdot cm^{-3}$	LTD is related to resource acquisition, indicating the ability of plants to store nutrients and water and resist external interference; the higher the value, the stronger the ability to resist interference.
LC	$g \cdot kg^{-1}$	The higher the LC value, the stronger the water supply capacity of the plant in a xerophytic environment.
LN	$g \cdot kg^{-1}$	The higher the LN value, the better the chlorophyll synthesis and photosynthetic efficiency.
LP	$g \cdot kg^{-1}$	LP promotes protein synthesis and physiological repair, and improves plant cold tolerance.
Leaf C:N ratio	-	C:N is proportional to the growth rate; the higher the value, the higher the carbon fixation advantage and nutrient utilization strategy, and the stronger the carbon assimilation ability.
Leaf C:P ratio	-	C:P represents the ability of plants to assimilate carbon when absorbing nutrients and the efficiency of carbon fixation in plants; the higher the value, the higher the carbon fixation advantage and nutrient utilization strategy, and the stronger the carbon assimilation ability.
Leaf N:P ratio	-	N:P indicates that plants are limited by nitrogen and phosphorus. If the value is >16, the plants are limited by phosphorus, if it is <14, the plants are limited by nitrogen, and between 14 and 16, both elements are limiting plant growth.

"-" indicates that the unit is dimensionless. LT, leaf thickness; SLA, specific leaf area; LDMC, leaf dry-matter content; LWC, leaf water content; Chl, chlorophyll; LTD, leaf tissue density; LC, leaf carbon content; LN, leaf nitrogen content; LP, leaf phosphorus content.

2.5. Data Analysis

The Kolmogorov-Smirnov method was used to test the normality of each index. With a normal distribution, one-way analysis of variance (ANOVA) was performed using SPSS

20.0 (version 20.0, IBM SPSS, Armonk, NY, USA) to test the variability of the soil properties and leaf functional traits. The LSD test was used for post hoc multiple comparisons. Dunnett's T3 method was adopted when the distribution was not normal. The coefficient of variation (CV) is equal to the ratio of the standard deviation and mean value. Generally, CV $\leq$ 20% shows weak variation; 20% < CV $\leq$ 50% reflects moderate variation; and CV > 50% indicates strong variation [29]. The plasticity index (PI) indicates the degree of the response of traits to the planting combinations. The higher the value, the more sensitive the plant is to the external environment. For the calculation method, refer to Valladares et al. [30]:

$$\text{PI} = (\text{maximum} - \text{minimum})/\text{maximum} \quad (6)$$

The values used in the formula were all leaf functional traits. The nonlinear normal curve model was used to fit the relevant parameters of leaf functional traits. Pearson's method was used to analyze the correlation between leaf functional traits, and the "corrplot" program package in R4.1.2 software was used to plot the heatmap. Principal components (PC) analysis was used to screen out the main indexes that affected the variation in the leaf functional traits of *Z. planispinum*. Due to the different dimensions between the indicators, they were standardized and pretreated before evaluation. Then, the plant adaptability scores (PAS) of *Z. planispinum* with different planting combinations were calculated. The PAS calculation was combined with the weighted method, using the following formula:

$$\text{PAS} = \sum W_i \times F_i \quad (7)$$

where W_i is the contribution rate of each PC, and F_i is the PC score of each planting combination. By weighting the variance contribution rate (W_i) and factor score (F_i) of each PC factor, the PASs of different planting combinations are obtained.

Stepwise regression analysis was used to explore the effects of soil factors on the leaf functional traits of *Z. planispinum*. The data are expressed as mean $\pm$ standard value.

3. Results

3.1. Characteristics of Leaf Functional Traits of Z. planispinum in Different Planting Combinations

The change law of leaf functional traits of *Z. planispinum* in the five plantations are shown in Figure 2. The LT was highest in Trt 4 and was significantly greater than that in Trts 1 and 2; there was no significant difference between the other treatments. The SLA value in Trt 2 was the highest, significantly higher than that of other treatments, while that in Trt 4 was the smallest, significantly lower than that of Trts 2 and 3. The LDMC in Trt 1 was the highest, whereas that in Trt 2 was the lowest, but there was no significant difference among the five treatments. The LWC in Trt 1 was significantly lower than that in other treatments, and there was no significant difference among the other treatments. The LTD of Trt 1 was significantly higher than that of Trt 2. The Chl contents in Trts 1 and 5 were significantly higher than those in the other three treatments. The CV among different plantations was 5.8~26.9%, with the largest CV seen in Chl (26.9%), which indicated moderate variation, followed by LT (19.1%), LTD (18.0%), SLA (13.6%), and LDMC (9.1%); LWC had the lowest CV (5.8%).

The ANOVA results show that LC, LN, LP, leaf C:N, leaf C:P, and leaf N:P were not significantly different among the five plantations (Table 4). This indicated strong stability in the leaf nutrition index.

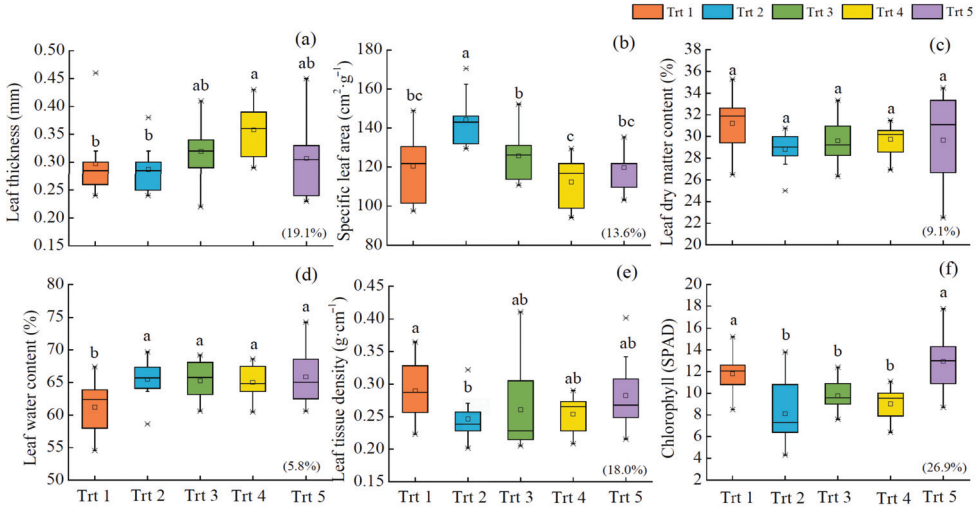

Figure 2. Leaf thickness (**a**), specific leaf area (**b**), leaf dry matter content (**c**), leaf water content (**d**), leaf tissue density (**e**) and chlorophyll (**f**) of *Z. planispinum* in different planting combinations. Trts 1–5, five plantations, representing the research objects of this article. Bars show mean ± standard deviation, n = 30. "□" in the box plot indicates the mean value of individual plant traits; different lowercase letters indicate significant differences between trait values ($p < 0.05$); percentages in parentheses are the CV.

Table 4. Carbon, nitrogen, and phosphorus contents and stoichiometric ratios of *Z. planispinum* leaves.

Plantation Type	LC (g·kg^{-1})	LN (g·kg^{-1})	LP (g·kg^{-1})	Leaf C:N Ratio	Leaf C:P Ratio	Leaf N:P Ratio
Trt 1	46.38 ± 1.43 a	2.79 ± 0.08 a	2.74 ± 0.34 a	16.60 ± 0.01 a	17.02 ± 1.58 a	1.03 ± 0.10 a
Trt 2	44.64 ± 4.21 a	2.93 ± 0.11 a	3.42 ± 0.72 a	15.23 ± 0.86 a	13.49 ± 4.07 a	0.88 ± 0.22 a
Trt 3	45.33 ± 4.39 a	3.11 ± 0.23 a	3.00 ± 0.16 a	14.58 ± 0.33 a	15.16 ± 2.27 a	1.04 ± 0.13 a
Trt 4	44.40 ± 2.83 a	3.20 ± 0.14 a	2.92 ± 0.42 a	13.88 ± 0.28 a	15.31 ± 1.21 a	1.10 ± 0.11 a
Trt 5	42.98 ± 0.90 a	2.85 ± 0.45 a	3.46 ± 0.51 a	15.28 ± 2.74 a	12.57 ± 2.12 a	0.82 ± 0.01 a
Coefficient variation/%	5.8	8.1	14.8	9.0	16.7	15.2

Trts 1–5, five plantations, representing the research objectives of this article. LC, leaf carbon content; LN, leaf nitrogen content; LP, leaf phosphorus content. Means followed by the same lowercase letter are not significantly different ($p > 0.05$) among root types as determined by the LSD test. Data are presented as mean ± standard deviation.

3.2. Plasticity of Leaf Functional Traits of Z. planispinum in Different Planting Combinations

The PI values for Chl, LT, and LTD were higher than those for the other traits (PI > 0.50), indicating that they were sensitive to the planting combinations. In contrast, the plasticity change of LC was the least sensitive (PI < 0.20) and inert in response to the planting combination (Figure 3). These findings imply that the Chl content as a physiological trait, and LT and LTD as structural traits were more sensitive to the planting combinations.

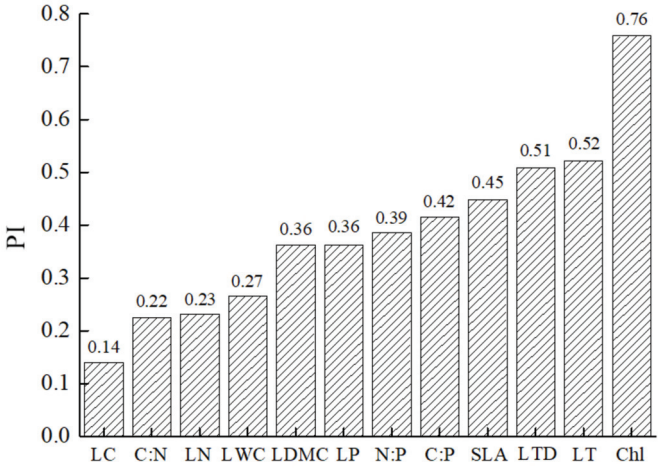

Figure 3. Plasticity index of the leaf functional traits of *Z. planispinum*. LT, leaf thickness; SLA, specific leaf area; LDMC, leaf dry-matter content; LWC, leaf water content; Chl, chlorophyll; LTD, leaf tissue density; LC, leaf carbon content; LN, leaf nitrogen content; LP, leaf phosphorus content; C:N, leaf C:N ratio; C:P, leaf C:P ratio; N:P, leaf N:P ratio.

3.3. Correlation Analysis of the Leaf Functional Traits of Z. planispinum in Different Planting Combinations

Leaf thickness had significant negative correlations with SLA. Three pairs of traits were significantly positively correlated: Chl and LTD, LC and leaf C:P, and leaf N:P and C:P, respectively. Leaf water content was negatively and positively correlated with LDMC and LN, respectively. Leaf nitrogen content was significantly negatively correlated with leaf C:N, as was LP with leaf C:P and N:P. The correlations between LC, LN, and LP contents and their ratios were more significant than those between the other leaf functional traits (Figure 4).

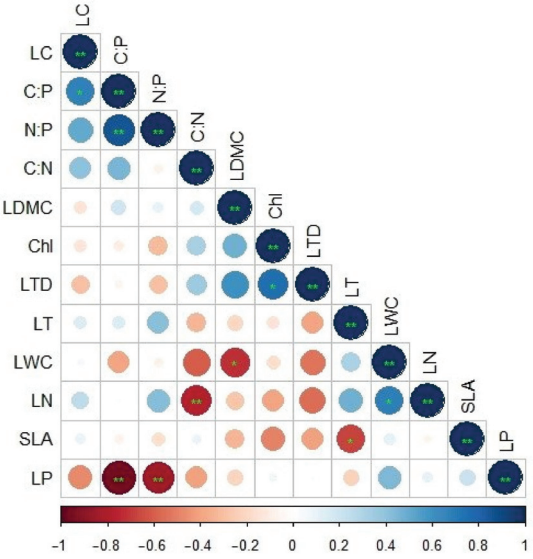

Figure 4. Correlation analysis of the leaf functional traits of *Z. planispinum*. LT, leaf thickness; SLA,

specific leaf area; LDMC, leaf dry-matter content; LWC, leaf water content; Chl, chlorophyll; LTD, leaf tissue density; LC, leaf carbon content; LN, leaf nitrogen content; LP, leaf phosphorus content; C:N, leaf C:N ratio; C:P, leaf C:P ratio; N:P, leaf N:P ratio. Red indicates negative correlation, blue indicates positive correlation, and the darker the color, the stronger the significance. * Correlation is significant at the 0.05 level (2-tailed). ** Correlation is significant at the 0.01 level (2-tailed).

3.4. Analysis of the Adaptability of *Z. planispinum* in Different Planting Combinations

Following a PC analysis of the leaf functional traits of *Z. planispinum*, four principal components were extracted, which explained 88.41% of the cumulative variance. This finding indicated that these principal components could explain most of the information about the original variables (Table 5). Among them, the first was significantly positively correlated with LC, leaf C:P, and N:P, while it was significantly negatively correlated with LP. The second principal component was greatly affected by LN and had a positive effect on leaf C:N. The first and second principal components represented the LC, LN, and LP contents and their ratios. The third principal component had a significant negative correlation with LDMC and a significant positive correlation with LWC, representing the nutrients and water stored in the leaves. The fourth principal component was mainly controlled by SLA.

Table 5. Principal component analysis of leaf functional traits of *Z. planispinum*.

Factors	Load Matrix of Principal Component			
	PCA1	**PCA2**	**PCA3**	**PCA4**
LT	0.291	−0.508	0.309	0.625
SPAD	−0.235	0.534	−0.249	0.647
SLA	−0.097	0.114	0.210	**−0.943**
LDMC	0.104	0.115	**−0.873**	0.212
LWC	−0.305	−0.440	**0.769**	0.090
LTD	−0.217	0.520	−0.614	0.388
LC	**0.727**	0.196	0.452	−0.018
LN	0.107	**−0.823**	0.364	0.091
LP	**−0.928**	−0.076	0.220	−0.088
Leaf C:N ratio	0.366	**0.912**	−0.047	−0.055
Leaf C:P ratio	**0.979**	0.121	−0.107	−0.009
Leaf N:P ratio	**0.887**	−0.406	−0.076	0.052
Eigenvalue	3.905	3.586	2.068	1.050
Variance contribution rate/%	29.838	23.051	19.480	16.035
Cumulative variance contribution rate/%	29.838	52.889	72.370	88.405

LT, leaf thickness; SLA, specific leaf area; LDMC, leaf dry-matter content; LWC, leaf water content; Chl, chlorophyll; LTD, leaf tissue density; LC, leaf carbon content; LN, leaf nitrogen content; LP, leaf phosphorus content. Bold font is the relatively large influence factor of each main component load factor.

The plant adaptability scores of *Z. planispinum* in different planting combinations were calculated (Table 6). The results showed that the *Z. planispinum* in Trt 1 had the strongest adaptability, followed by Trt 4, while Trt 2 had the lowest adaptability. The factor 3 score of Trt 1 was the lowest, indicating that it was mainly affected by the LDMC and LMC. The factor 4 score of Trt 2 was the lowest, and the SLA of Trt 2 was significantly higher than that of other treatments, which indicated that the SLA of *Z. planispinum* in Trt 2 was mainly affected by the high SLA. Trts 3 and 4 had the lowest factor 2 scores, indicating that they were highly restricted by LN and leaf C:N. The factor 1 score of Trt 5 was the lowest, indicating that it was mainly affected by LC, LP, and leaf C:P and N:P.

Table 6. Factor scores of leaf functional traits of *Z. planispinum*.

Sample Site	Factor Score				Soil Quality Index	Rank
	F_1	F_2	F_3	F_4		
Trt 1	1.409	1.934	**−2.516**	0.959	0.530	1
Trt 2	−0.93	−0.187	1.526	**−3.292**	−0.552	5
Trt 3	0.466	**−0.746**	0.631	−0.178	0.061	3
Trt 4	0.904	**−1.821**	0.731	1.303	0.201	2
Trt 5	**−1.844**	0.820	−0.373	1.208	−0.240	4

Trts 1–5, five plantations, representing the research objectives of this article. The bold font indicates the factor with the lowest score.

3.5. Effects of Soil Factors on Leaf Functional Traits

The Shapiro-Wilk normality test was performed for the 12 functional trait indicators (dependent variables). The data analysis revealed that the significance level of all indicators was greater than 0.05, indicating that the dependent variables obeyed a normal distribution, so the next step of the stepwise regression analysis was carried out.

The relationship between the leaf functional traits of *Z. planispinum* in response to soil factors was analyzed by stepwise regression (Table 7). The results showed that LT, Chl, SLA, LTD, and soil C:N were significantly correlated with the soil factor ($p < 0.05$), while the correlations between the remaining indicators and the soil factor were not ($p > 0.05$). LT was significantly correlated with MBP ($p < 0.05$). Chl was significantly correlated with soil N:P and MBN ($p < 0.01$), and in its regression equation, the standard regression coefficient of soil N:P (−0.937) was greater than that of MBN (−0.373), indicating that soil N:P was the main factor affecting Chl, while MBN was the secondary factor. SLA was highly significantly correlated with TP, SWC, and AN ($p < 0.01$), and the standardized coefficient of SWC (0.515) greater than that of TP (−0.412) and AN (−0.396), indicating that SWC was the main factor affecting SLA, followed by TP and AN. LTD was highly significantly correlated with soil N:P, soil C:P, MBC, SWC, and soil C:N ($p < 0.01$), where the standard regression coefficient was soil C:P (4.493) > soil N:P (−4.464) > soil C:N (−1.474) > MBC (−0.321) > SWC (0.21), indicating that LTD was mainly influenced by soil C:P and soil N:P. Leaf C:N had a significant correlation with ACa and MBC (p <0.05), and the standardized coefficient of ACa (−0.908) was greater than that of MBC (0.564), indicating that the main factor affecting leaf C:N was ACa, with MBC a secondary factor. In summary, leaf functional traits were jointly influenced by SWC, MBC, MBN, MBP, AN, TP, ACa, soil C:N, C:P, and N:P.

Table 7. Stepwise regression analysis of leaf functional traits and soil quality.

Leaf Functional Traits	Stepwise Regression Equation	Standardized Regression Coefficients	R-Square	*P*
LT	LT = 0.071 + 0.002 × MBP	B_{MBP} = 0.715	0.449	0.020
Chl	Chl = 29.749 – 3.814 × N:P−0.65 × MBN	$B_{N:P}$ = −0.937, B_{MBN} = −0.373	0.796	0.002
SLA	SLA = 127.27 – 17.515 × TP + 1.067 × SWC − 0.055 × AN	B_{TP} = −0.412, B_{SWC} = 0.515, B_{AN} = −0.396	0.960	0.000
LTD	LTD = 0.868–0.226 × N:P + 0.017 × C:P − 0.001 × MBC + 0.001 × SWC − 0.033 × C:N	$B_{N:P}$ = −4.464, $B_{C:P}$ = 4.493, B_{MBC} = −0.321, B_{SWC} = 0.21, $B_{C:N}$ = −1.474	0.983	0.000
Leaf C:N ratio	C:N = 20.979 – 0.058 × ACa + 0.055 × MBC	B_{ACa} = −0.908, B_{MBC} = 0.564	0.628	0.013

P is significant. C:N, soil C:N ratio; C:P, soil C:P ratio; N:P, soil N:P ratio.

4. Discussion

4.1. Effect of Planting Combinations on the Leaf Functional Traits of Z. planispinum

Plants adapt to changes in the environment by adjusting their leaf morphology and internal physiological characteristics, resulting in a rich combination of traits [31,32]. After being combined with *P. salicina*, *Z. planispinum* improved nutrient acquisition by decreasing SLA to reduce water loss from the organism [33], which is a strategy for resisting water deficit stress. After planting with *L. japonica*, *Z. planispinum* formed a combination of drought-tolerant traits, with large LT values and a small SLA. It cooperatively resisted

drought stress and adapted to the arid and barren living environment by reducing the SLA, strengthening defense tissues, storing nutrients, reducing water dissipation and improving drought tolerance and defense capabilities [34]. In general, the above two plantations had higher adaptive capacity than the other three plantations because, in addition to their stronger resource acquisition and defense functions, the former may also have more litter input to change the habitat quality. After planting with *S. tonkinensis*, *Z. planispinum* showed a rapid investment strategy of low LT, LDMC, and Chl, as well as high SLA and LWC, which met growth demands by reducing adaptability. The reasons are that the light supply to *Z. planispinum* was relatively stable after planting with *S. tonkinensis*, which is an understory crop. The thinner leaves lowered the required light intensity and CO_2 transmission distance and improved the photosynthetic capacity of the leaves [35]. It can be inferred that, in a habitat with abundant light, the *Z. planispinum* has less competitive pressure and mostly adopts a fast growth strategy. The results showed that there was a close relationship between the economic spectrum and the adaptive capacity of the leaves, but the mechanism of action needs to be studied in depth.

Apart from Chl, LT, and LTD, the overall plasticity of the leaf functional traits in *Z. planispinum* was relatively small. The reasons are as follows: (1) Due to the fragile habitat in karst areas (where the superposition of geological and seasonal drought causes a tendency for the environment to be xeric and there is a shallow soil layer and low soil reserves), *Z. planispinum* resists environmental stress by improving its stability; (2) In order to adapt to the nutrient poor environment, *Z. planispinum* adopts a conservative strategy of slow investment, which ultimately leads to a relatively low growth rate and low plasticity in the variation of traits. The structural traits of the leaves in this study were more plastic than the chemical traits, reflecting the different adaptation strategies adopted by *Z. planispinum* to cope with environmental changes [36]. The reason is that structural traits respond more sensitively and intuitively to changes in the external environment and adapt to dynamic changes in the resource environment through rapid adjustment. The LC, LN, and LP contents and their stoichiometric ratios in *Z. planispinum* in different planting combinations were not significantly different, and the CVs were all small, indicating that the biological organism was able to maintain the relative stability of its chemical composition [37]. This phenomenon showed that, as a suitable dominant species, *Z. planispinum* has higher internal stability and a more conservative approach to nutrient utilization, making it more suitable for water- and nutrient-deficient habitats [38,39]. In the future, the adaptation strategies and driving mechanisms of *Z. planispinum* need to be investigated further in conjunction with its internal stability mechanisms.

4.2. Coupling Relationship between the Leaf Functional Traits of Z. planispinum

Plants adapt to different environments through synergistic or trade-off relationships among leaf functional traits [40]. This study showed a significant negative correlation between LDMC and LWC, confirming that an increase in plant LDMC reduces LWC. This combination of traits is common in plant communities [41] because *Z. planispinum* can resist water stress by increasing its element retention capacity. Chlorophyll and SLA were negatively correlated with LTD and LT as the physical support structures, respectively, reflecting the resource balancing and allocation strategy of the leaves in terms of ecological function [41,42] and structure construction. *Z. planispinum*, therefore, improved the efficiency of resource allocation by adjusting the relationship between the photosynthetic capacity (fast growth) and material accumulation (slow growth), and thus alleviated habitat stress. There were strong correlations between LC, LN, LP, and their stoichiometry in *Z. planispinum*. This occurred because the plant's use of nutrients was influenced by the environment and its own demands. *Z. planispinum* adjusted its own leaf nutrient elements and stoichiometric ratio to adapt to the nutrient supply in the environment [43], which also verified the internal stability theory of ecological stoichiometry. Among the stoichiometric relationships, leaf C:P was significantly positively correlated and extremely significantly negatively correlated with LC and LP, respectively, indicating that the accumulation and

consumption of C and P in *Z. planispinum* were not synchronized, and there was a trade-off effect, which may be related to the different cycling paths of C and P nutrient elements [44].

4.3. Response of Leaf Functional Traits to Soil Factors

This study found that leaf functional traits were affected mainly by the SWC, different forms of massive elements, element stoichiometric balance, and microbial biomass. Soil water affected the ecological adaptation strategy of *Z. planispinum*, and the reasons for this are as follows: (1) The characteristics of a dry and hot valley, shallow soils, and deeply burial groundwater in the study area made water the dominant factor, and the impact of the plantations on the water cycle of the micro-habitat may have aggravated the water restriction [45]; (2) Soil water is closely related to plant health [46], and drought stress makes trees more vulnerable to insect pests and pathogens [47]; shallow-rooted species such as *Z. planispinum* are particularly susceptible to water deficits; (3) Soil water and nutrients have a strong coupling relationship which, together, affect C fixation and microbial activity [48], as well as nutrient content and stoichiometry [49], which in turn have an impact on plant growth. This indicates that the effect of water on the adaptive capacity of plantations is worthy of further study.

Mineral nutrients affected the photosynthetic rate and plant composition of *Z. planispinum* [50], and there was also a strong synergistic effect between photosynthetic productivity and nutrients [51]. Therefore, the levels of mineral elements affected plant growth and adaptation. Both N and P are limiting elements that constitute the body and are important fertility indicators [52] which restrict the formation of ecosystem productivity and are therefore key factors that affect plant survival. However, C had no significant effect on plant adaptation, which is related to the fact that it is mainly derived from the atmosphere and can be conserved through photosynthetic fixation. In addition, the forms of N and P that affected plant growth were not the same, which may be due to the higher degree of N restriction in this area [53]. Furthermore, the relatively abundant P had a dilution effect on N [54], resulting in the limitation of AN. The P saturation caused an imbalance in the C:N:P ratios, leading to element deficiency and limiting ecosystem functions [55]. In addition, plants can absorb small molecular substances, such as free amino acids in the soil [56], and the degradation of soil organic structure in this area may also have been a reason for the lack of AN. Phosphorous is mainly derived from the geological environment and is less affected by soil structure and biological activity, and its main component forms are also different. Calcium is a characteristic element in karst areas, which is mainly inherited from the parent rock, and has both nutrient supply and signal transduction functions [57,58] with strong ecological regulation, so it has a significant effect on the growth of *Z. planispinum*, which is mainly composed of more active quick acting components.

Soil microbial biomass plays an important role in forest ecosystems by acting as a storage reservoir of biologically active nutrients [59]. It is a nutrient pool that is easy to decompose and turn over. It drives the biogeochemical cycle of biogenic elements [60], has a crucial impact on the terrestrial ecosystem, and plays an important role in the soil [61]. Moreover, ecological stoichiometry regulates the cycle of C, N, and other elements [62]; influences the balance of elements; determines the processes of nutrient mineralization, absorption, and utilization; and ultimately affects the productivity of the ecosystem [55]. Therefore, soil microbial biomass and element stoichiometry jointly affect plant growth and adaptation, and plant functional traits have synchronous responses to them. The comprehensive results of this study show that cultivating the organic structure of the soil is particularly important to improving the ecological adaptation traits of plants and is a key measure to improving their adaptive capacity. However, stoichiometry is dependent on water [63], and there is a strong coupling effect between soil components. Therefore, the comprehensive influence of soil action on leaf functional traits needs further study.

5. Conclusions

(1) *Z. planispinum* tended to have a slow investment strategy after planting with *P. salicina*. The combination with the *S. tonkinensi* showed a rapid growth strategy. Following combination with *L. japonica*, *Z. planispinum* tended to form a combination of traits that resisted drought and infertile environmental stress. The combination with *L. japonica* made the investment strategy of *Z. planispinum* adopt a transition from slow to fast. The results showed that species combination could affect the adaptive mechanism of *Z. planispinum*.

(2) *Z. planispinum* was relatively more adaptive when combined with *P. salicina* or *L. japonica*. However, the lowest adaptive capacity occurred when the *Z. planispinum* was planted in combination with *S. tonkinensis*. The results indicated that planting combinations can promote or inhibit the growth of *Z. planispinum*.

(3) The leaf functional traits of *Z. planispinum* were affected by SWC, MBC, MBN, MBP, AN, TP, ACa, C:N, C:P, and N:P, involving the effects of soil physical properties, soil elements, and their stoichiometry and microbial properties. In the future, it will be necessary to further study the comprehensive effect of soil action on leaf functional traits across a wider range of sites.

Author Contributions: Conceptualization, Y.Y.; formal analysis, Y.L. and Y.Y.; software, Y.L. and Y.S.; investigation, Y.L. and Y.S.; writing—original draft preparation, Y.L.; writing—review and editing, Y.Y. All authors have read and agreed to the published version of the manuscript.

Funding: This research was funded by the Guizhou Province Science and Technology Support Plan Project (Qian-ke-he Zhicheng [2022] Yiban 103).

Institutional Review Board Statement: Not applicable.

Informed Consent Statement: Not applicable.

Conflicts of Interest: The authors declare no conflict of interest.

References

1. Kattge, J.; Bönisch, G.; Díaz, S.; Lavorel, S.; Prentice, I.C.; Leadley, P.; Tautenhahn, S.; Werner, G.D.A.; Aakala, T.; Abedi, M.; et al. TRY plant trait database–Enhanced coverage and open access. *Glob. Chang. Biol.* **2020**, *26*, 119–188. [CrossRef] [PubMed]
2. Li, S.J.; Wang, H.; Gou, W.; White, J.F.; Kingsley, K.L.; Wu, G.Q.; Su, P.X. Leaf functional traits of dominant desert plants in the Hexi Corridor, Northwestern China: Trade-off relationships and adversity strategies. *Glob. Ecol. Conserv.* **2021**, *28*, e01666. [CrossRef]
3. Wang, M.; Wan, P.C.; Guo, J.C.; Xu, J.S.; Chai, Y.F.; Yue, M. Relationships among leaf, stem and root traits of the dominant shrubs from four vegetation zones in Shaanxi Province, China. *Isr. J. Ecol. Evol.* **2017**, *63*, 25–32. [CrossRef]
4. Hou, X.L.; Han, H.; Tigabu, M.; Cai, L.P.; Meng, F.R.; Liu, A.Q.; Ma, X.Q. Changes in soil physico-chemical properties following vegetation restoration mediate bacterial community composition and diversity in Changting, China. *Ecol. Eng.* **2019**, *138*, 171–179. [CrossRef]
5. Wang, L.X.; Pang, X.Y.; Li, N.; Qi, K.B.; Huang, J.S.; Yin, C.Y. Effects of vegetation type, fine and coarse roots on soil microbial communities and enzyme activities in eastern Tibetan plateau. *Catena* **2020**, *194*, 104694. [CrossRef]
6. Lü, X.T.; Reed, S.; Yu, Q.; He, N.P.; Wang, Z.W.; Han, X.G. Convergent responses of nitrogen and phosphorus resorption to nitrogen inputs in a semiarid grassland. *Glob. Chang. Biol.* **2013**, *19*, 2775–2784. [CrossRef]
7. Thoms, C.; Gattinger, A.; Jacob, M.; Thomas, F.M.; Gleixner, G. Direct and indirect effects of tree diversity drive soil microbial diversity in temperate deciduous forest. *Soil Biol. Biochem.* **2010**, *42*, 1558–1565. [CrossRef]
8. Zhou, L.; Sun, Y.J.; Saeed, S.; Zhang, B.; Luo, M. The difference of soil properties between pure and mixed Chinese fir (*Cunninghamia lanceolata*) plantations depends on tree species. *Glob. Ecol. Conserv.* **2020**, *22*, e01009. [CrossRef]
9. Bongers, F.J.; Schmid, B.; Bruelheide, H.; Bongers, F.; Li, S.; von Oheimb, G.; Li, Y.; Cheng, A.P.; Ma, K.P.; Liu, X.J. Functional diversity effects on productivity increase with age in a forest biodiversity experiment. *Nat. Ecol. Evol.* **2021**, *5*, 1594–1603. [CrossRef]
10. Wang, J.; Fu, B.J.; Wang, L.X.; Lu, N.; Li, J.Y. Water use characteristics of the common tree species in different plantation types in the Loess Plateau of China. *Agr. For. Meteorol.* **2020**, *288*, 108020. [CrossRef]
11. Peng, C.J.; Song, M.H.; Zhou, C.L.; Li, Y.K.; Li, X.J.; Cao, G.M. Relationship between leaf functional traits of herbaceous plants and soil factors in different coverage gradients of *Potentilla fruticosa* shrub under grazing. *Acta Bot. Boreal. Occident. Sin.* **2020**, *40*, 870–881. [CrossRef]

12. Li, X.E.; Song, X.Y.; Zhao, J.; Lu, H.F.; Qian, C.; Zhao, X. Shifts and plasticity of plant leaf mass per area and leaf size among slope aspects in a subalpine meadow. *Ecol. Evol.* **2021**, *11*, 14042–14055. [CrossRef]
13. Zhang, J.H.; Li, M.X.; Xu, L.; Zhu, J.X.; Dai, G.H.; He, N.P. C:N:P stoichiometry in terrestrial ecosystems in China. *Sci. Total Environ.* **2021**, *795*, 148849. [CrossRef]
14. Elser, J.J.; Fagan, W.F.; Kerkhoff, A.J.; Swenson, N.G.; Enquist, B.J. Biological stoichiometry of plant production: Metabolism, scaling and ecological response to global change. *New Phytol.* **2010**, *186*, 593–608. [CrossRef]
15. Gong, H.D.; Cui, Q.J.; Gao, J. Latitudinal, soil and climate effects on key leaf traits in northeastern China. *Glob. Ecol. Conserv.* **2020**, *22*, e00904. [CrossRef]
16. Li, Y.Q.; He, W.; Wu, J.; Zhao, P.; Chen, T.; Zhu, L.W.; Ouyang, L.; Ni, G.Y.; Hölscher, D. Leaf stoichiometry is synergistically-driven by climate, site, soil characteristics and phylogeny in karst areas, Southwest China. *Biogeochemistry* **2021**, *155*, 283–301. [CrossRef]
17. Bauters, M.; Verbeeck, H.; Doetter, S.; Ampoorter, E.; Baert, G.; Vermeir, P.; Verheyen, K.; Boeckx, P. Functional Composition of Tree Communities Changed Topsoil Properties in an Old Experimental Tropical Plantation. *Ecosystems* **2017**, *20*, 861–871. [CrossRef]
18. Wang, K.L.; Zhang, C.H.; Chen, H.S.; Yue, Y.M.; Zhang, W.; Zhang, M.Y.; Qi, X.K.; Fu, Z.Y. Karst landscapes of China: Patterns, ecosystem processes and services. *Landsc. Ecol.* **2019**, *34*, 2743–2763. [CrossRef]
19. Hao, Z.; Kuang, Y.W.; Kang, M. Untangling the influence of phylogeny, soil and climate on leaf element concentrations in a biodiversity hotspot. *Funct. Ecol.* **2015**, *29*, 165–176. [CrossRef]
20. Tu, Y.L.; Wei, C.S.; Zou, Z.L.; Lu, Y.M. A new *Zanthoxylum* Genus—*Z. planipinum* var. *dingtanensis* and the research of its species classification. *Guizhou Sci.* **2001**, *19*, 77–80. (In Chinese)
21. Yu, Y.H.; Song, Y.P.; Li, Y.T. Management practices effects on *Zanthoxylum planispinum* 'dintanensis' fruit quality. *Agron. J.* **2022**, *114*, 2095–2104. [CrossRef]
22. Zou, J.; Yu, L.F.; Huang, Z.S. Variation of Leaf Carbon Isotope in Plants in Different Lithological Habitats in a Karst Area. *Forests* **2019**, *10*, 356. [CrossRef]
23. Li, Y.T.; Yu, Y.H.; Song, Y.P. Stoichiometry of Soil, Microorganisms, and Extracellular Enzymes of *Zanthoxylum planispinum* var. *dintanensis* Plantations for Different Allocations. *Agronomy* **2022**, *12*, 1709. [CrossRef]
24. Bao, S.D. *Soil Agrochemical Analysis*, 3rd ed.; China Agriculture Press: Beijing, China, 2000; pp. 22–173. (In Chinese)
25. Lu, R.K. *Methods for Soil and Agriculture Chemistry Analysis*, 3rd ed.; Chinese Agricultural Science and Technology Press: Beijing, China, 1999. (In Chinese)
26. Vance, E.D.; Brookes, P.C.; Jenkinson, D.S. An extraction method for measuring soil microbial biomass C. *Soil Biol. Biochem.* **1987**, *19*, 703–707. [CrossRef]
27. Pan, Q.; Zheng, H.; Wang, Z.H.; Wen, Z.; Yang, T.Z. Effects of plant functional traits on ecosystem services: A review. *Chin. J. Plant Ecol.* **2021**, *45*, 1140–1153. [CrossRef]
28. Perez-Harguindeguy, N.; Diaz, S.; Garnier, E.; Lavorel, S.; Poorter, H.; Jaureguiberry, P.; Bret-Harte, M.S.; Cornwell, W.K.; Craine, J.M.; Gurvich, D.E.; et al. New handbook for standardised measurement of plant functional traits worldwide. *Aust. J. Bot.* **2016**, *64*, 715–716. [CrossRef]
29. Qin, J.; Kong, H.Y.; Liu, H. Stoichiometric characteristics of soil C, N, P and K in different *Pinus massoniana* forests. *J. Northwest A&F Univ. (Nat. Sci. Ed.)* **2016**, *44*, 68–82. (In Chinese)
30. Valladares, F.; Wright, S.J.; Lasso, E.; Kitajima, K.; Pearcy, R.W. Plastic phenotypic response to light of 16 congeneric shrubs from a Panamanian rainforest. *Ecology* **2000**, *81*, 1925–1936. [CrossRef]
31. Wright, I.J.; Ackerly, D.D.; Bongers, F.; Harms, K.E.; Ibarra-Manriquez, G.; Martine-Ramos, M.; Mazer, S.J.; Muller-Landau, H.C.; Paz, H.; Pitman, N.C.A.; et al. Relationships among ecologically important dimensions of plant trait variation in seven Neotropical forests. *Ann. Bot.-Lond.* **2007**, *99*, 1003–1015. [CrossRef]
32. Faucon, M.P.; Houben, D.; Lambers, H. Plant functional traits: Soil and ecosystem services. *Trends Plant Sci.* **2017**, *22*, 385–394. [CrossRef]
33. Wilson, P.J.; Thompson, K.; Hodgson, J.G. Specific leaf area and leaf dry matter content as alternative predictors of plant strategies. *New Phytol.* **1999**, *143*, 155–162. [CrossRef]
34. Thomas, F.M.; Yu, R.D.; Schafer, P.; Zhang, X.M.; Lang, P. How diverse are *Populus* "*diversifolia*" leaves? Linking leaf morphology to ecophysiological and stand variables along water supply and salinity gradients. *Flora* **2017**, *233*, 68–78. [CrossRef]
35. Parkhurst, D.F. Diffusion of CO_2 and other gases inside leaves. *New Phytol.* **1994**, *126*, 449–479. [CrossRef]
36. Wu, T.H.; Long, L.C.; Xiong, L.; Liu, Q. Variation and adaptation of leaf functional traits of different growth type in Karst forests. *Chin. J. Appl. Environ. Biol.* **2023**, *29*, 1–10. [CrossRef]
37. Sterner, R.W.; Elser, J.J. *Ecological Stoichiometry: The Biology of Elements from Molecules to Biosphere*; Princeton University Press: Princeton, NJ, USA, 2002.
38. Persson, J.; Fink, P.; Goto, A. To be or not to be what you eat: Regulation of stoichiometric homeostasis among autotrophs and heterotrophs. *Oikos* **2010**, *119*, 741–751. [CrossRef]
39. Zhang, T.T.; Liu, W.Y.; Huang, J.B.; Hu, T.; Tang, D.D.; Chen, Q. Characteristics of plant ecological stoichiometry homeostasis. *Guihaia* **2019**, *39*, 701–712. [CrossRef]
40. Reich, P.B.; Oleksyn, J. Global patterns of plant leaf N and P in relation to temperature and latitude. *Proc. Natl. Acad. Sci. USA* **2004**, *101*, 11001–11006. [CrossRef]

41. Wright, I.J.; Reich, P.B.; Westoby, M.; Ackerly, D.D.; Baruch, Z.; Bongers, F.; Cavender-Bares, J.; Chapin, T.; Cornelissen, J.H.C.; Diemer, M.; et al. The worldwide leaf economics spectrum. *Nature* **2004**, *428*, 821–827. [CrossRef]
42. Ordoñez, J.C.; van Bodegom, P.M.; Witte, J.P.M.; Wright, I.J.; Reich, P.B.; Aerts, R. A global study of relationships between leaf traits, climate and soil measures of nutrient fertility. *Glob. Ecol. Biogeogr.* **2009**, *18*, 137–149. [CrossRef]
43. Ma, F.; Xu, T.T.; Liu, J.L.; Xiao, G.J.; Li, M.; Bi, J.T.; Na, X.F. Variations in Carbon, Nitrogen and Phosphorus Stoichiometry of Caragana liouana Originated from Nine Provenances in a Common Garden. *Acta Bot. Boreal. Occident. Sin.* **2017**, *37*, 1381–1389. [CrossRef]
44. Bertolet, B.L.; Corman, J.R.; Casson, N.J.; Sebestyen, S.D.; Kolka, R.K.; Stanley, E.H. Influence of soil temperature and moisture on the dissolved carbon, nitrogen, and phosphorus in organic matter entering lake ecosystems. *Biogeochemistry* **2018**, *139*, 293–305. [CrossRef]
45. Cortes, S.S.; Whitworth-Hulse, J.I.; Piovano, E.L.; Gurvich, D.E.; Magligano, P.N. Changes in rainfall partitioning caused by the replacement of native dry forests of *Lithraea molleoides* by exotic plantations of *Pinus elliottii* in the dry Chaco mountain forests, central Argentina. *J. Arid Land* **2020**, *12*, 717–729. [CrossRef]
46. Singh, S.P.; Mahapatra, B.S.; Pramanick, B.; Yadav, V.R. Effects of irrigation levels, planting methods and mulching on nutrient uptake, yield, quality, water and fertilizer productivity of field mustrad (*Brassica rapa* L.) under sandy loam soil. *Agric. Water Manag.* **2021**, *244*, 106539. [CrossRef]
47. Whyte, G.; Howard, K.; Hardy, G.E.S.; Burgess, T.I. The Tree Decline Recovery Seesaw; a conceptual model of the decline and recovery of drought stressed plantation trees. *For. Ecol. Manag.* **2016**, *370*, 102–113. [CrossRef]
48. Mahajan, G.R.; Das, B.; Manivannan, S.; Manjunath, B.L.; Verma, R.R.; Desai, S.; Kulkarni, R.M.; Latare, A.M.; Sale, R.; Murgaonkar, D.; et al. Soil and water conservation measures improve soil carbon sequestration and soil quality under cashews. *Int. J. Sediment Res.* **2021**, *36*, 190–206. [CrossRef]
49. Lin, Y.M.; Chen, A.M.; Yan, S.W.; Rafay, L.; Du, K.; Wang, D.J.; Ge, Y.G.; Li, J. Available soil nutrients and water content affect leaf nutrient concentrations and stoichiometry at different ages of *Leucaena leucocephala* forests in dry-hot vally. *J. Soil Sediment* **2019**, *19*, 511–521. [CrossRef]
50. Hu, H.Q.; Wang, L.H.; Li, Y.L.; Sun, J.W.; Zhou, Q.; Huang, X.H. Insight into mechanism of lanthanum (III) induced damage to plant photosynthesis. *Ecotoxicol. Environ. Saf.* **2016**, *127*, 43–50. [CrossRef]
51. Amoozager, A.; Mohammadi, A.; Sabzalian, M.R. Impact of light-emitting diode irradiation on photosynthesis, phytochemical composition and mineral element content of lettuce cv. Grizzly. *Photosynthetica* **2017**, *55*, 85–95. [CrossRef]
52. Xu, C.H.; Xiang, W.H.; Gou, M.M.; Chen, M.M.; Chen, L.; Lei, P.F.; Fang, X.; Deng, X.W.; Ouyang, S. Effects of forest restoration on soil carbon, phosphorus, and their stoichiometry in Hunan, Southern China. *Sustainability* **2018**, *10*, 1874. [CrossRef]
53. Zhang, W.; Zhao, J.; Pan, F.J.; Li, D.J.; Chen, H.S.; Wang, K.L. Changes in nitrogen and phosphorus limitation during secondary succession in a karst region in southwest China. *Plant Soil* **2015**, *391*, 77–91. [CrossRef]
54. He, L.H. *Quality Formation and Regulation of Wheat in Shanxi*; China Agricultural Science and Technology Press: Beijing, China, 2012. (In Chinese)
55. Sun, Y.; Wang, C.T.; Chen, X.L.; Liu, S.R.; Lu, X.J.; Chen, H.Y.H.; Ruan, H.H. Phosphorus additions imbalance terrestrial ecosystem C:N:P stoichiometry. *Glob. Chang. Biol.* **2022**, *28*, 7353–7365. [CrossRef]
56. Paungfoo-Lonhienne, C.; Visser, J.; Lonhienne, T.G.A.; Schmidt, L. Past, present and future of organic nutrients. *Plant Soil* **2012**, *359*, 1–18. [CrossRef]
57. Zhang, R.; Sun, Y.; Liu, Z.; Jin, W.; Sun, Y. Effects of melatonin on seedling growth, mineral nutrition, and nitrogen metabolism in cucumber under nitrate stress. *J. Pineal Res.* **2017**, *62*, e12403. [CrossRef]
58. Hashem, A.; Alqarawi, A.A.; Radhakrishnan, R.; Al-Arjani, A.B.F.; Aldehaish, H.A.; Egamberdieva, D.; Abd Allah, E.F. Arbuscular mycorrhizal fungi regulate the oxidative system, hormones and ionic equilibrium to trigger salt stress tolerance in *Cucumis sativus* L. *Saudi J. Biol. Sci.* **2018**, *25*, 1102–1114. [CrossRef]
59. Heuck, C.; Weig, A.; Spohn, M. Soil microbial biomass C:N:P stoichiometry and microbial use of organic phosphorus. *Soil Biol. Biochem.* **2015**, *85*, 119–129. [CrossRef]
60. Li, P.; Yang, Y.H.; Han, W.X.; Fang, J.Y. Global patterns of soil microbial nitrogen and phosphorus stoichiometry inforest ecosystems. *Glob. Ecol. Biogeogr.* **2014**, *23*, 979–987. [CrossRef]
61. Medlyn, B.E.; Zaehle, S.; De Kauwe, M.G.; Walker, A.P.; Dietze, M.C.; Hanson, P.J.; Hickler, T.; Jain, A.K.; Luo, Y.; Parton, W.; et al. Using ecosystem experiments to improve vegetation models. *Nat. Clim. Chang.* **2015**, *5*, 528–534. [CrossRef]

62. Chen, L.L.; Deng, Q.; Yuan, Z.Y.; Mu, X.M.; Kallenbach, R.L. Age-related C:N:P stoichiometry in two plantation forests in the Loess Plateau of China. *Ecol. Eng.* **2018**, *120*, 14–22. [CrossRef]
63. Murray, D.S.; Shattuck, M.D.; McDowell, W.H.; Wymore, A.S. Nitrogen wet deposition stoichiometry: The role of organic nitrogen, seasonality, and snow. *Biogeochemistry* **2022**, *160*, 301–314. [CrossRef]

forests

MDPI

Article

Identifying the Landscape Security Pattern in Karst Rocky Desertification Area Based on Ecosystem Services and Ecological Sensitivity: A Case Study of Guanling County, Guizhou Province

Bin Ying, Ting Liu, Li Ke, Kangning Xiong *, Sensen Li, Ruonan Sun and Feihu Zhu

School of Karst Science, Guizhou Normal University, Guiyang 550003, China; keli202303@163.com (L.K.)
* Correspondence: xiongkn@gznu.edu.cn

Abstract: Ecological environmental security in karst areas is an issue of global concern. Identifying the ecological landscape security pattern (ELSP) is key to promoting environmental protection and alleviating the land development and utilization impacts. Ecological sources (ESs) and ecological corridors (ECs) are important bases for constructing an ELSP. We used five influencing factors (land use type, digital elevation model (DEM), rocky desertification degree, normalized difference vegetation index (NDVI) and slope) to obtain the distribution of the importance and sensitivity values of ecosystem services in Guanling County, Guizhou Province. The probability of the connectivity index (PC) was calculated, and the ES was extracted by combining the importance of ecosystem services, ecological sensitivity, and landscape connectivity. According to the topographic and geomorphological characteristics of Guanling County, seven indicators of elevation, slope, landscape type, degree of stone desertification, distance from rivers, distance from settlements, and distance from roads were selected as resistance factors for the outward expansion of the ESs to calculate the comprehensive resistance surface of Guanling County. Based on the gravity model, an interaction matrix between 10 ESs was constructed, and the magnitude of the interaction forces between the source sites was quantitatively evaluated to distinguish the important ECs and general ECs. The study showed that the total length of the ECs in Guanling County was 509.78 km, and the core area of Guanling County was large, accounting for 65.73% of the ecological landscape area. By assessing the importance of ecosystem services, ecological sensitivity, and landscape connectivity, 10 ES and 45 EC were obtained based on ArcGIS10.8, which constituted the landscape security pattern of Guanling County by ESs and ECs. Suggestions were proposed for a planning layout that will benefit the ecological restoration of Guanling County and environmental protection of the karst region according to the study area characteristics.

Keywords: landscape security pattern; ecosystem services; sensitivity; landscape connectivity; Guanling County; Guizhou

Citation: Ying, B.; Liu, T.; Ke, L.; Xiong, K.; Li, S.; Sun, R.; Zhu, F. Identifying the Landscape Security Pattern in Karst Rocky Desertification Area Based on Ecosystem Services and Ecological Sensitivity: A Case Study of Guanling County, Guizhou Province. *Forests* **2023**, *14*, 613. https://doi.org/10.3390/f14030613

Academic Editor: José Aranha

Received: 7 February 2023
Revised: 8 March 2023
Accepted: 16 March 2023
Published: 19 March 2023

1. Introduction

With the acceleration of urbanization, frequent human activities have led to the fragmentation of ecosystems. Ecological security issues have increasingly become the focus of attention of experts and researchers at home and abroad. The construction of regional security patterns is an effective way to improve the ecological environment and achieve regional sustainable development. Yu (1995) [1] proposed the theory of landscape security patterns based on the landscape ecological planning method advocated by Forman [2]. This theory satisfied the theoretical requirements of the reasonable regulation of ecological processes in ecological security research and became an effective way to guide the theory and practice of landscape ecology spatial pattern-ecological process coupling [3]. Ecological

security patterns focus on biodiversity conservation, landscape restoration, ecosystem service supply, etc. It is of great significance to analyze the interaction between key elements and ecological processes for ecological security such as ecosystem integrity, reasonable structure, and normal function [4]. At present, the theory of landscape security patterns has been widely used in empirical research. For example, Li et al. (2015), using Changzhou as an example, used the minimum cumulative resistance model (MCR) to construct the resistance surface, determine the quantity and pattern optimization of urban ecological land, and solve urban environmental problems [5]. Based on the distance cost analysis method, Su et al. (2016) constructed an urban regional composite ecological security pattern (ESP) to protect the survival and habitat security of important vegetation, wild animals, and human beings [6]. Liang et al. (2018) comprehensively analyzed the priority protection area and the minimum cost EC, established a more representative, connected, and efficient EC network system, and proposed a new framework for a protection area network composed of protection priority and EC [7]. Peng et al. (2018) evaluated the ecological land risk, quantified the value of ecological land, identified the ESs of Shenzhen, and constructed EC to provide a theoretical framework for the study of urban ecological security patterns [8]. A large number of ES and EC studies have also been carried out in karst areas [9–12]. However, the research on ELSPs has mainly focused on cities, watersheds, and other regions, and few in karst areas. The construction method of ELSP is divided into three steps: the selection of ESs, the construction of comprehensive resistance surfaces, and the extraction of ECs [13]. The traditional method is subjective when selecting the ESs and usually selects areas with the highest ecological values as the ES, which lacks a certain scientific rigor. Therefore, some researchers have introduced more scientific methods such as the importance of ecosystem services [14], morphological spatial pattern analysis (MSPA) [15], and landscape connectivity analysis to identify ES.

Ecosystem services are the direct or indirect contributions of ecosystems to human well-being. They reflect the human need for ecosystems and are the frontiers of ecological, geographic and economic research [16]. At present, ecosystem services have made many contributions to human development. Researchers at home and abroad have studied the function, quantitative evaluation, and ecosystem service flow of ecosystem services [17–19]. Ecological sensitivity is mainly used in ecological environmental protection and spatial planning. Researchers have also combined ecological sensitivity evaluation with spatial security patterns, making it an important indicator for the selection of ESs [20–22]. Ecosystem services and ecological sensitivity assessments have gradually been applied to the study of regional security patterns, but little attention has been given to ecological protection and ecological security pattern construction in karst areas.

The term karst originates from the karst plateau of the former Yugoslavia, coupled with the atmosphere, hydrosphere, and biosphere to form the natural ecological environment of karst. It is widely distributed, accounting for 10% of the total Earth area [23,24]. The distribution of karst areas in China exceeds 1.24 million km^2, which is concentrated in Yunnan, Guizhou, Guangxi, etc., among which Guizhou karst has a continuous distribution and a wide area of carbonate rocks. Due to the lack of water and soil components in the ecological environment, the Guizhou karst area has low ecological capacity, poor environmental stability, and high sensitivity to variation, and is prone to disasters such as soil erosion, rocky desertification, drought, and flood. The special geomorphic conditions result in complex landforms and strong spatial heterogeneity in the karst areas. At present, the research into environmental governance and rocky desertification control in karst regions has achieved much success [25], and is mainly concentrated on the environment monitoring of karst [26–29], the spatial distribution of rocky desertification [30–32], the evolution process and patterns of rocky desertification [33–35], driving factor analysis [36–40], and rocky desertification control, etc. [41–43]. Guanling County in Guizhou Province is a typical karst landform area in China. With the acceleration of urbanization and the development of a large number of urban construction facilities, the originally fragile karst environment has been continuously affected by human activity and economic development, and the landscape pattern in the

area has changed dramatically [44]. The vegetation coverage has been reduced, cave cracks have developed, water leakage has become serious, the terrain has become extremely fragmented, landscape connectivity has declined, and the ecological environment has become fragile [45]. It is of great significance for the sustainable development of the ecological environment in this karst region to construct a security pattern and optimize its spatial layout. This paper identifies the ecological source of Guanling County based on the importance of ecosystem services, ecological sensitivity, and landscape connectivity, and constructs a comprehensive resistance surface of the study area from the aspects of landscape, terrain, human interference, etc. ArcGIS spatial analysis was used to calculate the potential ecological corridor of Guanling County, and identified the important ecological corridor based on the gravity model to construct the landscape security pattern of Guanling County and provide effective scientific support for the planning and construction of the study area.

2. Materials and Methods

2.1. Overview of the Study Area

Guanling County (Figure 1) is located in central Guizhou Province, the eastern ridge slope of the Yunnan-Guizhou Plateau to the south of the Guangxi hilly slope, within the city of Anshun, 105°15′~105°49′ E, 25°19′~26°05′ N, which is adjacent to Zhenning County, Zhenfeng County, Qinglong County, etc. The total area of the county is 1464 km^2. The terrain is high in the northwest and low in the southeast. The elevation is between 370 and 1850 m. The mountainous area accounts for 89% of the total area of the county, and the surface is rugged. The climate in the region is mainly a subtropical monsoon humid climate with sufficient heat, concentrated summer rainfall, and serious soil erosion. The mountains in the territory are part of the Wumeng Mountains. The landform types are complex and diverse. Carbonate rocks are widely distributed, and karst development is strong. Guanling County is a typical karst plateau mountainous area and the area of karst landforms encompasses 83.83% of the county. With socioeconomic development and the influence of human activities, the regional terrain is more fragmented, and the ecological environment has been seriously damaged.

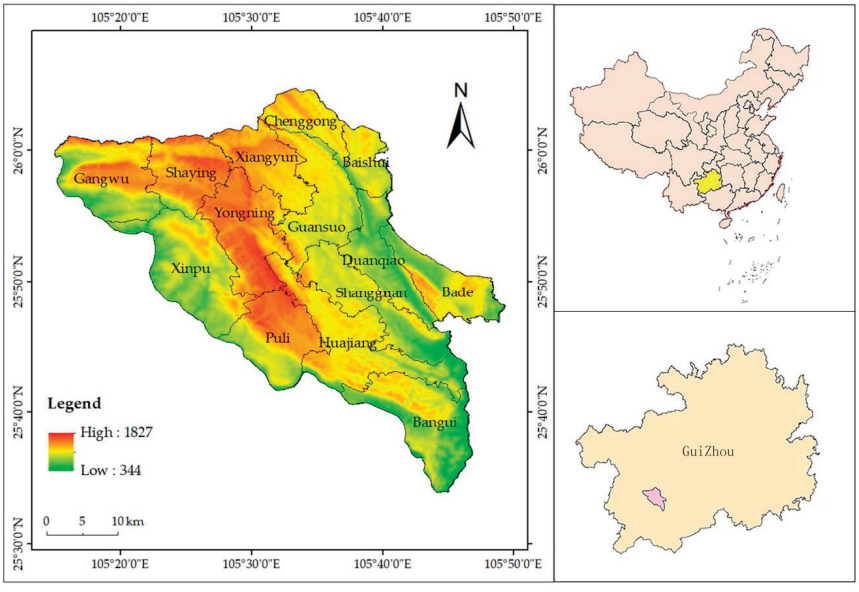

Figure 1. Geographical location map of Guanling County.

2.2. Data Sources

The basic data used in this study include land use data, digital elevation model (DEM) data, rocky desertification data, and normalized difference vegetation index (NDVI) data.

(1) Land use data: Derived from the results of the third national land survey (the third national land survey) in Guanling County, according to the land use classification system of the third national land survey (land use status classification GB/T21010-2017) [46]; the data are divided into seven categories.
(2) DEM data: Obtained from the Chinese Academy of Sciences Data Sharing Center (https://www.resdc.cn/), accessed on 17 May 2022, with a resolution of 30 m, and using ArcGIS10.8 surface analysis to extract the slope data.
(3) NDVI data: Obtained from the National Ecological Science Data Center (http://www.nesdc.org.cn/), accessed on 19 February 2022, with a resolution of 30 m.
(4) Rocky Desertification data: Rocky desertification data from Xiong et al. [47], and corrected by the visual interpretation of remote sensing and field survey observations.

2.3. Research Methods

2.3.1. Importance and Sensitivity Analysis of Ecosystem Services

The ecosystem service value is the benefit to humankind from ecosystems [48–50]. The ecosystem service value per unit area of land use type was obtained according to the ecosystem service value evaluation research of Xie et al. (2008). (Table 1).

Table 1. Ecosystem service value of land use types.

Value of Ecosystem Services	Land Use Type	Importance of Ecological Services
5	Water body	Extremely important
4	Forestland and grassland	Highly important
3	Garden plot	Moderately Important
2	Cultivated land	Slightly important
1	Construction land and other land	Unimportant

Ecological sensitivity is a comprehensive index used to evaluate the regional ecological environmental quality, land use rationality, and economic development. It is the basis of regional ecological environment planning and management [51]. This paper, combined with the principle of data availability and objectivity, chose five indicators (land use data, DEM, rocky desertification data, NDVI and slope) according to the current research [52] to evaluate the ecological sensitivity of the study area (Table 2).

Table 2. Ecological environment sensitivity the evaluation factor classifications and weights.

Sensitivity Assignment	NDVI	DEM/m	Slope/°	Land Use Type	Rocky Desertification
1	≤0.35	≤500	≤5	Construction Land	Extremely strong rocky desertification
3	(0.35, 0.50]	(500, 800]	(5, 15]	Other land	Intense rocky desertification
5	(0.50, 0.65]	(800, 1100]	(15, 25]	Cultivated land	Moderate rocky desertification
7	(0.65, 0.75]	(1100, 1500]	(25, 35]	Grassland and Garden land	Mild rocky desertification
9	>0.75	>1500	>35	Forestland and Water body	No rocky desertification

2.3.2. Landscape Connectivity Analysis

Landscape connectivity refers to the degree to which the landscape promotes or hinders movement between patches [53], which can be reflected by the size of the patches, the distance between similar patches, and the presence of corridors [54], and promotes the communication and exchange of species and biodiversity between patches. MSPA is an

image processing method based on mathematical morphology principles such as corrosion, expansion, open operations, and closed operations to measure, identify, and segment raster images [55]. This method can suitably identify the important ecological patches in the study area and obtain seven kinds of landscape elements (core, edge, bridge, islet, perforation, loop and branch) for a clear spatial topological relationship between the target pixel set and the structural elements [56]. Based on the Guidos software, this paper examined the landscape structure of Guanling County by MSPA. The forestland, grassland, water area, cultivated land, and garden land in the seven types of land use in the study area were used as the foreground data, and the other types were used as the background data to extract the core areas. All values were binarized and imported into the Guidos Toolbox software for the MSPA analysis of the images using the eight-neighborhood analysis method.

Next, we used Conefor 2.6 software (available at http://www.conefor.org/ (accessed on 2 March 2023), as proposed by Saura and Torne (2009), to calculate the *dPC* of the core area. Finally, according to their *dPC* value from high to low, the patches were divided into four levels, and the importance pattern of the Guanling County landscape connectivity was finally obtained. The calculation formula of *dPC* is:

$$dPC = \frac{PC - PC_{i-remove}}{PC}$$

where *PC* is the possible connectivity index of the whole landscape when all patches exist in the landscape and $PC_{i-remove}$ is the possible connectivity index value of the remaining patch composition landscape after removing patch *i*. The higher the *dPC* value, the higher the importance of the patch in landscape connectivity, and the more obvious its core position in the landscape. The calculation formula of *PC* is:

$$PC = \frac{\sum_{i=1}^{n} \sum_{j=1}^{n} a_i \times a_j \times a_{ij}}{A_L^2}$$

where n is the total number of habitat nodes in the landscape; a_i and a_j are the areas of plaque i and plaque j, respectively; A is the total area of the study area; and a_{ij} is the maximum final connectivity of all paths between plaque i and plaque j.

2.3.3. Construction of Ecological Resistance Surface

The flow of matter and energy needs to overcome a certain resistance, and the resistance encountered in the outward diffusion of ESs constitutes the comprehensive resistance surface [57]. Based on previous studies [58,59], seven indicators were selected from landscape, topography, and human interference including the elevation, slope, landscape type, degree of stone desertification, distance from rivers, distance from settlements and distance from roads as the resistance factors for the outward expansion of ESs, and these resistance factors were assigned resistance values (from 1 to 9, where the higher the value, the higher the degree of resistance) in a hierarchy (Table 3). Using ArGIS10.8, these seven types of factors were superimposed by finding the mean value to obtain the comprehensive resistance surface of Guanling County.

2.3.4. Construction of ELSP

The core steps of ecological security pattern construction include ecological source identification, ecological resistance surface construction, and key ecological corridor extraction. Among these, the ecological source is the starting point for the outward diffusion of species, which can promote the development of ecological processes and is the key area to ensure regional ecological security [60]. The identification of ESs in Guanling County is mainly based on the analysis of the importance of ecosystem services, ecological sensitivity, and landscape connectivity. ECs are corridors that can provide protection for biodiversity and prevent soil erosion and the loss of ecosystem services [61]. They are the pathways of material and energy flow in the region and key factors in maintaining ecological sta-

bility, ecological processes, and ecological function in the region [62]. According to the constructed comprehensive resistance surface, the ECs between the sources were extracted. Using the center point of the ESs as the ecological node, the minimum cost distance from each source to other ESs was calculated by the cost distance using the distance analysis tool in ArcGIS, and then the cost path was used to calculate the minimum cost path between the sources. Finally, the key EC in the study area, which were the channels with the smallest resistance value between the sources, were obtained. Based on the gravity model, we quantitatively evaluated the interaction between each ecological source and determined the importance of the potential corridor (the greater the interaction, the higher the importance of the corridor). The calculation formula of gravity model is as follows:

$$G_{ij} = \frac{N_i * N_j}{D_{ij}^2} = \frac{\frac{\ln s_i}{P_i} * \frac{\ln s_j}{P_j}}{\left(\frac{L_{ij}}{L_{max}}\right)^2} = \frac{L_{max}^2 * \ln(s_i) * \ln(s_j)}{L_{ij}^2 * P_i * P_j}$$

where G_{ij} is the interaction force between source patches i and j; N_i and N_j is the weight value of source patches, D_{ij} is the potential corridor resistance value between source patches i and j; P_i and P_j is the resistance value of source patches i and j; L_{ij} is the potential corridor resistance value from source patches i to j; L_{max} is the maximum resistance value of all potential corridors in the study area.

Table 3. Ecological resistance surface evaluation system.

Resistance Value	Distance from River/m	Distance from the Settlement/m	Distance from Road/m	Degree of Stone Desertification	Landscape Type	Elevation/m	Slope/°
1	≤500	>1000	≤1000	No rocky desertification	Forestland and Water body	≤500	≤5
3	(500, 1000]	(1000, 800]	(500, 1000]	Mild rocky desertification	Grassland and Garden land	(500, 800]	(5, 10]
5	(1000, 1500]	(800, 500]	(200, 500]	Moderate rocky desertification	Cultivated land	(800, 1100]	(10, 15]
7	(1500, 2000]	(200, 500]	(100, 200]	Intense rocky desertification	Other land	(1100, 1500]	(15, 25]
9	>2000	≤200	≤100	Extremely strong rocky desertification	Cultivated land	>1500	>25

3. Results and Analysis

3.1. Land Use Analysis of Guanling County

According to the land use distribution in Guanling County (Figure 2), the largest area was that of cultivated land at 404.34 km^2, accounting for 27.94% of the total area; the forestland area was 345.48 km^2, accounting for 23.87% of the total area; the grassland area was 246.31 km^2, accounting for 17.02% of the total area; the garden land area was 16.38 km^2, accounting for 1.13% of the total area; the water body area was the smallest, at only 15.73 km^2, accounting for 1.09% of the total area; and the construction land area was 42.31 km^2, accounting for 2.92% of the total area. The area of bare land and other land was 376.50 km^2, accounting for 26.02% of the total area. There was more cultivated land, bare land, and other land in Guanling County (Table 4), and the ecological environment was poor. Forest protection and the Grain for Green Project are recommended. The water area was relatively small, and thus water resource protection should be improved.

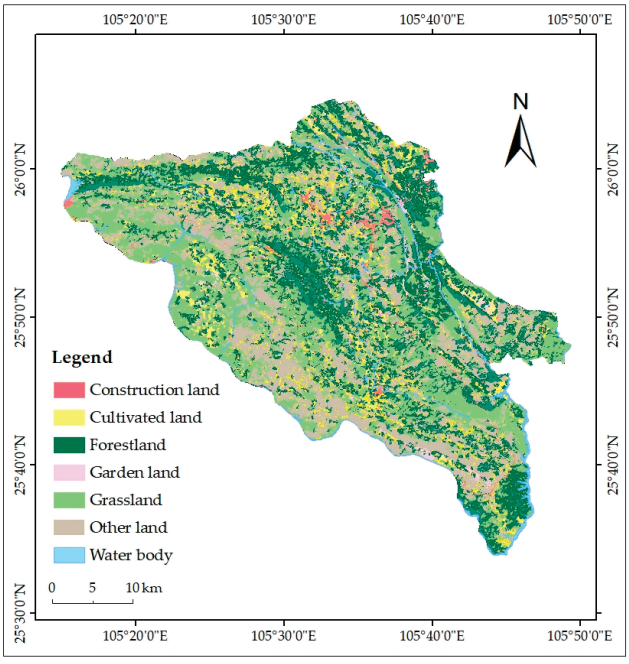

Figure 2. Guanling County land use distribution map.

Table 4. Areas of various land use types in Guanling County.

Land Use Types	Area (km^2)	Proportion (%)
Forestland	345.48	23.87
Grassland	246.31	17.02
Garden land	16.38	1.13
Water body	15.73	1.09
Cultivated land	404.34	27.94
Construction land	42.31	2.92
Other land	376.50	26.02

3.2. Analysis of Importance and Ecological Sensitivity of Ecosystem Services

The importance of ecosystem services can be calculated for different ecosystems to analyze regional differentiation rules and clarify the important areas of ecosystem services. According to research on the evaluation of ecosystem service value by Xie et al. (2008), water areas, forestlands and grasslands, garden lands, cultivated lands, and construction lands were assigned an importance value of 5, 4, 3, 2, and 1, respectively (where the higher the value, the higher the value of the ecosystem services). Then, a distribution map of the importance of ecosystem services in Guanling County (Figure 3) was obtained. The area of extremely important and important areas of ecosystem service value was 607.38 km^2, accounting for 41.98% of the total area of the county.

Ecological environmental sensitivity is an important factor restricting urban development. The more sensitive the ecological environment, the more likely environmental problems are to occur in the area. Through the superposition of ecological sensitivity evaluation factors, the ecological sensitivity evaluation results were obtained. The natural breakpoint method was used to divide the ecological sensitivity into five grades: insensitive, mildly sensitive, moderately sensitive, highly sensitive, and extremely sensitive (Figure 4). The highly sensitive and extremely sensitive area of Guanling County was 526.5 km^2, accounting for 36.37% of the total area of the county, mainly in the northwest,

central, east, and south; the insensitive area was 53.5 km^2, accounting for 3.70% of the total area of the county, mainly distributed in the western and southern fringes of the study area. The ecological environment of Guanling County is relatively fragile.

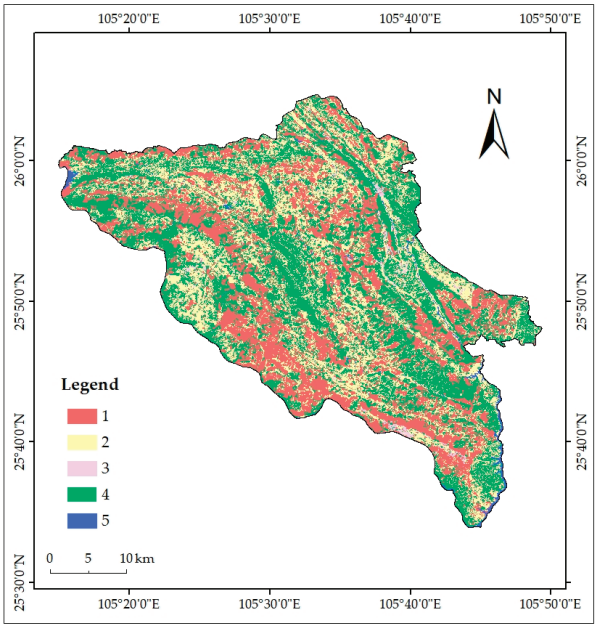

Figure 3. Importance distribution map of ecosystem services in Guanling County.

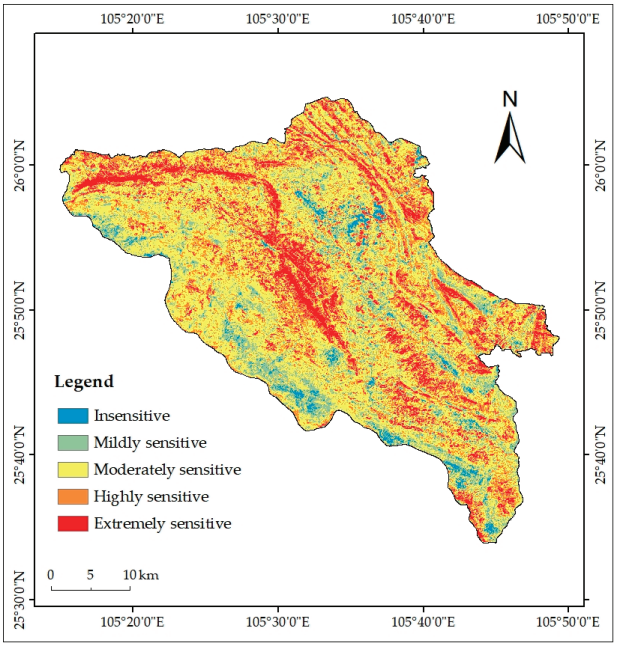

Figure 4. Ecological sensitivity distribution map of Guanling County.

3.3. Analysis of Landscape Connectivity and Landscape Types in Guanling County

There are many indicators used to measure landscape connectivity. The integral index of connectivity (IIC) and probability of connectivity (PC) proposed by Pascual-Hortal and Saura (2006) can evaluate landscape connectivity more effectively than other indicators [63]. Both the IIC and PC are landscape connectivity evaluation indices based on graph theory, but the PC has more advantages and is more rational than the IIC index [64]. *Guidos* software was used to analyze the landscape structure of Guanling County by MSPA, and the core patches of Guanling County were extracted. Combined with Conefor 2.6 software, the *dPC* index value of each patch was calculated. According to the level of *dPC*, the landscape connectivity of Guanling County was divided into four levels: extremely high, high, medium, and low. In the landscape type of Guanling County (Figure 5), the core area was an important species habitat, with an area of 608.61 km^2, accounting for 65.73% of the ecological landscape area, and was widely distributed. The loop area had a certain buffer effect on species migration, covering an area of 70.59 km^2, accounting for 7.62% of the ecological landscape area. The islet area was the smallest and was the supplementary part of the core area. This area was only 11.71 km^2, accounting for 1.30% of the ecological landscape area. The perforation distribution in the study area was relatively uniform, with an area of 45.15 km^2, accounting for 4.88% of the ecological landscape area. The edge area was the external boundary of the core area, with an area of 120.06 km^2, accounting for 12.97% of the ecological landscape area. The connecting bridge, with an area of 31.30 km^2, accounting for 3.39% of the ecological landscape area, had a certain effect on the communication between species. The area of the branch line was 38.53 km^2, accounting for 4.16% of the ecological landscape (Table 5).

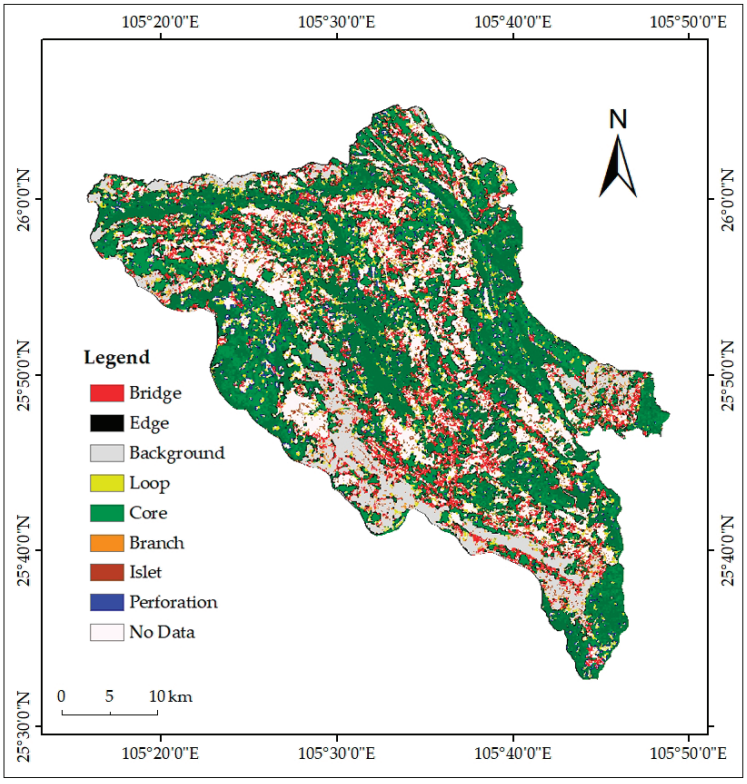

Figure 5. MSPA landscape type map of Guanling County.

Table 5. Landscape types in Guanling County.

Landscape Type	Area (km^2)	Proportion of Total Area of Ecological Landscape (%)
Core	608.61	65.73
Islet	11.71	1.26
Perforation	45.15	4.88
Edge	120.06	12.97
Loop	70.59	7.62
Bridge	31.30	3.38
Branch	38.53	4.16

In the analysis of landscape connectivity in Guanling County (Figure 6), the area of very high and highly connected patches was 518.26 km^2, accounting for 35.82% of the total area, mainly in the central, western, and eastern parts of the study area. The area of medium and low connectivity patches was 929.04 km^2, accounting for 64.20% of the total area, mainly distributed in the northern and southern regions of the study area, with a relatively large area and wide distribution. The landscape patches in Guanling County are relatively fragmented, and the connectivity between the landscapes is poor, which is mainly related to the special topography of the karst region.

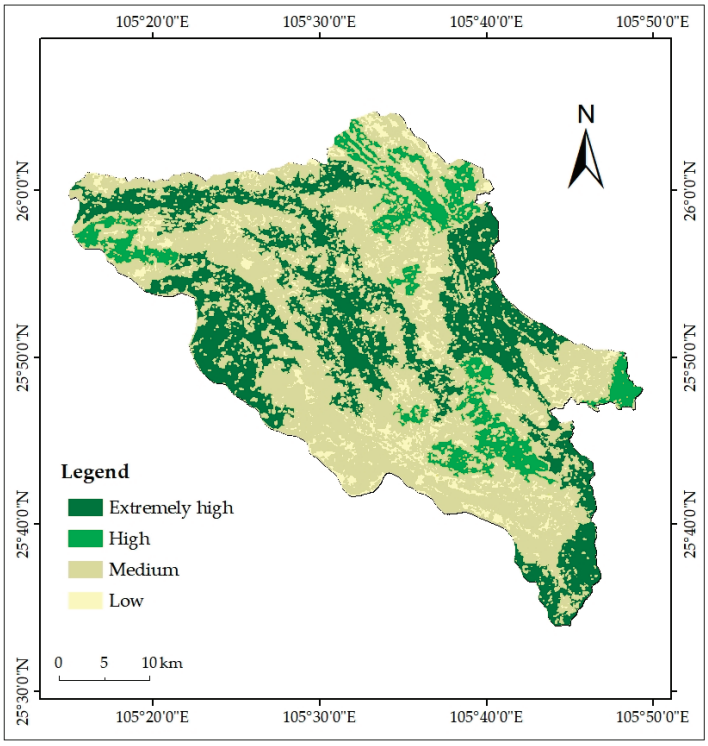

Figure 6. Guanling County landscape connectivity distribution map.

3.4. Comprehensive Resistance Surface and ES

We used the reclassification tool in ArcGIS10.8 to derive the resistance surface of seven single factors, and then superimposed these seven types of factors to find the mean value to obtain the comprehensive resistance surface distribution map of Guanling County (Figure 7). The results show that there is a high resistance area mainly located in the north, central, and south of Guanling County, and the patches in this area are fragmented and

the landscape connectivity is poor. The low resistance areas are mainly located in the western and southern fringes, where the landscape connectivity is relatively good and mainly consists of woodlands and grasslands. The selection of ES sites was based on the analysis of ecosystem service importance, ecological sensitivity, and landscape connectivity in Guanling County, and the ecosystem service importance, ecological sensitivity, and landscape connectivity were divided into four levels: very high, high, medium and low, respectively. Patches with two levels, very high and high after overlaid analysis with ArcGIS, were selected as ecological source sites. Finally, 10 ESs were obtained, with an area of 387.48 km^2, accounting for 26.78% of the total area. As far as the landscape components are concerned, the source sites were mainly woodlands, waters, and grasslands, and the ecological values of construction land and bare land were relatively low, mostly non-source sites. In terms of distribution area, the southwest region of Guanling County had less distribution, while the central, western, and eastern regions had more distribution. The distribution of ESs was fragmented, and there were many fine patches in the area, with poor inter-patch connectivity and high landscape fragmentation, which is very unfavorable for species dispersal.

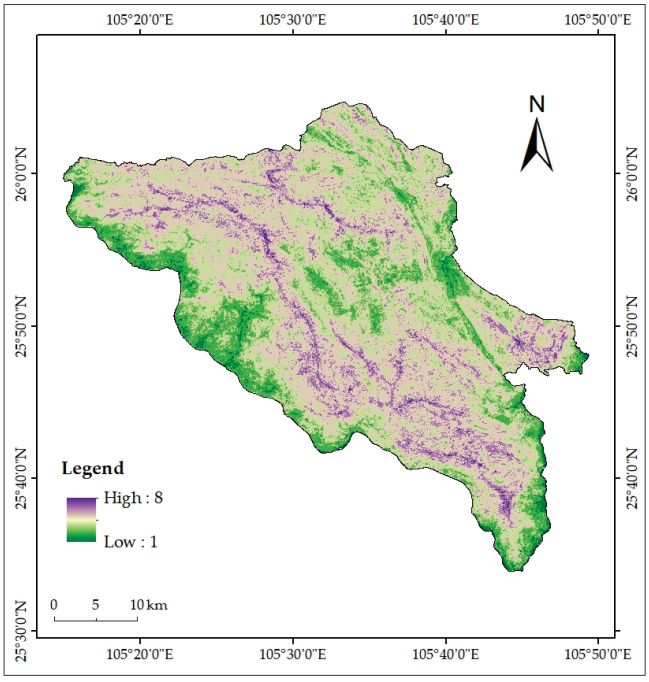

Figure 7. Guanling County comprehensive resistance surface distribution map.

3.5. EC Identification and ELSP Construction

EC are the links between each ecological source and the pathways of material flow, allowing species to avoid disturbance during migration [65]. According to the results of the ecological source distribution, using the distance analysis tool in ArcGIS10.8, combined with the comprehensive resistance surface of the study area, the minimum consumption distance between the ecological source points in the study area was calculated, and a total of 45 EC were obtained. The total length of the EC was 509.78 km, the maximum resistance value was 2.06 and the minimum resistance value was 0.23. Twenty of these ECs had resistance values above 1. Based on the gravity model, the interaction matrix between the 10 ecological source sites was constructed (Table 6), which could quantitatively evaluate the magnitude of the interaction between the source sites and discern the importance of potential ECs, and

the corridors with interaction forces greater than 10 were identified as important ECs, while the rest were general ECs. The interaction between source 6 and source 8 was the largest with 168.1243, which indicates that the material exchange and transportation between the two sources were more convenient and less costly. The interaction between source 3 and 9 was the smallest at 2.2473, which indicates that the exchange between the two sources requires a higher cost distance and a higher difficulty factor for material exchange and transportation. The ELSP is mainly composed of ecological nodes and EC. Under certain social, economic development and ecological protection conditions, this pattern plays an important role in the regional ecosystem. The ELSP of Guanling County is composed of ESs and ECs (Figure 8).

Table 6. Interaction matrix between sources based on gravity model calculations.

Number of Source	1	2	3	4	5	6	7	8	9	10
1	0	23.556	4.1539	4.7667	4.765	8.9556	7.954	9.5467	43.4106	19.5628
2		0	7.0123	8.5573	4.9466	24.6238	24.6462	21.9493	6.4892	23.4465
3			0	22.3342	17.3254	16.2479	32.0352	10.4792	2.2473	4.4374
4				0	19.6368	12.927	32.9607	8.1683	2.2863	3.911
5					0	10.362	16.8525	7.2889	2.4914	3.4039
6						0	78.5538	168.1243	3.9237	17.3001
7							0	30.9580	3.5073	9.6917
8								0	5.3442	39.4447
9									0	9.4984
10										

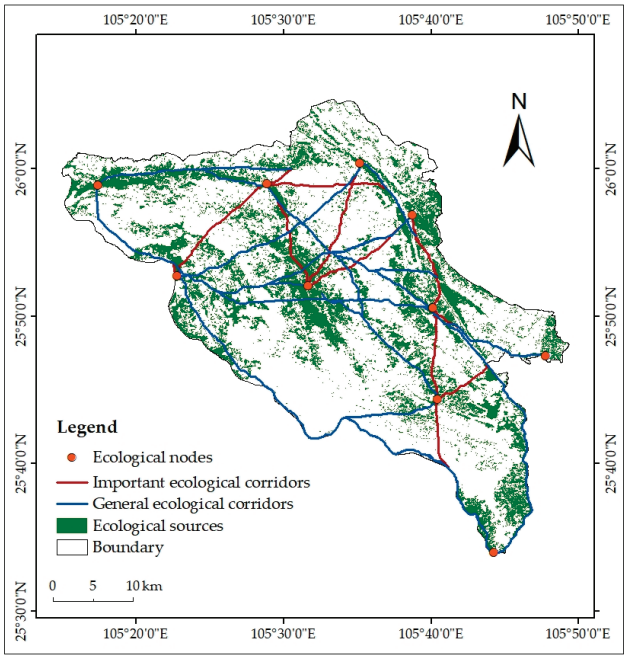

Figure 8. Landscape security pattern layout of Guanling County.

3.6. Discussion

This study combined ecosystem service values and landscape connectivity to determine the ESs, which is more scientific than previous methods and avoids the subjective

selection of ESs. According to the particular topography and geomorphology in the study area and considering the influence of various factors on regional development, the five evaluation factors of rocky desertification degree, land use, NDVI, DEM, and slope were selected to analyze the sensitivity of the study area. The selection of indicators takes into account the geomorphological characteristics of the karst region, which provides a more scientific basis for the construction of the comprehensive resistance surface and the extraction of EC in the study area.

According to the results from this research, we suggest that the protection of the core source area should first be strengthened in the process of ecological land use planning. The ES is a key part of the region. The ecological source area in Guanling County is small, with a low proportion and scattered distribution, which is very unfavorable for the exchange of materials in the region. Therefore, it should be protected in the landscape planning process and development, and construction should be prohibited. Second, ECs should be established, native species should be used as much as possible, and corresponding widths should be set according to the source distribution and the topographic and geomorphic characteristics of the study area to promote species migration and minimize artificial facilities. An organic combination of the ECs identified in this study and the original corridor to form an EC system can improve landscape connectivity between patches. In corridor planning, the potential corridors identified in this study can be organically combined with the original corridors; important ECs can be built in combination with the current corridors to enhance the connectivity between the corridors and the source sites; the construction of general ECs can be combined with some scattered fragmented patches using the existing spatial pattern to increase the connectivity between the source sites. Third, we should focus on the restoration of landscape patches. The general landscape of Guanling County is relatively fragmented. In the planning process, we should focus on the reconstruction and restoration of landscape patches with poor patch connectivity and high ecologically sensitive areas to minimize human interference.

4. Conclusions

This research selected five factors of land use type, DEM, slope, NDVI, and rocky desertification to analyze the ecological sensitivity of Guanling County in Guizhou Province with ArcGIS10.8 software. Through the superposition of various factors, the distribution status of the ecological sensitivity of Guanling County was obtained. Based on the natural breakpoint method, the calculation results were divided into five grades: insensitive, mildly sensitive, moderately sensitive, highly sensitive, and extremely sensitive, and the distributions of seven landscape types (core, islet, perforation, branch, bridge, edge, loop) in the study area were identified. The core area was the main landscape in the study area and an important habitat for species. The total core area was 608.61 km^2, accounting for 65.73% of the ecological landscape area, with a wide distribution range. Using Conefor 2.6 software, the *dPC* index value of each patch was calculated, and the distribution of landscape connectivity in Guanling County was obtained and divided into four grades: extremely high, high, medium, and low. The results showed that the very high and high connectivity patches in Guanling County had an area of 518.26 km^2, accounting for 35.82% of the total area, and were mainly distributed in the central, western, and eastern parts of the study area; the medium and low connectivity patches had an area of 929.04 km^2, accounting for 64.20% of the total area, and were mainly distributed in the northern and southern parts of the study area, with a relatively large area share and wide distribution. The landscape fragmentation of Guanling County was serious, and the connectivity was poor. According to the overlay of ecosystem service importance, ecological sensitivity, and landscape connectivity in Guanling County, 10 ESs were obtained with an area of 387.48 km^2, accounting for 26.78% of the total area of the county. Using the distance analysis tool in ArcGIS10.8, combined with the comprehensive resistance surface of the study area, the minimum consumption distance between each ecological source point was calculated, and a total of 45 ECs were obtained. The maximum resistance value was

2.06 and the minimum resistance value was 0.23, among which 20 ECs had resistance values over 1. Based on the gravity model, the interaction matrix between 10 ESs was constructed to quantitatively evaluate the magnitude of the interaction forces between the source sites and identify the important EC and general EC in Guanling County. Together, ESs and ECs constitute the ELSP of Guanling County. In the southwest part of the study area, the connectivity of landscape patches was relatively poor, the distribution of ES was limited, and the sensitivity was high. In future planning and construction efforts, we should focus on the ecological protection of this area and reduce human interference. However, there were still shortcomings in this study: the study of EC in the study area was mainly based on the minimum cost distance, the width of the corridor was determined by many factors together, influenced by topography, climate change, etc. In this study, the article did not study the width of the corridor in detail because we were limited by the data acquisition and, at the same time, there was not enough time to conduct detailed experiments. The width of the corridor has an important impact on the ecological function of the landscape [66]. Future research will address these inadequacies to improve the scientific accuracy of the study.

Author Contributions: Conceptualization, B.Y. and T.L.; methodology, B.Y. and T.L.; software, T.L. and L.K.; validation, B.Y., T.L. and L.K.; formal analysis, B.Y. and T.L.; investigation, T L., S.L. and R.S.; resources, B.Y. and K.X.; data curation, T.L. and L.K.; writing—original draft preparation, B.Y. and T.L.; writing—review and editing, B.Y. and F.Z.; project administration, B.Y.; funding acquisition, B.Y. All authors have read and agreed to the published version of the manuscript.

Funding: This research was funded by the National Natural Science Foundation of China (42261056, 42061028); the Key Science and Technology Program of Guizhou Provence: Poverty alleviation model and technology demonstration for eco-industries derivated from the karst desertification control (No. 5411 2017 Qiankehe Pingtai Rencai); the Oversea Expertise Introduction Program for Discipline Innovation of China: Overseas expertise introduction center for South China Karst eco-environment discipline innovation (No. D17016).

Data Availability Statement: Data supporting this study can be obtained from the Chinese Academy of Sciences Data Sharing Center (https://www.resdc.cn/, accessed on 17 May 2022) and the National Ecological Science Data Center (http://www.nesdc.org.cn/, accessed on 19 February 2022).

Conflicts of Interest: The authors declare no conflict of interest.

References

1. Yu, K. Security Patterns in Landscape Planning with a Case in South China. Ph.D. Thesis, Harvard University, Cambridge, MA, USA, 1995.
2. Formam, R.T.T. *Land Mosaics: The Ecology of Landscape and Regions*; Cambridge University Press: Cambridge, UK, 1995; pp. 32–76.
3. LI, H.; Yi, N.; Yao, W.J.; Wang, S.Q.; Li, Z.Y.; Yang, S.H. Shangri-La county ecological land use planning based on landscape security pattern. *Acta Ecol. Sin.* **2011**, *37*, 587–596. (In Chinese)
4. Du, Y.Y.; Hu, Y.N.; Yang, Y.; Peng, J. Building ecological security patterns in southwestern mountainous areas based on ecological importance and ecological sensitivity: A case study of Dali Bai Autonomous Prefecture, Yunnan Province. *Acta Ecol. Sin.* **2017**, *37*, 8241–8253. (In Chinese)
5. Li, F.; Ye, Y.P.; Song, B.W.; Wang, R.S. Evaluation of urban suitable ecological land based on the minimum cumulative resistance model: A case study from Changzhou, China. *Ecol. Model.* **2015**, *318*, 194–203. [CrossRef]
6. Su, Y.; Chen, X.; Liao, J.; Zhang, H.; Wang, C.; Ye, Y.; Wang, Y. Modeling the optimal ecological security pattern for guiding the urban constructed land expansions. *Urban For. Urban Green.* **2016**, *19*, 35–46. [CrossRef]
7. Liang, J.; He, X.; Zeng, G.; Zhong, M.; Gao, X.; Li, X.; Li, X.; Wu, H.; Feng, C.; Xing, W.; et al. Integrating priority areas and ecological corridors into national network for conservation planning in China. *Sci. Total Environ.* **2018**, *626*, 22–29. [CrossRef]
8. Peng, J.; Yang, Y.; Liu, Y.X.; Hu, Y.N.; Du, Y.Y.; Meersmans, J.; Qiu, S.J. Linking ecosystem services and circuit theory to identify ecological security patterns. *Sci. Total Environ.* **2018**, *644*, 781–790. [CrossRef]
9. Dai, L.; Wang, Z.J. Construction and optimization strategy of ecological security pattern based on ecosystem services and landscape connectivity: A case study of Guizhou Province, China. *Environ. Sci. Pollut. Res.* **2023**, 1–17. [CrossRef]
10. Shuai, N.; Hu, Y.; Gao, M.; Guo, Z.; Bai, Y. Construction and optimization of ecological networks in karst regions based on multi-scale nesting: A case study in Guangxi Hechi, China. *Ecol. Inform.* **2023**, *74*, 101963. [CrossRef]
11. Wu, Z.; Xiong, K.; Zhu, D.; Xiao, J. Revelation of coupled ecosystem quality and landscape patterns for agroforestry ecosystem services sustainability improvement in the karst desertification control. *Agriculture* **2023**, *13*, 43. [CrossRef]

12. Jiang, Y.; Gao, J.; Wu, S.; Jiao, K. Mediation effect as the component to ecosystem? Establishing the chain effect framework of ecosystem services across typical karst basin in China. *CATENA* **2023**, *221*, 106761. [CrossRef]
13. Beier, P.; Majkad, R.; Spencer, W.D. Forks in the road: Choices in procedures for designing wildland linkages. *Conserv. Biol.* **2008**, *22*, 836–851. [CrossRef]
14. Wang, H.; Ma, X.; Du, Y. Constructing ecological security patterns based on ecological service importance and ecological sensitivity in Guangdong Province. *Acta Ecol. Sin.* **2021**, *41*, 1705–1715. (In Chinese) [CrossRef]
15. Yao, C.Y.; An, R.; Dou, C.; Liu, Y.L. Construction and evaluation of forest ecological network in the Three Gorges Reservoir area based on MSPA and MCR models. *J. Resour. Environ. Yangtze River Basin* **2022**, *31*, 1953–1962. (In Chinese)
16. Costanza, R.; Kubiszewski, l. The authorship structure of "ecosystem services" as a transdisciplinary field of scholarship. *Ecosyst. Serv.* **2012**, *1*, 16–25. [CrossRef]
17. Li, D.; Wu, S.; Liu, L.; Liang, Z.; Li, S. Evaluating regional water security through a freshwater ecosystem service flow model: A case study in Beijing-Tianjin-Hebei region, China. *Ecol. Indic.* **2017**, *81*, 159–170. [CrossRef]
18. Darvill, R.; Lindo, Z. The inclusion of stakeholders and cultural ecosystem services in land management trade-off decisions using an ecosystem services approach. *Landsc. Ecol.* **2016**, *31*, 533–545. [CrossRef]
19. Shi, Y.; Shi, D.; Zhou, L.; Fang, R. Identification of ecosystem services supply and demand areas and simulation of ecosystem service flows in Shanghai. *Ecol. Indic.* **2020**, *115*, 106418. [CrossRef]
20. Zhang, Q.; Zhang, T. Land consolidation design based on an evaluation of ecological sensitivity. *Sustainability* **2018**, *10*, 3736. [CrossRef]
21. Chi, Y.; Zhang, Z.; Gao, J.; Xie, Z.; Zhao, M.; Wang, E. Evaluating landscape ecological sensitivity of an estuarine island based on landscape pattern across temporal and spatial scales. *Ecol. Indic.* **2019**, *101*, 221–237. [CrossRef]
22. Ersayin, K.; Tagil, S. Ecological sensitivity and risk assessment in the Kizilirmak Delta. *Fresenius Environ. Bull.* **2018**, *26*, 6508–6516.
23. Gao, G.L.; Deng, Z.M.; Xiong, K.N.; Su, X.L. *The Call and Hope of Karst*; Guizhou Science and Technology Press: Guiyang, China, 2003. (In Chinese)
24. Yuan, D.X. Global view on Karst rock desertification and integrating control measures and experiences of China. *J. Grassl. Sci.* **2008**, *9*, 19–25. (In Chinese)
25. Lu, Y.R. Karst Development Mechanism and Research Directions of Developing Engineering Construction Effect. *J. Earth Sci.* **2016**, *37*, 419–432. (In Chinese) [CrossRef]
26. Xiong, K.N.; LI, J.; Long, M.Z. Features of Soil and Water Loss and Key Issues in Demonstration Areas for Combating Karst Rocky Desertification. *J. Geogr.* **2012**, *67*, 878–888. (In Chinese)
27. Yue, Y.; Liu, B.; Wang, K.; Li, R.; Zhang, B.; Zhang, C.; Chen, H. RETRACTED ARTICLE: Using remote sensing to quantify the fractional cover of vegetation and exposed bedrock within a complex landscape: Applications for karst rocky desertification monitoring. *Environ. Monit. Assess.* **2013**, *185*, 1025. [CrossRef]
28. Tong, X.; Brandt, M.; Yue, Y.; Horion, S.; Wang, K.; De Keersmaecker, W.; Tian, F.; Schurgers, G.; Xiao, X.; Luo, Y.; et al. Increased vegetation growth and carbon stock in China karst via ecological engineering. *Nat. Sustain.* **2018**, *1*, 44–50. [CrossRef]
29. Qi, X.; Zhang, C.; Wang, K. Comparing remote sensing methods for monitoring Karst rocky desertification at sub-pixel scales in a highly heterogeneous Karst Region. *Sci. Rep.* **2019**, *9*, 13368. [CrossRef] [PubMed]
30. Jiang, Y.; Li, L.; Groves, C.; Yuan, D.; Kambesis, P. Relationships between rocky desertification and spatial pattern of land use in typical karst area, Southwest China. *Environ. Earth Sci.* **2009**, *59*, 881–890. [CrossRef]
31. Bai, X.-Y.; Wang, S.-J.; Xiong, K.-N. Assessing spatial-temporal evolution processes of karst rocky desertification land: Indications for restoration strategies. *Land Degrad. Dev.* **2013**, *24*, 47–56. [CrossRef]
32. Yang, Q.; Jiang, Z.; Yuan, D.; Ma, Z.; Xie, Y. Temporal and spatial changes of karst rocky desertification in ecological reconstruction region of Southwest China. *Environ. Earth Sci.* **2014**, *72*, 4483–4489. [CrossRef]
33. Yue, Y.; Wang, K.; Zhang, B.; Jiao, Q.; Liu, B.; Zhang, M. Remote sensing of fractional cover of vegetation and exposed bedrock for karst rocky desertification assessment. *Procedia Environ. Sci.* **2012**, *13*, 847–853. [CrossRef]
34. Ying, B.; Xiao, S.Z.; Xiong, K.N.; Cheng, Q.W.; Luo, J.S. Comparative studies of the distribution characteristics of rocky desertification and land use/land cover classes in typical areas of Guizhou province, China. *Environ. Earth Sci.* **2014**, *71*, 631–645. [CrossRef]
35. Gao, J.; Wang, H. Temporal analysis on quantitative attribution of karst soil erosion: A case study of a peak-cluster depression basin in Southwest China. *CATENA* **2019**, *172*, 369–377. [CrossRef]
36. Jiang, Z.; Lian, Y.; Qin, X. Rocky desertification in Southwest China: Impacts, causes, and restoration. *Earth Sci. Rev.* **2014**, *132*, 1–12. [CrossRef]
37. Yan, X.; Cai, Y.L. Multi-scale anthropogenic driving forces of karst rocky desertification in southwest China. *Land Degrade. Dev.* **2015**, *26*, 193–200. [CrossRef]
38. Zhang, S.; Zhang, Y.; Xiong, K.; Yu, Y.; Min, X. Changes of leaf functional traits in karst rocky desertification ecological environment and the driving factors. *Glob. Ecol. Conserv.* **2020**, *24*, e01381. [CrossRef]
39. Peng, X.D.; Dai, Q.H. Drivers of soil erosion and subsurface loss by soil leakage during karst rocky desertification in SW China. *Int. Soil Water Conserv. Res.* **2022**, *10*, 217–227. [CrossRef]
40. Guo, B.; Wei, C.; Yu, Y.; Liu, Y.; Li, J.; Meng, C.; Cai, Y. The dominant influencing factors of desertification changes in the source region of Yellow River: Climate change or human activity? *Sci. Total Environ.* **2022**, *813*, 152512. [CrossRef] [PubMed]

41. Yan, D.; Zhong, C.J. Characteristic of rocky desertification and comprehensive improving model in karst peak-cluster depression in Guohua, Guangxi, China. *Procedia Environ. Sci.* **2011**, *10*, 2449–2452. [CrossRef]
42. Wu, Z.; Zhu, D.; Xiong, K.; Wang, X. Dynamics of landscape ecological quality based on benefit evaluation coupled with the rocky desertification control in South China Karst. *Ecol. Indic.* **2022**, *138*, 108870. [CrossRef]
43. Yao, B.; Yue, X.J.; Huang, P.; Li, Y.-H. The Qing-Long model: China provides a solution to the karst rocky desertification challenge. *Acta Ecol. Sin.* **2022**. [CrossRef]
44. Li, Y.X.; Li, J.; Chen, H.; Wang, Z.J. Landscape connectivity evaluation and temporal-spatial characteristics of Guiyang City from 2008 to 2017 based on MSPA and MCR models. *J. Ecol.* **2022**, *41*, 1240–1248. (In Chinese) [CrossRef]
45. Wang, S.J.; Li, Y.B.; Li, R.L. Background, evolution and management of karst rocky desertification. *J. Quat. Study* **2003**, *1*, 657–666. (In Chinese)
46. General Administration of Quality Supervision; Inspection and Quarantine of the People's Republic of China, National Standardization Administration of China. *GB/T21010-2017*; Land Use Status Classification. Standards Publishing House: Beijing, China, 2017. Available online: https://openstd.samr.gov.cn/bzgk/gb/newGbInfo?hcno=224BF9DA69F053DA22AC758AAAADEEAA (accessed on 22 September 2022). (In Chinese)
47. Xiong, K.N.; Yuan, J.Y.; Fang, Y.; Lan, A.J.; Chen, Q.W.; Zeng, F.Q.; Ying, B.; Zhang, W.W.; Hu, J.; Zhou, Z.F.; et al. *Atlas of Comprehensive Prevention and Control of Karst Rocky Desertification in Guizhou (2006–2050)*; Guizhou People's Publishing House: Guiyang, China, 2007. (In Chinese)
48. Ahern, J.; Cilliers, S.; Niemelä, J. The concept of ecosystem services in adaptive urban planning and design: A framework for supporting innovation. *Landsc. Urban Plan.* **2014**, *125*, 254–259. [CrossRef]
49. Warsame, A.A.; Abdi, A.H. Towards sustainable crop production in Somalia: Examining the role of environmental pollution and degradation. *Cogent Food Agric.* **2023**, *9*, 2161776. [CrossRef]
50. Raihan, A.; Pavel, M.I.; Muhtasim, D.A.; Farhana, S.; Faruk, O.; Paul, A. The role of renewable energy use, technological innovation, and forest cover toward green development: Evidence from Indonesia. *Innov. Green Dev.* **2023**, *2*, 100035. [CrossRef]
51. Xu, W.; Wang, J.; Zhang, M.; Li, S. Construction of landscape ecological network based on landscape ecological risk assessment in a large-scale opencast coal mine area. *J. Clean. Prod.* **2021**, *286*, 125523. [CrossRef]
52. Yang, T.R.; Kuang, W.H.; Liu, W.D.; Liu, A.L.; Pan, T. Optimization of ecological spatial structure of Guanzhong urban agglomeration based on ecological security pattern. *J. Geogr. Res.* **2017**, *36*, 441–452. (In Chinese)
53. Taylor, P. Connectivity is a vital element of landscape structure. *Oikos* **1993**, *68*, 571–573. [CrossRef]
54. Chen, L.D.; Fu, B.J. The ecological significance and application of landscape connectivity. *J. Ecol.* **1996**, *15*, 37–42.
55. Gandini, M.L.; Lara, B.D.; Moreno, L.B.; Cañibano, M.A.; Gandini, P.A. Landscape dynamics of Paspalum quadrifarium grasslands analyzed by Morphological Spatial Pattern Analysis (MSPA). *PeerJ* **2018**. [CrossRef]
56. Xu, F.; Yin, H.W.; Kong, F.H.; Xu, J.G. Developing ecological networks based on mspa and the least-cost path method: A case study in bazhong western new district. *J. Ecol.* **2015**, *35*, 6425–6434. (In Chinese)
57. Gao, X.W.; Feng, Z.J.; Ge, J.F. Analysis of landscape security pattern in Western Mountains of Shijiazhuang. In Proceedings of the Geoinformatics 2008 and Joint Conference on GIS and Built Environment: Geo-Simulation and Virtual GIS Environments, Guangzhou, China, 28–29 June 2008; Volume 7145, p. 71451. [CrossRef]
58. Xiao, S.; Wu, W.; Guo, J.; Ou, M.; Pueppke, S.G.; Ou, W.; Tao, Y. An evaluation framework for designing ecological security patterns and prioritizing ecological corridors: Application in Jiangsu Province, China. *Landsc. Ecol.* **2020**, *35*, 2517–2534. [CrossRef]
59. Su, X.; Zhou, Y.; Li, Q. Designing ecological security patterns based on the framework of ecological quality and ecological sensitivity: A case study of Jianghan Plain, China. *Int. J. Environ. Res. Public Health* **2021**, *18*, 8383. [CrossRef]
60. Wang, Z.; Shi, P.; Zhang, X.; Tong, H.; Zhang, W.; Liu, Y. Research on landscape pattern construction and ecological restoration of Jiuquan city based on ecological security evaluation. *Sustainability* **2021**, *13*, 5732. [CrossRef]
61. Liu, Z.; Gan, X.; Dai, W.; Huang, Y. Construction of an ecological security pattern and the evaluation of corridor priority based on ESV and the "importance–connectivity" index: A case study of Sichuan province, China. *Sustainability* **2022**, *14*, 3985. [CrossRef]
62. Wu, M.Q.; Hu, M.M.; Wang, T.; Fan, C.; Xia, B.C. Recognition of urban ecological source area based on ecological security pattern and multi—Scale landscape connectivity. *Acta Ecol. Sin.* **2019**, *39*, 4720–4731. (In Chinese) [CrossRef]
63. Xiong, C.N.; Wei, H. Lan Mingjuan. Landscape connectivity of urban green space in Chongqing. *Chin. J. Ecol.* **2008**, *5*, 2237–2244. (In Chinese)
64. Garcia-Lozano, C.; Varga, D.; Pintó, J.; Roig-Munar, F. Landscape connectivity and suitable habitat analysis for wolves (*Canis lupus* L.) in the Eastern Pyrenees. *Sustainability* **2020**, *12*, 5762. [CrossRef]
65. Yu, K. Security patterns and surface model in landscape ecological planning. *Landsc. Urban Plan.* **1996**, *36*, 1–17. [CrossRef]
66. Chen, X.; Peng, J.; Liu, Y.X.; Yang, Y.; Li, G. Construction of ecological security pattern of Yunfu City based on 'importance-sensitivity-connectivity' framework. *Geogr. Res.* **2017**, *36*, 471–484. (In Chinese) [CrossRef]

forests

MDPI

Article

Research on the Resilience Assessment of Rural Landscapes in the Context of Karst Rocky Desertification Control: A Case Study of Fanhua Village in Guizhou Province

Bin Ying [1,2], Sensen Li [1], Kangning Xiong [1,*], Yufeng Hou [3], Ting Liu [1] and Ruonan Sun [1]

[1] School of Karst Science, Guizhou Normal University, Guiyang 550000, China
[2] Institute of Guizhou Rural Revitalization, Guiyang 550000, China
[3] China Railway Construction Fifth Survey and Design Institute Group Co., Ltd., Tianjin 300000, China
* Correspondence: xiongkn@126.com

Abstract: The ecological rehabilitation project has greatly curbed the serious problem of karst rocky desertification (KRD) in southern China and significantly changed the ecological environment and landscape pattern of the karst rocky desertification control areas (KRDCA). As one of the most important social–ecological fragile areas in the world, rural landscapes in KRDCA still show a strong sensitivity to disturbance. To reduce risks and improve the resilience of landscapes, this paper constructs a framework for assessing rural landscape resilience in KRDCA from the three dimensions of ecology, engineering, and social culture, based on the concept of resilience defined by the United Nations International Agency for Disaster Reduction. Considering the characteristics of rural landscapes in KRDCA, we select typical villages for empirical study. The results show the following: (1) The KRDCA is highly sensitive to natural disasters due to its special dual geomorphic structure characteristics. The disaster preparedness capacity of villages is the key factor determining the resilience of rural landscapes. The analysis of the disaster preparedness capacities of rural landscape structures with different vulnerability characteristics can be used as an effective means of evaluating the resilience level of rural landscapes in KRDCA. (2) Based on the empirical analysis of Fanhua village, which is a typical KRDCA in southern China, we found that the ecological system and engineering system of the village landscape have high resilience, while the resilience of the social and cultural systems are weak. This is due to the fact that the large number of rural population emigration in recent years has resulted in villages being at the key node of the reorganization of the social and cultural value system. The unstable sociocultural value system reduces the ability of rural landscapes to adapt to disturbance or environmental change. The study results could guide improvement strategies for subsequent landscape planning and inspire new ideas and methods for the implementation of rural revitalization strategies and the improvement of landscape resilience in KRDCA.

Keywords: resilient landscape; rural planning; resilience assessment; karst rocky desertification control areas

Citation: Ying, B.; Li, S.; Xiong, K.; Hou, Y.; Liu, T.; Sun, R. Research on the Resilience Assessment of Rural Landscapes in the Context of Karst Rocky Desertification Control: A Case Study of Fanhua Village in Guizhou Province. *Forests* **2023**, *14*, 733. https://doi.org/10.3390/f14040733

Academic Editor: Julia Jones

Received: 16 February 2023
Revised: 16 March 2023
Accepted: 2 April 2023
Published: 3 April 2023

1. Introduction

1.1. Karst Rocky Desertification in Southern China

The world's karst landforms are mainly distributed in southern China, central and southern Europe, and eastern North America, accounting for 12% of the world's total land area [1]. Karst landforms account for more than 30% of the total land area in China. Karst areas in Southwest China centered on the Yunnan-Kweichow Plateau are characterized as the most intense karst development and acute human–land conflict, which makes this area a typical ecologically fragile region [2]. Karst rocky desertification (KRD) is caused by various factors and is considered to be a major socio-environmental problem in karst areas. It is a typical ecological degradation process governed by vegetation degradation and succession,

surface water and soil erosion, and land productivity degradation, and, finally, shows a desert-like landscape on the ground surface [3–5]. The result of KRD in southern China triggers a serious threat to the ecological security and downgrades sustainable economic and social development in this region. In the past 30 years, the Chinese government has realized the problems of KRD in southwest China and implemented many ecological projects in the karst region to mitigate the severity of rocky desertification [6], such as the projects of Grain for Green and Natural Forest Protection.

1.2. The Progress Karst Rocky Desertification Control in China

Since the beginning of the 21st century, the Chinese government has attached great importance to the control of KRD. During the 10th Five-Year Plan period, "promoting the comprehensive control of KRD in Guizhou, Guangxi and Yunnan" was listed as a national goal. Since then, the 11th, 12th, and 13th Five-Year Plans clearly stated that efforts will continue to be intensified to comprehensively promote karst rocky desertification control (KRDC). The world's largest KRD ecological restoration and protection project has been carried out in 300 counties [7], forming a complete set of technical systems with ecological governance technology and biological and engineering management technology [5]. Under the background of the Chinese government's implementation of KRDC and ecological civilization construction, China's ecological environment and landscape pattern have undergone significant changes [8–10]. The serious KRD problem in karst areas of Southwest China has been gradually addressed, the degree of KRD has been reduced, and the impact of ecological damage has diminished [11–13]. The results of China KRD monitoring showed that the area of KRD in Guizhou Province decreased by 8457 km^2 in 2016 compared with 2005 [14]. In addition, the comprehensive management model of the fragile ecological environment, the ecological agriculture construction model, the agroforestry model, the poverty alleviation and ecological construction model, the returning farmland to forest and forest ecological construction model, the nature reserve and forest park model, ecological tourism and scenic area construction, and other models have achieved outstanding results in karst areas [15,16]. In particular, the rich biodiversity and unique geomorphic landscapes in karst areas have high aesthetic, scientific, and conservation values [17,18]. At present, there are 32 national geoparks with karst landscapes as the main or auxiliary land type, accounting for 23.2% of the national geoparks. Among them, Shilin Karst in Yunnan, Libo Karst in Guizhou, Wulong Karst in Chongqing, Guilin Karst in Guangxi, Shibing Karst in Guizhou, Jinfoshan Karst in Chongqing, and Huanjiang Karst in Guangxi are nominated as World Natural Heritage Sites, highlighting the global value and importance of the karst landscape in Southwest China [19,20]. In general, China's KRDC measures have achieved remarkable progress, effectively supporting the sustainable development of Southwest China. However, in vast rural areas, due to the constraints of the karst geological background (overground–underground water and soil dual structure, slow soil formation and a shallow and discontinuous soil layer, rapid hydrological process, etc.) and the influence of human–land conflict, there are some problems in the process of KRDC, such as difficulty in consolidating control effects and lack of sustainability [21].

1.3. Rural Landscape in Karst Rocky Desertification Control Area

In 2017, the Chinese government put forward the strategy of rural revitalization, with the strategic goals of accelerating the modernization of agriculture and rural areas and improving the living environment [22], introducing a new connotation to rural environmental governance in KRDCA. Rural landscape systems usually refer to the expression of rural ecology, engineering, and social culture in the landscape, which can not only provide a livable residential environment and activity space for people, but also promote the sustainable and diversified development of rural areas [23,24]. Villages developed on KRD are extremely vulnerable to the external environment, posing a serious threat to the landscape pattern of rural human–land systems. The practical problem of how to improve rural landscapes in KRDCA based on the consideration of ecological, social, and

cultural factors must be urgently addressed. The concept of "resilience", first proposed by Canadian ecologist Holling in 1973 [25], provides a new perspective for the study of the anti-disturbance capacity of rural landscapes in KRDCA. Resilience refers to the ability of ecosystems to recover quickly without collapse in the face of disturbance, and was gradually introduced into the fields of landscape planning and risk management to identify potential risks and maintain the operational capacity of landscape systems [26–28]. In recent years, due to the impact of global climate change and the frequent occurrence of natural disasters, rural vulnerability in KRD areas has become prominent. The assessment of landscape resilience by identifying the potential risks and system stability ability of the landscape system can not only be used as an effective means to detect the effect of rocky desertification control, but also can be based on the principle of landscape ecology to enhance the ability of the village system in rocky desertification areas to respond to land degradation through the optimization and coordination of landscape patches. It has the potential to be an effective measure to control rocky desertification.

Currently, research on landscape resilience is gradually increasing, mainly focusing on the connotation and representation of resilient landscapes [29], the maintenance and management of resilient landscapes [30,31], the relationship between resilient landscapes and climate [32], and the planning and design of resilient landscape cases [33]. Due to the complexity of the influencing factors of landscape resilience, there have been relatively few empirical studies that truly involve the assessment of landscape resilience. The quantitative assessment of rural resilience has mainly focused on the dynamic changes in village livelihood and the assessment of individual resilience adaptability, but has ignored the role of rural landscape resilience, which is an important factor in rural development. Therefore, it is necessary to construct a rural landscape resilience assessment framework for KRDCA and to analyze the systematic adaptation and resilience of human–land landscape systems to the interference of natural disasters in the context of KRDC. To provide strategies for improving the resilience of karst rural landscapes and controlling KRD, this research constructs the analysis framework of rural landscape resilience identification in KRDCA based on the concept of resilience proposed by the United Nations International Agency for Disaster Reduction [34], and selects typical karst villages in southern China to carry out empirical research.

2. Assessment Framework for rural Landscape Resilience in Karst Areas Desertification Control Areas in Southern China

Since the concept of ecological resilience was introduced in different fields, researchers have begun to explore the quantitative evaluation of resilience, and a relatively complete theoretical system has been developed. Bruneau et al. (2003) proposed that resilience could be measured by the functional performance of infrastructure before and after a community disaster [35]. Building on the research of Bruneau's group, Henry et al. (2017) suggested that resilience can be analyzed from key parameters such as disturbance events, system resilience, and overall resilience strategies [36], and Equation (1) was also proposed, where resilience is defined as the ratio between the recovery status of the system to be evaluated at t_1 after the disturbance and the loss status at t_0 after the disturbance.

$$R(t) = \text{recovery}(t_1) \Big/ \text{loss}(t_0) \quad (1)$$

Referring to the definition of resilience proposed by the United Nations International Agency for Disaster Reduction, Kusumastuti (2014) defined resilience as the ratio between disaster preparedness and vulnerability, as shown in Equation (2) [37,38]. On this basis, Xu (2020) conducted an empirical study on resilience assessment by identifying the disaster preparedness and vulnerability of complex urban public spaces [39]. Due to the special geomorphological characteristics of KRDCA, the difference in the disaster preparedness capacity of rural communities before disasters determines the degree of disaster damage to rural landscapes. Improving disaster preparedness capacity can effectively reduce the

negative impact caused by disturbance events. Vulnerability is defined as a sensitive state in which rural landscapes in KRDCA are susceptible to external disturbance or internal pressure damage due to a lack of adaptability or defects in the landscape structure itself [40]. This is the regional background characteristic of the eco-social system in KRDCA, which plays a decisive role in the resilience level of rural landscapes. Therefore, this paper also defines rural landscape resilience in KRD management areas as the ratio of landscape preparedness capacity and vulnerability.

$$\text{Resilience Index } (RI) = \frac{\text{Preparedness Index } (PI)}{\text{Vulnerability Index } (VI)} \quad (2)$$

RI is the resilience level score of the village landscape in the KRDCA to be evaluated, which is the ratio between the system disaster preparedness index (*PI*) and vulnerability index (*VI*). If $RI > 1$, it means that the disaster preparedness capacity of the rural landscape system can overcome its own vulnerability when facing disturbance events, it can use its own resources, skills and social organizations to manage or deal with adverse conditions or risks, and can restore to the original state; that is, the rural landscape system is resilient in the face of risks. However, when $RI \leq 1$, it means that the disaster preparedness capacity is not enough to make up for vulnerability when disturbance events occur, and great losses will result; that is, the rural landscape system has poor resilience in the face of risk.

The evaluation index system for the disaster preparedness capacity and vulnerability level of the village landscape is constructed from the rural ecosystem, engineering facility system, and social and cultural system in KRDCA. Disaster preparedness refers to the ability of people, organizations, and systems to use all available resources and skills to cope with adverse conditions, disasters, or risks [34]. This study mainly refers to the ability of rural landscapes in KRDCA to cope with disturbances and reduce losses by using their main components, the ecosystem, the engineering facility system, and the social and cultural system. If the vulnerability is improperly handled, it can directly lead to the reduction or cessation of some functions of the system [41]. In this study, it refers to the potential threat caused by the defects and inadequacies of rural landscape ecosystems, engineering facility systems, and social and cultural systems in KRDCA. Under the same vulnerability status, the disaster preparedness capacity of village landscapes to natural disasters is a key factor determining the resilience level of rural landscapes. The disaster preparedness and vulnerability assessment of rural landscapes in KRDCA could be used to effectively assess the resilience level of rural landscape systems in karst areas against the background of the Chinese government's KRDC. The disaster preparedness capacity of rural landscapes is positively correlated with landscape resilience, while vulnerability is negatively correlated with landscape resilience. In the face of external disturbance, if the disaster preparedness capacity could resist the vulnerability caused by its own structural defects, the landscape system is resilient; otherwise, the rural landscape system had no resilience or insufficient resilience. The specific evaluation framework is shown in Figure 1.

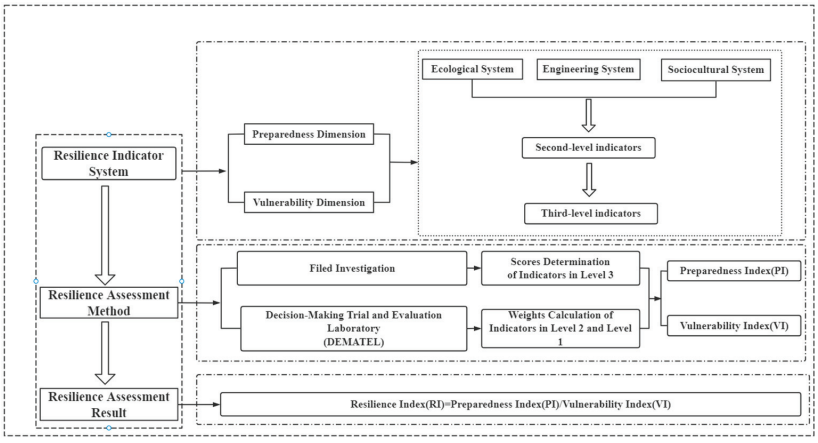

Figure 1. Rural resilient landscape assessment framework.

3. Data Source and Processing

3.1. Study Area

Centered on the Yunnan-Kweichow Plateau, South China karst area is one of the world's outstanding karst landscape, covering eight provinces and municipalities, including Guizhou, Guangxi, Chongqing, Yunnan, Sichuan, Hunan, Hubei, and Guangdong [42]. Guizhou is a part of the plateau and mountains of Southwest China, located on the eastern slope of the Yunnan-Kweichow Plateau, with complex karst types, complete morphology, and a large, concentrated distribution area, accounting for 61.9% of the total area of the province [43]. Affected by Himalayan movement, the Qinghai-Tibet Plateau has been rapidly uplifted, and the karst areas in Guizhou have developed a typical plate-canyon landform. The basic characteristics of the surface are broken and rugged terrain, a thin soil layer, a small area of cultivated land with poor quality, low land carrying capacity, and extremely fragile ecosystems [44,45]. Farmers living in this area have long been affected by natural disasters such as soil erosion, landslides, debris flows, drought, and floods, which have gradually led to large areas of KRD [46]. The China KRDC project has improved the karst ecological environment and effectively curtailed the expansion of KRD by adopting ecological control, engineering control, and biological control measures [47]. However, due to the closed influence of the karst mountain environment, the rural landscape in KRDCA in Guizhou still shows typical characteristics of high sensitivity to disasters.

Based on the rural landscape resilience analysis framework of karst areas, this research selected Fanhua village in Guanling County, a typical county of KRDC in South China, as a case study to carry out empirical research and analysis (the specific location is shown in Figure 2). The main part of the village is in the southeast to northwest trend of the peak cluster basin, covering an area of about 6 km^2, and the lithology is mainly dominated by limestone. The climate type of the study area is a subtropical monsoon climate that characterized by sufficient heat and rain in the summer; the cumulative average annual temperature, average maximum temperature, and average minimum temperature are 16.2 °C, 16.9 °C, and 15.4 °C, respectively. The annual precipitation is 1205.1 mm, and the average annual humidity is 81%. The terrain of the study area is relatively gentle, and is suitable for the growth of all kinds of vegetation and crops. However, long-term unreasonable land utilization has led to low vegetation coverage and serious soil erosion in the village. In addition, due to the influence of ground and underground dual structures in karst areas, surface water carries an amount of soil that easily leaks into the underground river system, which leads to significant trend of KRD. The local government has curbed the trend of KRD in a timely manner through measures such as mountain closure and forest cultivation, construction of water conservation facilities, vegetation management and

protection, scientifically accelerated vegetation restoration, and soil fertility improvements. The village landscape pattern and villagers' livelihood modes have been significantly improved, providing a good platform for the study of rural landscape resilience assessment in KRDCA.

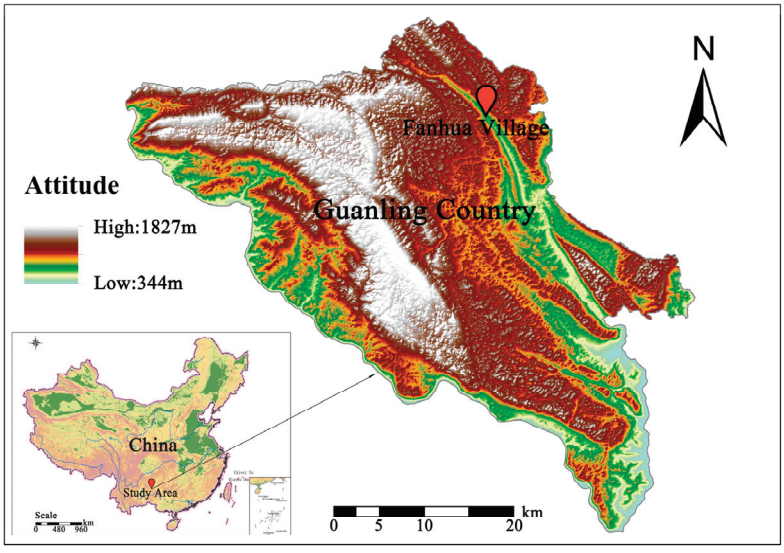

Figure 2. Regional location map of Fanhua Village.

3.2. Data Sources

3.2.1. Questionnaire Inquiry

In July 2022, the research group carried out a field survey of Fanhua village. First, the village cadres were interviewed to understand the KRDC measurements and technologies in Fanhua village, and then the field survey and data collection were carried out from the three viewpoints of ecosystem, engineering system, and social and cultural system. The survey and data collection included assessment indicators of the rural landscape preparedness and vulnerability of Fanhua village. The quantitative indicators were mainly evaluated by on-site data collection and local statistical data, while the qualitative indicators were mainly analyzed and evaluated by villager interviews. The interviewees were mainly residents over 40 years old who had a certain understanding of landscape pattern changes and KRDC effects. A total of 44 people were interviewed, including 3 village cadres with an average interview duration of 3.5 h, and 41 villagers with an average interview duration of 2 h. With the help of village cadres, on-site data collection and local statistical data reviews were conducted. The Likert scale method was used in the study, and the evaluation index score information was divided into five levels: very low (1), low (2), moderate (3), high (4), and very high (5).

3.2.2. Assessment Indicators

Rural landscapes in karst areas have unique local characteristics. The existing landscape resilience evaluation index system was developed mostly for urban areas, and is not suitable for the assessment of rural landscape resilience in KRDCA. Combined with the rural regional characteristics of karst areas, this paper constructs an evaluation index system based on the three dimensions of ecological system, engineering system, and social culture system proposed in the evaluation theoretical framework (specific indicators are shown in Tables 1 and 2).

Table 1. Assessment index of disaster preparedness of rural landscapes in KRDCA.

First-Level Indicators	Second-Level Indicators	Third-Level Indicators	Indicator Score Description
Ecological system	Ecological pattern	Ratio of green space	0%–20% (1), 21%–30% (2), 31%–40% (3), 41%–50% (4), More than 50% (5)
		Diversity of species	The proportion of vegetation species in the total number of suitable plants in the area: less than 30% (1), 31%–50% (2), 51%–70% (3), 71%–90% (4), and more than 90% (5)
	Ecological governance	The proportion of KRDCA	0%–20% (1), 21%–30% (2), 31%–40% (3), 41%–50% (4), More than 50% (5)
Engineering system	Building facilities	Building structure	The proportion of brick or reinforced concrete structure: less than 50% (1), 51%–60% (2), 61%–70% (3), 71%–80% (4), more than 80% (5)
		Proportion of new homes built in the last decade	Less than 40% (1), 41%–50% (2), 51%–60(3), 61%–70% (4), more than 70% (5)
	Water conservation engineering	Kilometers of new aqueducts	Less than 0.3 (1), 0.3–0.5 (2), 0.5–0.8 (3), 0.8–1.0 (4), more than 1.0 (5)
		Number of new cisterns	0 (1), 1–2 (2), 3 (3), 4 (4), more than 5 (5)
	Fire protection facilities	Fire station service radius	More than 7 km^2 (1), 4 km^2–5 km^2 (2), 5 km^2–6 km^2 (3), 6 km^2–7 km^2 (4), Less than 4 km^2 (5)
	Road engineering	Proportion of concrete roads	Less than 50% (1), 51%–60% (2), 61%–70% (3), 71%–80% (4), more than 80% (5)
		Road supporting facilities	0 (1), 1–2 (2), 3 (3), 4 (4), more than 5 (5)
Sociocultural system	Cultural disaster preparedness	Number of disaster avoidance strategy training per year	0 (1), 1–2 (2), 3 (3), 4 (4), more than 5 (5)
		KRDC knowledge propaganda	0 (1), 1–2 (2), 3 (3), 4 (4), more than 5 (5)
	Cultural landscape protection	Establishment of cultural reserve	0 (1), 1–2 (2), 3 (3), 4 (4), more than 5 (5)
		Awareness of cultural protection	Less than 30% (1), 30%–50% (2), 50%–70% (3), 70%–90% (4), more than 90% (5)

Table 2. Assessment indicators of rural landscape vulnerability in KRDCA.

First-Level Indicators	Second-Level Indicators	Third-Level Indicators	Indicator Score Description
Ecological system	Ecological pressure	The proportion of crops requiring large amounts of water	0%–20% (1), 21%–30% (2), 31%–40% (3), 41%–50% (4), more than 50% (5)
		Proportion of invasive alien plants	0%–10% (1), 11%–20% (2), 21%–30% (3), 31%–40% (4), more than 40% (5)
	Ecological vegetation sensitivity	Threat assessment of native vegetation	Number of endangered species of native vegetation: 0 (1), 1–2 (2), 3–4 (3), 5–6 (4), more than 6 (5)
	Building instability	Old buildings with security risks	The number of buildings with security risks: 0 (1), 1–2 (2), 3–4 (3), 5–6 (4), more than 6 (5)
	Water supply and drainage pressure	Annual water supply and drainage facilities failure days	Less than 15 days (1), 15–50 (2), 50–80 (3), 80–100 (4), more than 100 days (5)
	Fire protection pressure	Frequency of failure of fire protection facilities in the past five years	0 (1), 1–3 (2), not checked (3), 4–5 (4), more than 5 times (5)
Engineering system	Road sensitivity	Annual frequency of road failure	0 (1), 1–2 (2), 3 (3), 4 (4), more than 5 (5)
		Proportion of unrepaired roads	0%–10% (1), 11%–20% (2), 21%–30% (3), 31%–40% (4), more than 40% (5)
Sociocultural system	Cultural resource loss	Idle cultural facilities	0 (1), 1–2 (2), 3 (3), 4 (4), more than 5 (5)
		Damage to traditional buildings	0 (1), 1–2 (2), 3 (3), 4 (4), more than 5 (5)
	Disaster sensitivity	Setting of disaster sensitive area	1–2 (1), 3 (2), no disaster sensitive zones were set (3), 4–5 (4), more than 5 (5)

Ecosystems are an important part of rural landscapes that can not only bring good landscape effects, but also regulate climate, alleviate pollution, and purify air [48]. When the rural landscape system in KRDCA suffers from external disturbances, a good ecosystem can effectively act as a buffer to address disasters. This paper measures the quality of ecosystems from the two dimensions of ecological patterns and ecological governance [49,50]. Reasonable ecological patterns both create a good landscape effect and also effectively alleviate the impact of floods and other disasters and enhance the disaster preparedness ability of landscapes [51]. The ecological treatment project has improved the vegetation coverage rate in KRDCA and effectively alleviated the threat of heavy rainfall and other disasters to the rural landscape and to the safety of villager lives and property [52,53]. From

the perspective of ecosystem vulnerability, this paper considers the two dimensions of ecological pressure and ecological vegetation sensitivity to evaluate the status quo of rural ecosystem vulnerability. When invasive alien vegetation and water-intensive crops account for a high proportion of the total local green vegetation, the village ecological balance is affected and the vulnerability of the village ecosystem increases. Ecological vegetation is the basis of human survival and sustainable social development. The threat of the ecological vegetation survival environment will inevitably lead to the loss of biodiversity and affect the balance of the ecosystem so that the rural landscape system will show stronger sensitivity to external impacts [54].

Engineering systems mainly refer to the use of people's skills to plan various landscape infrastructures and recreational facilities, which can be used to mitigate and recover from the negative effects of disasters when they occur. This paper analyses the disaster preparedness capability of engineering systems from four perspectives: building facilities, water conservation engineering, fire protection facilities, and road engineering. In the face of natural disasters or human disturbance, healthy and safe living environments or building facilities can be used as a refuge to exhibit their disaster preparedness capabilities. Water conservation projects can effectively alleviate the negative impact of surface water leakage caused by ground and underground dual structures in karst areas and reduce the impact of drought and flood disasters on rural landscape systems [55]. Fire protection facilities can manage the threat caused by potential fire hazards, and their logical use can enhance the disaster preparedness ability of rural landscape systems. When natural disasters or human interference occur, a perfect road system can help people safely evacuate or provide emergency refuge places and enhance the ability of rural landscape systems to avoid disasters. The vulnerability of engineering systems is analyzed from the following perspectives: building instability, water supply and drainage pressure, fire protection pressure, and road sensitivity. Building instability refers to the vulnerability of the residential environment or building facilities in the face of disasters when they have certain security risks or have difficulty performing their established functions; this can both damage the rural landscape system and affect people's life and safety. When water supply and drainage facilities are not sufficient to cope with the impact of droughts and floods, the vulnerability of rural landscape systems has increased, impacting landscape systems. The failure of fire protection facilities makes it difficult for them to perform their intended functions, thereby reducing their disaster preparedness ability. The imperfect or defective road system causes potential threats to people's disaster avoidance actions, which may enhance the destructive power of disaster behavior on rural landscape systems.

The sociocultural system mainly refers to the use of social organization norms and local culture to build and maintain the landscape, which can enhance people's sense of identity and belonging to the place [56]. Karst areas in southern China show a high sensitivity to natural disasters, and the local cultural landscape contains the wisdom of ancient people accumulated over thousands of years to deal with natural disasters. However, there is a lack of in-depth, targeted, and comprehensive research covering both natural and social sciences on the understanding of disaster culture in ethnic areas, the discovery of local knowledge of disaster reduction, the changes in social and traditional culture caused by disasters, and the construction of localized disaster prevention and reduction systems. In this paper, we measure the disaster preparedness of the social culture system from two perspectives: cultural disaster preparedness and cultural landscape protection. Cultural disaster preparedness refers to the assessment of the existing cultural disaster perception and response ability, which reflects the inheritance of traditional survival wisdom and disaster avoidance and reduction skills in karst areas and the degree of integration with modern science, including the popularization of the knowledge and achievements of rock desertification control. Traditional cultural landscapes embody the folk experience of karst area residents in adapting to habitat. If the traditional cultural landscape cannot be used, the loss of cultural landscape leads to the loss of local disaster preparedness ability, which enhances the vulnerability of the landscape system and reduces the resilience level of karst

rural landscapes. This paper measures the vulnerability of the social culture system from the two perspectives of cultural resource loss and disaster sensitivity. Traditional culture is the crystallization of the wisdom of local ancient people, which contains rich knowledge and survival skills. Abandoning traditional culture has increased the vulnerability of rural landscapes in karst areas of South China and reduced landscape resilience. Identifying disaster sensitive areas in different regions is conducive to formulating targeted risk response strategies and reducing the disaster sensitivity of high-risk areas.

3.3. Data Processing

3.3.1. Index Weight Calculation Method

The DEMATEL method was used to determine the weight of each index. DEMATEL is a graph theory and a matrix tool for system analysis that was proposed by A. Gabus and E. Fontela in the Battelle Laboratory in 1971 to solve the problem of complex system evaluation [57], which can be used to describe the logical relationship between system elements and has been widely accepted [58,59]. All the elements of the system to be evaluated are considered together, affecting one another. Based on the direct influence relationship between the elements as the starting point, the influence matrix is analyzed to obtain the influence degree of each element on other elements, and the centrality and cause degree of each element are obtained as the basis for the construction of the model to determine the weight of each element in the system. The specific steps are as follows:

Step 1. Implement the acquisition of the matrix. The rural landscape resilience assessment index system in KRDCA in southern China is determined to be composed of n elements, and m experts are invited to compare each other to determine the degree of direct influence between elements. Factor i and factor j are compared twice, which is the direct influence of factor i on factor j and the direct influence of factor j on factor i. The specific function is shown in Equation (3), where M is the $n \times n$ direct influence matrix and a_{ij} is the direct influence matrix that is the degree to which element i affects element j. The direct influence matrix comparison scale has five levels: no impact (0), low impact (1), medium impact (2), high impact (3), and very high impact (4), and the direct impact matrix is obtained based on the scoring judgement of experts [50].

$$M = \left(a_{ij}\right)_{n \times n} \tag{3}$$

Step 2. Calculate the normative influence matrix. The normalized influence matrix is obtained by normalizing the direct influence matrix, and the specific function is shown in Equation (4):

$$N = \left(\frac{a_{ij}}{Maxvar}\right)_{n \times n} \tag{4}$$

$$Maxvar = max\left(\sum_{j=i}^{n} a_{ij}\right) \tag{5}$$

where $Maxvar$ is summed in each row of the matrix (Equation (5)), takes the maximum value among these values, and then uses the obtained $Maxvar$ to calculate the normative influence matrix N.

Step 3. The total influence matrix is derived. The direct influence matrix multiplication of the specification represents the increased indirect influence between elements. The total influence matrix T is represented by adding all the indirect influences together, as shown in Equation (6).

$$T = \left(N + N^2 + N^3 + \ldots N^k\right) = \sum_{k=1}^{\infty} N^k \tag{6}$$

where T is the total influence matrix and N is the canonical influence matrix.

Step 4. Calculation of impact degree. The impact degree represents the comprehensive influence value of each corresponding element on all other elements, and the set is denoted as D, as shown in Equation (7). The method of obtaining D_i is shown in Equation (8).

$$D = (D_1 + D_2 + D_3 + \ldots D_n) \tag{7}$$

$$D_i = \sum_{j=1}^{n} t_{ij} (i = 1, 2, 3, \ldots n) \tag{8}$$

where t_{ij} represents the degree of direct influence and indirect influence brought by factor i on factor j, that is, the degree of comprehensive influence. It also indicates the comprehensive impact of factor j on factor i.

Step 5. Calculation of influence degree. The degree of influence represents the comprehensive influence value of each corresponding element by all other elements, namely, the degree of influence. This set is denoted as C, as shown in Equation (9). The method of obtaining C_i is shown in Equation (10).

$$C = (C_1, C_2, C_3 \ldots C_n) \tag{9}$$

$$C_i = \sum_{j=1}^{n} t_{ij} (i = 1, 2, 3, \ldots n) \tag{10}$$

Step 6. Calculation of centrality. The degree of influence (D_i) and the degree of influence (C_i) of an element i were added to obtain the centrality of the element, denoted as M_i. Centrality indicates the position of the factor in the evaluation index system and the size of its role, as shown in Equation (11).

$$M_i = D_i + C_i \tag{11}$$

By normalizing the centrality of all elements in the system to be evaluated, the status and weight of corresponding elements in the system are obtained. In this study, the weights of indicators at all levels are shown in the evaluation results table, below.

3.3.2. Disaster Preparedness and Vulnerability Scoring Method

According to the above analysis of resilience assessment Equation (2) and the understanding of the concept of resilience, the score of disaster preparedness (PI) is the weighted sum of the scores of all first-level indicators (PD), the calculation method of PD is the weighted sum of all second-level indicators, PS is the average score of all third-level indicators (PC), and the score of third-level indicators is the average of the field survey [59]. The specific function is shown in Equation (12).

$$PI = \sum_{i=1}^{i=NP} w_i PD_i \; PD_i = \sum_{j=1}^{j=MP_i} u_{ij} PS_{ij} \; PS_{ij} = \frac{\sum_{k=1}^{k=LP_j} PC_{ijk}}{LP_j} \tag{12}$$

where PI represents the disaster preparedness score of the system to be evaluated. PD_i, PS_{ij}, and PC_{ijk} correspond to the scores of the first-level index i, the second-level index j, and the third-level index k, respectively. At the same time, NP, MP_i, and LP_j correspond to the number of indicators of the first-level index, the second-level index, and the third-level index, respectively, while w_i and u_{ij} represent the corresponding weight of the first-level index i and the second-level index j in the resilience evaluation of the system.

The calculation method of vulnerability and disaster preparedness capacity is the same, and the specific function is shown in Equation (13):

$$VI = \sum_{i=1}^{i=NV} y_i VD_i \; VD_i = \sum_{j=1}^{j=MV_i} x_{ij} VS_{ij} \; VS_{ij} = \frac{\sum_{k=1}^{k=LV_j} VC_{ijk}}{LV_j} \quad (13)$$

where VI represents the vulnerability score of the system to be evaluated. VD_i, VS_{ij}, and VC_{ijk} correspond to the scores of the first level index i, the second level index j, and the third level index k, respectively. At the same time, NV, MV_i, and LV_j correspond to the number of indicators of the first level index, the second level index, and the third level index, respectively, while Y_i and X_{ij} represent the corresponding weight of the first level index i and the second level index j in the system resilience evaluation.

4. Result

4.1. Ecological Resilience Assessment

The resilience score of the Fanhua village ecosystem is 2.08 (Table 3), and its disaster preparedness and vulnerability scores are 1.39 and 0.67, respectively, indicating that the village ecological landscape subsystem has a high level of resilience. Among them, the scores of the two dimensions of "ecological pattern" and "ecological governance", which are indicators of ecosystem disaster preparedness, are five and three (very low (one), low (two), average (three), high (four) and very high (five)), respectively, indicating that ecosystem disaster preparedness capacity is strong. There are abundant ecological elements in Fanhua village. Forests, grasslands, rivers, and farmland form the basis of the ecological pattern of Fanhua village. Under the policy of Closing Hillsides to Facilitate Afforestation of the local government, the green area of Fanhua village accounts for more than 60% of the total area of the village with diverse species; most of them are suitable local species adapted to local climatic conditions and well-growth condition. To maintain the existing ecological landscape pattern, the local government has implemented ecological control measures such as afforestation, high-standard farmland construction, and the construction of diversion channels [60]. The area of KRDCA accounts for approximately 40% of the total area of the village. The scores of "ecological pressures" and "ecological vegetation sensitivity" reflecting the evaluation dimension of ecosystem vulnerability are three and one, respectively. The main reason for the increase in vulnerability to "ecological pressure" is that the score of "the proportion of crops requiring large amounts of water" is five, and most of the crops in the village were rice and corn with high water demand. To effectively reduce the water demand for industrial development in Fanhua village and to enhance the ability of industry to cope with drought, the village has begun to promote the planting of water-saving crops such as Sichuan peppercorn and yellow ginger. In general, in the face of natural disasters, the existing ecological elements of the ecological landscape structure of Fanhua village could have a greater buffer capacity against drought and flood disasters. According to the evaluation results, two methods were used to enhance the landscape resilience of Fanhua Village: (1) the planting area of crops with large water requirement was further reduced, and the landscape design of farmland was carried out without destroying the disaster preparedness capacity of the ecosystem. (2) The appropriate reduction of the paving of hard road permeable paving brick.

Table 3. Assessment results of ecological resilience in Fanhua village.

Evaluative Dimension	Weight	Evaluation Index	Score		Evaluation Attribute	RI
Ecological pattern	0.167	Ratio of green space	5	5	PI = 1.39	2.08
		Diversity of species	5			
Ecological governance	0.184	The proportion of KRDCA	3	3		
Ecological pressure	0.172	The proportion of crops requiring large amounts of water	5	3	VI = 0.67	
		Proportion of invasive alien plants	1			
Ecological vegetation sensitivity	0.151	Threat assessment of native vegetation	1	1		

4.2. Engineering Resilience Assessment

The disaster preparedness capability and vulnerability scores of the engineering system of Fanhua village are 1.05 and 0.84, respectively, and the engineering resilience score is 1.24 (Table 4), indicating that the engineering facility system of Fanhua village also has high resilience. Among them, the disaster preparedness capability indicators of engineering systems "Building facilities" and "Road engineering" both are 4, "Water conservation engineering" is 3.5, and "Fire protection facilities" is 1. The village has relatively perfect infrastructure, and housing, education, medical, and other buildings are mostly newly built concrete structures and good environments. The village has a diverse road system with complete supporting facilities, and the landscape along the road is mostly designed professionally. To cope with the structural water shortage in karst areas, the Fanhua village has built diversion channels and reservoirs that can be combined with the landscape. The reason for the low disaster preparedness score of "Fire facilities" is that the service radius of fire facilities in the village is greater than 7 km^2, making it difficult to deal with sudden fires. In the dimension of vulnerability of the engineering system in Fanhua village, the scores of "Building instability" and "Fire protection facility pressure" are four and three, respectively, while the scores of "Water supply and drainage facility pressure" and "Road sensitivity" are one and two, respectively. The reason for the increase in vulnerability to "building instability" is that there are scattered dilapidated buildings in the village that have been uninhabited for a long time, and their structural safety is poor. In response to greater rain and flood damage, they may easily collapse. The reason for the high vulnerability score of "Fire facilities pressure" is mainly because the fire facilities in the village are not regularly repaired. The system of engineering facilities is often closely connected, and the collapse of one element may reduce the stability and self-recovery ability of the whole landscape system [61,62]. However, in general, Fanhua village can still contribute to disaster prevention and the reduction of existing engineering facilities in response to external disturbances so that it has high stability and self-sustaining ability, which can effectively enhance the engineering resilience of the landscape system. According to the evaluation results, the following two improvement methods can reduce the vulnerability of the engineering system of Fanhua Village and enhance its landscape resilience: (1) Plan the location and number of firefighting facilities in the village, and check whether they can be used normally on time. (2) Repair buildings or facilities with cultural significance and demolish abandoned buildings without cultural value.

Table 4. Assessment results of engineering resilience in Fanhua village.

Evaluative Dimension	Weight	Evaluation Index	Score		Evaluation Attribute	RI
Building facilities	0.103	Building structure	5	4	PI = 1.05	1.24
		Proportion of new homes built in the last decade	3			
Water conservation engineering	0.075	Kilometers of new aqueducts	5	3.5		
		Number of new cisterns	2			
Fire protection facilities	0.056	Fire station service radius	1	1		
Road engineering	0.079	Proportion of concrete roads	5	4		
		Road supporting facilities	3			
Building instability	0.091	Old buildings with security risks	4	4	VI = 0.84	
Water supply and drainage pressure	0.072	Annual water supply and drainage facilities failure days	1	1		
Fire protection pressure	0.074	Frequency of failure of fire protection facilities in the past five years	3	3		
Road sensitivity	0.092	Annual frequency of road failure	2	2		
		Proportion of unrepaired roads	2			

4.3. Sociocultural Resilience Assessment

The disaster preparedness capacity and vulnerability scores of the sociocultural system of Fanhua village are 0.93 and 1.04, respectively, and the sociocultural resilience score is 0.89 (Table 5). The cultural landscape system is less than one, indicating that the sociocultural resilience is insufficient. The scores of "cultural disaster preparedness capacity" and "cultural landscape protection" are 3 and 2.5, respectively. Every year, disaster prevention knowledge popularization and KRDC publicity activities are held in Fanhua village, and the villagers have a certain understanding of disaster prevention strategies and knowledge of KRDC. From the perspective of cultural landscape protection, although the village has a long history and important cultural elements, it has formed a unique cultural value system and art carrier. For example, although the ancestral hall of the Chen family, a symbol of village history and culture, is still regarded as the spiritual bond between villagers, its importance in the hearts of teenagers has been greatly diminished, and the preservation of local opera is mainly carried out by elderly individuals, without the introduction of new members. These traditional cultural concepts and landscape carriers contain ancient people's understanding of the relationship between human society and the ecological environment, and they are increasingly being recognized as pivotal to disaster mitigation [63]. For example, traditional buildings in this region are often built on a high foundation, while new buildings are located on a low foundation. Rain and flood damage due to heavy rainfall is prone to have a great impact on new buildings, and the ability to deal with flood disasters is reduced. In the dimension of sociocultural system vulnerability in Fanhua village, the vulnerability scores of "cultural resource loss" and "disaster sensitivity" are both three. In village landscape transformation, traditional cultural elements are deliberately explored and applied in landscape design. However, with the development of the times, many people in the village have ventured out for work and study, introducing foreign cultural values that impact the original social and cultural value system, and the local traditional knowledge of disaster prevention and reduction in the traditional culture has been gradually lost. Facilities for young and middle-aged people have been idle for a long time, and no protection measures have been implemented for the former residence of Jiang and Chen, which symbolizes the history of Fanhua village, causing it to become a potential safety hazard. According to the evaluation results, the following three approaches can be used to improve the resilience level of Fanhua Village landscape: (1) Continue to excavate and protect traditional culture and its related landscape carriers. (2) Explore the modern landscape forms of disaster risk reduction knowledge in traditional culture. (3) Perform reasonable excavation of the economic benefits of traditional culture.

Table 5. Assessment results of sociocultural resilience in Fanhua village.

Evaluative Dimension	Weight	Evaluation Index	Score		Evaluation Attribute	RI
Cultural disaster preparedness	0.171	Number of disaster avoidance strategy training per year	3	3	PI = 0.93	0.89
		KRDC knowledge propaganda	3			
Cultural landscape protection	0.165	Establishment of cultural reserve	3	2.5		
		Awareness of cultural protection	2			
Cultural resource loss	0.150	Idle cultural facilities	3	3	VI = 1.04	
		Damage to traditional buildings	3			
Disaster sensitivity	0.198	Setting of disaster sensitive area	3	3		

4.4. Resilience Assessment of the Rural Landscape in Fanhua Village

In summary, the disaster preparedness and vulnerability scores of Fanhua village are 3.37 and 2.56, respectively, and the overall resilience score of the landscape is 1.32, with a calculation result >1 (Table 6), indicating that the village landscape is resilient, the disaster preparedness ability can cope with its vulnerability, and the existing landscape system structure can resist the impact caused by external disturbances or its own defects. Taking the ratio of disaster preparedness and vulnerability of ecological, engineering, and sociocultural systems as the resilience of corresponding dimensions, the resilience scores of the Fanhua village landscape system are 2.08, 1.24, and 0.89, respectively. That is, the resilience of the Fanhua village landscape system is the highest in terms of ecological elements, followed by engineering resilience, while it is insufficient in terms of sociocultural resilience.

Table 6. Landscape resilience assessment results of Fanhua village.

	Ecological System	Engineering System	Sociocultural System	Total
PI	1.39	1.05	0.93	3.37
VI	0.67	0.84	1.04	2.55
RI		1.32		

5. Discussion

Through the analysis of the rural landscape resilience of Fanhua village, we found that villages in typical KRDCA in Guizhou Province have developed a unique system in terms of economy and culture, which has allowed a large number of traditional villages and local cultures to be well preserved. However, the fragile ecological environment has greatly restrained rural development in karst areas. With the promotion of the KRDC project of the Chinese government, the KRD problem in karst areas in southern China has diminished, and the rural landscape ecological pattern and infrastructure engineering facilities have gradually improved [64]. However, with the large flow of the rural population in China in recent years, the local cultural values in karst areas of southern China are suffering from external cultural impacts [65]. The weakening of local culture is also accompanied by the loss of knowledge and skills for resisting interference accumulated by ancient people. These internal changes are manifested in the external rural landscape. Therefore, the results of this study may be helpful for formulating corresponding strategies to promote the comprehensive development of Fanhua village.

6. Conclusions

Based on disaster preparedness and vulnerability, this paper constructs an index system of rural landscape resilience evaluation in KRDCA in southern China from the three dimensions of ecology, engineering, and social culture. The disaster preparedness ability of rural landscapes in the KRDCA in southern China is reflected in the fact that the nature of the system can be used to reduce the negative impact of disturbance. Ecological elements can serve as a buffer against natural disasters and reduce the destructive power of floods and other disasters, while engineering elements can effectively reduce the damage degree

of disasters to village buildings. The social and cultural elements of the village system's ability to adapt to external shocks or environmental changes involve more local knowledge and skills developed over a long period of time. The disadvantageous factors of ecology, engineering, and social culture strengthen its vulnerability to disturbance. In view of this, this research constructs a rural landscape resilience assessment framework based on the combination of disaster preparedness and vulnerability of rural landscapes in KRDCA. In addition, Fanhua village in Guanling county of Guizhou Province, a typical KRDCA, was selected as study area to empirically analyze the rural landscape resilience. However, this was an exploratory study on the quantitative assessment of landscape resilience, and, as such, it has certain local characteristics in index selection. In future studies, assessment systems can be developed based on the specific situations.

The results of the study indicated that the rural landscape resilience of Fanhua village was higher from the three dimensions of ecology, engineering, and social culture. Specifically, the scores for ecological resilience, engineering resilience, and sociocultural resilience, which constitute the rural landscape resilience of Fanhua village, were 2.08, 1.24, and 0.88, respectively. The ecological resilience was the highest, but the sociocultural resilience was insufficient. In terms of the disaster preparedness of rural landscapes, the disaster preparedness of the ecological system was the highest, and that of the social cultural system was the lowest, with values of 1.39 and 0.92, respectively. From the perspective of the vulnerability of rural landscapes, the vulnerability of the social cultural system was the highest, and that of the ecological system was the lowest, with values of 1.04 and 0.67, respectively. Therefore, the rural landscape system of Fanhua village can use ecological elements and engineering facilities to cope with the impact of disturbances. In contrast, the social cultural system has weak disaster preparedness ability and high vulnerability, and it is difficult to use cultural knowledge to resist the impact of external disturbances. This indicates that Fanhua village is in the key stage of the transformation and adjustment of its rural development structure. It also presents complex features in landscape construction.

Author Contributions: Conceptualization, B.Y. and S.L.; methodology, S.L. and Y.H.; software, S.L. and Y.H.; validation, B.Y. and S.L.; formal analysis, B.Y.; investigation, S.L., T.L., and R.S.; writing—original draft preparation, B.Y. and S.L.; writing—review and editing, B.Y. and K.X. All authors have read and agreed to the published version of the manuscript.

Funding: This research was funded by the National Natural Science Foundation of China (42261056); the National Key R&D Program of China (SQ2020YFC1522300); the Key Science and Technology Program of Guizhou Provence: Poverty alleviation model and technology demonstration for eco-industries derived from the karst desertification control (No. 5411 2017 Qiankehe Pingtai Rencai) and the Oversea Expertise Introduction Program for Discipline Innovation of China: Overseas expertise introduction center for South China Karst ecoenvironment discipline innovation (No. D17016).

Data Availability Statement: Not applicable.

Acknowledgments: Thanks to the villagers of Fanhua Village for their help in our questionnaire survey and data collection.

Conflicts of Interest: The authors declare no conflict of interest.

References

1. Chen, C.; Yuan, D.; Cheng, H.; Yu, T.; Shen, C.; Edwards, R.L.; Wu, Y.; Xiao, S.; Zhang, J.; Wang, T.; et al. Human activity and climate change triggered the expansion of rocky desertification in the karst areas of southwestern China. *Sci. J. China Earth Sci.* **2021**, *64*, 1761–1773. [CrossRef]
2. Chen, Q.; Lu, S.; Xiong, K.N.; Zhao, R. Coupling analysis on ecological environment fragility and poverty in South China karst. *J. Environ. Res.* **2021**, *201*, 111650. [CrossRef] [PubMed]
3. Yuan, D.X. Rock desertification in the subtropical karst of south China. *Ztschrift Fur Geomorphol.* **1997**, *108*, 81–90.
4. Xiong, K.N.; Li, P.; Zhou, Z.F.; An, Y.L. *Remote Sensing of Karst Rocky Desertification-A Typical Research of GIS: Taking Guizhou Province as an Example*; Geology Publishing House: Beijing, China, 2002; p. 18. (In Chinese)
5. Wang, S.J.; Liu, Q.M.; Zhang, D.F. Karts rocky desertification in south-west China geomorphology, land use, impact and rehabilitation. *Land Degrad. Dev.* **2004**, *15*, 115–121. [CrossRef]

6. Tong, X.W.; Wang, K.L.; Yue, Y.M.; Brandt, M.; Liu, B.; Zhang, C.H.; Liao, C.J.; Fensholt, R. Quantifying the effectiveness of ecological restoration projects on long-term vegetation dynamics in the karst regions of Southwest China. *Int. J. Appl. Earth Obs. Geoinf.* **2017**, *54*, 105–113. [CrossRef]
7. Li, L.; Xiong, K.N.; Dan, W.H. Study progress and prospect of ecological industrial market models for control of karst rocky desertification. *J. Int. J. Environ. Pollut.* **2020**, *67*, 2–4. [CrossRef]
8. Tong, X.W.; Brandt, M.; Yue, Y.M.; Horion, S.; Wang, K.L.; De, K.W.; Tian, F.; Schurgers, G.; Xiao, X.M.; Luo, Y.Q.; et al. Increased vegetation growth and carbon stock in China karst via ecological engineering. *J. Nat. Sustain.* **2018**, *1*, 44–50. [CrossRef]
9. Liu, Y.S. Research on the urban-rural integration and rural revitalization in the new era in China. *J. ACTA Geogr. Sin.* **2018**, *4*, 73. (In Chinese) [CrossRef]
10. Wu, Z.G.; Zhu, D.Y.; Xiong, K.N. Dynamics of landscape ecological quality based on benefit evaluation coupled with the rocky desertification control in South China Karst. *Ecol. Indic.* **2022**, *138*, 108870. [CrossRef]
11. Yang, W.L.; Chu, W.C.; Zhou, L.M. Evaluating the impact of karst rocky desertification on regional climate in Southwest China with WRF. *J. Theor. Appl. Climatol.* **2019**, *137*, 481–492. [CrossRef]
12. Lv, Y.X.; Jiang, Y.J.; Hu, W.; Cao, M.; Mao, Y. A review of the effects of tunnel excavation on the hydrology, ecology, and environment in karst areas: Current status, challenges, and perspectives. *J. Hydrol.* **2020**, *586*, 124891. [CrossRef]
13. Macias-Fauria, M. Satellite images show China going green. *Nature* **2018**, *553*, 411–413. [CrossRef] [PubMed]
14. Wang, X.F.; Yang, G.B. Analysis on the Change Characteristics and Control Effect of Karst Rocky Desertification in Beipanjiang River Basin of Guizhou Province. *J. Yangtze River Sci. Res. Inst.* **2022**, *1*, 9. (In Chinese) [CrossRef]
15. Zhang, J.; Dai, M.; Wang, L.; Su, W. Household livelihood change under the rocky desertification control project in karst areas, Southwest China. *J. Land Use Policy* **2016**, *56*, 8–15. [CrossRef]
16. Xiao, J.; Xiong, K.N. A review of agroforestry ecosystem services and its enlightenment on the ecosystem improvement of rocky desertification control. *J. Sci. Total Environ.* **2022**, *852*, 158538. [CrossRef]
17. Yang, M.D. The Characteristics and Protection of Karst Cave Tourism Resources. *J. Carsologica Sin.* **1998**, *17*, 51–56. (In Chinese)
18. Yang, S.; Li, C.; Lou, H.; Wang, P.; Wu, X.; Zhang, Y.; Zhang, J.; Li, X. Role of the countryside landscapes for sustaining biodiversity in karst areas at a semi centennial scale. *Ecol. Indic.* **2021**, *123*, 107315. [CrossRef]
19. Wu, Q.; Zheng, W.; Rao, C.J.; Wang, E.W.; Yan, W.D. Soil Quality Assessment and Management in Karst Rocky Desertification Ecosystem of Southwest China. *J. For.* **2022**, *13*, 1513. [CrossRef]
20. Wang, L.; Xiao, S. Tourism space reconstruction of a world heritage site based on actor network theory: A case study of the Shibing Karst of the South China Karst World Heritage Site. *Int. J. Geoheritage Park.* **2020**, *8*, 140–151. [CrossRef]
21. Ying, B.; Xiong, K.N.; Wang, Q.; Wu, Q.M. Can agricultural biomass energy provide an alternative energy source for karst rocky desertification areas in Southwestern China? investigating Guizhou Province as example. *J. Environ. Sci. Pollut. Res.* **2021**, *28*, 44315–44331. [CrossRef]
22. Liu, Y.S.; Zang, Y.Z.; Yang, Y.Y. China's rural revitalization and development: Theory, technology and management. *J. Geogr. Sci.* **2020**, *30*, 1923–1942. [CrossRef]
23. Schippers, P.; Vander, H.C.M.; Koelewijn, H.P.; Schouten, M.A.H. Landscape diversity enhances the resilience of populations, ecosystems and local economy in rural areas. *J. Landsc. Ecol.* **2015**, *30*, 193–202. [CrossRef]
24. Holmes, G.; Clemoes, J.; Marriot, K.; Jones, S.W. The politics of the rural and relational values: Contested discourses of rural change and landscape futures in west wales. *Geoforum* **2022**, *133*, 153–164. [CrossRef]
25. Holling, C.S. Resilience and Stability of Ecological Systems. *J. Annu. Rev. Ecol. Syst.* **1973**, *4*, 1–23. [CrossRef]
26. Martha, S. The Designer's Geoengineering Toolkit: Crisis Creates Opportunities for Landscape Architects to Reverse, Repair and Regenerate the Earth's Climate. *J. Landsc. Archit.* **2020**, *27*, 10–25. (In Chinese) [CrossRef]
27. Niall, U. Resilient Landscapes—Dimensions of Future Landscape Architectural Practices. *J. Chin. Landsc. Archit.* **2010**, *26*, 10–14. (In Chinese)
28. Eriksson, M.; Samuelson, L.; Jagrud, L.; Mattsson, E.; Celander, T.; Malmer, A.; Bengtsson, K.; Johansson, O.; Schaaf, N.; Svending, O.; et al. Water, Forests, People: The Swedish Experience in Building Resilient Landscapes. *J. Environ. Manag.* **2018**, *62*, 45–57. [CrossRef]
29. Matthias, I.; Semmler, M.S.S.; Giesecke, T. Pollen diversity captures landscape structure and diversity. *J. Ecol.* **2015**, *103*, 880–890. [CrossRef]
30. Abrams, J.; Greiner, M.; Schultz, C. Can Forest Managers Plan for Resilient Landscapes? Lessons from the United States National Forest Plan Revision Process. *J. Environ. Manag.* **2021**, *67*, 574–588. [CrossRef]
31. Hossain, M.S.; Ramirez, J.A.; Haisch, T.; Speranza, C.I.; Martius, O.; Mayer, H.; Keiler, M. A coupled human and landscape conceptual model of risk and resilience in Swiss Alpine communities. *Sci. Total Environ.* **2020**, *730*, 138322. [CrossRef]
32. Sara, B.; Sophie, N.; Kathleen, L.W.; Angie, W.; Erin, D.; Stephen, R.J.S. Greening Blocks: A Conceptual Typology of Practical Design Interventions to Integrate Health and Climate Resilience Co-Benefits. *J. Environ. Res. Public Health* **2019**, *16*, 4241. [CrossRef]
33. Long, N.V.; Cheng, Y. Flood-resilient urban design based on the indigenous landscape in the city of Can Tho, Vietnam. *J. Urban Ecosyst.* **2020**, *23*, 675–687. [CrossRef]
34. United Nations International Strategy for Disaster Reduction. UNISDR Terminology on Disaster Risk Reduction. 2009. Available online: https://www.undrr.org/publication/2009-unisdr-terminology-disaster-risk-reduction (accessed on 28 July 2022).

35. Bruneau, M.; Chang, S.E.; Eguchi, R.T.; Lee, G.C.; O'Rourke, T.D.; Reinhorn, A.M.; Shinozuka, M.; Tierney, K.; Wallace, W.A.; Von Winterfeldt, D. A framework to quantitatively assess and enhance the seismic resilience of communities. *J. Earthq. Spectra* **2003**, *19*, 733–752. [CrossRef]
36. Henry, D.; Emmanuel Ramirez-Marquez, J. Generic metrics and quantitative approaches for system resilience as a function of time. *Reliab. Eng. Syst. Saf.* **2012**, *99*, 114–122. [CrossRef]
37. Kusumastuti, R.D.; Husodo, Z.A.; Suardi, L.; Danarsari, D.N. Developing a resilience index towards natural disasters in Indonesia. *Int. J. Disaster Risk Reduct.* **2014**, *10*, 327–340. [CrossRef]
38. Simpson, D.M.; Katirai, M. Indicator Issues and Proposed Framework for a Disaster Preparedness Index (DPi), Draft Version 1.0. 2006. Available online: http://www.fritzinstitute.org/PDFs/WhitePaper/DaveSimpsonIndicatorsRepor.pdf (accessed on 19 July 2022).
39. Hui, X.; Yang, L.; Lin, W. Resilience Assessment of Complex Urban Public SpacesInt. *J. Environ. Res. Public Health* **2020**, *17*, 524. [CrossRef]
40. Rani, M.; Rehman, S.; Sajjad, H.; Chaudhary, B.S.; Sharma, J.; Bhardwaj, S.; Kumar, P. Assessing coastal landscape vulnerability using geospatial techniques along Vizianagaram-Srikakulam coast of Andhra Pradesh, India. *J. Nat. Hazards* **2018**, *94*, 711–725. [CrossRef]
41. Khademi, N.; Balaei, B.; Shahri, M.; Mirzaei, M.; Sarrafi, B.; Zahabiun, M.; Mohaymany, A.S. Transportation network vulnerability analysis for the case of a catastrophic earthquake. *Int. J. Disaster Risk Reduct.* **2015**, *12*, 234–254. [CrossRef]
42. Peng, X.D.; Dai, Q.H.; Ding, G.J.; Shi, D.M.; Li, C.L. Impact of vegetation restoration on soil properties in near-surface fissures located in karst rocky desertification regions. *J. Soil Tillage Res.* **2020**, *200*, 104620. [CrossRef]
43. Tang, X.; Xiao, J.; Ma, M.; Yang, H.; Li, X.; Ding, Z.; Yu, P.; Zhang, Y.; Wu, C.; Huang, J.; et al. Satellite evidence for China's leading role in restoring vegetation productivity over global karst ecosystems. *J. For. Ecol. Manag.* **2022**, *507*, 120000. [CrossRef]
44. Cao, Z.; Zhang, K.; He, J.; Yang, Z.; Zhou, Z. Linking rocky desertification to soil erosion by investigating changes in soil magnetic susceptibility profiles on karst slopes. *J. Geoderma* **2021**, *389*, 114949. [CrossRef]
45. Guo, B.; Yang, F.; Fan, Y.W.; Zang, W.Q. The dominant driving factors of rocky desertification and their variations in typical mountainous karst areas of southwest China in the context of global change. *J. CATENA* **2023**, *220*, 1066674. [CrossRef]
46. Peng, X.D.; Dai, Q.H. Drivers of soil erosion and subsurface loss by soil leakage during karst rocky desertification in SW China. *J. Int. Soil Water Conserv. Res.* **2022**, *10*, 217–227. [CrossRef]
47. Deng, X.H.; Xiong, K.N.; Yu, Y.H.; Zhang, S.H.; Kong, L.W.; Zhang, Y. A Review of Ecosystem Service Trade-Offs/Synergies: Enlightenment for the Optimization of Forest Ecosystem Functions in Karst Desertification Control. *J. For.* **2023**, *14*, 88. [CrossRef]
48. Saklaurs, M.; Lībiete, Z.; Donis, J.; Kitenberga, M.; Elferts, D.; Jūrmalis, E.; Jansons, Ā. Provision of Ecosystem Services in Riparian Hemiboreal Forest Fixed-Width Buffers. *J. For.* **2022**, *13*, 928. [CrossRef]
49. Zhang, H.; Liang, X.Y.; Chen, H.; Shi, Q.Q. Spatio-temporal evolution of the social-ecological landscape resilience and management zoning in the loess hill and gully region of China. *J. Environ. Dev.* **2021**, *39*, 100616. [CrossRef]
50. Jiang, S.L.; Xiong, K.N.; Xiao, J. Structure and Stability of Agroforestry Ecosystems: Insights into the Improvement of Service Supply Capacity of Agroforestry Ecosystems under the Karst Rocky Desertification Control. *J. For.* **2022**, *13*, 878. [CrossRef]
51. Donatella, V.; María, V.M.; Erica, M.L.; Cosimo, G.G.; Irene, P. Fostering the Resiliency of Urban Landscape through the Sustainable Spatial Planning of Green Spaces. *J. Land* **2022**, *11*, 367. [CrossRef]
52. Liu, Y.F.; Guo, B.; Lu, M.; Zang, W.Q.; Yu, T.; Chen, D.H. Quantitative distinction of the relative actions of climate change and human activities on vegetation evolution in the Yellow River Basin of China during 1981–2019. *J. Arid Land* **2023**, *03*, 91–108. [CrossRef]
53. Guo, B.; Lu, M.; Fan, Y.W.; Wu, H.W.; Yang, Y.; Wang, C.L. A novel remote sensing monitoring index of salinization based on three-dimensional feature space model and its application in the Yellow River Delta of China. *J. Geomat. Nat. Hazards Risk* **2023**, *14*, 95–116. [CrossRef]
54. Khan, A.; Pan, X.D.; Najeeb, U.; Tan, D.K.Y.; Fahad, S.; Zahoor, R.; Luo, H.H. Coping with drought: Stress and adaptive mechanisms, and management through cultural and molecular alternatives in cotton as vital constituents for plant stress resilience and fitness. *J. Biol. Res.* **2018**, *51*, 47. [CrossRef] [PubMed]
55. Lu, Y.R. Karst Development Mechanism and Research Directions of Developing Engineering Construction Effect. *J. Acta Geogr. Sin.* **2016**, *37*, 419–432. (In Chinese) [CrossRef]
56. Stanik, N.; Aalders, I.; Miller, D. Towards an indicator-based assessment of cultural heritage as a cultural ecosystem service—A case study of Scottish landscapes. *J. Ecol. Indic.* **2019**, *95*, 288–297. [CrossRef]
57. Si, S.L.; You, X.Y.; Liu, H.C.; Zhang, P. DEMATEL Technique: A Systematic Review of the State-of-the-Art Literature on Methodologies and Applications. *J. Math. Probl. Eng.* **2018**, *2018*, 3696457. [CrossRef]
58. Ghosh, S.; Chatterjee, N.D.; Dinda, S. Urban ecological security assessment and forecasting using integrated DEMATEL-ANP and CA-Markov models: A case study on Kolkata Metropolitan Area, India. *J. Sustain. Cities Soc.* **2021**, *68*, 102773. [CrossRef]
59. Buyukozkan, G.; Guleryuz, S. An integrated DEMATEL-ANP approach for renewable energy resources selection in Turkey. *J. Int. J. Prod. Econ.* **2016**, *182*, 435–448. [CrossRef]
60. Xu, G.Y.; Xiong, K.N.; Shu, T.; Shi, Y.J.; Chen, L.S.; Zheng, L.L.; Fan, H.X.; Zhao, Z.M.; Yang, Z.H. Bundling evaluating changes in ecosystem service under karst rocky desertification restoration: Projects a case study of Huajiang-Guanling, Guizhou province, Southwest China. *Environ. Earth Sci.* **2022**, *81*, 302. [CrossRef]

61. Wang, L.; Xue, X.; Wang, Z.; Zhang, L. A unified assessment approach for urban infrastructure sustainability and resilience. *J. Adv. Civ. Eng* **2018**, *2018*, 2073968. [CrossRef]
62. Dong, S.J.; Malecha, M.; Farahmand, H. Integrated infrastructure-plan analysis for resilience enhancement of post-hazards access to critical facilities. *Cities* **2021**, *117*, 103318. [CrossRef]
63. Lambert, S.; Scott, J. International Disaster Risk Reduction Strategies and Indigenous Peoples. *Int. Indig. Policy J.* **2019**, *10*, 1–21. [CrossRef]
64. Zhang, Y.; Xiong, K.N.; Yu, Y.H.; Yang, S.; Liu, H.Y. Stoichiometric characteristics and driving mechanisms of plants in karst areas of rocky desertification of southern China. *Appl. Ecol. Environ. Res.* **2020**, *18*, 1961–1979. [CrossRef]
65. Chen, Y.; Tan, Y.; Gruschke, A. Rural vulnerability, migration, and relocation in mountain areas of Western China: An overview of key issues and policy interventions. *Chin. J. Popul. Resour. Environ.* **2021**, *19*, 110–116. [CrossRef]

forests

MDPI

Article

Forest Plant Water Utilization and the Eco-Hydrological Regulation in the Karst Desertification Control Drainage Area

Bo Fan [1,2], Kangning Xiong [1,2,*] and Ziqi Liu [1,2]

[1] School of Karst Science, Guizhou Normal University, Guiyang 550001, China; 17793689707@163.com (B.F.); 201511004@gznu.edu.cn (Z.L.)
[2] State Engineering Technology Institute for Karst Desertification Control, Guiyang 550001, China
* Correspondence: xiongkn@163.com

Abstract: Subtropical forests in southwestern karst areas are the top priority for ecosystem restoration, as studying the water absorption strategies of the major plants in these regions is crucial to determining the species distribution and coexistences within these seasonal subtropical forests, which will help us to cope with the forest ecosystem crisis under future climate change. We used the stable isotope ratios (δD and δ^{18}O) of tree xylem and soil water to assess the seasonal changes in the water use patterns and hydrological niche separations of four dominant tree species in seasonal subtropical forests in southwestern karst areas. The results showed that the soil water's isotopic composition varied gradiently in the vertical direction and that the variation of the soil water's isotopic composition was greater in the shallow layer than in its depths. Juglans regia (HT) mainly depended on soil water at a depth of 30–60 cm (41.8 $\pm$ 6.86%) and fissure water (32.5 $\pm$ 4.21%), while Zanthoxylum bungeanum Maxim (HJ) and Eriobotrya japonica Lindl (PP) had the same water use pattern. In the dry season, HT competed with HJ and PP for water resources, and in the rainy season, HJ and PP competed with Lonicera japonica (JYH), while HJ competed with PP all the time. JYH and HT were in a separate state of hydrologic niche and they did not pose a threat to each other. Coexisting trees are largely separated along a single hydrological niche axis that is defined by their differences in root depth, which are closely related to tree size. Our results support the theory of hydrological niche isolation and its potential responses in relation to drought resistance. This study provides a method for determining more efficient plant combinations within karst forest vegetation habitats and its results will have important implications for ecosystem vegetation restoration.

Keywords: karst forest; vegetation water use strategy; hydrogen and oxygen stable isotopes; hydrologic niche separation

Citation: Fan, B.; Xiong, K.; Liu, Z. Forest Plant Water Utilization and the Eco-Hydrological Regulation in the Karst Desertification Control Drainage Area. *Forests* **2023**, *14*, 747. https://doi.org/10.3390/f14040747

Academic Editor: Roberto Tognetti

Received: 17 February 2023
Revised: 29 March 2023
Accepted: 4 April 2023
Published: 5 April 2023

1. Introduction

According to the Global Forest Resources Assessment 2020, the average global forest coverage rate is 31.7% [1], and these forests play an irreplaceable role in maintaining the Earth's ecological and hydrological cycles. Forest distribution and abundance are mainly restricted by water resources [2,3]. Over the last few decades, due to major changes in the climate because of human influence, droughts have become more severe and frequent [4], which will have an obvious influence on the survival of forest vegetation species and the hydrological cycle [5]. Therefore, studying the water use of forest vegetation is crucial for forest ecohydrological regulation [6]. Forest vegetation is a participant in various important processes of the terrestrial hydrological cycle, and its ecological processes and hydrological processes are intertwined. The forest water cycle is an important part of the land water cycle [7,8], as it not only affects the structure, function, and distribution pattern of forest vegetation, but also affects the energy budget, conversion, and distribution of the Earth's surface system. It plays an important role in the carbon and nitrogen balance of terrestrial ecosystems [9–11]. The hydrological function of the forest ecosystem is not only

an important part of its service function, but also affects the system's productivity, nutrient cycle, and other functions [12–14]. Water is a key factor affecting the material circulation and plant growth in forest ecosystems [15]. Plants absorb water from the soil through their roots and store it in their xylem, and they use this water in photosynthesis or lose the water through evaporation via their stomata to complete the hydrological cycle [16].

Affected by the subtropical climate, subtropical forests are mainly found in karst areas in southwest China [17], where water and energy are abundant in the region. However, seasonal droughts always occur due to the inconsistent distribution of temperature and precipitation during the summer [18,19]. In the current extreme arid climate, more and more species are suffering from water stress [20]. The main problem of karst forest ecosystem restoration is vegetation restoration [21]. Understanding the physiological characteristics, ecological characteristics, and water use patterns of the different vegetation in these regions is a necessary means for this vegetation restoration. Stable hydrogen (δ^2H) and oxygen (δ^{18}O) isotopes are the most effective tools for determining plant water sources. Previous studies have shown that the isotopic fractionation of water does not occur during root absorption and transport. Thus, the relative contributions of different water sources can be inferred by comparing the δ^2H and δ^{18}O values of xylowater with the potential water sources (e.g., soil water, groundwater, and rainwater) [22]. Previous studies on subtropical forests have shown that multiple species living in the same habitat may have different water use patterns; this makes it possible for these species to coexist [23], which is called hydroecological niche separation [24]. Symbiotic plants often adopt different water use patterns due to differences in their root size, root depth, and leaf water use, resulting in the spatial–temporal distribution of their water use [25]. Some studies have shown that grasses and herbs tend to draw water from shallow soils throughout the growing season [26,27]. In contrast, some trees and shrubs often have the ability to obtain water from deep soil [22]. In addition, some species have the ability to switch between these shallow and deep soil layers to absorb their water, which is related to the plant's root morphology, as two forms of roots provide them with the ability to use water flexibly, have a high ecological plasticity, and can greatly adapt to changes in the external environment [17,28]. Based on this, plant species with hydrologic niche separation can have symbiosis within the same lifetime without water competition, which is an important mechanism for influencing the plant community structure and maintaining the plant coexistence in ecosystems with limited water resources.

The Guizhou Province is the most threatened area of rocky desertification in southwest China, so the growth and development of its forest plants have received strong attention. The region is widely mountainous, with a high bare rock leakage rate and shallow and discontinuous soil layers [21]. An inappropriate species selection for its forest ecosystem restoration would result in soil dryness vegetation degradation and reforestation difficulties. We know very little about the water uptake of its local species and whether the mix of these species within the small habitats of its subtropical forests is reasonable; therefore, it is urgent to understand the water use strategies of its forest vegetation and whether there is water competition or hydrologic niche separation among its different species.

In this study, stable hydrogen (δ^2H) and oxygen (δ^{18}O) isotopes were used to analyze the water use patterns of forest plants in a karst rocky desertification area. Our objectives were to: (1) explore the water use strategies and seasonal variations of the functional vegetation within the forest, and (2) determine whether there was hydroecological niche separation among the forest's species within the same lifetime. We hypothesized that: (i) the water use patterns of the four plants were different, and (ii) there was a significant hydrologic niche separation among the plants within the study habitat. The results of this study will elucidate the characteristics of the water use patterns of plants in karst forests and provide a scientific basis for the coexistence of plants in native territories.

2. Materials and Methods

2.1. Study Area

This study was conducted in the Guizhou Plateau canyon landform-type area in southwest China, which represents the general structure of the karst environmental types in southern China, specifically in the Huajiang section of the Beipanjiang Gorge, Guizhou Province (105°36′30″~105°46′30″ E, 25°39′13″~25°41′00″ N) (Figure 1). Karst landforms account for 87.92% of the total area, with a subtropical hot and dry valley climate, rain, and heat all co-occurring in time. The seasonal distribution of its precipitation is uneven, with most of the rain being concentrated within the period of May to October, accounting for 83% of the annual rainfall, for an average annual rainfall total of 1100 mm [29]. Its average annual temperature is 18.4 °C, with hot and humid summers and autumns and warm and dry winters and springs. The sample area is 607–890 m above sea level. This area has strong karstification, abundant underground cracks, karst caves, and serious soil erosion. Its soil average thickness is only about 30 cm and its lithology is Middle Triassic dolomitic limestone.

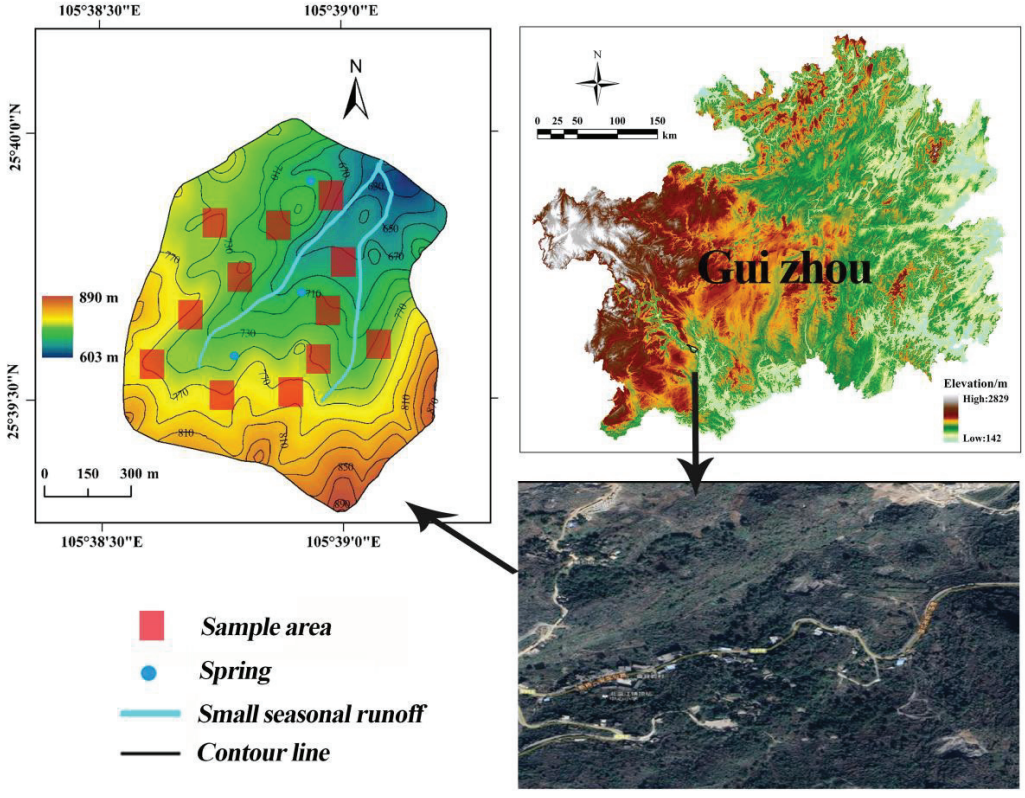

Figure 1. Geographical location of the study area. The left is a sampling point map, and the right is a regional satellite map. *Juglans regia*, *Zanthoxylum bungeanum Maxim*, *Eriobotrya japonica*, and *Lonicera japonica* these four plants are represented by their Chinese abbreviations in the following articles and charts, which are HT, HJ, PP, and JYH in the above order.

In the early 1970s, this area was a vast original forest with various types of vegetation, with the forest accounting for about 74% of the basin area. Subsequently, its artificial cultivation resulted in large-scale deforestation, with many plants recovering after a comprehensive conversion of farmland to forest in 2002. Nonetheless, the native vegetation

in the region has been seriously degraded, and the land is now occupied by secondary vegetation, mainly broadleaved forest, coniferous and broad-leaved mixed forest, and shrub. Its land use types are agricultural land and abandoned forestland, etc. The study area is rich in plant species, including *Lonicera japonica*, *Eriobotrya japonica Lindl*, *Pinus massoniana Lamb*, *Hylocereus undulatus Britt*, *Zanthoxylum bungeanum Maxim*, *Juglans regia*, and *Broussonetia papyrifera*. Among them, *Juglans regia*, *Zanthoxylum bungeanum Maxim*, *Eriobotrya japonica*, and *Lonicera japonica* (these four plants are represented by their Chinese abbreviations in the following articles and charts, which are HT, HJ, PP, and JYH in the above order) are the dominant species, with the largest local planting scales; they not only exhibit a great adaptability to the karst environment, but also bring considerable economic benefits to local residents.

2.2. Experimental Design and Sampling Collection

At the start of the experiment, the team performed a preliminary survey of the main plant species within the area's forests. The results showed that HT, HJ, PP, and JYH had the highest coverage compared to other plant species. Therefore, these four plants were selected as samples. The team found 360 plants of these four species across the region. After a statistical analysis of their physiological characteristics, such as the plant size and growth years of the samples, according to the average level of samples, a total of 12 representative sample plots (10 m × 10 m) were selected. The numbers of the four plant species in each plot tended to be consistent, with 4–5 from each species, totaling 217 tree species. The sample trees were the same in age, and their physiological characteristics, such as tree height, base diameter, and DBH, were roughly similar. The soil, plant, and spring water samples were collected once in each of the following months: September 2021, January 2022, April 2022, and July 2022 (the study area was located in southwest China, which is affected by subtropical monsoons and has a dry and hot valley climate. January, April, July, and September fall in winter, spring, summer, and fall. There would be significant changes in the rainfall and plant growth within the study area. Therefore, this paper chose these four months for sampling, which could be more representative).

On each sampling date, two plants with a similar growth morphology were randomly selected from each sample plot as sample trees (Table 1). A sample of each plant's xylem was collected from all four sides of its canopy. To avoid an isotope fractionation of the xylem water and a contamination with isotopically enriched water, the phloem tissue of the branches was removed [30]. All the plant samples were cut into 3–4 cm segments, placed in a high-boric-acid glass bottle, sealed with polyethylene film, and kept frozen in the refrigerator (4 °C) until the isotopic analysis. The fully expanded leaves of at least 10 individuals from each plant species on three slopes were collected to produce one composite sample for a carbon isotopic composition analysis. The leaves were dried at 60 °C and ground into a uniform powder that was sieved through a 1 mm mesh for the analysis of the carbon isotopic composition.

Table 1. Basic information of sampled plant species.

Species	Family	Life Feom	Height (m) (Mean ± SD)	DBH (cm)	Coverage Area (m^2)	Sample Number
Juglans regia	Walnut genus	Arbor	11.28 ± 3.19	21.48 ± 2.72	35.46 ± 5.31	49
Zanthoxylum bungeanum Maxim	Peppercorn genus	Small deciduous trees	3.39 ± 0.21	5.52 ± 0.11	5.83 ± 0.19	55
Eriobotrya japonica Lindl	Loquat genus	Small deciduous trees	2.76 ± 0.24	5.31 ± 0.13	2.86 ± 0.34	53
Lonicera japonica	Honeysuckle genus	Evergreen	0.89 ± 0.23	2.31 ± 1.31	4.33 ± 1.29	60

The soil samples were collected at the same time as the plant samples. On each sampling date, using a ring cutter, the soil samples were collected separately under each sampled tree at depths of 10, 20, 30, 40, 50, and 60 cm. The soil samples were divided into two parts: one part was stored in a freezer for the isotope analysis and the other was used to obtain the soil water content by weight (the subsequent soil moisture content is represented by "SWC" %). The root samples were collected at 10 cm intervals of depth, separated from the soil, and washed with water. The diameters and lengths of all the root segments within each 10 cm deep segment were measured with calipers and rulers to determine the root surface area within each segment. Fine roots with diameters of less than 0.001 m and roots with decayed surfaces were not recorded.

The surface of a karst area tends to be rugged and fragmented, with widespread fissures; as a result, fissure water is also a possible source of plant water. After a statistical survey of all the fissures in the region, the research team separately selected three representative fissures within the sampling area of each slope position. These fissures were located at an average distance of 2–3 m from the sample trees and had depths that varied from 0.4–1.5 m, and some plant roots extended to this point. Alternatively, either an underground water source that contributed to the pore leakage into a spring or the spring itself could be used [17]. Because a spring was located at each of the upper and middle slope positions, we also collected spring water in glass bottles and refrigerated these water samples. The fissure soil and spring samples were collected at the same time as the soil and plant samples, with a total of 72 fissure soil samples and 48 spring samples. The sampling time was similar to that of the plant soil. Because the water used to irrigate the HJ and PP was derived from precipitation, it was not separately included in this study.

In addition, a funnel device was used to collect the precipitation directly. The rainwater samples were also placed into glass bottles and sealed with film before the isotope analysis. The meteorological data were monitored over time by a small weather station in the study area (ATMOS, Meter Company, NC, USA). The equipment recorded the precipitation, air temperature, relative humidity, atmospheric pressure, and photosynthetically active radiation, at a frequency of 30 min per sampling record.

2.3. Isotopic Analysis

Water was extracted from the collected plant and soil samples using a low-temperature vacuum extraction instrument (LI-2100, LICA, Beijing, China), with the extraction process taking 2 to 3 h. Using this approach, the extraction efficiency exceeded 98%, which was sufficient for obtaining appropriate water samples [28]. The extracted water samples and rainwater samples were filtered through a 0.22 μm filter to eliminate any impurities and organic contaminants. Isotope measurements were performed on the filtered water samples using a liquid water isotope analyzer (TLWIA, Lijia, Beijing, China). The accuracy of the liquid water isotope analyzers for the $\delta^{18}O$ and $\delta^{2}H$ is usually better than 0.1‰ and 0.3‰, respectively [31]. Due to the spectral contamination of the water samples that were extracted at a low temperature, the spectra of the test results were corrected according to the instrument's calibration procedure [32]. The weighted averages ($\delta_{p,mean}$) of the $\delta^{2}H$ and $\delta^{18}O$ in the monthly precipitation were calculated as follows:

$$\delta_{p,mean} = \frac{(\sum_{i=1}^{n} \delta_{p,i} \times PPT_i)}{(\sum_{i=1}^{n} PPT_i)} \quad (1)$$

where $\delta_{p,i}$ is the $\delta^{18}O$ and $\delta^{2}H$ of the ith precipitation event, and PPT_i is the amount of the ith precipitation.

2.4. MixSIAR Analysis

The stable isotopes of the xylem water were compared to those of the potential water sources, and the intersections of the two were then used as initial indications of the depth from which each plant was absorbing water. The current proportion of the water used by plants is usually estimated by the Bayesian mixing model MixSIAR (version 4.2.0),

which includes the uncertainties and discriminant factors that are associated with multiple water sources [33]. The initial xylem isotope values, δ^2H and δ^{18}O, for the four plants were used as mixed data inputs for MixSIAR, and the means and standard errors of the isotope values (δ^2H and δ^{18}O) at the different soil layers (0–10 cm, 10–20 cm, 20–30 cm, 30–40 cm, 40–50 cm, 50–60 cm, fissure water, and groundwater) were used as the source data within the MixSIAR program. There was no concentration dependence in the source data. Because isotope fractionation did not occur due to the plant water absorption, the discrimination data were set to zero [34]. The run length of the Markov chain Monte Carlo (MCMC) was set to 'long' (chain length = 300,000; burn = 200,000; thin = 100; and chains = 3). Gelman-Rubin and Geweke diagnostic tests were used to determine whether the model was close to convergence [33] and the model's predictions were expressed as the mean values. Previous sample surveys found that the soil layers in the study area were generally unevenly distributed and shallow; therefore, only the 0–60 cm soil samples were retrieved. When analyzing the soil water, the soil isotope values between the different soil layers at 0–60 cm of depth were not readily apparent, so the water sources from the different soil layers were combined into two larger layers (0–30 cm and 30–60 cm) to facilitate a subsequent analysis and comparison. The two layers were identified based on the following approach [22]:

(1) The shallow layer (0–30 cm): The SWC and isotope values from the first 30 cm were close to each other, with a small variation along the vertical profile. In addition, the soil that resided close to the surface could easily be affected by rainfall and evaporation, so the soil water isotope value and SWC tended to exhibit a large range of variation between the seasons.
(2) The deep layer (30–60 cm): The SWC and isotope values in this layer changed less than those in shallow soil, because the soil layer was deeper and thus less affected by external precipitation and evaporation. As a result, the changes between the seasons were smaller.

2.5. Data Analyses

A K-S was used to test the normality of all the parameter sets and a linear regression analysis was used to understand the relationship between the δ^{18}O and δ^2H of each plant and its potential water source. After a box plot detection, the outliers were removed and the best fitting line was drawn to determine the equation, R coefficient, and p value. The differences in the xylem water content's δ^{18}O and δ^2H at $p < 0.05$ were analyzed by a one-way ANOVA and minimum significance difference (LSD) analysis. Then, the differences in the soil water isotope composition of each plant in the same month and the significant differences in the water sources of the different plants, with seasonal variations, were detected by a post-Tukey test and the minimum significant difference. An IBM SPSS 23-line statistical analysis was used for all the data, and Excel 2019 and Origin 2018 were used for the data editing and visualization.

3. Results

3.1. Precipitation Distribution and Isotopic Composition

The precipitation and temperature in the study area from August 2020 to July 2022 are shown in Figure 2, revealing a daily rainfall that ranged from 0 mm to 76 mm. Throughout the rainy season, a total of 1197.96 mm of rainfall occurred, accounting for 81.7% of the annual precipitation, of which the highest monthly rainfall was recorded at 283.4 mm in June. This latter value alone accounted for 19.33% of the annual total rainfall. The average daily rainfall was 6.65 mm during the rainy season and only 1.48 mm during the dry season. The daily temperature ranged from 4.16 °C to 30.98 °C and the average temperatures during the rainy season and dry season were 24.84 °C and 14.73 °C, respectively. In comparison, the rainfall increased by 10.11% in 2022 compared to 2021 (Figure 2).

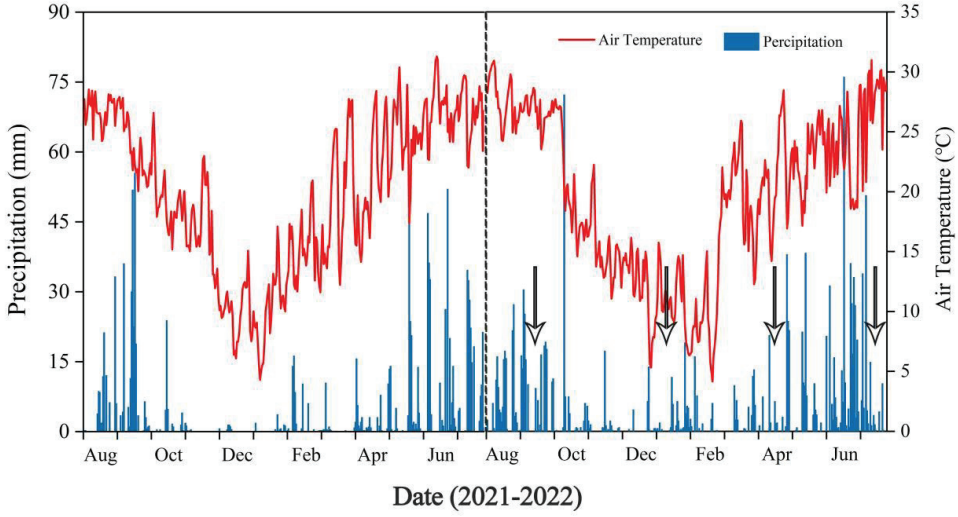

Figure 2. Precipitation and temperature in the study area from August 2020 to August 2022. The black arrow in the figure represents the sampling date.

The isotopic composition of the precipitation showed great changes during the sampling period, with the $\delta^{18}O$ ranging from −5.15‰ to −11.36‰, with an average of −7.57‰. The range of the $\delta^{2}H$ was −37.41‰ to −83.51‰, with an average of −60.48‰ (Figure 3). The local atmospheric precipitation line (LMWL), which was fitted according to the precipitation data (Figure 4), showed that the slope and intercept of the LMWL were smaller than those of the global atmospheric precipitation line (GMWL) [35]. The isotope values of the four plants mostly fell to the right of the LMWL, meaning that the soil water came from rain and underwent a degree of evaporation. It can also be seen from the soil water line (SWL) for the different slope positions of the four plants that the soil water source within each soil layer was precipitation (Figure 4).

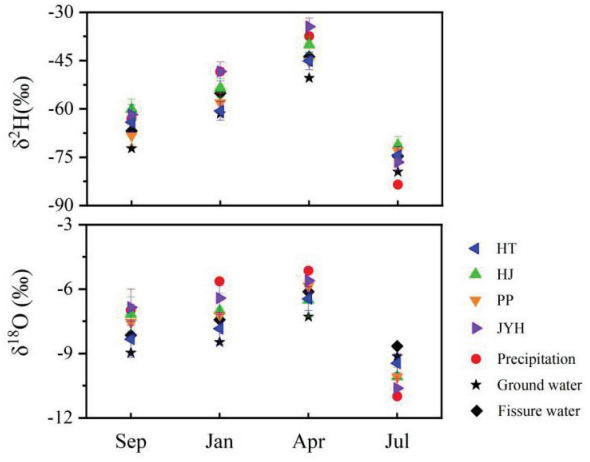

Figure 3. Seasonal variation of $\delta^{2}H$ and $\delta^{18}O$ values in xylem water of different water bodies and four plant species. The error bar represents the standard deviation. The $\delta^{2}H$ and $\delta^{18}O$ in rainwater represent the values of weighted averages per month.

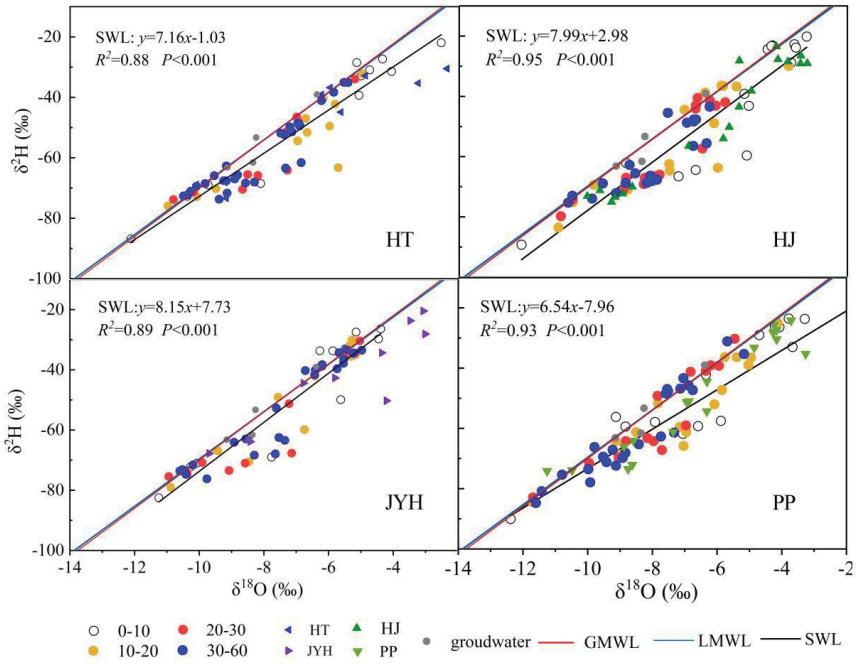

Figure 4. The linear regression relationship between δ^2H and δ^{18}O of soil moisture of four plant species in the study area. SWL represents soil water line based on isotopic data of soil water. LMWL represents the local meteoric water line (y = 7.86x + 9.02, R^2 = 0.98, and $p < 0.01$). GMWL is the global meteoric water line (y = 8x + 10) [35]. LMWL and GMWL are plotted in each panel for reference. The isotopic compositions of xylem water from four species are shown in the Figure 4.

3.2. Isotopic Composition and Variation of Xylem Water

The isotopic values of the xylem water varied with the sampling time and species. For HT, the δ^2H ranged from −46.37‰ to −77.24‰ and the δ^{18}O ranged from −6.42‰ to −10.22‰; for the HJ, the δ^2H ranged from −38.85‰ to −76.34‰ and the δ^{18}O ranged from −5.72‰ to −10.22‰; for the PP, the δ^2H values of the loquat ranged from −41.24‰ to −79.99‰ and the δ^{18}O values ranged from −5.85‰ to −10.69‰. The variation ranges of the δ^2H and δ^{18}O of JYH were the largest (Figure 3) and it is speculated that the water source of JYH was shallow and most affected by the surface rainfall evaporation. Overall, there was no significant difference between HJ and PP ($p > 0.05$) when averaging the xylem water isotope values across all the sampling dates, suggesting that both species were absorbing water from similar soil layers. However, the analysis on the sampling dates showed that the four planting covers had significant differences between the seasons ($p < 0.05$), indicating that the water absorption of the plants had an obvious time variability. From September 2021 to July 2022, the δ^2H and δ^{18}O in the xylem water of the four plants increased first and then decreased, and the change trend was basically the same, with the maximum value appearing in April and the minimum value in July (Figure 3). Meanwhile, the isotopic composition of HT and HJ was close to the fractured water and 30–60 cm water source in most cases, and occasionally close to the groundwater and precipitation, while the honeysuckle mainly depended on the 0–30 cm surface soil water and precipitation, and PP changed significantly between the deep and shallow water sources (Figure 3). In combination with Figure 4, the isotopic values of the plant xylem water were distributed across the different soil layers, indicating that soil water was still the main source of water for all four species. Among them, the water utilization of HJ and PP was very similar.

3.3. Soil Moisture and Isotopic Composition

The soil moisture's δ^2H and δ^{18}O experienced significant seasonal variations by depth and month (Figures 4 and 5). Because the soil layers in karst areas are shallow, there was no significant difference in the soil water content in the upper 0–30 cm soil layer (0–10, 10–20, and 20–30) depth in the vertical section ($p > 0.05$), and the variation value within a single season was only about ±4%. The SWC of the HT, HJ, and PP samples showed a similar trend at each depth. The water content of all the soil layers gradually increased from 0–40 cm and showed a turning point from 40 cm (Figure 4), gradually decreasing or increasing slowly. This may be because 0–40 cm was greatly affected by the surface rainfall, and the soil thickness in karst areas is generally about 40 cm. Further down, it is difficult to store precipitation due to the influence of gravel and cracks, etc., and the distribution being extremely uneven. In different months, the soil water content in the rainy season was generally higher than that in the dry season, with the lowest occurring in January and April and the highest in July. In July, the soil water content of HT reached 37.15%, which was the best water-retaining species among the four plants; HJ and PP followed, reaching 36.08% and 35.76%. The lowest SWCS of HT, HJ, PP, and JYH were 27.24%, 26.15%, 24.10%, and 24.06%, respectively. During the sampling period, the SWC in the shallow soil layer (0–30 cm) changed more than that in the other soil layers, while the SWC in the deep soil layer (30–60 cm) was relatively stable, and the same trend was observed for all four species.

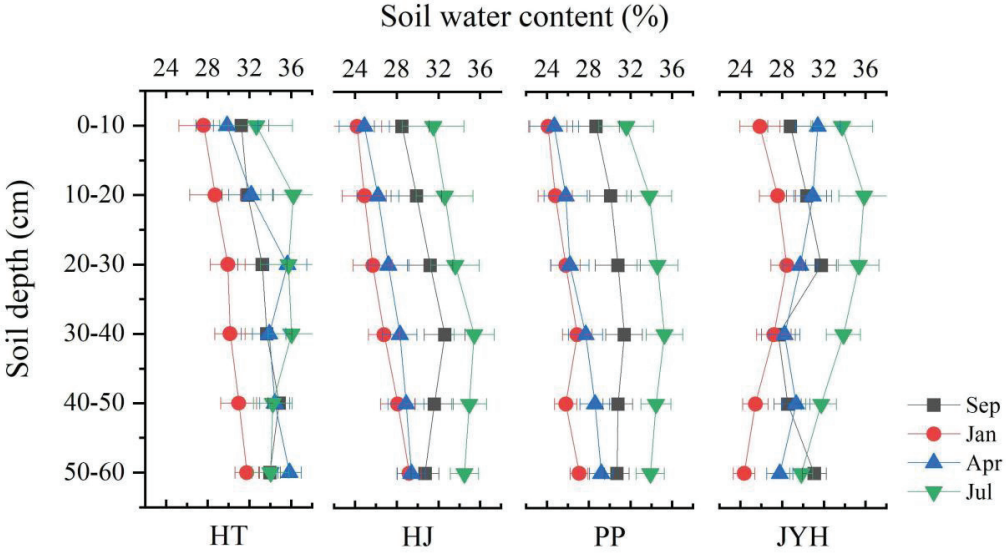

Figure 5. Changes in soil water content between HT, HJ, PP, and JYH in 0–60 cm section. The error bar represents the standard deviation.

The isotopic composition of the soil water varied with the soil depth and plant species. During the sampling period, the isotopic composition of the soil water became poorer as the soil depth increased, and the difference in the isotopic values and variations in the shallow soil water (0–30 cm) was higher than that in the deep soil water (30–60 cm). From a seasonal point of view, there was no significant difference between the shallow and deep soil water isotopic compositions of HJ and PP ($p > 0.05$). The δ^2H and δ^{18}O values of HT ranged from −21.94‰ to 86.83‰, and from −2.55‰ to 12.21‰, respectively. The δ^2H and δ^{18}O values of HJ ranged from −32.17‰ to 77.34‰, and from −5.04‰ to 10.91‰, respectively. Those of PP ranged from −31.41‰ to −77.76‰ and −5.26‰ to 9.59‰, while those of JYH ranged from −3.26‰ to −11.25‰ and −20.87‰ to −82.51‰, respectively.

From January to July, the δ^2H and $\delta^{18}O$ in the xylem water of the four species decreased gradually and increased in September (Figure 3).

3.4. Variations in the Proportion of Plant Water Uptake

According to the graph inference method, the isotopic ratios of the xylem water, crack water, and soil water of the four plants overlapped at several soil depths during the study period (Figures 6 and 7), suggesting that the plants could obtain water from several sources. Using the MixSIAR model further to predict the water absorption ratios of the plants, HT mainly depended on 30–60 cm deep water sources (41.8 ± 6.86%) and crack water (32.5 ± 4.21%) during the rainy season in July and September, while its use of surface water sources 0–30 cm (22.5 ± 2.86%) was relatively small (Figure 8). This was related to the sufficient precipitation during the rainy season, which increased the water content of the surface layer (Figure 5), while the dry season mainly relied on deep and fissure water. For HJ during the dry season, deep soil water was dominant (45.24 ± 4.16%) and shallow soil water was secondary (25.5 ± 4.38%). However, in the rainy season, the water source was mainly shallow soil water (45.6 ± 3.94%), which was supplemented by deep soil water (22.03 ± 4.22%).

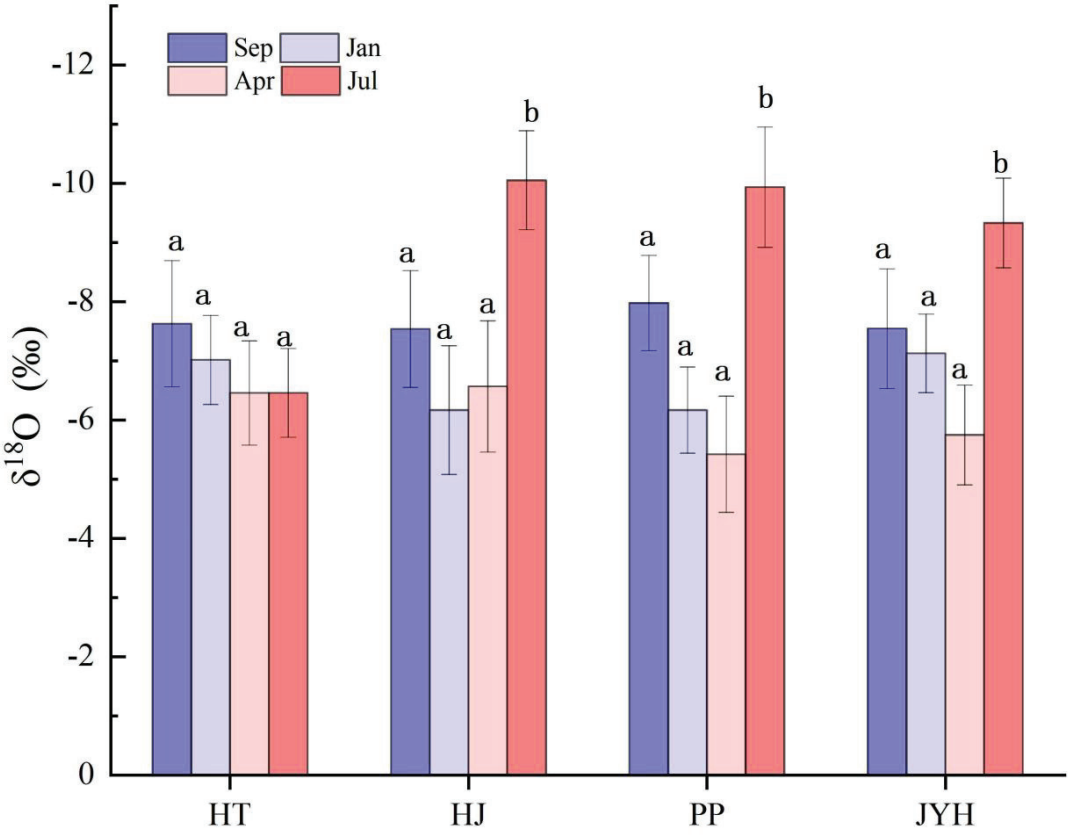

Figure 6. Significant differences in soil water isotope composition of four plants in the same month. a and b represent different significant differences. Error bars represent standard deviations, $p < 0.05$.

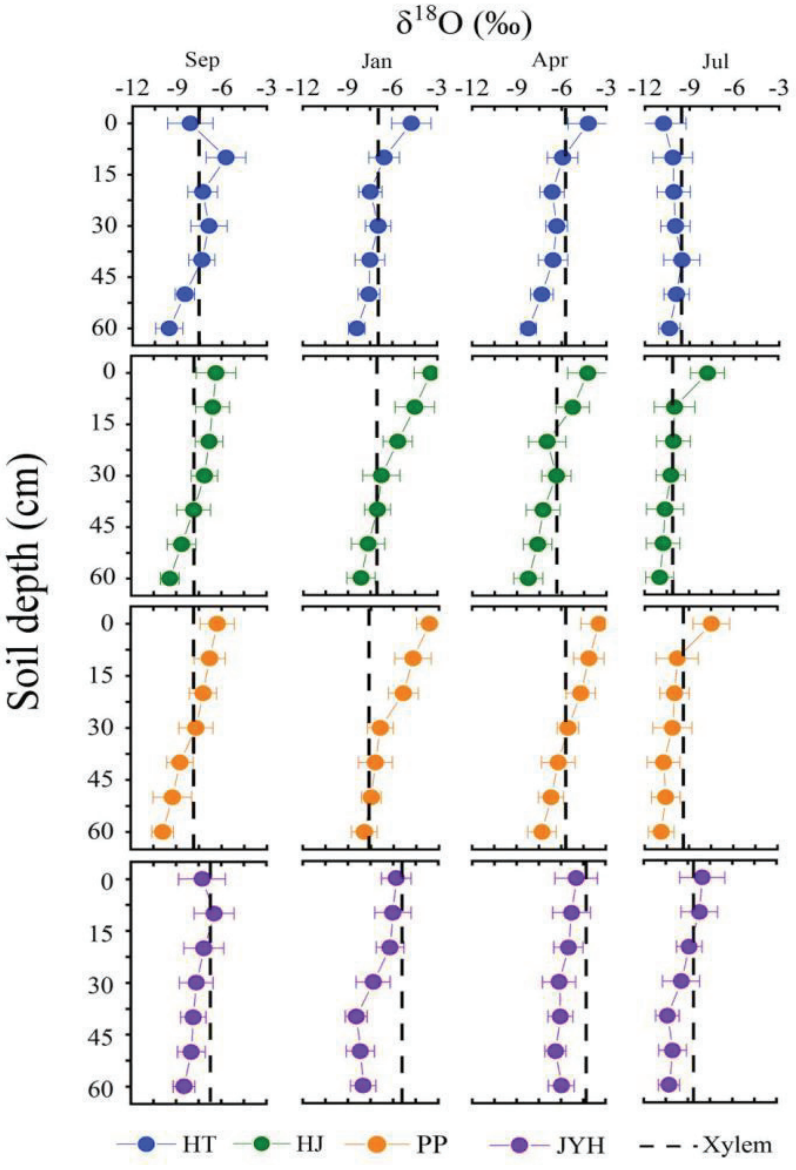

Figure 7. Seasonal variation in $\delta^{18}O$ in soil layer (0–60 cm) and xylem water (vertical dashed line) of four species. From left to right are September 2021, and January, April, and July 2022. Error bars represent standard deviations ($p < 0.05$).

In contrast, the water absorption pattern of PP was the same, and the difference was only slightly different in numerical value (Figure 8); for example, the absorption of shallow water in the rainy season reached 54.31 ± 3.36%, while that in the dry season was only 12.53 ± 4.24% (Figure 8). In contrast, the water absorption ratio of JYH was significantly different, as JYH was dominated by 0–30 cm surface water (61.3%) in both the dry and rainy seasons (Figure 8). Individual plants may have also reached as deep as 40 cm into the water, which was mainly related to JYH's root system. In addition, the proportion of water sources for HT was relatively balanced and the change was slightly small, as the main body of HT

relied on a 30–60 cm water source and fissure water (70 ± 3.22%) (Figure 8). HJ and PP transferred flexibly between the shallow layer during the rainy season and the deep layer during the dry season, and it can also be clearly seen from Table 2 that the proportion of the water sources in the loquat varied significantly between the seasons. During the sampling period, there was no significant difference in the water absorption patterns between HJ and PP ($p > 0.05$), but there was a difference in the water absorption ratio between the seasons ($p < 0.05$), as shown in Table 2. The utilization of shallow water by JYH was significantly higher than that by the other plants in the dry rainy season, and the utilization of deep water from 30–60 cm by the other three plants was significantly higher than that by JYH in the dry rainy season.

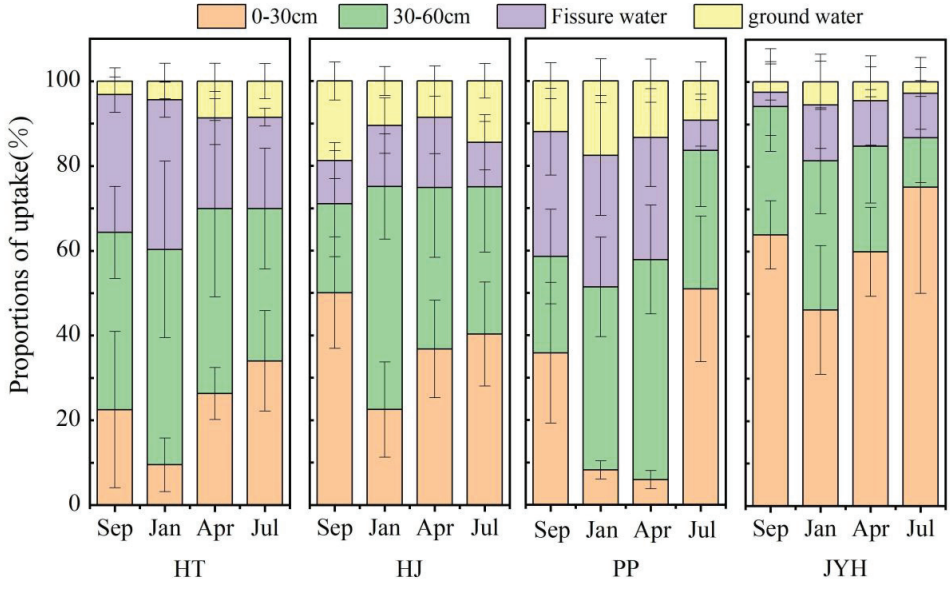

Figure 8. Seasonal variations in proportion of water uptake from different soil layers based on MixSIAR for HT, HJ, PP, and JYH. Error bars represent standard deviation.

Table 2. Changes in water use ratio of four species in dry rainy season.

Water Source Plants	*Juglans regia*		*Zanthoxylum bungeanum Maxim*		*Eriobotrya japonica Lindl*		*Lonicera japonica*	
	Dry	**Rainy**	**Dry**	**Rainy**	**Dry**	**Rainy**	**Dry**	**Rainy**
0–30 cm	17.9% ^{c}	28.3% ^{c}	29.6% ^{b}	45.2% ^{b}	7.1% ^{d}	43.4% ^{b}	53.1% ^{a}	69.6% ^{a}
30–60 cm	47.2% ^{a}	38.9% ^{a}	45.4% ^{a}	27.8% ^{b}	47.6% ^{a}	27.7% ^{b}	30.1% ^{b}	20.9% ^{c}
Fissure water	28.4% ^{a}	27.1% ^{a}	15.5% ^{b}	10.4% ^{c}	29.9% ^{a}	18.3% ^{b}	12.0% ^{b}	6.9% ^{c}
Ground water	6.6% ^{b}	5.9% ^{b}	9.6% ^{b}	16.7% ^{a}	15.5% ^{a}	10.6% ^{a}	4.9% ^{b}	2.6% ^{b}

By contrast, in the table, ^{a}, ^{b}, ^{c}, and ^{d} represent the significant difference in water utilization ratio of the four plants in the same season, $p < 0.05$.

3.5. Changes of Carbon Isotopes in Plant Leaves

The seasonal variation in the $\delta^{13}C$ in the leaves of the four plant species was measured during the study period. The results showed that leaf $\delta^{13}C$ of the four planting species changed from high to low from the dry season to the rainy season (Figure 9). Under drought conditions in January, the $\delta^{13}C$ was generally high, and HJ and HT were the highest, at −26.24‰ and −26.37‰, respectively. In the rainy season, the $\delta^{13}C$ values were generally low, especially in July, when the precipitation was sufficient and the plants were not affected

by drought stress, adopting a low water use efficiency (Figure 9). The WUE of each plant species was at a low level. In addition, by analyzing the $\delta^{13}C$ value, HT, HJ, and PP, in descending order, were HT > HJ > PP. This is the same as the result that was obtained in Figure 8, where HT and HJ had a higher water use efficiency and higher survival rate than the other two species.

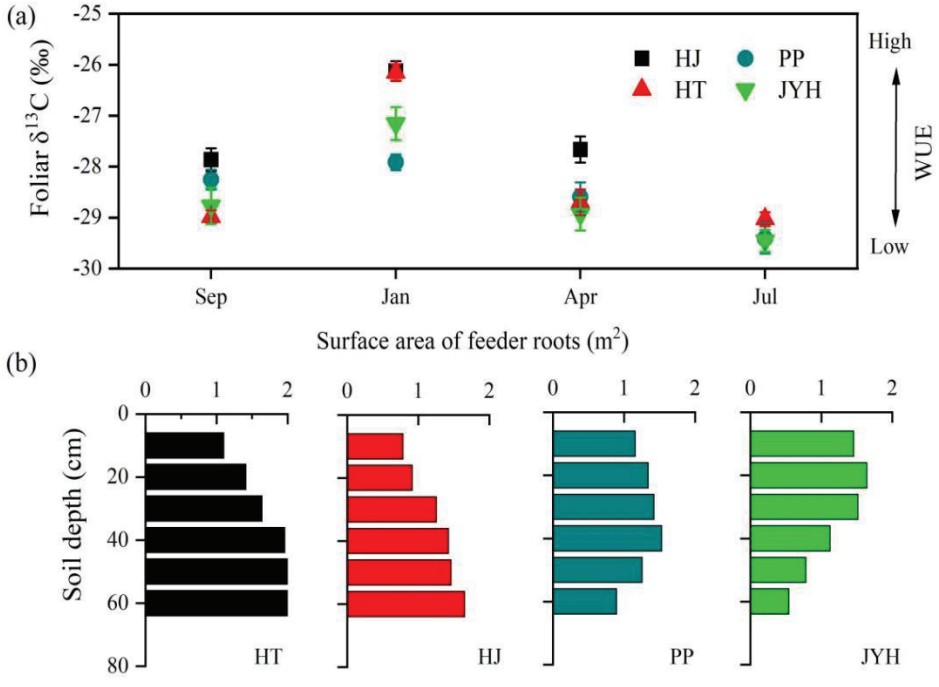

Figure 9. (**a**) Seasonal variation of $\delta^{13}C$ values in leaves of HT, HJ, PP, and JYH. (**b**) Profile distribution of root surface area of four species. Error bars represents standard error.

4. Discussion

4.1. Vertical Gradients of Forest Soil Water Isotopic Composition

In subtropical forests, the vertical gradient of soil water isotopes is mainly affected by evaporation and infiltration, as well as the mixing of old and new rainwater [36]. It could be clearly seen that 0–60 cm, from the surface to the deep layer, presented a clear trend of gradual depletion. It only showed significant changes at about 0–15 cm, because it was close to the surface and was greatly affected by precipitation and evaporation. The further down the soil was, the less the external precipitation evaporation had an influence, so the water isotope of deep soil tended to be stable. The stable isotope ratios of the four plants from 0–60 cm decreased, as shown in Figure 7. As the authors make clear, there was no significant difference between the different months and different depths among some plants (HJ and PP), as only the range and trend of the variation were described. Due to the small data gap, the data analysis showed that there was no statistically significant difference (Figures 6 and 7). As the soil depth increased, the $\delta^{2}H$ and $\delta^{18}O$ in the soil moisture became more depleted. Compared to the deeper soil profiles in January and April, the isotopic composition in the surface 0–30 cm soil water was more abundant (Figures 6 and 7). This is attributed to the decreased rainfall and increased evaporation in the surface soil layer [37]. However, due to the influence of rainfall with poor isotopic values in the summer, this trend was reversed in the topsoil during July and September, suggesting that precipitation was also an important factor controlling the soil water isotopic composition [22,38,39]. The

isotopic ratios of the surface soil displayed larger variances than those of the deep soil, due to the combined influences of evaporation and precipitation. In this study, the $\delta^{18}O$ values of the 30–60 cm soil changed less by depth and sampling date than those of the 0–30 cm soil (Figures 6 and 7). HJ and PP showed the same change pattern, suggesting that the influence of evaporation on the deep soil was limited [36,40]. The fissure water in the study area often came from rainwater that had seeped into the soil, and the vertical changes in the soil isotope composition were caused by the mixing old and new water [41,42], which would then infiltrate into the deeper soil layers [43].

The isotopes in precipitation generally show the seasonal variation characteristics of being low in summer and high in winter, which is mainly related to the water vapor sources in the winter and summer half years and the meteorological conditions during precipitation [17,28,44]. In the summer half year, southwest China is mainly affected by the oceanic warm and humid air masses of southwest monsoons and southeast monsoons, with sufficient water vapor, a high humidity, and weak evaporation [44]. According to the Rayleigh fractionation principle, the heavy isotopes in precipitation would be depleted with a decrease in the water vapor content during the transport process of air mass, and the $\delta^{18}O$ would be low. In the winter half year, the region is mainly affected by the westerly dry and cold water vapor mass and the local evaporation of water vapor, with the water vapor content being low, the air being relatively dry, the evaporation being strong, the heavy isotope being gradually enriched in precipitation, and the $\delta^{18}O$ being high [45,46]. Compared to the GMWL, the slope and intercept of the atmospheric precipitation line in the study area were relatively small, indicating that the climate in this region is warm and humid, that there is a certain degree of secondary evaporation in the precipitation process, and that the unbalanced evaporation effect is larger. This is mainly related to the temperature of the water vapor condensation, the evaporation conditions, the water vapor source, and the transportation mode [46].

4.2. Differences in Seasonal Water Uptake Patterns among Species

According to the regression diagram of the soil water's $\delta^{2}H$ and $\delta^{18}O$ in Figure 4, the xylem isotopic compositions of the four plants were distributed in 0–60 cm of the soil and water, suggesting that most of the water sources for the subtropical forest plants during the study period came from the 0–60 cm soil layer [47]. Figure 8 also shows that about 71.67% of the water sources for the four plants came from 0–60 cm of the soil water. During the study period, HJ and PP were concentrated in deep water absorption during the dry season and shallow water absorption during the rainy season. HT, however, was always dominated by deep water sources and fissure water sources, and the reason for this was that the three plants belonged to different functional types. As a macrophanerophytes, HT has numerous root systems and goes deep underground, so it can use deep water sources and water that is stored in rock cracks with great efficiency [48]. As small trees and shrubs, HJ and PP have small and shallow roots, and, in order to achieve a higher water use efficiency, their absorbed water sources can be flexibly converted between deep and shallow layers. In a study of aspen and other plants, Flanagan et al. also found that plants not only absorb soil water, but also involve groundwater [49]. It could be seen that the water absorption patterns of HJ and PP showed the same "dimorphic root system" [48,50,51], which indicates that their water resource utilization had a certain plasticity level. Wang et al. found that Huangjing could switch between deep and shallow water sources with seasonal changes, which was similar to our experimental results [47].

In contrast, JYH's water absorption was more extreme between the seasons, with the difference between the dry season and rainy season in the 0–30 cm soil layer being only about 16.7% (Figure 8). The contribution ratio of the water absorption was significantly different from that of the other three plants ($p < 0.05$). Karakis and other researchers found in their experiments on grape that the depth of a vine's water-absorbing root system could vary over time. Shallow roots used rainwater as their main source during spring, and with the advance of the growing season, the roots could gradually penetrate into the soil

profile [52]. Similar results have been found for other ecosystems [25,53], and shrubs or small trees will gradually increase their water absorption depth during the growing season. This also had some similarity to our study, but it remains to be seen whether the roots of plants gradually infiltrated into the soil layers with the growing season, due to a lack of data [54,55]. In addition, although both belong to the "dimorphic root system", PP still showed different characteristics to HJ, as its water source segmentation was more severe during the dry season and the rainy season (Figure 8), which may be related to the root systems of both [56,57]. At the same time, during a precipitation event in July, PP was greatly affected by precipitation [58], and the contribution ratio of the surface water increased rapidly (Figure 8), while that of the deep water decreased slightly. However, HJ is relatively slow and its rise is not obvious. This is influenced by the root system of HJ, as, compared to PP, the root system of HJ has a deeper distribution and fewer fibrous roots on the surface, which is less responsive to surface rainfall (Figure 9).

The four plants, all belonging to subtropical forest vegetation, showed different levels of ecological plasticity under the same precipitation conditions. The shallow root system of PP, coupled with small evergreen trees, resulted in a low plasticity level for its water resource utilization [56,59]. Especially during dry years, many cases of dry death occurred when there was no rain for a long time [13]. Furthermore, both PP and HJ belong to small trees and have similar water use patterns, meaning that water competition exists between these species. Adequate water sources during the rainy season can ensure the survival of both, but under severe water stress, PP will be more passive [58]. Zhang et al. found that, in plants from subalpine habitats that mainly absorb water from the surface layer (0–30 cm), subalpine shrubs compete for water resources at similar depths during the drought and growing seasons, with a high water demand, resulting in plant dieback [60].

4.3. Hydrological Niche Separation and Ecohydrological Regulation of Forest Vegetation

During the dry season and rainy season, the water source of each plant in the same habitat of a subtropical forest is different. With a change in water conditions, their water use strategies will also change, showing a greater drought tolerance [12,15,61]. In this study, HT, as a deciduous tree with stout branches and deep roots, had the same water use pattern in both the rainy and dry seasons, with soil water of a 30–60 cm depth and fissure water always being its main sources (Figure 7). Thus, in the dry season, HT would compete for water with HJ and PP within the same lifetime. Moreover, HJ and PP had the same water use pattern, indicating that they would compete for water resources at a similar depth. With a small body size and shallow root system, the latter showed obvious weakness in its water absorption [62]. In the rainy season, with sufficient precipitation, HJ and PP turned to the shallow water source of 0–30 cm, while HT was still dominated by the deep water, so there was no competition between them and a clear separation of hydrological niche. However, as a perennial semi-evergreen shrub, the root system of JYH was mainly concentrated at around 0–40 cm (Figure 8) and its water resources throughout the whole year came from this. It was in competition with HJ and PP, and the water use capacity of the three factors determined the survival status of the species, with HJ usually winning. It follows that there are complex water use patterns among plants within the same lifetime of these subtropical forests. HT competed with HJ and PP during the dry season and HJ and PP competed with JYH during the rainy season, while HJ competed with PP all the time. JYH and HT were in a state of hydrologic niche separation, and they did not pose a threat to each other; therefore, large swaths of JYH were often seen growing around HT in the study area. The hydroecological niche isolation (HNS) hypothesis proposes that, within a community, plants may differ in their hydraulic characteristics in order to avoid or tolerate drought along the water availability gradients, thus avoiding competition [23]. These features include water absorption (e.g., different rooting depths or possibly leaf water absorption), differences in their stomatal control, and differences in their xylem structures [63]. The four plants in this study belong to different functional types of vegetation, with significant differences in their plant sizes.

The root depth of HT was much greater than that of the other three species, so it could utilize deeper water. Deciduous trees reduce water evaporation during the dry season and greatly improve their water use efficiency. In fact, these characteristics can have a significant impact on hydrological processes [64].

Previous studies have shown that tree size is also related to effective rooting depth [65] and demonstrated that this interdependence is related to different hydraulic strategies. Rooting depth increases with tree height, compensating for the greater evaporation requirements at the top of the canopy [66] and allowing larger trees to be photosynthetically active during the dry season. Our data in this study show a coordination between the rooting depth and water absorption sources in seasonal subtropical forests, suggesting a trade-off between drought avoidance (i.e., deep roots) and drought tolerance [64,67]. Drought-resistant species are characterized by their deep roots, such as tall trees and shrubs, which enable the plants to survive close to the hydraulic safety limit [68,69]. This is the main strategy of most vegetation within a forest, and these complementary strategies allow for a niche partitioning within forest ecosystems and influence the structure of the dominant species in communities that are driven by water resources and light [70]. At the surface, trees take advantage of the abundant sunlight in the upper layers, shrubs take advantage of the weaker light in the middle layers, and herbs gather at the ground level. In the underground space, plant roots are interwoven layer by layer to gather soil nutrients on the one hand, and prevent soil erosion on the other. This is especially evident in the above-ground and subsurface binary structure space, with serious leakage in southwest karst areas [21]. Due to the community structure of forest vegetation, it is highly possible to gather precipitation and facilitate the successful completion of the forest ecohydrological process between the atmosphere, vegetation, and soil. The dense canopy in a forest system can reduce the flushing of the surface soil through rain [71], accumulate soil nutrients, further promote vegetation growth during the dry season, and increase productivity [72,73].

Due to the limited availability of soil water, plants during the drought and rain seasons are subjected to different levels of water stress [74,75]. Plants in hot, dry river valleys respond to drought in different ways. One way is that some deciduous species drop their leaves to reduce transpiration and remain dormant throughout the drought; another way is through changing the water absorption strategy according to the available water source [22]. HJ is not only a small deciduous tree, but also has a dimorphic root system, which can stably change its water source pattern between the seasons. This flexible water use strategy can greatly improve its survival rate [19]. Although PP also has a dimorphic root system, it also has a shallow root system, making it difficult for it to penetrate deeper and thus relatively dependent on shallow soil water [58]. This extreme shallow and deep water conversion between the seasons indicates its high dependence on the water environment. Moreover, as an evergreen tree [56], PP has a greater need for water [76], which makes it more likely to die than prickly ash in the same habitat.

5. Conclusions

In this study, we used a Bayesian mixing model (MixSIAR) combined with stable isotopes of hydrogen (δ^2H) and oxygen (δ^{18}O) to investigate the seasonal variations in the water uptake patterns of four plantations in a karst subtropical forest. The soil water isotopic composition varied in gradient along the vertical direction, and the variation in the soil water isotopic composition was greater in the shallow layer than in the deep layer. HT mainly relied on deep soil water and fissure water, while JYH mainly relied on shallow water. They did not compete with each other for water, but had a seasonal hydrologic niche separation from the other two species, which reduced the water competition. The stony desertification intensity in the study area was relatively high and there were a variety of vegetation types within the subtropical artificial forest, which led to water competition among the various species with the same water use pattern. The result of this inter-species competition led to plant drying and death. A reasonable species combination (for example, the deep planting of PP, with timely irrigation during the dry season; HT, HJ, and PP being

as far away from each other as possible; the adoption of grass irrigation, Joe irrigation, Joe grass, and other planting methods) would facilitate their symbiosis with each other. Staggered water uptake would greatly improve the survival of species and their adaptation to changing future environments, maintain the hydrological cycle of forest ecosystems, promote the transfer of water between the atmosphere, vegetation, and soil, and help the ecological restoration of karst areas. This study provides a method for determining more efficient plant combinations for karst forest vegetation habitats, and its results will have important implications for ecosystem vegetation restoration.

Author Contributions: Conceptualization, K.X.; methodology, B.F., Z.L.; software, B.F.; formal analysis, B.F.; writing—original draft preparation, B.F.; writing—review and editing, B.F., K.X.; visualization, B.F.; supervision, K.X., Z.L.; project administration, K.X., Z.L.; funding acquisition, K.X. All authors have read and agreed to the published version of the manuscript.

Funding: This study was supported by the Science and Technology Program of Guizhou Province (No. 5411 2017 Qiankehe Pingtai Rencai), the China Overseas Expertise Introduction Program for Discipline Innovation (No. D17016) and the National Major Research and Development Program of China (2016YFC0502607).

Institutional Review Board Statement: Not applicable.

Informed Consent Statement: Not applicable.

Data Availability Statement: Not applicable.

Conflicts of Interest: The authors declare no conflict of interest.

References

1. Forzieri, G.; Miralles, D.G.; Ciais, P.; Alkama, R.; Ryu, Y.; Duveiller, G.; Cescatti, A. Increased control of vegetation on global terrestrial energy fluxes. *Nat. Clim. Change* **2020**, *10*, 356–362. [CrossRef]
2. Brandt, M.; Yue, Y.; Wigneron, J.P.; Tong, X.; Tian, F.; Jepsen, M.R.; Fensholt, R. Satellite-observed major greening and biomass increase in south China karst during recent decade. *Earth's Future* **2018**, *6*, 1017–1028. [CrossRef]
3. Konapala, G.; Mishra, A.K.; Wada, Y. Climate change will affect global water availability through compounding changes in seasonal precipitation and evaporation. *Nat. Commun.* **2020**, *11*, 3044. [CrossRef]
4. Yang, X.-D.; Wu, N.-C.; Gong, X.-W. Plant Adaptation to Extreme Environments in Drylands. *Forests* **2023**, *14*, 390. [CrossRef]
5. Yang, H.B.; Yang, D.W. Derivation of climate elasticity of runoff to assess theeffects of climate change on annual runoff. *Water Resour.* **2011**, *47*. [CrossRef]
6. Wang, J.; Fu, B.J.; Wang, L.X. Water use characteristics of the common tree species in different plantation types in the Loess Plateau of China. *Agric. For. Meteorol.* **2020**, *288–289*, 108020. [CrossRef]
7. Bode, S.; De Wispelaere, L.; Hemp, A. Water-isotope ecohydrology of Mount Kilimanjaro. *Ecohydrology* **2020**, *13*, e2171. [CrossRef]
8. Zhang, S.; Xiong, K.; Qin, Y.; Min, X.; Xiao, J. Evolution and determinants of ecosystem services: Insights from South China karst. *Ecol. Indic.* **2021**, *133*, 108437. [CrossRef]
9. Tie, Q.; Hu, H.C.; Tian, F.Q. Environmental and physiological controls on sap flow in a subhumid mountainous catchment in North China. *Agric. For. Meteorol.* **2017**, *240–241*, 46–57. [CrossRef]
10. Tang, Y.K.; Wen, X.F.; Sun, X.M. The limiting effect of deep soil water on evapotranspiration of a subtropical coniferous plantation subjected to seasonal drought. *Adv. Atmos. Sci.* **2014**, *31*, 385–395. [CrossRef]
11. Fu, T.; Chen, H.; Wang, K. Structure and water storage capacity of a small karst aquifer based on stream discharge in South China. *J. Hydrol.* **2016**, *534*, 50–62. [CrossRef]
12. Song, L.; Yang, B.; Liu, L.L.; Mo, Y.X.; Liu, W.J.; Meng, X.J.; Zhang, Y.J. Spatial-temporal differentiations in water use of coexisting trees from a subtropical evergreen broadleaved forest in Southwest China. *Agric. For. Meteorol.* **2022**, *316*, 108862. [CrossRef]
13. Wang, X.; Liu, Z.; Xiong, K.; He, Q.; Li, Y.; Li, K. Characteristics and controlling factors of soil dissolved organic matter in the rainy season after vegetation restoration in a karst drainage area, South China. *Catena* **2022**, *217*, 106483. [CrossRef]
14. Brinkmann, N.; Seeger, S.; Weiler, M. Employing stable isotopes to determine the residence times of soil water and the temporal origin of water taken up by Fagus sylvatica and Picea abies in a temperate forest. *New. Phytol.* **2018**, *219*, 1300–1313. [CrossRef] [PubMed]
15. Rowland, L.; da Costa, A.C.; Galbraith, D.R.; Oliveira, R.S.; Binks, O.J. Death from drought in tropical forests is triggered by hydraulics not carbon starvation. *Nature* **2015**, *528*, 119–122. [CrossRef]
16. Xiao, J.; Xiong, K. A review of agroforestry ecosystem services and its enlightenment on the ecosystem improvement of rocky desertification control. *Sci. Total Environ.* **2022**, *856*, 158538. [CrossRef]

17. Nie, Y.P.; Chen, H.S.; Wang, K.L.; Tan, W.; Deng, P.Y.; Yang, J. Seasonal water use patterns of woody species growing on the continuous dolostone outcrops and nearby thin soils in subtropical China. *Plant Soil.* **2011**, *341*, 399–412. [CrossRef]
18. Tu, Z.; Chen, S.; Chen, Z.; Ruan, D.; Zhang, W.; Han, Y.; Han, L.; Wang, K.; Huang, Y.; Chen, J. Hydrological Properties of Soil and Litter Layers of Four Forest Types Restored in the Gully Erosion Area of Latosol in South China. *Forests* **2023**, *14*, 360. [CrossRef]
19. Tang, Y.K.; Wu, X.; Chen, Y.M.; Wen, J.; Xie, Y.; Lu, S. Water use strategies for two dominant tree species in pure and mixed plantations of the semiarid Chinese Loess Plateau. *Ecohydrology* **2018**, *11*, e1943. [CrossRef]
20. Seneviratne, S.I.; Corti, T.; Davin, E.L. Investigating soil moisture–climate interactions in a changing climate: A review. *Earth Sci. Rev.* **2010**, *99*, 125–161. [CrossRef]
21. Xu, Q.; Xiong, K.; Chi, Y. Effects of intercropping on fractal dimension and physicochemical properties of soil in karst areas. *Forests* **2021**, *12*, 1422. [CrossRef]
22. Rothfuss, Y.; Javaux, M. Reviews and syntheses: Isotopic approaches to quantify root water uptake: A review and comparison of methods. *Biogeosciences* **2017**, *14*, 2199–2224. [CrossRef]
23. Wu, H.; Li, X.Y.; Jiang, Z.; Chen, H. Contrasting water use pattern of introduced and native plants in an alpine desert ecosystem, Northeast Qinghai–Tibet Plateau, China. *Sci. Total Environ.* **2016**, *542*, 182–191. [CrossRef] [PubMed]
24. Herberich, M.M.; Gayler, S.; Anand, M.; Tielbörger, K. Hydrological niche segregation of plant functional traits in an individual-based model. *Ecol. Model.* **2017**, *356*, 14–24. [CrossRef]
25. Liu, W.; Chen, H.; Zou, Q.; Nie, Y. Divergent root water uptake depth and coordinated hydraulic traits among typical karst plantations of subtropical China: Implication for plant water adaptation under precipitation changes. *Agric. Water Manag.* **2021**, *249*, 106798. [CrossRef]
26. Asbjornsen, H.; Shepherd, G.; Helmers, M. Seasonal patterns in depth of water uptake under contrasting annual and perennial systems in the Corn Belt Region of the Midwestern US. *Plant Soil* **2008**, *308*, 69–92. [CrossRef]
27. Fu, A.; Chen, Y.; Li, W. Water use strategies of the desert riparian forest plant community in the lower reaches of Heihe River Basin, China. *Sci. China Earth Sci.* **2014**, *57*, 1293–1305. [CrossRef]
28. Yang, B.; Wen, X.F.; Sun, X.M. Seasonal variations in depth of water uptake for a subtropical coniferous plantation subjected to drought in an East Asian monsoon region. *Agric. For. Meteorol.* **2015**, *201*, 218–228. [CrossRef]
29. Li, Y.; Liu, Z.; Liu, G. Dynamic Variations in Soil Moisture in an Epikarst Fissure in the Karst Rocky Desertification Area. *J. Hydrol.* **2020**, *591*, 1–12. [CrossRef]
30. Querejeta, J.I.; Estrada-Medina, H.; Allen, M.F.; Jimenez-Osornio, J. Water source partitioning among trees growing on shallow karst soils in a seasonally dry tropical climate. *Oecologia* **2007**, *152*, 26–36. [CrossRef]
31. Wen, X.; Lee, X.; Sun, X.; Wang, J.; Hu, Z.; Li, S.; Yu, G. Dew water isotopic ratios and their relationships to ecosystem water pools and fluxes in a cropland and a grassland in China. *Oecologia* **2012**, *168*, 549–561. [CrossRef]
32. Schultz, N.M.; Griffis, T.J.; Lee, X.; Baker, J.M. Identification and correction of spectral contamination in 2H/1H and 18O/16O measured in leaf, stem, and soil water. *Rapid Commun. Mass Spectrom.* **2011**, *25*, 3360–3368. [CrossRef]
33. Stock, B.; Semmens, B. *MixSIAR GUI User Manual v3. 1.*; Scripps Institution of Oceanography, UC San Diego: San Diego, CA, USA, 2016.
34. Fan, J.; Wang, Q.; Jones, S.B. Soil water depletion and recharge under different land cover in China's Loess Plateau. *Ecohydrology* **2016**, *9*, 396–406. [CrossRef]
35. Craig, H. Isotopic variations in meteoric waters. *Science* **1961**, *133*, 1702–1703. [CrossRef]
36. Renée Brooks, J.; Barnard, H.R.; Coulombe, R.; McDonnell, J.J. Ecohydrologic separation of water between trees and streams in a Mediterranean climate. *Nat. Geosci.* **2010**, *3*, 100–104. [CrossRef]
37. Geris, J.; Tetzlaff, D.; McDonnell, J.J. Spatial and temporal patterns of soil water storage and vegetation water use in humid northern catchments. *Sci. Total. Environ.* **2017**, *595*, 486–493. [CrossRef]
38. Han, C.; Chen, N.; Zhang, C.; Liu, Y. Sap flow and responses to meteorological about the Larix principis-rupprechtii plantation in Gansu Xinlong mountain, northwestern China. *For. Ecol. Manag.* **2019**, *451*, 117519. [CrossRef]
39. Dong, Z.; Li, S.; Zhao, Y.; Lei, J.; Wang, Y.; Li, C. Stable oxygen-hydrogen isotopes reveal water use strategies of Tamarix taklamakanensis in the Taklimakan Desert, China. *J. Arid Land* **2020**, *12*, 115–129. [CrossRef]
40. Jiang, Z.C.; Lian, Y.Q.; Qin, X.Q. Rocky desertification in Southwest China:impacts, causes, and restoration. *Earth-Sci. Rev.* **2014**, *132*, 1–12. [CrossRef]
41. Xiang, W.; Si, B.C.; Biswas, A.; Li, Z. Quantifying dual recharge mechanisms in deep unsaturated zone of Chinese Loess Plateau using stable isotopes. *Geoderma* **2019**, *337*, 773–781. [CrossRef]
42. Demand, D.; Blume, T.; Weiler, M. Spatio-temporal relevance and controls of preferential flow at the landscape scale. *Hydrol. Earth Syst. Sci.* **2019**, *23*, 4869–4889. [CrossRef]
43. Gazis, C.; Feng, X. A stable isotope study of soil water: Evidence for mixing and preferential flow paths. *Geoderma* **2004**, *119*, 97–111. [CrossRef]
44. Chen, F.; Huang, C.; Lao, Q.; Zhang, S.; Chen, C.; Zhou, X.; Zhu, Q. Typhoon control of precipitation dual isotopes in southern China and its palaeoenvironmental implications. *J. Geophys. Res. Atmos.* **2021**, *126*, e2020JD034336. [CrossRef]
45. Tian, L.; Yao, T.; Sun, W.; Stievenard, M.; Jouzel, J. Relationship between δD and δ^{18}O in precipitation on north and south of the Tibetan Plateau and moisture recycling. *Sci. China Ser. D Earth Sci.* **2001**, *44*, 789–796. [CrossRef]

46. Wu, X.; Pan, M.; Zhu, X.; Yin, J.; Wang, Z.; Zhang, M.; Cao, J. Effect of the El Niño–Southern Oscillation on hydrogen and oxygen isotope ratios of precipitation in Guilin, SW China. *Isot. Environ. Health Stud.* **2021**, *57*, 67–81. [CrossRef] [PubMed]
47. Wang, J.; Fu, B.J.; Lu, N.; Zhang, L. Seasonal variation in water uptake patterns of three plant species based on stable isotopes in the semi-arid Loess Plateau. *Sci. Total Environ.* **2017**, *609*, 27–37. [CrossRef]
48. Gao, X.D.; Zhao, X.N.; Wu, P.T.; Brocca, L.; Zhang, B.Q. Effects of large gullies on catchment-scale soil moisture spatial behaviors: A case study on the Loess Plateau of China. *Geoderma* **2016**, *261*, 1–10. [CrossRef]
49. Flanagan, L.B.; Orchard, T.E.; Tremel, T.N. Using stable isotopes to quantify water sources for trees and shrubs in a riparian cottonwood ecosystem in flood and drought years. *Hydrol. Process.* **2019**, *33*, 3070–3083. [CrossRef]
50. Leite, P.A.; Wilcox, B.P.; McInnes, K.J. Woody plant encroachment enhances soil infiltrability of a semiarid karst savanna. *Environ. Res. Commun.* **2020**, *2*, 115005. [CrossRef]
51. Hoekstra, N.J.; Finn, J.A.; Hofer, D. The effect of drought and interspecific interactions on depth of water uptake in deep- and shallow-rooting grassland species as determined by δ18O natural abundance. *Biogeosciences* **2014**, *11*, 4493–4506. [CrossRef]
52. Karakis, S.; Gulbranson, E.; Cameron, B. Insight into the source of grapevine water acquisition during key phenological stages using stable isotope analysis. *Aust. J. Grape Wine Res.* **2018**, *24*, 252–259. [CrossRef]
53. Barbeta, A.; Mejía-Chang, M.; Ogaya, R.; Voltas, J.; Dawson, T.; Peñuelas, J. The combined effects of a long-term experimental drought and an extreme drought on the use of plant-water sources in a Mediterranean forest. *Glob. Change Biol.* **2015**, *21*, 1213–1225. [CrossRef] [PubMed]
54. Feng, X.; Fu, B.; Piao, S.; Wang, S.; Ciais, P.; Zeng, Z.; Wu, B. Revegetation in China's Loess Plateau is approaching sustainable water resource limits. *Nat. Clim. Change* **2016**, *6*, 1019–1022. [CrossRef]
55. Luo, Y.; Gong, Y. α Diversity of Desert Shrub Communities and Its Relationship with Climatic Factors in Xinjiang. *Forests* **2023**, *14*, 178. [CrossRef]
56. Apostolakis, A.; Schöning, I.; Michalzik, B.; Ammer, C.; Schall, P.; Hänsel, F.; Nauss, T.; Trumbore, S.; Schrumpf, M. Forest Structure and Fine Root Biomass Influence Soil CO2 Efflux in Temperate Forests under Drought. *Forests* **2023**, *14*, 411. [CrossRef]
57. Jiang, Y.; Huang, A.; Wu, H.; Zhang, X. GIS-based research on climate suitable region of Loquat in Lishui, Zhejiang province of China. *Environ. Res. Commun.* **2022**, *4*, 015006. [CrossRef]
58. Zhang, Y.; Yao, Q.; Li, J.; Wang, Y.; Liu, X.; Hu, Y.; Chen, J. Contributions of an arbuscular mycorrhizal fungus to growth and physiology of loquat (*Eriobotrya japonica*) plants subjected to drought stress. *Mycol. Prog.* **2015**, *14*, 1–11. [CrossRef]
59. Mao, Q.; He, B.; Ma, M.; Wang, L.; Koike, T.; Agathokleous, E. Effects of biochar on Karst lime soil nutrients, soil microbial communities, and physiology of Sichuan pepper plants. *Ann. Appl. Biol.* **2022**, *181*, 357–366. [CrossRef]
60. Zhang, F.; Jia, W.; Zhu, G.; Zhang, Z.; Shi, Y.; Yang, L.; Zhang, M. Using stable isotopes to investigate differences of plant water sources in subalpine habitats. *Hydrol. Process.* **2022**, *36*, e14518. [CrossRef]
61. Li, T.; Liu, Y.; Cai, Q.; Duan, X.; Li, P.; Ren, M.; Ye, Y. Water Stress-Induced Divergence Growth of Picea schrenkiana in the Western Tianshan and Its Forcing Mechanisms. *Forests* **2023**, *14*, 354. [CrossRef]
62. Taufik, M.; Torfs, P.J.; Uijlenhoet, R.; Jones, P.D.; Murdiyarso, D.; Van Lanen, H.A. Amplification of wildfire area burnt by hydrological drought in the humid tropics. *Nat. Clim. Change* **2017**, *7*, 428. [CrossRef]
63. Sterck, F.; Markesteijn, L.; Schieving, F.; Poorter, L. Functional traits determine trade- offs and niches in a tropical forest community. *Proc. Natl. Acad. Sci. USA* **2011**, *108*, 20627–20632. [CrossRef] [PubMed]
64. Jiang, S.; Xiong, K.; Xiao, J. Structure and Stability of Agroforestry Ecosystems: Insights into the Improvement of Service Supply Capacity of Agroforestry Ecosystems under the Karst Rocky Desertification Control. *Forests* **2022**, *13*, 878. [CrossRef]
65. Ivanov, V.Y.; Hutyra, L.R.; Wofsy, S.C.; Munger, J.W.; Saleska, S.R.; De Oliveira, R.C.; De Camargo, P.B. Root niche sepa-ration can explain avoidance of seasonal drought stress and vulnerability of overstory trees to extended drought in a mature Amazonian forest. *Water Resour. Res.* **2012**, *48*, 1–21. [CrossRef]
66. McDowell, N.G.; Allen, C.D. Darcy's law predicts widespread forest mortality under climate warming. *Nat. Clim. Change* **2015**, *5*, 669–672. [CrossRef]
67. Karger, D.N.; Kessler, M.; Lehnert, M.; Jetz, W. Limited protection and ongoing loss of tropical cloud forest biodiversity and ecosystems worldwide. *Nat. Ecol. Evol.* **2021**, *5*, 854–862. [CrossRef]
68. Silvertown, J.; Araya, Y.; Gowing, D. Hydrological niches in terrestrial plant communities: A review. *J. Ecol.* **2015**, *103*, 93–108. [CrossRef]
69. Restrepo-Coupe, N.; Levine, N.M.; Christoffersen, B.O.; Albert, L.P.; Wu, J.; Costa, M.H.; Saleska, S.R. Do dynamic global vege-tation models capture the seasonality of carbon fluxes in the Amazon basin? A data-model intercomparison. *Glob. Change Biol.* **2016**, *23*, 1–18. [CrossRef]
70. Meinzer, F.C.; Johnson, D.M.; Lachenbruch, B.; McCulloh, K.A.; Woodruff, D.R. Xylem hydraulic safety margins in woody plants: Coordination of stomatal control of xylem tension with hy-draulic capacitance. *Funct. Ecol.* **2009**, *23*, 922–930. [CrossRef]
71. Deng, X.; Xiong, K.; Yu, Y.; Zhang, S.; Kong, L.; Zhang, Y. A Review of Ecosystem Service Trade-Offs/Synergies: Enlightenment for the Optimization of Forest Ecosystem Functions in Karst Desertification Control. *Forests* **2023**, *14*, 88. [CrossRef]
72. Guo, W.; Liu, H.; Wu, X. Vegetation greening despite weakening coupling between vegetation growth and temperature over the boreal region. *J. Geophys. Res. Biogeosci.* **2018**, *123*, 2376–2387. [CrossRef]
73. Feng, H.; Zou, B. A greening world enhances the surface-air temperature difference. *Sci. Total Environ.* **2019**, *658*, 385–394. [CrossRef]

74. Yang, J.; Chen, H.; Nie, Y.; Wang, K. Dynamic variations in profile soil water on karst hillslopes in South China. *Catena* **2019**, *172*, 655–663. [CrossRef]
75. Huo, G.P.; Zhao, X.N.; Gao, X.D.; Wang, S.F.; Pan, Y.H. Seasonal water use patterns of rainfed jujube trees in stands of different ages under semiarid plantations in China. *Agric. Ecosyst. Environ.* **2018**, *265*, 392–401. [CrossRef]
76. Ellsworth, P.Z.; Sternberg, L.S. Seasonal water use by deciduous and evergreen woody species in a scrub community is based on water availability and root distribution. *Ecohydrology* **2015**, *8*, 538–551. [CrossRef]

forests

MDPI

Article

Influence of Different Planting Combinations on the Amino Acid Concentration in Pericarp of *Zanthoxylum planispinum* 'Dintanensis' and Soil

Yitong Li [1], Yanghua Yu [1,*], Yanping Song [1] and Changsheng Wei [2]

[1] School of Karst Science, State Engineering Technology Institute for Karst Decertification Control, Guizhou Normal University, Guiyang 550001, China
[2] Forestry Bureau of Zhenfeng County, Zhenfeng 562200, China
* Correspondence: yuyanghua2003@163.com

Abstract: In this study, the effect of different planting combinations on the amino acid concentration in the pericarp of *Zanthoxylum planispinum* 'dintanensis' (hereafter referred to as *Z. planispinum*) was studied, and the response of amino acid concentration to soil factors was clarified. The aim of this study was to screen optimal planting combinations and provide a theoretical basis for improving pericarp quality. Five planting combinations of *Z. planispinum* in a karst rocky desertification area were selected as the research objects, and the concentration and accumulation of free amino acids in the pericarp of *Z. planispinum* were analyzed. Then, combined with existing soil quality data, the pericarp quality of *Z. planispinum* was comprehensively evaluated by principal component analysis, and the effect of soil factors on amino acid concentrations was clarified by redundancy analysis. The results are as follows: (1) except for arginine, serine, proline, alanine, tyrosine and cystine, the concentrations of other free amino acids significantly differed among the five planting combinations. In general, the planting combination has a great influence on the concentration of free amino acids in the pericarp of *Z. planispinum*, especially essential amino acids; (2) free amino acid concentration in the pericarp of *Z. planispinum* mostly increased in combination with *Sophora tonkinensis* Gagnep. (hereafter referred to as *S. tonkinensis*) and decreased in combination with *Prunus salicina* Lindl; (3) principal component analysis showed that the concentration of free amino acid in the pericarp of *Z. planispinum* was generally at a high level when combined with *S. tonkinensis* or *Lonicera japonica* Thunb. (hereafter referred to as *L. japonica*). Among them, the amino acids in the pericarp of *Z. planispinum* with *S. tonkinensis* were closer to the ideal protein standard of FAO/WHO; (4) soil-available potassium, available phosphorus, microbial biomass nitrogen, available calcium and microbial biomass phosphorus in soil factors had significant effects on amino acid concentration after a redundancy analysis. It can be seen that the available nutrients and soil microbial biomass contribute greatly to the amino acid concentration of the pericarp. According to the soil quality and the amino acid quality of the pericarp, planting with *L. japonica* can improve the amino acid quality of the pericarp of *Z. planispinum*, as well as selecting *Z. planispinum* + *L. japonica* as the optimal planting combination.

Keywords: principal component analysis; redundancy analysis; karst rocky desertification area

Citation: Li, Y.; Yu, Y.; Song, Y.; Wei, C. Influence of Different Planting Combinations on the Amino Acid Concentration in Pericarp of *Zanthoxylum planispinum* 'Dintanensis' and Soil. *Forests* **2023**, *14*, 843. https://doi.org/10.3390/f14040843

Academic Editor: Gaetano Distefano

Received: 24 February 2023
Revised: 9 April 2023
Accepted: 18 April 2023
Published: 20 April 2023

1. Introduction

As a type of organic nitrogen, amino acids are the most basic element of proteins and are an important primary metabolite for maintaining plant growth, reproduction and development [1]. Amino acids are also common small molecular precursors of synthesized organic compounds, such as nucleic acid, chlorophyll and hormone and secondary metabolism in plants [2]. In addition, as one of the existing forms of amino acids, free amino acids (FAAs) are important flavoring substances. Their types and concentrations are often used as important indicators to evaluate the nutritional value and taste of fruits and

have an important impact on the formation of fruit quality [3,4]. Free amino acids are generally grouped according to their taste as bitter (valine, leucine, isoleucine, methionine and arginine), sweet (glycine, alanine, serine, threonine, proline and histidine), delicious (lysine, glutamate and aspartate) and aromatic (phenylalanine, tyrosine and cystine) [5]. Therefore, the study of amino acid concentration is particularly important to further identify the flavor of *Zanthoxylum planispinum* 'dintanensis' (hereafter referred to as *Z. planispinum*).

The chemical elements in the soil are the direct source of nutrients for fruit formation, the raw material storage for nutrients and determine the main chemical reaction processes and rates such as photosynthesis, respiration and transpiration [6]. Nitrogen (N), phosphorus (P) and other macro elements play an important role in the growth and development of plants, as well as the regulation of various physiological functions [7,8]. Nitrogen is an important component of protein and other metabolites, participating in the amino acid synthesis of secondary metabolites [9,10]. Phosphorus is an important chemical element that constitutes the metabolites of deoxyribonucleic acid, ribonucleic acid and adenosine triphosphate. It also directly participates in the biochemical reaction of some primary metabolite synthesis [11,12]. In addition, calcium, as the second messenger, is used to activate the resistance gene of plant cells and regulate the response to the stimulation signal of whole plant somatic cells [13,14].

Microorganisms in soil can decompose plant residues into humus, thus participating in the assimilation of secondary metabolism in plants [15]. In addition, the decomposition and mineralization of organic matter by soil microorganisms affect soil nutrient cycling, thereby changing the balance of soil nutrient elements. Ecological stoichiometry is a combination of the basic principles of ecology and stoichiometry to explore the energy balance and nutrient element balance of the ecosystem [16]. The change in element stoichiometry has an obvious correlation with the change in metabolites, which can regulate molecular synthesis in the organism and further affect the metabolic reaction [17]. It can be seen that the changes in soil elements, microorganisms and their stoichiometry are of great significance to the synthesis of metabolites.

Z. planispinum is a small deciduous tree of *Zanthoxylum planispinum* in the family Rutaceae. It is a medicinal and edible homologous plant with rich protein and complete amino acid species [18]. It has become a unique dominant tree species for karst rocky desertification control in Guizhou due to its calcium (Ca) preference and drought-resistant and lithogenic characteristics. However, in recent years, due to the continuous planting of monoculture forests, soil fertility decline, improper management measures and other reasons, the pericarp quality of *Z. planispinum* has decreased, and plant growth has declined. Adopting the combination planting method of different plants can effectively increase the diversity of plant communities, make full use of space and resources [19] and have the following advantages: increased crop yield; optimized crop quality; efficient use of nutrients; increased biodiversity; and reduced disease [20,21]. Based on this, this study selected four common planting combinations of *Z. planispinum* and compared them with a *Z. planispinum* monoculture forest. The effects of different planting combinations on the amino acid quality in the pericarp of *Z. planispinum* and their response to soil were studied. The purpose of this is to solve the following problems: (1) concentration characteristics, flavor contribution and quality evaluation of FAAs in the pericarp of *Z. planispinum* with different planting combinations; and (2) effects of soil properties on the pericarp quality of *Z. planispinum*. To do so, the plants suitable for planting with *Z. planispinum* were selected, and the basis for the selection of planting combinations and the cultivation management of *Z. planispinum* was provided.

2. Materials and Methods

2.1. Overview of the Research Site

The research area is located in Beipanjiang Town, Zhenfeng County, Guizhou Province, China (105°38′35″ E, 25°39′37″ N). It belongs to a subtropical humid monsoon climate, with rainfall concentrated from May to October and an annual average rainfall of about

1100 mm. The annual average temperature is 18.4 °C. It is a valley terrain with an altitude of 370–1473 m. The soil type is mainly lime soil with carbonate rock accounting for 78.45%, pH > 6.5. The soil is rich in Ca. Most of the study area is moderately and intensively a rocky desertification area, with a rock exposure rate of 50%–80%. The environment is highly heterogeneous, with many kinds of niche types, such as stone surface, stone ditch, stone crevice, stone groove, stone cave, etc. *Z. planispinum* has the largest planting area in the study area. In addition, there were *Zea mays* L. (hereafter referred to as *Z. mays*), *Lonicera japonica* Thunb. (hereafter referred to as *L. japonica*), *Prunus salicina* Lindl. (hereafter referred to as *P. salicina*), *Sophora tonkinensis* Gagnep. (hereafter referred to as *S. tonkinensis*), *Arachis hypogaea* L. (hereafter *A. hypogaea*) and other associated species.

2.2. Treatment Setting

In order to ensure the typicality, representativeness and comparability of the selected sample plots, some common local planting combinations were screened. The final allocation of tree species determined that *P. salicina* represented the arbor, *S. tonkinensis* represented the dwarf medicinal material, *A. hydropogaea* represented the legume plant, and *L. japonica* represented the liana plant (*Z. planispinum* + *P. salicina*; *Z. planispinum* + *S. tonkinensis*; *Z. planispinum* + *A. hydropogaea*; *Z. planispinum* + *L. japonica*). The *Z. planispinum* monoculture forest was used as a control. One treatment with similar environmental elements was set for each plantation (Figure 1 & Table 1). Before planting research plantations, all treatments were mainly planted with *Z. mays*, and the management measures were the same in order to make the soil background value similar. In 2012, *Z. planispinum* was planted in 5 treatments. After 2018, *L. japonica*, *S. tonkinensis*, *A. hydropogaea* and *L. japonica* were planted around *Z. planispinum*. The annual plant *A. hydropogaea* was continuously planted according to the phenological season. Other perennial plants were regularly maintained to maintain the dynamic stability of the community. The age of *Z. planispinum* in the 5 treatments was 8 years, and the slopes were 10°. Li et al. [22] introduced the planting density of interplanting plants and forest land management measures in detail.

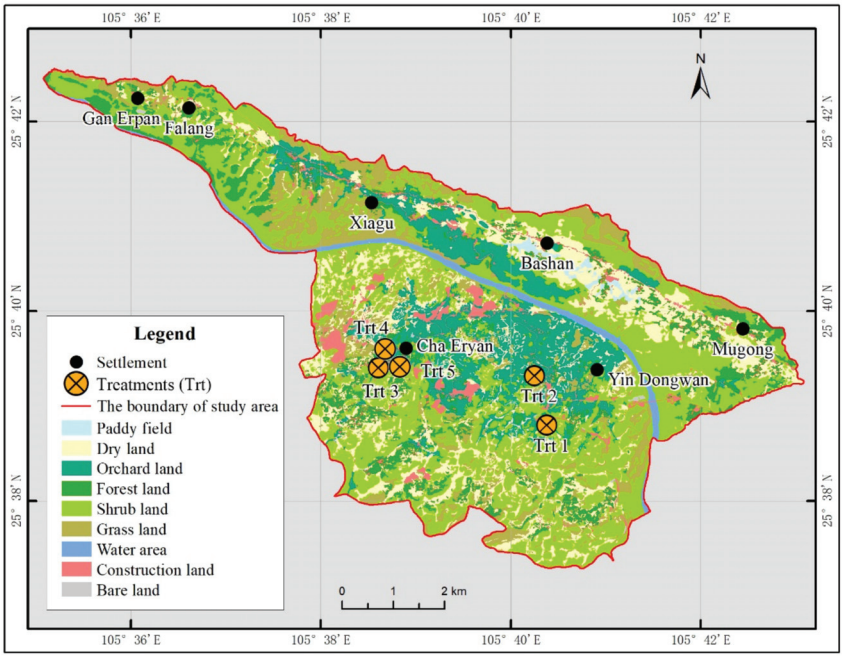

Figure 1. Distribution of treatments (Trt).

Table 1. Descriptions of the plantation types.

Plantation Types	Species Combinations	Longitude	Latitude	Growing Area (ha)	Altitude (m asl)	Density (m)	Height (m)	Crown Width (m)	Coverage (%)
Trt 1	*Z. planispinum* + *P. salicina*	105°40′28.33″ E	25°37′57.41″ N	1.34	764	3 × 3	3.5	2 × 2.3	70
Trt 2	*Z. planispinum* + *S. tonkinensis*	105°40′19.79″ E	25°39′25.75″ N	0.67	728	2 × 2	2.0	1.2 × 1.8	60
Trt 3	*Z. planispinum* + *A. hypogaea*	105°38′36.32″ E	25°39′23.64″ N	0.67	791	2 × 2	2.5	2.5 × 2.8	85
Trt 4	*Z. planispinum* + *L. japonica*	105°38′36.35″ E	25°39′22.29″ N	6.67	814	3.5 × 3	2.5	1.5 × 2.5	70
Trt 5	*Z. planispinum*	105°38′35.64″ E	25°39′23.35″ N	33.35	788	3 × 4	2.2	2.5 × 2.3	65

2.3. Soil Sample Collection and Soil Parameters

Three 10 m × 10 m sample squares were arranged in each treatment, and multiple sampling points were arranged within each sample square. At each sampling point, equal amounts of soil were collected in layers of 0–10 cm and 10–20 cm, and samples of the same soil layer were uniformly mixed. The soil sample parameters in this study were taken as the average of the data from 2 soil layers to ensure that the number of observations of soil samples was consistent with the number of observations of the FAAs (15 observations in total over 5 treatments).

The soil water content of Trt 5 was significantly lower than that of other treatments, indicating that combined planting can significantly improve soil water content. Soil organic carbon (SOC), total N and total P were the highest in Trt 4. Total N, total P and total potassium (K) were significantly lower in Trt 2. Trt 5 had the highest concentration of total Ca. The concentration of available N and available Ca in Trt 4 was significantly higher than that in other treatments. There was no significant change in available P concentration among treatments. Available K concentration in Trt 1 was significantly higher than that in other treatments. There was no significant difference in the C:N value among the 5 treatments. C:P and N:P values of Trt 2 were significantly higher than that of Trt 5. The values of microbial biomass carbon, microbial biomass nitrogen (MBN) and microbial biomass phosphorus (MBP) had no significant difference among the 5 treatments, indicating that soil microorganisms have strong stability. Relevant data are shown in Table 2. Li et al. [23] described the soil sample collection, index determination and data analysis in detail.

Table 2. Soil parameters in different planting combinations.

Soil Parameters	Trt 1	Trt 2	Trt 3	Trt 4	Trt 5
Soil water content	31.60 ± 6.29 ab	36.73 ± 2.65 a	25.05 ± 1.38 bc	28.69 ± 0.30 bc	21.15 ± 0.14 c
Soil organic carbon concentration	37.73 ± 7.32 ab	29.40 ± 0.57 ab	28.68 ± 12.62 ab	50.83 ± 13.33 a	26.50 ± 2.19 b
Total nitrogen concentration	3.53 ± 0.46 ab	2.64 ± 0.07 b	2.78 ± 0.74 b	4.60 ± 0.44 a	2.76 ± 0.23 b
Total phosphorus concentration	1.37 ± 0.02 a	0.82 ± 0.03 b	1.10 ± 0.43 ab	1.52 ± 0.17 a	1.26 ± 0.04 ab
Total potassium concentration	6.95 ± 0.34 b	6.11 ± 1.51 b	12.33 ± 0.25 a	11.88 ± 0.53 a	10.88 ± 0.03 a
Total calcium concentration	0.95 ± 0.28 b	1.48 ± 0.39 b	1.85 ± 0.71 b	1.88 ± 0.18 b	6.05 ± 0.21 a
Available nitrogen concentration	275.00 ± 74.25 ab	160.00 ± 5.66 b	161.75 ± 61.87 b	350.00 ± 55.15 a	153.75 ± 15.91 b

Table 2. *Cont.*

Soil Parameters	Trt 1	Trt 2	Trt 3	Trt 4	Trt 5
Available phosphorus concentration	45.80 ± 13.29 a	23.38 ± 11.63 a	26.55 ± 10.54 a	36.68 ± 10.01 a	20.08 ± 2.44 a
Available potassium concentration	393.00 ± 107.48 a	195.85 ± 32.03 b	172.75 ± 57.63 b	223.75 ± 98.64 ab	141.25 ± 2.47 b
Available calcium concentration	317.50 ± 14.85 b	334.75 ± 0.35 b	347.75 ± 24.40 ab	371.00 ± 8.49 a	350.50 ± 7.07 ab
Soil C:N ratio	10.65 ± 0.70 a	11.13 ± 0.53 a	10.07 ± 1.85 a	10.97 ± 1.85 a	9.59 ± 0.00 a
Soil C:P ratio	27.68 ± 5.79 abc	35.83 ± 0.79 a	25.82 ± 1.33 bc	33.10 ± 4.99 ab	21.03 ± 2.38 c
Soil N:P ratio	2.59 ± 0.37 ab	3.22 ± 0.22 a	2.60 ± 0.34 ab	3.02 ± 0.05 a	2.19 ± 0.25 b
Microbial biomass carbon	243.00 ± 4.95 a	254.75 ± 2.47 a	252.00 ± 2.83 a	262.75 ± 21.57 a	262.25 ± 26.52 a
Microbial biomass nitrogen	12.40 ± 1.70 a	13.58 ± 1.31 a	14.38 ± 0.60 a	13.90 ± 1.06 a	14.08 ± 0.18 a
Microbial biomass phosphorus	128.00 ± 23.33 a	144.50 ± 4.95 a	148.00 ± 8.49 a	154.50 ± 13.44 a	139.00 ± 3.54 a

Trts 1–5, five plantations, representing the research objectives of this article. Means followed by the same lowercase letter are not significantly different ($p > 0.05$) among root types as determined by the least significance difference test. Data are presented as mean ± standard deviation.

2.4. Fruit Sample Collection

In the first ten days of June 2021, the fresh fruit of *Z. planispinum* was collected in 5 treatments, at which time the fruit was mature. We selected 5 healthy-growing *Z. planispinum* from each sample square discussed above and collected about 200 g of mature and disease-free *Z. planispinum* fruit from different directions, taking care to eliminate the edge effect. The collected fruits were naturally air-dried in nylon bags, and 5 plant fruit samples from each sample square were mixed into 1 (15 observations in total over 5 treatments). After the pericarps were separated, dried at 45 °C, crushed and screened for the determination of FAAs. Because the pericarp of *Z. planispinum* was rich in amino acids, aromatic oil, fatty acids and other substances and was the main part of utilization, this paper studied the changes in free amino acid concentration in its pericarp.

2.5. Free Amino Acid Analysis

The free amino acids were determined by high-performance liquid chromatography [24,25], and phenylisothiocyanate acetonitrile solution was used as the pre-column derivatization reagent. The UV detector wavelength was 254 nm; the chromatographic column was C18SHISEIDO (4.6 mm × 250 mm × 5 μm). The column temperature was 40 °C, the flow rate was 1 mL/min, the injection volume was 10 μL, mobile phase A was sodium acetate-acetonitrile solution, mobile phase B was 80% acetonitrile aqueous solution and the mobile phase was gradient-eluted. N-leucine was used as the internal standard. The accumulation of essential and nonessential amino acids was calculated by reference.

2.6. Data Analysis

A 1-way analysis of variance and Duncan's method were used for multiple comparisons to analyze the difference in free amino acid concentration in the pericarp of *Z. planispinum* with different planting combinations. The data of free amino acid concentration were standardized and then analyzed by principal component analysis to evaluate the quality of FAAs in the pericarp of *Z. planispinum*. Redundancy analysis was used to reveal the influence mechanism of soil properties on pericarp quality. The data are presented as mean ± standard deviation. Microsoft Excel 2013 (version 2013, Microsoft, Redmond, WA, USA), SPSS 20.0 (version 20.0, IBM SPSS, Armonk, NY, USA) and Origin 8.6 (version 8.6, OriginLab Corporation, Northampton, MA, USA) software were used to complete data sorting, analysis and mapping.

3. Results

3.1. Amino Acid Concentrations in the Pericarp of Z. planispinum in Different Planting Combinations

As shown in Table 3, 17 kinds of FAAs were detected in the pericarp of *Z. planispinum* from 5 planting combinations. Among them, arginine, serine, proline, alanine, tyrosine and cystine had no significant differences among the five plantations, while the concentration of the remaining 11 FAAs had significant differences in different degrees. The results showed that the combination planting had a great influence on the free amino acid concentration of the peel of *Z. planispinum*, especially the essential amino acids. Among the 11 amino acids with significant differences mentioned above, the FAAs in the pericarp of *Z. planispinum* were lowest at Trt 1 and highest at Trt 2 (except phenylalanine).

Table 3. Amino acid concentrations in the pericarp of *Z. planispinum* in different planting combinations.

Amino Acid		Trt 1	Trt 2	Trt 3	Trt 4	Trt 5
Essential amino acids (mg/kg)	Valine	376.51 ± 10.86 b	500.15 ± 87.33 a	420.97 ± 10.85 ab	438.20 ± 8.85 ab	409.29 ± 22.74 ab
	Threonine	282.72 ± 7.50 b	368.39 ± 58.89 a	314.29 ± 6.22 ab	337.44 ± 16.76 ab	304.01 ± 22.22 ab
	Phenylalanine	8.46 ± 1.40 c	33.19 ± 2.62 b	23.96 ± 8.93 bc	20.92 ± 8.22 bc	55.35 ± 11.82 a
	Methionine	33.71 ± 0.04 b	46.81 ± 8.85 a	41.84 ± 3.45 ab	34.09 ± 4.92 ab	41.17 ± 3.22 ab
	Leucine	471.19 ± 10.18 b	608.99 ± 98.29 a	514.84 ± 1.06 ab	555.49 ± 24.27 ab	507.19 ± 25.65 ab
	Lysine	347.38 ± 0.42 b	470.78 ± 90.79 a	361.81 ± 47.02 ab	384.33 ± 16.50 ab	386.29 ± 2.37 ab
	Isoleucine	43.18 ± 6.89 b	458.46 ± 90.71 a	375.71 ± 12.23 a	370.20 ± 25.94 a	380.95 ± 12.11 a
	Total	1563.14 ± 36.47 b	2486.75 ± 437.47 a	2053.41 ± 68.29 ab	2140.67 ± 27.30 a	2084.22 ± 70.05 a
Nonessential amino acids (mg/kg)	Histidine	175.01 ± 1.83 b	224.90 ± 36.95 a	189.15 ± 11.31 ab	205.69 ± 7.85 ab	187.80 ± 10.38 ab
	Arginine	367.86 ± 21.83 a	496.41 ± 125.63 a	439.46 ± 43.59 a	420.37 ± 6.47 a	396.40 ± 12.56 a
	Serine	325.79 ± 12.94 a	447.59 ± 98.81 a	380.91 ± 22.85 a	406.63 ± 16.93 a	366.69 ± 25.24 a
	Proline	427.79 ± 36.36 a	608.59 ± 128.90 a	458.82 ± 88.71 a	601.17 ± 21.00 a	533.05 ± 87.49 a
	Glycine	381.66 ± 17.76 b	491.17 ± 83.21 a	422.02 ± 14.86 ab	437.38 ± 9.76 ab	416.49 ± 0.92 ab
	Glutamate	738.39 ± 30.78 b	1012.02 ± 203.02 a	863.35 ± 9.32 ab	899.38 ± 18.59 ab	846.80 ± 22.80 ab
	Aspartate	477.48 ± 48.72 b	744.83 ± 181.96 a	646.66 ± 126.96 ab	597.16 ± 8.89 ab	578.21 ± 1.11 ab
	Alanine	363.17 ± 9.57 a	454.11 ± 69.92 a	386.75 ± 0.01 a	406.52 ± 20.65 a	377.00 ± 29.29 a
	Tyrosine	232.20 ± 8.64 a	270.88 ± 19.56 a	245.27 ± 11.75 a	273.96 ± 10.92 a	221.14 ± 37.96 a
	Cystine	52.02 ± 4.85 a	48.37 ± 2.22 a	39.48 ± 8.34 a	54.93 ± 12.49 a	37.41 ± 4.61 a
	Total	2998.50 ± 87.20 b	4077.54 ± 783.16 a	3443.26 ± 236.39 ab	3677.10 ± 59.48 ab	3376.77 ± 209.43 ab
Total free amino acids (mg/kg)		5104.49 ± 147.33 b	7285.59 ± 1383.21 a	6125.28 ± 359.58 ab	6443.82 ± 88.16 ab	6045.19 ± 302.42 ab
EAAs/TFAAs (%)		30.62	34.13	33.52	33.22	34.48
EAAs/NEAAs (%)		44.14	51.82	50.43	49.75	52.62

Trts 1–5, five plantations, representing the research objectives of this article. EAAs/TFAAs, the ratio of essential amino acids to total amino acids; EAAs/NEAAs, the ratio of essential and nonessential amino acids. Means followed by the same lowercase letter are not significantly different ($p > 0.05$) among root types as determined by the least significance difference test. Data are presented as mean ± standard deviation.

The concentration of essential amino acids (EAAs), nonessential amino acids (NAAs) and total free amino acids (TAAs) in the pericarp of *Z. planispinum* in different planting combinations were 1563.12–2486.75, 2998.50–4077.54 and 5104–7285.59 mg/kg, respectively, with Trt 2 being the highest, significantly higher than Trt 1, in which the lowest amino acid concentration was found. The ideal protein standard proposed by the Food and Agriculture Organization of the United Nations/World Health Organization (FAO/WHO) in 1973 is that the essential amino acid divided by the total amino acid (EAAs/TFAAs) is 40.00%, and the essential amino acid divided by the nonessential amino acid (EAAs/NEAAs) is higher than 60.00%. The EAAs/TFAAs of *Z. planispinum* in each plantation were 30.62%–34.48%, and the EAAs/NEAAs were 44.14%–52.62%, of which *Z. planispinum* + *S. tonkinensis* and *Z. planispinum* monoculture forest were closest to this standard.

3.2. Accumulation of Flavoring Amino Acids in Pericarp of Z. planispinum in Different Planting Combinations

According to Table 4, in general, the concentration of sweet amino acids (SAAs) (1956.13–2594.73 mg/kg) was the highest, and the concentration of aromatic amino acids (AAAs) (292.68–352.43 mg/kg) was the lowest. The concentration of bitter amino acids (BAAs) (1292.44–2110.81 mg/kg) was similar to that of delicious amino acids (DAAs) (1563.25–2227.62 mg/kg). The concentration of various flavoring amino acids of *Z. planispinum* in all planting combinations was SAAs > DAAs > BAAs > AAAs. The concentration of

four kinds of flavored amino acids in Trt 2 was the highest, and that in Trt 1 was the lowest, indicating that planting with *S. tonkinensis* is the most beneficial to the accumulation of amino acids and the formation of the special flavor in *Z. planispinum*.

Table 4. Accumulation of flavoring amino acids in the pericarp of *Z. planispinum* in different planting combinations.

Amino Acid	Trt 1	Trt 2	Trt 3	Trt 4	Trt 5
Bitter amino acid (mg/kg)	1292.44 ± 49.82 b	2110.81 ± 410.80 a	1792.82 ± 62.15 a	1818.35 ± 4.21 a	1734.99 ± 69.83 ab
Sweet amino acid (mg/kg)	1956.13 ± 13.25 b	2594.73 ± 476.69 a	2151.94 ± 101.79 ab	2394.82 ± 50.96 ab	2185.03 ± 175.55 ab
Delicious amino acid (mg/kg)	1563.25 ± 79.08 b	2227.62 ± 475.77 a	1871.82 ± 183.31 ab	1880.86 ± 26.21 ab	1811.29 ± 26.28 ab
Aromatic amino acid (mg/kg)	292.68 ± 5.19 b	352.43 ± 19.97 a	308.71 ± 12.34 ab	349.79 ± 15.20 a	313.89 ± 30.76 ab

Trts 1–5, five plantations, representing the research objectives of this article. Means followed by the same lowercase letter are not significantly different ($p > 0.05$) among root types as determined by the least significance difference test. Data are presented as mean ± standard deviation.

Due to the different taste perception thresholds of different amino acids, a higher concentration of amino acids does not necessarily correlate to a greater contribution to food flavor. Therefore, the taste activity value (TAV), calculated as the ratio of concentration to its taste threshold, was used to further analyze the impact of flavoring amino acids on the pericarp flavor of *Z. planispinum* [26]. The TAVs of each flavoring amino acid in the five planting combinations are shown in Table 5. When the TAV ≥ 1, it indicates that the amino acid contributes to the flavor effect. The TAVs of arginine (3.68–4.96) in BAAs, glutamate (14.77–20.24) and aspartate (15.92–24.83) in DAAs and cystine (1.87–2.75) in AAAs were all greater than 1. In addition, the TAVs of histidine were both greater than 1 at Trt 2 (1.03) and Trt 4 (1.12). Therefore, aspartate, glutamate, arginine, cystine and histidine played an important role in the formation of the unique flavor of *Z. planispinum*. In addition, the combination of *Z. planispinum* with *S. tonkinensis* (Trt 2) or *L. japonica* (Trt 4) was more conducive to the accumulation of amino acids and the formation of the special flavor. The delicious amino acids among the four flavoring amino acids had the highest contribution rate to the flavor of *Z. planispinum*, which was more consistent with the unique freshening flavor of *Z. planispinum*.

Table 5. Taste activity values of flavoring amino acids in the pericarp of *Z. planispinum* in different planting combinations.

Amino Acid		Taste Threshold [27] (mg/g)	Taste Activity Value				
			Trt 1	Trt 2	Trt 3	Trt 4	Trt 5
Bitter amino acid	Valine	1.50	0.25	0.33	0.28	0.29	0.27
	Leucine	3.80	0.12	0.16	0.14	0.15	0.13
	Isoleucine	0.90	0.05	0.51	0.42	0.41	0.42
	Methionine	0.30	0.11	0.16	0.14	0.11	0.14
	Arginine	0.10	3.68	4.96	4.39	4.20	3.96
Sweet amino acid	Glycine	1.10	0.35	0.45	0.38	0.40	0.38
	Alanine	0.60	0.61	0.76	0.64	0.68	0.63
	Serine	1.50	0.22	0.30	0.25	0.27	0.24
	Threonine	2.60	0.11	0.14	0.12	0.13	0.12
	Proline	3.00	0.14	0.20	0.15	0.20	0.18
	Histidine	0.20	0.88	1.12	0.95	1.03	0.94

Table 5. *Cont.*

Amino Acid		Taste Threshold [27] (mg/g)	Taste Activity Value				
			Trt 1	Trt 2	Trt 3	Trt 4	Trt 5
Delicate amino acid	Lysine	0.50	0.69	0.94	0.72	0.77	0.77
	Glutamate	0.05	14.77	20.24	17.27	17.99	16.94
	Aspartate	0.03	15.92	24.83	21.56	19.91	19.27
Aromatic amino acid	Phenylalanine	1.50	0.01	0.02	0.02	0.01	0.04
	Tyrosine	2.60	0.09	0.10	0.09	0.11	0.09
	Cystine	0.02	2.60	2.42	1.97	2.75	1.87

3.3. Principal Component Analysis of Free Amino Acids in Pericarp of *Z. planispinum*

The free amino acids in the pericarp of *Z. planispinum* were analyzed by principal component analysis. It can be seen from Table 6 that the cumulative variance contribution rate of two principal component eigenvalues greater than 1 was 89.63%. Therefore, selecting these two main components as effective components for data analysis can reflect most of the amino acid information and can characterize the quality of amino acids. The variance contribution rate of the first principal component was 72.56%, which had the greatest impact on the accumulation of amino acid concentration in the pericarp of *Z. planispinum*. Among them, except cystine, methionine and phenylalanine, the load values of amino acids were higher and positively correlated. The variance contribution rate of the second principal component was 17.08%, which indicated that it had a certain impact on the peel of *Z. planispinum*, but this effect was small. Cystine had a greater negative impact, while phenylalanine had a greater positive impact.

Table 6. Principal component load matrix and coefficient.

Factors	Principal Component Load Matrix	
	PC1	PC2
Aspartate	**0.866**	0.378
Glutamate	**0.971**	0.212
Serine	**0.988**	0.102
Histidine	**0.993**	0.031
Glycine	**0.951**	0.174
Threonine	**0.989**	−0.021
Arginine	**0.916**	0.249
Alanine	**0.986**	−0.034
Tyrosine	**0.811**	−0.458
Cystine	0.157	**−0.915**
Valine	**0.989**	0.123
Methionine	0.563	0.673
Phenylalanine	0.111	**0.881**
Isoleucine	**0.702**	0.513
Leucine	**0.993**	0.019
Lysine	**0.901**	0.231
Proline	**0.838**	0.055
Eigenvalue	12.639	2.599
Variance contribution rate/%	72.557	17.076
Cumulative variance contribution rate/%	72.557	89.633

The bold font is the relatively large influence factor of each principal component load factor.

The variance contribution rate (W_i) and factor score (F_i) of the two principal component factors extracted were further weighted. Finally, the comprehensive score (CS) and ranking of *Z. planispinum* plantation of five planting combinations were obtained, and the CS reflected the comprehensive quality level of FAAs in the pericarp of *Z. planispinum* under

each combination. The comprehensive score calculation was combined with the weighted method using the following formula:

$$CS = \sum W_i \times F_i$$

where W_i is the contribution rate of each principal component, and F_i is the principal component score of each plantation type. By weighting the variance contribution rate (W_i) and factor score (F_i) of each principal component factor, the CSs of different plantation types are obtained.

It can be seen from Table 7 that the CS was ranked from high to low as Trt 2 > Trt 4 > Trt 3 > Trt 5 > Trt 1. Among them, after planting with *S. tonkinensis* (Trt 2) or *L. japonica* (Trt 4), the CS of fruit pericarp quality of *Z. planispinum* was positive, indicating that the FAAs in the pericarp of *Z. planispinum* in these two treatments were higher than the average level.

Table 7. Factor score and comprehensive evaluation of *Z. planispinum* in different planting combinations.

Plantation Types	Factor Score		Comprehensive Score	Ranking
	PC1	PC2		
Trt 1	−3.78	−2.71	−3.20	5
Trt 2	4.46	1.69	3.52	1
Trt 3	−0.52	0.56	−0.28	3
Trt 4	0.94	−1.23	0.47	2
Trt 5	−1.10	1.70	−0.51	4

Trts 1–5, five plantations, representing the research objectives of this article.

3.4. Effects of Soil Properties on Amino Acid Concentration of Pericarp

Soil factors were used as explanatory variables (red arrows), and amino acid concentrations were used as response variables (blue arrows) to carry out redundancy analysis to reveal the interaction rules between them. According to Figure 2, the cumulative interpretation rates of the first and second ranking axes were 83.60% and 10.20%, respectively, with the cumulative contribution rate as high as 93.80%. Among them, the effect of soil factors on the concentration of FAAs in the pericarp of *Z. planispinum* was available K > available P > MBN > available Ca > MBP, reaching a significant level (Table 8). In general, the contribution rate of available nutrients was higher than that of total nutrients, while the contribution rate of stoichiometric ratio and soil water content was lower.

Effects of available K, total P and available P on amino acids were all negative (except cystine), reflecting the inhibition of K and P on the accumulation of amino acids (Figure 2). Total Ca had a strong negative effect on cystine and a positive effect on phenylalanine, but it had little effect on other amino acids, while available Ca had a significant enhancement effect on amino acids, indicating that available forms of Ca had different effects on amino acids and available Ca was beneficial to the accumulation of amino acids. Soil water content, SOC, total N, available N and element stoichiometry had a great influence on cystine and tyrosine in aromatic amino acids, and the influence of the stoichiometric ratio on amino acids was mostly positive. The effect of microbial biomass on amino acids was one of enhancement.

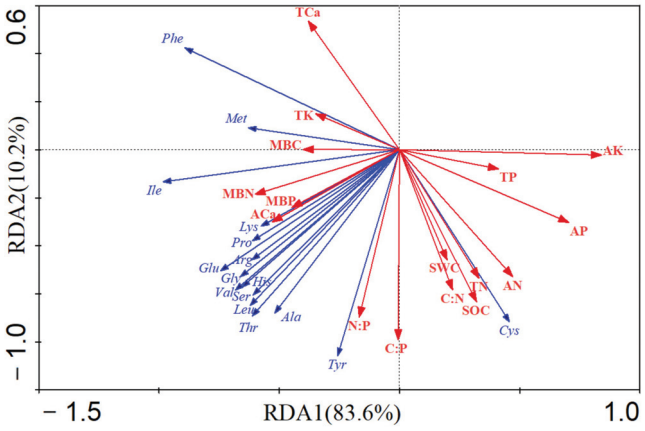

Figure 2. Redundancy analysis of free amino acids and soil. SWC, soil water content; SOC, soil organic carbon; TN, total nitrogen; TP, total phosphorus; TK, total potassium; TCa, total calcium; AN, available nitrogen; AP, available phosphorus; AK, available potassium; ACa, available calcium; MBC, microbial biomass carbon; MBN, microbial biomass nitrogen; MBP, microbial biomass phosphorus; Val, valine; Thr, threonine; Phe, phenylalanine; Met, methionine; Leu, leucine; Lys, lysine; Iso, isoleucine; His, histidine; Arg, arginine; Ser, serine; Pro, proline; Gly, glycine; Glu, glutamate; Asp, aspartate; Ala, alanine; Tyr, tyrosine; Cys, cystine.

Table 8. Importance sequencing and significance test of soil factors.

Soil Factors	Contribution/%	Pseudo-*F*	*p*
Available potassium	0.646	23.763	0.002
Available phosphorus	0.472	11.626	0.002
Microbial biomass nitrogen	0.365	7.458	0.012
Available calcium	0.286	5.217	0.018
Microbial biomass phosphorus	0.235	3.989	0.038
Available nitrogen	0.218	3.633	0.052
Microbial biomass carbon	0.191	3.062	0.076
Total calcium	0.171	2.691	0.066
Total phosphorus	0.156	2.402	0.15
Total potassium	0.134	2.02	0.174
Soil organic carbon	0.131	1.955	0.146
Total nitrogen	0.125	1.854	0.15
Soil N:P ratio	0.087	1.233	0.276
Soil C:N ratio	0.078	1.106	0.354
Soil water content	0.072	1.012	0.354
Soil C:P ratio	0.071	0.995	0.364

4. Discussion

4.1. Effects of Planting Combinations on Amino Acids in the Pericarp of Z. planispinum

Previous studies have shown that plant varieties [28], altitude [29], environmental stress [30], water and fertilizer coupling treatment [31], season [32], etc. affect the concentration and accumulation of FAAs in the pericarp. In this study, it was found that the planting combination had a greater impact on the concentration of FAAs in the pericarp of *Z. planispinum*, especially on essential amino acids. This is because the combination of planting can effectively reduce the leaching and loss of water and fertilizer in the soil. It can also keep the soil loose, and its thermal insulation effect creates a good environment for the survival of microorganisms. The litter and root exudates produced by combined plants change the soil's micro-ecological environment and soil nutrient status [33,34]. Secondly, the combination of plant species, planting density and other factors can cause spatial

niche differences; directly affect the air temperature and humidity, CO_2 concentration, wind speed, light intensity and light quality distribution; and form different field microclimates [35]. Different planting combinations change the soil water status, fertilizer status and microenvironment; affect the acquisition and utilization of plant resources; lead to changes in the stress factors of *Z. planispinum*; and ultimately affect its C and N metabolism balance and amino acid accumulation. Cannabinoid has a significant contribution to the spicy taste of *Z. planispinum*, and valine and leucine are considered to be precursors for the synthesis of the nitrogen-containing portion of cannabinoid [36]. In this study, the concentration of valine and leucine in the pericarp of *Z. planispinum* with *S. tonkinensis* (Trt 2) was significantly the highest, followed by *L. japonica* (Trt 4). From the perspective of TAV value, aspartate, glutamate, arginine, cystine and histidine had a significant impact on the formation of the flavor. In summary, the combination of *Z. planispinum* with *S. tonkinensis* (Trt 2) or *L. japonica* (Trt 4) was more conducive to the accumulation of amino acids and the formation of the special flavor.

Principal component analysis showed that the amino acid quality of the pericarp of *Z. planispinum* was the best and was closest to the standard of ideal protein after planting with *S. tonkinensis* (Trt 2). However, soil nutrient concentration under this mode was generally low. This is similar to the conclusion of Lin et al. [37], who found that adverse environmental factors can improve the quality of *Ganoderma lucidum* to some extent. It is speculated that when faced with environmental stress, *Z. planispinum* can promote the accumulation of FAAs and the synthesis of secondary metabolites by reducing yield and improving nutrient reabsorption, finally improving the quality of the pericarp. In addition, when plants are stressed by adverse environmental factors, they can inhibit the growth of other plants by releasing secondary metabolites to the external environment to improve their competitiveness [38], which may limit the N fixation effect of *S. tonkinensis*, which is not conducive to the improvement in soil quality. The concentration of FAAs in the pericarp of *Z. planispinum* after planting with *L. japonica* (Trt 4) was also relatively rich, ranking second in the comprehensive score. In addition, previous research showed that soil quality under this mode was the best [23]. This is because *L. japonica* produces a rich decomposable litter, which provides rich materials for the C and N metabolism of *Z. planispinum*, and promotes the formation of *Z. planispinum* pericarp quality. *Z. planispinum* has a large root system and strong ability to sprout, which improves soil conditions in the rhizosphere, thus enhancing the ability of its root system to absorb nutrients and water in the lower layer, increasing the supply of the N metabolism substrate in the upper part, which is conducive to the improvement in N-metabolism-related enzyme activities, such as glutamine synthetase activity, thus affecting the accumulation of FAAs [39]. It can be seen from Table 2 that the soil water content of *Z. planispinum* + *L. japonica* plantation was significantly lower than that of *Z. planispinum* + *P. salicina*/*S. tonkinensis* (Trt 1 or Trt 2). It is speculated that under the condition of relative water deficit, FAAs are synthesized and accumulated in large quantities to improve the osmoregulation ability of *Z. planispinum*. In addition, FAAs also protect plants from water stress by participating in redox balance and energy metabolism, as well as regulating mitochondrial function as signal molecules [40,41]. The pericarp quality of *Z. planispinum* after planting with *P. salicina* (Trt 1) was the lowest in this study. This is due to the fact that *P. salicina* is a tall tree, which has formed a strong nutrient competition with *Z. planispinum*, limiting the accumulation of amino acids in *Z. planispinum* [42]. Moreover, *Z. planispinum* is a photophilic plant. After being blocked by *P. salicina*, the photosynthesis of *Z. planispinum* is inhibited, resulting in a lower C assimilation rate of leaves, which in turn leads to a lower amino acid assimilation rate, further leading to the reduction of FAAs [43,44]. In the future, based on this research, we need to pay more attention to secondary metabolites and their formation mechanism that forms the aroma and hemp of *Z. planispinum* to lay a theoretical basis for comprehensive quality control.

4.2. Relationship between Soil Nutrients and Pericarp Quality

Soil nutrient stress affects the secondary metabolism process of plants and changes the accumulation of C-based secondary metabolites in plants, but different nutrient elements have different effects on the secondary metabolism process of plants [45]. This study showed that soil-available K contributed the most to the accumulation of FAAs in fruit pericarp and showed a negative effect. This is because K can significantly affect N metabolism, especially amino acid and protein metabolism. K deficiency leads to an increase in protease and peptidase activity and promotes protein degradation, which leads to the accumulation of low-molecular-weight substances, such as FAAs, and confirms that the accumulation of metabolites is the result of environmental adaptation [46,47]. In this study, soil-available P had a significant negative impact on the concentration of FAAs in the pericarp of *Z. planispinum*, and the previous study showed that the soil of five planting combinations had phosphorus saturation [22]. This may be due to excessive soil available phosphorus leading to the consumption of beneficial microorganisms in plants and increasing the abundance of pathogenic microorganisms, which ultimately affects the growth of *Z. planispinum* [48]. The number of beneficial microorganisms in soil can be increased by adding organic fertilizer or soil conditioner to promote the coordinated development of soil microbial flora of *Z. planispinum* [49]. In this study, the contribution rate of soil-available Ca to FAAs was large and had a promoting effect. It indicated that Ca could improve the quality and stress resistance of crops, which is consistent with the research conducted by Li et al. [50]. The reason for this is that Ca is one of the essential nutrients for plant growth and development, which can promote the transport and transformation of plant carbohydrates and the absorption of mineral elements [51]. Ca deficiency can cause the vacuolar membrane of mesophyll cells to break, destroy the lamellar structure of thylakoids and inhibit the photosynthetic capacity of plants. Moreover, Ca, as the second messenger in the process of cell signal transduction, is involved in the regulation of the synthesis and metabolism of amino acids and proteins [52,53]. It can accelerate the absorption and metabolism of N by plants, as well as promote the growth and development of plants and the formation of fruit quality [54]. This study found that soil microbial biomass nitrogen and microbial biomass phosphorus had a significant positive effect on the accumulation of free amino acid concentration in the pericarp of *Z. planispinum*. This is because soil microorganisms can secrete a variety of enzymes to decompose animal and plant residues and other organic substances, as well as accelerate the transformation and transportation of carbon. Some metabolites can promote the decomposition of minerals to help plants absorb and use them [55]. This study also found that the contribution rate of the soil stoichiometric ratio to the concentration of amino acids in the pericarp was low, which was related to the extremely strong internal stability of the soil-nutrient-element stoichiometric ratio of five plantations [22]. In the future, it is worth further studying the influence of different element components on amino acid accumulation in the pericarp of *Z. planispinum*, especially the determination of the threshold value of the influence direction. Based on the mechanism of the soil microbial community improving soil nutrient status and plant nutrient absorption, as well as the cascade relationship of the soil microorganism and the nutrient element, fruit quality is further constructed to provide a scientific basis to formulate a soil-nutrient-optimization plan. It is also necessary to further study the effects of total nutrients and available nutrients on the FAAs in the pericarp and explore the specific reasons. The mechanisms of soil microbial community-improving plant nutrition should also be deeply explored. Furthermore, the mechanisms of planting combinations improving mineral nutrition should be fully and comprehensively understood, and targeted soil-nutrient-optimization programs for different planting combinations should be formulated.

5. Conclusions

(1) Planting with *S. tonkinensis* or *L. japonica* can significantly increase the concentration of FAAs in the pericarp of *Z. planispinum*, which is conducive to the formation of pericarp quality. Based on the results of soil quality analysis in the early research and

the amino acids in the pericarp, the optimal planting combination was found to be *Z. planispinum* + *L. japonica*;

(2) As a characteristic element of karst, available Ca had a high contribution rate to the accumulation of FAAs in the pericarp, which had a positive impact;

(3) The effect of available nutrients on FAAs in the pericarp was greater than that of total nutrients. Soil management in plantations should involve paying more attention to the concentration and proportion of available nutrients.

Author Contributions: Conceptualization, Y.Y.; formal analysis, Y.L. and Y.Y.; software, Y.L. and Y.S.; investigation, Y.L. and Y.S.; writing—original draft preparation, Y.L.; writing—review and editing, Y.Y. and C.W. All authors have read and agreed to the published version of the manuscript.

Funding: This research was funded by the Guizhou Province Science and Technology Support Plan Project (Qian-ke-he Zhicheng [2022] Yiban 103) and the Guizhou Province Science and Technology 457 Support Plan Project (Qian-ke-he Zhicheng (2020) 1Y120).

Institutional Review Board Statement: Not applicable.

Informed Consent Statement: Not applicable.

Data Availability Statement: Not applicable.

Conflicts of Interest: The authors declare no conflict of interest.

References

1. Dinkeloo, K.; Boyd, S.; Pilot, G. Update on amino acid transporter functions and on possible amino acid sensing mechanisms in plants. *Semin. Cell Dev. Biol.* **2018**, *74*, 105–113. [CrossRef] [PubMed]
2. Wu, G.Y. Amino acids: Metabolism, functions, and nutrition. *Amino Acids* **2009**, *37*, 1–17. [CrossRef]
3. Mandrioli, R.; Mercolini, L.; Raggi, M.A. Recent trends in the analysis of amino acids in fruits and derived foodstuffs. *Anal. Bioanal. Chem.* **2013**, *405*, 7941–7956. [CrossRef] [PubMed]
4. Ardo, Y. Flavour formation by amino acid catabolism. *Biotechnol. Adv.* **2006**, *24*, 238–242. [CrossRef] [PubMed]
5. Li, Z.Q.; Hong, T.N.; Shen, G.H.; Gu, Y.T.; Guo, Y.Z.; Han, J. Amino Acid Profiles and Nutritional Evaluation of Fresh Sweet–Waxy Corn from Three Different Regions of China. *Nutrients* **2022**, *14*, 3887. [CrossRef] [PubMed]
6. Jafarikouhini, N.; Kazemeini, S.A.; Sinclair, T.R. Sweet corn nitrogen accumulation, leaf photosynthesis rate, and radiation use efficiency under variable nitrogen fertility and irrigation. *Field Crops Res.* **2020**, *257*, 107913. [CrossRef]
7. Sardans, J.; Penuelas, J. Tree growth changes with climate and forest type are associated with relative allocation of nutrients, especially phosphorus, to leaves and wood. *Glob. Ecol. Biogeogr.* **2013**, *22*, 494–507. [CrossRef]
8. The, S.V.; Snyder, R.; Tegeder, M. Targeting Nitrogen Metabolism and Transport Processes to Improve Plant Nitrogen Use Efficiency. *Front. Plant Sci.* **2021**, *11*, 628366. [CrossRef]
9. Aires, A.; Rosa, E.; Carvalho, R. Effect of nitrogen and sulfur fertilization on glucosinolates in the leaves and roots of broccoli sprouts (*Brassica oleracea* var. *italica*). *J. Sci. Food Agric.* **2006**, *86*, 1512–1516. [CrossRef]
10. Krapp, A. Plant nitrogen assimilation and its regulation: A complex puzzle with missing pieces. *Curr. Opin. Plant Biol.* **2015**, *25*, 115–122. [CrossRef]
11. Vance, C.P.; Uhde-Stone, C.; Allan, D.L. Phosphorus acquisition and use: Critical adaptations by plants for securing a nonrenewable resource. *New Phytol.* **2003**, *157*, 423–447. [CrossRef] [PubMed]
12. Becquer, A.; Trap, J.; Irshad, U.; Ali, M.A.; Claude, P. From soil to plant, the journey of P through trophic relationships and ectomycorrhizal association. *Front. Plant Sci* **2014**, *5*, 548. [CrossRef] [PubMed]
13. Thor, K. Calcium-Nutrient and Messenger. *Front. Plant Sci.* **2019**, *10*, 440. [CrossRef] [PubMed]
14. Ciesla, A.; Mitula, F.; Misztal, L.; Fedorowicz-Stronska, O.; Janicka, S.; Tajdel-Zielinska, M.; Marczak, M.; Janicki, M.; Ludwikow, A.; Sadowski, J. A Role for Barley Calcium-Dependent Protein Kinase CPK2a in the Response to Drought. *Front. Plant Sci.* **2016**, *7*, 1550. [CrossRef] [PubMed]
15. Kuzyakov, Y.; Xu, X.L. Competition between roots and microorganisms for nitrogen: Mechanisms and ecological relevance. *New Phytol.* **2013**, *198*, 656–669. [CrossRef] [PubMed]
16. Anderson, T.R.; Boersma, M.; Raubenheimer, D. Stoichiometry: Linking elements to biochemicals. *Ecology* **2004**, *85*, 1193–1202. [CrossRef]
17. Rivas-Ubach, A.; Sardans, J.; Pérez-Trujillo, M.; Estiarte, M.; Penuelas, J. Strong relationship between elemental stoichiometry and metabolome in plants. *Proc. Natl. Acad. Sci. USA* **2012**, *109*, 4181–4186. [CrossRef]
18. Tu, Y.L. The study of nutritive components and trace elements of flash of *Zhnthoxylum planispinum* var. dingtanensis. *J. Guizhou Norm. Univ. (Nat. Sci.)* **2000**, *18*, 31–36. (In Chinese)

19. Duchene, O.; Vian, J.F.; Celette, F. Intercropping with legume for agroecological cropping systems: Complementarity and facilitation processes and the importance of soil microorganisms. A review. *Agric. Ecosyst. Environ.* **2017**, *240*, 148–161. [CrossRef]
20. Dong, Y.; Tang, L.; Zheng, Y.; Wei, L.F. Effects of N application on rhizosphere microflora and fusarium wilt occurrence of intercropped faba bean. *Acta Ecol. Sin.* **2010**, *30*, 1797–1805. (In Chinese)
21. Yang, Z.X.; Tang, L.; Zheng, Y.; Dong, K.; Dong, Y. Effects of different wheat cultivars intercropped with faba bean on faba bean Fusarium wilt, root exudates and rhizosphere microbial community functional diversity. *J. Plant Nutr. Fertil.* **2014**, *20*, 570–579. (In Chinese) [CrossRef]
22. Li, Y.T.; Yu, Y.H.; Song, Y.P. Stoichiometry of Soil, Microorganisms, and Extracellular Enzymes of *Zanthoxylum planispinum* var. *dintanensis* Plantations for Different Allocations. *Agronomy* **2022**, *12*, 1709. [CrossRef]
23. Li, Y.T.; Yu, Y.H.; Song, Y.P. Soil properties of different planting combinations of *Zanthoxylum planispinum* var. *dintanensis* plantations and their driving force on stoichiometry. *Agronomy* **2022**, *12*, 2562. [CrossRef]
24. do Nascimento, T.M.T.; Mansano, C.F.M.; Peres, H.; Rodrigues, F.H.F.; Khan, K.U.; Romaneli, R.S.; Sakomura, N.K.; Fernandes, J.B.K. Determination of the optimum dietary essential amino acid profile for growing phase of Nile tilapia by deletion method. *Aquaculture* **2020**, *523*, 735204. [CrossRef]
25. Lu, P.Y.; Wang, J.; Wu, S.G.; Gao, J.; Dong, Y.; Zhang, H.J.; Qi, G.H. Standardized ileal digestible amino acid and metabolizable energy content of wheat from different origins and the effect of exogenous xylanase on their determination in broilers. *Poult. Sci.* **2020**, *99*, 992–1000. [CrossRef]
26. Chen, D.; Zhang, M. Non-volatile taste active compounds in the meat of Chinese mitten crab (*Eriocheir sinensis*). *Food Chem.* **2007**, *104*, 1200–1205. [CrossRef]
27. Liu, Y.; Qiu, C.P. Calculated Taste Activity Values and Umami Equivalences Explain Why Dried Sha-chong (*Sipunculus nudus*) Is a Valuable Condiment. *J. Aquat. Food Prod. Technol.* **2016**, *25*, 177–184. [CrossRef]
28. Turkiewicz, I.P.; Wojdyło, A.; Tkacz, K.; Nowicka, P. Carotenoids, chlorophylls, vitamin E and amino acid profile in fruits of nineteen Chaenomeles cultivars. *J. Food Compos. Anal.* **2020**, *93*, 103608. [CrossRef]
29. Guevara-Terán, M.; Padilla-Arias, K.; Beltrán-Novoa, A.; Gonzalez-Paramas, A.M.; Giampieri, F.; Battino, M.; Vasquez-Castillo, W.; Fernandez-Soto, P.; Tejera, E.; Alvarez-Suarez, J.M. Influence of Altitudes and Development Stages on the Chemical Composition, Antioxidant, and Antimicrobial Capacity of the Wild Andean Blueberry (*Vaccinium floribundum* Kunth). *Molecules* **2022**, *27*, 7525. [CrossRef]
30. Ozturk, M.; Unal, B.T.; Garcia-Caparros, P.; Khursheed, A.; Gul, A.; Hasanuzzaman, M. Osmoregulation and its actions during the drought stress in plants. *Physiol. Plant.* **2021**, *172*, 1321–1335. [CrossRef]
31. Schreiner, R.P.; Scagel, C.F.; Lee, J. N, P, and K supply to Pinot noir grapevines: Impact on berry phenolics and free amino acids. *Am. J. Enol. Vitic.* **2014**, *65*, 43–49. [CrossRef]
32. Wang, D.C.; Fu, Y.R.; Yu, Y.H.; Chen, M.; Wei, C.S. Amino acid accumulation characteristics in pericarp of germinating branches of *Zanthoxylum planispinum* var. *dintanensis* in different seasons. *J. South. Agric.* **2022**, *53*, 1963–1972. (In Chinese) [CrossRef]
33. Gargallo–Garriga, A.; Preece, C.; Sardans, J.; Oravec, M.; Urban, O.; Penuelas, J. Root exudate metabolomes change under drought and show limited capacity for recovery. *Sci. Rep.* **2018**, *8*, 12696. [CrossRef] [PubMed]
34. Ma, T.; Zhu, S.S.; Wang, Z.H.; Chen, D.M.; Dai, G.H.; Feng, B.W.; Su, X.Y.; Hu, H.F.; Li, K.H.; Han, W.X.; et al. Divergent accumulation of microbial necromass and plant lignin components in grassland soils. *Nat. Commun.* **2018**, *9*, 3480. [CrossRef] [PubMed]
35. Du, Q.; Chen, P.; Liu, S.S.; Luo, K.; Zheng, B.C.; Yang, H.; He, S.; Yang, W.Y.; Yong, T.W. Effect of field microclimate on the difference of soybean flower morphology under maize-soybean relay strip intercropping system. *Sci. Agric. Sin.* **2021**, *54*, 2746–2758. (In Chinese) [CrossRef]
36. Greger, H. Alkamides: A critical reconsideration of a multifunctional class of unsaturated fatty acid amides. *Phytochem. Rev.* **2016**, *15*, 729–770. [CrossRef]
37. Lin, Z.N.; Lu, Z.; Lin, Y.; Li, Y.C.; Liu, M.X. Growth and Quality of *Ganoderma lucidum* at Tea Plantations under Relay Cropping. *Fujian J. Agric. Sci.* **2020**, *35*, 532–537. (In Chinese) [CrossRef]
38. Jiang, D.Q.; Wang, H.Y.; Tang, C.Z.; Jiang, J.Y.; Du, Y.X.; Zhang, Y.; Wang, S.; Guo, L.P. Influence and mechanism of stress combination on medicinal plants secondary metabolism. *China J. Chin. Mater. Med.* **2020**, *45*, 2009–2016. (In Chinese)
39. Reggiani, R.; Nebuloni, M.; Mattana, M.; Brambilla, I. Anaerobic accumulation of amino acids in rice roots: Role of the glutamine synthetase/glutamate synthase cycle. *Amino Acids* **2000**, *18*, 207–217. [CrossRef]
40. Slama, I.; Abdelly, C.; Bouchereau, A.; Flowers, T.; Savoure, A. Diversity, distribution and roles of osmoprotective compounds accumulated in halophytes under abiotic stress. *Ann. Bot.* **2015**, *115*, 433–447. [CrossRef]
41. Zhong, C.; Jian, S.F.; Huang, J.; Jin, Q.Y.; Cao, X.C. Trade-off of within-leaf nitrogen allocation between photosynthetic nitrogen-use efficiency and water deficit stress acclimation in rice (*Oryza sativa* L.). *Plant Physiol. Biochem.* **2019**, *135*, 41–50. [CrossRef] [PubMed]
42. Pan, W.K.; Tang, S.; Zhou, J.J.; Liu, M.J.; Xu, M.; Kuzyakov, Y.; Ma, Q.X.; Wu, L.H. Plant-microbial competition for amino acids depends on soil acidity and the microbial community. *Plant Soil* **2022**, *475*, 457–471. [CrossRef]
43. Kishor, P.B.K.; Sreenivasulu, N. Is proline accumulation per se correlated with stress tolerance or is proline homeostasis a more critical issue? *Plant Cell Environ.* **2014**, *37*, 300–311. [CrossRef] [PubMed]

44. Nam, T.G.; Kim, D.O.; Eom, S.H. Effects of light sources on major flavonoids and antioxidant activity in common buckwheat sprouts. *Food Sci. Biotechnol.* **2018**, *27*, 169–176. [CrossRef]
45. Wang, Z.B.; Zhang, Y.Z.; Bo, G.D.; Zhang, Y.P.; Chen, Y.; Shen, M.C.; Zhang, P.; Li, G.T.; Zhou, J.; Li, Z.F.; et al. Ralstonia solanacearum infection disturbed the microbiome structure throughout the whole Tobacco Crop Niche as well as the nitrogen metabolism in soil. *Front. Bioeng. Biotechnol.* **2022**, *10*, 903555. [CrossRef]
46. Hu, W.; Lv, X.B.; Yang, J.S.; Chen, B.L.; Zhao, W.Q.; Meng, Y.L.; Wang, Y.H.; Zhou, Z.G.; Oosterhuis, D.M. Effects of potassium deficiency on antioxidant metabolism related to leaf senescence in cotton (*Gossypium hirsutum* L.). *Field Crops Res.* **2016**, *191*, 139–149. [CrossRef]
47. Raddatz, N.; de los Ríos, L.M.; Lindahl, M.; Quintero, F.J.; Pardo, J.M. Coordinated Transport of Nitrate, Potassium, and Sodium. *Front. Plant Sci.* **2020**, *11*, 247. [CrossRef]
48. Li, P.F.; Liu, M.; Li, G.L.; Liu, K.; Liu, T.S.; Wu, M.; Saleem, M.; Li, Z.P. Phosphorus availability increases pathobiome abundance and invasion of rhizosphere microbial networks by Ralstonia. *Environ. Microbiol.* **2021**, *23*, 5992–6003. [CrossRef]
49. Song, X.H.; Xie, K.; Zhao, H.B.; Li, Y.L.; Dong, C.X.; Xu, Y.C.; Shen, Q.R. Effects of different organic fertilizers on tree growth, yield, fruit quality, and soil microorganisms in a pear orchard. *Eur. J. Hortic. Sci.* **2012**, *77*, 204–210.
50. Li, H.; Liu, S.Q.; Chen, X.; Wang, Y.; Feng, L.; Liu, J.K. Effects of calcium on growth, photosynthetic characteristics and quality of aquicultural garlic seedlings. *J. Plant Nutr. Fertil.* **2013**, *19*, 1118–1128. (In Chinese). Available online: https://x.cnki.net/kcms/detail/detail.aspx?dbcode=CJFD&dbname=CJFD2013&filename=ZWYF201305012&v=x0QVnnll88REIYoqsflQFp%mmd2Fokke2LEPXJdqx1nK4ZPctjFPpE3eziAAq5Di%mmd2F7FXw (accessed on 23 February 2023).
51. Li, H.; Liu, S.Q.; Liu, Z.L.; Feng, L.; Liu, J.K.; Chen, X.W.; Wang, Y. Effects of Calcium on Physiological Characteristics and Main Mineral Elements Absorption of Garlic. *Sci. Agric. Sin.* **2013**, *46*, 3626–3634. (In Chinese) [CrossRef]
52. Poovaiah, H.W.; Redd, A.S.N. Calcium and signal transduction in plants. *Crit. Rev. Plant Sci.* **1993**, *12*, 185–211. [CrossRef] [PubMed]
53. Hang, Y.; Wen, L.; Pang, Y.Z.; Hang, B.Y.; Wang, J.; Lü, X.L. Effect of spraying calcium on sugar and acid accumulation in 'Summer Black' grape. *Soil Fertil. Sci. China* **2020**, *2*, 166–172. (In Chinese) [CrossRef]
54. Yue, Y.K.; Jin, Z.Y.; Zhang, M.; Li, Z.Y. Effects of different nitrogen and calcium levels on fruit quality of protected peach. *China Fruits* **2021**, *4*, 55–58. (In Chinese) [CrossRef]
55. Sneha, G.R.; Swarnalakshmi, K.; Sharma, M.; Reddy, K.; Bhoumik, A.; Suman, A.; Kannepalli, A. Soil Type Influence Nutrient Availability, Microbial Metabolic Diversity, Eubacterial and Diazotroph Abundance in Chickpea Rhizosphere. *World J. Microbiol. Biotechnol.* **2021**, *37*, 167. [CrossRef]

forests

MDPI

Article

Agroforestry Ecosystem Structure and the Stability Improvement Strategy in Control of Karst Desertification

Shilian Jiang [1,2], Kangning Xiong [1,2,*], Jie Xiao [1,2], Yiling Yang [1,2], Yunting Huang [1,2] and Zhigao Wu [1,2]

[1] School of Karst Science, Guizhou Normal University, Guiyang 550001, China; sljiang@gznu.edu.cn (S.J.); mhxj47@gznu.edu.cn (J.X.); yyl980730@163.com (Y.Y.); yunting11183024@163.com (Y.H.); wuzg1224@163.com (Z.W.)
[2] State Engineering Technology Institute for Karst Desertification Control, Guiyang 550001, China
* Correspondence: xiongkn@gznu.edu.cn

Abstract: Agroforestry systems (AFS) are priority semi-natural ecosystems in fragile ecological zones. The complexity and diversity of their species structure play a crucial role in maintaining AFS stability. To explore the optimization of improvement strategies in AFS' structure and stability for control of karst desertification (KD), in this study, we chose typical desertification control areas in the southern China karst region. The study included homegarden (HG), agrisilviculture (ASV), and multipurpose woodlots (MWLs) as three AFS. We quantified the AFS' structural characteristics using descriptive statistics and spatial structure parameters. We used the fuzzy integrated evaluation method with structural and functional indicators as guidelines, and stand structure, plant species diversity, soil fertility, and environmental factors as first-level evaluation indicators. The entropy weight method calculates the weights of indicators at all levels. The fuzzy comprehensive evaluation method establishes an evaluation index system to evaluate the grading of AFS' stability. The results showed that: (i) The species composition of the AFS in the KD control areas had a simple structure, the overall diversity level was low, and the diversity level of herbaceous plants was better than that of woody plants. (ii) The overall distribution curves of diameter at breast height (DBH), tree height (TH), and crown width (CW) of woody plants in the AFS in the KD control areas were slight to the left, with a single-peaked pattern, mostly randomly and unevenly distributed in space, with a low degree of tree species isolation and relatively weak stand stability. (iii) There was variability in the stability classes of different types of AFS, overall reflecting the ranking HG > ASV > MWLs. (iv) When structural optimization was applied, corresponding measures can be taken according to farmers' wishes for different types of AFS and their primary business purposes. The improvement of stability depends mainly on the utility of the structural optimization applied coupled with positive human interference (for example, pruning, dwarfing, and dense planting). This study provides a scientific reference for maintaining the stability of AFS and promoting service provision.

Keywords: agroforestry; structure; species diversity; evaluation indicator systems; fuzzy integrated evaluation

Citation: Jiang, S.; Xiong, K.; Xiao, J.; Yang, Y.; Huang, Y.; Wu, Z. Agroforestry Ecosystem Structure and the Stability Improvement Strategy in Control of Karst Desertification. *Forests* **2023**, *14*, 845. https://doi.org/10.3390/f14040845

Academic Editor: Ernesto I. Badano

Received: 8 March 2023
Revised: 13 April 2023
Accepted: 18 April 2023
Published: 20 April 2023

1. Introduction

We are facing the threat of a rapid decline in global terrestrial biodiversity [1]. In contrast, habitat loss and environmental degradation due to population growth, agricultural intensification, and deforestation are the leading causes of loss of biodiversity (BD) and associated ecosystem functions and services [2]. Numerous studies have found that agroforestry is essential in maintaining biodiversity, improving the ecological environment in ecologically fragile areas, slowing down agricultural intensification, optimizing ecosystem services, and keeping farmers' livelihoods [3–8]. Compared to traditional intensive agroecosystems, agroforestry systems (AFS) have structural characteristics such as multi-level, multi-plant species composition and configuration in time and space, and the complexity of

AFS structure will influence the internal functions of the system and determine the supply of ecosystem services [9–11]. Regarding structure, higher connectivity, modularity, and nestedness can contribute to the dynamic stability or structural stability of intercropping ecosystems [12]. The more specific and complex the structure of an ecosystem, the more stable the design of the ecosystem [13,14]. Therefore, identifying AFS structural characteristics and analyzing the stability status of AFS to propose effective improvement strategies that will optimize the functions of AFS and enhance their service provisioning capacity are the focus and difficulty of current research [15].

The AFS are priority semi-natural ecosystems in fragile ecological zones. The proper structure has a crucial role in vegetation restoration, water conservation, soil conservation, increasing biodiversity, maintaining the system's stability, and improving the environment [16,17]. Agroforestry systems structure can be understood as an ecosystem attribute based on the composition of species and their quantitative relationships in the species structure, stratification in the vertical form, and mosaicism in the horizontal structure [18,19]. The AFS stability is dynamic, not static. It is a comprehensive characteristic of the system's ecological equilibrium state, such as system movement efficiency, resistance, and interactions between biotic and abiotic elements [20]. It reflects the interdependence and interaction relationships such as system structure and function over a certain period [9,21], and stability is a decisive factor in the system structure and service function [22]. Therefore, quantifying the AFS' structure, evaluating its stability, exploring the factors influencing its stability, and proposing strategies for structural optimization and stability improvement will be beneficial in maximizing the benefits brought by optimally adjusted AFS [23,24].

Karst, as a component of the world's major ecologically vulnerable areas [25], has become a priority research topic in the United Nations Sustainable Development Goals for restoring degraded ecosystems [26]. The local vulnerability of the karst ecosystems, combined with irrational human activities, has led to karst desertification (KD) as a critical ecological degradation problem in karst areas worldwide [27–30]. This has left karst regions with low disaster resilience and environmental capacity, limiting land use and economic development [31,32]. To promote economic growth and ecological restoration, scholars subsequently proposed AFS as one of the environmental restoration programs to apply in KD areas [33,34]. This would gradually be developed into homegarden (HG), which is mainly self-sufficient and distributed around the houses of the farmers. This increases the economic income of farmers and maintains ecological benefits as does agrisilviculture (ASV). It also has multiple uses, such as timber production, and provides various products, such as fruit, fodder, food, and industrial raw materials, such as multipurpose woodlots (MWLs). After years, it has been shown that the development of AFS in KD areas not only maximizes its soil and water conservation benefits [12,13,35] but also has a positive effect on improving the productivity of KD areas and maintaining soil faunal diversity [36,37]. It highlights the promising development of AFS in KD areas. In particular, the ecosystem services provided by AFS are essential for improving the overall ecosystem quality of the region and developing environmentally friendly industries that are compatible with the resources and environment. Studies indicate that the AFS structure is the essential dominant factor in providing ecosystem services [10,14], as it directly influences ecological processes and indirectly affects the supply of ecosystem services [11]. However, current studies on the structure and stability of AFS in the late stage are scarce [15].

Therefore, first, we focused on quantifying the species composition and diversity in the stand structure characteristics of woody plants in the AFS in the KD control areas. Second, taking the structure and function of the AFS as the standard layer, taking the stand structure, plants species diversity, soil fertility, and topographic factors as the first-level evaluation index indicators of stability, we used the fuzzy comprehensive evaluation method to construct a stability evaluation index system to evaluate the stability of different types of AFS in the KD control areas. Finally, the relationship between structure and stability and the influencing factors were explored, and practical strategies for structure optimization and stability improvement are proposed. To this end, we assumed that: (i) The

richness and diversity of species composition in the three AFS show MWLs > HG > ASV, but in terms of stand structure, HG is more reasonable, followed by MWLs and ASV are the worst. An urgent need is to take appropriate disturbance measures for optimization and adjustment. (ii) Considering the intensity of anthropogenic disturbance, the results of the stability evaluation showed the best stability of MWLs, followed by HG, and poor stability of ASV. (iii) From the weight values of each level of indicators, we can obtain that plant species diversity and stand structure were the main drivers of stability, and soil fertility and topographic factors were less influential, and we need to focus on species composition and their adaptability in the stability improvement strategy. To verify the above hypotheses, we quantified the structural characteristics of AFS in the KD region of southern China, evaluated its stability, and classified it into different classes. We explored the influencing factors of structure and stability and proposed strategies for structural optimization and stability improvement. It provides a scientific reference for maintaining AFS stability in the KD control areas and promoting the improvement of their service provisioning capacity.

2. Materials and Methods

2.1. Study Area

As early as China's 9th National Development Five-Year Plan in year, agroforestry (AF) was attempted to be adopted to combat the KD [33,34]. It was found that the blind value-addition of a population in karst areas, especially in mountainous areas where the slopes are dominated by agriculture, and where not enough attention is paid to forestry and pastoralism, resulted in an imbalance in the ratio of agriculture to other land uses. Forestry and pastoralism eventually led to the degradation of arable land, pastureland, and forest land, soil erosion, and increased floods and droughts. Furthermore, the deterioration of the ecological environment will become an inevitable consequence [38]. In turn, it has prompted various experts and scholars to consider different AF models in areas with varying levels of KD. Later, with further development, different types of AFS were gradually formed, such as homegarden (HG), mainly for farmers' self-sufficiency, and agrisilviculture (ASV), that primarily increases the economy and ecological restoration. In addition, it is not easy to distinguish the type of AFS (which has both the common characteristics HG and ASV) that combines the classification criteria of AFS by [39,40] to name it multipurpose woodlots (MWLs). Accordingly, based on the management experience of AFS in the study area, the representativeness and typicality of the study area, we selected the following three KD areas on the Guizhou plateau, to represent the overall ecological environment of karst in southern China (Figure 1).

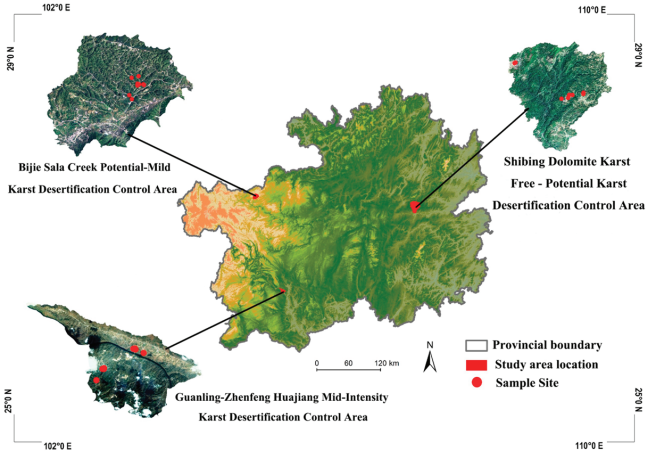

Figure 1. Study area.

First, the example area of potential–light KD in the karst plateau mountains of Bijie Salaxi was selected as the first study area (hereafter referred to as BJ). The study area (105°01′11″–105°08′38″ E, 27°11′09″–27°17′28″ N) has diverse geomorphic types and fragmented topography, and positive and negative topography such as peaks, depressions, funnels, dark rivers, and water caves are widely developed in the area. Elevations range from 1495 to 2200 m with a relative elevation difference of 705 m [41]. The northern subtropical humid monsoon climate has an average annual temperature of 12 °C and an average annual rainfall of about 984.4 mm. The area is mainly dryland, with a few paddy fields, dam terraces, and more slopes [42]. The AFS mainly comprises fruit trees such as walnuts, prickly pears, plums, apples, peaches, and loquats with crops such as ryegrass, white clover, maize, potatoes, and beans (Figure 2).

Figure 2. Schematic diagram of three types of AFS used in the control of KD in BJ.

Second, the Guanling-Zhenfeng Huajiang Karst Plateau Canyon moderate intensity KD area was selected as the second study area (hereafter referred to as HJ) (25°39′20″–25°41′20″ N, 106°37′30″–106°39′49″ E). There are various types of landforms and fragmented terrain. The favorable and hostile landscape, such as peaks, depressions, funnels, dark rivers, and water caves, are widely developed in the area. The elevation ranges from 370 to 1473 m with a relative elevation difference of 1103 m; the study area has a dry and hot southern subtropical valley climate, with warm and dry winters and springs and hot and humid summers and autumns, with an average annual temperature of about 18.4 °C and an average yearly precipitation of about 1100 mm [41]. The soil is predominantly developed on limestone with high soil fertility, but the soil layer is shallow and discontinuous, with poor water retention and drought tolerance [43]. The AFS in the KD area mainly comprises walnut, prickly pear, plum, apple, peach, loquat, and other fruit trees with ryegrass, white clover, and other forage grasses, corn, potatoes, beans, and other crops (Figure 3).

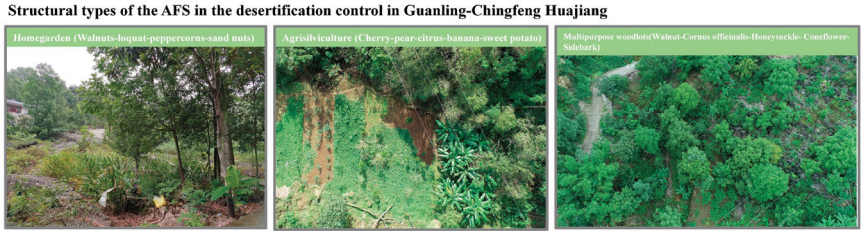

Figure 3. Schematic diagram of three types of AFS used in the control of KD in HJ.

Finally, the example area of no–potential KD in the Karst Plateau trough valley of Shibing was selected as the third study area (hereafter this is referred to as SB) (108°01′36″–108°10′52″ E, 27°13′56″–27°04′51″ N). The topography is high in the north and low in the south. Elevation ranges from 600 to 1250 m, with an average height of 912 m. It is a subtropical humid monsoon climate, with warm spring and cool summer, four seasons, an annual average temperature of 16 °C, and an average yearly rainfall of 1220 mm. The area has a thick soil layer, mainly lime soil, high soil fertility, and traditional agriculture

is well-developed. Therefore, the AFS in this KD area is composed chiefly of golden pear, peach, cherry, plum, and other fruit trees with medicinal plants or forage grasses such as yellow essence, prunus seeds, and white hyacinth (Figure 4).

Figure 4. Schematic diagram of three types of AFS used in the control of KD.

2.2. Sample Site Selection and Survey

2.2.1. Sample Site Selection

Based on the above classification of different AFS for the KD areas, and through field survey by combining previous research results, we classified them into three types of AFS: HG, ASV, and MWLs. Three 20 m × 20 m test plots were set up for each AFS type in the three study areas, totaling nine plots per study area and 27 test plots for the three study areas.

2.2.2. Structural Investigation

First, each study plot's geographic coordinates and elevation were recorded with GPS (Garmin 639csx USA Kansas) [44] and the slope direction and gradient were measured with a slope meter (Supplementary Materials Table S1). Within each parcel, all tree species present in the sample square were recorded, the diameter at breast height of all plants was measured with a diameter at breast height ruler (cm), the crown width (m) was measured with a 50 m long measuring tape, and the tree height (m) was measured with a 15 m long telescopic height gauge. After that, two small diagonal sample squares with an area of 5 m × 5 m were selected for the survey, and all shrub species present in these sample squares were recorded, and their basal diameter (cm), crown width (m), and height (m) were measured. Finally, all herbaceous species occurring in five 1 m × 1 m small sample squares located at the corners and center of the sample square were measured and recorded. Their height (cm), the number of plants, multiplicity, and cover were also measured. For the above, species that were difficult to identify in the field, we harvested their leaves and brought them back to the laboratory to identify them concerning the references Flora of Yunnan, Flora of China, Higher Flora of China, Flora of China, and so on, to establish a database of information on plant species in each plot. We chose to conduct all the above surveys at the peak of plant growth (July 2022).

Therefore, combined with field investigation and research, we used Excel (Version 2019, Washington, DC, USA) to determine the plant species composition of the AFS in KD control areas and calculate the index parameters, SPSS (Version 25.0, Chicago, IL, USA) for descriptive statistical analysis, and Origin 2018(Version 9.0, Northampton, MA, USA) for mapping, aiming to explore the structural characteristics and stability of AFS.

2.2.3. Collection and Determination of Physical and Chemical Properties of Soils

In each 20 m × 20 m sample plot designed above, five small sample squares were distributed on the four corners and the center point. First, we collected samples of soil from 0–10 cm and 10–20 cm depth with a ring knife from the root system after removing the humus and brought it back to the laboratory to determine soil bulk density and capillary porosity. We collected 1 kg samples of soil separately from 0–10 cm and 10–20 cm depths in plastic bags and brought them back to the laboratory to determine the chemical properties

of soil organic matter, total nitrogen, total phosphorus, and total potassium. The details and equations for the collection and experimental operation of soil physical properties were calculated by referring to the method of Li Ke et al. [45]. Specific indicators are shown in Table 1.

Table 1. Indicators and measurement methods [45].

Indicators	Measurement Methods
Soil pH (pH)	By water leaching-potentiometric method (National Standard GB7859-87)
Soil bulk density (SBD)	Soaking method and ring knife method
Soil capillary porosity (WFPS)	Soaking method and ring knife method
Soil organic matter (SOM)	National standard GB7857-87 oxidation of potassium dichromate -external heating method
Soil total nitrogen (TN)	National standard GB7173-87 semi-trace Kelvin method
Soil total phosphorus (TP)	Sodium hydroxide alkali fusion—molybdenum antimony anti-colorimetric method
Total potassium in soil (TK)	By flame photometry

Soil Physical Indexes Were Determined

First, the fresh weight was determined by weighing the sample in the field, then it was brought back to the laboratory, and soaked for 12 h. Second, the ring knives and their contained samples were placed on absorbent paper for 2 h after full soaking and then weighed. Finally, the weighted ring knives were dried in an oven at 115 °C and then weighed once dry and the soil's physical properties were calculated [45]. The calculation formulae are:

$$\text{Soil bulk density } (g{\cdot}cm^3)\ (SBD) = \text{Soil capacity } (g{\cdot}cm^3) = \text{wet soil weight inside the ring knife/ring knife volume} \times (1 \pm \text{natural soil water content}) \quad (1)$$

$$\text{Soil capillary water holding capacity} = (\text{soil weight at 12 h of water absorption-dry soil weight})/\text{dry soil} \times 100 \quad (2)$$

$$\text{Soil capillary porosity (WFPS)} = \text{capillary water holding capacity} \times \text{capacity} \quad (3)$$

Soil Chemical Properties Determined

The soil brought back to the laboratory was air-dried and the chemical properties were determined by taking the determination method in Table 1, and calculated according to the following equation:

$$\text{Soil organic matter } (g{\cdot}kg^{-1}) = \text{soil organic carbon } (g{\cdot}kg^{-1}) \times 1.724 \quad (4)$$

$$\text{Soil organic carbon (SOC, } g{\cdot}kg^{-1}) = \frac{\frac{c \times 5}{V_0} \times (V_0 - V) \times 10^{-3} \times 3.0 \times 1.1}{m \times k} \times 1000 \quad (5)$$

where: c—0.8000 mol·L^{-1}($K_2Cr_2O_7$), 5—the volume of potassium dichromate standard solution added (mL), V_0—the volume of $FeSO_4$ used for blank titration (mL), V—the volume of $FeSO_4$ used for sample titration (mL), 3.0—$\frac{1}{4}$ molar mass of carbon atoms (g-mol^{-1}), 10^{-3}—Converting mL to L, 1.1—Oxidation correction factor, m—the mass of air-dried soil sample (g), k—the coefficient of converting air-dried soil to dried soil, 1.724—Average conversion factor for conversion of soil organic carbon to soil organic matter.

$$\text{Soil total nitrogen (TN, } g{\cdot}kg^{-1}) = \frac{(V_0 - V) \times c\left(\frac{1}{2}H_2SO_4\right) \times 14.0 \times 10^{-3}}{m} \times 10^3 \quad (6)$$

where: V—the volume of the acid standard solution used in the titration of the test solution (mL); V_0—the volume of the acid standard used in titration blank (mL); c—0.01 mol·L^{-1}

($K_2Cr_2O_7$) or the concentration of HCL standard solution; 14.0—the molar mass of nitrogen atoms ($g \cdot mol^{-1}$); 10^{-3}—Converting mL to L, m—the mass of the dried soil sample (g).

$$\text{Soil total phosphorus } \left(\text{TP, } g \cdot kg^{-1}\right) = \rho \times \frac{V_1}{m} \times \frac{V_2}{V_3} \times 10^{-3} \times \frac{100}{100 - H} \quad (7)$$

where: ρ—the mass concentration of phosphorus in the solution of the sample to be measured ($mg \cdot L^{-1}$) as found from the calibration curve; m—weighing sample mass (g); V_1—the volume of the fixed volume of the sample after melting (mL); V_2—the volume of solution fixation when developing color (mL); V_3—volume dispensed from the molten sample after volume fixing (mL); 10^{-3}—Conversion factor for converting $mg \cdot L^{-1}$ concentration units to kg mass; $\frac{100}{100-H}$—Conversion factor for converting air-dried soil to dried soil; H—the percentage of moisture content in air-dried soil.

$$\text{Soil total potassium } \left(\text{TK, } g \cdot kg^{-1}\right) = \frac{\rho \times MVC \times SM}{m \times 10^6} \times 1000 \quad (8)$$

where: ρ—the mass concentration of K in the solution to be measured from the standard curve ($\mu g \cdot mL^{-1}$); MVC—Constant volume of the measuring solution; SM—Score multiplier; m—weighing sample mass (g); 10^6—Conversion of μg to g divisor.

2.2.4. Determination of the Rate of Rock Outcrop

We collected rock outcrops rate specimens by the mechanical pointing method and photography method (Figure 5). First, holding a 1 m long bamboo pole, we walked along the edge of the 20 × 20 m sample, clicked on the ground every meter, determined whether the point was in contact with a rock, and counted the rocks. The absence of rocks was not measured, rather it was the number of sample points clicked on rock outcrops that were counted [46]. The rock exposure rate was calculated as the rock outcrops rate (BRR) = the number of sample points in contact with rocks/total number of sample points.

Figure 5. Measuring the percentage of surrounding limestone rock outcrops in AFS. The (**a**) is the original photo of 1 m × 1 m, and the (**b**) shows the rock area that was measured in the 1 m × 1 m.

Second, the size and area of rocks covered by the soil surface (1 × 1 m) were determined by digital photography and later by using ImageJ processing software (Version 1.8.0.112, New York, NY, USA) [47]. The above data were collected at the peak of plant growth (July 2022).

2.3. Parameter Calculation and Model Construction

2.3.1. Calculation of Parameters of AFS Structure

This research used the spatial structure analysis method of a stand with one reference tree and four nearest neighboring trees. The angular scale (W), mixing degree (M), and

stand size ratio (U) were selected to establish the distribution of three spatial structure parameters to analyze the spatial distribution pattern [48,49], the degree of species isolation, and the degree of individual differentiation of woody plant distribution in ASF of the KD control area.

Angular Scale

Angular scale (W_i). The angular scale reflects the distribution pattern of individual trees in an agroforest and refers to the proportion of α angles smaller than the standard angle α_0 ($\alpha_0 = 72^\circ$) to the four α angles examined [48], which is calculated by equation.

$$W_i = \frac{1}{n}\sum_{j=1}^{n} Z_{ij} \quad (9)$$

where: W_i is the angular scale of reference tree I; the z_{ij} is a discrete variable; $z_{ij} = 1$ when the jth α-angle is smaller than the standard angle α_0, and $z_{ij} = 0$ vice versa.

The five values and significance of W_i: $W_i = 0$, indicates that the stand is particularly uniformly distributed; $W_i = 0.25$, indicates that the stand is uniformly distributed; Wi = 0.5 indicates that the stand is randomly distributed; $W_i = 0.75$, indicates that the stand is unevenly distributed; and $W_i = 1$ indicates that the stand is very unevenly distributed. For the overall stand mean, the range of the random distribution is (0.475, 0.517), and for the overall stand mean ($\overline{w}$), the range of random distribution is within (0.475, 0.517), with $\overline{w} > 0.517$ being a clumped distribution and $\overline{w} < 0.475$ being a uniform distribution.

Mixing Degree

Mixing degree (M_i). The degree of admixture was used to examine the spatial isolation of tree species. It is described as the proportion of the four nearest neighbors of reference tree I that is not of the same species as the proportion of individuals in the four nearest neighbors of reference tree i that are not of the same species as reference tree i. It was calculated by see equation:

$$M_i = \frac{1}{n}\sum_{j=1}^{n} V_{ij} \quad (10)$$

where: Mi is the mixing degree of reference tree I; the V_{ij} is the discrete variable $v_{ij} = 1$ when the reference tree i is not the same species as the jth neighboring tree, $v_{ij} = 0$, otherwise, $v_{ij} = 0$ [49].

The five values and meanings of M_i: $M_i = 0$, indicates that the stand is zero-mixed; $M_i = 0.25$, indicates that the stand is weakly mixed; $M_i = 0.5$, indicates moderate mixing; $M_i = 0.75$, indicates strong mixing; $M_i = 1$, indicates that the stand is very strong. For the overall stand mean value ($\overline{M}$), the larger the value indicates the higher the degree of species isolation, and the more stable the stand.

Size Ratio

Size ratio (U_i). The size ratio refers to the ratio of the number of neighboring trees with diameters larger than the reference. The ratio of the number of neighboring trees with a diameter at breast height greater than that of the reference tree to the four nearest neighboring trees examined. The calculation method is shown in equation.

$$U_i = \frac{1}{n}\sum_{j=1}^{n} K_{ij} \quad (11)$$

where: U_i is the size ratio of the reference tree I; the k_{ij} is the discrete variable If the neighboring tree j is smaller than the reference tree i, $k_{ij} = 0$, otherwise, $k_{ij} = 1$ [48].

The five values and meanings of U_i. $U_i = 0$ indicates that the reference tree is dominant; $U_i = 0.25$, indicates that the reference tree is subdominant; $U_i = 0.75$, indicates that the reference tree is inferior; $U_i = 1$, indicates that the reference tree is inferior. It can be seen that the size ratio quantifies the relationship between the reference tree and its neighbors, and the lower the value (U_i), the fewer neighbors have a larger diameter at breast height

than the reference tree. For the mean size-ratio value ($\overline{U}$), the statistics by species can better understand the competition among species in the stand, and there are five values and meanings: when the $\overline{U} = 0$, the species is preferred. When $0 < \overline{U} \leq 0.33$, the species is suboptimal. When $0.33 < \overline{U} \leq 0.67$, the species is in the intermediate state. When $0.67 < \overline{U} < 1$, the species is in an inferior condition. When $\overline{U} = 1$, it means that the species is inferior. Among them, those in superior and suboptimal states are dominant species, and those in inferior and absolute inferior states are inferior tree species.

2.3.2. Species Diversity

Based on the field survey data, the plant species and animal species in the AFS were surveyed, and the importance value (IV) of plant species in the sample site was calculated, as well as its species diversity index, with the importance value IV = (relative abundance + relative frequency + relative dominance)/3 [44].

$$\text{Shannon Diversity Index } H' : \ H' = -\sum_{i=1}^{s} P_i ln p_i \tag{12}$$

$$\text{Pielou Uniformity Index } E : \ E = \frac{H'}{lnS} \tag{13}$$

$$\text{Simpson dominance index C} : \ \text{C} = \sum_{i=1}^{s} \frac{N_i(N_i - 1)}{N(N-1)} \tag{14}$$

$$\text{Margalef Richness Index D} : \ D_{MG} = \frac{S-1}{lnN} \tag{15}$$

where: in Equations (12)–(15): Pi is the frequency; $P_i = N_i/N$, S is the number of taxa; Ni is the number of individuals of the "i" taxon; and N is the total number of individuals of all taxa.

2.3.3. Establishment of Evaluation Index System

Selection Criteria and Principles of Evaluation Indicators

As a semi-natural ecosystem, the AFS cannot escape the interaction between material cycles and energy transfer with the surrounding environmental conditions. It makes them into a non-linear zone far from equilibrium. To better understand the structure and stability of AFS, the concept of multi-indicator evaluation based on information entropy theory can provide us with a measure of uncertainty or confusion of information in AFS so that we can better rely on important information from them to achieve the improvement of AFS stability. Therefore, we comprehensively consider the actual situation of AFS in KD areas. To ensure the system reliability of the evaluation system, we aimed to evaluate the AFS stability in KD control areas and develop the principles and criteria for constructing the index system. (Supplementary Materials Tables S2 and S3).

Establishment of Evaluation Indicators

We divided the evaluation factors into the target, criterion, and indicator layers according to the dissipative structure information entropy theory. The target layer is agroforestry ecosystem stability. The criterion layer is the AFS structure and KD standing environment factors. The indicator layer is divided into primary indicators and secondary indicators. The first-level hands are four, including forest stand structure, species diversity, soil fertility, and topographic factors. There are 20 secondary indicators, including angular scale, hybridization, size ratio, depression, tree height, crown width, plant richness index, diversity index, uniformity index, dominance index, soil organic matter, total soil nitrogen, total soil phosphorus, total soil potassium, soil bulk, soil capillary porosity, soil pH, slope, elevation, and rock outcrops rate. Based on the above target layer, criterion layer, and indicator layer, we constructed the evaluation index system (Table S4 in Supplementary Materials), which provides support for further construction of the weight matrix and affiliation matrix, and fuzzy matrix based on the indicators in the criterion layer and target layer, respectively.

Among them, the primary index is expressed as U= {U_1, U_2, U_3..., U_n}, and the secondary index is expressed as U_i= {U_{i1}, U_{i2}, U_{i3}, ..., U_{in}} (i = 1, 2, 3, ..., n), and Uin denotes the nth index of the ith level of evaluation [50,51].

Calculation of Indicator Weight Values

a. Assume that there are mth agroforestry samples and nth evaluation indicators.

From this, the original matrix $X' = [X'_{ij}]_{mn}$ for stability evaluation can be established as follows:

$$X' = \begin{bmatrix} x'_{11} & x'_{12} & \cdots & x'_{1n} \\ x'_{21} & x'_{22} & \cdots & x'_{1n} \\ \vdots & \vdots & \vdots & \vdots \\ x'_{m1} & x'_{m2} & \cdots & x'_{mn} \end{bmatrix} \tag{16}$$

where: x'_{ij} is the value of the j evaluation indicator in the ith AFS sample.

b. Data standardization.

The data of the sample matrix X′ is dimensionless, and this paper uses the extreme value method to process:

When the indicator data response is a positive effect:

$$X_{ij} = \frac{x'_{ij} - min(x'_{ij})}{max(x'_{ij}) - min(x'_{ij})} \tag{17}$$

When the indicator data response is a negative effect:

$$X_{ij} = \frac{max(x'_{ij}) - x'_{ij}}{max(x'_{ij}) - min(x'_{ij})} \tag{18}$$

where: X_{ij} is the normalized value, where $1 \leq i \leq m$, and i is an integer; max(X'_{ij}) and min(X'_{ij}) are the maximum and minimum values in row i of the matrix X′, respectively.

The matrix X after data normalization is:

$$X = \begin{bmatrix} x_{11} & x_{12} & \cdots & x_{1n} \\ x_{21} & x_{22} & \cdots & x_{2n} \\ \vdots & \vdots & \vdots & \vdots \\ x_{m1} & x_{m2} & \cdots & x_{mn} \end{bmatrix} \tag{19}$$

c. Calculate the entropy value of the jth evaluation index.

The formula for calculating the entropy value of each evaluation index is:

$$E_j = -\frac{\sum_{i=1}^{m} f_{ij} ln f_{ij}}{lnm} \tag{20}$$

$$f_{ij} = \frac{x_{ij}}{\sum_{i=1}^{n} x_{ij}} \tag{21}$$

where: E_j is the entropy value, $E_j \geq 0$; f_{ij} is the frequency of evaluation index j in the ith sample, $0 \leq f_{ij} \leq 1$.

d. Calculation of weight values:

$$W_j = \frac{1 - E_i}{\sum_{i=1}^{n}(1 - E_i)} - \frac{1 - E_i}{n - \sum_{i=0}^{n} E_i} \tag{22}$$

where: $0 \leq W_j \leq 1$, $\sum_{i=1}^{n} W_i = 1$. After calculating the weight of each index, the entropy weight matrix W_i= {W_{i1}, Wi_2, . . . , W_{i3}}, for the second level evaluation index is determined first, and then the entropy weight matrix W= {W_1, W_2, . . . , W_n}, for the first level evaluation index is determined.

Establishment of the Evaluation Set

Based on the available research results and the nature and specific conditions of the evaluated objects, the evaluation set $V = \{V_1, V_2, \ldots, V_k\}$ is created for the first and second levels of evaluation indicators, where k is the number of evaluation levels and k = 5. The evaluation indexes were classified into I, II, III, IV, and V classes, which were excellent, good, moderate, poor, and very poor, respectively. There is no uniform classification standard for some evaluation indicators, so this paper uses the extreme difference method to classify them according to the actual measurement results (Supplementary Materials Table S5. Evaluation Table S6).

Creation of Fuzzy Matrix

According to the established evaluation set, V distinguishes the affiliation degree $r_{ij}(0 \leq r_{ij} \leq 1))$ of the set to which each evaluation factor Ui belongs. The descending semi-trapezoidal affiliation function is used to calculate the affiliation of negative effect indicators; the ascending semi-trapezoidal affiliation function is used to calculate the association of positive effect indicators. The fuzzy relationship matrix R (i.e., the affiliation matrix) is obtained according to the established affiliation function.

$$R = \begin{bmatrix} r_{11} & r_{12} & \cdots & r_{1k} \\ r_{21} & r_{22} & \cdots & r_{2k} \\ \vdots & \vdots & \vdots & \vdots \\ r_{n1} & r_{n2} & \cdots & r_{nk} \end{bmatrix} \tag{23}$$

where: r_{ij} is the affiliation degree of the "j" evaluation level to which the "i" evaluation index belongs.

Comprehensive Evaluation

First, the fuzzy comprehensive evaluation of the second-level indicators; the fuzzy evaluation vector S_i of the second-level indicators are obtained.

$$S_i = w_i \cdot R_i = \{w_{i1}, w_{i2}, \ldots, w_{ij}\} \cdot \begin{bmatrix} r_{11} & r_{12} & \cdots & r_{1k} \\ r_{21} & r_{22} & \cdots & r_{2k} \\ \vdots & \vdots & \vdots & \vdots \\ r_{n1} & r_{n2} & \cdots & r_{nk} \end{bmatrix} \tag{24}$$

where: S_i is the affiliation vector of the evaluation set V to which the second-level evaluation factor Ui belongs, $1 \leq i \leq 3$, and i is an integer. Then the fuzzy comprehensive evaluation is calculated for the first-level indexes.

$$A = W \cdot S \tag{25}$$

where: W is the weight vector of the first-level indicators; S is the affiliation vector of the evaluation set *V* to which the first-level evaluation factor *U* belongs; A is the affiliation vector of the evaluation set *V* to which the study area's AFS stability belongs. According to the principle of maximum affiliation, the affiliation level of A can be determined.

3. Results

3.1. Plant Species Components

Components are the elements that make up the system. The most important feature of the AFS, unlike agricultural (mainly plantation) and forestry systems, is that they have many structural components; as the number of components increases, the diversity, complexity, and stability of the system increase, and the processes of material cycling and energy flow in the system change, and productivity increases. In the case of AFS, the main components are crops and forest trees, whose presence and quantity play an essential role

in maintaining the balance and stability of the ecosystem. Therefore, this section aimed to explore the species composition and diversity of AFS in KD control areas.

3.1.1. Types of AFS Structure

The fieldwork and statistics revealed that the primary structure types of the homegarden (HG), the agrisilviculture (ASV), and the multipurpose woodlots (MWLs) in the three study areas had significant differences.

Firstly, in terms of the HG, the BJ study area vegetation was mainly comprised of walnut (*Juglans regia* L.), prickly pear (*Rosa roxburghii* Tratt.), apple (*Malus pumila* Mill.), plum (*Prunus salicina* Lindl.), loquat (*Eriobotrya japonica* Lindl), and other woody plants and vegetables with understory beekeeping, understory chicken farming, and different primary structure types such as walnut-prickly pear-beekeeping, walnut-apple-chicken keeping, apple-plum-vegetable, farming etc. The spatial relationship is mainly clumped mixed species and contour belt-type hybrid species. The HJ study area vegetation primarily comprised walnut, loquat, pear (*Pyrus* spp.), pepper (*Zanthoxylum bungeanum* Maxim.), persimmon (*Diospyros kaki* Thunb.), cherry (*Prunus pseudocerasus* Lindl.), citrus (rosa peach clementine), and other woody plants combined with amomi fructus (*Amomum villosum* Lour.), sweet potato (*Ipomoea batatas* (L.) Poir.), cabbage (*Brassica rapa* var. Glabra regel), eggplant (*Solanum melongena* L.), and other crops such as walnut-loquat-pear-sand-potato, walnut-pepper-sand, citrus-persimmon-cherry-vegetable, etc. The spatial relationships were mainly vertical spatial structures and clumped mixed species. In SB, which is primarily composed of woody plants such as peach (Pesca), cherry, and plum in combination with crops such as cabbage, eggplant, pepper, and tomato (*Solanum tuberosum* L.). Its primary structure types peach-plum-cherry-vegetable, peach-corn-vegetable, and peach-potato-vegetable, were mainly dominated by the spatial relationship of clumped mixed species.

Secondly, as far as the ASV is concerned, the BJ study area mainly comprised woody plants such as walnut, apple(malus), and prickly pear with ryegrass (*Lolium perenne* L.), maize (*Zea mays* L.), white clover (*Trifolium repens* L.), etc. The primary structure types of walnut-apple-white clover, walnut-prickly pear-corn, walnut-corn-rye grass, etc., are mainly dominated by clumped mixed species with vertical spatial structure. The HJ study area vegetation mainly consists of pepper, dragon fruit (*Hylocereus undulatus* Britt), plum, citrus, and other woody plants with corn, sugarcane (*Saccharum officinarum* L.), peanut (*Arachis hypogaea* L.), and different structural types such as pepper-dragon fruit-sugarcane, pepper-plum, pepper-dragon fruit, citrus-plum-corn, intercropping and double-layer structure. The SB study area vegetation mainly consists of golden pear (*Pyrus pyrifolia* (Burm.f.) Nakai), peach, and other woody plants with pasture (*Arthraxon* P.Beauv.), corn, roasted tobacco (*Nicotiana tabacum* L.), and different structural types of golden pear-pasture, peach-roasted tobacco peach-corn, mainly for the double-layer structure.

Finally, regarding the MWLs, the BJ study area vegetation is mainly comprised of walnut, prickly pear, firethorn (*Pyracantha fortuneana* (Maxim.) H.L.Li), single flower (*Hypericum monogynum* L.), lacquer tree (*Rhus verniciflua* Stokes), and other woody plants combined with pasture and different structural types such as walnut-prickly pear-pasture, prickly pear-goldenrod-pasture, walnut-firethorn-lacquer tree-pasture, which are mainly clumped mixed species. The HJ study area vegetation primarily consists of woody plants such as walnuts, paper mulberry (*Broussonetia papyrifera* (L.) L'Hér. ex Vent.), medicinal evodia fruit (*Euodia* sp.), oriental arborvitae (*Platycladus orientalis* (L.) Franco), loquat (*Eriobotrya japonica* (Thunb.) Lindl.) with honeysuckle flower (*Lonicera* L.), banana (*Musa* × *paradisiaca* L.), bamboo (Bambuseae), etc. The structure types of walnuts-honeysuckle flower-medcinal evodia fruit, walnuts-paper mulberry-banana, oriental arborvitae-walnuts-honeysuckle flower, etc., are mainly in the form of clumped mixed planting and intercropping structure. The study area of SB mainly consists of golden pear combined with perennial herbs such as many flower Solomonseal rhizome (*Polygonatum sibiricum* Redouté), hyacinth orchid (*Bletilla striata* (Thunb.) Rchb.f.), heterophylly falsestarwort root (Radix Pseudostellariae), grass family (Gramineae). Such as the golden pear- many floSolomonsealseal rhizome-grass

families, golden pear- hyacinth orchid-grass family, golden pear- heterophylly falsestar-wort root-grass family, and other structural types, mainly intercropping mixed and double layer structure.

3.1.2. Species Composition and Importance Values

In the AFS, crops and forest trees are notable species that play a key role in the balance and stability of the ecosystem. First, forest trees are an integral part of AFS, providing wood, fiber, and other biomass needed by humans and critical ecological services to the ecosystem. Second, crops offer food and other necessities humans need while providing ecological benefits, promoting ecosystem diversity, and providing food and habitat for other organisms. Developing AFS can also contribute to ecosystem diversity by providing food and habitat for other organisms. Statistical analysis of the species composition of the three study areas resulted in the following (Supplementary Materials Tables S7 and S8).

Firstly, in the HG, the BJ study area had 29 species of plants belonging to 20 families and 29 genera, among which nine species of plants of Asteraceae accounted for 21.95% of the total, four species of plants of Gramineae accounted for 9.76% of the total, two species of plants of Labiatae, Caryophyllaceae, Polygonaceae, and Urticaceae respectively, and 4.88% of the total respectively, and the rest of the families had only one species of plants. The HJ study area had 19 species of plants belonging to 15 families and 17 genera, among which two *Asteraceae* and *Leguminosae*, respectively, accounted for 10.53% of the total, and the rest had only one species. The SB study area had a total of 43 species of plants belonging to 19 families and 42 genera, including seven species of Asteraceae, accounting for 16.28% of the total, four species of Labiatae and Solanaceae, accounting for 9.30% of the total, three species of Gramineae, accounting for 6.98%, Rosaceae, Primulaceae, liliaceae, and Polygonaceae all had two species, accounting for 4.65% of the total. In comparison, the rest of the families had only one species. Taken together, the above species structures of Asteraceae, Gramineae, and Labiatae were present in both the BJ and SB study areas, indicating their greater dominance in the development of HG, while the HJ study area showed more significant differences.

Secondly, in the ASV, the BJ study area had 27 species of plants belonging to 19 families and 27 genera, including five species of Asteraceae (16.22% of the total), four species of Gramineae (13.51% of the total), three species of Rosaceae (10.81%) and three species of Labiatae (8.11%). The SB study area had 21 species of plants, belonging to 10 families and 21 genera, including four species of grasses, accounting for 19.05% of the total, four species of Labiatae, and four species of Asteraceae, accounting for 9.52% of the total, and only one species of plants in each family. In the above AS species structure, plants of Asteraceae were all present, indicating that they had a more significant advantage in developing AS.

Finally, in the MWLs, the BJ study area had 30 plant species belonging to 13 families and 21 genera, among which seven species of Asteraceae accounted for 26.67% of the total, four species of Gramineae accounted for 13.33% of the total, two species of Leguminosae accounted for 6.67% of the total, and the rest had only one species of plants in each family. The HJ study area had 14 plant species, belonging to 10 families and 12 genera, among which two species of Asteraceae and two species of Gramineae accounted for 14.29% of the total, and the rest had only one species of plant in each family. The SB study area had 32 species of plants belonging to 17 families and 22 genera, including five species of Asteraceae, accounting for 15.63% of the total, four species of Gramineae, accounting for 12.50% of the total, two species of Amaranthaceae, accounting for 9.38% of the total, and two species of Xanthate, accounting for 6.25% of the total. The rest of the families had only one species of plants. In the above species structure, Asteraceae were present in all three study areas, indicating that Asteraceae have a tremendous advantage in developing AFS.

3.1.3. Plant Diversity

The analysis of plant species diversity (Supplementary Materials Table S9) reveals the plant species diversity for the different types of AFS in the KD areas. Overall, the AFS

formed by KD has a simpler structure and lower species diversity and generally shows a higher level of herbaceous plant species diversity than woody plant species diversity. In particular, it was found that the AFS formed by the KD mainly consisted of a two-layer structure consisting of trees and herbs or shrubs and herbs, indicating that their hierarchical structure was relatively like HG. The H' diversity index of different types of the AFS in the various study areas was ranked BJ > HJ > SB, indicating that the overall species diversity level in the BJ study area was higher than that in the other two study areas. The evenness index E reflected the uniformity of plant species in AFS, and the overall performance was ranked HJ > BJ > SB, indicating that the general distribution of AFS in the HJ study area was more uniform. The C dominance index showed an opposite pattern to the H diversity index. The SB study area with a lower species diversity index value had a lower overall diversity level and higher dominance.

3.2. Forest Stand Structure in the AFS

For the AFS, the main components are crops and perennial woody plants. It is an artificial system configured with perennial woody plants and produced in a particular time and space to imitate the natural ecosystem according to individual functional needs. It has not only the properties of the natural ecosystem but also the properties of the plantation ecosystem [9,16]. It has also been pointed out that in the study of AFS, not only the horizontal properties (such as species composition and their diversity) should be considered, but it is also necessary to pay attention to their vertical spatial structural characteristics (such as the spatial location of woody plants and their relationships) to make possible to maintain the AFS total development. On the one hand, the diameter at breast height, crown width, and tree height in the non-spatial structure are essential indicators of woody plant growth and ecosystem health. They can provide information about the stand structure and species diversity of AFS, which can better reveal the structural characteristics of AFS and are essential for the adequate protection and maintenance of healthy development of ecosystems. On the other hand, spatial structural characteristics describe the properties of the spatial location of forest trees and their arrangement relationships, which largely determine the functions played by agroforestry. A complete understanding of its spatial structural characteristics is necessary to develop more appropriate agroforestry management strategies to guide its management practices.

Therefore, we analyzed the characteristics of the AFS structure in the KD control areas from both non-spatial and spatial systems of forest stands to provide theoretical support for optimizing the AFS structure.

3.2.1. Nonspatial Structure

In this section, we describe the nonspatial structural characteristics of three agroforestry systems (AFS) types. They are homegarden (HG), agrisilviculture (ASV), and multipurpose woodlots (MWLs).

Nonspatial Structural Characteristics of the HG

In the HG (Figure 6), the values for diameter at breast height, tree height, and crown width of agroforestry woody plants in the BJ study area were 8.05 $\pm$ 1.23 cm, 4.21 $\pm$ 0.61 m, and 2.94 $\pm$ 0.31 m, respectively. The values for diameter at breast height, tree height, and crown width of the HJ study area woody plants were 8.30 $\pm$ 1.23 cm, 4.16 $\pm$ 0.47 m, and 3.14 $\pm$ 0.34 m, respectively. In the SB study area, the values for woody plants' diameter at breast height, tree height, and crown width were 6.01 $\pm$ 0.86 cm, 3.40 $\pm$ 0.38 m, and 2.89 $\pm$ 0.22 m, respectively. Among them, the values for diameter at breast height, tree height, and crown width of woody plants in the BJ and HJ study areas were larger than those in the SB study area, indicating that woody plants in the BJ and HJ study areas were more luxuriant. In addition, from the perspective of kurtosis and skewness, the overall distribution curve of the non-spatial structure of woody plants in the BJ and HJ study areas was leftward and spiky. In contrast, the canopy width distribution of woody plants in the

SB study area was more dispersed, and the peaks were flat. The woody plants in the BJ and HJ study areas showed more concentrated distribution characteristics, while those in the SB study area were more dispersed.

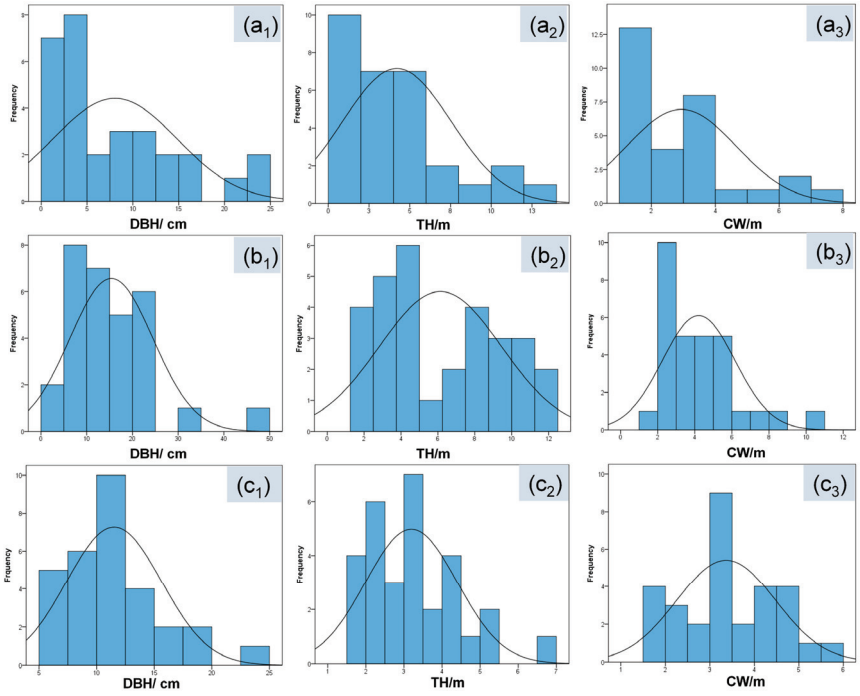

Figure 6. Nonspatial structure in HG. DBH, TH, and CW in the figure indicate the diameter at breast height (cm), tree height (m), and crown width (m), respectively (the same in the figure below); in addition, (**a$_1$**–**a$_3$**) indicate the BJ, (**b$_1$**–**b$_3$**) indicate the HJ, (**c$_1$**–**c$_3$**) indicate the SB.

Nonspatial Structural Characteristics of the ASV

In the ASV (Figure 7), the values for diameter at breast height, tree height, and crown width of agroforestry woody plants in the BJ study area were 15.39 ± 1.66 cm, 6.14 ± 0.61 m, and 4.21 ± 0.36 m, respectively. The values for diameter at breast height, tree height, and crown width of agroforestry woody plants in the HJ study area were 8.59 ± 1.02 cm, 3.10 ± 0.52 m, and 2.64 ± 0.28 m, respectively. The values for diameter at breast height, tree height, and crown width of agroforestry woody plants in the SB study area were 10.93 ± 0.88 cm, 4.13 ± 0.49 m, and 2.99 ± 0.27 m, respectively. The diameter values at breast height, height, and crown width of woody plants in the SB study area were 10.93 ± 0.88 cm, 4.13 ± 0.49 m, and 2.99 ± 0.27 m. In conclusion, among the ASV, the parameters diameter at breast height, tree height, and crown width of woody plants in the BJ study area were the largest, while those for the diameter at breast height, tree height, and crown width of woody plants in the HJ study area were the smallest. The SB study area was at an intermediate level. In addition, the kurtosis and skewness values of diameter at breast height, tree height, and crown width in the three study areas were greater than zero except for the HJ tree height distribution, which was less than zero, indicating that the overall distribution curve of the non-spatial structure of this type of ASV was slightly left and spiky.

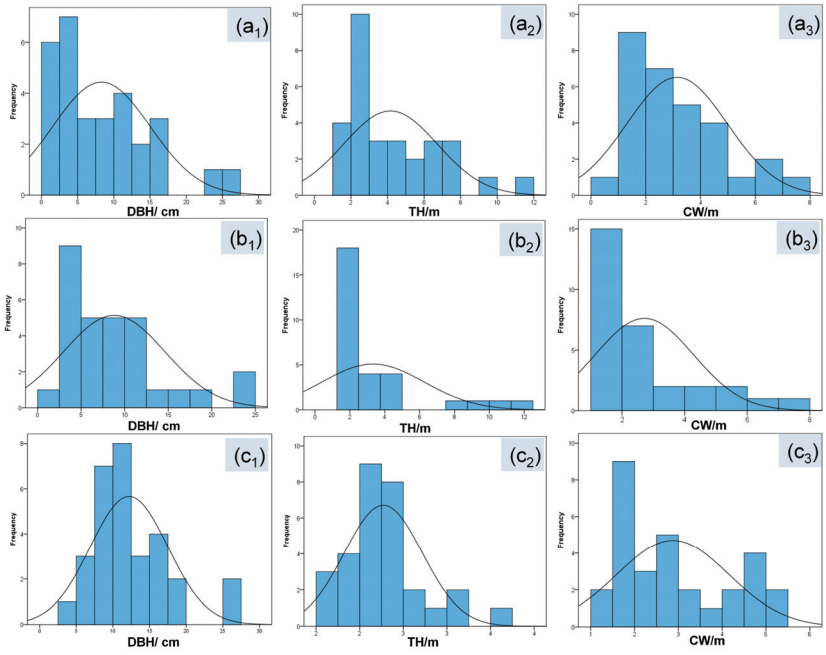

Figure 7. Nonspatial structure in ASV. DBH, TH, and CW in the figure indicate the diameter at breast height (cm), tree height (m), and crown width (m), respectively (the same in the figure below); in addition, (**a1**–**a3**) indicate the BJ, (**b1**–**b3**) indicate the HJ, (**c1**–**c3**) indicate the SB.

Nonspatial Structural Characteristics of the MWLs

In the MWLs (Figure 8), the values for diameter at breast height, height, and crown width of agroforestry woody plants in the BJ study area were 11.52 ± 0.75 cm, 3.19 ± 0.22 m, and 3.37 ± 0.20 m, respectively. The values for diameter at breast height, tree height, and crown width of the HJ study area woody plants were 11.34 ± 1.25 cm, 2.68 ± 0.42 m, and 2.97 ± 0.38 m, respectively. The values for diameter at breast height, tree height, and crown width of the SB study area woody plants were 9.30 ± 0.81 cm, 2.04 ± 0.11 m, and 1.97 ± 0.11 m, respectively. Among them, the kurtosis values of the canopy width distribution of the diameter at breast height of the BJ study area woody plants were less than zero, and the skewness values were more significant than zero, which indicated that the canopy width distribution was more dispersed, and the peaks were flat. The kurtosis values of the diameter distribution at breast height and height of the SB study area trees were less than zero, indicating that the distribution of diameter at breast height and crown width was more dispersed, and the peaks were flat. The distribution of woody plants in the BJ study area was more concentrated, while the SB study area was more scattered. In addition, the HJ study area had the most significant tree height distribution with kurtosis and skewness values greater than zero, indicating that its tree height distribution was to the left of the distribution curve and had a spike shape, saying that the tree height distribution of the HJ study area woody plants was more concentrated compared to the diameter at breast height and crown width.

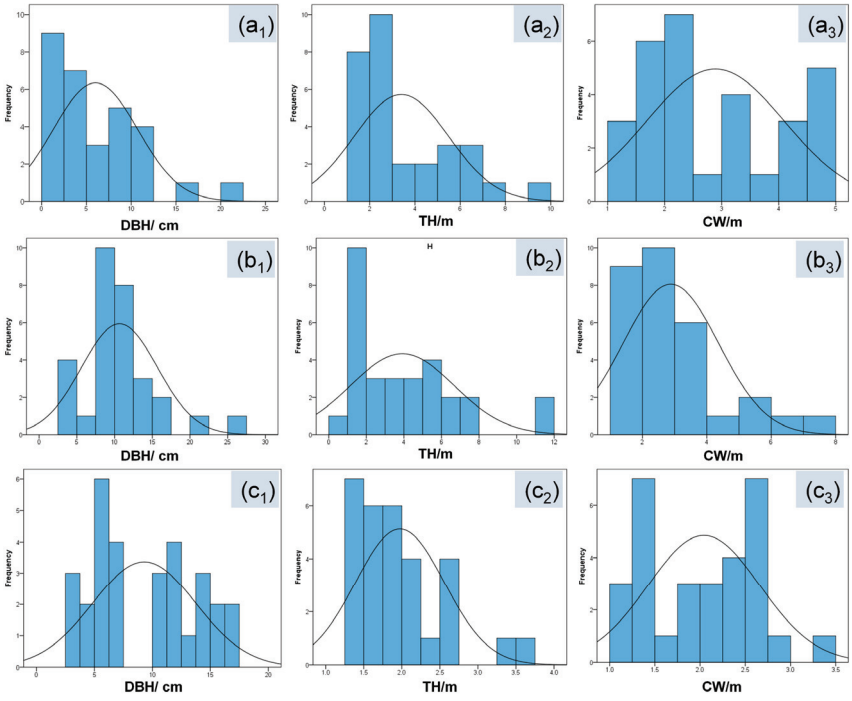

Figure 8. Nonspatial structure in MWLs. DBH, TH, and CW in the figure indicate the diameter at breast height (cm), tree height (m), and crown width (m), respectively (the same in the figure below); in addition, (**a1**–**a3**) indicate the BJ, (**b1**–**b3**) indicate the HJ, (**c1**–**c3**) indicate the SB.

3.2.2. Spatial Structure

In this section, we describe the spatial structural characteristics of three agroforestry systems (AFS) types. They are homegarden (HG), agrisilviculture (ASV), and multipurpose woodlots (MWLs).

Spatial Structural Characteristics of the HG

In the HG (Figure 9), first, the distribution pattern of stand level shows that the average angular scale distribution frequency in the BJ study area was slowly decreasing between W = 0.25 and W = 1. The distribution frequency (33.33%) was maximum and equal at W = 0.25 and W = 0.5, indicating that woody plants were primarily in a random and uniform distribution. The frequency of distribution (33.33%) was the most extensive and equal in the HJ study area at W = 0.25 and W = 0.75, respectively, and the frequency of distribution (26.67%) was relatively small at W = 0.5, indicating that the spatial distribution pattern of HJ mainly was in a random and uneven distribution (6.67%), the spatial distribution pattern of the SB study area was random and irregular.

Second, from the degree of species segregation, it can be seen that the distribution frequency was the largest at M = 0.75 (26.67%). The smallest at M = 0.5 (13.33%) in the BJ study area, and the proportion of the remaining mixed degree was 20%, indicating that the overall species segregation was strong, and the stand was relatively stable; the distribution frequency was the largest at M = 0.5 (33.33%) and M = 0.25 (26.67%) in the HJ study area. In addition, the frequency of distribution at M = 0.75 and M = 0.1 (20%) was equal, indicating that the study area has strong species segregation and a relatively stable stand; in the SB study area, the frequency of distribution at M = 0.75 was the highest (66.67%), and the frequency of distribution at M = 0.5 was the second highest (26.67%), indicating that the study area had a low species segregation and low stand stability. The distribution frequency

at M = 0.5 was the second highest (26.67%), implying that all tree species in the study area were quite isolated and it had low stability.

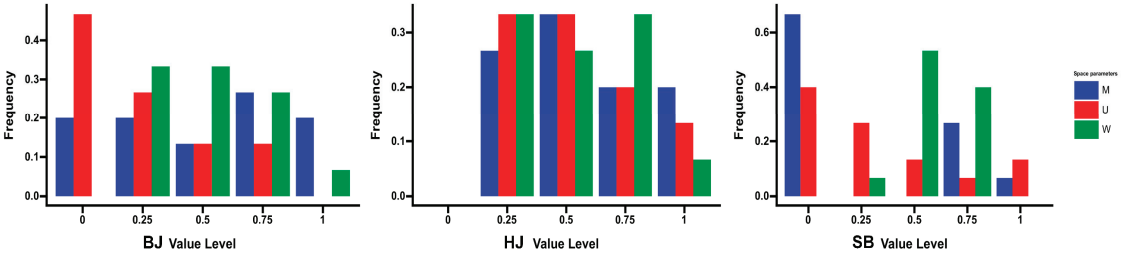

Figure 9. Spatial structure of HG. The W stands for angular scale, M stands for mixing degree, and U stands for the size ratio.

Finally, regarding the degree of stand size differentiation, the proportion of single trees with absolute dominance in the BJ study area reached 46.67%, while those at a complete disadvantage were 0. The average size ratio (0.52), which was between 0.33 and 0.67, indicated that the reference trees were mostly in an intermediate state; the HJ study area showed a trend of decreasing with the increase of the value level from absolute dominance to absolute disadvantage. The highest distribution frequency (33.33%) was found in the HJ study area at U = 0.25 and U = 0.5, indicating that the reference trees were mostly moderate; the proportion of single trees in absolute dominance in the SB study area reached 40% and showed a decreasing trend from dominance to complete sovereignty, indicating that the number of reference trees in this study area was gradually decreasing from dominant to absolutely inferior trees.

Spatial Structural Characteristics of the ASV

In the ASV (Figure 10), first of all, the distribution pattern at the stand level shows that the most significant distribution frequency (46.67%) was at W = 0.50 in the BJ study area. In comparison, the distribution frequency was the same at 26.67% at W = 0.25 and W = 0.75, and there was no W = 1.00, indicating that woody plants in this agroforestry type primarily reside in a random and uneven distribution; the distribution frequency in the HJ study area was the largest (46.67%) at W = 0.25. In the HJ study area, the distribution frequency was the highest at W = 0.25 (46.67%), and the distribution frequencies were equal at W = 0.5 and W = 0.75 (26.67%), indicating that woody plants in this type of agroforestry were mostly randomly and unevenly distributed; in the SB study area, the distribution frequency was the highest at W = 0.5 (66.67%), indicating that more tree species in this type of agroforestry were randomly and evenly distributed.

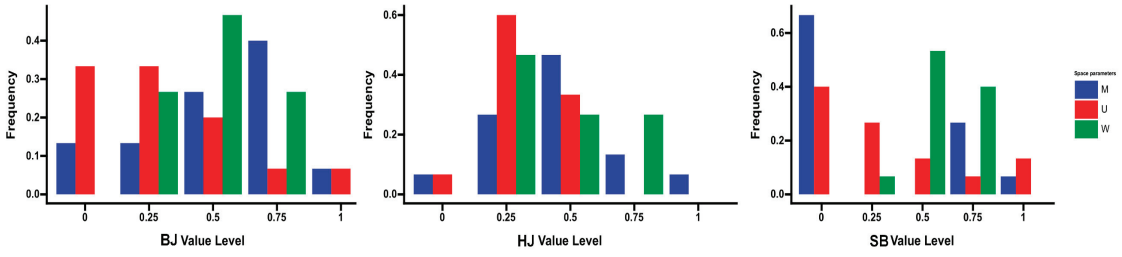

Figure 10. Spatial structure of ASV. The W stands for angular scale, M stands for mixing degree, and U stands for the size ratio.

Secondly, the distribution frequency at M = 0.75 was the highest in the BJ study area (40%). It shows that this type of agroforestry has a high degree of species isolation and relatively stable forest stands. The distribution frequency at M = 0.5 was the highest in the HJ study area (46.67%). The trend decreased from M = 0.5 to both ends, indicating a substantial degree of species segregation and a relatively stable stand in this type of agroforestry. The distribution frequency was the highest at M = 0 (33.33%) in the SB, indicating that the degree of species segregation in this type of agroforestry was low, and the stand was unstable.

Finally, regarding the degree of stand size differentiation, the proportion of woody plant size ratios in the BJ study area that were dominant and subdominant was the same (33.33%), indicating that the reference trees in this system were dominant. Subdominant species were the same, indicating that the number of reference trees in inferior and absolute inferior strains was low, and all were in the transition between dominant and subdominant to intermediate state; the proportion of single trees in complete dominance in the SB study area was 30%, while the proportion of single trees in subdominants was 30%. The balance of single trees at absolute authority reached 30%, while the proportion of single trees at subdominant and moderate was the lowest (33%). The ratio of single trees at inferiority and absolute inferiority (20%) indicates that the number of reference trees at inferiority and absolute inferiority was low. The overall state was excessive, from dominance to inferiority.

Spatial Structural Characteristics of the MWLs

In MWLs (Figure 11), first, the distribution pattern at stand level shows that the frequency of distribution was maximum (33.33%) at W = 0.50 in the BJ study area, equal at W = 0.25 and 0.50, and minimum (13.33%) at W = 1.00, indicating that woody plants in this study area were mostly in random and uneven distribution; the frequency of distribution was maximum (40%) at W = 0.75 and minimum (13.33%) at W = 1.00 in the HJ study area, indicating that woody plants in this agroforestry type were primarily in random and uneven distribution. The distribution frequency was the highest at W = 0.75 (40%) and the lowest at W = 1.00 (13.33%) in the HJ study area, indicating that woody plants in this agroforestry type were mostly randomly and unevenly distributed. It indicates that woody plants in AFS were mostly randomly and uniformly distributed and show a decreasing trend from a uniform distribution to random and uneven distribution.

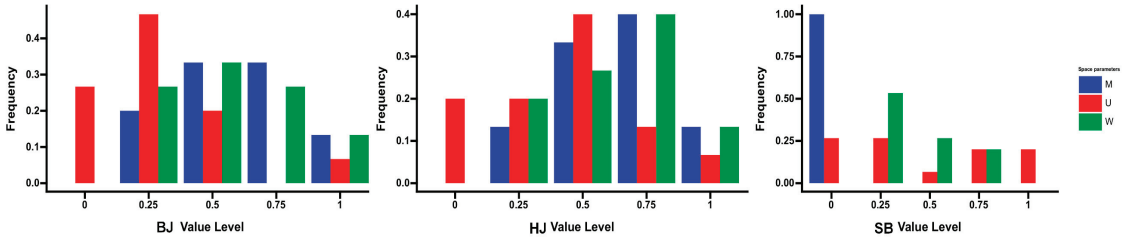

Figure 11. Spatial structure of MWLs. The W stands for angular scale, M stands for mixing degree, and U stands for the size ratio.

Second, in terms of species segregation, the distribution frequencies of M = 0.5 and M = 0.75 in the BJ study area were the highest and the same (33.33%), indicating that all types of AFS in the study area were in a relatively large proportion of medium-intensity mixing, indicating that the overall species segregation was strong, and the forest stands were relatively stable. The frequency of M = 0.5 and M = 0.75 in the HJ study area was the highest (33.33%), and there was a decreasing trend from the center of M = 0.75 to the two ends, indicating that the tree species in this type of agroforestry ecosystem were more segregated and the stand was more stable. The maximum distribution frequency (100%) was found at M = 0.00 in the multifunctional agroforestry ecosystem, indicating that species segregation was extremely low, and the stability was low in this study area.

Finally, in terms of stand size differentiation, the distribution frequency of U = 0.25 was the largest in the BJ study area (46.67%), followed by the distribution frequency at U = 0.00 (26.67%), which showed a "single-peaked" and decreasing trend distribution from the center to both ends of the subdominant distribution state. The proportion of absolute dominant and subdominant trees was the same in the SB study area (26.67%), the proportion of moderate trees was the lowest (6.67%), and the balance of inferior and absolute inferior trees was the same (20%). This indicates that the reference species in ASV were mostly dominant and subdominant trees.

3.3. Stability Analysis

3.3.1. Calculation of Evaluation Index Weights and Analysis of the Results

We can draw the following conclusions based on the weight values of each indicator in Table 2. First, soil fertility had the most significant contribution in the first-level hand with a weight of 0.3402, which is an essential factor affecting the AFS stability. In the first-level index of soil fertility, the weight of the soil's total potassium content was 0.0886, which is an extremely significant influencing factor. Potassium, phosphorus, and organic matter content in soil are essential nutrients in soil fertility, which play a decisive role in plant growth and development.

Table 2. Weights of indicators at each level.

First-Class Index			Second-Class Index		
Ordinal	**Indicator Name**	**Weight**	**Ordinal**	**Indicator Name**	**Weight**
1	U_1	0.2983	1	U_{11}	0.0462
			2	U_{12}	0.0722
			3	U_{13}	0.0374
			4	U_{14}	0.0274
			5	U_{15}	0.0604
			6	U_{16}	0.0546
2	U_2	0.1909	7	U_{21}	0.0466
			8	U_{22}	0.0323
			9	U_{23}	0.0366
			10	U_{24}	0.0754
3	U_3	0.3402	11	U_{31}	0.0547
			12	U_{32}	0.0550
			13	U_{33}	0.0567
			14	U_{34}	0.0886
			15	U_{35}	0.0301
			16	U_{36}	0.0300
			17	U_{37}	0.0250
4	U_4	0.1706	18	U_{41}	0.0587
			19	U_{42}	0.0658
			20	U_{43}	0.0461

Second, the contribution of stand structure in the first-level index was second only to soil fertility, with a weight value of 0.2983, which is also a key factor affecting the AFS stability. Among the first-level indicators of stand structure, the degree of stand mixing with a weight of 0.0722 was an important influence factor in this indicator, which describes the degree of spatial segregation of tree species in AFS, interspecific relationships. The degree of stand mixing not only influences the nutrient uptake and photosynthesis of a single stand but also significantly impacts the growth and development of shrubs, herbs, and soil animals in the understory, which plays an essential role in the configuration of the agroforestry ecosystem.

Once again, the weight value of plant species diversity in the primary index was 0.1909, in which the diversity index and richness index were significant influencing factors. Finally, among the topographic factors, elevation was the main influencing factor; however,

the contribution rate of each secondary index is in a more balanced state, and they were all critical influencing factors in stability.

In conclusion, it is clear from the weight values of each indicator that there was not a single factor driving the stability of AFS, but all the influencing factors worked together. Therefore, in the planning and management of AFS, each indicator's contribution and influencing factors need to be considered comprehensively to achieve the stability and sustainable development of the system.

3.3.2. Multilevel Fuzzy Comprehensive Evaluation

Based on the evaluation level criteria, the evaluation affiliation matrix R of the evaluation index set Ui to the evaluation domain V was determined. Establishing the evaluation affiliation R is the key to fuzzy comprehensive evaluation. According to the effects of the evaluation fingers, the fuzzy relationship matrix affecting different AFS stability in the KD areas can be obtained by substituting the above affiliation function formula. According to the established fuzzy relationship matrix and the weight values of the secondary evaluation indexes (Table 2), the second evaluation was conducted using equation (24), and the secondary fuzzy evaluation matrix S11 of the first AFS in the BJ study area is obtained.

$$S_{11} = \begin{bmatrix} 0.0000 & 0.0000 & 0.2987 & 0.1603 & 0.0000 \\ 0.1895 & 0.3380 & 0.0000 & 0.0000 & 0.0000 \\ 0.0442 & 0.0662 & 0.0681 & 0.0382 & 0.0650 \\ 0.2857 & 0.0000 & 0.0677 & 0.0000 & 0.0128 \end{bmatrix}$$

Similarly, the secondary fuzzy evaluation matrix of the other two types of AFS can be obtained as:

$$S_{12} = \begin{bmatrix} 0.0211 & 0.1291 & 0.2381 & 0.0377 & 0.0000 \\ 0.0645 & 0.2623 & 0.1309 & 0.0000 & 0.0000 \\ 0.0442 & 0.1276 & 0.0000 & 0.1968 & 0.0000 \\ 0.0000 & 0.2497 & 0.0656 & 0.0000 & 0.0035 \end{bmatrix} \quad S_{13} = \begin{bmatrix} 0.0000 & 0.0000 & 0.2003 & 0.2588 & 0.0000 \\ 0.0000 & 0.2399 & 0.2032 & 0.0961 & 0.0000 \\ 0.0804 & 0.0675 & 0.1276 & 0.0000 & 0.0407 \\ 0.3442 & 0.0624 & 0.0000 & 0.0000 & 0.0406 \end{bmatrix}$$

The secondary level fuzzy evaluation matrix of the AFS in HJ is obtained as:

$$S_{21} = \begin{bmatrix} 0.3227 & 0.1412 & 0.1221 & 0.0827 & 0.0000 \\ 0.2283 & 0.0995 & 0.0000 & 0.0765 & 0.0000 \\ 0.3107 & 0.1710 & 0.0000 & 0.0000 & 0.0290 \\ 0.2858 & 0.0000 & 0.1822 & 0.0000 & 0.1363 \end{bmatrix} \quad S_{22} = \begin{bmatrix} 0.0000 & 0.0607 & 0.2646 & 0.0397 & 0.0000 \\ 0.0000 & 0.0000 & 0.0000 & 0.0000 & 0.3327 \\ 0.0163 & 0.1661 & 0.0715 & 0.0709 & 0.0120 \\ 0.3805 & 0.0209 & 0.0000 & 0.0000 & 0.1318 \end{bmatrix}$$

$$S_{23} = \begin{bmatrix} 0.0000 & 0.1533 & 0.1068 & 0.2686 & 0.0000 \\ 0.2277 & 0.1095 & 0.0000 & 0.0852 & 0.0000 \\ 0.0898 & 0.0219 & 0.0000 & 0.1543 & 0.0000 \\ 0.3455 & 0.0000 & 0.0000 & 0.0000 & 0.3585 \end{bmatrix}$$

The secondary level fuzzy evaluation matrix of the AFS in SB is:

$$S_{31} = \begin{bmatrix} 0.0000 & 0.0000 & 0.1660 & 0.1896 & 0.0784 \\ 0.0545 & 0.4597 & 0.0000 & 0.0000 & 0.0000 \\ 0.1108 & 0.0642 & 0.1809 & 0.0528 & 0.0000 \\ 0.0000 & 0.2608 & 0.1777 & 0.0000 & 0.0000 \end{bmatrix} \quad S_{32} = \begin{bmatrix} 0.0000 & 0.0620 & 0.0690 & 0.0801 & 0.1003 \\ 0.0000 & 0.0000 & 0.1326 & 0.1917 & 0.0404 \\ 0.1073 & 0.0000 & 0.1212 & 0.0613 & 0.0934 \\ 0.0288 & 0.2469 & 0.1822 & 0.0000 & 0.0000 \end{bmatrix}$$

$$S_{33} = \begin{bmatrix} 0.0000 & 0.0000 & 0.1537 & 0.0439 & 0.0241 \\ 0.0000 & 0.0000 & 0.1230 & 0.2366 & 0.0000 \\ 0.0953 & 0.2046 & 0.1164 & 0.0785 & 0.0000 \\ 0.0000 & 0.2454 & 0.0000 & 0.1327 & 0.0000 \end{bmatrix}$$

3.3.3. Distribution of Stability Levels

When conducting the first-level evaluation, we used the Formula (25) based on the second-level fuzzy evaluation matrix S1 and the first-level evaluation index weight values

W (Table 2). The affiliation degree A value is calculated, the level is determined according to the principle of maximum affiliation, and the results are shown in (Table 3).

Table 3. Evaluation results.

Structure Type	Area	Level					Rating
		I	II	III	IV	V	
HG	BJ	0.1000	0.0870	0.1238	0.0608	0.0243	III
	HJ	0.2929	0.1193	0.0675	0.0393	0.0331	I
	SB	0.0481	0.1541	0.1414	0.0745	0.0234	II
ASV	BJ	0.0336	0.1746	0.1072	0.0782	0.0006	II
	HJ	0.0705	0.0809	0.1032	0.0360	0.0901	III
	SB	0.0414	0.0606	0.1183	0.0813	0.0694	III
MWLs	BJ	0.1330	0.0741	0.0319	0.1489	0.0612	IV
	HJ	0.0324	0.1115	0.1089	0.1076	0.0072	II
	SB	0.0861	0.0794	0.1420	0.0772	0.0208	III

First, in the HG stability evaluation grade, the affiliation degree (0.1238) of the BJ study area corresponding to the evaluation grade III was the largest and the level to which it belongs in general. The affiliation degree (0.2929) of the HJ study area corresponding to the evaluation grade I was the largest, and the level to which it belongs is excellent. The SB study area's affiliation degree (0.1541) related to the evaluation grade II was the largest, and the level to which it belongs is good. Second, among the ASV stability evaluation levels, the BJ study area had the largest affiliation (0.1746) corresponding to evaluation level II and belongs to the level of good. The HJ study area had the most significant association (0.1023) related to evaluation level II and belongs to the reasonable level. The SB study area had the largest affiliation (0.1183) corresponding to evaluation level III and belongs to the level of the fair. Finally, among the stability evaluation levels of MWLs, the BJ study area had the highest affiliation (0.1489) for evaluation level IV, and the affiliation level is poor. The HJ study area had the highest affiliation (0.1115) for evaluation level II, and the affiliation level is good. The SB study area had the highest affiliation (0.1420) for evaluation level III, and the affiliation level is fair.

In conclusion, there were significant differences in the evaluation grades of the AFS stability of the same type in different KD control demonstration areas. It indicates that the maintenance of the AFS stability and the intensity of anthropogenic disturbance may have some correlation.

4. Discussion

4.1. AFS Species Composition and Species Diversity

We found that the species composition of the AFS of KD control areas is simple, and the diversity level is low according to the data analysis (For details, please refer to Tables S7–S9 of the Supplementary Materials), the results of this study better support our hypothesis (i). The species composition was mainly shown in the configuration with crops, livestock breeding, or pasture crops, with fewer species of woody plants, and their diversity levels were lower than those of understory species. Similar findings have been better explained in related research reports. For example, studies on the characteristics of karst biodiversity and its reconstruction mechanism pointed out that there are few plant species (1–4 species) in each community in karst areas, and the species diversity level is generally low. Especially in some plantation forest areas planted to KD control, the species diversity level of vegetation is deficient [52–54]. Combined with the actual conditions in KD areas, the following mechanisms can be supported to explain this result: the gradient stress hypothesis, due to the existence of different gradients and stresses in the KD areas, bearing the multiple stresses of topography, karst drought, and high soil calcium, changing their structure as well as physiological and biochemical processes in the process of survival, through a complex and diverse response mechanism (cross-adaptation) to gain resistance to

adapt to the environment [55,56]. Therefore, favorable interactions and complementarities among species face an extraordinary test.

4.2. AFS Structural Features

Through data analysis (Figures 6–11), we obtained the following main conclusions: first, in terms of non-spatial structure, the distribution curves of diameter at breast height, tree height, and crown width of woody plants in different types of AFS under KD control areas were generally left and monoclinic, but HG was usually better than the remaining two types. Second, in terms of spatial structure, the spatial distribution pattern of woody plants in the HG and MWLs was mostly random and uneven distribution, with better segregation of tree species and more stable stands. In contrast, the ASVs were mainly in a uniform distribution, with relatively low stand isolation and poor stability. The above conclusions better support our hypothesis (ii) and have been better explained in the existing studies. On the one hand, with the growth and development of the stand, the demand for sunlight, water, and nutrients increases, which is subject to self-thinning and some human interference, making the stand aggregation weaker and will eventually develop into a random distribution pattern [57]. On the other hand, habitat heterogeneity and seed dispersal limitations force tree populations to aggregate and thus increase their survival potential [58]. In addition, the species composition and their number influence the degree of isolation of tree species and their stability levels, which are mainly related to species composition and biological characteristics [59]. We also argue that in poor KD areas, farmers' perceptions of agroforestry affect their management strategies. For example, failure to achieve the expected economic income in the short-term triggers them to change their planting strategy by changing tree species or directly cutting them down, thus leading to a reduction in tree species composition and a return to a single agroforestry ecosystem, which will be detrimental to the development of agroforestry. Therefore, farmers' willingness to participate should be added to the management strategy, which is similar to the view of agroforestry development in Ethiopia [60].

4.3. Driving Factor of AFS Stability

The distribution of the weight values of the primary indicators (Table 2) reflects the AFS stability constraints rather than solely the vulnerability of a singular karst ecological environment. They mainly consist of the interaction of site conditions such as soil physical and chemical properties and topographic factors and AFS structural factors such as species diversity and stand structure. This conclusion is somewhat different from our hypothesis (iii). However, it is better to show that the scientific analysis method can identify the influence of factors of stability and thus effectively explore the improvement strategies for AFS stability.

As far as the site conditions are concerned, in the KD area, on the one hand, due to the mismatch in the spatial distribution of soil water and soil resources, high spatial and temporal heterogeneity of water and heat factors, and extreme deficiency of nitrogen, phosphorus, and potassium, and in the process of vegetation restoration, with the accumulation of biomass and changes in species, the reserves of nitrogen, phosphorus, and potassium in the soil will decrease, which is hugely limiting for plant self-growth and diversity is highly limiting. In addition, the strongly developed karst dual hydrogeological structure leads to the unique "karst drought" phenomenon [61], the mosaic of rocks and shallow soils, the high heterogeneity of karst habitats and the significant differences in soil ecological functions, and the tendency of the microenvironment in KD areas to dry out and heat [62], lead to the development of AF in KD areas and a low survival rate and species diversity of AFS in KD areas [63]. Therefore, although studies have shown that AFS play a crucial role in providing ecosystem services [11,64], they are subject to significant stress effects on plant growth due to KD site conditions, resulting in low AFS stability.

As far as AFS structure is concerned, the higher number of plants and the greater the mixedness index, the higher the degree of isolation of its species and the more stable

the forest stand; the influence of plant species diversity on ecosystem stability should not be ignored. Ecological theory suggests that ecosystem stability is closely related to plant diversity [65,66]. The higher the number of species in an ecosystem, the higher its level of diversity, the more complex its trophic structure will be, the more resistant it will be to external disturbances, and the more stable it will be [9,67,68]. Therefore, plant stands construction and plant species diversity also influence stability factors.

4.4. Stability Improvement Strategy

According to the stability evaluation results, we can see that (Table 3) there is variability in the stability classes of different types of the AFS, among which, in HG, it mainly shows the ranking HJ (excellent) > SB (good) > BJ (fair); for ASV, it shows the ranking BJ (good) > HJ (fair) = SB (fair); for MWLs, it shows the ranking HJ (good) > SB (fair) > BJ (poor). Overall, this reflects HG > ASV > MWLs. Based on the above findings, combined with previous practical experience in AFS structure optimization and stability improvement, more targeted strategies are discussed around the relationship between species composition with its diversity and stability and the current situation of the AFS in KD control for reference stability enhancement strategies.

4.4.1. Species Composition and Its Diversity Strategy

Regarding species diversity and complexity, the core of biodiversity is species diversity, which enables ecosystems with higher diversity to use limited resources more fully and maintain their productivity at a higher level through complementary ecological niches [69]. As a result, different species have complex linkages in their quantitative and spatial, and temporal distributions, and species' trait differences, their respective survival strategies, and the relationships and interactions among species have essential effects on population survival and development dynamics and community structure, function, and succession [70–72]. In addition, the stability and diversity hypothesis theory suggests that desert vegetation communities are less stable due to the lack of redundant species, and their ecological functions are mainly carried out by dominant or community-building species, with a low number of other species [73,74]. Because of this, vegetation community simplicity, diversity, and structural indicators are low in AFS stability in KD. Therefore, it is essential to increase the number of plant community species in maintaining stability and pay special attention to introducing some fast-growing community dominant or community-building species to configure so that AFS generates disturbance resistance and resilience stability to maintain the strength of its system itself.

Species Composition Strategy in the HG

The composition of woody plants and crops in HG primarily resides in the random selection of farmers and rarely follows a specific rule or guiding scheme for configuration. Regarding site conditions, they are mainly distributed around the courtyard with certain practicality and ornamental properties. It is primarily based on physiological and ecological growth habits of long-term competition, adaptation, and evolution of a mosaic pattern of different woody plants, crops, and other vegetation. Its dominant species are not prominent, primarily common species, and most of the plants are calcium-loving, lithophytic, drought-tolerant, and barren [15]. Due to the complexity of KD habitats, there are not only one species that can adapt to the same successional stage habitat but also a species group composed of multiple species with the same adaptations [38,75]. Therefore, if the dominance of the dominant tree species does not decrease, different colors and seasonal phases can be changed according to the season and phenology of the tree species. The temporal relationship structure can be fully utilized to appropriately increase the native ornamental tree species to improve their species diversity level and thus enhance the beauty of the landscape.

Species Composition Strategy in the ASV

The ASV is mainly located in or around farmland to maintain farmers' economic income while taking ecological benefits into account. The species composition should consider the types of products and their uses and select native species to meet the needs of local people and markets. However, it should be regarded that woody plants and herbaceous crops can improve the soil and the small environment, which is beneficial for enhancing the fertility of the agroforestry land and thus increasing species diversity. The KD areas are locally fragile. The AF in KD areas should follow the unique local natural environment and moisture conditions and select complementary, less water-demanding drought-tolerant plants. In addition, the thin soil layer and poor continuity in KD areas should select for trees that can grow in rock crevices and ravines [76–78].

Species Composition Strategy in the MWLs

The MWLs are mainly balanced to maintain ecological, economic, and social functions and contain some of the main tasks of HG and ASV, such as timber production and food production. For this type of AFS, crop species, and woody plants should be reasonably selected and deployed, and various woody plants can be configured together. Still, the inhibitory effect between plants should be considered. In terms of spatial utilization, we should choose to match the height of trees, shrubs, and grasses and to match loose and compact plants; in terms of root depth, we should choose to match deep-rooted and shallow-rooted crops, which can efficiently utilize water and nutrients at different levels in the soil and choose shade-tolerant crops with better shade woody plants to fully use light energy resources for light energy utilization. The AFS comes after intercropping, crop set, or strip planting in the collocation [16,20]. Implementing intercropping or strip planting will change the group structure of crops, create edge row advantage, and allow good ventilation and light conditions for plants.

4.4.2. Artificial Interference Strategy

Regarding anthropogenic disturbances, KD areas are locally fragile. In its ecological context of exposed bedrock, shallow soil, and marked water infiltration, it must undergo strict natural screening to enable plant populations with calcium-loving, drought-tolerant, and lithophytic characteristics to survive [78]. Therefore, the species selection and configuration should be based on various highly resistant woody plants, giving full play to their resistance to disturbance stability in the KD environment against spatial heterogeneity of small habitats, drought stress, high calcium, and pests and diseases. It should carry out the reasonable transformation of multi-species, appropriate trees for the right place, take native species as auxiliary species and appropriately increase the numbers of species of trees and shrubs so that the structure and function of each species are complementary. Build a rich diversity of AFS. In addition, configure decoy tree species and set up isolation zones; implement pruning, nurturing, truncation, and sanitary felling. The theory of creating AFS with multi-species configuration and the technique of implementing dynamic management of agroforestry ecosystem is developed. Strengthen the role of natural enemies and simultaneously carry out appropriate chemical and biological control measures. On the one hand, we should try to avoid the occurrence of harmful human interference and reduce the factors that cause AFS instability; on the other hand, we should strengthen the management of stand nurturing and ecosystem management, enhance the screening and trait improvement of highly resistant strains of trees, and fundamentally change the low-quality afforestation.

5. Conclusions

Our research has quantified the AFS structural characteristics by descriptive statistics and structural parameter calculation methods. The AFS stability in the KD evaluation index system was constructed using the fuzzy comprehensive evaluation method, the weights of each index were calculated by the entropy weight method, and the stability was evaluated and graded by establishing an evaluation set. The structure and stability influencing factors

were explored. The structure optimization and stability enhancement strategies were proposed to provide a reference basis for studying AFS's sustainable operation and service supply capability. The main conclusions are as follows:

(i) The species composition of the AFS in the KD control areas has a simple structure, the overall diversity level is low, and the diversity level of herbaceous plants is better than that of woody plants.
(ii) The overall distribution curves of diameter at breast height (DBH), tree height (TH), and crown width (CW) of woody plants in the AFS in the KD control areas were slight to the left, with a single-peaked pattern, mostly randomly and unevenly distributed in space, with a low degree of tree species isolation and relatively weak stand stability.
(iii) There is variability in the stability classes of different types of AFS, among which, in HG, it mainly shows the ranking in study areas of HJ (excellent) > SB (good) > BJ (fair); in ASV, it shows BJ (good) > HJ (fair) = SB (fair); in MWLs, it shows HJ (good) > SB (fair) > BJ (poor). Overall reflecting HG > ASV > MWLs.
(iv) When structural optimization was applied, corresponding measures can be taken according to farmers' wishes for different AFS and their primary business purposes. The improvement of stability depends mainly on the utility of structural optimization coupled with positive human interference (for example, pruning, dwarfing, and dense planting). This study provides a scientific reference for maintaining the stability and sustainable development of the AFS in the KD control areas.

Our study still needs to be improved in that the drivers of the structure and stability of AFS in KD control areas are not only biological and environmental interactions. Although anthropogenic disturbances were mentioned in our manuscript, no specific analysis was made. Further explanation of the effects of anthropogenic disturbances on KD-managed AFS is necessary for future studies.

Supplementary Materials: The following supporting information can be downloaded at https://www.mdpi.com/article/10.3390/f14040845/s1. Table S1: Geographical information of AFS sample sites; Table S2: Principles and description of the construction of the index system; Table S3: Stability evaluation index screening criteria and meaning; Table S4: AFS Stability evaluation indicators and their ecological significance; Table S5: Evaluation Indicators; Table S6: Evaluation index standard grading; Table S7: AFS plant composition and importance values; Table S8: Changes in ecosystem plant composition; Table S9: AFS species diversity index.

Author Contributions: Conceptualization, S.J.; methodology, S.J. and J.X.; software, S.J., and J.X.; validation, S.J.; formal analysis, S.J.; and J.X.; investigation, S.J., Y.Y., Y.H.; Z.W. and J.X.; resources, S.J.; data curation, S.J.; writing—original draft preparation, S.J.; writing—review and editing, S.J. and J.X.; visualization, S.J.; supervision, K.X.; project administration, K.X.; funding acquisition, K.X. All authors have read and agreed to the published version of the manuscript.

Funding: This study was supported by the Key Project of Science and Technology Program of Guizhou Province (No. 5411 2017 Qiankehe Pingtai Rencai), the China Overseas Expertise Introduction Program for Discipline Innovation (No. D17016), and the National Major Research and Development Program of China (2016YFC0502607).

Institutional Review Board Statement: Not applicable.

Informed Consent Statement: Not applicable.

Data Availability Statement: Our data are placed in the Supplementary Materials.

Acknowledgments: Thanks to Shuzhen Song and Xiaobi Wu for our guidance in the experiment.

Conflicts of Interest: The authors declare no conflict of interest.

References

1. IPBES. *Assessment Report on Land Degradation and Restoration: Summary for Policymakers IPBES Secretariat*; The Intergovernmental Science-Policy Platform on Biodiversity and Ecosystem Services: Bonn, Germany, 2018.
2. Millennium Ecosystem Assessment. *Ecosystem and Human Well-Being*; Island Press: Washington, DC, USA, 2005.

3. Vivian, V.; Luis, G.B.; Paige, W.; Eleanor, J.; Sterling, S.N. The role of coffee agroforestry in the conservation of tree diversity and community composition of native forests in a Biosphere Reserve. *Agric. Ecosyst. Environ.* **2014**, *189*, 154–163.
4. FAO. *Agroforestry for Landscape Restoration: Exploring the Potential of Agroforestry to Enhance the Sustainability and Resilience of Degraded Landscapes*; Food, and Agriculture Organization of the United Nations: Rome, Italy, 2017. [CrossRef]
5. Santos, M.; Cajaiba, R.L.; Bastos, R.; Gonzalez, D.; Petrescu Bakış, A.L.; Ferreira, D.; Mosquera-Losada, M.R. Why do agroforestry systems enhance biodiversity? Evidence from habitat amount hypothesis predictions. *Front. Ecol. Evolut.* **2022**, *9*, 1008. [CrossRef]
6. Jose, S. Agroforestry for ecosystem services and environmental benefits: An overview. *Agrofor. Syst.* **2009**, *76*, 1–10. [CrossRef]
7. Bayala, J.; Wallace, J.S. Tree-crop interactions: Agroforestry in a changing climate. In *The Water Balance of Mixed Tree-Crop Systems*; CABI: Wallingford, UK, 2015; pp. 146–190.
8. Jose, S.; Udawatta, R.P. Agroforestry for Ecosystem Services: An Introduction. In *Agroforestry and Ecosystem Services*; Udawatta, R.P., Jose, S., Eds.; Springer: Cham, Switzerland, 2021; pp. 1–17.
9. Hu, Y.H.; Chen, Q.B.; Zhou, Z.D. *Ecological Engineering of Tropical Agroforestry Complexes*; China Forestry Press: Beijing, China, 2006.
10. Marais, Z.E.; Baker, T.P.; O'Grady, A.P.; England, J.R.; Tinch, D.; Hunt, M.A. A Natural Capital Approach to Agroforestry Decision-Making at the Farm Scale. *Forests* **2019**, *10*, 980. [CrossRef]
11. Xiao, J.; Xiong, K. A review of agroforestry ecosystem services and its enlightenment on the ecosystem improvement of the karst desertification control. *Sci. Total Environ.* **2022**, *852*, 158538. [CrossRef]
12. Chen, H.; Zhu, D.Y.; Chen, H.; Wen, Y.Q. Impact of agroforestry on soil environment in rocky desertification areas and its application. *World For. Res.* **2019**, *32*, 13–18.
13. Wu, Q.; Liang, H.; Xiong, K.; Li, R. Eco-benefits coupling of agroforestry and soil and water conservation under KRD environment: Frontier theories and outlook. *Agrofor. Syst.* **2019**, *93*, 1927–1938. [CrossRef]
14. Marais, Z.E.; Thomas, P.; Baker, M.A.; Hunt, D.M. Shelterbelt species composition and age determine structure: Consequences for ecosystem services. *Agric. Ecosyst. Environ.* **2022**, *329*, 107884. [CrossRef]
15. Jiang, S.; Xiong, K.; Xiao, J. Structure and Stability of Agroforestry Ecosystems: Insights into the Improvement of Service Supply Capacity of Agroforestry Ecosystems under the Karst Rocky Desertification Control. *Forests* **2022**, *13*, 878. [CrossRef]
16. Li, W.H.; Lai, S.D. *Agroforestry Complex Management in China*; Science Press: Beijing, China, 1994; pp. 20–21.
17. António, C.B.S.; Obieze, C.; Jacinto, J.; Maquia, I.S.A.; Massad, T.; Ramalho, J.C.; Ribeiro, N.S.; Máguas, C.; Marques, I.; Ribeiro-Barros, A.I. Linking Bacterial Rhizosphere Communities of Two Pioneer Species, *Brachystegia boehmii* and *B. spiciformis*, to the Ecological Processes of Miombo Woodlands. *Forests* **2022**, *13*, 1840. [CrossRef]
18. Deheuvels, O.; Avelino, J.; Somarriba, E.; Malezieux, E. Vegetation structure, and productivity in cocoa-based agroforestry systems in Talamanca, Costa Rica. *Agric. Ecosyst. Environ.* **2012**, *149*, 181–188. [CrossRef]
19. Notaro, M.; Deheuvels, O.; Gary, C. Participative design of the spatial and temporal development of improved cocoa agroforestry systems for yield and biodiversity. *Eur. J. Agron.* **2022**, *132*, 126395. [CrossRef]
20. Feng, Z.W.; Wang, X.K.; Wu, G. *Structure and Function of Agroforestry Systems: A Study of the Northern Part of Henan and Huaihai Plain*; China Science and Technology Press: Beijing, China, 1992.
21. Ripoche, A.; Autfray, P.; Rabary, B.; Randriamanantsoa, R.; Blanchart, E.; Trap, J.; Sauvadet, M.; Becquer, T.; Letourmy, P. Increasing plant diversity promotes ecosystem functions in rainfed rice-based short rotations in Malagasy highlands. *Agric. Ecosyst. Environ.* **2021**, *320*, 107576. [CrossRef]
22. Lin, K.H.; Ye, G.F. A review of the stability of planted forest ecosystems. *J. Southwest For. Acad.* **2010**, *30*, 88–94.
23. Altieri, M.A.; Nicholls, C.I.; Henao, A.; Lana, M.A. Agroecology and the design of climate change-resilient farming systems. *Agron. Sustain. Dev.* **2015**, *35*, 869–890. [CrossRef]
24. Qin, Y. *Strategies for Optimizing the Structure and Improvement the Stability of Forest Ecosystem in Karst Desertification Control*; Guizhou Normal University: Guiyang, China, 2022.
25. Ford, D.C.; Williams, P.W. *Karst Hydrogeology and Geomorphology*; Wiley: Hoboken NJ, USA, 2007; p. 1.
26. Cao, J.; Yuan, D.; Pei, J. *Karst Ecosystems in Southwest China Constrained by Geological Conditions*; Geological Press: Beijing, China, 2005.
27. Kranjc, A. Dinaric karst: An example of deforestation and desertification of lime rocky terrain. In *Deforestation Around the World*; Moutinho, P., Ed.; Intech Open: London, UK, 2012; pp. 73–94.
28. Sunkar, A. Deforestation and rocky desertification processes in Gunung Sewu karst landscape. *Media Konserv.* **2008**, *13*, 1–7.
29. Xiong, K.N.; Chi, Y.K. Problems and countermeasures facing karst ecosystems in southern China. *Ecol. Econ.* **2015**, *31*, 23–30.
30. Febles González, J.M.; Febles Díaz, J.M.; Sobrinho, N.M.B.A.; Tolón-Becerra, A.; Lastra-Bravo, X.; Botta, G.F. Resilience of Red Ferralitic soils in the karst regions of Mayabeque Province, Cuba. *Land Degrad. Dev.* **2019**, *30*, 109–116. [CrossRef]
31. Zuo, T.A.; Zhang, F.T.; Yu, S.J.; Li, J.; Fan, H.; Ye, D. Progress of research on rocky desertification poverty in karst areas of China. *China Karst* **2021**, *6*, 1–13.
32. Chen, H.S.; Yue, Y.M.; Wang, K.K. Comprehensive management of rocky desertification in a southwest karst region: Effectiveness, problems, and countermeasures. *China Karst* **2018**, *37*, 37.
33. Su, W.C.; Zhu, W.X. The connotation and concept of sustainable agricultural development in karst ecologically fragile areas of Guizhou. *Econ. Geogr.* **2000**, *05*, 75–79.

34. Mei, Z.M.; Xiong, K.N. The basic model of ecological reconstruction in the Karst mountains of Guizhou and its environmental benefits. *J. Guizhou Norm. Univ. Nat. Sci. Ed.* **2000**, *4*, 9–17.
35. Luo, D.; Xiong, K.; Wu, C.; Gu, X.; Wang, Z. Soil Moisture and Nutrient Changes of Agroforestry in Karst Plateau Mountain: A Monitoring Example. *Agronomy* **2022**, *13*, 94. [CrossRef]
36. Cui, L. *Technology, and Demonstration of Rock Desertification Land Preparation Based on Plant Diversity Restoration and Conservation*; Guizhou Normal University: Guizhou, China, 2016.
37. Liu, Q.S.; Chen, H.; Li, L.Z.; Wang, C.L.; Chen, J.; Yang, Y.W.; Zhang, H.M. Marginal effects of soil mite communities in agroforestry areas of rocky desertification management. *J. Appl. Environ. Biol.* **2020**, *26*, 370–377.
38. Xiong, K.; Li, P.; Zhou, Z.; An, Y.; Lv, T.; Lan, A. *Remote Sensing of Karst Rock Desertification: A Typical Study of GIS: Guizhou Province as an Example*; Geological Publishing House: Beijing, China, 2002.
39. Nair, P.K.R. Classification of an agroforestry system. *Agrofor. Syst.* **1985**, *3*, 97–182. [CrossRef]
40. Nair, P.K.R. *An Introduction to Agroforestry*; Kluwer Academic Publishers: Dordrecht, The Netherlands, 1993.
41. Zhang, Y.; Xiong, K.N.; Yu, Y.H.; Xu, M.; Cheng, W.; Tan, D.J. Characteristics of daily dynamics of soil respiration in three economic forests in karstic rocky desertification areas of southern China. *J. Cent. South Univ. For. Sci. Technol.* **2019**, *01*, 92–99.
42. Song, S.; Xiong, K.N.; Chi, Y.; Guo, W.; Liao, J. A review of research on degraded grassland improvement in the management of karstic rock desertification in southern China. *J. Domest. Anim. Ecol.* **2019**, *3*, 82–87, 96.
43. Yang, S.; Yu, Y.H.; Xiong, K.; Zhang, S.; LI, T.; Wang, Z.; Hu, T. Influence of soil nutrients on functional traits of pickled walnut in KD areas. *Guangxi Plant* **2022**, *6*, 927–937.
44. Fang, J.; Wang, X.; Shen, Z.; Tang, Z.; He, J.; Yu, D.; Guo, Z. Main contents, methods and technical specifications of plant community inventory. *Biol. Divers.* **2009**, *6*, 533–548.
45. Li, K.; Li, Z.J. *Methods of Soil Agrochemical Analysis*; China Agricultural Science and Technology Press: Beijing, China, 2019; pp. 33–41.
46. Liu, J.; Shen, Y.; Zhao, Z.; Zhao, G. A method for measuring surface rock exposure rate in rocky desert areas. *J. Mt. Sci.* **2018**, *6*, 973–980.
47. Zhu, Y.; Shao, M. Spatial distribution of surface rock fragment on hill-slopes in a small catchment in wind-water erosion crisscross region of the Loess Plateau. *Sci. Chin.* **2008**, *51*, 862–870. [CrossRef]
48. Hui, G. Angular scale-a structural parameter describing the distribution pattern of individual trees. *Sci. For.* **1999**, *1*, 25.
49. Li, J. Treasureday Oak Natural Secondary Forest Stand Structure Quantitative Analysis. Master's Thesis, Henan Agricultural University, Henan, China, 2008.
50. Sun, C.; Qin, F.; Yang, Z.; Dong, X.; Tai, H.; Ren, X. Study on the stability of typical artificial forest ecosystem in the Arsenic sandstone region based on information entropy. *Res. Soil Water Conserve.* **2021**, *6*, 90–97.
51. Zhang, L.; Li, S.; Miu, N.; Zeng, Y.; Li, J.; Wang, Y.; Sun, H. Stability evaluation of Chinese fir ecosystem based on information entropy in the pelvic region of Sichuan Province. *J. Cent. South Univ. For. Technol.* **2020**, *7*, 79–88.
52. Tang, C.Q.; Li, Y.H.; Zhang, Z.Y. Species diversity patterns in natural secondary plant communities and man-made forests in a subtropical mountainous karst area, Yunnan, SW China. *Mt. Res. Dev.* **2010**, *30*, 244–251. [CrossRef]
53. Du, Y.; Wu, C.; Zhou, S.; Huang, L.; Han, S.; Xu, X.; Ding, Y. Forest soil organic carbon density and its distribution characteristics along an altitud in algradient in Lushan Mountains of China. *J. Appl. Ecol.* **2011**, *7*, 1675–1681.
54. Sheng, M.; Xiong, K.; Cui, G.; Liu, Y. Plant diversity and soil physicochemical properties in karstic desertification areas of Guizhou. *J. Ecol.* **2015**, *2*, 434–448.
55. Cao, J.; Yuan, D.; Zhang, C.; Jiang, L. Karst ecosystems in southwest China constrained by geological conditions. *Earth Environ.* **2004**, *32*, 1–8.
56. Zhang, S.; Xiong, K.; Qin, Y.; Min, X.; Xiao, J. Evolution and determinants of ecosystem services: Insights from South China Karst. *Ecol. Indic.* **2021**, *133*, 108437. [CrossRef]
57. Zhang, J.; Huang, Y. Advances in the study of biodiversity and stability mechanisms. *J. Ecol.* **2016**, *13*, 3859–3870.
58. Condit, R.; Ashton, P.S.; Baker, P.; Bunyavejchewin, S.; Gunatilleke, S.; Gunatilleke, N.; Hubbell, S.P.; Foster, S.P.; Itoh, R.B.; LaFrankie, A.; et al. Spatial patterns in the distribution of tropical tree species. *Science* **2000**, *288*, 1414–1418. [CrossRef] [PubMed]
59. Li, Y.; He, J.; Yu, S. Spatial structures of different-sized tree species in a secondary forest in the early succession stage. *Eur. J. For. Res.* **2020**, *139*, 709–719. [CrossRef]
60. Sahle, M.; Saito, O.; Demissew, S. Characterization and mapping of inset-based home-garden agroforestry for sustainable landscape management of the Gurage socioecological landscape in Ethiopia. *Environ. Sci. Pollut. Res.* **2022**, *29*, 24894–24910. [CrossRef] [PubMed]
61. Williams, P.W. The role of the epi karst in karst and cave hydrogeology: A review. *Int. J. Speleol.* **2008**, *37*, 1–10. [CrossRef]
62. Sweeting, M.M. Reflections on the development of Karst geomorphology in Europe and a comparison with its development in China. *Z. Geomorphol.* **1993**, *37*, 127–136.
63. Li, S.; Ren, H.; Yao, X. Influence of land use patterns on the daily dynamics of environmental microclimate in karst areas. *J. Appl. Ecol.* **2009**, *20*, 387–395.
64. Xiong, K.N.; Xiao, J.; Zhu, D.Y. Advances in the study of agroforestry ecosystem services. *J. Ecol.* **2022**, *42*, 851–861.
65. Tilma, D.; Dowuin, J.A. Biodiversity and stability in grasslands. *Nature* **1994**, *367*, 363–365. [CrossRef]

66. Lehman, C.L.; Tilman, D. Biodiversity, stability, and productivity in competitive communities. *Am. Nat.* **2000**, *156*, 534–552. [CrossRef]
67. Loreau, L.; Mazancourt, C. Biodiversity and ecosystem stability: A synthesis of underlying mechanisms. *Ecol. Lett.* **2013**, *16*, 106–115. [CrossRef]
68. Li, Z.Y.; Ye, X.Z.; Wang, S.P. Ecosystem stability and its relationship with biodiversity. *J. Plant Ecol.* **2021**, *12*, 1127. [CrossRef]
69. Gross, K.; Cardinale, B.J.; Fox, J.W.; Gonzalez, A.; Loreau, M.; Wayne Polley, H. Species richness and the temporal stability of biomass production: A new analysis of recent biodiversity experiments. *Am. Nat.* **2014**, *183*, 1–12. [CrossRef]
70. Geng, S.; Shi, P.; Song, M.; Zong, N.; Zu, J.; Zhu, W. The diversity of vegetation composition enhances ecosystem stability along elevational gradients in the Taihang Mountains, China. *Ecol. Ind.* **2019**, *104*, 594–603. [CrossRef]
71. Ma, Z.; Liu, H.; Mi, Z.; Zhang, Z.; Wang, Y.; Xu, W.; He, J. Climate warming reduces the temporal stability of plant community biomass production. *Nat. Commun.* **2017**, *8*, 15378. [CrossRef]
72. Wu, Z.; Xiong, K.; Zhu, D.; Xiao, J. Revelation of Coupled Ecosystem Quality and Landscape Patterns for Agroforestry Ecosystem Services Sustainability Improvement in the Karst Desertification Control. *Agriculture* **2023**, *13*, 43. [CrossRef]
73. Hou, W.J.; Gao, J.B.; Peng, T.; Wu, S.H.; Dale, F. Progress of research on the vulnerability of karst ecosystems in southwest China under the structure-function-habitat framework. *Adv. Geosci.* **2016**, *03*, 320–330.
74. Guo, K.; Liu, C.; Dong, M. Ecological Adaptation of Karst Plants and Rock Desertification Management in Southwest China. *J. Pl. Ecol.* **2011**, *10*, 991–999.
75. Song, T.Q.; Peng, L.X.; Du, H.; Wang, K.L.; Zeng, F.P. Spatial and temporal evolution characteristics, occurrence mechanism and regulation measures of karstic desertification in southwest China. *J. Ecol.* **2014**, *34*, 5328–5341.
76. He, F.Y.; Xiong, K.N.; Zhu, D.Y. Research progress on moisture effects of agroforestry in karst mountains. *China Forage* **2020**, *07*, 22–27.
77. Li, S.; Ren, H.; Xue, L.; Chang, J.; Yao, X. Influence of bare rocks on surrounding soil moisture in the karst rocky desertification regions under drought conditions. *Catena* **2014**, *116*, 157–162. [CrossRef]
78. Li, S.; Xue, L.; Wang, J.; Ren, H.; Yao, S.; Leng, X.; Wu, Z. Surface temperature and air temperature and humidity dynamics of bare rock in rocky desertification areas. *J. Ecol.* **2019**, *2*, 436–442. [CrossRef]

forests

MDPI

Article

Temporal and Spatial Variations in Carbon/Nitrogen Output in the Karst Critical Zone and Its Response to the Forest Ecosystem of Karst Desertification Control

Chenpeng Hu [1,2], Ziqi Liu [1,2], Kangning Xiong [1,2,*], Xiaoxi Lyu [1,2], Yuan Li [1,2] and Renkai Zhang [1,2]

[1] School of Karst Science, Guizhou Normal University, Guiyang 550001, China
[2] State Engineering Technology Institute for Karst Desertification Control, Guiyang 550001, China
* Correspondence: xiongkn@gznu.edu.cn

Abstract: Rocky desertification is a common phenomenon in karst areas. Soil carbon and nitrogen storage is of great significance to the formation and evolution of ecosystems. Soil leakage is one of the important indicators in evaluating ecosystem stability. There are few studies on the response of carbon and nitrogen leakage below the surface of karst critical zones to forest ecosystems. The karst springs in the study area of Shibing Heichong, Bijie Salaxi and Guanling-Zhenfeng Huajiang in Guizhou, China, were selected to determine the variation characteristics of carbon and nitrogen content and karst spring outputs and their response to soil leakage. The results showed the following: (1) The content and output of carbon and nitrogen in karst springs in the three study areas showed obvious spatial differences. The carbon and nitrogen output of karst spring water was mainly concentrated in the rainy season. The carbon and nitrogen contents and output of karst springs in the Shibing Heichong study area were higher than those in the Bijie Salaxi and Guanling-Zhenfeng Huajiang study areas. (2) The carbon and nitrogen outputs of karst springs were mainly affected by flow. Land cover and land use in forests affect the carbon and nitrogen contents of karst springs and thus affect the output. (3) The higher the soil leakage of the karst spring was, the higher the carbon and nitrogen output. The leakage of the overlying soil in the Shibing Heichong study area was high, but the soil decline was small, and the stability of the forest ecosystem was relatively good. In summary, a lower degree of rocky desertification results in higher leakage from karst springs and higher risks of soil leakage; however, the ecosystem was relatively stable. Evaluating forest soil carbon and nitrogen loss and ecosystem stability in karst areas through the nutrient output of karst springs is of great significance for the prevention and control of rocky desertification areas.

Keywords: karst spring; soil; dissolved organic carbon/nitrogen; rocky desertification; terrestrial ecosystem

Citation: Hu, C.; Liu, Z.; Xiong, K.; Lyu, X.; Li, Y.; Zhang, R. Temporal and Spatial Variations in Carbon/Nitrogen Output in the Karst Critical Zone and Its Response to the Forest Ecosystem of Karst Desertification Control. *Forests* **2023**, *14*, 1121. https://doi.org/10.3390/f14061121

Academic Editors: Thomas H. DeLuca and Timothy A. Martin

Received: 5 March 2023
Revised: 4 May 2023
Accepted: 11 May 2023
Published: 29 May 2023

1. Introduction

Earth's critical zone refers to a heterogeneous near-surface environment that vertically covers various spheres, including plant canopies, soil layers, air envelopes and aquifers, and is a key area for human survival and the functioning of Earth's ecosystems [1,2]. The Earth's critical zone is at the intersection of the atmosphere, biosphere, lithosphere, soil sphere and hydrosphere. The input of solar energy, as well as atmospheric processes and their gases and sediments, interact with biota, soil and rocks to provide ecosystem services. The hydrosphere cannot be divided as precisely as other spheres, and the hydrological cycle connects every link in the Earth's critical zone [1,3]. The hydrological cycle is also accompanied by material and energy transfer [2]. Approximately 10 to 15% of the Earth's land is covered by karst landforms, which are home to a quarter of the world's population [4]. The karst region of Southwest China, with the karst plateau of Guizhou as the centre, covers an area of more than 550,000 km^2 and is one of the three major continuous karst regions in the world. It is in the subtropical monsoon climate zone and has sufficient

hydrothermal conditions and geological conditions, making this area the most complex, typical and diverse karst region in tropical and subtropical karst development in China and even the world [5]. Due to the extremely fragile karst ecological environment and unsustainable human activities in the local area, soil erosion is serious, resulting in bare surface bedrock and a poor rocky desertification environment. Critical zones of the earth control the surface ecological environment, change the surface morphology and stabilize life resources mainly through the process of rock weathering and soil formation. The karst critical zone is a type of critical zone developed against the background of carbonate rocks. The karst critical zone has the characteristics of a fast rock weathering rate and a slow soil formation rate [6], which are different from other areas. Its ecological environment is fragile, material energy exchange is frequent, and ecological and biogeochemical processes are extremely sensitive to climate change [7].

The year 2015 was the International Year of Soil, indicating the global importance of soil in ecosystem sustainability [8]. Soil not only facilitates many ecological processes but is also an important component of terrestrial ecosystems. Carbon and nitrogen storage in the soil is also very important for terrestrial ecosystems. Soil nitrogen storage is closely related to soil organic carbon storage [9,10]. Nitrogen deficiency affects plant growth and forest ecosystem stability [11,12]. Soil carbon and nitrogen content is affected by the dynamic balance of input and output [13], as well as the quantity and quality of litter, microorganisms and environmental factors [14–17]. The unique geological background and hydrological process in karst areas create a fragile ecosystem that is sensitive to human disturbance [18–20]. Different land use patterns will affect the soil carbon and nitrogen contents in forests. Compared with non-karst areas, forest ecosystems in karst areas are more sensitive. Different land use patterns have an impact on the basin, and deforestation increases the concentration and flux of dissolved organic carbon in surface water [21,22]. Previous research has demonstrated that soil C:N and tree species have a considerable influence on nitrogen release in forest watersheds [23]. The hydrological process of forest ecosystems includes the hydrological regulation process of the forest canopy, litter layer and soil layer [24]. Litter is a participant in the nutrient and hydrological cycle of forest ecosystems [25,26]. Spring water serves as an outlet for underground forest catchments and is used to monitor groundwater and interflow-related processes in headwaters and material flows in biogeochemical cycles [27]. Karst springs are the final manifestation of the results of groundwater lithospheric circulation in karst critical zones [28]. In karst regions, karst stores CO_2 in the atmosphere and soil as dissolved inorganic carbon (DIC) in karst water bodies [29]. Dissolved organic carbon (DOC) is not only an important component of organic carbon in water bodies but also an important component of the activated carbon pool in karst ecosystems [30,31]. Until now, research on carbon and nitrogen in water bodies has mainly focused on aquatic ecosystems. DOC is particularly important for organisms in water bodies and is the main source of energy [32]. While carbon and nitrogen in water are affected by organisms, environmental factors such as overlying vegetation, land use topography and hydrology will also affect the source, nature, distribution and migration of carbon and nitrogen in water bodies. Karst spring water is an important node of the carbon and nitrogen cycle and the output port of nutrient leakage, and it is also a typical medium for analysing the process and mechanism of the key carbon and nitrogen cycle of karst. The spring water in the karst key zone's central part was used to study the carbon and nitrogen output law and its influencing factors, as well as to reveal the relationship between carbon and nitrogen nutrient output and soil leakage in the forest ecosystem of rocky desertification control.

Karst desertification areas in southern China face serious problems such as soil erosion, soil nutrient loss and water scarcity. In the mountainous area of the Guizhou Plateau, which is representative of the overall structure of the karst ecological environment type in the south, Guanling-Zhenfeng Huajiang, Bijie Salaxi and Shibing Heichong were selected as the research areas. In this study, the carbon and nitrogen contents of karst spring water and overlying soil in the forests of the three study areas are assessed. The main objectives

of this study are as follows: (1) to understand the variation characteristics of carbon and nitrogen content and output of karst spring water in this area, (2) to determine the factors influencing the carbon and nitrogen content and output in karst springs, and (3) to evaluate the response of karst spring water carbon and nitrogen output to surface forest ecosystems. This study can provide a scientific basis and theoretical support for karst underground leakage control and comprehensive management of rocky desertification.

2. Materials and Methods

2.1. Study Area

The selected demonstration areas are in the northwest and southwest of the Guizhou Plateau, and the karst landforms are widely developed and typical, representative of the landforms of plateau mountains, plateau canyons and mountain canyons of the karst plateau. The Bijie Salaxi Demonstration Area belongs to the karst plateau mountainous potential-mild rocky desertification area, and the Guanling-Zhenfeng Huajiang demonstration area belongs to the medium-intensity rocky desertification area of the karst plateau canyon and the no-potential rocky desertification area of the Shibing Heichong karst mountain canyon, which is typical of rocky desertification type areas in Guizhou and even the whole country (Figure 1).

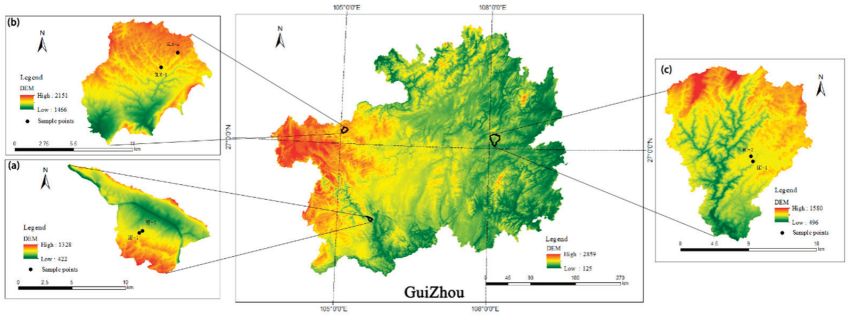

Figure 1. Overview of study area ((**a**) is Guanling-Zhenfeng Huajiang study area, (**b**) is Bijie Salaxi study area, (**c**) is Shibing Heichong study area).

The Guanling-Zhenfeng Huajiang Demonstration Area is a karst plateau canyon with an annual rainfall of 1052 mm, most of which forms surface runoff into the river; a small part enters groundwater, and the source of drinking and irrigation is mainly spring water. The rocky desertification control demonstration area of the Guanling-Zhenfeng Huajiang Plateau Canyon is in the slope area from the cattle farm basin to the Beipan River Gorge, and the Beipan River constitutes the erosion datum of the entire area. The lithology is mainly Middle and Upper Triassic limestone and grey matter dolomite, the soil erosion problem is serious, and the rocky desertification grade is primarily medium and intense. The Bijie Salaxi demonstration area belongs to the karst plateau mountainous area and has a potential-mild rocky desertification grade, with an annual rainfall of 984 mm and a lack of water resources. In terms of geology and geomorphology, the Bijie Salaxi Plateau Mountain Rocky Desertification Control Demonstration Area is in the upper reaches of the Wujiang River Basin in the transition slope zone from the Eastern Yunnan Plateau to the Qianzhong Mountain Plain Hills, with large undulating terrain, mainly peaks, troughs and hilly depressions. The outcropping rock layer is mainly the middle and thick limestone of the Lower Permian, the groundwater level is shallow, and the soil is primarily limestone. Shibing Karst Plateau trough valley no-potential rocky desertification area, annual rainfall of 1130 mm, sufficient water resources, high utilization rate of water resources, agriculture and tourism developed. The Shibing Karst Demonstration Area is in northern Shibing County, Guizhou Province, on the slope of the transition from the Qianzhong Mountains

to Xiangxi Hills, which belongs to a typical dolomite karst and has typical and complete geomorphological development.

The lithology of HJ-1 and HJ-2 in the Guanling-Zhenfeng Huajiang study area is mainly dolomite limestone, with a high exposure rate of surrounding rocks and low vegetation coverage. There are sparse low shrubs on both sides of HJ-1, and pepper is planted. The overlying land is primarily used for corn planting, and the spring area is 0.05 km^2. HJ-2 is surrounded by herbs, with the left and right sides of the pepper forest, thin and very little overlying soil, scattered tall shrubs, and a spring area of 0.06 km^2. The lithology of SLX-1 and SLX-2 in the Bijie Salaxi study area is limestone. SLX-1 is located at the foot of the mountain, surrounded by herbaceous plants, and covered with tall shrubs, and the secondary vegetation on the slope is mainly secondary vegetation. The closer to the steep slope, the higher the rock exposure rate, and the spring area is 0.08 km^2. SLX-2 is located at the bottom of the depression at the foot of the mountain. The overlying vegetation is mainly grass and shrub, with a small amount of exposed rock, surrounding depressions or slopes, and the spring area is 0.11 km^2. The lithology of HC-1 and HC-2 in the Shibing Heichong study area is dolomite. HC-1 is in the depression, and pine forests are distributed in the surrounding mountains. The overlying land is mainly used for planting tobacco, and there is a small area of artificially planted peach trees. The spring area is 0.12 km^2; HC-2 is surrounded by farmland, mainly rice farms, and the overlying land is also planted with corn. The spring area is 0.13 km^2.

2.2. Sample Collection and Preparation

2.2.1. Sampling and Pre-Treatment

From July 2020 to June 2021, karst spring water samples were collected and monitored monthly. A 100 mL polyethylene bottle, nitric acid and mercuric chloride solution were used for water sample collection and flow monitoring. Spring water samples were collected, a 100 mL polyethylene bottle was used to test soluble organic carbon, and a 100 mL polyethylene bottle was used for TN and NO_3-N. Each sample was collected and covered with a sealing film, sealed with Parafilm, and stored at 4 °C. Water level meters (HOBO U20, Onset, Bourne, MA, USA) were installed near karst springs. The monitoring frequency of the recorder was 30 min/time, and the runoff was monitored by the water level metre. The overlying soil of karst spring water under different rocky desertification conditions was collected in the rainy season and dry season. According to the principle of uniform distribution and representativeness, three soil profiles were selected in the overlying environment of spring water for soil collection. Before sampling, 1 kg of chemical soil was collected to determine the chemical properties of soil soluble organic carbon and nitrate nitrogen, with litterfall removed. The depth of soil collection in the Guanling-Zhenfeng Huajiang study area was 0 to 15 cm, the depth of soil collection in the Bijie Salaxi study area was 0 to 25 cm, and the depth of soil collection in the Shibing Heichong study area was 0 to 30 cm.

2.2.2. Laboratory Analysis

In the process of field sample collection, a HQ40d portable water quality analyser (HACH, Loveland, CO, USA) was used to test water temperature, pH and conductivity, and an alkalinity metre (Merck, Darmstadt, Germany) was used to titrate HCO_3^- on site and record. The soil samples were dried at 60 °C for 48 h, passed through a 0.25 mm sieve, and acidified with 1 mol L^{-1} HCl for analysis of soil soluble organic carbon. The sieved soil sample was added to super pure water, shaken and centrifuged for NO_3-N analysis. The water samples were filtered and tested for nitrate nitrogen and total nitrogen by a flow analyser (SYSTEA, Zona Industriale Paduni-Selciatella, Italy). DOC was measured using a TOC analyser (multi N/C 3100, Analytik Jena, Jena, Germany).

2.3. Data Analysis

2.3.1. Estimation of Carbon and Nitrogen Output from Karst Springs [33]

The monthly soluble organic carbon output (Fi_{DOC}) was calculated as follows:

$$Fi_{DOC} = Ci_{DOC} \times Qi \times Di \times 24 \times 60 \times 60 \quad (1)$$

where Ci_{DOC} is the *i*-month carbon-nitrogen output (mg), C*i* is the *i*-month carbon-nitrogen content (mg L^{-1}), Q*i* is the *i*-month flow rate (mL/s), and D*i* is the *i*-month number of days (d). The monthly output of DIC, TN, and NO_3-N was calculated in the same way.

In this study, the total one-year carbon and nitrogen output Fs_{DOC} was determined as follows:

$$Fs_{DOC} = \sum_{i=1}^{n} Fi_{DOC} \quad (2)$$

where Fi_{DOC} represents the monthly soluble organic carbon output (mg). The annual output of DIC, TN, and NO_3-N was calculated in the same way.

2.3.2. Soil Carbon and Nitrogen Stocks [34]

The soil carbon and nitrogen density (DOCD) of each layer was calculated as follows:

$$DOCDi = DOCi \times B \times Di \times 10^{-2} \quad (3)$$

where DOCD*i* is the organic carbon density of layer *i* (kg/m^2), DOC*i* is the soluble organic carbon content of layer *i* (g/kg), bulk density (g/cm^3), and D*i* is the depth of layer *i* (cm). The NO_3-N density (DNO_3-N) was calculated in the same way

In this study, the total DOCS determination method of the spring area was as follows:

$$DOCS = \sum_{i=1}^{n} DOCDi \times Si \quad (4)$$

where DOCS represents the total soluble organic carbon storage of soil in the plot (kg C), DOCD*i* represents the soluble organic carbon density of layer I (kg/m^2), and S*i* represents the soil area (m^2). NO_3-N RESERVES (NO_3-NS) were calculated in the same way.

2.4. Statistical Analysis

Excel 2019 (Microsoft Corporation, Albuquerque, NM, USA) was used to complete the statistical analysis. Origin2021b for drawing (OriginLab, Northampton, MA, USA) and Origin2021b were used for correlation analysis plotting. Statistical significance was defined as $p < 0.05$, and Spearman correlation analysis was used to determine the relationship between carbon and nitrogen output and carbon and nitrogen content, flow rate and water physical and chemical parameters. The study area was mapped using ArcGIS 10.7 (ESRI, RedLands, CA, USA).

3. Results

3.1. Carbon and Nitrogen Content and Category of Karst Spring Water

The DIC of HC-2 reached a maximum of 474 mg/L in November. That of SLX-2 reached a minimum of 174 mg/L in December. The DIC concentration in the karst spring water in the Shibing Heichong study area was 300~474 mg/L, which was significantly higher than that in the Guanling-Zhenfeng Huajiang study area and the Bijie Salaxi study area (Figure 2). The dissolved organic carbon (DOC) of HJ-2 reached a maximum value of 5.11 mg/L in October. The DOC of SLX-2 reached a minimum value of 1.60 mg/L in June. The concentration of DOC in the spring water in the Guanling-Zhenfeng Huajiang study area ranged from 2.01 to 5.11 mg L^{-1}, which was higher than that in the Bijie Salaxi study area and Shibing Heichong study area. The total nitrogen (TN) of HJ-1 reached a maximum value of 3.19 mg/L in October. The TN of HJ-2 reached a minimum value

of 0.35 mg/L in November. The nitrate nitrogen (NO_3-N) reached a maximum value of 2.38 mg/L in April. The NO_3-N of HJ-2 reached a minimum value of 0.33 mg/L in September. The concentrations of TN and NO_3-N in spring water in the Shibingheichong study area were 1.15–2.65 mg/L and 1.12–2.38 mg/L, respectively, which were significantly higher than those in the Guanling-Zhenfeng Huajiang study area and Bijie Salaxi study area. The carbon and nitrogen contents of the spring water in the study area of the Guanling-Zhenfeng Huajiang River changed greatly, and the carbon and nitrogen contents of the spring water in the Bijie Salaxi study area changed slightly (Figure 2).

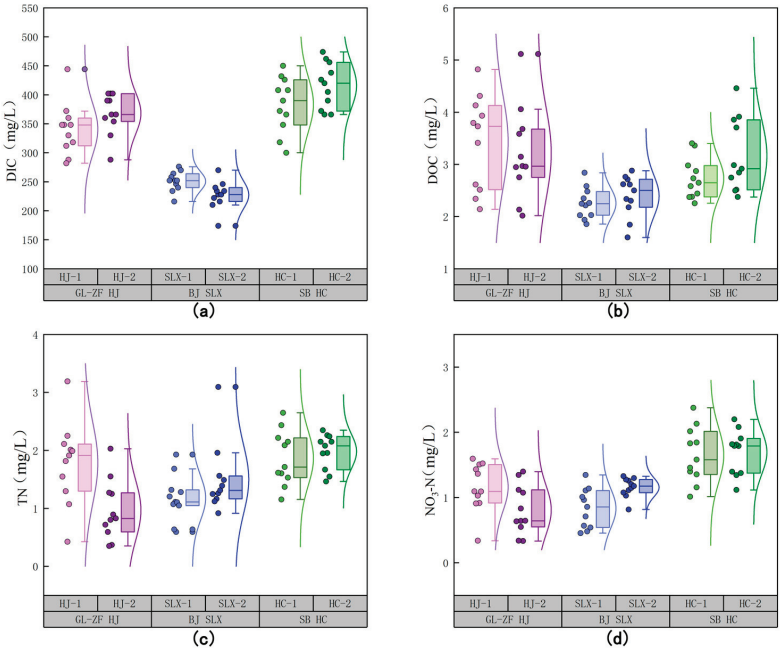

Figure 2. Comparison of DIC (**a**), DOC (**b**), TN (**c**) and NO_3-N (**d**) contents in karst spring water in the Guanling-Zhenfeng Huajiang Research Area, Bijie Salaxi Research Area and Shibing Heichong Research Area.

3.2. Flow Change Characteristics of Karst Springs

In the three study areas, the changes in karst spring flow showed obvious spatial and temporal differences (Figure 3). In the Guanling-Zhenfeng Huajiang study area, the overall flow rate of spring water was small, ranging from 11.15 mL/s to 101.63 mL/s, and the variation was small. The HJ-1 flow (42.10 mL/s) was slightly smaller than that of HJ-2 (45.72 mL/s), exhibited an upwards trend from July to October and from March to June, and stopped during the dry season. In the study area of Bijie Salaxi, the overall flow rate of spring water was 20.64 mL/s to 313.20 mL/s. The SLX-2 flow (154.16 mL/s) was larger than that of SLX-1 (117.67 mL/s), showing a downwards trend from July to August, an upwards trend from August to September and April to June, and a discontinuous trend in November, January and February during the dry season. In the Shibing Heichong study area, the overall flow rate of spring water was 13.08 to 527.03 mL/s, with a large variation. The HC-1 flow (131.24 mL/s) was slightly smaller than that of HC-2 (237.23 mL/s), showing a downwards trend from May to June, July to August, and September to January, an upwards trend from August to September and March to May, and a discontinuous trend in February during the dry season. In one hydrological year, the measured flow of karst springs was 43.91 mL/s (average) in the Guanling-Zhenfeng Huajiang study area, 135.92 mL/s (average) in the Bijie Salaxi study area, and 184.23 mL/s (average) in the Shibing Heichong study area.

From the measured flow rate, the monthly flow rate varied greatly; the maximum monthly flow was 527.03 mL/s (Shibing Heichong Research Area), and the minimum monthly flow was 11.15 mL/s (Guanling-Zhenfeng Huajiang Research Area). The monthly flow of karst springs in the Shibing Heichong Research Area was large, and the interruption time was short, while the monthly flow of karst springs in the Guanling-Zhenfeng Huajiang Research Area was small, and the interruption time was long. Atmospheric precipitation is the main source of groundwater recharge in spring basins [35,36]. In the three study areas, rainfall decreased at different times, and flow also decreased rapidly. The results showed that the trends of rainfall and flow were consistent (Figure 3). From April to June, the rainfall in the Bijie Salaxi study area increased from 84.8 mm to 234.60 mm, and the flow rates of SLX-1 and SLX-2 increased rapidly. The same phenomenon was observed in other study areas, indicating that the dynamic change in flow was sensitive to atmospheric precipitation.

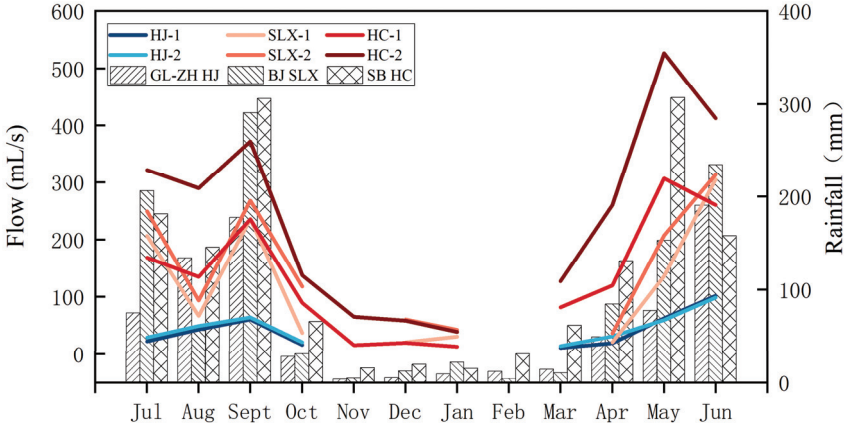

Figure 3. Trends of karst spring flow and rainfall.

3.3. Carbon and Nitrogen Contents in the Overlying Soil of Karst Springs

The contents of DOC and soil nitrate nitrogen (NO_3-N) in the overlying soil of the six karst springs showed a clear vertical change trend, that is, the surface layer > middle layer > lower layer (Figure 4). In the Guanling-Zhenfeng study area, the DOC content in the overlying soil of HJ-2 (9.76 mg/kg) was higher than that of HJ-1 (7.54 mg/kg), and the NO_3-N content was 7.13 mg/kg, which was less than that of HJ (7.96 mg/kg). The variation in the carbon and nitrogen contents in the soil of HJ-1 was greater than that of HJ-2. In the study area of Bijie Salaxi, the contents of DOC and NO_3-N in the overlying soil of SLX-2 were higher than those of SLX-1, and the change range was also greater than that of SLX-1. The contents of DOC and NO_3-N in the soil overlying HC-2 were higher than those of HC-1. In the three study areas, soil DOC and NO_3-N also showed obvious spatial characteristics, that is, Shibingheichong study area > Bijie Salaxi study area > Guanling-Zhenfenghuajiang study area. Additionally, the soil DOC content was higher in the dry season than in the rainy season. In the Guanling-Zhenfeng Huajiang research area and Shibing Heichong research area, the NO_3-N content in the overlying soil of the karst spring was higher in the rainy season than in the dry season (Figure 4).

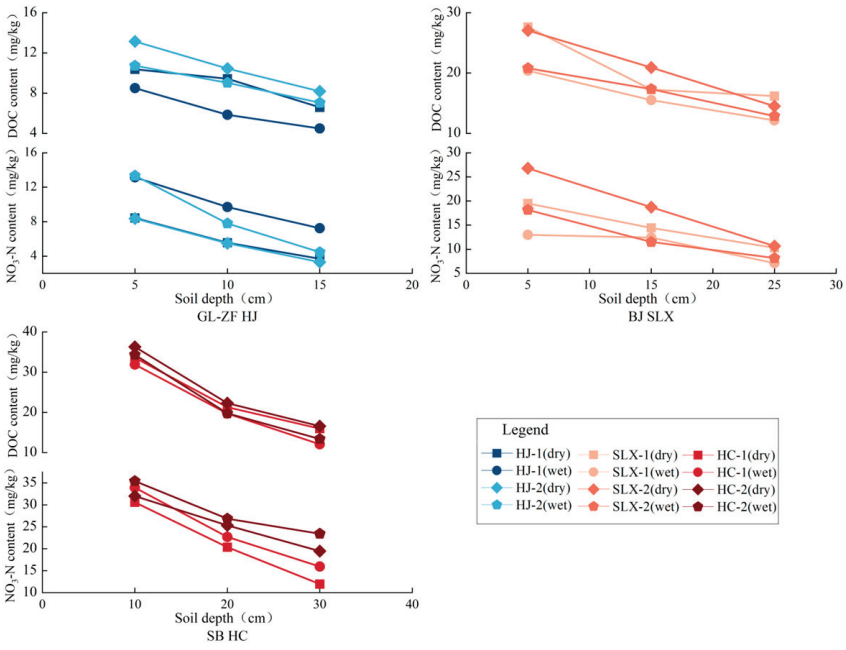

Figure 4. Comparison of DOC and NO_3-N contents in overlying soil of karst springs in Guanling-Zhenfeng Huajiang Research Area, Bijie Salaxi Research Area and Shibing Heichong Research Area.

3.4. Carbon and Nitrogen Output of Karst Springs

In the three study areas, the carbon and nitrogen outputs of karst spring water exhibited obvious spatial and temporal differences (Figure 5). The maximum monthly carbon and nitrogen output of karst springs occurs during the rainy season, and the output is also concentrated in summer and autumn. Karst spring water in the Bijie Salaxi Research Area accounted for the highest proportion of carbon and nitrogen output in summer and autumn at 71% to 80%. The maximum was reached in June 2021, with DOC fluxes of SLX-1 and SLX-2 of 1.60 kg and 1.30 kg, DIC fluxes of 213.47 kg and 189.96 kg, TN fluxes of 1.01 kg and 1.21 kg, and NO_3-N fluxes of 0.90 kg and 1.05 kg, respectively. The carbon and nitrogen outputs in the Guanling-Zhenfeng Huajiang Research Area and the Bijie Salaxi Research Area reached their highest values in June, and the carbon and nitrogen outputs in the Shibing Heichong Research Area reached their maximum values in May. The DOC fluxes of HC-1 and HC-2 were 1.79 kg and 2.67 kg, DIC fluxes were 246.68 kg and 397.61 kg, TN fluxes were 1.49 kg and 2.30 kg, and NO_3-N fluxes were 1.36 kg and 2.04 kg, respectively. During the dry season, the flow rate of karst springs continues to be low, and even the flow is interrupted to varying degrees, resulting in a low monthly output of carbon and nitrogen. In March of the dry season, the flow rate of HJ-2 (13.91 mL/s) in the Guanling-Zhenfeng Huajiang Study Area was slightly greater than that of HJ-1 (11.15 mL/s), but the nitrogen output of HJ-2 was slightly lower than that of HJ-1 because the nitrogen content of HJ-1 was higher than that of HJ-2. In this study, we observed that the seasonal variation characteristics of carbon and nitrogen fluxes in karst spring water were consistent with the research phenomenon of river flux in the Zhujiang River [37].

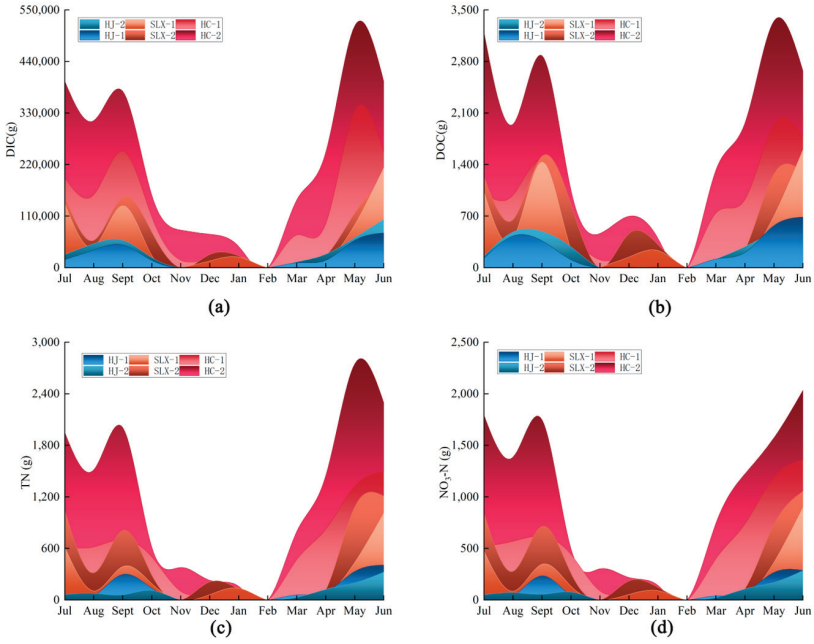

Figure 5. Monthly carbon and nitrogen output of karst springs ((**a**) is DIC monthly output. (**b**) is DOC monthly output. (**c**) is TN monthly output. (**d**) is NO_3-N monthly output.)

4. Discussion

4.1. Influencing Factors of the Carbon and Nitrogen Outputs of Karst Spring Water

The carbon and nitrogen outputs of karst springs also exhibited obvious spatial characteristics. The annual output of carbon and nitrogen in Shibing Heichong spring water is 1.25 to 4.71 times that of the Bijie Salaxi research area and 3.46~14.25 times that of the Guanling-Zhenfeng Huajiang research area. In the above, the flow rate and carbon and nitrogen output showed obvious spatial characteristics. There was a significant correlation between carbon and nitrogen output and the flow rate of karst spring water ($p < 0.001$), indicating that the carbon and nitrogen output of karst spring water was mainly affected by the flow. Previous studies have also shown that differences in nutrient flux were mainly due to differences in flow [38]. The annual carbon and nitrogen output of spring water in the Bijie Salaxi Research Area was 1.89, which was 5.24 times that of spring water in the Guanling-Zhenfeng Huajiang Research Area. In the Guanling-Zhenfeng Huajiang study area, the HJ-2 flow rate (45.71 mL/s) was slightly greater than that of HJ-1 (42.10 mL/s). The annual output of DOC and DIC (2.84 kg/a, 368.04 kg/a) of HJ-2 was higher than that of HJ-1 (2.62 kg/a, 278.73 kg/a), while the annual output of TN and NO_3-N (0.99 kg/a, 0.84 kg/a) of HJ-2 was slightly lower than that of HJ-1 (1.44 kg/a, 1.05 kg/a). In the Guanling-Zhenfeng Huajiang study area, the difference in karst spring flow was small, and the nitrogen output of HJ-2 was lower than that of HJ-1 due to the influence of carbon and nitrogen content. As shown in Figure 6, there was a significant correlation between carbon and nitrogen content and output ($p < 0.01$), and the output was also affected by the content. The carbon and nitrogen output of karst springs is mainly affected by the flow rate, followed by the carbon and nitrogen content.

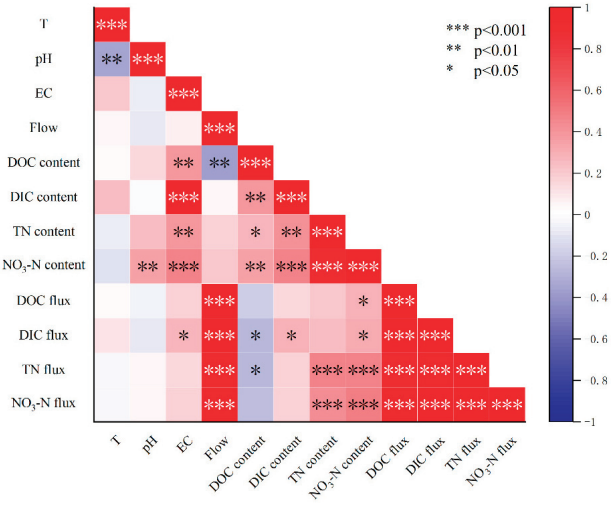

Figure 6. Spearman correlation coefficient of carbon and nitrogen output, carbon and nitrogen content and water chemical parameters in karst springs.

We found that karst spring water carbon and nitrogen output was mainly affected by the flow. The karst spring water in the three study areas had different degrees of disconnection. For the Shibing Heichong study area, the cut-off time was shorter, and the flow was much higher than that in the other two study areas. Thicker soil, higher vegetation coverage, soil cover and vegetation litter can also improve soil water retention and water storage capacity [39] and increase field water holding capacity and soil water content, which is conducive to the continuity of spring water flow. The Guanling-Zhenfeng Huajiang study area belongs to the karst plateau canyon with a steep slope (22°–30°), resulting in groundwater infiltration [40,41], and low vegetation coverage leads to poor rainfall interception [42]. Therefore, the karst spring water flow in the study area is 43.91 mL/s (mean), and the cut-off time is longer.

4.2. Influencing Factors of the Carbon and Nitrogen Contents of Karst Spring Water

The contents of DIC, TN and NO_3-N in the karst spring were much higher than those in the Guanling-Zhenfeng Huajiang study area and Bijie Salaxi study area. DIC in karst spring water is mainly composed of dissolved CO_2, H_2CO_3, HCO_3^- and CO_3^{2-} [43]. When the pH in the water body is between 6.35 and 9.33 and is weakly alkaline, the DIC in the water body is mainly HCO_3^- [44]. In field tests of spring water in the three study areas, CO_3^{2-} values were lower and free CO_2 content in the water was also small, so DIC levels in the study areas could be expressed by HCO_3^- concentrations. The concentration of DIC in karst spring water in the Shibing Heichong research area ranged from 300 to 474 mg/L, which was significantly higher than that in the Huajiang Research Area and Salaxi Research Area. DIC in karst areas is mainly affected by carbonate rocks, and the solubility of different carbonate rocks is also different. The lithology of the Shibing Heichong Research Area is dolomite, the lithology of the Bijie Salaxi Research Area is limestone, and the lithology of the Guanling-Zhenfeng Huajiang Research Area is grey dolomite [33,45]. The litter of vegetation in the Shibing-Heichong study area had relatively stable nutrient input [46–48], which maintained the stability of the soil carbon and nitrogen contents, so the soil carbon and nitrogen contents were significantly higher than those of the other study areas (Figure 4). The differences in the DOC, TN and NO_3-N contents in spring water in the Shibing Heichong study area were relatively small.

A higher degree of rocky desertification limits the growth of plants, resulting in a fragile ecosystem [49–51]. The vegetation and soil coverage in the Guanling-Zhenfeng

Huajiang study area of moderate-intensity rocky desertification were low. The vegetation types were mainly economic crops, corn, pepper, loquat seedlings, etc., and the planting mode was relatively simple. The ecosystem was relatively fragile, and the soil carbon and nitrogen contents were low. At the same time, farming leads to small and large differences in the carbon and nitrogen contents in spring water (Figure 2). Areas with low rocky desertification provide a better environment for vegetation survival and more plant species due to low degradation, and the species richness in these areas is higher than that in areas with high rocky desertification [52,53]. The study area of Bijie Salaxi in the Shibing Heichong study area belongs to the no-potential rocky desertification grade and potential-mild rocky desertification grade. The vegetation type and coverage rate were higher than those in the Guanling-Zhenfeng Huajiang study area, and the DOC content in soil was also relatively high. The concentration of DOC in spring water in the Guanling-Zhenfeng Huajiang study area ranged from 2.01 to 5.11 mg/L, which was higher than that in the Bijie Salaxi study area and Shibing Heichong study area. HJ-1 and HJ-2 contained a large number of phytoplankton and bacteria, and biological mechanisms such as phytoplankton and bacteria production are considered to be an important source of DOC [54], resulting in a higher DOC content. Different land-use patterns and vegetation cover affect the variation in the carbon and nitrogen contents in water [55–57]. The soil thickness of karst spring water in the Guanling-Zhenfeng Huajiang research area was thin, the vegetation coverage was low, and it was agricultural land, which is affected by agricultural farming. The carbon and nitrogen contents of spring water in the Guanling-Zhenfeng Huajiang research area more were concentrated than those in the other research areas, and the change range was large (Figure 2). The contents of carbon and nitrogen in karst springs in the study area of Salaxi Spring in Bijie were relatively concentrated, and the change range was small because the water cover vegetation is mainly secondary vegetation and is not affected by human activities.

4.3. Response of Karst Spring Water Carbon and Nitrogen Output to the Surface Ecosystem

Karst is a typical ecologically fragile area. Soil carbon and nitrogen storage is key to the formation and evolution of local ecosystems. As the most active components of soil carbon and nitrogen [58–61], soluble carbon and nitrogen are extremely sensitive to environmental changes. Water resources carry nutrients into groundwater through soil circulation [3,8]. The aboveground-underground dual hydrological structure in karst areas leads to the characteristics of aboveground-underground double loss of nutrients. Spring water is an important output port of forest groundwater [3,62,63] and plays a very important role in underground leakage in karst areas.

When comparing carbon and nitrogen storage, we found that the DOC storage in the dry season was significantly higher than that in the rainy season (Figure 7), which was consistent with the results of other studies on carbon storage [60,61]. The NO_3-N storage in the Shibing Heichong study area and the Guanling-Zhenfeng Huajiang study area was greater in the wet season than in the dry season. This is because the soil NO_3-N storage increased in the rainy season due to the influence of agricultural fertilization. Agricultural activities seriously affect soil nitrogen content and storage and decrease the stability of soil organic matter [64,65]. In contrast, in the Bijie Salaxi research area, the karst spring was not affected by agriculture, and the NO_3-N reserves in the dry season were greater than those in the rainy season. We observed significant differences in karst springs and carbon and nitrogen outputs with different carbon and nitrogen reserves. Due to land use/cover change, there are significant differences in soil carbon and nitrogen storage [66–68]. The vegetation and soil cover rate of the study area was as high as >50%, which was higher than that of the Bijie Salaxi study area (30%~50%) and Guanling-Zhenfeng Huajiang study area (10%~35%) [33]. The carbon and nitrogen storage in the Shibing Heichong study area was significantly higher than that in the Bijie Salaxi study area and the Guanling-Zhenfeng Huajiang study area (Figure 7). As shown in the figure, the carbon and nitrogen reserves of the spring area in the Bijie Salaxi study area were 2.33 to 10.64 times those of the

Guanling-Zhenfeng Huajiang study area. In the above analysis, karst spring water carbon and nitrogen output measurements were in the following order: Shibing Heichong study area > Bijie Salaxi study area > Guanling-Zhenfeng Huajiang study area. In the study area of Shibing Heichong, the carbon and nitrogen storage of HC-2 spring was greater than that of HC-1, and the carbon and nitrogen output of HC-2 karst spring was also greater than that of HC-1. The Bijie Salaxi area and Guanling-Zhenfeng Huajiang study area also exhibited the same phenomenon. The results showed that the higher the carbon and nitrogen storage in the karst spring area was, the higher the carbon and nitrogen output of the karst spring. Comparing the annual output and soil leakage of six karst springs, we found that the DOC leakage and output in the HC-2 spring area were the largest, which were 136.75 kg and 19.94 kg, respectively. In the Guanling-Zhenfeng Huajiang study area, the DOC output of HJ-2 spring water was slightly larger than that of HJ-1. The difference in DOC reserves in HJ-1 is 23.91 kg, which was greater than that of 18.24 kg in the HJ-2 spring area. The increase in NO_3-N storage in the HJ-1 spring area was higher than that in the HJ-2 spring area, indicating that HJ-1 was more affected by agriculture, resulting in more serious soil leakage [69–71]. The overlying soil environment of different karst springs has different carbon and nitrogen reserves. Due to the continuous supply of soil with high carbon and nitrogen contents, the annual output of carbon and nitrogen in karst spring water is relatively high, resulting in relatively high soil nutrient leakage. Due to the continuous supply of low-carbon nitrogen content soil, the annual output of carbon and nitrogen in karst spring water is relatively low, and the resulting soil nutrient leakage is also relatively low.

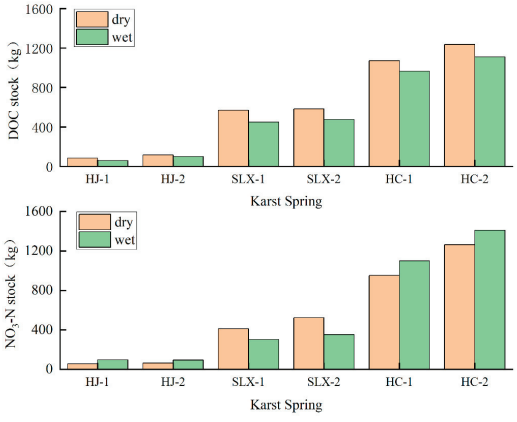

Figure 7. Comparison of DOC and NO_3-N storage in overlying soil of karst spring.

Stability refers to the ability of ecosystems to maintain and restore their own functions and structures, representing the reliability of ecosystems to provide normal service functions [72,73]. Disturbance or disturbance refers to changes affecting ecosystems [74–76]. The response of ecosystems to disturbance is a multilevel and multiscale process. Evaluating ecosystem stability is a way to quantify the response of a specific level and scale. Soil is the medium for storing a large amount of nutrients and is essential for plant growth. Therefore, the soil nutrient loss rate is an important indicator for evaluating ecosystem stability. It is concluded that greater carbon and nitrogen storage above the karst spring results in higher annual outputs of carbon and nitrogen in the spring and more soil nutrient leakage in the forest ecosystem. This result indicates that the risk of soil nutrient loss in areas with low rocky desertification grades is also higher than that in areas with high rocky desertification grades. In the study area of Shibing Heichong, the soil loss, karst spring water output and output rate were relatively high. At the same time, there are many types of vegetation and high coverage, and the nutrient input to the ecosystem through rich litter

is stable and high [77,78]. The decline in soil carbon and nitrogen storage (leakage rate) in the Shibingheichong study area was far less than that in the other two study areas. In the Guanling-Zhenfeng Huajiang study area, soil loss, karst spring water output and output rate were relatively low, soil cover and vegetation cover were low, rocky desertification degree was high and nutrient input was low. The soil carbon and nitrogen storage in the Guanling-Zhenfeng Huajiang research area decreased greatly (leakage rate). The Bijie Salaxi study area was at an intermediate level.

5. Conclusions

In the three study areas, the carbon and nitrogen contents and output of karst springs showed obvious spatial and temporal variation characteristics. The contents of DIC, TN and NO_3-N in karst springs in the Shibing Heichong study area were significantly higher than those in the Bijie Salaxi study area and Guanling-Zhenfeng Huajiang study area. The DOC content of karst springs in the Guanling-Zhenfeng Huajiang study area was higher than that in the other two study areas. Karst spring carbon and nitrogen contents were affected by local lithology, land use, zooplankton and other factors. The output of carbon and nitrogen in karst springs was found to be in the following order: Shibing Heichong research area > Bijie Salaxi research area > Guanling-Zhenfeng Huajiang research area. Karst spring carbon and nitrogen output was mainly concentrated in the rainy season and was mainly affected by the flow, followed by carbon and nitrogen content. The carbon and nitrogen outputs of the karst spring were more sensitive to the response to rainfall.

The contents of carbon and nitrogen in the overlying soil of karst springs also showed temporal and spatial characteristics. No potential rocky desertification Shibing Heichong studied soil cover, vegetation coverage was high, and soil carbon and nitrogen contents were significant in the other two study areas. The DOC content in soil was affected by litter, and the DOC content in the dry season was greater than that in the rainy season. Affected by agriculture, the NO_3-N content in the soil of the Shibing Heichong study area and Guanling-Zhenfeng Huajiang study area was higher in the rainy season than in the dry season. The lower the carbon and nitrogen output of the karst spring in the Guanling-Zhenfeng Huajiang research area was, the lower the carbon and nitrogen leakage of the overlying soil. The carbon and nitrogen output of karst springs in the study area was higher, and the soil carbon and nitrogen leakage were also higher, but at the same time, the soil carbon and nitrogen input were also high, and the soil decline was low. This result shows that the overlying forest ecosystem of karst springs was relatively stable and had strong anti-interference in the Shibing Heichong research area. Karst springs play a vital role in the carbon and nitrogen cycles in the karst critical zone. This study can provide a scientific foundation and theoretical support for comprehensively studying forest water and soil nutrient loss in karst areas by examining the interannual change in carbon and nitrogen compounds in karst springs and soil.

Author Contributions: C.H. writing—original draft preparation, software, and formal analysis; Z.L. conceptualization, methodology, and data curation; K.X. methodology, writing—review and editing, and funding acquisition; X.L. validation, investigation, and supervision; Y.L. investigation, validation, and resources. R.Z. investigation and validation. All authors have read and agreed to the published version of the manuscript.

Funding: This research was supported by the Key Science and Technology Program of Guizhou Provence (No. 5411 2017 QKHPTRC), the Science and Technology Program of Guizhou Province (No. Yiban 185 2021 Qiankehe Jichu-ZK) and the China Overseas Expertise Introduction Program for Discipline Innovation (D17016).

Data Availability Statement: The data presented in this study are available on request from the corresponding author.

Conflicts of Interest: The authors declare no conflict of interest.

References

1. Brantley, S.L.; Goldhaber, M.B.; Ragnarsdottir, K.V. Crossing Disciplines and Scales to Understand the Critical Zone. *Elements* **2007**, *3*, 307–314. [CrossRef]
2. Lin, H. Earth's Critical Zone and hydropedology: Concepts, characteristics, and advances. *Hydrol. Earth. Syst. Sci.* **2010**, *14*, 25–45. [CrossRef]
3. Reiss, M.; Chifflard, P. An Opinion on Spring Habitats within the Earth's Critical Zone in Headwater Regions. *Water* **2017**, *9*, 645. [CrossRef]
4. Yang, M. On the Fragility of Karst Environment. *Yunnan Geogr. Environ. Res.* **1990**, *2*, 21–29. (In Chinese)
5. Xiong, K.; Chen, Y.; Chen, X.; Lan, A.; Sui, J. *Stone into Gold-Guizhou Rocky Desertification Control Technology and Mode*; Guizhou Science and Technology Press: Guiyang, China, 2011.
6. Jiang, Z.C.; Zhang, C.; Qin, X.; Pu, J.; Bai, B. Structural Features and Function of the Karst Critical Zone. *Acta Geol. Sin.* **2019**, *93*, 109–112. [CrossRef]
7. Liu, M.; Xu, X.; Wang, D.; Sun, A.Y.; Wang, K. Karst catchments exhibited higher degradation stress from climate change than the non-karst catchments in southwest China: An ecohydrological perspective. *J. Hydrol.* **2016**, *535*, 173–180. [CrossRef]
8. Zhu, Y.; Meharg, A.A. Protecting global soil resources for ecosystem services. *Ecosyst. Health Sust.* **2015**, *1*, 11. [CrossRef]
9. Zhu, G.Y.; Zhou, L.H.; He, X.J.; Wei, P.; Lin, D.M.; Qian, S.H.; Zhao, L.; Luo, M.; Yin, X.H.; Zeng, L.; et al. Effects of Elevation Gradient on Soil Carbon and Nitrogen in a Typical Karst Region of Chongqing, Southwest China. *J. Geophys. Res. Biogeosci.* **2022**, *127*, e2021JG006742. [CrossRef]
10. Hu, L.; Li, Q.; Yan, J.H.; Liu, C.; Zhong, J.X. Vegetation restoration facilitates belowground microbial network complexity and recalcitrant soil organic carbon storage in southwest China karst region. *Sci. Total Environ.* **2022**, *820*, 153137. [CrossRef]
11. Mueller, K.E.; Hobbie, S.E.; Tilman, D.; Reich, P.B. Effects of plant diversity, N fertilization, and elevated carbon dioxide on grassland soil N cycling in a long-term experiment. *Glob. Chang. Biol.* **2013**, *19*, 1249–1261. [CrossRef]
12. Mudge, P.L.; Schipper, L.A.; Baisden, W.T.; Ghani, A.; Lewis, R.W. Changes in soil C, N and $\delta^{15}N$ along three forest–pasture chronosequences in New Zealand. *Soil Res.* **2014**, *52*, 27–37. [CrossRef]
13. Albaladejo, J.; Ortiz, R.; Garcia-Franco, N.; Navarro, A.R.; Almagro, M.; Pintado, J.G.; Martínez-Mena, M. Land use and climate change impacts on soil organic carbon stocks in semi-arid Spain. *J. Soil. Sediment* **2013**, *13*, 265–277. [CrossRef]
14. Li, D.; Niu, S.; Luo, Y. Global patterns of the dynamics of soil carbon and nitrogen stocks following afforestation: A meta-analysis. *New Phytol.* **2012**, *195*, 172–181. [CrossRef]
15. Feng, W.T.; Liang, J.Y.; Hale, L.; Jung, C.G.; Chen, J.; Zhou, J.Z.; Xu, M.G.; Yuan, M.T.; Wu, L.Y.; Bracho, R.; et al. Enhanced decomposition of stable soil organic carbon and microbial catabolic potentials by long-term field warming. *Glob. Chang. Biol.* **2017**, *23*, 4765–4776. [CrossRef] [PubMed]
16. Qiu, L.; Xiao, T.; Bai, T.; Mo, X.; Huang, J.; Deng, W.; Liu, Y. Seasonal Dynamics and Influencing Factors of Litterfall Production and Carbon Input in Typical Forest Community Types in Lushan Mountain, China. *Forests* **2023**, *14*, 341. [CrossRef]
17. Filipiak, M.; Filipiak, Z.M. Application of ionomics and ecological stoichiometry in conservation biology: Nutrient demand and supply in a changing environment. *Biol. Conserv.* **2022**, *272*, 109622. [CrossRef]
18. Lv, Y.; Jiang, Y.; Hu, W.; Cao, M.; Mao, Y. A review of the effects of tunnel excavation on the hydrology, ecology, and environment in karst areas: Current status, challenges, and perspectives. *J. Hydrol.* **2020**, *586*, 124891. [CrossRef]
19. Jiang, Y.; Hou, W.; Gao, J.; Wu, S. Refined revealing the chain path of multiple ecosystem services under diverse environmental factor gradients. *Sci. Total Environ.* **2022**, *865*, 161187. [CrossRef]
20. Vilhar, U.; Kermavnar, J.; Kozamernik, E.; Petrič, M.; Ravbar, N. The effects of large-scale forest disturbances on hydrology–An overview with special emphasis on karst aquifer systems. *Earth Sci. Rev.* **2022**, *235*, 104243. [CrossRef]
21. Oni, S.; Tiwari, T.; Ledesma, J.L.; Ågren, A.M.; Teutschbein, C.; Schelker, J.; Laudon, H.; Futter, M.N. Local- and landscape-scale impacts of clear-cuts and climate change on surface water dissolved organic carbon in boreal forests. *J. Geophys. Res. Biogeosci.* **2015**, *120*, 2402–2426. [CrossRef]
22. Dogan, F.N.; Karpuzcu, M.E. Effect of land use change on hydrology of forested watersheds. *Ecohydrology* **2022**, *15*, e2367. [CrossRef]
23. Lovett, G.M.; Weathers, K.C.; Arthur, M.A. Control of Nitrogen Loss from Forested Watersheds by Soil Carbon: Nitrogen Ratio and Tree Species Composition. *Ecosystems* **2022**, *5*, 712–718. [CrossRef]
24. Sun, Z.Y. Study on Hydrological Regulation Ability of Typical Forest Ecosystem in Changbai Mountain. Master's Thesis, Changchun University of Science and Technology, Changchun, China, 2022.
25. Austin, A.T.; Ballaré, C.L. Dual role of lignin in plant litter decomposition in terrestrial ecosystems. *Proc. Natl. Acad. Sci. USA* **2010**, *107*, 4618–4622. [CrossRef]
26. Sayer, E.J.; Rodtassana, C.; Sheldrake, M.; Bréchet, L.M.; Ashford, O.S.; Lopez-Sangil, L.; Kerdraon-Byrne, D.; Castro, B.; Turner, B.L.; Wright, S.J.; et al. Revisiting nutrient cycling by litterfall—Insights from 15 years of litter manipulation in old-growth lowland tropical forest. *Adv. Ecol. Res.* **2020**, *62*, 173–223. [CrossRef]
27. Williams, D.D. The spring as an interface between groundwater and lotic faunas and as a tool in assessing groundwater quality. *Int. Ver. Theor. Angew. Limnol. Verh.* **1991**, *24*, 1621–1624. [CrossRef]
28. Iván, V.; Stevenazzi, S.; Pollicino, L.C.; Masetti, M.; Mádl-Szőnyi, J. An Enhanced Approach to the Spatial and Statistical Analysis of Factors Influencing Spring Distribution on a Transboundary Karst Aquifer. *Water* **2020**, *12*, 2133. [CrossRef]

29. Jiang, Y.J.; Lei, J.Q.; Hu, L.C.; Xiao, Q.; Wang, J.L.; Zhang, C.; Ali, H.D. Biogeochemical and physical controls on the evolution of dissolved inorganic carbon (DIC) and δ^{13}CDIC in karst spring-waters exposed to atmospheric CO_2(g): Insights from laboratory experiments. *J. Hydrol.* **2020**, *583*, 124294. [CrossRef]
30. Aitkenhead, J.A.; McDowell, W.H. Soil C:N ratio as a predictor of annual riverine DOC flux at local and global scales. *Glob. Biogeochem. Cycles* **2000**, *14*, 127–138. [CrossRef]
31. Simon, C.; Pimentel, T.P.; Monteiro, M.T.; Candido, L.A.; Gastmans, D.; Geilmann, H.; Oliveira, R.D.; Rocha, J.B.; Pires, E.; Quesada, C.A.; et al. Molecular links between whitesand ecosystems and blackwater formation in the Rio Negro watershed. *Geochim. Cosmochim. Acta* **2020**, *311*, 274–291. [CrossRef]
32. Mentges, A.; Feenders, C.; Deutsch, C.A.; Blasius, B.; Dittmar, T. Long-term stability of marine dissolved organic carbon emerges from a neutral network of compounds and microbes. *Sci. Rep.* **2019**, *9*, 17780. [CrossRef]
33. Hu, C.P. Temporal and Spatial Variations of Carbon and Nitrogen Output in the Karst Critical Zone and Its Environmental Significance. Master's Thesis, Guizhou Normal University, Guiyang, China, 2022.
34. Li, Y.; Xiong, K.N.; Liu, Z.Q.; Li, K.P.; Luo, D. Distribution and influencing factors of soil organic carbon in a typical karst catchment undergoing natural restoration. *Catena* **2022**, *212*, 106078. [CrossRef]
35. Zheng, W.; Wang, S.; Sprenger, M.; Liu, B.; Cao, J. Response of soil water movement and groundwater recharge to extreme precipitation in a headwater catchment in the North China Plain. *J. Hydrol.* **2019**, *576*, 466–477. [CrossRef]
36. Wu, Y.; Zhou, X.; Wang, M.; Zhuo, L.; Xu, H.; Liu, Y. Comparison of hydrogeological characteristics and genesis of the Xiaguan Hot Spring and the Butterfly Spring in Yunnan of China. *J. Hydrol.* **2021**, *593*, 125922. [CrossRef]
37. Zhang, L.; Yang, Y.; He, W.; Xu, J.; Li, R. Fluxes of riverine nutrient to the Zhujiang River Estuary and its potential eutrophication effect. *Acta Oceanol. Sin.* **2022**, *41*, 88–98. [CrossRef]
38. Oehler, T.; Eiche, E.; Putra, D.P.; Adyasari, D.; Hennig, H.; Mallast, U.; Moosdorf, N. Seasonal variability of land-ocean groundwater nutrient fluxes from a tropical karstic region (southern Java, Indonesia). *J. Hydrol.* **2018**, *565*, 662–671. [CrossRef]
39. Zhang, H. *Study on Soil Property and Water Holding Characteristics of Different Vegetation Belt in the Loess Plateau*; Northwest A&F University: Xi'an, China, 2021.
40. Bai, Y.E.; Liu, Q.F.; Gu, Z.R.; Lu, Y.; Sheng, Z.P. The dissolution mechanism and karst development of carbonate rocks in karst rocky desertification area of Zhenfeng–Guanling–Huajiang County, Guizhou, China. *Carbonate Evaporite* **2019**, *34*, 45–51. [CrossRef]
41. Liu, Q.; Wang, T.J.; Liu, C.Q.; Mikouendanandi, E.B.J.; Chen, X.J.; Peng, T.; Zhang, L. Characterizing the spatiotemporal dynamics of shallow soil water stable isotopic compositions on a karst hillslope in Southwestern China. *J. Hydrol.* **2022**, *610*, 127964. [CrossRef]
42. Han, D.D.; Deng, J.C.; Gu, C.J.; Mu, X.M.; Gao, P.; Gao, J.J. Effect of shrub-grass vegetation coverage and slope gradient on runoff and sediment yield under simulated rainfall. *Int. J. Sediment Res.* **2021**, *36*, 29–37. [CrossRef]
43. Clark, I.; Fritz, P. *Environmental Isotopes in Hydrogeology*; Lewis Publishers: New York, NY, USA, 1997.
44. Li, K.; Liu, C.; Ma, Y.; Wang, X. Land-based dissolved organic nitrogen dynamics and bioavailability in Jiaozhou Bay, China. *Estuar. Coast. Shelf Sci.* **2019**, *220*, 13–24. [CrossRef]
45. Hu, C.; Liu, Z.; Xiong, K.; Lyu, X.; Li, Y.; Zhang, R. Characteristics of and Influencing Factors of Hydrochemistry and Carbon/Nitrogen Variation in the Huangzhouhe River Basin, a World Natural Heritage Site. *Int. J. Environ. Res. Public Health* **2021**, *18*, 13169. [CrossRef]
46. Dawoe, E.K.; Isaac, M.E.; Quashie-Sam, J.S. Litterfall and litter nutrient dynamics under cocoa ecosystems in lowland humid Ghana. *Plant Soil* **2010**, *330*, 55–64. [CrossRef]
47. Oddi, L.; Celi, L.; Cremonese, E.; Filippa, G.; Galvagno, M.; Palestini, G.; Siniscalco, C. Decomposition processes interacting with microtopography maintain ecosystem heterogeneity in a subalpine grassland. *Plant Soil* **2019**, *434*, 379–395. [CrossRef]
48. Ahmad, A.; Liu, Q.; Nizami, S.M.; Mannan, A.; Saeed, S. Carbon emission from deforestation, forest degradation and wood harvest in the temperate region of Hindukush Himalaya, Pakistan between 1994 and 2016. *Land Use Policy* **2018**, *78*, 781–790. [CrossRef]
49. Ma, T.; Deng, X.; Chen, L.; Xiang, W. The soil properties and their effects on plant diversity in different degrees of rocky desertification. *Sci. Total Environ.* **2020**, *736*, 139667. [CrossRef] [PubMed]
50. Zhang, S.H.; Zhang, Y.; Xiong, K.N.; Yu, Y.H.; Min, X.Y. Changes of leaf functional traits in karst rocky desertification ecological environment and the driving factors. *Glob. Ecol. Conserv.* **2020**, *24*, e01381. [CrossRef]
51. Wang, X.W.; Liu, Z.Q.; Xiong, K.; He, Q.F.; Li, Y.; Li, K.P. Characteristics and controlling factors of soil dissolved organic matter in the rainy season after vegetation restoration in a karst drainage area, South China. *Catena* **2022**, *217*, 106483. [CrossRef]
52. Tang, M.; Liu, J.; Hou, W.; Stubbendieck, R.M.; Xiong, H.; Jin, J.; Gong, J.; Cheng, C.; Tang, X.; Liu, Y.; et al. Structural variability in the bulk soil, rhizosphere, and root endophyte fungal communities of Themeda japonica plants under different grades of karst rocky desertification. *Plant Soil* **2021**, *475*, 105–122. [CrossRef]
53. Zheng, W.; Wu, Q.; Rao, C.X.; Chen, X.; Wang, E.; Liang, X.; Yan, W. Characteristics and interactions of soil bacteria, phytocommunity and soil properties in rocky desertification ecosystems of Southwest China. *Catena* **2023**, *220*, 106731. [CrossRef]
54. Keller, D.P.; Hood, R.R. Comparative simulations of dissolved organic matter cycling in idealized oceanic, coastal, and estuarine surface waters. *J. Mar. Syst.* **2013**, *109*, 109–128. [CrossRef]

55. Alexander, R.B.; Smith, R.A.; Schwarz, G.E.; Boyer, E.W.; Nolan, J.V.; Brakebill, J. Differences in phosphorus and nitrogen delivery to the Gulf of Mexico from the Mississippi River Basin. *Environ. Sci. Technol.* **2008**, *42*, 822–830. [CrossRef]
56. Potthast, K.; Meyer, S.; Crecelius, A.; Schubert, U.S.; Tischer, A.; Michalzik, B. Land-use and fire drive temporal patterns of soil solution chemistry and nutrient fluxes. *Sci. Total Environ.* **2017**, *605*, 514–526. [CrossRef]
57. Ni, X.; Parajuli, P.B.; Ouyang, Y.; Dash, P.; Siegert, C.M. Assessing land use change impact on stream discharge and stream water quality in an agricultural watershed. *Catena* **2021**, *198*, 105055. [CrossRef]
58. Wood, C.W.; Edwards, J.H. Agroecosystem management effects on soil carbon and nitrogen. *Agric. Ecosyst. Environ.* **1992**, *39*, 123–138. [CrossRef]
59. Gaspar, L.; Quijano, L.; Lizaga, I.; Navas, A. Effects of land use on soil organic and inorganic C and N at 137Cs traced erosional and depositional sites in mountain agroecosystems. *Catena* **2019**, *181*, 104058. [CrossRef]
60. Lozano-García, B.; Muñoz-Rojas, M.; Parras-Alcántara, L. Climate and land use changes effects on soil organic carbon stocks in a Mediterranean semi-natural area. *Sci. Total Environ.* **2017**, *579*, 1249–1259. [CrossRef] [PubMed]
61. Lindén, L.; Riikonen, A.; Setälä, H.; Yli-Pelkonen, V. Quantifying carbon stocks in urban parks under cold climate conditions. *Urban For. Urban Green.* **2020**, *49*, 126633. [CrossRef]
62. Horsák, M.; Horsáková, V.; Polášek, M.; Coufal, R.; Hájková, P.; Hájek, M. Spring water table depth mediates within-site variation of soil temperature in groundwater-fed mires. *Hydrol. Process.* **2021**, *35*, e14293. [CrossRef]
63. Singha, K.; Navarre-Sitchler, A. The Importance of Groundwater in Critical Zone Science. *Groundwater* **2022**, *60*, 27–34. [CrossRef]
64. Garcia-Pausas, J.; Rabissi, A.; Rovira, P.; Romanyà, J. Organic Fertilisation Increases C and N Stocks and Reduces Soil Organic Matter Stability in Mediterranean Vegetable Gardens. *Land. Degrad. Dev.* **2017**, *28*, 691–698. [CrossRef]
65. Kiriyama, H.; Matsuda, H.; Kamiji, Y.; Morita, S. Nitrogen stock and farmer behaviour under rice policy change in Japan. *J. Environ. Manag.* **2021**, *299*, 113438. [CrossRef]
66. Li, Z.W.; Liu, C.R.; Dong, Y.T.; Chang, X.F.; Nie, X.D.; Liu, L.; Xiao, H.B.; Lu, Y.M.; Zeng, G.M. Response of soil organic carbon and nitrogen stocks to soil erosion and land use types in the Loess hilly–gully region of China. *Soil Tillage Res.* **2017**, *166*, 1–9. [CrossRef]
67. Rytter, R. Stone and gravel contents of arable soils influence estimates of C and N stocks. *Catena* **2012**, *95*, 153–159. [CrossRef]
68. Pellikka, P.; Heikinheimo, V.; Hietanen, J.; Schäfer, E.; Siljander, M.; Heiskanen, J. Impact of land cover change on aboveground carbon stocks in Afromontane landscape in Kenya. *Appl. Geogr.* **2018**, *94*, 178–189. [CrossRef]
69. Zhao, Z.Q.; Bai, Z.H.; Wei, S.; Ma, W.Q.; Wang, M.R.; Kroeze, C.L.; Ma, L. Modeling farm nutrient flows in the North China Plain to reduce nutrient losses. *Nutr. Cycl. Agroecosyst.* **2017**, *108*, 231–244. [CrossRef]
70. Gomes, L.; Simões, S.J.; Dalla Nora, E.; de Sousa-Neto, E.; Forti, M.C.; Ometto, J.P. Agricultural Expansion in the Brazilian Cerrado: Increased Soil and Nutrient Losses and Decreased Agricultural Productivity. *Land* **2019**, *8*, 12. [CrossRef]
71. Wojciechowska, E.; Pietrzak, S.; Matej-Łukowicz, K.; Nawrot, N.; Zima, P.; Kalinowska, D.; Wielgat, P.; Obarska-Pempkowiak, H.; Gajewska, M.; Dembska, G.; et al. Nutrient loss from three small-size watersheds in the southern Baltic Sea in relation to agricultural practices and policy. *J. Environ. Manag.* **2019**, *252*, 109637. [CrossRef] [PubMed]
72. Pimm, S.L. The complexity and stability of ecosystems. *Nature* **1984**, *307*, 321–326. [CrossRef]
73. Keersmaecker, W.D.; Lhermitte, S.; Honnay, O.; Farifteh, J.; Somers, B.; Coppin, P.R. How to measure ecosystem stability? An evaluation of the reliability of stability metrics based on remote sensing time series across the major global ecosystems. *Glob. Chang. Biol.* **2014**, *20*, 2149–2161. [CrossRef]
74. Donohue, I.; Hillebrand, H.; Montoya, J.M.; Petchey, O.L.; Pimm, S.L.; Fowler, M.S.; Healy, K.; Jackson, A.L.; Lurgi, M.; McClean, D.; et al. Navigating the complexity of ecological stability. *Ecol. Lett.* **2016**, *19*, 1172–1185. [CrossRef]
75. Wohlgemuth, D.; Solan, M.; Godbold, J.A. Species contributions to ecosystem process and function can be population dependent and modified by biotic and abiotic setting. *Proc. R. Soc. B* **2017**, *284*, 20162850. [CrossRef]
76. Gottschall, F.; Cesarz, S.; Auge, H.; Kovach, K.; Mori, A.S.; Nock, C.A.; Eisenhauer, N. Spatio-temporal dynamics of abiotic and biotic properties explain biodiversity-ecosystem functioning relationships. *Ecol. Monogr.* **2021**, *92*, e01490. [CrossRef]
77. Yang, H.L.; Li, L.Y.; Zhan, J.; Bao, C.; Luo, Y.Q. Effects of litter chemical traits and species richness on soil carbon cycling changed over time. *Front. Environ. Sci.* **2022**, *10*, 1023831. [CrossRef]
78. Fung, T.; Richards, D.R.; Leong, R.A.; Ghosh, S.; Tan, C.W.J.; Drillet, Z.; Leong, K.L.; Edwards, P.J. Litter decomposition and infiltration capacities in soils of different tropical urban land covers. *Urban Ecosyst.* **2022**, *25*, 21–34. [CrossRef]

forests

MDPI

Article

Afforestation Influences Soil Aggregate Stability by Regulating Aggregate Transformation in Karst Rocky Desertification Areas

Dayun Zhu [1,2,*], Qian Yang [1,2], Yingshan Zhao [1,2], Zhen Cao [1,2], Yurong Han [1,2], Ronghan Li [1,2], Ju Ni [1,2] and Zhigao Wu [1,2]

[1] School of Karst Science, Guizhou Normal University, Guiyang 550001, China; 20010170506@gznu.edu.cn (Q.Y.); 222100170561@gznu.edu.cn (Y.Z.); 21010170525@gznu.edu.cn (Z.C.); 222200171823@gznu.edu.cn (Y.H.); 21010170571@gznu.edu.cn (R.L.); 222100170581@gznu.edu.cn (J.N.); 1060374627@gznu.edu.cn (Z.W.)

[2] State Engineering Technology Institute for Karst Desertification Control, Guiyang 550001, China

* Correspondence: zhudayun163@163.com or zhudayun@gznu.edu.cn

Abstract: Surface vegetation has a substantial impact on soil aggregate stability, which is an important indicator of soil quality. However, there is still limited research on the response of soil aggregate stability indicators and the organic carbon, total nitrogen, and total phosphorus content in soil aggregates for different vegetation patterns in rocky desertification fragile ecological areas. Therefore, in order to study the effects of different vegetation restoration models on soil aggregate stability and aggregate related nutrient content and their promoting relationships in the karst rocky desertification areas in southwest China, soil samples under three artificial restoration vegetation measures (*Juglans regia* L.-*Rosa roxburghii* Tratt., *Rosa roxburghii* Tratt.-*Lolium perenne* L., *Juglans regia* L.-*Lolium perenne* L.) were collected in 0–10 cm and 10–20 cm soil, and the traditional farmland (*Zea mays* L.) was used as the control, combined with dry and wet sieving experiments for the research and analysis. The results showed that there were significant differences in the distribution of aggregates and soil nutrients among the four types of plots. Compared with traditional agricultural land, artificial afforestation increased the content of soil large macroaggregates (LMAs) and decreased the proportion of microaggregates (MIAs) and silt+clay (SCA), which enhanced the soil aggregate stability and reduced the soil fragmentation and erodibility. The afforestation restoration increased the content of soil aggregate-related SOC, TN, and TP, and increased with the decrease in the aggregate particle size. Research has found that soil aggregate stability indicators are significantly influenced by the particle size distribution of soil aggregates. In the positive succession process of vegetation types, soil nutrient accumulation is controlled by changes in the soil aggregate particle size, which affects the soil aggregate stability and reduces soil erodibility, thereby protecting the soil nutrient loss. The composite management of forest and irrigation in degraded ecological areas has certain reference and indicative significance for ecological restoration in rocky desertification areas.

Keywords: soil aggregate stability; soil nutrients; vegetation restoration; karst rocky desertification

Citation: Zhu, D.; Yang, Q.; Zhao, Y.; Cao, Z.; Han, Y.; Li, R.; Ni, J.; Wu, Z. Afforestation Influences Soil Aggregate Stability by Regulating Aggregate Transformation in Karst Rocky Desertification Areas. *Forests* **2023**, *14*, 1356. https://doi.org/10.3390/f14071356

Academic Editor: Choonsig Kim

Received: 18 May 2023
Revised: 9 June 2023
Accepted: 28 June 2023
Published: 30 June 2023

1. Introduction

Irrational land use can lead to soil degradation, deplete soil nutrients, and change the stability of soil structure [1,2], which seriously affects the natural environment and agroecological sustainability. As an important measure to prevent soil degradation, artificial afforestation can alter the soil structure by the accumulation of plant root exudates and litter to reduce the soil erodibility [3]. Karst areas are among the highest nutrient loss and soil erosion areas in the world [4], including the European Mediterranean region, Dinaric karst, and southwest China [5], and ecological problems have attracted great attention. Therefore, understanding the influence of soil aggregate stability on soil nutrients under different vegetation restoration types in karst rocky desertification areas is thus critical to studying karst ecological restoration.

Soil aggregates, a key component of soil structure, are critical for improving soil fertility, carbon sequestration, soil aggregate stability, and resistance to water erosion [6]. At the same time, its stability is intimately tied to the rainfall erosivity, surface runoff, and soil loss rate [7,8]. Soil erodibility is a term used to describe the sensitivity of the soil to water erosion, which can impair soils' ability to support ecosystem functions, including food production, pollution prevention, flood control, and climate change mitigation [9]. Investigating the changes in soil structure and erosion resistance during vegetation restoration measures is important for analyzing the effectiveness of ecological management measures in rocky desertification areas and providing a basis for further management.

The type of vegetation has been shown to influence the accumulation of the C, N, and P contents in soil, and irrational agricultural activities have been shown to significantly affect the distribution of aggregates and changes in aggregate-related nutrients [10,11], In addition, soil nutrients play an important role in soil growth [12], and the ability to resist erosion also affects the potential changes in soil nutrients [13,14]. However, in karst rocky desertification areas, most studies have concentrated only on the ability of vegetation types to increase nutrients or improve erodibility, and it is not clear how the differences in soil aggregate stability and the resulting ability to affect soil nutrients are improved by artificial afforestation patterns [15,16], and most use the mean weight diameter (MWD) and the geometric mean diameter (GMD) to evaluate soil aggregate stability [17,18] without combining stability with the promotion relationship of nutrients in aggregates. Therefore, it is necessary to combine various stability indicators to elaborate the ability of different vegetation types in rocky desertification areas to improve soil aggregate stability and nutrients, as well as to determine the promotion relationship between them, which will help to develop more effective vegetation restoration strategies in order to maximize the ecological advantages of vegetation restoration.

As a result, we chose the demonstration area of integrated management of rocky desertification in the Plateau Mountain, Bijie Salaxi, to further investigate the impact of vegetation restoration on soil aggregate stability and soil nutrients in karst rocky desertification areas in southern China, as well as to provide a foundation for preventing soil erosion and the development of effective management strategies for sustainable ecosystem functions in rocky desertification areas. The main research contents are (1) an investigation into the capacity of different vegetation types to improve soil nutrients and ameliorate soil aggregate stability and (2) to reveal the promotion relationship between the aggregate particle size on soil aggregate stability and aggregate nutrients under different vegetation restoration measures.

2. Materials and Methods

2.1. Study Area and Soil Sampling

The Bijie Salaxi rocky desertification comprehensive management demonstration area was taken as the study area (Figure 1). The research area is in Southwest China's karst region, covering an area of 86 km^2, of which 74% is a karst landform, the rocky desertification grade is mainly potential–mild, and the region is dominated by highland mountainous terrain, with an altitude of 1600–2081 m. The climate is subtropical monsoon climate, with an annual temperature variation range of −7.2–30.1 °C, an annual average temperature of 12.7 °C, and an accumulated temperature of ≥10 °C between 3717 and 4109 °C. The total annual rainfall is 984 mm, with the rainy season from June to September, during which the rainfall accounts for 52% of the total annual rainfall. In addition, the soil in the area is mainly yellow soil, with a small amount of yellow brown soil and calcareous soil distributed in some mountain valleys and depressions. The vegetation is mainly composed of secondary evergreen deciduous coniferous broad-leaved mixed forests, covering two major categories, 130 families, 426 genera, and 697 species of seed and spore plants. Since the implementation of ecological management in this area, a certain scale of forest and grass vegetation restoration models have gradually emerged, including single and mixed species of *Juglans regia* L., *Rosa roxburghii* Tratt., *Lolium perenne* L. In April 2019, four land

use types (*Zea mays* L., *Juglans regia* L.-*Rosa roxburghii* Tratt., *Rosa roxburghii* Tratt.-*Lolium perenne* L., and *Juglans regia* L.-*Lolium perenne* L.) were selected in the study area(Table 1), and three quadrats were laid out on each study plot with a size of 10 m × 10 m. According to the "S" type of spotting, five sample locations were chosen, and 1 kg of undisturbed soil samples were collected at depths that varied between 0 and 10 cm and 10 and 20 cm. Each soil sample was immediately placed in a PE plastic bag and sealed before being transported to the lab in an ice box for the analyses of the physical and chemical parameters.

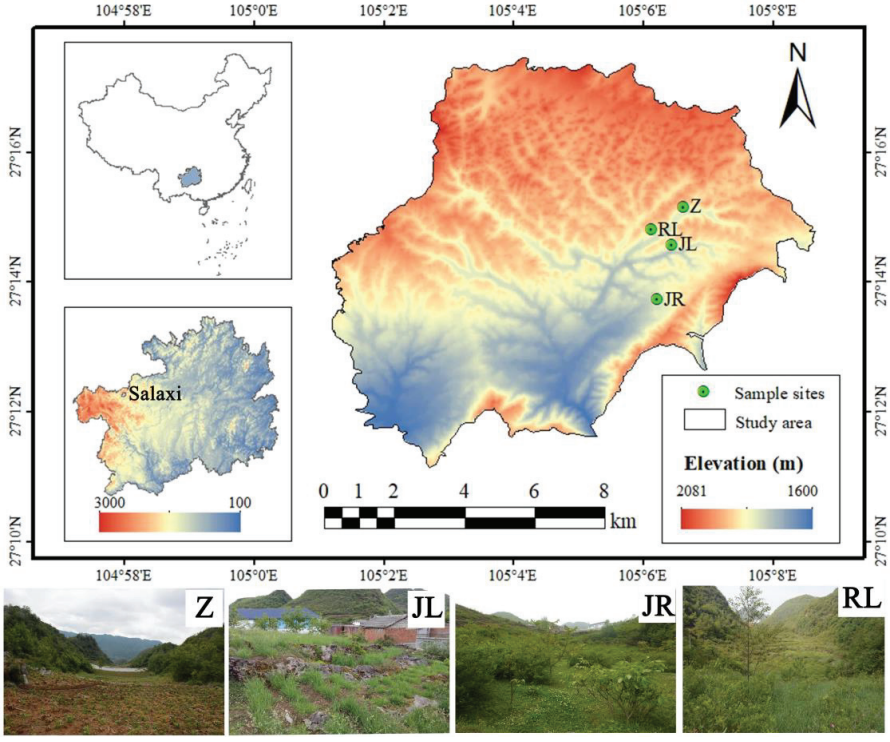

Figure 1. The location of the study area and the distribution of sample sites.

Table 1. Basic information about the sample plot.

Land Use Type	Longitude	Latitude	Altitude/m	Slope Inclination/○	Slope Aspect	Land Use
Zea mays L. (Z)	105°06′38″E	27°15′10″ N	1760	17	Half shady slope	Still growing *Zea mays* L.
Rosa roxburghii Tratt.-Lolium perenne L. (RL)	105°06′08″E	27°14′49″ N	1826	16	Half shady slope	Reforestation in 2010
Juglans regia L.-*Lolium perenne* L. (JL)	105°06′27″E	27°14′35″ N	1892	19	Half shady slope	Reforestation in 2010
Juglans regia L.-*Rosa roxburghii Tratt.* (JR)	105°06′13″E	27°13′44″ N	1751	14	Half shady slope	Reforestation in 2009

2.2. Soil Analysis

The soil was screened by a 10 mm sieve after natural air-drying, and then the soil aggregate content was determined by two experimental methods, dry sieving and wet sieving, under natural water content and water erosion conditions, respectively [19]. The experiment obtained the mass of four grade aggregates: >2 mm large macroaggregates

(LMA), 0.25–2 mm small macroaggregates (SMA), 0.053–0.25 mm microaggregates (MIAs), and <0.053 mm silt+clay (SCA).

Take soil samples from various levels of aggregates obtained through wet sieving analysis and pass them through a 0.05 mm sieve to determine the content of soil organic carbon (SOC), total nitrogen (TN), and total phosphorus (TP) [20]. The SOC was determined by wet digestion with a mixture of 5 mL of 0.8 mol/L potassium dichromate ($K_2Cr_2O_7$) and 5 mL of concentrated sulfuric acid (H_2SO_4), TN and (TP) are digested by sulfuric acid-potassium sulfate: copper sulfate (9:1) and sulfuric acid-perchloric acid respectively, and the filtrate is measured by a continuous flow analyzer.

2.3. Soil Aggregate Stability Index

The mean weight diameter (MWD) [21], geometric mean diameter (GMD) [22], K factor [23], fractal dimension (Dm) [24], and structure failure rate (PAD) [25] were used to express the soil aggregate stability.

The following equations [21,22] were used to calculate the mean weight diameter (MWD) and geometric mean diameter (GMD):

$$\mathrm{MWD} = \frac{\sum_{i=1}^{n} W_i \bar{X}_i}{\sum_{i=1}^{n} W_i} \tag{1}$$

$$\mathrm{GMD} = EXP\left[\frac{\sum_{i=1}^{n} W_i \ln \bar{X}_i}{\sum_{i=1}^{n} W_i}\right] \tag{2}$$

where n is the number of aggregate size fractions, X_i is the i-th aggregate particle size mean diameter, W_i is the i-th aggregate particle size weight.

The following equation [24] was used to determine the fractal dimension (Dm):

$$\mathrm{Dm} = 3 - \frac{\log[\mathrm{W}(\delta < \mathrm{R_i})/\mathrm{W_0}]}{\log(\mathrm{R_i}/\mathrm{R_{max}})} \tag{3}$$

where R_i is the average value of two adjacent grain sizes (mm), R_{max} is the average value of the largest grain size aggregate (mm), W is the accumulation of the mass of aggregate with diameters less than R_i (g), and W_0 is the total sum of aggregate content of each grain size (g).

In order to express the soil erodibility, the K factor [23] was calculated using the following equation:

$$\mathrm{K} = 7.954 \times \{0.0017 + 0.0494 \times \exp[-0.5 \times (\lg \mathrm{H_{GMD}} + 1.675/0.6986)^2]\} \tag{4}$$

The structure failure rate (PAD) of the soil aggregates is a crucial indicator for assessing the erosion durability, and was calculated with the following equation:

$$\mathrm{PAD} = \frac{a - b}{a} \tag{5}$$

where a is the percentage of aggregates >0.25 mm, measured by Yoder's method (dry sieving) [19], and b is the percentage of aggregates >0.25 mm, measured by Yoder's method [19]. Higher p values imply a lower soil aggregate stability.

2.4. Statistical Analysis

Excel 2010 and SPSS 22 were used to organize and evaluate the data collected after the studies, using one-way ANOVA and Duncan's test, the study data were evaluated for significance of differences (a = 0.05). The correlation analysis used the Pearson coefficient. We compared the standardized values of various indicators. The plotting was performed in Origin 2018.

Standardization can eliminate the impact of different factor dimensions. The factors were separated into positive and negative indicators, and their ranges were normalized to 0–1. The factors' main components were then extracted using principal component analysis.

Positive indicator:

$$y_i = \frac{x_i - x_{min}}{x_{max} - x_{min}} \quad (6)$$

Negative indicator:

$$y_i = \frac{x_{max} - x_i}{x_{max} - x_{min}} \quad (7)$$

where y_i was the standardized value of the i-th index. x_i was the original value. x_{max} and x_{min} were the maximum and minimum values, respectively.

3. Results

3.1. Soil Aggregate Size Distribution

Figure 2 indicates the characteristics of the aggregate particle size distribution under different land use methods and soil depths, and, under the various plant patterns, there are clear changes in the distribution of each soil particle size. The results of the dry sieving experiments showed (Figure 2a,b) that the LMA (>2 mm) content dominated the aggregates (40.17%–72.61%) in all sample sites, and the LMA content increased significantly after the transformation of cultivated land (Z) into plantation grassland, while the MIAs showed the opposite trend. The LMA content decreased with an increasing soil depth except for cultivated land (Z), and the SMA content showed an opposite trend. In the outcomes of the wet sieving tests (c and d), JL and JR were dominated by the SMA content (40.23%–44.46%), while RL and Z had the most MIA content (32.94%–54.23%). When cultivated land was converted to artificial grassland, the LMA content showed an increasing trend, and the MIA content decreased significantly. Compared to Z, the RL distribution decreased by 75.21%, 46.52%, and 61.67%. This result shows that afforestation has a major impact on the soil aggregation findings.

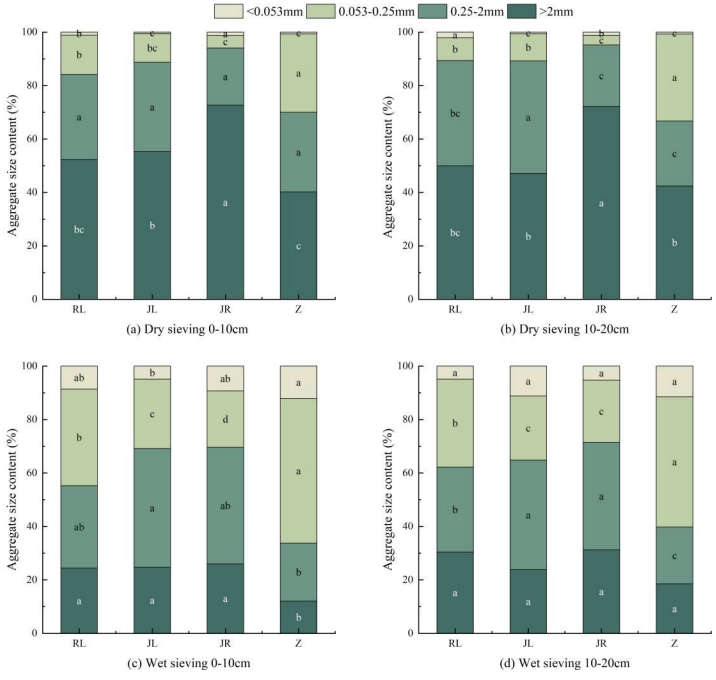

Figure 2. Soil aggregate particle size distribution characteristics. Note: various lowercase letters indicate significant differences ($p < 0.05$) in the same soil layer at various sites for the same grain size, as shown below.

3.2. Soil Aggregate Stability

Statistical analysis of soil aggregate stability indicators (MWD, GMD, Dm, PAD, and K) for each site (Figure 3) showed that the one-way ANOVA showed that the type of planting in the sample site had a remarkable influence on each soil aggregate stability index ($p < 0.05$). The cultivated land has the lowest MWD and GMD values, and the stability indexes were improved after the transformation of cultivated land into artificial forest grassland, with the highest in JR. Compared with the cultivated land, MWD increased 1.65 times and GMD increased 2.76 times in the dry sieving results and 1.98 and 2.81 times in the wet sieving results, respectively. The Dm values in sample plot Z were slightly higher than those in the rest of the sample plots. At the same time, both PAD and K values showed a decline with increasing depth of the soil layer (Figure 4), and the fragmentation rate of the soil aggregates and erodibility K values were significantly greater in the cultivated area than in the other sample sites. This shows that the plantations not only enhance the soil structure and aggregate stability, but also reduce soil erodibility. Among the three plantation types, the combination of *Juglans regia* L.-*Rosa roxburghii* Tratt. was superior to *Rosa roxburghii* Tratt.-*Lolium perenne* L. and *Juglans regia* L.-*Lolium perenne* L.

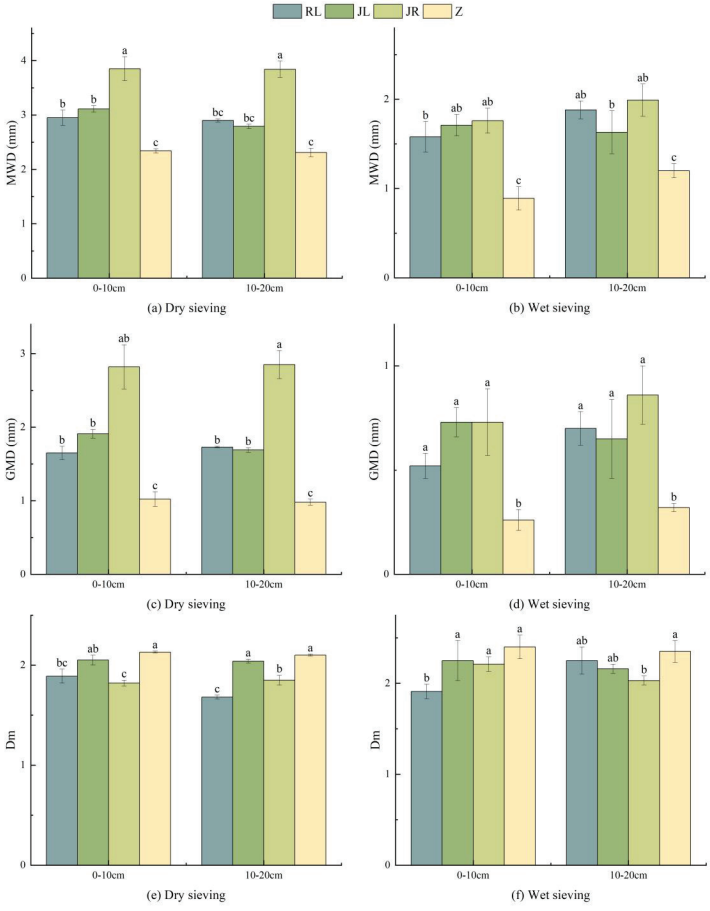

Figure 3. Distribution characteristics of MWD, GMD, and Dm values of soils. Note: various Minuscule indicate significant differences ($p < 0.05$) in the same soil layer at different locations.

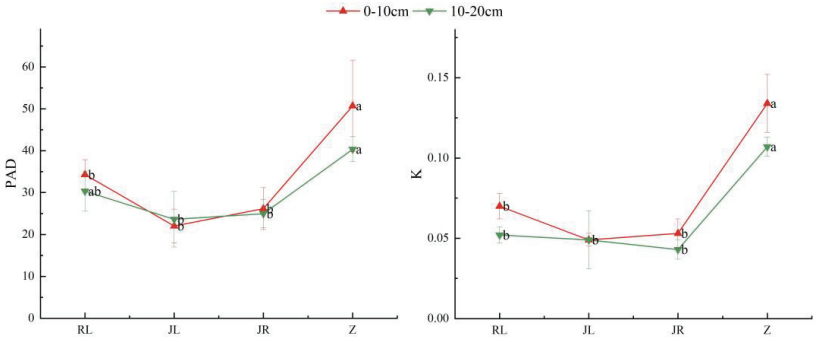

Figure 4. Distribution characteristics of soil PAD and erodibility K values. Note: various Minuscule indicate significant differences ($p < 0.05$) in the same soil layer at different locations.

3.3. Soil Nutrients of Different Vegetation Restoration Types

Aggregate-related SOC, TN, and TP were significantly influenced by the land use type and soil depth (Figure 5). The nutrient content was higher at the 10 cm layer, and the soil aggregate-related SOC and TN content was significantly increased by 7.89–26.96 g/kg and 0.38–1.95 g/kg for RL, JL, and JR, compared to the cultivated land (Figure 5a,b), and the TP content increased by 0.03–0.37 g/kg for RL and JR compared to the cultivated land. In addition, in different land use types, the content of nutrients associated with aggregates was negatively correlated with the aggregate diameter and increased with a decreasing particle size, and the cultivated land had the lowest SOC content among all the aggregate particle sizes. In the 10–20 cm soil layer, the SOC1, SOC2, SOC3, and SOC4 (LMAs, SMAs, MIAs, SCAs, aggregate SOCs) were significantly lower than those in the rest of the sample plots. The TN content also showed a similar pattern. The TN4 (<0.053 mm aggregate TN) content of the cultivated land was significantly lower than that of the other plots, and the TN3 (0.053–0.25 mm aggregate TN) content was the highest in RL. The total phosphorus content of the aggregates at all levels in the range of 0–20 cm ranged from 0.67 to 1.28 g/kg, and the content of the 10–20 cm soil layer was slightly lower than that of the 0–10 cm soil layer. The variation in total phosphorus content in different particle sizes between different types of plots was poor. In conclusion, afforestation contributes to the accumulation of soil nutrients.

3.4. Relationships between Aggregate Stability and Soil Nutrients

To see how different plant restoration categories affect the soil aggregate stability, further analysis of the correlation between aggregate particle size and soil structure and soil nutrients was conducted. Based on the measured data, the structure of soil was divided into two categories: the stability factor SST (MWD, GMD, Dm, PAD) and erodibility factor (K). The standardized average value of each factor extreme value was taken as the input parameter of the correlation analysis. The soil nutrient data were processed similarly by taking the average of the standardized values of SOC, TN, and TP, and the combined nutrients of different particle size aggregates were expressed as LMAN, SMAN, MIAN, and SCAN. The findings showed that the aggregate size was closely related to the soil structure index and aggregate nutrients, and LMA and MIA aggregates were particularly well represented. As shown in Table 2, the LMA clusters showed significant positive and negative correlations with the SST and K values, respectively, while in contrast, the MIA clusters showed significant negative and positive correlations with SST and K values, respectively. The SMA and SCA aggregates showed different degrees of a negative correlation with SST and K, and most of them did not reach the significance level. In addition, there was a high positive relationship between the SST and different grain size soil nutrients with the highest correlation coefficient of 0.606 ($p < 0.001$) with the LMA large particle size aggregate nutrients, indicating that macro-aggregates are more favorable for

the soil nutrient aggregation. Unlike SST, the relationship between the K values and all four grain sizes of soil nutrients was significantly negatively correlated, showing that the smaller the grain size, the higher the negative correlation coefficient. This shows that the aggregate size shift has a direct effect on promoting the soil structure and soil nutrient changes.

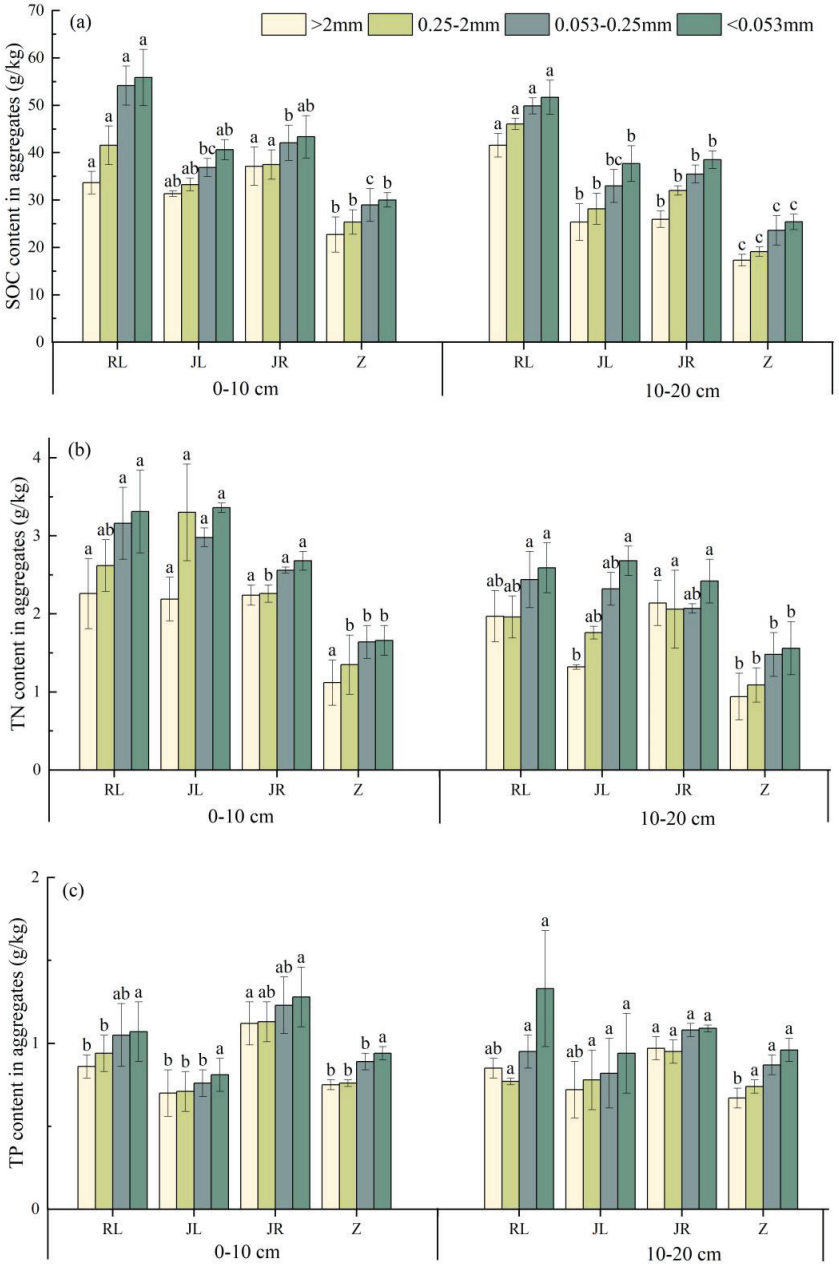

Figure 5. Nutrient content distribution characteristics of soil aggregates. Note: (**a**) SOC content in aggregates; (**b**) TN content in aggregates; (**c**) TP content in aggregates. Various lowercase letters indicate significant differences ($p < 0.05$) in the same soil layer at various sites for the same grain size.

Table 2. Correlation of aggregate size with the soil structure and stability indicators.

	LMA	SMA	MIA	SCA	SST	K	LMAN	SMAN	MIAN	SCAN
LMA	1	−0.55 **	−0.74 **	0.36	0.83 **	−0.61 **	0.63 **	0.56 **	0.53 **	0.40
SMA		1	−0.15	−0.06	−0.14	−0.12	−0.17	−0.05	−0.06	0.14
MIA			1	−0.42 *	−0.87 **	0.82 **	−0.63 **	−0.64 **	−0.60 **	−0.60 **
SCA				1	0.51 *	−0.36	0.54 **	0.47*	0.58 **	0.51 *
SST					1	−0.90 **	0.61 **	0.59 **	0.60 **	0.55 **
K						1	−0.52 **	−0.55 **	−0.56 **	−0.56 **
LMAN							1	0.95 **	0.91 **	0.82 **
SMAN								1	0.95 **	0.89 **
MIAN									1	0.92 **
SCAN										1

Note: The use of an asterisk indicates statistically significant differences. * $p < 0.05$; ** $p < 0.01$.

In addition, the differences in the standardized values of the soil aggregate stability indicators between the plantation grass model and the conventional tillage model were further compared (Figure 6). By comparison, it was found that the LMAs' large particle size aggregates of the three plantation grasslands were obviously higher than those of the cultivated land, while the MIA microaggregates were all smaller than those of the cropland, with the highest standardized value of macroaggregates for the mixed use of *Juglans regia* L. and *Lolium perenne* L., which was approximately 1.76 times higher than that of the cropland. Mixed land forestry and grass use not only promoted changes in aggregate particle size types but were also visualized in soil structure, with substantial increases in stability and erosion resistance. The average SST of the three land use types, RL, JL, and JR, is approximately three times greater than that of cropland, while the average K is only 42% of that of cropland. In terms of standardized values of soil nutrients, the LMANs, SMANs, MIANs, and SCANs of the three mixed land use types were significantly greater than that of the arable monoculture, and the larger the particle size of the aggregates, the higher the degree of soil nutrient aggregation. Compared with traditional cultivated land, artificial afforestation in rocky desertification areas promotes the transformation of microaggregates to macroaggregates to a certain extent, which in turn improves soil nutrients and enhances the soil aggregate stability and is of significant indicative importance for fragile eco-restoration of rocky desertification.

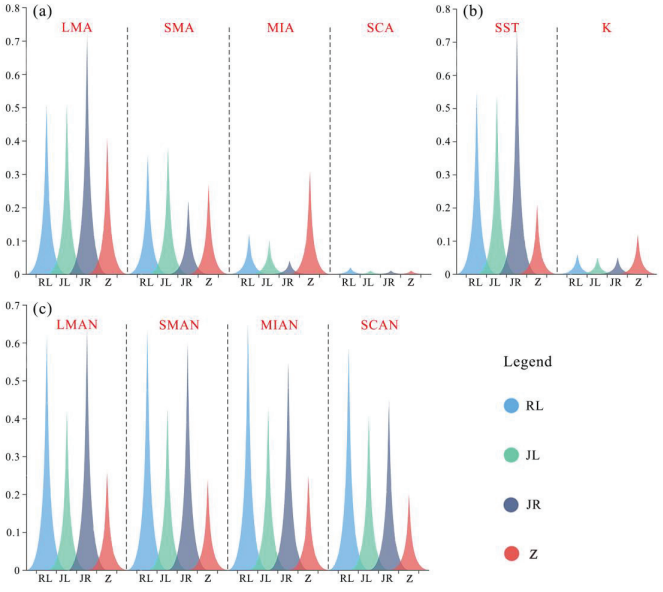

Figure 6. Comparison of aggregate structure and nutrients under different land use patterns. Note: (**a**) Soil aggregates particle size; (**b**) Soil aggregate stability; (**c**) Soil aggregate nutrients.

4. Discussion

4.1. Effects of Artificial Afforestation on Soil Aggregate and Chemical Properties

In this study, the karst rocky desertification area had a high degree of soil fragmentation and low land use efficiency. Land use types have a major effect on soil structure and stability (Figures 2–4). Cultivated land had the greatest MIA and SCA content of all land use types, which was in line with the findings of earlier research [26]. Rainfall-induced soil erosion is a significant factor in the rocky desertification process in karst regions [27], which makes the macroaggregates decompose into MIAs and SCAs, thus reducing the stability of the test soil [28]. The higher LMA content in the three different forest grasslands compared to the cultivated land, with similar trends to the SMA content, was mainly attributed to the breakdown of soil macroaggregates by long-term tillage [29], suggesting that the conversion of cultivated land to forest grassland influences the distribution characteristics of soil aggregates by regulating the LMA aggregate content [30].

In addition, we found that forest-irrigated land had the highest stability, and forest-grassland and forest-irrigated land had the best erosion resistance, followed by irrigated land. On the one hand, plant roots and plant residues in the soil produce more stable compounds [31]; on the other hand, the binding agents of fungi and organic matter in plantation forestland increase with apoplast, forming organic binders that enhance the stability of soil aggregates [32]. The instability of soil aggregates on agricultural land is a major factor in soil erosion. which leads to soil nutrient loss, and natural forestland, due to the vegetation cover, prevents the direct destruction of soil aggregates by heavy rainfall [33]. Soil nutrients such as in woodlands can bind the soil together more [34,35]. Therefore, the planting patterns of *Juglans regia* L.-*Rosa roxburghii* Tratt., *Rosa roxburghii* Tratt.-*Lolium perenne* L., and *Juglans regia* L.-*Lolium perenne* L. in the vegetation restoration used in the management process of karst areas are feasible.

Soil nutrients are regulated by the plant and soil features and have a favorable role in preserving the soil productivity and reducing soil deterioration. In this study, aggregate particle size-related SOC, TN, and TP were strongly impacted by land use type. For example, compared with other sample soils, the highest organic carbon and total nitrogen contents were found in the irrigated grassland, and the highest total phosphorus contents were found in the forested irrigated land, while the nutrients associated with each grain size cluster were significantly lower in the cultivated land than in the other sample soils. Rocky desertification areas have different effects on the nutrients associated with aggregates due to sediment transport under different land use types [31,36]. Additionally, aggregate-associated nutrients were slightly higher in the topsoil layer than in the 10–20 cm soil layer; this might be the result of artificially disturbed soil and factors such as root secretions and surface apoplast influencing the loss and accumulation of aggregate-associated nutrients. In contrast, the TP content associated with forest grassland increased with an increasing soil depth, probably due to the different particle size distributions of the aggregates with increasing soil depth [26]. The fact that the carbon and nitrogen contents of the soil and aggregates were lower in the 10–20 cm soil layer than in the 0–10 cm soil layer suggests that the forest and grass vegetation restoration techniques used in the study area significantly increased the soil's ability to sequester elements by enhancing the vegetation cover and boosting the source of organic matter. The nutrient content in SCA aggregates was slightly higher than in other aggregate particle sizes. Zheng et al. [37] and Liu et al. [38] also reported similar results. More and more organic matter will be absorbed as the aggregates' specific surface area and smaller particle size increase. Thus, small particle size aggregates have a greater surface area of the soil particles, which in turn leads to a greater nutrient content.

4.2. Differences in Soil Structure and Chemical Properties of Different Vegetation Types

Soil properties, environmental factors, land use types, rainfall erosivity, and other factors all influence soil aggregate stability [2,39], and soil nutrients are also closely related to soil structure [17,26,40]. The research results show that there is a significant correlation between the content of large and small soil aggregates, soil aggregate stability indicators,

and aggregate nutrients. The transformation of vegetation type has a significant impact on the particle size of aggregates [41]. Compared with traditional cultivated land, a plantation increases the content of soil macroaggregates, changes the soil structure, enhances the soil aggregate stability, and reduces the soil K, Dm, and PAD, and the anthropogenic disturbance in cultivation activities makes the soil fragmentation rate higher in this environment. In contrast, the vegetation cover, litter in the surface soil, and plant roots of planted forests protect the soil and effectively mitigate the impact of natural factors such as precipitation on the soil structure [42].

Most of the nutrients in soils are found in aggregates, the formation of which is critical to the accumulation of nutrients in aggregates, and the disruption of aggregates can lead to nutrient losses [43], affecting the content of nutrients associated with soil aggregates at all levels. In this study, all nutrient levels were higher in the artificial afforestation pattern than in the traditional cultivated land pattern. Compared to traditional cultivated land, afforestation changes the distribution characteristics of soil aggregates, and this change is related to the intensity of disturbance and overstory plant species under different restoration patterns [44]. The change in plant species reduces runoff, and sediment significantly reduces nutrient loss and promotes nutrient accumulation [45–47]. At the same time, plants secrete large amounts of organic matter, which promotes the growth and secretion of microorganisms, together with the increase in the plant apoplast, helps to regulate nutrient cycling and soil fertility [48], and improves the availability of soil nutrients [49]. The low correlation between the soil aggregate characteristics and soil TP content in this study maybe as a result of the changing soil microbial characteristics and functions during afforestation, which affect microbial metabolism through the enzymatic activities of soil cellulase, β-1,4-N-acetylglucosamnidase, etc., and directly increase the accumulation of soil carbon and nitrogen without directly affecting the accumulation of phosphorus [50].

The statistical analysis of this paper shows that the stability structure and nutrient structure of soil aggregates under the artificial mixed afforestation pattern are superior to those under the traditional single tillage pattern. Compared with the mixed land use type, the vegetation coverage of cultivated land is low and has obvious seasonal differences. When rainfall occurs, microaggregates are more likely to be splashed by raindrops, resulting in the mineralization of the organic matter inside them. Additionally, after harvest, the nutrients in plants cannot be returned to the soil, which is unfavorable to the buildup of soil nutrients [40]. The shift from cultivated land to a plantation mode induces the aggregation of MIAs into LMA macroaggregates, leading to changes in stability indicators such as soil aggregate fragmentation rate, PAD, and erodibility K values, and an increase in the physical protection of nutrients, with a significant accumulation of soil nutrients realized in typical degraded karst areas [51]. Therefore, in terms of the nutrient fixation and stability of the soil, the anthropogenic configuration of forest, irrigation, and grass complex planting in rocky desertification areas has a positive influence on fragile ecological restoration.

4.3. Limitations and Prospects

Long-term artificial plant restoration can significantly improve the soil aggregate stability and encourage nutrient buildup, which is of practical significance for ecosystem vegetation restoration and land use regulation in karst areas. However, the ecological environment of the southwest karst region is complex, and many factors affect the soil environment [52]. Therefore, in subsequent studies, multiple sampling can be performed to increase the number of comparative experiments in the time scale and to explore the variability of the dual spatial and temporal scales. We should not only combine the factors of field differences such as different topography and altitude, but also consider multi-disciplinary intersections and combine factors such as surface plant nutrient differences, surface moss crust characteristics, and soil microbial activity in rocky desertification areas to conduct in-depth research on soil aggregates and their nutrients in karst areas.

5. Conclusions

Through the present study, we analyzed the impact of vegetation restoration on the structure of soil aggregates, soil aggregate stability, and the distribution of aggregate-related organic carbon, total nitrogen, and total phosphorus, as well as the nutrient content response to the soil aggregate stability in the rocky desertification area of the Karst Plateau Mountains in southern China, using four typical land use practices and two soil layers. Research has shown that (1) vegetation restoration significantly affects the LMA content of soil; (2) among the three types of artificial forests, the soil aggregate stability of *Juglans regia* L.-*Rosa roxburghii* Tratt. is better than that of *Rosa roxburghii* Tratt.-*Lolium perenne* L. and *Juglans regia* L.-*Lolium perenne* L.; (3) soil nutrients have significantly improved with the restoration of vegetation; and (4) compared to traditional cultivated land, artificial afforestation in rocky desertification areas has to some extent promoted the transformation of microaggregates to macroaggregates, and the larger the particle size of aggregates, the higher the soil nutrient aggregation. In general, afforestation influences soil aggregate stability by regulating aggregate transformation in karst desertification areas. This study provides a theoretical reference for promoting ecological restoration in rocky desertification areas.

Author Contributions: Conceptualization, D.Z.; methodology, Q.Y.; software, Q.Y.; validation, D.Z. and Q.Y.; formal analysis, Q.Y., Y.Z. and Z.C.; investigation, Z.W. and R.L.; resources, Y.H. and J.N.; data curation, Q.Y.; writing—original draft preparation, D.Z.; writing—review and editing, D.Z. All authors have read and agreed to the published version of the manuscript.

Funding: This work was supported by the National Natural Science Foundation of China (No. 41907042) and the special project of Guizhou Normal University on Academic Seedling Cultivation and Innovation Exploration (Grant No. 2019).

Data Availability Statement: The processed data required to reproduce these findings cannot be shared at this time as the data also forms part of an ongoing study.

Conflicts of Interest: The authors state no conflict of interest.

References

1. Liu, X.B.; Zhang, X.Y.; Wang, Y.X.; Sui, Y.Y.; Zhang, S.L.; Herbert, S.J.; Ding, G. Soil degradation: A problem threatening the sustainable development of agriculture in Northeast China. *Plant Soil Environ.* **2010**, *56*, 87–97. [CrossRef]
2. Dong, L.B.; Li, J.W.; Liu, Y.L.; Hai, X.Y.; Li, M.Y.; Wu, J.Z.; Wang, X.Z.; Shangguan, Z.P.; Zhou, Z.C.; Deng, L. Forestation delivers significantly more effective results in soil C and N sequestrations than natural succession on badly degraded areas: Evidence from the Central Loess Plateau case. *Catena* **2022**, *208*, 105734. [CrossRef]
3. Lan, J. Changes of soil aggregate stability and erodibility after cropland conversion in degraded karst region. *J. Soil Sci. Plant Nutr.* **2021**, *21*, 3333–3345. [CrossRef]
4. He, J.H.; Zhang, K.L.; Cao, Z.; Ke, Q.H. Tracer vertical movement and its affecting factors in karst soil profiles in simulated leaching context. *J. Soils Sediments* **2021**, *22*, 229–237. [CrossRef]
5. Jiang, Z.; Lian, Y.; Qin, X. Rocky desertification in Southwest China: Impacts, causes, and restoration. *Earth-Sci. Rev.* **2014**, *132*, 1–12. [CrossRef]
6. Six, J.; Bossuyt, H.; Degryze, S.; Denef, K. A history of research on the link between (micro) aggregates, soil biota, and soil organic matter dynamics. *Soil Tillage Res.* **2004**, *79*, 7–31. [CrossRef]
7. Le Bissonnais, Y. Aggregate stability and assessment of soil crustability and erodibility: I. Theory and methodology. *Eur. J. Soil Sci.* **1996**, *47*, 425–437. [CrossRef]
8. Wuddivira, M.N.; Stone, R.J.; Ekwue, E.I. Clay, organic matter, and wetting effects on splash detachment and aggregate breakdown under intense rainfall. *Soil Sci. Soc. Am. J.* **2009**, *73*, 226–232. [CrossRef]
9. Zhang, K.L.; Shu, A.P.; Xu, X.L.; Yang, Q.K.; Yu, B. Soil erodibility and its estimation for agricultural soils in China. *J. Arid. Environ.* **2008**, *72*, 1002–1011. [CrossRef]
10. Park, S.I.; Yang, H.I.; Park, H.J.; Seo, B.S.; Jeong, Y.J.; Lim, S.S.; Kwak, J.H.; Kim, H.Y.; Yoon, K.S.; Lee, S.M.; et al. Rice straw cover decreases soil erosion and sediment-bound C, N, and P losses but increases dissolved organic C export from upland maize fields as evidenced by $\delta^{13}C$. *Sci. Total Environ.* **2021**, *753*, 142053. [CrossRef]
11. Lan, M.; Xue, C.; Yang, J.; Wang, N.; Sun, C.; Wu, G.; Chen, H.; Su, Z. Changes in Plant Diversity and Soil Factors under Different Rocky Desertification Degrees in Northern Guangdong, China. *Forests* **2023**, *14*, 694. [CrossRef]
12. Yılmaz, E.; Çanakcı, M.; Topakcı, M.; Sönmez, S.; Ağsaran, B.; Alagöz, Z.; Çıtak, S.; Uras, D.S. Effect of vineyard pruning residue application on soil aggregate formation, aggregate stability and carbon content in different aggregate sizes. *Catena* **2019**, *183*, 104219. [CrossRef]

13. Guo, M.M.; Chen, Z.X.; Wang, W.L.; Wang, T.C.; Wang, W.X.; Cui, Z.Q. Revegetation induced change in soil erodibility as influenced by slope situation on the Loess Plateau. *Sci. Total Environ.* **2021**, *772*, 145540. [CrossRef]
14. Wang, H.; Wang, J.; Zhang, G. Impact of landscape positions on soil erodibility indexes in typical vegetation-restored slope-gully systems on the Loess Plateau of China. *Catena* **2021**, *201*, 105235. [CrossRef]
15. Guan, Y.J.; Zhou, W.; Bai, Z.K.; Cao, Y.G.; Huang, Y.H.; Huang, H.Y. Soil nutrient variations among different land use types after reclamation in the Pingshuo opencast coal mine on the Loess Plateau, China. *Catena* **2020**, *188*, 104427. [CrossRef]
16. Dong, L.; Li, J.; Zhang, Y.; Bing, M.Y.; Liu, Y.L.; Wu, J.Z.; Hai, X.Y.; Li, A.; Wang, K.B.; Wu, P.X.; et al. Effects of vegetation restoration types on soil nutrients and soil erodibility regulated by slope positions on the Loess Plateau. *J. Environ. Manag.* **2022**, *302*, 113985. [CrossRef]
17. Yan, H.; Wang, L.; Wang, T.W.; Wang, Z.; Shi, Z.H. A synthesized approach for estimating the C-factor of RUSLE for a mixed-landscape watershed: A case study in the Gongshui watershed, southern China. *Agric. Ecosyst. Environ.* **2020**, *301*, 107009. [CrossRef]
18. Zheng, J.Y.; Zhao, J.S.; Shi, Z.H.; Wang, L. Soil aggregates are key factors that regulate erosion-related carbon loss in citrus orchards of southern China: Bare land vs. grass-covered land. *Agric. Ecosyst. Environ.* **2021**, *309*, 107254. [CrossRef]
19. Yoder, R.E. A direct method of aggregate analysis of soils and a study of the physical nature of erosion losses. *Soil Sci. Soc. Am. J.* **1936**, *28*, 337–351. [CrossRef]
20. Bao, S.D. *Analysis of Soil Agrochemical*, 3rd ed.; Agriculture Press: Beijing, China, 2000.
21. Van Bavel, C.H.M. Mean weight-diameter of soil aggregates as a statistical index of aggregation. *Proc. Soil Sci. Soc. Am.* **1950**, *14*, 20–23. [CrossRef]
22. Gardner, W.R. Representation of soil aggregate-size distribution by a logarithmic-normal distribution. *Soil Sci. Soc. Am. J.* **1956**, *20*, 151–153. [CrossRef]
23. Shirazi, M.A.; Boersma, L. A unifying quantitative analysis of soil texture. *Soil Sci. Soc. Am. J.* **1984**, *48*, 142–147. [CrossRef]
24. Yang, P.L.; Luo, Y.P.; Shi, Y.C. Soil fractal characteristics characterized by weight distribution of particle size. *Chin. Sci. Bull.* **1993**, *20*, 1896–1899.
25. Liu, W.L.; Wu, J.G.; Fu, M.J.; Liang, Y.J.; Zhao, X.Y. Effect of different cultivation years on composition and stability of soil aggregate fractions in orchard. *J. Soil Water Conserv.* **2014**, *28*, 129–135.
26. Tang, X.; Qiu, J.; Xu, Y.; Li, J.H.; Chen, J.H.; Li, B.; Lu, Y. Responses of soil aggregate stability to organic C and total N as controlled by land-use type in a region of south China affected by sheet erosion. *Catena* **2022**, *218*, 106543. [CrossRef]
27. Zhu, D.; Xiong, K.; Xiao, H. Multitime scale variability of rainfall erosivity and erosivity density in the karst region of southern China, 1960–2017. *Catena* **2021**, *197*, 104977. [CrossRef]
28. Zhang, J.; Yang, M.; Deng, X.; Liu, Z.; Zhang, F. The effects of tillage on sheet erosion on sloping fields in the wind-water erosion crisscross region of the Chinese Loess Plateau. *Soil Tillage Res.* **2019**, *187*, 235–245. [CrossRef]
29. Barreto, R.C.; Madari, B.E.; Maddock, J.E.L.; Machado, P.L.; Torres, E.; Franchini, J.; Costa, A.R. The impact of soil management on aggregation, carbon stabilization and carbon loss as CO_2 in the surface layer of a Rhodic Ferralsol in Southern Brazil. *Agric. Ecosyst. Environ.* **2009**, *132*, 243–251. [CrossRef]
30. He, Y.; Zhang, Q.; Wang, S.; Jiang, C.; Lan, Y.; Zhang, H.; Ye, S. Mixed Plantations Induce More Soil Macroaggregate Formation and Facilitate Soil Nitrogen Accumulation. *Forests* **2023**, *14*, 735. [CrossRef]
31. Li, H.; Zhu, H.; Liang, C.; Wei, X.; Yao, Y. Soil erosion significantly decreases aggregate-associated OC and N in agricultural soils of Northeast China. *Agric. Ecosyst. Environ.* **2022**, *323*, 107677. [CrossRef]
32. Zeng, Q.; Darboux, F.; Man, C.; Zhu, Z.; An, S. Soil aggregate stability under different rain conditions for three vegetation types on the Loess Plateau (China). *Catena* **2018**, *167*, 276–283. [CrossRef]
33. Ruiz-Colmenero, M.; Bienes, R.; Eldridge, D.J.; Marques, M.J. Vegetation cover reduces erosion and enhances soil organic carbon in a vineyard in the central Spain. *Catena* **2013**, *104*, 153–160. [CrossRef]
34. Ayoubi, S.; Karchegani, P.M.; Mosaddeghi, M.R.; Honarjoo, N. Soil aggregation and organic carbon as affected by topography and land use change in western Iran. *Soil Tillage Res.* **2012**, *121*, 18–26. [CrossRef]
35. Wang, X.; Cammeraat, E.L.H.; Cerli, C.; Kalbitz, K. Soil aggregation and the stabilization of organic carbon as affected by erosion and deposition. *Soil Biol. Biochem.* **2014**, *72*, 55–65. [CrossRef]
36. Liu, M.; Han, G.; Li, X. Contributions of soil erosion and decomposition to SOC loss during a short-term paddy land abandonment in Northeast Thailand. *Agric. Ecosyst. Environ.* **2021**, *321*, 107629. [CrossRef]
37. Zheng, Z.C.; He, S.Q.; Li, T.X.; Wang, Y.D. Effect of land use patterns on stability and distributions of organic carbon in the hilly region of Western Sichuan, China. *Afr. J. Biotechnol.* **2011**, *10*, 13107–13114. [CrossRef]
38. Liu, D.; Ju, W.; Jin, X.; Li, M.; Shen, G.T.; Duan, C.J.; Guo, L.; Liu, Y.; Zhao, W.; Fang, L. Associated soil aggregate nutrients and controlling factors on aggregate stability in semiarid grassland under different grazing prohibition timeframes. *Sci. Total Environ.* **2021**, *777*, 146104. [CrossRef]
39. Nciizah, A.D.; Wakindiki, I.I.C. Physical indicators of soil erosion, aggregate stability and erodibility. *Arch. Agron. Soil Sci.* **2015**, *61*, 827–842. [CrossRef]
40. Guo, Y.; Fan, R.; Zhang, X.; Zhang, Y.; Wu, D.; Mclaughlin, N.; Zhang, S.; Chen, X.; Jia, S.; Liang, A. Tillage-induced effects on SOC through changes in aggregate stability and soil pore structure. *Sci. Total Environ.* **2020**, *703*, 134617. [CrossRef]

41. Fonte, S.J.; Nesper, M.; Hegglin, D.; Velásquez, J.E.; Ramirez, B.; Rao, I.M.; Bernasconi, S.M.; Bünemann, E.K.; Frossard, E.; Oberson, A. Pasture degradation impacts soil phosphorus storage via changes to aggregate-associated soil organic matter in highly weathered tropical soils. *Soil Biol. Biochem.* **2014**, *68*, 150–157. [CrossRef]
42. Yan, Y.C.; Wang, X.; Guo, Z.J.; Chen, J.Q.; Xin, X.P.; Xu, D.W.; Yan, R.R.; Chen, B.R.; Xu, L.J. Influence of wind erosion on dry aggregate size distribution and nutrients in three steppe soils in northern China. *Catena* **2018**, *170*, 159–168. [CrossRef]
43. Jiang, W.; Li, Z.; Xie, H.; Ouyang, K.; Yuan, H.; Duan, L. Land use change impacts on red slate soil aggregates and associated organic carbon in diverse soil layers in subtropical China. *Sci. Total Environ.* **2023**, *856*, 159194. [CrossRef]
44. Robert, J.H.; Sarah, J.R.; Ian, A.D.; Duane, A.P.; David, A.C. Species-and community-level patterns in fine root traits along a 120,000-year soil chronosequence in temperate rainforest. *J. Ecol.* **2011**, *99*, 954–963. [CrossRef]
45. Cleveland, C.C.; Townsend, A.R.; Taylor, P.; Alvarez-Clare, S.; Bustamante, M.M.C.; Chuyong, G.; Dobrowski, S.Z.; Grierson, P.; Harms, K.E.; Houlton, B.Z.; et al. Relationships among net primary productivity, nutrients and climate in tropical rainforest: A pan-tropical analysis. *Ecol. Lett.* **2011**, *14*, 939–947. [CrossRef]
46. Wang, S.Q.; Huang, Y.Z.; Ye, S.M. Distribution of organic carbon and nutrients in soil aggregates under different stand types of *Cunninghamia lanceolata* in southern Guangxi of China. *Soil Sci. Plant Nutr.* **2021**, *67*, 427–438. [CrossRef]
47. Hou, E.Q.; Wen, D.Z.; Jiang, L.F.; Luo, X.Z.; Kuang, Y.W.; Lu, X.K.; Chen, C.R.; Allen, K.T.; He, X.J.; Huang, X.Z.; et al. Latitudinal patterns of terrestrial phosphorus limitation over the globe. *Ecol. Lett.* **2021**, *24*, 1420–1431. [CrossRef]
48. Zhang, Y.; Zhang, B.; Xu, Q.; Gao, D.; Xu, W.; Ren, R.; Jiang, J.; Wang, S. The effects of plant and soil characteristics on partitioning different rainfalls to soil in a subtropical Chinese fir forest ecosystem. *Forests* **2022**, *13*, 123. [CrossRef]
49. Philippot, L.; Raaijmakers, J.M.; Lemanceau, P.; Van der Putten, W.H. Going back to the roots: The microbial ecology of the rhizosphere. *Nat. Rev. Microbiol.* **2013**, *11*, 789–799. [CrossRef]
50. Luo, X.; Hou, E.; Zhang, L.; Kuang, Y.; Wen, D. Altered soil microbial properties and functions after afforestation increase soil carbon and nitrogen but not phosphorus accumulation. *Biol. Fertil. Soils* **2023**, 1–14. [CrossRef]
51. Lan, J.; Long, Q.; Huang, M.; Jiang, Y.; Hu, N. Afforestation-induced large macroaggregate formation promotes soil organic carbon accumulation in degraded karst area. *For. Ecol. Manag.* **2022**, *505*, 119884. [CrossRef]
52. Wang, X.; Huang, X.; Xiong, K.; Hu, J.; Zhang, Z.; Zhang, J. Mechanism and Evolution of Soil Organic Carbon Coupling with Rocky Desertification in South China Karst. *Forests* **2022**, *13*, 28. [CrossRef]

forests

MDPI

Article

Changes in Ecosystem Service Values of Forests in Southwest China's Karst Regions from 2001–2020

Zhongfa Zhou [1,*], Lu Zhang [1,2], Tangyin Wu [1], Dan Luo [1], Lan Wu [1], Quan Chen [3] and Qing Feng [3]

[1] School of Karst Science, Guizhou Normal University, Guiyang 550001, China; sophiazl@gznu.edu.cn (L.Z.); 21010170545@gznu.edu.cn (T.W.); 21010170535@gznu.edu.cn (D.L.); 21010170543@gznu.edu.cn (L.W.)
[2] Real Estate Registration Center of Guizhou Province, Guiyang 550001, China
[3] The State Key Laboratory Incubation Base for Karst Mountain Ecology Environment of Guizhou Province, Guiyang 550001, China; 201407075@gznu.edu.cn (Q.C.); 20030170040@gznu.edu.cn (Q.F.)
* Correspondence: fa6897@gznu.edu.cn

Abstract: Forests, serving as crucial custodians of our planet's ecological balance, also constitute a significant source of livelihood for humanity. Karst regions, recognized as some of the world's most susceptible landscapes, grapple with the dual predicaments of ecological restoration and resident impoverishment. To bridge the gap between environmental and economic concerns, this manuscript employs an amalgamation of remote sensing and socio-economic methodologies to devise a comprehensive assessment framework, thereby scrutinizing the alterations in forest ecosystems from 2001 to 2020.The investigation reveals that over the past two decades, forest rehabilitation within the study area has yielded commendable outcomes, substantially mitigating various ecological dilemmas instigated by rocky desertification in this region. The forested area has increased significantly, and the ecosystem service value has more than doubled. These improvements are largely attributed to compulsory forest conservation measures, demonstrating their decisive influence. The study advocates meticulous management and conservation strategies to safeguard these unique ecosystems and ensure their sustainability. This research underscores the significance of striking a balance between maintaining ecological integrity and fostering economic development, thereby contributing to the broader discourse on sustainable forest management in vulnerable landscapes.

Keywords: forest; ecosystem services; karst

Citation: Zhou, Z.; Zhang, L.; Wu, T.; Luo, D.; Wu, L.; Chen, Q.; Feng, Q. Changes in Ecosystem Service Values of Forests in Southwest China's Karst Regions from 2001–2020. *Forests* **2023**, *14*, 1534. https://doi.org/10.3390/f14081534

Academic Editors: Mathias Neumann and Timothy A. Martin

Received: 4 June 2023
Revised: 21 July 2023
Accepted: 24 July 2023
Published: 27 July 2023

1. Introduction

Forests, encompassing approximately one-third of Earth's terrestrial surface [1], serve as crucial constituents in maintaining our planet's ecological balance while providing an array of indispensable ecosystem services vital to human well-being. Forests are geographically unevenly distributed across the globe. Russia, Brazil, Canada, the United States, and China collectively account for 54% of the world's forested areas [2], thereby conferring upon these nations a heightened responsibility for safeguarding forest ecosystems. Moreover, forests function as crucial components within the Earth's biosphere, contributing not only to global energy and material cycles, but also furnishing a variety of direct and indirect products essential for human life and economic development. Forests represent a principal source of livelihood for innumerable communities [3], particularly in rural areas. However, factors such as anthropogenic activities, wildfires, pests, diseases, and other environmental perturbations can degrade forests, resulting in diminished supply of forest products and services, biodiversity value, productivity, and health [4]. Forest degradation can also precipitate other adverse environmental consequences, including deterioration of downstream water quality and increased greenhouse gas emissions [5,6]. Although a multitude of measures have been enacted globally to ensure the sustainable utilization of forest resources, the rate of forest area loss has slowed, yet forested areas continue to

decrease worldwide. This issue is particularly acute in developing countries, especially in impoverished regions.

The sustainable use of forests is intimately linked to societal challenges such as eradicating poverty and addressing global climate change [7]. To bridge the gap between environmental and economic concerns, scientists across the world have conducted extensive research and devised comprehensive frameworks to quantify the myriad benefits of forest ecosystems and account for the stock and flow of forest resources within the environmental and economic systems [8,9]. The System of Environmental-Economic Accounting—Ecosystem Accounting (SEEA EA) proffers a systematic approach for measuring and reporting the economic, social, and environmental values of forest ecosystems [10], predicated on the principles of the System of Environmental-Economic Accounting Central Framework (SEEA-CF) [11]. Concurrently, it is a spatially based comprehensive statistical framework [12] employed to organize biophysical information about ecosystems, measure ecosystem services, monitor changes in ecosystem scope and conditions, evaluate ecosystem services and assets, and integrate this information with measurements of economic and human activities.

This framework has yielded some noteworthy findings in the appraisal of forest ecosystem value. Countries such as the UK and the Netherlands have published the most comprehensive accounting results thus far, and the EU has developed supranational accounting [13]. However, the implementation of SEEA EA typically necessitates detailed and comprehensive data, which is relatively accessible in developed countries but often unattainable in remote or economically disadvantaged developing countries. Additionally, the imperfect national economic accounting systems of developing countries hinder the integration of data procured from various statistical measurements using unified standards, precluding comprehensive analysis. Consequently, there remain numerous limitations and challenges in the promotion and application process. Despite the backing of several pilot projects by the World Bank and the United Nations [14], such as the Natural Capital Accounting and Valuation of Ecosystem Services (NCAVES) project [15,16], these constraints cannot be entirely surmounted. For instance, in Indonesia, the government favors planning land use over mapping spatial data on forest scope, conditions, and use [17,18], thereby rendering it incapable of monitoring forest resource use and fluctuations in forest ecosystem conditions and values using statistical data. This underscores a pressing gap that needs to be addressed in developing nations, particularly in economically deprived areas: how can we employ limited biophysical parameters to rapidly evaluate the ecosystem changes in the range, quality, and value of these regions, thereby fostering the sustainable development of the local economy and society? To address these limitations, an increasing number of geographers have become engaged in this work. Owing to advancements in remote sensing and geographic information technology, scientists have been able to employ remote sensing data to monitor forests globally, including their distribution, health status, and other relevant attributes. Satellite data reveals that China's net growth in leaf area between 2000 and 2017 accounted for 25% of the global total, with 42% of this greening stemming from forests [19,20]. By harnessing remote sensing technology, researchers can access an abundance of data on forest ecosystems, which can be analyzed in tandem with socio-economic data to furnish a more comprehensive understanding of the value of forest ecosystem services and the factors influencing their changes. Integrating remote sensing data with socio-economic data can yield more accurate and spatially explicit assessments of forest ecosystem services, as well as their value and temporal changes [21,22]. This approach holds the potential to surmount the data limitations faced in poverty-stricken and remote areas, contributing to a more accurate and holistic comprehension of forest ecosystems and their role in supporting human well-being. Simultaneously, policymakers and forest managers can acquire a more comprehensive understanding of the implications of different management options for both ecosystems and human well-being.

Our analysis of remote sensing data on global forest change over the past 20 years indicates that forest change in China is highly significant, with a substantial proportion

of karst mountainous areas in the Southwest experiencing reforestation [23,24]. These areas serve as vital ecological barriers in the upper reaches of the Yangtze River and represent ecologically fragile regions characterized by a widespread distribution of karst landforms. The karst area in southwest China, influenced by both natural and human factors, underwent severe degradation of karst rocky desertification from the 1950s to the 1990s. The ecosystem in this region is exceptionally fragile, and the poverty rate among farmers is high, resulting in a pronounced conflict between humans and land [25–27]. For instance, in karst areas where farmland is scarce, numerous impoverished farmers increase their income by deforesting. However, deforestation leads to a larger scale of rocky desertification, which further exacerbates the difficulties in agricultural production, creating a phenomenon of "the more deforestation, the poorer; the poorer, the more deforestation". Therefore, the objective of this research is to harness remote sensing and socioeconomic data to scrutinize changes in the forest ecosystem of the area from 2001 to 2020. By doing so, we aim to evaluate the impacts of forest conservation implementations, investigate the delicate balance between ecosystem protection and economic growth, and thereby provide guidance to policy makers. This assistance would be instrumental in facilitating prudent forest management decisions, considering ecosystem functionality and human welfare considerations.

2. Materials and Methods

2.1. Overview of the Study Area

Nestled within the karst mountainous expanse of southwest China lies the study area, a unique and intricate ecosystem distinguished by its remarkable topography and diverse vegetation (Figure 1). This region, predominantly composed of limestone and dolomite formations [28], stands as a quintessential exemplar of global karst landforms, with an extensive karst development encompassing over 73.8% of the total area [29–31].

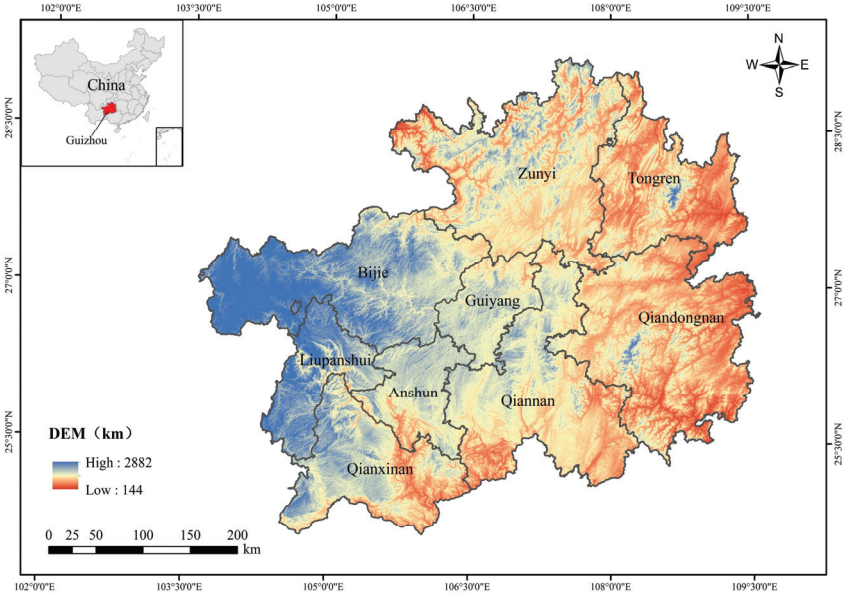

Figure 1. Location of the study area.

The region's climate is classified as subtropical monsoon, characterized by high temperatures and abundant rainfall. The average annual temperature ranges from 14 °C to 16 °C, and the annual precipitation averages between 1000 mm and 1300 mm. This climate, in conjunction with the region's distinctive karst topography, has catalyzed a rapid

greening process. The region's vegetation is as multifaceted as its topography, including a variety of co-existing forest types. Economically significant and ubiquitously distributed coniferous forests, primarily composed of Chinese fir (*Cunninghamia lanceolata*), Mason pine (*Pinus massoniana*), Yunnan pine (*Pinus yunnanensis*), and cypress forests (*Cupressus* spp.), intermingle with broad-leaved forests. The latter predominantly comprise species from the Fagaceae family, including *Fagus* spp., Lauraceae family with *Laurus* spp., Magnoliaceae family with *Magnolia* spp., and Camelliaceae family with *Camellia* spp. [32]. These forests are interspersed with bamboo forests, shrubs, and swamp and aquatic vegetation, contributing to the region's rich biodiversity.

The strata of the research area predominantly consist of sedimentary rocks and slightly metamorphosed sedimentary rocks, with igneous rocks and highly metamorphosed rocks being sparse. Among the sedimentary rocks, carbonate rocks are the most developed, with an accumulated thickness of up to 20,000 m. Due to the restriction of parent-rock properties in soil formation, the research area exhibits lithogenic soils such as calcareous and purple soils. Soil types, distributed roughly from south to north, encompass ferruginous tropical soil, lateritic red soil, yellowish-red soil, yellow soil, yellow-brown soil, and montane meadow soil. Karst landforms in this region are characterized by a variety of dissolution features, including sinkholes, caves, and disappearing streams, formed as a consequence of the dissolution of the underlying soluble rock by slightly acidic water. These areas typically possess complex subterranean drainage systems, with water infiltrating the ground through sinkholes and other surface features and coursing through a network of subterranean channels and caves. This results in sparse surface water, with streams and rivers often disappearing underground. The soil in this region, often thin and rocky due to the karst topography, has given rise to unique vegetation patterns [33–35]. Plants must adapt to the rocky soil and fluctuating water availability [36].

The vegetation in this region exhibits zonality driven by thermal conditions and water constraints. The subtropical monsoon climate, in conjunction with the region's distinctive karst topography, has catalyzed a rapid greening process, particularly in the Karst Peak-Cluster Depression and Karst Trough Valley [37]. However, in non-karst areas of the west highland in the Karst Fault Basin and Karst Plateau, decreasing rainfall has caused recent degradation. Vertically, a distinct zonal pattern is observable under the comprehensive influence of water, heat, and other environmental factors [38]. The interplay of these factors has resulted in a diverse range of forest types, from coniferous and broad-leaved forests to bamboo forests, shrubs, and swamp and aquatic vegetation.

Simultaneously, as the region embarks on ecological restoration initiatives such as the reforestation of agricultural land, it is also hosting industries such as distinctive fruit forestry, under-forest economy, and forest ecotourism. These endeavors aim to augment the economic value of forestry products, thereby striking a balance between ecological preservation and economic development.

2.2. Dataset

In this investigation, we utilized both spatial and socio-economic data to evaluate alterations in forest resources. The spatial data, procured from the Google Earth Engine Platform, were juxtaposed with socio-economic data, encompassing forest products and forest-related disasters, sourced from the Guizhou Statistical Yearbook spanning the years 2001 through 2021. We procured land-cover data (the MCD12Q1 V6 product) from 2001 to 2020 with a resolution of 500 m, which derived from supervised classifications of MODIS Terra and Aqua reflectance data. These land-cover data were generated by a decision-tree classification algorithm. This algorithm utilizes various data layers, including surface reflectance, brightness temperature, land-surface temperature, vegetation indices, and derived-texture metrics. The classification scheme included 5 legacy classification schemes (IGBP, UMD, LAI, BGC, and PFT). The International Geosphere-Biosphere Programme (IGBP) scheme is used in this research, which classifies land cover into 17 classes, including various types of forests, shrublands, savannas, wetlands, and urban areas [39]. The Land-

sat net primary production CONUS (NPP) was ascertained and the Global Precipitation Measurement (GPM) data (Monthly Global Precipitation Measurement v6) were utilized to amend the pre-existing findings pertaining to ecological value. The Global Precipitation Measurement signifies an international satellite endeavor that furnishes cutting-edge observations of precipitation in the form of rain and snow on a global scale, with an update interval of three hours. The Integrated Multi-Satellite Retrievals for GPM (IMERG) represents a consolidated algorithm that generates rainfall estimates by amalgamating data from all passive-microwave instruments integrated within the GPM Constellation. Additionally, we employed a digital elevation model (DEM) with a resolution of 12.5 m to generate the slope, elevation, and aspect of the study area (Table 1).

Table 1. Data sources for assessing forest resources changes.

	Resource Type	Data Sources
Spatial Data	Digital elevation models (DEM) Land Cover Landsat net primary production (NPP) Global precipitation measurement (GPM)	Google Earth Engine Platform (https://developers.google.cn/earth-engine/datasets) accessed on 4 December 2022
Socio-economic Data	Forest Products Forest Fire Insect pests and rat infestations	Guizhou Statistical Yearbook (2001–2021) (http://stjj.guizhou.gov.cn/) accessed on 4 December 2022

2.3. Methods

2.3.1. Indicator Framework

This investigation presents an exhaustive and multi-dimensional methodology to scrutinize the alterations in forest resources within the karst mountainous expanse of southwest China. Initially, the remote sensing examination employs land-cover data to delineate the scope and categorization of forests within the research zone, and a change detection analysis is executed in Google Earth Engine (GEE) to pinpoint regions of forest augmentation and depletion throughout the investigation years. This necessitates a comparison of land-cover data (IGBP classification system. Appendix A) across various years and the identification of pixels that have transitioned from one forest classification to another, or from forest to non-forest, and vice versa. The Digital Elevation Model (DEM) data are utilized to generate topographic variables that could potentially impact the distribution of forests, such as slope, elevation, and aspect.

The statistical analysis incorporates landscape indices to mirror alterations in the landscape configuration of the research zone. These indices, computable via Python, provide quantitative assessments of landscape fragmentation, connectivity, diversity, and other attributes. These indices are computed for each year of the investigation duration, facilitating a quantitative appraisal of alterations in the landscape configuration over time.

Finally, through the amalgamation of remote sensing data, socio-economic data, field surveys, and community surveys, this manuscript establishes two accounts (Table 2), specifically, physical condition and ecosystem services to monitor the spectrum of forest resources, health status, yield of forest products, and alterations in ecosystem services within the research zone. The fusion of qualitative and quantitative analysis enables a comprehensive appraisal of alterations in forest resources. This methodology enhances the insights derived from the remote sensing and landscape analysis, offering a more intricate and nuanced comprehension of the complex interplay between natural and human factors within the research zone.

Table 2. Indicators for assessing forests.

Account Types	First-Level Indicators	Second-Level Indicators
Physical Condition	Extent	Area
	Livelihood provision	Forest Production
	Site conditions	Elevation
		Slope
	Landscape index	NP
		PD
		LPI
		ED
		AREA_MN
		SHAPE_MN
		FRAC_MN
		COHESION
		DIVISION
		AI
	Threats	Forest Fire
		Pests and Rats
Ecosystem Services	Provisioning Services	Food production
		Raw Material Production
		Water Supply
	Regulating Services	Gas Regulation
		Climate Regulation
		Environmental Purification
		Hydrological Regulation
	Supporting Services	Soil Conservation
		Maintenance of Nutrient Cycles
		Biodiversity
	Cultural Services	Aesthetic Landscape

2.3.2. Landscape Index

The research zone has experienced substantial population migration and adjustments in land-use policy over the past two decades. The examination of landscape-pattern evolution can elucidate the mechanism of interaction between frequent human disturbances and the process of forest transformation [40,41]. Consequently, this manuscript has chosen a suite of indices—Number of Patch (NP), Patch Density (PD), Largest Patch Index (LPI), Edge Density (ED), Mean Area Index (AREA_MN), Mean Shape Index (SHAPE_MN), Mean Patch Fractal Dimension (FRAC_MN), Patch Cohesion Index (COHESION), Landscape Division Index (DIVISION), and Aggregation Index (AI)—to holistically represent the evolution of the landscape pattern within the research zone. The calculation of these landscape indices involved the use of MCD12Q1 V6 land-cover data. These data were transmuted into binary maps, facilitating the extraction of four distinct forest cover categories: Evergreen Needleleaf Forest, Evergreen Broadleaf Forest, Deciduous Broadleaf Forest, and Mixed Forest. Simultaneously, non-forest background data was assigned a value of 9999. This process yielded a sequence of landscape indices for the study area, with the computation method as follows (Table 3):

Table 3. Landscape indexes.

Landscape Index	Indicator Description	Calculation Formula	Reference
Number of Patch (NP)	The number of patches, or the number of patches of a certain type of landscape	N	[42]

Table 3. *Cont.*

Landscape Index	Indicator Description	Calculation Formula	Reference
Patch Density (PD)	PD represents the density of a certain patch in the landscape, which can reflect the heterogeneity and fragmentation of the landscape as a whole and the degree of fragmentation of a certain type, as well as the heterogeneity of the landscape per unit area.	$PD = \frac{NP}{A}$	[42]
Largest Patch Index (LPI)	LPI is the ratio of the largest patch area to the total area in line, which is a positive correlation indicator of the contiguous situation, reflecting the size of the dominant patch in the landscape.	$LPI = A_{max}/A$	[41]
Edge Density (ED)	ED is the ratio of the total perimeter to the total area of the patch, which is a negative correlation indicator of the contiguous situation, reflecting the degree of fragmentation of the patch.	$ED = \frac{P}{A}$	[43]
Mean Area (AREA_MN)	It represents an average situation, which indicates the degree of fragmentation of the landscape.	$AREA_{MN} = A/N$	[43]
Mean Shape (SHAPE_MN)	It is the mean shape index, which reflects the degree of disturbance of human activities to the landscape pattern.	$SPI_{MN} = \frac{\sum_{i=1}^{n} 0.25P_i/\sqrt{a_i}}{N}$	[44]
Mean Patch Fractal Dimension (FRAC_MN)	It indicates the complexity of the plate. If the result is 1.0, it indicates the simplest square plate.	$FRAC_{MN} = \frac{\sum 2ln(\frac{P_i}{4})/ln^4}{N}$	[44]
Patch Cohesion Index (COHESION)	It reflects the aggregation and dispersion of patches in the landscape, and the value is between −1 and 1. When the index result is −1, the patches are completely dispersed, and when the result is 1, the patches are clustered.	$C = \frac{(1 - \frac{\sum_{j=1}^{m} p_{ij}}{\sum_{j=1}^{m} p_{ij}\sqrt{a_{ij}}})}{(1 - \frac{1}{\sqrt{A}})} \times 100$	[45]
Landscape Division Index (DIVISION)	It refers to the separation degree of individual distribution of different plates in a certain landscape type.	$D = [1 - \sum_{j=1}^{m} (\frac{a_{ij}}{A})^2]$	[45]
Aggregation Index (AI)	AI examined the connectivity between patches of each landscape type. The smaller the value, the more discrete the landscape.	$AI = [\frac{g_{ii}}{\max \rightarrow g_{ii}}](100)$	[46]

A is the total area of landscape or patch (hm^2). P is the total perimeter of all cropland patches. a_i is the patch area. P_i is the perimeter of the patch. g_{ii} is the number of similar adjacent patches of the corresponding landscape type.

2.3.3. Ecosystem Services Value-Equivalent Model

Forests, as an important ecosystem, provide four categories of ecosystem services for human beings, which are provisioning services (PS), regulating services (RS), supporting services (SS) and cultural services (CS) [47]. Our investigation employed a revised version of the ecosystem service value-estimation methodology proposed by Costanza et al. [48,49]. This approach was further refined by Chinese researchers including Xie Gaodi et al. to accommodate the economic conditions, land usage, and vegetation types particular to China. The methodology initially calculates the value of various ecosystem services as an equivalent to the value of food production from farmland, that is, setting the equivalent value of ecological services for food production in farmland as 1, and calculating the value of other types of ecosystem services based on the willingness to consume or pay. This value is the ratio of the welfare obtained from the annual food production of farmland, forming the equivalent value of various ecosystems. For the study area, the grain crops of the farmland ecosystem are rice, wheat, and corn, so the output of these three major food crops is used to measure the value of various ecosystems (58.5 2007\$/hm^2).

$$V_i = S_{ri} \times F_{ri} + S_{wi} \times F_{wi} + S_{ci} \times F_{ci}$$

In the formula, V_i represents the value of ecosystem services of a standard equivalent factor (\$/hm^2); S_{ri}, S_{wi}, S_{ci}, respectively, represent the percentage (%) of the sown area

of rice, wheat, and corn in the total sown area of the three crops in the i-th year; F_{ri} , F_{wi} , F_{ci} represent the average net profit per unit area of rice, wheat, and corn in the i-th year ($/hm^2).

Next, given that the ecosystem services such as food supply, climate regulation, and biodiversity of the ecosystem are generally positively correlated with biomass, and the supply of water resources and the regulation of water temperature are highly correlated with changes in precipitation, in conjunction with the research results of other scholars, this study revised the equivalent values to attain an equivalent that can more accurately reflect spatial heterogeneity [50]. The specific process is illustrated in the following diagram (Figure 2):

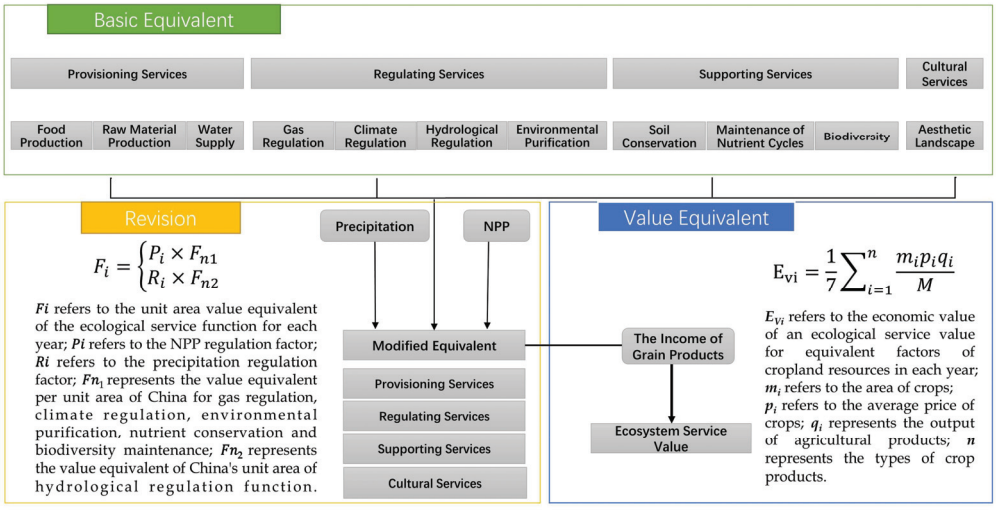

Figure 2. Ecosystem services value-equivalent calculation.

3. Results

3.1. Changes in Physical Condition

3.1.1. Extent Changes and Area Transfer

During this investigation, we discerned that those four types of forests—namely, Evergreen Needleleaf Forest (ENF), Evergreen Broadleaf Forest (EBF), Deciduous Broadleaf Forest (DBF), and Mixed Forest (MF)—underwent significant transformations. This was determined by analyzing the spatial pattern evolution of forest-cover data from 2001 to 2020 and calculating the characteristics of forest augmentation or diminution. It is evident (Figure 3a) that the distribution of forests within the research zone has conspicuously expanded and exhibited regional disparities over the past two decades, with the exception of a partial decline in the southeast region (Figure 3a-3). Owing to the elevated altitude and low annual average temperature in the western region, the primary increase is observed in Deciduous Broadleaf Forest (Figure 3a-2), while the southern region, with ample precipitation and heat conditions, predominantly experienced an increase in Evergreen Broadleaf Forest [51,52] (Figure 3a-5). Moreover, the terrain in the southeast is relatively flat with inconspicuous karstification, primarily constituting a non-karst area [30,53]. Contrasting with the relatively dispersed patches in other regions, various types of forests in this region have expanded over a substantial area. Lastly, in the northern region, characterized by the most intricate comprehensive effects of altitude, precipitation, and temperature, the four types of forests have augmented to varying extents.

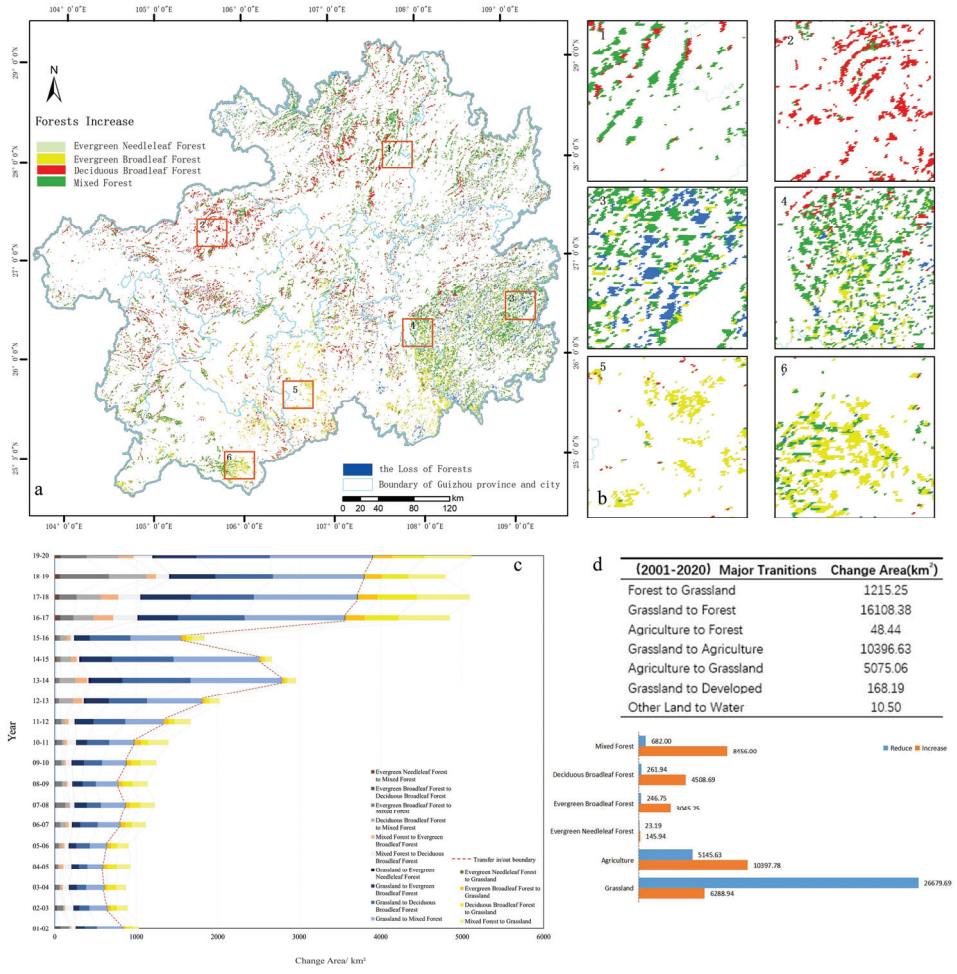

Figure 3. Spatial and temporal pattern change of forests. (**a**) is the increase or loss of forests over the past 20 years. (**b**) is a characteristic area of forest increase or loss. (**c**) is the proportion of transfers in/out between various forest types. (**d**) is the transfer area between various land cover types.

Subsequently, the alteration in forest area is concomitant with the conversion of forests to other land categories and the conversion of other land types into forests. Concurrently, the four types within forests also undergo conversion between each other (Figure 3c). As depicted in the figure (Figure 3c), the change in forest area can be approximately bifurcated into two phases. Prior to 2012, the area transfer between forest and other land types remained relatively stable, with the ratio of transfer-in to transfer-out approximating 2 (Table 4). "Transferred in" refers to the area increase resulting from the conversion of various other land categories into forests, while "transferred out" refers to the area decrease resulting from the transformation of forests into other land categories. Post 2012, the transformation within the research zone underwent a dramatic shift. The forest area expanded significantly, with the maximum value of the transfer-in to transfer-out ratio exceeding 16, and the net increased area escalated from 635.31 km^2 in 2002 to 2677 km^2 in 2020.

Table 4. Area of forest transferred in/out by year.

	01–02	02–03	03–04	04–05	05–06	06–07	07–08	08–09	09–10	10–11	11–12	12–13	13–14	14–15	15–16	16–17	17–18	18–19	19–20
Trans-in Area (km^2)	833.88	646.88	605.63	590.69	639.13	800.50	865.00	777.63	874.94	972.25	1339.13	1806.31	2786.44	2510.38	1548.19	3554.63	3708.44	3791.50	3895.06
Trans-out Area (km^2)	198.56	248.63	270.19	337.75	266.44	317.25	363.38	361.44	372.06	423.06	327.88	216.75	172.00	154.06	288.56	1290.94	1382.88	1001.75	1218.06
Ratio	4.2	2.6	2.2	1.7	2.4	2.5	2.4	2.2	2.4	2.3	4.1	8.3	16.2	16.3	5.4	2.8	2.7	3.8	3.2

The primary catalyst for the augmentation of forest within the research zone is substantiated to be the consistent transformation of grassland into forest over the past two decades (Figure 3d), encompassing a total area of 16,108.28 square kilometers. The alteration in Mixed Forest is the most conspicuous, with an increase of 8456 km^2 and a decrease of 682 km^2, succeeded by Deciduous Broadleaf Forest (an increase of 4508.69 km^2 and a decrease of 261.94 km^2). In contrast to other types, the transformation of Evergreen Coniferous Forest is a bit less.

3.1.2. Forest Products

The hydrothermal conditions within the research zone are highly favorable for plant growth. The primary economic forests encompass fruit trees (*Rosaceae*), tea trees (*Camellia sinensis*), woody oil plants (*Euphorbiaceae*), lacquer plants (*Toxicodendron vernicifluum*), and Chinese medicinal herbs. As depicted (Figure 4a), the yield of forest products in this region prior to 2006 was exceedingly low, with minimal annual fluctuations. From 2007 to 2013, it transitioned into a phase of gradual growth, after which the yield of various forest products commenced a rapid escalation. Among these, tea and its subsidiary products, walnuts (*Juglans regia*) and chestnuts (*Castanea sativa*) emerged as the primary forest products, with the output amplifying 11-fold. Regarding the yield of fruit (Figure 4b), the output of citrus (*Citrus* spp.) significantly surpasses that of other fruits, thereby conferring a distinct advantage in the region. Additionally, the local area is abundant in a variety of prickly pear (*Opuntia* spp.), which yielded more than 440,000 tons in 2020. Another notable transformation is that post-2014, the yield of apple (*Malus domestica*) (from 0.79 million tons to 34.46 million tons) and kiwi (*Actinidia deliciosa*) (0.99 million tons to 26.01 million tons) also escalated significantly, increasing by over 25-fold.

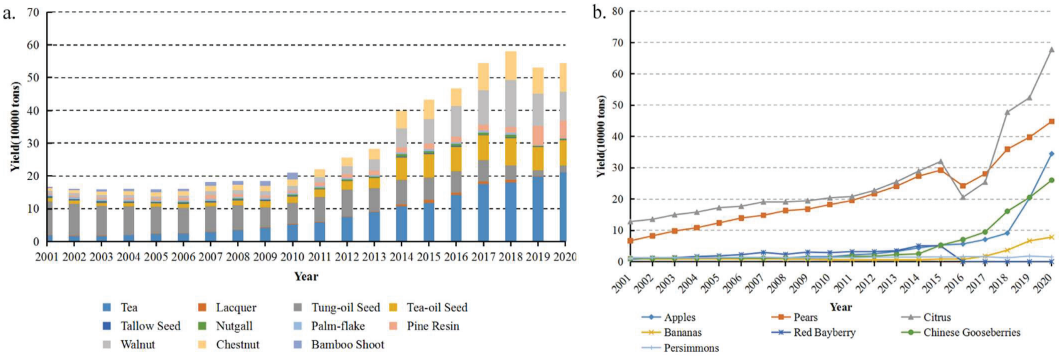

Figure 4. Changes of main forest products in the study area. (**a**) is the yield of forest products. (**b**) is the economic fruit yield.

3.1.3. Changes in Landscape

Through the analysis of landscape indexes, we can discern the differentiation regularity of the landscape pattern within the research zone (Figure 5). According to the NP, LPI, and Area-MN indices, the number of patches of Evergreen Coniferous Forest *(Pinaceae*) and Deciduous Coniferous Forest (*Larix decidua*) within the region is relatively minimal and essentially stable, while the patches of Evergreen Broadleaf Forest (*Fagaceae*) and Mixed Forest are on the rise. LPI indicates that the Mixed Forest is the dominant landscape type

here, but its maximum patch area exhibits a downward trend, and the DIVISION degree is ascending. By integrating ED, PD, and Area-MN indices, it becomes evident that the forest landscape in this area is relatively fragmented due to the karst topography, particularly the coniferous forest.

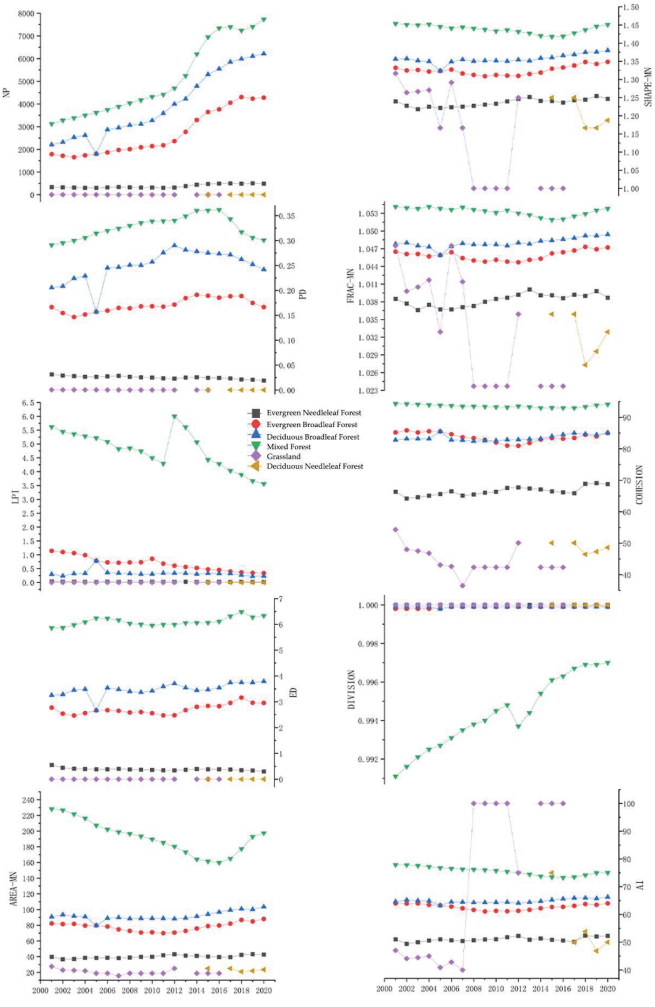

Figure 5. Temporal series diagram of landscape index.

From the perspective of various indices, the Mixed Forest, Deciduous Broadleaf Forest (*Fagaceae*), Evergreen Broadleaf Forest, and Evergreen Coniferous Forest cluster significantly, and the landscape pattern is stable. However, in certain years, Closed Shrub Forest and Deciduous Coniferous Forest were not monitored, resulting in discontinuity in the distribution of the index. The ED, LPI, PD, and other indices have undergone abrupt changes in certain years, primarily affecting the Mixed Forest and Deciduous Broadleaf Forest. This indicates that the natural state of the forest has been severely disrupted during this period.

3.1.4. Slope and Elevation Changes

This study conducted statistics on the slope and elevation of forests at five-year intervals (Figure 6). The results revealed that the distribution of Mixed Forest and Deciduous Broadleaf Forest (*Fagaceae*) is essentially unrestricted by slope, while Evergreen Broadleaf Forest (*Fagaceae*) and Evergreen Coniferous Forest (*Pinaceae*) are more prevalently distributed in hilly regions with relatively gentle slopes. Concurrently, post-2015, the distribution proportion of Mixed Forests on all slopes has diminished, as the proportion of other Broadleaf Forests has escalated. Furthermore, through observing the elevation changes of various forests, it is discerned that Evergreen Broadleaf Forest and Mixed Forest tend to proliferate in low-altitude areas, constituting more than 90% of the forest types in areas below 500 m above sea level. However, Deciduous Broadleaf Forest is primarily distributed in the mid-altitude area. In the elevation range of 1500 m to 2500 m, the area of Deciduous Broadleaf Forest comprises more than half, and the high-altitude area is dominated by Coniferous Forest.

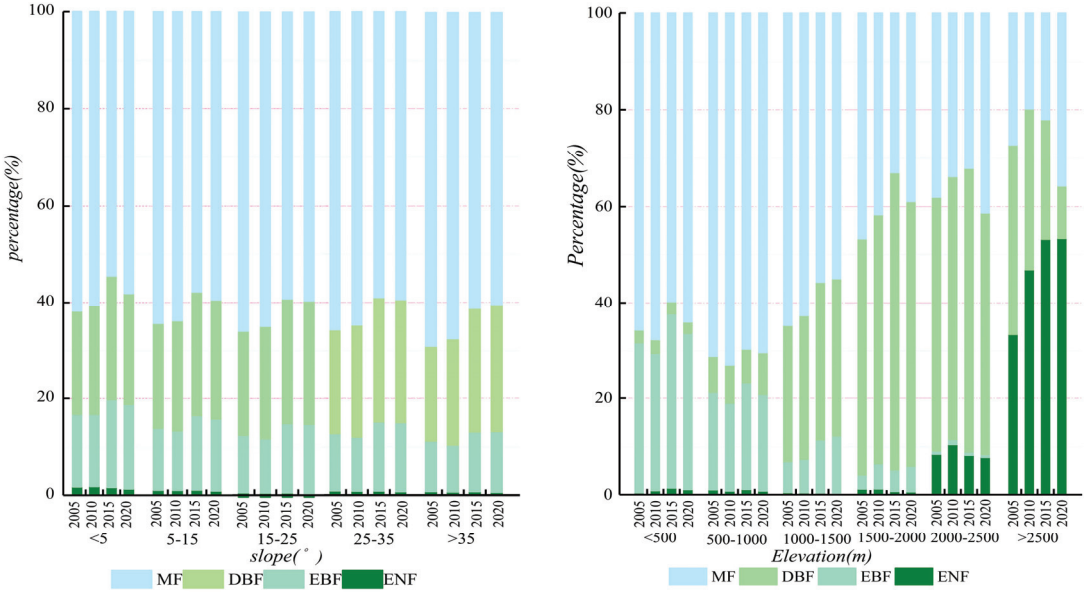

Figure 6. Slope and elevation distribution of forests.

3.1.5. Threats

Mountain fires and insect pests pose significant threats to the vitality of forest ecosystems, potentially instigating drastic transformations in forest ecosystems and diminishing their ecological and economic functions. In alignment with the classification system provided by the International Union for Conservation of Nature (IUCN), wildfires fall under the broad category of "Changes to Natural Systems", specifically as a threat pertaining to "Fire & Fire Suppression". Concurrently, diseases and pest infestations can be classified within the sphere of "Invasive Species & Diseases" [54]. In addressing these menaces, it is paramount to diligently monitor and manage the distribution of pests and diseases as well as the impacts of wildfires. Furthermore, proactive measures should be implemented for prevention [55].

At the dawn of the 21st century, due to the obsolescence of forest management methodologies and awareness, the incidence rate of mountain fires remained elevated (Figure 7). For example, local funeral customs, such as the burning of incense, candles, and joss paper, can readily lead to forest fires. Moreover, due to the forest monitoring measures being

limited to sporadic cameras and periodic drone inspections, it is challenging to detect fires promptly, resulting in the spread of wildfires [56]. There were 2154 forest fires in 2003 and 2612 in 2008. Although the scale of the fires was minimal and the proportion of affected forests was low, the local forest pattern would undergo alterations. Conversely, with the implementation of the disease and pest control project, the affected forests within the research zone have been promptly managed, and the prevention rate has exceeded 90% in the period from 2017 to 2020.

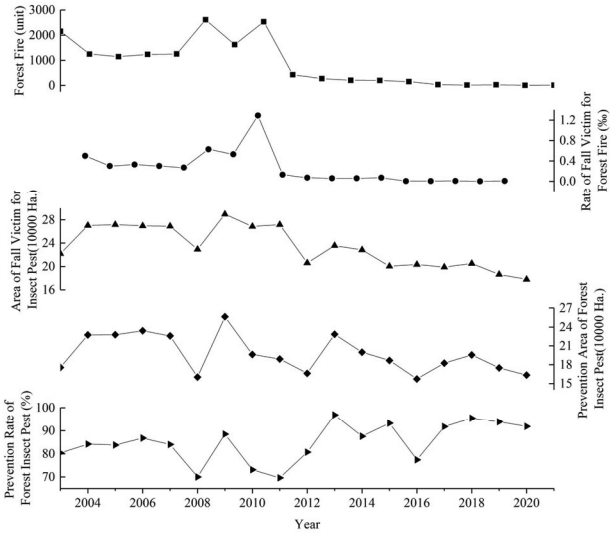

Figure 7. Forest-fire and insect-pest situation in the study area.

3.2. Changes in Ecosystem Services

3.2.1. Changes of Spatial-Temporal Pattern

In this investigation, we employed the value-equivalent model to compute the value of ecosystem services within the research zone [57,58]. We spatialized the calculation results of Provisioning Services Value (PSV), Regulating Services Value (RSV), Supporting Services Value (SSV), and Cultural Services Value (CSV) through the method of Geographic Information System (GIS), allowing for an intuitive representation of the spatial distribution of PS in the study area on the map (Figure 8). The study discovered that the high-value areas of forest ecosystem services were distributed in Zunyi City in the north, Tongren City in the east, and Qiandongnan Autonomous Prefecture in the southeast. Among these three cities, there are Alsophila spinulosa (*Cyatheaceae*) National Nature Reserve in the north, Fanjing Mountain National Nature Reserve in the east, and Leigong Mountain Nature Reserve in the southeast, thereby forming a forest cluster with high ecosystem service value. By comparing the ecosystem services value (ESV) data at five-year intervals, the service capacity of PSV and CSV remained nearly unchanged, and SSV improved in 2010 compared to 2005. Subsequently, compared to 2010, the maximum value of ESV in 2015 experienced a slight decline, but the distribution area of middle and low values significantly expanded, and a new high value-gathering area emerged. In 2020, the service value of the four ecosystems improved. Specifically, the high-value gathering area in the southeast expanded significantly, the low-value area in the southwest evolved into a median area, while the high-altitude area in the northwest formed a new ESV cluster.

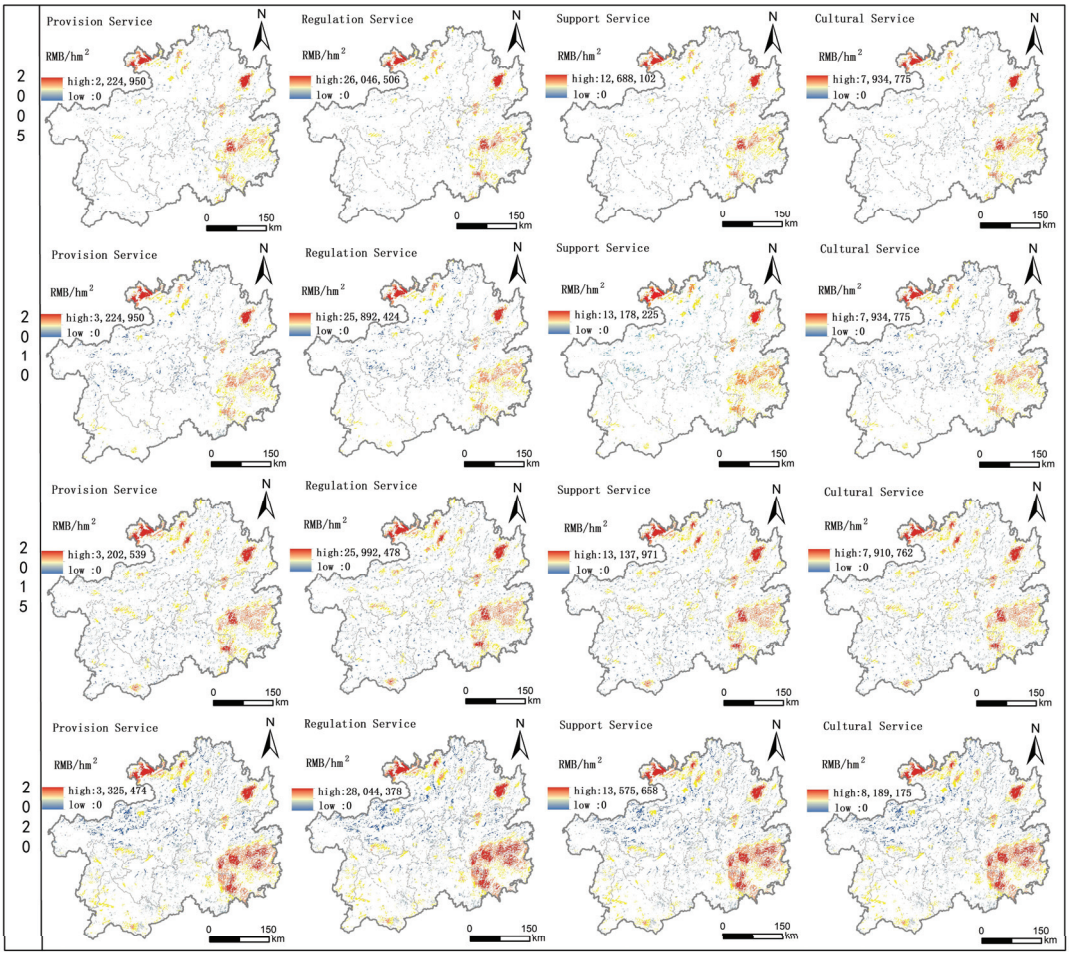

Figure 8. Spatial-temporal changes of ecosystem services.

3.2.2. Changes of Ecosystem Services Value

The value of ecosystem services within the research zone ranks foremost in terms of Regulating Services (RS), succeeded by Supporting Services (SS). This indicates that, compared to the circulation value of forest products as commodities in human society, the forest ecological utility in this area is more pronounced. Furthermore, the value of the four ecosystem services has amplified by 2.3–2.5 times over the past two decades (Table 5). However, the total regional ESV reached 7.25 billion dollars in 2020, of which 4.74 billion dollars is the contribution of RS. This implies that the value of RS surpasses the sum of the other three values, which is markedly unbalanced. It appears that a more effective forest policy is required to balance the ecological functions and the provision functions of forest products, thereby enabling forest resources to provide more sustainable support for local development.

Table 5. Forest ecosystem services value of Guizhou Province. (Unit: 100 million dollars).

Year	PSV	RSV	SSV	CSV	Total
2001	1.78	19.77	7.29	1.47	30.31
2002	1.85	20.48	7.55	1.52	31.39
2003	1.88	20.79	7.66	1.54	31.87
2004	1.90	21.10	7.77	1.56	32.33
2005	1.91	21.19	7.80	1.57	32.47
2006	1.94	21.56	7.93	1.59	33.03
2007	1.99	22.07	8.12	1.63	33.80
2008	2.03	22.55	8.30	1.67	34.54
2009	2.07	22.91	8.43	1.69	35.11
2010	2.11	23.47	8.63	1.73	35.94
2011	2.16	24.00	8.81	1.77	36.75
2012	2.28	25.43	9.32	1.87	38.91
2013	2.49	27.71	10.15	2.04	42.38
2014	2.85	31.78	11.62	2.34	48.59
2015	3.19	35.59	13.00	2.61	54.39
2016	3.35	37.48	13.69	2.75	57.27
2017	3.56	39.81	14.52	2.92	60.80
2018	3.77	42.18	15.38	3.09	64.41
2019	4.00	44.70	16.34	3.29	68.33
2020	4.25	47.44	17.35	3.49	72.53

4. Discussion

4.1. The Framework Design

The present study proposes an ecosystem service-evaluation method based on remote sensing data and socio-economic data. This approach, to a certain extent, alleviates the dilemma of inadequate on-site survey data in underdeveloped areas, enables GIS analysis, and facilitates swift and continuous monitoring of ecosystem changes, providing assistance to decision-makers. However, the improvement of this framework is an ongoing process.

The current framework has a limited selection of indicators. For example, only two categories of threats were selected, which might result in less accurate assessment results. Secondly, we found that, with the current framework, it is possible only to perform analysis and calculations on an annual basis. A smaller time interval of the research area would not allow for the collection of remote-sensing and socio-economic data to achieve variations.

Furthermore, this framework only conducts an evaluation from the overall perspective of the ecosystem. However, more detailed features, such as individual situations in the forest (crown width, diameter at breast height, plant height, age group), are overlooked, which may result in limited application scenarios of the evaluation results.

4.2. Insufficiency of the Value-Equivalent Model

While the value-equivalent model employed in this study provides an intuitive reflection of ecosystem value and is straightforward to calculate, it primarily focuses on the feedback of macro patterns and phenomena, thereby circumventing the mechanisms at play when the ecosystem performs its ecological functions.

Meanwhile, we also noticed that the unit value in this model is calculated through the willingness-to-pay method [59]; thus, the result depends heavily on the personal willingness of the respondents selected in the survey. Moreover, such willingness can change with the development of the economy and the guidance of public opinion. For instance, when people tend to choose virtual entertainment rather than getting close to nature, their willingness to pay for tourism will decline, and the corresponding value will change accordingly. However, since it is impossible to conduct the willingness-to-pay survey annually, this study used a fixed unit price for the calculation, which might cause some bias in the results.

Another point worth noting is that, although we attempted to make the value-equivalence factor more accurate and made some adjustments, our current adjustment method ignores the spatial heterogeneity of the entire research area. We simply treated the research area, taking the annual average precipitation, among other averages, for adjustment. However, due to the significant differences in area, altitude, and climatic conditions across the research area, it is still challenging to obtain accurate results even after adjustment.

5. Conclusions

Utilizing remote sensing images and socio-economic data, this study maps the transformations of the forest ecosystem in the core area of the karst mountain regions in southwest China from 2001 to 2020. Based on the analysis of alterations in the forest's physical conditions and the calculation of the evolution pattern of its ecosystem service value, the following conclusions can be drawn:

1. Over the past two decades, forest rehabilitation within the study area has yielded commendable outcomes, substantially mitigating various ecological dilemmas instigated by rocky desertification in this region. The forested area has increased significantly, and the ecosystem service value has more than doubled.
2. The restoration of the forest ecosystem in the research area has clear stages. The physical accounts and ecosystem service accounts of the forest ecosystem in the second stage show more significant changes in terms of range expansion, area increase, and value enhancement compared to the first stage. The main reason is that a number of ecological restoration policies were implemented locally during this stage, including the conversion of farmland to forests, migration and relocation, and the promotion of the development of the forestry industry.
3. Human intervention has a significant impact on the changes in the ecosystem, and reasonable forestry management policies can effectively and quickly enhance the service value of the forest ecosystem. By establishing an evaluation system that combines remote-sensing data and socio-economic data, we can provide excellent technical support for finding a balance between the sustainable development of forests and human life.

Author Contributions: Conceptualization, Z.Z. and L.Z.; methodology, T.W.; software, T.W., L.W. and D.L; formal analysis, L.Z. and Q.C.; investigation, L.W., D.L. and T.W.; data curation, Q.F.; writing—original draft preparation, L.Z.; writing—review and editing, Z.Z. and Q.C.; visualization, L.Z.; supervision, Q.C.; project administration, L.Z.; funding acquisition, Z.Z. All authors have read and agreed to the published version of the manuscript.

Funding: This research was funded by the NSFC regional project, "Research on the coupling mechanism between ecological assets and regional poverty in karst rocky desertification areas (41661088)", by "Guizhou Province's high-level innovative talent training plan 'hundred' level talents (Qiankehe platform talents [2016] 5674)" and a special study of Guizhou Provincial Department of natural resources on the "Construction of evaluation system of real estate economic operation system in Guizhou Province" (520000215RSUFG5DLMENO/52000021C4D958906C150).

Institutional Review Board Statement: Not applicable.

Informed Consent Statement: Not applicable.

Data Availability Statement: Not applicable.

Acknowledgments: Our deepest appreciation goes to the funding bodies for their indispensable support. We also extend our gratitude to our esteemed colleagues, whose insightful expertise and contributions substantially enhanced this research. Our profound thanks go to the anonymous reviewers who generously gave their time and expertise in critiquing our manuscript. Their invaluable comments and suggestions have markedly elevated the quality of our work.

Conflicts of Interest: The authors declare no conflict of interest.

Appendix A

Table A1. International Geosphere-Biosphere Programme (IGBP) legend and class descriptions.

Name	Description
Evergreen Needleleaf Forests	Dominated by evergreen conifer trees (canopy >2 m). Tree cover >60%.
Evergreen Broadleaf Forests	Dominated by evergreen broadleaf and palmate trees (canopy >2 m). Tree cover >60%.
Deciduous Needleleaf Forests	Dominated by deciduous needleleaf (larch) trees (canopy >2 m). Tree cover >60%.
Deciduous Broadleaf Forests	Dominated by deciduous broadleaf trees (canopy >2 m). Tree cover >60%.
Mixed Forests	Dominated by neither deciduous nor evergreen (40–60% of each) tree type (canopy >2 m). Tree cover >60%.
Closed Shrublands	Dominated by woody perennials (1–2 m height) >60% cover.
Open Shrublands	Dominated by woody perennials (1–2 m height) 10–60% cover.
Woody Savannas	Tree cover 30–60% (canopy >2 m).
Savannas	Tree cover 10–30% (canopy >2 m).
Grasslands	Dominated by herbaceous annuals (<2 m)
Permanent Wetlands	Permanently inundated lands with 30–60% water cover and >10% vegetated cover.
Croplands	At least 60% of area is cultivated cropland.
Urban and Built-up Lands	At least 30% impervious surface area including building materials, asphalt, and vehicles.
Cropland/Natural Vegetation Mosaics	Mosaics of small-scale cultivation 40–60% with natural tree, shrub, or herbaceous vegetation.
Permanent Snow and Ice	At least 60% of area is covered by snow and ice for at least 10 months of the year.
Barren	At least 60% of area is non-vegetated barren (sand, rock, soil) areas with less than 10% vegetation.
Water Bodies	At least 60% of area is covered by permanent water bodies. Unclassified 255 Has not received a map label because of missing inputs.

References

1. FAO. *Global Forest Resources Assessment 2020—Key Findings*; FAO: Rome, Italy, 2020.
2. Available online: https://www.Fao.org/Forest-Resources-Assessment/En/ (accessed on 1 March 2023).
3. Campbell, E.T.; Tilley, D.R. Valuing ecosystem services from Maryland forests using environmental accounting. *Ecosyst. Serv.* **2014**, *7*, 141–151. [CrossRef]
4. FAO. *Global Forest Resources Assessment 2020. Guidelines and Specifications Fra 2020*; FAO: Rome, Italy, 2018.
5. Grammatikopoulou, I.; Vačkářová, D. The value of forest ecosystem services: A meta-analysis at the European scale and application to national ecosystem accounting. *Ecosyst. Serv.* **2021**, *48*, 101262. [CrossRef]
6. Helseth, E.V.; Vedeld, P.; Framstad, E.; Gómez-Baggethun, E. Forest Ecosystem Services in Norway: Trends, Condition, and Drivers of Change (1950–2020). *Ecosyst. Serv.* **2022**, *58*, 101491. [CrossRef]
7. Available online: https://Sustainabledevelopment.un.org/ (accessed on 1 December 2022).
8. Dardonville, M.; Legrand, B.; Clivot, H.; Bernardin, C.; Bockstaller, C.; Therond, O. Assessment of ecosystem services and natural capital dynamics in agroecosystems. *Ecosyst. Serv.* **2022**, *54*, 101415. [CrossRef]
9. Edens, B.; Maes, J.; Hein, L.; Obst, C.; Siikamaki, J.; Schenau, S.; Javorsek, M.; Chow, J.; Chan, J.Y.; Steurer, A.; et al. Establishing the SEEA Ecosystem Accounting as a global standard. *Ecosyst. Serv.* **2022**, *54*, 101413. [CrossRef]
10. UN; FAO. *System of Environmental-Economic Accounting for Agriculture, Forestry and Fisheries (SEEA AFF)*; The Food and Agriculture Organization of the United Nations and United Nations Statistical Division: Rome, Italy, 2020.
11. UN; EC; IMF; FAO; WB; OECD. *System of Environmental-Economic Accounting (Central Framework)*; United Nations Department of Economic and Social Affairs: New York, NY, USA, 2014.
12. Guerry, A.D.; Polasky, S.; Lubchenco, J.; Chaplin-Kramer, R.; Daily, G.C.; Griffin, R.; Ruckelshaus, M.H.; Bateman, I.J.; Duraiappah, A.; Elmqvist, T.; et al. Natural capital and ecosystem services informing decisions: From promise to practice. *Proc. Natl. Acad. Sci. USA* **2015**, *112*, 7348–7355. [CrossRef] [PubMed]
13. Available online: https://Seea.un.org/Home/Natural-Capital-Accounting-Project (accessed on 1 March 2023).
14. Available online: https://Seea.un.org/News/Release-Ncaves-China-Project-Reports-During-Closing-Workshop (accessed on 1 March 2023).
15. Available online: https://Seea.un.org/Content/China-0 (accessed on 1 March 2023).
16. Hein, L.; Bagstad, K.J.; Obst, C.; Edens, B.; Schenau, S.; Castillo, G.; Soulard, F.; Brown, C.; Driver, A.; Bordt, M.; et al. Progress in natural capital accounting for ecosystems. *Science* **2020**, *367*, 514–515. [CrossRef]
17. Polasky, S.; Daily, G. An Introduction to the Economics of Natural Capital. *Rev. Environ. Econ. Policy* **2021**, *15*, 87–94. [CrossRef]

18. Chen, C.; Park, T.; Wang, X.; Piao, S.; Xu, B.; Chaturvedi, R.K.; Fuchs, R.; Brovkin, V.; Ciais, P.; Fensholt, R.; et al. China and India lead in greening of the world through land-use management. *Nat. Sustain.* **2019**, *2*, 122–129. [CrossRef]
19. Macias-Fauria, M. Satellite images show China going green. *Nature* **2018**, *553*, 411–413. [CrossRef]
20. Bagstad, K.J.; Ingram, J.C.; Lange, G.M.; Masozera, M.; Ancona, Z.H.; Bana, M.; Kagabo, D.; Musana, B.; Nabahungu, N.L.; Rukundo, E.; et al. Towards Ecosystem Accounts for Rwanda: Tracking 25 Years of Change in Flows and Potential Supply of Ecosystem Services. *People Nat.* **2019**, *2*, 163–188. [CrossRef]
21. Brandon, C.; Brandon, K.; Fairbrass, A.; Neugarten, R. Integrating Natural Capital into National Accounts: Three Decades of Promise and Challenge. *Rev. Environ. Econ. Policy* **2021**, *15*, 134–153. [CrossRef]
22. Tong, X.; Brandt, M.; Yue, Y.; Horion, S.; Wang, K.; De Keersmaecker, W.; Tian, F.; Schurgers, G.; Xiao, X.; Luo, Y.; et al. Increased vegetation growth and carbon stock in China karst via ecological engineering. *Nat. Sustain.* **2018**, *1*, 44–50. [CrossRef]
23. Zhang, C.; Qi, X.; Wang, K.; Zhang, M.; Yue, Y. The application of geospatial techniques in monitoring karst vegetation recovery in southwest China. *Prog. Phys. Geogr. Earth Environ.* **2017**, *41*, 450–477. [CrossRef]
24. Chen, Q.; Xiong, K.; Dan, W.; Niu, L. Analysis of the coupling characteristics of ecology and poverty in typical karst areas: A case study of 9000 provincial poor villages in Guizhou Province. *Acta Ecol. Sin.* **2021**, *41*, 2968–2982.
25. Wu, Y.; Zhou, Z.; Zhu, C.; Ma, G.; Huang, D. Measurement and spatial differentiation of rural poverty in karst mountainous areas: A case study of Panzhou City. *Resour. Environ. Yangtze River Basin* **2020**, *29*, 1247–1256.
26. Yang, R.; Zhong, C.; Yang, Z.; Liu, F.; Peng, H. Analysis of Poverty Influencing Factors in Deep Poverty Counties of Southwest Karst Rocky Desertification. *World Geogr. Res.* **2022**, *31*, 1298–1309.
27. Guizhou Provincial Local Chronicles Compilation Committee. *Guizhou Provincial Chronicle Geographical Chronicles*; Guizhou People's Publishing House: Guiyang, China, 1988.
28. Qian, C. Remote Sensing Inversion of Forest Biomass and Spatiotemporal Dynamic Analysis in Karst Region. Ph.D. Thesis, Nanjing Forestry University, Nanjing, China, 2022.
29. Su, W. Current Causes of Rocky Desertification in Karst Mountainous Areas of Southwest China and Optimization Model of Governance. *J. Soil Water Conserv.* **2002**, *2*, 29–32+79.
30. Xiong, K.; Li, J.; Long, M. Characteristics and key problems of soil erosion in typical karst rocky desertification control areas. *Acta Geogr.* **2012**, *67*, 878–888.
31. Guizhou Provincial Local Chronicles Compilation Committee. *Guizhou Province (1978–2010) Forestry*; Guizhou People's Publishing House: Guiyang, China, 2019; Volume 16.
32. Feng, N.; Liu, D.; Li, Y.; Liu, P. Soil net N mineralization and hydraulic properties of carbonate-derived laterite under different vegetation types in Karst forests of China. *Sci. Total. Environ.* **2023**, *856*, 159116. [CrossRef] [PubMed]
33. Peng, D.; Zhou, Q.; Tang, X.; Yan, W.; Chen, M. Changes in soil moisture caused solely by vegetation restoration in the karst region of southwest China. *J. Hydrol.* **2022**, *613*, 128460. [CrossRef]
34. Zhong, F.; Xu, X.; Li, Z.; Zeng, X.; Yi, R.; Luo, W.; Zhang, Y.; Xu, C. Relationships between lithology, topography, soil, and vegetation, and their implications for karst vegetation restoration. *Catena* **2022**, *209*, 105831. [CrossRef]
35. Guizhou Provincial Local Chronicles Compilation Committee. *Guizhou Province Chronicle (1978–2010) XVI Vols*; Guizhou People's Publishing House: Guiyang, China, 2017; Volume Agriculture.
36. He, Y.; Wang, L.; Niu, Z.; Nath, B. Vegetation recovery and recent degradation in different karst landforms of southwest China over the past two decades using GEE satellite archives. *Ecol. Informatics* **2022**, *68*, 101555. [CrossRef]
37. Peng, J.; Jiang, H.; Liu, Q.; Green, S.M.; Quine, T.A.; Liu, H.; Qiu, S.; Liu, Y.; Meersmans, J. Human activity vs. climate change: Distinguishing dominant drivers on LAI dynamics in karst region of southwest China. *Sci. Total. Environ.* **2020**, *769*, 144297. [CrossRef] [PubMed]
38. Available online: https://Doi.org/10.5067/Modis/Mcd12q1.061 (accessed on 6 July 2023).
39. Hu, X.; Chen, Z.; Mo, L.; Yan, C.; Wang, W.; Luo, X. Analysis of Forest Landscape Pattern of Danxiashan National Nature Reserve Based on Remote Sensing Imagery. *Ecol. Sci.* **2023**, *42*, 155–163.
40. Liu, Y.; Cai, X.; Ning, X.; Wang, H. Urban Forest Mapping Study of Landscape Ecological Index Model. *Sci. Surv. Mapp.* **2022**, *47*, 185–195.
41. Chen, S.; Feng, X.; Ma, R.; Hong, Q. Evaluation Method and Empirical Study of Cultivated Land Fragmentation: A Case Study of Ningbo City, Zhejiang Province. *China Land Sci.* **2016**, *30*, 80–87.
42. Liu, Y.; Liao, H.; Wu, X.; Guo, Q.; Mao, X.; Li, C. A Study on the Spatial Coupling Relationship between Arable Land Fragmentation and Poverty in Southwest Karst Region. *J. Southwest Univ. Nat. Sci. Ed.* **2019**, *41*, 10–20.
43. Wang, S. Remote Sensing Monitoring and Spatiotemporal Analysis of Forest Change Characteristics in Southwest China in the Past 20 Years. Master's Thesis, Southwest University, Chongqing, China, 2022.
44. Xiong, C.; Wu, Z.; Zeng, Z.; Gong, J.; Li, J. Research on the temporal and spatial evolution of forest landscape pattern in the Guangdong-Hong Kong-Macao Greater Bay Area based on "spatial form-fragmentation-aggregation". *Acta Ecol. Sin.* **2023**, *43*, 3032-44.
45. Wan, W. Spatial differentiation of cultivated land fragmentation in Zhejiang Province based on county scale. *Environ. Ecol.* **2021**, *3*, 15–21+48.
46. Yang, J.; Xie, B.; Zhang, D. Spatial–temporal evolution of ESV and its response to land use change in the Yellow River Basin, China. *Sci. Rep.* **2022**, *12*, 13103. [CrossRef]

47. Costanza, R.; de Groot, R.; Farber, S.; Grasso, M.; Hannon, B.; Limburg, K.; Naeem, S.; Paruelo, J.; Raskin, R.G.; Sutton, P.; et al. The Value of the World's Ecosystem Services and Natural Capital. *Nature* **1997**, *387*, 253–260. [CrossRef]
48. Costanza, R.; Kubiszewski, I.; Giovannini, E.; Lovins, H.; McGlade, J.; Pickett, K.E.; Ragnarsdóttir, K.V.; Roberts, D.; De Vogli, R.; Wilkinson, R. Development: Time to Leave Gdp Behind. *Nature* **2014**, *505*, 283–285. [CrossRef]
49. Costanza, R.; de Groot, R.; Sutton, P.; van der Ploeg, S.; Anderson, S.J.; Kubiszewski, I.; Farber, S.; Turner, R.K. Changes in the global value of ecosystem services. *Glob. Environ. Chang.* **2014**, *26*, 152–158. [CrossRef]
50. Xie, G.; Zhang, C.; Zhang, L.; Chen, W.; Li, S. Improvement of Ecosystem Service Value Methodology Based on Value Equivalent Factor per Unit Area. *J. Nat. Resour.* **2015**, *30*, 1243–1254.
51. Xie, G.; Zhen, L.; Lu, C.; Xiao, Y.; Chen, C. A Valinization Approach to Ecosystem Services Based on Expert Knowledge. *J. Nat. Resour.* **2008**, *5*, 911–919.
52. Su, W.; Li, P.; He, W.; Zhu, W. Ecotourism in Guizhou Maolan Karst Forest Nature Reserve. *Carsologica China* **2001**, *1*, 67–71.
53. Wang, X.; Long, J.; Li, J.; Liu, L.; Liao, H.; Li, Y.; Yang, R. Soil eukaryotic microbial diversity under different successions of Maolan karst forest in Guizhou. *Environ. Sci.* **2020**, *41*, 4314–4321.
54. Su, W. The fragility of karst mountain ecosystems in Guizhou and its countermeasures. *Sci. Soil Water Conserv.* **2004**, *3*, 64–69.
55. Salafsky, N.; Salzer, D.; Stattersfield, A.J.; Hilton-Taylor, C.; Neugarten, R.; Butchart, S.H.M.; Collen, B.; Cox, N.; Master, L.L.; O'Connor, S.; et al. A Standard Lexicon for Biodiversity Conservation: Unified Classifications of Threats and Actions. *Conserv. Biol.* **2008**, *22*, 897–911. [CrossRef]
56. Salafsky, N.; Margoluis, R.; Redford, K.H.; Robinson, J.G. Improving the Practice of Conservation:A Conceptual Framework and Research Agenda for Conservation Science. *Conserv. Biol.* **2002**, *16*, 1469–1479. [CrossRef]
57. Macroeconomic Database of Guizhou Province, China. Available online: http://hgk.guizhou.gov.cn/publish/tj/index.html (accessed on 12 July 2023).
58. Xie, G.; Lu, C.; Leng, Y.; Zheng, D.; Li, S. Valuation of Ecological Assets on the Tibetan Plateau. *J. Nat. Resour.* **2003**, *2*, 189–196.
59. Xie, G.; Zhang, C.; Zhang, C.; Xiao, Y.; Lu, C. The Value of Ecosystem Services in China. *Resour. Sci.* **2015**, *37*, 1740–1746.

forests

MDPI

Article

Intercropping Peanut under Forests Can Reduce Soil N_2O Emissions in Karst Desertification Control

Tinghui Hu [1,2], Kangning Xiong [1,*] and Jun Wang [2]

[1] Guizhou Engineering Laboratory for Karst Desertification Control and Eco-Industry, School of Karst Science, Guizhou Normal University, Guiyang 550001, China; tinghuihu@gznu.edu.cn
[2] Guizhou Oil Research Institute, Guizhou Academy of Agricultural Sciences, Guiyang 550006, China; wangjun3931@163.com
* Correspondence: xiongkn@gznu.edu.cn

Abstract: In the process of vegetation restoration for karst desertification management, the lack of scientific and rational intercropping technology and the blind application of large amounts of nitrogen fertilizer have made the soil the main source of atmospheric N_2O in this region. How soil N_2O emissions vary under different intercropping modes is a scientific question worthy of study. This study took a three-year-old loquat (*Eribotrya japonica* L.) artificial forest in the karst plateau canyon as the experimental site and designed loquat intercropping with peanut, corn, and sweet potato (*Ipomoeabatatas* (L.) Lam.) as well as non-intercropping to analyze the differences in soil physicochemical properties and greenhouse gas emissions under different intercropping patterns. The results showed that intercropping with peanut significantly increased loquat yield, soil moisture, temperature, SOC, MBC, TN, and MBN content. The emissions of N_2O and CO_2were mainly positively correlated with soil moisture and temperature, while CH_4 showed a negative correlation with soil moisture and soil temperature. The soil absorbed CH_4 in the control of karst desertification. Karst area soils exhibited higher N_2O emissions. Intercropping patterns significantly influenced soil N_2O emissions, with N_2O-N cumulative emissions ranging from 5.28 to 8.13 $kg \cdot hm^{-2}$ under different intercropping conditions. The lowest N_2O-N cumulative emissions were observed for peanut intercropped under the forest. The peak N_2O emission occurred in April 2022, which may be attributed to the higher rainfall and soil moisture during that month. Intercropping peanut with loquat significantly reduced the global warming potential. Therefore, intercropping peanut in young forests can improve soil water and fertilizer conditions, reduce soil N_2O emissions and global warming potential, and serve as a nitrogen fixation and emission reduction technique suitable for karst desertification areas.

Keywords: karst desertification control; loquat; vegetation restoration; intercropping peanut; N_2O emission

Citation: Hu, T.; Xiong, K.; Wang, J. Intercropping Peanut under Forests Can Reduce Soil N_2O Emissions in Karst Desertification Control. *Forests* **2023**, *14*, 1652. https://doi.org/10.3390/f14081652

Academic Editor: Timothy A. Martin

Received: 26 June 2023
Revised: 24 July 2023
Accepted: 11 August 2023
Published: 15 August 2023

1. Introduction

The continuous increase in greenhouse gas (GHG) emissions, especially carbon dioxide (CO_2), nitrous oxide (N_2O), and methane (CH_4), is a major driving factor for global climate change [1]. Although the emissions of CH_4 and N_2O are much lower than those of CO_2, their global warming potential (GWP) is 25 times and 298 times greater than CO_2, respectively (over a 100-year horizon) [2]. Nitrous oxide (N_2O) is one of the main greenhouse gases, which can participate in photochemical reactions in the atmosphere to destroy the ozone layer in the stratosphere, thereby exacerbating the greenhouse effect [3]. N_2O has a long residence time in the atmosphere, and its continuous increase in concentration will further contribute to the greenhouse effect. Soil is the main source of N_2O emissions [4], and denitrification is the main process of N_2O production [5,6]. The main reason for this is the unreasonable use of synthetic fertilizers in agricultural production [7,8], especially in the karst areas of southern China centered around the Guizhou Plateau, where the soil is thin

and the ecosystem is fragile [9,10]. In order to increase yields, farmers blindly apply a large amount of nitrogen fertilizer, increasing the mineral nitrogen content in the soil nitrogen transformation process [11,12], causing the soil to become one of the main sources of atmospheric N_2O production in the karst area. Therefore, changes in N_2O concentration will have a significant impact on future climate change. Reducing or controlling N_2O emissions to improve the ecological environment and mitigate global change is of great significance.

Loquat (*Eriobotrya japonica* L.) is a subtropical evergreen fruit tree with rich nutrition and high economic value. Loquat has the characteristics of drought resistance, barrenness resistance, and wide adaptability, and it plays an important role in the control of karst desertification. By planting loquat in this area, the vegetation in the rocky desertification area can be effectively restored, and it has become an important source of income for local farmers [13,14]. However, during the vegetation restoration process, due to the lack of scientific and reasonable intercropping patterns, most farmers are accustomed to intercropping with crops such as corn and sweet potato (*Ipomoeabatatas* (L.) Lam.) and using a large amount of chemical fertilizers, which not only restrict the growth of loquat but also increase greenhouse gas emissions. Therefore, selecting suitable intercropping crops is of great significance for increasing farmers' income and promoting sustainable environmental development.

Afforestation is a major and long-term control method in karst desertification but does not meet the income needs of farmers for life within a year. Intercropping peanut under forests provides a good idea for a solution to this problem. Peanut (*Arachishypogaea* L.) is an important oil and economic crop worldwide, with China having the highest total peanut production in the world. It is one of the main export agricultural products and plays an important role in national economic development and food security. Due to its characteristics of dwarf stature, nitrogen fixation, low input, and high output, it has gradually become an ideal pioneer crop for intercropping with young tea gardens, orchards, medicinal gardens, and other economic forests [15–18]. Especially in karst areas, intercropping peanut under forests can not only increase the income of farmers in remote and poor areas and prevent water and soil loss on rocky desertification farmland but also effectively alleviate the conflict between food and oil land, playing an important role in ensuring China's food and oil security. Research has found that under conditions of no or low nitrogen application, the selection of crop varieties (such as peanut) can slow down global warming [19], and the N_2O emissions from peanut soil are significantly lower than those from nitrogen-fixing tree species [20]. Therefore, can intercropping loquat with peanut reduce greenhouse gas emissions in vegetation restoration and karst desertification control?

To this end, this study selected a loquat (*Eribotrya japonica* L.) site that had undergone karst canyon desertification control and restoration for three years as the experimental site and conducted intercropping patterns of loquat with peanut, corn, sweet potato, and other crops to study changes in soil temperature, moisture content, and greenhouse gas emission flux under different intercropping patterns. This study focused on analyzing changes in warming potential under different intercropping patterns to clarify the soil water–nutrient–gas cycle characteristics of the vegetation restoration system in ecologically fragile areas of karst desertification, and to provide technological support for the sustainable restoration of vegetation in karst desertification control areas.

2. Materials and Methods

2.1. Overview of the Experimental Site

The experiment was conducted in Guanling County, Anshun City, Guizhou Province, China, which represents the karst landscape of southern China. The site is located in Bangui Township, Huajiang Town, with coordinates of 25°41′33″ N and 105°37′32″ E. The area belongs to the medium- to high-intensity karst canyon desertification zone, with high rock exposure, scarce soil resources, rare surface runoff, and severe human–land conflicts. In order to control desertification, loquat, Sichuan pepper, dragon fruit, honeysuckle, and other crops have been widely promoted for planting. Currently, loquat has become one of

the dominant industries in the area. This experiment selected a loquat forest as the sample site for the restoration of karst desertification for three years. The soil is mainly yellow soil and yellow calcareous soil. The organic matter content in the 0–20 cm soil layer was 42.80 ± 1.25 g·kg^{-1}, the total nitrogen content was 2.61 ± 0.13 g·kg^{-1}, the total phosphorus content was 1.32 ± 0.22 g·kg^{-1}, the bulk density was 1.24 ± 0.10 g·cm^{-3}, and the pH was 7.64 ± 0.16. The average height of the loquat trees was 1.57 ± 0.12 m, the crown width was 1.52 ± 0.14 m (east–west) $\times$ 1.60 ± 0.17 m (north–south), and the ground diameter was 4.81 ± 0.37 cm.

2.2. Experimental Materials

The loquat variety used was "Wuxing Loquat", the peanut variety was Qian Peanut 1 (primarily harvested for its pods), and the sweet potato and corn were both local varieties (corn variety: Guanling White Corn, sweet potato variety: Bangui Red Heart Sweet Potato).

2.3. Experimental Design

The experiment was conducted in a loquat orchard planted in January 2018. Loquat trees with similar growth were selected, with a planting density of 830 trees per hectare, a row spacing of 4 m, and a plant spacing of 3 m. The experiment was conducted from February 2021 to May 2022, with four intercropping modes: intercropping with peanut (IP), intercropping with corn (IC), intercropping with sweet potato (IS), and no intercropping (SC) in the understory. Each plot had an area of 10 m $\times$ 10 m and was repeated four times, for a total of 16 plots. Among them, the distance between peanut, corn, and sweet potato and the loquat tree trunk was 0.80 m, and the planting row spacing for peanut, corn, and sweet potato was 0.40 m, with a plant spacing of 0.2 m. The field management was consistent during the experiment in each plot. Local commonly used compound fertilizer ($N:P_2O_5:K_2O$ = 15:15:15) was applied with a total amount of 337.5 kg·hm^{-2}, divided into two applications. The first application was carried out on 18 March 2021, with a dosage of 225.0 kg·hm^{-2}. Half of the fertilizer was evenly spread and incorporated into the soil in the interspace of the loquat trees using a hoe. The other half was applied by digging a 20 cm deep circular trench 40 cm away from the loquat tree trunk, and the fertilizer was evenly spread inside the trench, followed by backfilling. On 21 March 2021, intercropping of peanut, corn, and sweet potato was carried out, and after sowing, gas collectors were placed in the experimental field for gas emission collection. The second application was performed on 4 March 2022, using a fertilizer amount of 112.5 kg·hm^{-2}. A 20 cm deep circular trench was dug 50 cm away from the loquat tree trunk, and the fertilizer was evenly applied into the trench. Due to the absence of pest and disease infestation during the experimental period, no pesticides were used. The air temperature and rainfall were monitored by a small weather station during the experiment (Figure 1).

2.4. Soil Sample Collection and Analysis

Soil samples were collected using the "S" type 5-point sampling method at 0–20 cm soil depth in February, May, July, and October 2021 and January and April 2022 (if it rained, samples were collected 2 weeks after the rain). The samples were mixed and placed in aluminum boxes and brought back to the laboratory. After drying in an oven, the soil moisture content was measured. At the same time, a soil thermometer was used to measure the temperature of the 5 cm soil layer at 10 am. The formula for calculating soil moisture content is:

$$\text{Soil moisture content} = (\text{wet soil weight} - \text{dry soil weight})/\text{dry soil weight} \times 100\%. \quad (1)$$

The loquat yield was measured in May 2021 and April 2022 (during the loquat harvesting period). As there was no significant difference in loquat yield under different intercropping modes in 2021, 2022 yield data were used for analysis. Soil samples were collected in October 2021 (after the harvest of peanuts, corn, and sweet potatoes) and May 2022 (after the loquat harvest) using a soil corer (50 mm inner diameter), according to the "S"

curve sampling method at five points in the topsoil layer (0–20 cm). The collected soil was sieved to remove stones, debris, and roots; mixed; and then divided into two parts, one for nutrient analysis and the other, which was placed in a foam box at low temperature (4 °C), for soil microbial biomass carbon (MBC) and nitrogen (MBN) analysis in the laboratory.

After natural drying in the laboratory, the soil was ground using a ball mill and sieved using 0.15 mm and 2 mm screens. The soil organic carbon (SOC), total nitrogen (TN), and alkaline nitrogen (AN) content were determined using the "Soil Agricultural Chemistry Analysis" method set out by Bao [21]. The SOC content was determined using the high-temperature external heating potassium dichromate oxidation capacity method. The total nitrogen content of the soil was determined by digesting with H_2SO_4-$HClO_4$ and measuring using an automatic Kjeldahl nitrogen analyzer (Hanon K1160, Shandong, China). The alkaline nitrogen content of the soil was determined using the alkaline diffusion method. The determination of soil MBC and MBN content was performed by the chloroform fumigation–extraction method [22,23].

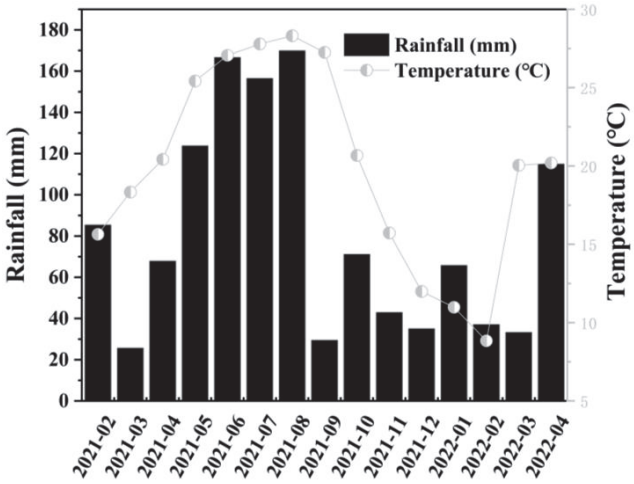

Figure 1. Monthly average rainfall and air temperature during the experiment.

2.5. Gas Collection and Analysis

Gas collection time was consistent with soil moisture collection time. The static box method was used for sampling, and the sampling box was made of acrylic material (20 cm long, 20 cm wide, and 30 cm high), with a three-way valve installed on the top for gas sampling. There was a small fan on the top of the box to mix the gas inside the box. The bottom of the sampling box was inserted into the soil between two loquat trees (10 cm), and the box was fastened to the groove on the base (sealed with water). During the sampling period, there were no crops or weeds in the box, which can represent the soil surface condition of the loquat orchard. Sampling was conducted from 9:00 to 11:00 on each sampling day. After the sampling box was fastened, the switch valve on the top of the sampling box was opened at 0, 15, 30, and 45 min, and 35 mL of gas was extracted with a 50 mL syringe and injected into a 12 mL headspace bottle that had been pre-evacuated. Each sampling was completed within 1 h. Gas concentration analysis was performed using an Agilent Technologies 7890A GC System (Agilent Technologies, Inc., Wilmington, DE, USA), and the CO_2, N_2O, and CH_4 gas emission fluxes were calculated according to the following formula [24]:

$$F = \frac{M}{22.4} \times \frac{273}{273 + T} \times H \times \frac{dc}{dt} \times 60$$

In the formula, F is the emission flux of CO_2, CH_4, and N_2O (the CO_2 unit is $mg \cdot m^{-2} \cdot h^{-1}$; CH_4 and N_2O units are $\mu g \cdot m^{-2} \cdot h^{-1}$); 60 is the conversion factor; H is the effective height of the sampling box (m); M is the molar mass of the gas; T is the temperature inside the sampling box (°C); and dc/dt is the slope of the regression curve of gas concentration and time.

The formula for calculating the cumulative greenhouse gas emissions is

$$G = \sum_{i=1}^{n} \frac{F_i + F_{i+1}}{2} \times (d_{i+1} - d_i) \times 24$$

In the formula, G is the total greenhouse gas emissions (kg/hm^2); F is the gas emission flux at the i-th sampling; d is the number of days between adjacent samplings; and n is the number of determinations.

As the CO_2 gas in the experiment is not a net emission, the global warming potential (GWP) is calculated based on a 100-year time scale. The warming effects per unit mass of CH_4 and N_2O are 25 and 298 times that of CO_2, respectively. The global warming potential values of soil CH_4 and N_2O fluxes are calculated using the following formula [2]:

$$GWP(kg\ CO_2\text{-}eq \cdot hm^{-2}) = 25 \times G(CH_4) + 298 \times G(N_2O)$$

GWP is the global warming potential ($kg \cdot hm^{-2}$); $G(CH_4)$ and $G(N_2O)$ are the cumulative emissions of CH_4 and N_2O, respectively ($kg \cdot hm^{-2}$).

2.6. Data Analysis

The experimental data were analyzed and processed using Excel 2016 and SPSS 13.0 software. Before conducting the statistical analysis, the normality of the dataset was evaluated, and a log10 transformation was performed if necessary to improve normality. One-way ANOVA was used to analyze the significance of soil moisture, soil greenhouse gas emissions, soil nutrient content, loquat yield, and economic benefits under different intercropping patterns at the same sampling time. Multiple comparisons between sampling months/years and intercropping patterns were conducted using the least significant difference (LSD) method. Pearson correlation analysis was used for correlation analysis. OriginPro 2021 (Originlab Lab, Northampton, MA, USA) was used for plotting.

3. Results

3.1. Seasonal Variation of Soil Moisture and Temperature under Different Intercropping Patterns

Soil moisture and soil water storage showed similar trends (Figure 2a,c). Intercropping patterns and sampling time significantly influenced soil moisture and water storage ($p < 0.001$) (Figure 2a). Throughout the experimental period, the average soil moisture content was highest in the IP treatment, followed by IC, IS, and SC, and IP was significantly higher than IS and SC ($p < 0.05$). The average water storage followed the order IP > IS > IC > SC (Figure 2d), with IP significantly higher than SC ($p < 0.05$). In October 2021, the soil moisture content and water storage were the lowest for all treatments, but IP significantly surpassed the other intercropping patterns. Compared to IC, IS, and SC, IP had 37.45%, 22.97%, and 42.40% higher soil moisture content, and 41.89%, 23.16%, and 47.95% higher water storage, respectively. This indicates that intercropping with peanut in the understory has a certain water conservation effect.

Soil temperature was significantly influenced by different sampling times ($p < 0.001$) (Figure 2b). The lowest soil temperature was recorded in January 2022, consistent with the trend of air temperature (Figure 2b), but there were no significant differences among the intercropping patterns.

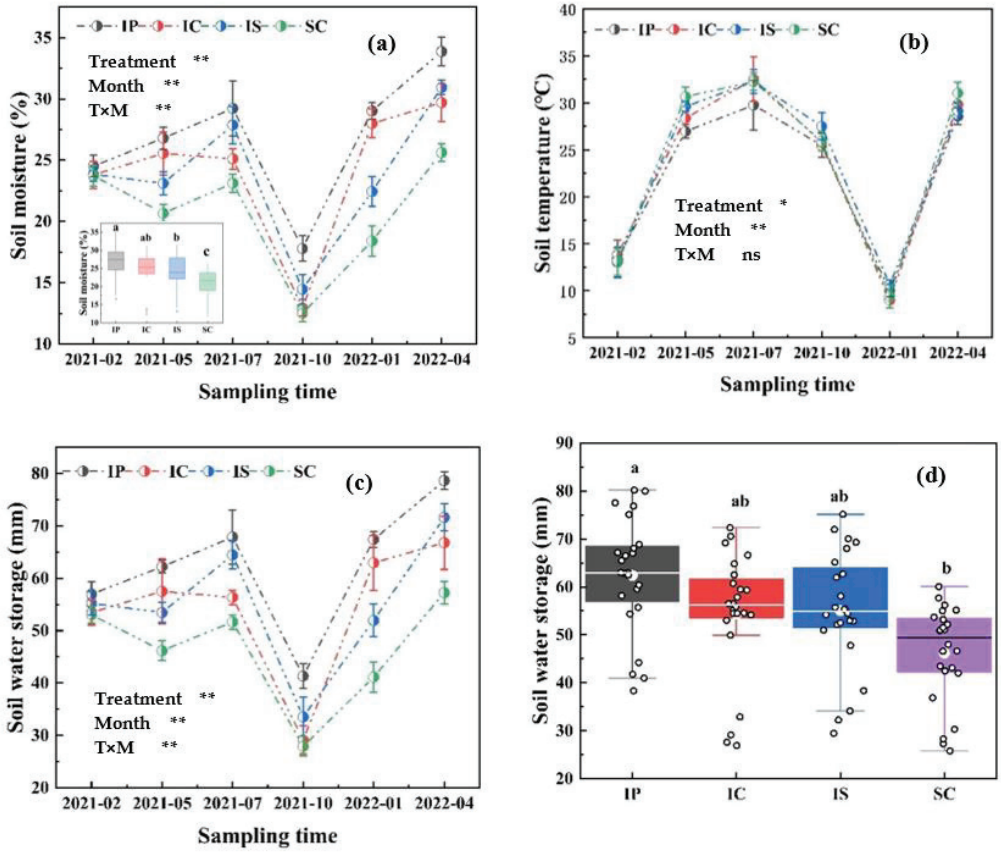

Figure 2. The seasonal variation of soil moisture (**a**), temperature (**b**), water storage (**c**), and average water storage (**d**) under different intercropping patterns of loquat with peanut (IP), corn (IC), sweet potato (IS), and no intercropping (SC). Error bars represent standard deviation ($n = 4$). * $p < 0.05$; ** $p < 0.01$; ns, not significant. Different lowercase letters indicate significant differences among different intercropping modes ($p < 0.05$). The same applies to the following.

3.2. Analysis of Soil Greenhouse Gas Emission Flux, Cumulative Emissions, and Their Global Warming Potential

The soil CO_2 emission flux exhibited significant seasonal dynamics ($p < 0.001$) (Figure 3a), and the intercropping pattern had a significant effect on it. Except for IC, the CO_2 emission flux gradually increased from February to July 2021 (Figure 3a) and then decreased, with the lowest emission in January 2022. The cumulative emissions were highest in SC, significantly higher than IP, IC, and IS ($p < 0.05$).

The intercropping pattern had a significant effect on the soil CH_4 emission flux ($p < 0.001$) (Figure 3b) and exhibited significant seasonal dynamics. The soil CH_4 emission flux showed a fluctuating trend during the experiment. The cumulative emissions of CH_4 were highest in SC (Figure 3d), followed by IS, significantly higher than IP and IC ($p < 0.05$). Overall, the cumulative CH_4 emission exhibited negative values, indicating that the soil had a certain absorption capacity for CH_4 during plant growth, and IP and IC had relatively high absorption rates, at 11.02 kg·hm^{-2} and 11.40 kg·hm^{-2}, respectively.

The soil N_2O emission flux exhibited significant seasonal dynamics ($p < 0.001$) (Figure 3c), and different intercropping patterns had a significant effect on it ($p < 0.001$). Except for IS in July 2021, which was significantly lower than other treatments, IP had the lowest emission

flux in other seasons. The highest N_2O emission flux among the same intercropping systems occurred in April 2022. IP had the lowest cumulative emissions (Figure 3d), with a value of 5.28 kg·hm^{-2}, followed by IS with a value of 6.02 kg·hm^{-2}, significantly lower than SC ($p < 0.05$).

The global warming potential of different intercropping systems was ranked as SC > IC > IS > IP, with IP, IC, and IS being 44.76%, 30.29%, and 34.25% lower than SC, respectively, and the differences were significant ($p < 0.05$) (Figure 3d).

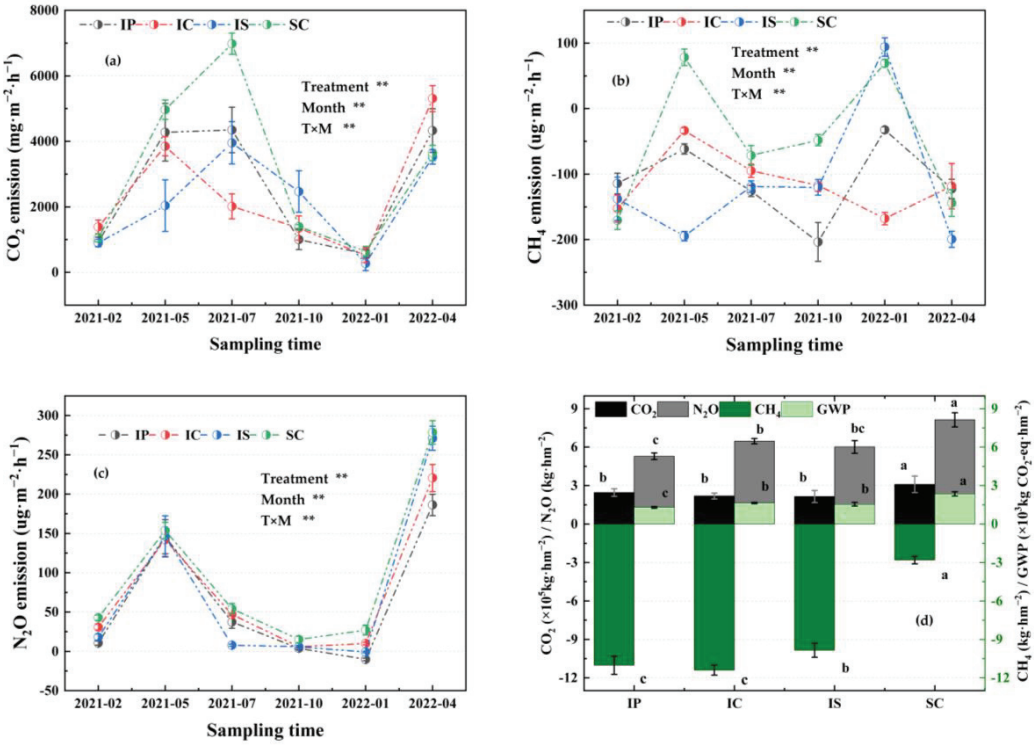

Figure 3. The soil CO_2 emission flux (**a**), soil CH_4 emission flux (**b**), soil N_2O emission flux (**c**), and cumulative emissions and global warming potential (**d**) under different intercropping patterns of loquat with peanut (IP), corn (IC), sweet potato (IS), and no intercropping (SC) ($n = 4$). ** $p < 0.01$; Different lowercase letters indicate significant differences among different intercropping modes ($p < 0.05$).

3.3. Analysis of Soil C and N Content

Soil SOC, TN, AN, MBC, and MBN content showed significant differences among different years and intercropping patterns ($p < 0.001$) (Figure 4). The trends of SOC under different intercropping treatments were basically consistent in 2021 and 2022 (Figure 4a). It showed that IP > IC > IS > SC, and IP was significantly higher than IS and SC ($p < 0.05$). Soil TN content in 2021 showed that IP > IS > IC > SC (Figure 4b), and IP was significantly higher than IC and SC ($p < 0.05$); in 2022, it showed that IS > IP > IC > SC, and IS, IP, and IC were all significantly higher than SC ($p < 0.05$). Soil AN content in 2021 showed that IP > IC > IS > SC (Figure 4c), and IP and IC were significantly higher than IS and SC ($p < 0.05$); in 2022, it showed that IP > IS > SC > IC, but the difference was not significant ($p > 0.05$).

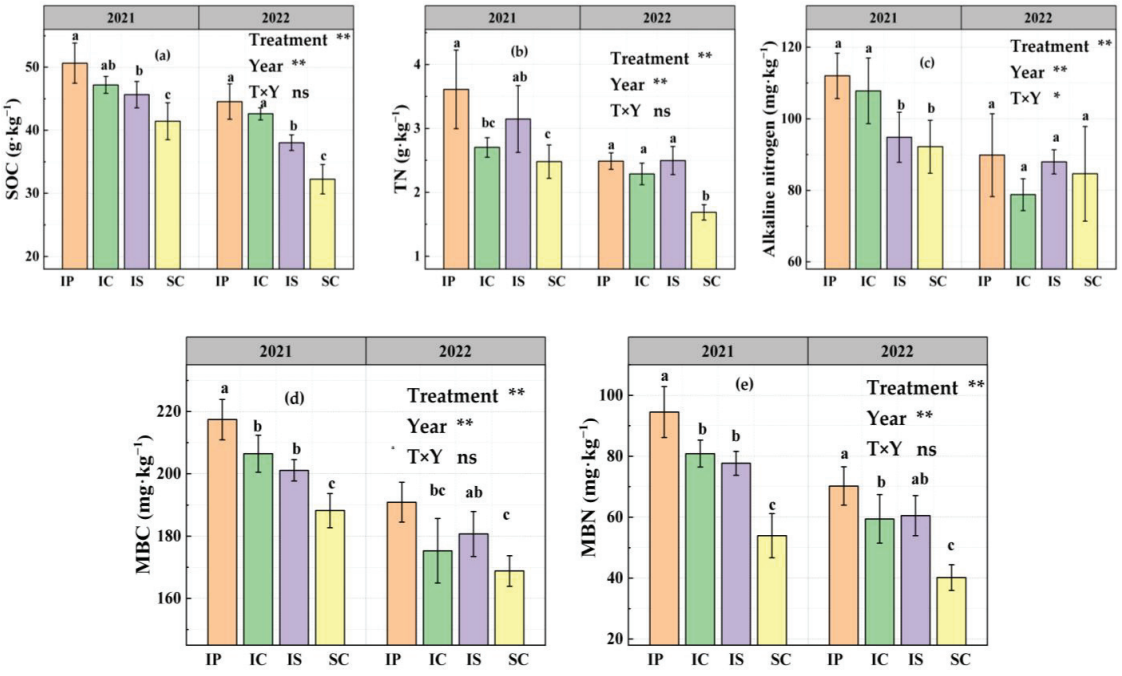

Figure 4. The soil organic carbon (SOC) (**a**), total nitrogen (TN) (**b**), alkaline nitrogen (AN) (**c**), soil microbial biomass carbon (MBC) (**d**), and soil microbial biomass nitrogen (MBN) (**e**) content of intercropped peanut (IP), intercropped corn (IC), intercropped sweet potato (IS), and non-intercropped (SC) in four replicates ($n = 4$). * $p < 0.05$; ** $p < 0.01$; ns, not significant. Different lowercase letters indicate significant differences among different intercropping modes ($p < 0.05$).

The trends in soil MBC and MBN contents were similar among different intercropping modes (Figure 4d,e). In 2021, both MBC and MBN showed the order of IP > IC > IS > SC, and in 2022 the order was IP > IS > IC > SC, with IP significantly higher than IC and SC ($p < 0.05$).

3.4. Yield and Economic Benefit Analysis

The yield and economic benefit analysis results for different intercropping modes are shown in Table 1. Loquat yield showed that IP > IS > IC > SC, and IP and IS were significantly higher than IC and SC ($p< 0.05$). IP had the highest total input cost, valued at 13,485 CNY·hm^{-2}, followed by IS at 13,275 CNY·hm^{-2}. The total output value and net profit of different intercropping modes exhibited consistent trends. The highest net profit was observed in the IP treatment, valued at 40,419.8 CNY·hm^{-2}, followed by IS at 35,473.4 CNY·hm^{-2}. In comparison to the non-intercropping mode (SC: 20,917.5 CNY·hm^{-2}), IP and IS demonstrated net profit increases of 93.2% and 69.6%, respectively, with significant differences ($p < 0.05$). The intercropping mode with the highest output–input ratio was IP (4.00), significantly higher than SC ($p < 0.05$).

3.5. Correlation Analysis

The soil temperature and soil moisture had a significantly positive correlation with CO_2 emissions and N_2O emissions ($p < 0.01$) (Figure 5a), while the CH_4 emissions showed a significant negative correlation with soil moisture ($p < 0.05$). There was a positive correlation between loquat yield and soil C and N content (Figure 5b) and a negative correlation with cumulative emissions of soil CO_2, CH_4, N_2O, and GWP. SOC, TN, MBC, and MBN content

showed a highly significant negative correlation with cumulative emissions of soil CH_4, N_2O, and GWP ($p < 0.01$).

Table 1. Yield and economic benefit analysis under different intercropping modes (mean ± SD).

Treatment	Loquat Yield ($kg \cdot hm^{-2}$)	Yield of Intercropped Crops ($kg \cdot hm^{-2}$)	Total Investment ($CNY \cdot hm^{-2}$)	Total Output Value ($CNY \cdot hm^{-2}$)	Net Profit ($CNY \cdot hm^{-2}$)	Output–Input Ratio
IP	9124.5 ± 845.6 a	920.3 ± 101.7	13,485	53,904.8 ± 4345.6 a	40,419.8 a	4.00 ± 0.32 a
IC	6833.1 ± 798.6 b	3511.6 ± 230.1	13,125	42,944.3 ± 3758.1 b	29,819.3 b	3.27 ± 0.29 ab
IS	8056.1 ± 752.1 a	5292.3 ± 401.7	13,275	48,748.4 ± 4375.6 ab	35,473.4 ab	3.67 ± 0.33 ab
SC	5758.5 ± 638.2 b		7875	28,792.5 ± 3190.8 c	20,917.5 c	3.66 ± 0.41 b

Note: IP, IC, IS, and SC, respectively, represent intercropping of peanut with loquat, intercropping of corn, intercropping of sweet potato, and no intercropping. Peanut yield was calculated based on dry weight of pods, corn yield was calculated based on dry weight of grains, and sweet potato and loquat yield were calculated based on fresh weight; total output value was calculated based on the local minimum prices, where the price of peanuts was 9.0 $CNY \cdot kg^{-1}$, loquat was 5.0 $CNY \cdot kg^{-1}$, corn was 2.5 $CNY \cdot kg^{-1}$,and sweet potato was 1.6 $CNY \cdot kg^{-1}$. Different lowercase letters within the same column indicate significant differences between different intercropping modes ($p < 0.05$).

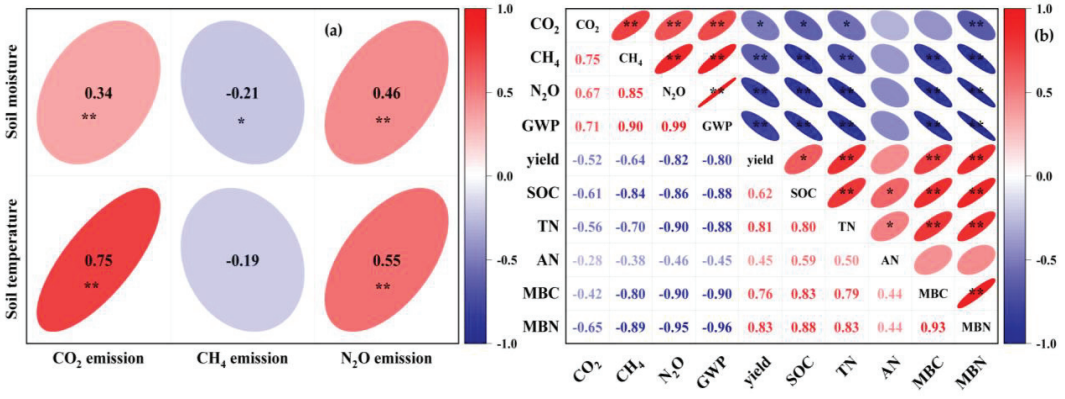

Figure 5. Correlation analysis of soil temperature, soil moisture content, and greenhouse gas emission flux (**a**), and the correlation analysis between loquat yield and soil C and N content, greenhouse gas cumulative emission, and warming potential (**b**). * The correlation is significant at the 0.05 level; ** significant at the 0.01 level.

4. Discussion

4.1. Intercropping Peanut Improved Loquat Yield and Soil Water and Fertilizer Environment in the Karst Plateau Canyon Desertification Control

Due to the high land and thermal resource utilization efficiency of intercropping systems [25], the area of intercropping peanuts with other crops has been increasing [26]. There are many factors that affect crop yield, and different intercropping treatments showed that IP and IS were significantly higher than IC and SC in loquat yield ($p < 0.05$) (Table 1). The IP treatment had the highest total output value, net profit, and output–input ratio, followed by the IS treatment, and these were both significantly higher than the IC and SC treatments ($p < 0.05$). This indicates that intercropping with dwarf nitrogen-fixing crops can promote loquat growth and yield formation, improve economic benefits, and achieve the purpose of promoting management through planting. Although intercropping with sweet potato can also achieve higher economic benefits, the nutrient requirements are high, making it unsuitable for intercropping in the poor and barren soil of karst desertification. There was a positive correlation between loquat yield and soil C and N content (Figure 5b). This indicates that soil C and N play an important role in crop growth, which is consistent with previous research results [27].

Some studies have shown that reasonable intercropping of leguminous crops can reduce soil erosion, reduce nitrogen loss, and increase soil organic matter and nitrogen content [28,29]. In this study, the average soil moisture content, soil water storage, SOC, TN, MBC, and MBN content of loquat intercropped with peanut were significantly higher than those of the non-intercropped plots ($p < 0.05$). Especially in October 2021, which experienced a long period of drought, the soil moisture content and water storage of loquat intercropped with peanut were significantly higher than the non-intercropping treatment (Figure 2a,c) ($p < 0.05$). This is consistent with previous studies on intercropping peanut in walnut forests [30]. This indicates that intercropping dwarf and nitrogen-fixing crops (peanut) can effectively improve soil water and fertilizer conditions in vegetation restoration of karst desertification control.

4.2. Intercropping Peanut with Young Loquat Forests Reduces N_2O Emissions

In agricultural production, there have been many reports on reducing soil N_2O emissions. Agronomic measures such as applying biochar [4,31,32], nitrification inhibitors [33], and slow-release fertilizers [34,35] and using optimized tillage methods [36] can reduce N_2O emissions. Previous studies have shown that reasonable intercropping and crop rotation with peanut can offset some of the external nitrogen input, increase crop nitrogen uptake, and reduce soil N_2O emissions [37–40], thereby ensuring the sustainability of the agricultural environment [41,42]. In this study, intercropping peanut with loquat significantly reduced the cumulative emissions of soil N_2O, CO_2, and CH_4 ($p < 0.05$) (Figure 3d). Among them, soil N_2O had the lowest cumulative emissions (Figure 3d), possibly because rhizobium is a diverse group of soil bacteria that can form symbiotic nitrogen-fixing associations with leguminous plants such as peanut, and many of these rhizobia can also perform denitrification [43]. Under anaerobic conditions, denitrifying microorganisms in the surrounding soil, including rhizobia cells released from decomposing nodules, can convert NO_3^- or NO_2^- to nitrogen gas [44,45], effectively reducing N_2O emissions [45–48]. The highest N_2O emissions under the same intercropping pattern were in April 2022 (Figure 3c). This may be related to the significantly positive correlation between soil N_2O emissions and soil temperature and moisture content (Figure 5a), and previous studies have shown that water management significantly affects soil N_2O emissions [49]. Therefore, this may be related to the higher rainfall (Figure 1), soil moisture content (Figure 2a), and soil temperature (Figure 2b) in April 2022.Furthermore, this study indicated that in July 2021, the N_2O emissions from the IS treatment were significantly lower than the other treatments, which may be due to the higher nitrogen consumption during the starch bulking period of sweet potatoes, resulting in lower N_2O emissions.

In addition, soil C and N content have a certain impact on soil greenhouse gas emissions. Previous studies [50–52] have shown that adding N reduces forest soil CO_2 and CH_4 emissions while increasing N_2O emissions; furthermore, increasing C reduces N_2O emissions. The cumulative CH_4 emissions in this study were negative, indicating that the soil has a certain absorption capacity for CH_4 during plant growth, especially in the IP and IC treatments, where the absorption was higher, which may be related to the higher availability of nitrogen in the soil under this intercropping pattern. In this study, it was found that SOC, TN, MBC, and MBN content showed a highly significant negative correlation with the cumulative emissions of soil CH_4, N_2O, and GWP ($p < 0.01$) (Figure 5b). This is different from the results of previous studies [51,52]. This may be related to the fact that the study area belongs to a severe karst desertification environment, with thin soil layers, high soil erosion, and long-term soil moisture deficiency (Figure 2a).

5. Conclusions

From the perspective of loquat yield and comprehensive economic benefits in the vegetation restoration of karst desertification, intercropping with peanut was a more suitable intercropping pattern, followed by intercropping with sweet potato. Understory intercropping of peanut improved soil moisture, water storage, soil carbon, and nitrogen

content. Karst area soils exhibited higher N_2O emissions, but intercropping with peanut effectively reduced soil N_2O emissions. The lowest cumulative N_2O-N emissions and global warming potential were observed when peanuts were intercropped under the forest. N_2O emissions primarily occurred in April and May, and the emission levels were strongly positively correlated with soil moisture and temperature. Additionally, the soils in karst desertification control demonstrated a certain capacity for CH_4 absorption.

Author Contributions: Conceptualization, methodology, writing—original draft preparation, T.H. and K.X.; validation, K.X.; formal analysis, investigation, data curation, software, supervision, T.H.; resources, funding acquisition, writing—review and editing, visualization, project administration, K.X. and J.W. All authors have read and agreed to the published version of the manuscript.

Funding: This research was funded by the Key Project of Science and Technology Program of Guizhou Province (Grant No. 5411 2017 QKHPTRC), the Projects of Geographical Sciety of Guizhou Province; Guizhou Provincial Science and Technology Projects (ZK 2021 (134)), National Key R&D Program of China (2022YFD1100303), Guizhou Provincial Science and Technology Projects (ZK 2022 (290)), Guizhou Provincial Science and Technology Projects (ZK 2023 (187)), and the China Agriculture Research System of MOF and MARA (CARS-13).

Data Availability Statement: All data supporting the results of this study are included in the manuscript, and data sets are available upon request.

Acknowledgments: We would like to thank Shan Yang and Zhifu Wang at the School of Karst Science, Guizhou Normal University, State Engineering Technology Institute for Karst Desertification Control, and JianweiLv, Liangqiang Cheng, Qinglin Rao, Jinhua Wang, and Min Jiang at the Guizhou Oil Research Institute, Guizhou Academy of Agricultural Sciences for their contributions.

Conflicts of Interest: The authors declare no conflict of interest.

References

1. IPCC. Climate change 2013: The physical science basis. In *Working Group I Contribution to the Fifth Assessment Report of the Intergovernmental Panel on Climate Change*; Stocker, T.F., Ed.; Cambridge University Press: Cambridge, UK; New York, NY, USA, 2013; p. 1535.
2. Tian, H.; Chen, G.; Lu, C.; Xu, X.; Hayes, D.J.; Ren, W.; Pan, S.; Huntzinger, D.N.; Wofsy, S.C. North American terrestrial CO_2 uptake largely offset by CH_4 and N_2O emissions: Toward a full accounting of the greenhouse gas budget. *Clim. Chang.* **2015**, *129*, 413–426. [CrossRef]
3. Raich, J.W.; Potter, C.S. Global patterns of carbon dioxide emissions fromsoil. *Glob. Biogeochem. Cycles* **1995**, *9*, 23–36. [CrossRef]
4. Wang, J.; Chen, Z.; Xu, C.; Elrys, A.S.; Shen, F.; Cheng, Y.; Chang, S.X. Organic amendment enhanced microbial nitrate immobilization with negligible denitrification nitrogen loss in an upland soil. *Environ. Pollut.* **2021**, *288*, 117721. [CrossRef] [PubMed]
5. Montzka, S.A.; Dlugokencky, E.J.; Butler, J.H. Non-CO_2 greenhouse gases and climate change. *Nature* **2011**, *476*, 43–50. [CrossRef]
6. Reay, D.S.; Davidson, E.A.; Smith, K.A.; Smith, P.; Melillo, J.M.; Dentener, F.; Crutzen, P.J. Global agriculture and nitrous oxide emissions. *Nat. Clim. Change* **2012**, *2*, 410–416. [CrossRef]
7. Alexandratos, N.; Bruinsma, J. *World Agriculture towards 2030/2050: The 2012 Revision*; ESA Working Paper No. 12–03; FAO: Rome, Italy, 2012.
8. Mueller, N.D.; Gerber, J.S.; Johnston, M.; Ray, D.K.; Ramankutty, N.; Foley, J.A. Closing yield gaps through nutrient and water management. *Nature* **2012**, *490*, 254–257. [CrossRef]
9. Xiao, J.; Xiong, K. A review of agroforestry ecosystem services and its enlightenment on the ecosystem improvement of rocky desertification control. *Sci. Total Environ.* **2022**, *852*, 158538. [CrossRef]
10. Yuan, D.X.; Jiang, Y.J.; Shen, L.C.; Pu, J.B.; Xiao, Q. *Modern Karstiology*; Volume Science Press: Beijing, China, 2016.
11. Wolf, I.; Brumme, R. Contribution of nitrification and denitrification sources for seasonal N_2O emissions in an acid german forest soil. *Soil Biol. Biochem.* **2002**, *34*, 741–744. [CrossRef]
12. Xu, W.B.; Hong, Y.T.; Chen, X.H.; Wang, Y. N_2O Emission from Upland Soils in Guizhou and lts Environmental Controlling Factors. *Chin. J. Enviromental Sci.* **2000**, *21*, 7–11.
13. Liu, H.Y.; Yu, Y.H.; Xiong, K.N. Response characteristics of photosynthesis to light intensity of three non-wood forests tree species in Karst habitat. *J. South. Agric.* **2021**, *6*, 1–14.
14. Hu, T.; Li, K.; Xiong, K.; Wang, J.; Yang, S.; Wang, Z.; Yu, X. Research Progress on Water–Fertilizer Coupling and Crop Quality Improvement and Its Implication for the Karst Rock Desertification Control. *Agronomy* **2022**, *12*, 903. [CrossRef]
15. Lin, H.X.; Pan, X.H.; Yuan, Z.Q.; Xiao, Y.P.; Liu, R.G.; Wang, R.Q.; Lv, F.J. Effects of nitrogen application and cassava-peanut intercropping on cassava nutrient accumulation and system nutrient utilization. *Sci. Agric. Sin.* **2018**, *51*, 3275–3290.

16. Jiao, N.Y.; Ning, T.Y.; Yang, M.K.; Fu, G.Z.; Yin, F.; Xu, G.W.; Li, Z.J. Effects of maize-peanut intercropping on photosynthetic characters and yield forming of intercropped maize. *Acta Ecol. Sin.* **2013**, *33*, 4324–4330. [CrossRef]
17. Zuo, Y.; Zhang, F.; Li, X.; Cao, Y. Studies on the improvement in iron nutrition of peanut by intercropping with maize on a calcareous soil. *Plant Soil* **2000**, *220*, 13–25. [CrossRef]
18. Hu, T.H.; Cheng, L.Q.; Wang, J.; Lv, J.W.; Rao, Q.L. Evaluation of Shade Tolerance of Peanut with Different Genotypes and Screening of Identification Indexes. *Sci. Agric. Sin.* **2020**, *53*, 1140–1153.
19. Li, Z.; Zhang, Z.; Lin, C.; Chen, Y.; Wen, A.; Fang, F. Soil-air greenhouse gas fluxes influenced by farming practices in reservoir drawdown area: A case at the three gorges reservoir in china. *J. Environ. Manag.* **2016**, *181*, 64–73. [CrossRef]
20. Dick, J.; Skiba, U.; Munro, R.; Deans, D. Effect of N-fixing and non N-fixing trees and crops on NO and N_2O emissions from Senegalese soils. *J. Biogeogr.* **2006**, *33*, 416–423. [CrossRef]
21. Bao, S.D. *Soil and Agriculture Chemistry Analysis*; China Agriculture Press: Beijing, China, 2010.
22. Wu, J.; Joergensen, R.G.; Pommerening, B.; Chaussod, R.; Brookes, P.C. Measurement of soil microbial biomass c by fumigation-extraction—An automated procedure. *Soil Biol. Biochem.* **1990**, *22*, 1167–1169. [CrossRef]
23. Vance, E.D.; Brookes, P.C.; Jenkinson, D.S. An extraction method for measuring soil microbial biomass c. *Soil Biol. Biochem.* **1987**, *19*, 703–707. [CrossRef]
24. Yang, Y.H.; Yi, J.T.; Zhang, C.; Chen, H.; Mu, Z.J. Effect of application of sewage sludge composts on greenhouse gas emissions in soil. *Environ. Sci.* **2017**, *38*, 1647–1653.
25. Tanwar, S.P.S.; Rao, S.S.; Regar, P.L.; Datt, S.; Kumar, P.; Jodha, B.S.; Santra, P.; Kumar, R.; Ram, R. Improving water and land use efficiency of fallow-wheat system in shallow lithic calcorthid soils of arid region: Introduction of bed planting and rainy season sorghum–legume intercropping. *Soil Tillage Res.* **2014**, *138*, 44–55. [CrossRef]
26. Wan, S.B.; Zheng, Y.P.; Liu, D.Z.; Cheng, B.; Wu, Z.F.; Chen, D.X.; Wang, C.B. Optinization of peanut-wheat intercropping system on date fertilizer and plant density. *Chin. J. Oil Crop Sci.* **2006**, *28*, 319–323.
27. Mariano, M.P.; Virginia, S.N.; Raúl, Z. Intercropping systems between broccoli and fava bean can enhance overall crop production and improve soil fertility. *Sci. Hortic.* **2023**, *312*, 111834.
28. Ma, Z.P.; Fan, M.P.; Chen, X.Q.; Wang, Z.L.; Yang, G.R.; Li, Y.M. Study on root system and red soil anti-erodibility of slope farmland under intercropping of maize and soybean. *J. Soil Water Conserv.* **2016**, *30*, 68–73.
29. Xu, Q.; Xiong, K.; Chi, Y.; Song, S. Effects of Crop and Grass Intercropping on the Soil Environment in the Karst Area. *Sustainability* **2021**, *13*, 5484. [CrossRef]
30. Yun, L.; Bi, H.; Ma, W.; Tian, X.; Cui, Z.; Zhou, H.; Gao, L. Spatial distribution of soil nutrient in fruit-crop intercropping in Loess Plateau of west Shanxi Province. *Trans. Chin. Soc. Agric. Eng.* **2010**, *26*, 292–299.
31. Agegnehu, G.; Bass, A.M.; Nelson, P.N.; Muirhead, B.; Wright, G.; Bird, M.I. Biochar and biochar-compost as soil amendments: Effects on peanut yield, soil properties and greenhouse gas emissions in tropical North Queensland, Australia. *Agric. Ecosyst. Environ.* **2015**, *213*, 72–85. [CrossRef]
32. Ibrahim, M.; Li, G.; Khan, S.; Chi, Q.; Xu, Y.; Zhu, Y. Biochars mitigate greenhouse gas emissions and bioaccumulation of potentially toxic elements and arsenic speciation in *Phaseolus vulgaris* L. *Environ. Sci. Pollut. Res.Int.* **2017**, *24*, 19524–19534. [CrossRef]
33. Li, H.-R.; Song, X.-T.; Bakken, L.R.; Ju, X.-T. Reduction of N_2O emissions by DMPP depends on the interactions of nitrogen sources (digestate vs. urea) with soil properties. *J. Integr. Agric.* **2023**, *22*, 251–264. [CrossRef]
34. Liu, Z.; Zhao, C.; Zhao, J.; Lai, H.; Li, X. Improved fertiliser management to reduce the greenhouse-gas emissions and ensure yields in a wheat-peanut relay intercropping system in china. *Environ. Sci. Pollut. Res.* **2021**, *29*, 22531–22546. [CrossRef]
35. Sompouviset, T.; Ma, Y.; Zhao, Z.; Zhen, Z.; Zheng, W.; Li, Z.; Zhai, B. Combined application oforganic and inorganic fertilizerseffects on the global warmingpotential and greenhouse gasemission in apple orchard in loessplateau region of China. *Forests* **2023**, *14*, 337. [CrossRef]
36. Cheng, S.; Xing, Z.-P.; Tian, C.; Liu, M.-Z.; Feng, Y.; Zhang, H.-C. Optimized tillage methods increased mechanically transplanted rice yield and reduced greenhouse gas emissions. *J. Integr. Agric.* **2023**. [CrossRef]
37. Tan, G.; Wang, H.; Xu, N.; Liu, H.; Zhai, L. Biochar amendment with fertilizers increases peanut N uptake, alleviates soil N(2)O emissions without affecting NH(3) volatilization in field experiments. *Environ. Sci. Pollut. Res. Int.* **2018**, *25*, 8817–8826. [CrossRef] [PubMed]
38. Xiao, H.; Es, H.M.; Amsili, J.P.; Shi, Q.; Sun, J.; Chen, Y.; Sui, P. Lowering soil greenhouse gas emissions without sacrificing yields by increasing crop rotation diversity in the North China Plain. *Field Crops Res.* **2022**, *276*, 108366. [CrossRef]
39. Rose, T.J.; Kearney, L.J.; Morris, S.; Van Zwieten, L.; Erler, D.V. Pinto peanut cover crop nitrogen contributions and potential to mitigate nitrous oxide emissions in subtropical coffee plantations. *Sci. Total. Environ.* **2019**, *656*, 108–117. [CrossRef] [PubMed]
40. Xiong, Z.; Xing, G.; Tsuruta, H.; Shen, G.; Shi, S.; Du, L. Field study on nitrous oxide emissions from upland cropping systems in China. *Soil Sci. Plant Nutr.* **2002**, *48*, 539–546. [CrossRef]
41. Chen, J.S.; Amin, A.S.; Hamani, A.K.M.; Wang, G.S.; Zhang, Y.Y.; Liu, K.; Gao, Y. Effects of maize (*Zea mays* L.) intercropping with legumes on nitrous oxide (N_2O) emissions. *Appl. Ecol. Environ. Res.* **2021**, *19*, 3393–3407. [CrossRef]
42. Huang, J.-X.; Chen, Y.-Q.; Sui, P.; Nie, S.-W.; Gao, W.-S. Soil Nitrous Oxide Emissions Under Maize-Legume Intercropping System in the North China Plain. *J. Integr. Agric.* **2014**, *13*, 1363–1372. [CrossRef]

43. Mania, D.; Woliy, K.; Degefu, T.; Frostegard, A. A common mechanism for efficient N(2) O reduction in diverse isolates of nodule-forming bradyrhizobia. *Env. Microbiol* **2020**, *22*, 17–31. [CrossRef]
44. Yang, L.; Cai, Z. The effect of growing soybean (*Glycine max.* L.) on N_2O emission from soil. *Soil Biol. Biochem.* **2005**, *37*, 1205–1209. [CrossRef]
45. Akiyama, H.; Hoshino, Y.T.; Itakura, M.; Shimomura, Y.; Wang, Y.; Yamamoto, A.; Tago, K.; Nakajima, Y.; Minamisawa, K.; Hayatsu, M. Mitigation of soil N_2O emission by inoculation with a mixed culture of indigenous *Bradyrhizobium diazoefficiens*. *Sci. Rep.* **2016**, *6*, 32869. [CrossRef]
46. Hénault, C.; Revellin, C. Inoculants of leguminous crops for mitigating soil emissions of the greenhouse gas nitrous oxide. *Plant Soil* **2011**, *346*, 289–296. [CrossRef]
47. Itakura, M.; Uchida, Y.; Akiyama, H.; Hoshino, Y.T.; Shimomura, Y.; Morimoto, S.; Tago, K.; Wang, Y.; Hayakawa, C.; Uetake, Y.; et al. Mitigation of nitrous oxide emissions from soils by *Bradyrhizobium japonicum* inoculation. *Nat. Clim. Change* **2012**, *3*, 208–212. [CrossRef]
48. Gao, Y.; Mania, D.; Mousavi, S.A.; Lycus, P.; Arntzen, M.Ø.; Woliy, K.; Frostegård, Å. Competition for electrons favours N_2O reduction in denitrifying Bradyrhizobium isolates. *Environ. Microbiol.* **2021**, *23*, 2244–2259. [CrossRef] [PubMed]
49. Islam, S.M.M.; Gaihre, Y.K.; Islam, M.R.; Akter, M.; Al Mahmud, A.; Singh, U.; Sander, B.O. Effects of water management on greenhouse gas emissions from farmers' rice fields in Bangladesh. *Sci. Total. Environ.* **2020**, *734*, 139382. [CrossRef]
50. Li, Q.; Cui, K.; Lv, J.; Zhang, J.; Peng, C.; Li, Y.; Song, X. Biochar amendments increase soil organic carbon storage and decrease global warming potentials of soil CH_4 and N_2O under N addition in a subtropical Moso bamboo plantation. *For. Ecosyst.* **2022**, *9*, 100054. [CrossRef]
51. Wang, J.; Wu, L.; Zhang, C.; Zhao, X.; Bu, W.; Gadow, K.V. Combined effects of nitrogen addition and organic matter manipulation on soil respiration in a Chinese pine forest. *Environ. Sci. Pollut. Res. Int.* **2016**, *23*, 22701–22710. [CrossRef]
52. Tian, J.; Dungait, J.A.J.; Lu, X.; Yang, Y.; Hartley, I.P.; Zhang, W.; Mo, J.; Yu, G.; Zhou, J.; Kuzyakov, Y. Long-term nitrogen addition modifies microbial composition and functions for slow carbon cycling and increased sequestration in tropical forest soil. *Glob. Chang. Biol.* **2019**, *25*, 3267–3281. [CrossRef]

forests

MDPI

Article

Multiple Factors Jointly Lead to the Lower Soil Microbial Carbon Use Efficiency of *Abies fanjingshanensis* in a Typical Subtropical Forest in Southwest China

Xianliang Wu [1], Zhenming Zhang [2,*], Jiachun Zhang [3], Yingying Liu [1], Wenmin Luo [1], Guiting Mou [1] and Xianfei Huang [4]

[1] Guizhou Institute of Biology, Guizhou Academy of Sciences, Guiyang 550009, China; wuxianliang1995@163.com (X.W.); liuyingying2019@126.com (Y.L.); luowenmin2006@163.com (W.L.); mugui6925@163.com (G.M.)
[2] College of Resource and Environmental Engineering, Guizhou University, Guiyang 550003, China
[3] Guizhou Botanical Garden, Guizhou Academy of Sciences, Guiyang 550004, China; zhangjiachun198806@163.com
[4] Guizhou Provincial Key Laboratory for Environment, Guizhou Normal University, Guiyang 550001, China; hxfswjs@gznu.edu.cn
* Correspondence: zhang6653579@163.com

Abstract: *Abies fanjingshanensis* trees are the only remaining Abies species in a type of subtropical forest of southwest China and are in imminent danger. Previous studies suggested that the massive death of Abies was caused by the unbalanced chemometrics and nutrients in the soil. To the best of our knowledge, for the first time, we evaluated the microbial carbon use efficiency (CUE) in the rhizospheric topsoil and subsoil of *A. fanjingshanensis*, at high elevation, middle elevation, and low elevation as well as investigated their physicochemical indices, soil enzyme activities, bacteria, fungi, and microbial biomass. The results showed that the physicochemical parameters (TP, SOC, AK, AP, MC, TN, NO_3-N, NH_4-N and cation exchange capacity) of the topsoil were higher than those of the subsoil. Acidobacteria, Proteobacteria, Planctomycetes, and Actinobacteria were the dominant phyla in the two soil layers. Candidatus_Koribacter was the main indicator species in the rhizospheric topsoil and subsoil. The positive correlation in the bacterial co-occurrence networks implied that cooperation was dominant between the bacteria in four soil types, and the same phenomenon was found in the co-occurrence networks of fungi. A structural equation model confirmed that pH was the most important factor affecting microbial CUE in the topsoil and subsoil. We inferred that the microorganisms in the acidic soil environment were forced to consume more energy to maintain cellular pH, while less energy was used for growth. The increased solubility of some toxic metals in the acidic soil affected the microbes, resulting in a lower microbial CUE in the *A. fanjingshanensis* rhizospheric soil. Our results highlight that pH values in soil mainly affected microbial CUE, and a lower microbial CUE may be another important factor in the death of large numbers of *A. fanjingshanensis*. Several measures must be carried out to improve the microbial CUE in the rhizospheric soil of *A. fanjingshanensis* by the department of forest management, such as adding the appropriate biochar and nitrogenous fertilizer.

Keywords: *Abies fanjingshanensis*; microbial carbon use efficiency; physicochemical indices; bacteria; fungus

Citation: Wu, X.; Zhang, Z.; Zhang, J.; Liu, Y.; Luo, W.; Mou, G.; Huang, X. Multiple Factors Jointly Lead to the Lower Soil Microbial Carbon Use Efficiency of *Abies fanjingshanensis* in a Typical Subtropical Forest in Southwest China. *Forests* **2023**, *14*, 1716. https://doi.org/10.3390/f14091716

Academic Editor: Robert G. Qualls

Received: 10 July 2023
Revised: 15 August 2023
Accepted: 19 August 2023
Published: 25 August 2023

1. Introduction

Soil microorganisms are important components of the soil and decomposers in the forest ecosystem [1,2], as they actively participate in the material circulation and energy flow and play a vital role in maintaining the structure and function of the ecosystem [3]. A variety of microorganisms inhabit the soil, and each has different physiological activities.

The metabolic functions of soil microorganisms are diverse, as they metabolize almost all organic substances that are biosynthesized [4]. Organic substances can also be mineralized into carbon dioxide and inorganic compounds, such as nitrogen, sulfur, phosphorus, and other elements, or transformed into another organic substance [5]. Soil microbial diversity indirectly reflects soil physicochemical properties [6]. Furthermore, the abundance and change in microorganisms reflect their adaptation to the environment [6]. Altitude also affects the forest soil environment and further affects the community structure and diversity of soil microorganisms [7]. Therefore, studying the relationship between altitude and soil microbial diversity reflects the changes in forest soil ecology and the microenvironmental climate.

Microbial carbon use efficiency (CUE) in soil microorganisms refers to the ratio of microbial growth to carbon absorption [8], reflecting the soil organic carbon (SOC) metabolism influenced by the microbial communities [9]. A high microbial CUE generally indicates high growth efficiency of the soil microorganisms, which is beneficial for accumulating and stabilizing microbial-sourced carbon in the soil [9]. In contrast, a low microbial CUE is beneficial for respiration and reduces soil carbon storage, indicating a decrease in soil carbon sequestration potential [10]. Xiong et al. [11] suggested that microbial CUE increased during the summer with increasing elevation in Wuyishan National Park, Fujian Province, China, while an opposite trend was observed during winter. Lv et al. [12] studied the changes and impact mechanism of soil microbial CUE in ancient woodland at different altitudes (980 to 1765 m) on Daiyun Mountain. The results showed that the microbial CUE varied from 0.1 to 0.4 and increased with elevation. Microbial CUE was negatively correlated with temperature, indicating that as altitude increased, the temperature decreased, which was a key factor promoting the increase in soil microbial CUE. Zhang et al. [13] selected six forest rhizosphere soils at different altitudes on Mount Taibai in the Qinling Mountains and measured their physicochemical properties, extracellular enzyme activities, microbial community, and vegetation characteristics. The results showed that the microbial CUE in the rhizosphere soil trended upward with increasing altitude. CUE increased by 4.36% from the lowest altitude of 0.505 to the highest altitude of 0.527 but decreased at elevations of 1603 and 2405 m. The variation in microbial CUE in the rhizosphere soil within the altitude gradient was affected by several environmental factors, and the influence of the soil matrix (such as soluble organic carbon and ammonium nitrogen content) dominated. Although several studies have been conducted on the CUE of forest soil, few studies have investigated perennial low-temperature areas in subtropical forest soil to study forest soil microorganisms. The soil microenvironment in these regions has gradually changed with global warming, leading to endangered plants growing on the soil. Therefore, further investigation of the soil microorganisms and CUE in these areas and revealing the relationship between soil microorganisms in subtropical regions and forest ecology in the region was of great significance for protecting local plants.

Fanjing Mountain is a complete and independent subtropical forest ecosystem that includes the globally unique Rhinopithecus brelichi and *Abies fanjingshanensis* [14]. However, A. *fanjingshanensis* has massively died in recent years. Several studies have been conducted on the cause of death of *A. fanjingshanensis* [15,16]. Liu et al. [14] demonstrated that total-C, total-N, hydrolyzed-N, and available-P contents of the forest soils were higher at higher altitudes, with median values for *A. fanjingshanensis* forest soil > Taxus chinensis var. mairei soil > Davidia involucrata soil. The C:N, C:P, and N:P ratios of the soil in *A. fanjingshanensis* stands were the largest and significantly higher than those of soils in T. chinensis var. mairei or D. involucrata stands. Li et al. [17] reported that the organic matter and alkaline nitrogen content in the 0–20 cm soil layer are significantly correlated with altitude. The organic matter content increased first and then decreased with altitude. The correlation between various indicators of soil in the 20–40 cm layer and altitude was relatively lower. However, although those studies considered the effect of elevation on soil physicochemical parameters, several factors caused the death of *A. fanjingshanensis*, according to an on-the-spot investigation. Furthermore, whether the death of *A. fanjingshanensis* was related to microbial CUE of the rhizosphere soil is unknown.

To fill these knowledge gaps, this study collected forest soil samples in high (HE), middle (ME), and low elevation (LE) areas of Fanjing Mountain and revealed the relationship between the physicochemical parameters, microorganisms, and CUE in the soil at different elevations. We hypothesized that (1) the difference in the microbial communities and their diversity would be relatively higher along with the changing elevation; (2) the CUE rate would play a relatively important role in the different elevations; (3) the soils of other tree species besides *A. fanjingshanensis* have more complex co-occurrence networks and higher network stability. Thus, this study aimed to (1) determine the physicochemical parameters of the *A. fanjingshanensis* soil and several altitudes; (2) evaluate the CUE and soil enzyme activities in different altitude soils; (3) investigate the diversity, dominant phyla, indicator species, and co-occurrence networks of bacteria and fungi in the soil, and (4) reveal the most important factor affecting the microbial CUE in rhizospheric soil.

2. Materials and Methods

2.1. Study Area

Fanjing Mountain (27°49′50″ to 28°1′30″ N, 108°45′55″ to 108°48′30″ E) is located in the Tongren area of northeastern Guizhou Province, southwest China and is a national nature reserve. It is the main peak of the Wuling Mountains, with the highest peak at an altitude of 2572 m. The nominated area for the World Natural Heritage site of Mount Fanjing is 402.75 km^2, with a buffer zone area of 372.39 km^2. Fanjing Mountain is one of the earliest areas in southern China to become land, with a long history of geologic evolution. Fanjing Mountain is mainly composed of metamorphic rock, surrounded by vast karst landforms with unique geological, ecological, biological, and landscape characteristics. The Fanjing Mountain ecosystem preserves many ancient relics and rare and endangered species and is the only habitat and distribution area for *Rhinopithecus brelichi* and *A. fanjingshanensis.* It is also the most important protected area for the Shuiqinggang forest in Asia. The typical dome-shaped mountain ecosystem forms spectacular subalpine mountains and hilly landforms. Fanjing Mountain is located in the middle of the mid-subtropical zone and the transitional slope zone between the Yunnan-Guizhou Plateau and the hills in western Hunan, with a height difference of 2000 m [14]. As influenced by the East Asian Monsoon and the large difference in mountain height, the mountain has a humid climate in a large area, and the three-dimensional climate in a small area is significantly different. In addition, there is little interference by human activity, which allows Fanjing Mountain to contain the richest biodiversity at the same latitude on earth and is an important species gene pool.

2.2. Soil Sample Collection and Chemical Analysis

Four soil samples, including those of *A. fanjingshanensis* (ABI, 2304 m), high elevation (HE, 2338 m), middle elevation (ME, 1427 m), and low elevation (LE, 634 m), were collected in June 2021. Three sampling points were randomly selected at the core area of each sample (20 m × 20 m). During sampling, the dead branches and fallen leaves were removed from the surface, and a 3.5 cm diameter soil drill was used to collect the topsoil (0–20 cm) and the subsoil (20–40 cm). The soil in the same layer was mixed, and about 500 g of mixed soil was placed in an ice bag and transported to the laboratory. The crushed stone and visible roots were removed, and the soil sample was divided into two parts after passing through a 2 mm sieve. One part was placed in 4 °C storage to determine soil available nutrients, microbial biomass C (MBC), and microbial biomass N (MBN). The other part of the soil was naturally air-dried, passed through 100 mesh, and was used to determine the physicochemical parameters.

Total carbon (C) and N in the soil were measured using a C and N element analyzer (Elemental Vario EL III, Elemental, Germany). A 5.0 g portion of fresh soil was extracted using a 2 mol/L KCI solution with a water-to-soil ratio of 4:1 to determine NH_4^+–N and NO_3^-–N. The supernatant was measured using a continuous flow analyzer (SAN++, Skalar, the Netherlands) [17]. Cation exchange capacity (CEC) in soil was analyzed by the Ammonium chloride-ammonium acetate exchange method. The mechanical composition in

soil was determined by a Laser particle analyzer (Mastersizer 3000, Malvern, The United Kingdom). Total phosphorous (TP) in the soil was determined using the $HClO_4$–H_2SO_4 method, and the sample was digested and decomposed, filtered (0.45 μm), and measured using the continuous flow analyzer [18]. Available phosphorus (AP) was extracted with Mehlich III, and the supernatant was measured using the continuous flow analyzer [19]. After MBC and MBN were determined by the fumigation–K_2SO_4 method, the content of total organic carbon in the filtrate was determined with a total organic carbon analyzer (TOC-VCPH/CPN, Shimadzu Instruments Co., Ltd., Japan) [20]. TN content was measured using a continuous flow analyzer, and the difference between the fumigated and non-fumigated soil samples was divided by the coefficients Kc = 0.45 and Ky = 0.54 to obtain the MBC and MBN content in the soil. The soil pH was tested by potentiometry using a soil-to-water ratio of 1:2.5 [21]. Three parallel samples were run for each sample. Moisture content (MC) was determined using the drying method (105 °C). The methods to determine β-glucosidase (βG), cellulosebiohydrolase (CBH), n-acetyl glucosaminidase (NAG), and acid phosphatase (AP-Tase) were taken from Xiong et al. [11].

2.3. Soil Enzymes Activities and Microbial Carbon Use Efficiency

βG, CBH, NAG, and AP-Tase were utilized to calculate microbial CUE. According to Sinsabaugh et al. [22], we calculated the ratios of C, N, and P by determining enzyme activity. Microbial CUE was calculated based on the following C:N stoichiometric equations [11]:

$$CUE_{C:N} = CUE_{max}[S_{C:N}/(S_{C:N} + K_N)] \quad (1)$$

$$S_{C:N} = (1/EEA_{C:N})(B_{C:N}/L_{C:N})] \quad (2)$$

where the meaning of $S_{C:N}$, the half-saturation constant K_N, CUE_{max} (0.6), $EEAC{:}N$ and $L_{C:N}$ are referred with Sinsabaugh et al. [22] and Xiong et al. [11].

2.4. DNA Extraction and Polymerase Chain Reaction (PCR) Amplification

lluminaMiSeq sequencing was performed on all of the soil samples. Total microbial DNA was extracted according to the E.Z.N.A. Soil DNA kit instructions (Omega Bio tek, Norcross, GA, USA) that included buffer SLX mlus, buffer SP2, HTR reagent, buffer XP2, DNA wash buffer, elution buffer, Hibind DNA micro elute column, 2 mL collection tubes. The special operated process can scan the official website (https://www.omegabiotek.com) (Accessed on 22 August 2023). A 1% agarose gel electrophoresis method was used to detect DNA extraction quality, and the NanoDrop2000 spectrophotometer was used to determine DNA concentration and purity. Bacterial primers were used, including 338F (5′-ACTCCTACCCCACCAG-3′) and 806R (5′-GACTACHVCCCTWTCTAAT-3′), while the fungal primers were ITSIF (5′-CTTCATTTAGAGAGATAA-3′) and ITIS2R (5′-GCTGCTTCTTCATCCATGC-3′). The amplification procedure was pre-denaturation at 95 °C for 3 min, 27 cycles (denaturation at 95 °C for 30 s, annealing at 55 °C for 30 s, and extension at 72 °C for 30 s), followed by stable extension at 72 °C for 10 min, and storage at 4 °C (PCR instrument: ABIGeneAmp 9700 Type). The PCR reaction system included 4 μL of 5× TransStart FastPfu buffer, 2 μL of 2.5 mmol/L dNTPs, 0.8 μL of the upstream primer (μmol/L), 0.8 μL of the downstream primer (5 pmol/L), 0.4 μL of transStart FastPfu DNA polymerase, 10 ng of template DNA, complement to 20 μL.

After mixing the PCR products from the same sample, 2% agarose gel electrophoresis was used to recover the PCR products. The AxyPrep DNA Gel Extraction Kit (Axygen-Biosciences, Union City, CA, USA) was utilized to purify the recovered products, and 2% agarose gel electrophoresis was used to detect the products. The Quantum Fluorometer (Promega, Madison, WI, USA) was used to detect and quantify the recovered products. The NEXTFLEX Rapid DNA-Seq Kit was employed to prepare the library. The Illumina Miseq PE300 platform was used for sequencing (Beijing Baimike Biotechnology Co., Ltd., Beijing, China). Fastp software was used for quality control of the original sequence [23], and FLASH software was employed for splicing [24]. OTU clustering was performed

on sequences based on 97% similarity with the chimeras removed using UPARSE software [25,26]. RDP classifiers were utilized to annotate the species classification for each sequence by comparing the bacteria to the Silva 16S rRNA database and fungi to the UNITE ITS database, with a matching threshold of 70%.

2.5. Statistical Analysis

The data were statistically analyzed using Excel 2019 (Microsoft Inc., Redmond, WA, USA), SPSS (SPSS Inc., Chicago, IL, USA), and R language (R 3.0.2). Redundancy analysis (RDA) was performed to reveal the relationship between microorganism (phylum level) and physicochemical indexes using the "Ape", "vegan", "psych", and "reshape2" packages in the R language. Single-factor analysis of variance and the least significant difference test were used to detect differences in the selected indicators. A structural equation model (SEM) was used to evaluate potential hypotheses and was analyzed using IBM SPSS Amos 24.

3. Results

3.1. The Physicochemical Indexes in Topsoil and Subsoil in ABI, HE, ME and LE

Most of the physicochemical parameters were not significantly different in the ABI rhizospheric topsoil or the subsoil (Table 1). The topsoil and subsoil pH values in the ABI rhizospheric topsoil were slightly higher than those at the same elevation but lower than those in the soil at the ME. SOC, TP, TN, AP, and C:N were significantly different between the ABI rhizospheric soil and the other elevations. The SOC and TP contents in ABI were significantly higher than those in the soil at HE, ME, and LE. The AP concentration increased in the topsoil and subsoil with an increase in elevation. TN content was significantly higher in the ABI rhizospheric topsoil than that at the other elevations. The C:N ratio in the ABI rhizospheric topsoil was lower than that in the soil at the other elevations, while the opposite was true in the lower soil layers. Taken together, except for pH, Cu, K, and TP, the selected physicochemical parameters were of higher magnitude in topsoil than in subsoil, and the ABI rhizospheric soil had greater contents than those at the same elevation (HE) and different elevations (ME and LE). CEC contents in the topsoil were higher than that in the subsoil, of which its CEC values in the topsoil of ME are highest. According to the international grading standards, the soil in this study was regarded as light clay.

Table 1. The physicochemical parameters in topsoil and subsoil of ABI, HE, ME and LE.

Indexes	0–20 cm				20–40 cm			
	ABI	HE	ME	LE	ABI	HE	ME	LE
pH	4.05 ± 0.34 ^{a}	4.04 ± 0.25 ^{a}	4.65 ± 0.23 ^{a}	4.03 ± 0.74 ^{a}	4.07 ± 0.52 ^{a}	4.31 ± 0.28 ^{a}	4.77 ± 0.29 ^{a}	4.69 ± 0.09 ^{a}
Ca	1.67 ± 0.47 ^{a}	0.42 ± 0.23 ^{a}	0.75 ± 0.68 ^{a}	1.07 ±631 ^{a}	1.98 ± 1.78 ^{a}	0.58 ± 0.12 ^{a}	0.72 ± 0.81 ^{a}	0.57 ± 0.18 ^{a}
Cu	26 ± 6 ^{a}	29 ± 24 ^{a}	23 ± 2 ^{a}	13 ± 2 ^{a}	28 ± 11 ^{a}	50 ± 54 ^{a}	26 ± 4.37 ^{a}	13 ± 1 ^{a}
Fe	28 ± 10 ^{a}	15 ± 4 ^{a}	22 ± 5 ^{a}	22 ± 3 ^{a}	31 ± 13	16 ± 1 ^{a}	27 ± 2 ^{a}	29 ± 5 ^{a}
K	2.26± 0.63 ^{b}	8.86 ± 0.65 ^{a}	2.79 ± 1.52 ^{b}	4.50 ± 0.29 ^{b}	2.20 ±0.13 ^{b}	10.58 ±0.34 ^{a}	3.35 ± 1.87 ^{b}	5.89 ± 1.55 ^{ab}
Zn	1.82 ± 0.89 ^{a}	1.56 ± 0.47 ^{a}	0.43 ± 0.19 ^{a}	0.50 ± 0.22 ^{a}	0.37 ± 0.01 ^{ab}	0.19 ± 0.01 ^{a}	0.41 ± 0.02 ^{ab}	0.32 ± 0.02 ^{b}
TP	0.63± 0.02 ^{a}	0.59 ± 0.01 ^{b}	0.64 ± 0.02 ^{ac}	0.41 ± 0.01 ^{d}	0.68 ± 0.15 ^{s}	0.82 ± 0.81 ^{b}	0.58 ± 0.18 ^{ac}	0.11 ± 0.03 ^{d}
SOC	235± 88 ^{a}	141 ± 11 ^{b}	196 ± 33 ^{c}	170 ± 37 ^{d}	160 ± 79 ^{a}	59 ± 24 ^{b}	51 ± 7 ^{b}	57 ± 24 ^{b}
AK	121 ± 39 ^{a}	101 ± 11 ^{a}	102 ± 28 ^{a}	128 ± 16 ^{a}	83 ± 27 ^{a}	49 ± 12 ^{a}	53 ± 10 ^{a}	41 ± 9 ^{a}
AP	109 ± 26 ^{a}	90 ± 22 ^{b}	63 ± 12 ^{c}	63 ± 10 ^{c}	67 ± 18 ^{a}	58 ± 28 ^{a}	38 ± 9 ^{b}	27 ± 3 ^{b}
MC	161 ± 2 ^{a}	100 ± 2 ^{b}	58 ± 2 ^{c}	38 ± 3 ^{d}	91 ± 3 ^{a}	48 ± 1 ^{c}	65 ± 27 ^{b}	35 ± 2 ^{d}
TN	9.99 ± 1.70 ^{a}	5.28 ± 0.42 ^{b}	3.52 ± 0.68 ^{b}	3.39 ± 0.82 ^{b}	5.04 ± 0.68 ^{a}	1.89 ± 0.52 ^{b}	2.29 ± 0.64 ^{b}	2.31 ± 0.41 ^{b}
C:N	24 ± 8 ^{a}	27 ± 4 ^{a}	56 ± 6 ^{b}	56 ± 23 ^{b}	31 ± 11 ^{a}	38 ± 27 ^{a}	25 ± 9 ^{a}	25 ±11 ^{a}
CEC	25 ± 2 ^{a}	10 ± 1 ^{b}	28 ± 2 ^{a}	11 ± 1^{b}	18 ± 1 ^{a}	6 ± 0 ^{b}	15 ±1 ^{a}	8 ± 0 ^{b}
0.25–1.00 mm	17 ± 3 ^{a}	25 ± 2 ^{b}	7 ± 0 ^{c}	13 ± 1 ^{a}	16 ± 1 ^{a}	16 ± 1 ^{a}	0.88 ± 0.09 ^{b}	17 ± 1 ^{a}
0.05–0.25 mm	15± 2 ^{a}	10 ± 0 ^{b}	26 ± 2 ^{c}	17 ± 1 ^{a}	10 ± 1 ^{a}	4 ± 0 ^{b}	19 ± 0 ^{c}	6 ± 0 ^{b}
0.01–0.05 mm	20 ± 2 ^{a}	19 ± 1 ^{a}	21 ± 3 ^{a}	15 ± 0 ^{a}	16 ± 1 ^{a}	21± 1 ^{a}	27 ± 1 ^{b}	22 ± 0 ^{a}
0.005–0.01 mm	7 ± 0 ^{a}	17 ± 2 ^{b}	16 ± 1 ^{b}	18 ± 1 ^{b}	21 ± 2 ^{a}	11 ± 1 ^{b}	11 ± 1 ^{b}	15 ± 1 ^{b}
0.001–0.005 mm	18 ± 1 ^{a}	14 ± 1 ^{a}	15 ± 1 ^{a}	22 ± 1 ^{a}	22 ± 3 ^{a}	22 ± 1 ^{a}	18 ± 1 ^{a}	22 ± 2 ^{a}
<0.001 mm	22 ± 2 ^{a}	15 ± 1 ^{b}	15 ± 1 ^{b}	15 ± 1^{b}	15 ± 1 ^{a}	26 ± 2 ^{b}	24 ± 0 ^{b}	18 ± 1 ^{a}

Note: The unit of Ca is g/kg, Cu is mg/kg, Fe is g/g; K is g/kg, Zn is mg/g, TP is g/kg, SOC is g/kg, AK is mg/kg, AP is mg/kg, MC is %, TN is g/kg, CEC is c mol/kg, and mechanical composition (0.25–1.00 mm, 0.05–0.25 mm, 0.01–0.05 mm, 0.005–0.01 mm, 0.001–0.005 mm and <0.001 mm) is %; Mean ± SD, n = 3. Different superscript letters in each row represent significant differences between different treatments (ANOVA, $p < 0.05$).

3.2. Microbial Biomass in Topsoil and Subsoil in ABI, HE, ME and LE

Figure 1 shows that the NO_3–N, NH_4–N, MBC, MBN, and MBP concentrations in the ABI rhizospheric topsoil were significantly higher than those at the HE, ME, and LE. The NH_3-N content in the LE topsoil was relatively lower than that of the other elevations. The MBC: MBN ratios in the ABI and HE topsoil were similar but significantly greater than that at ME and LE. Almost identical patterns were observed in the subsoil. In contrast, the MBC: MBN ratio in the ABI and LE subsoil was significantly higher than that of the HE and ME values. The higher the Chao1 and Ace values, the greater the number of operational taxonomic units contained in the community and the greater the community richness.

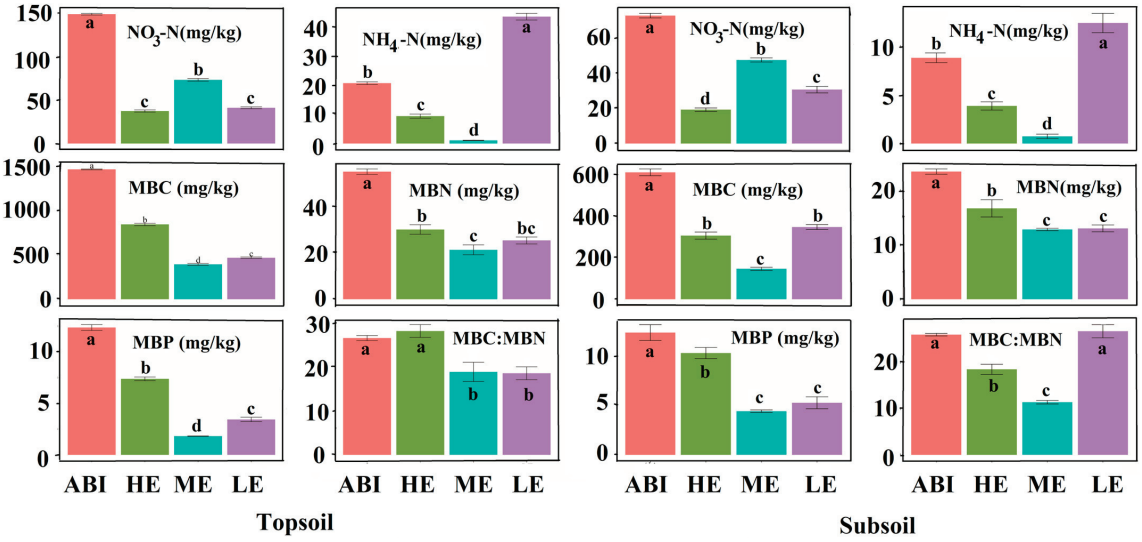

Figure 1. NO_3-N, NH_4-N, MBC, MBN, MBP and MBC:MBP concentrations in rhizospheric topsoil and subsoil. Note: Mean ± SD, n = 3. Different superscript letters in each row represent significant differences between different treatments (ANOVA, $p < 0.05$).

3.3. CUE and Soil Enzyme Activities

The differences in the CUE at different elevations in the soil are shown in Figure 2. The CUE values of ABI topsoil were significantly lower than those of the LE, ME, and HE soils ($p < 0.05$). Although the CUE value increased in the subsoil, the value was still lower in comparison with the other elevations. The contents of C-enzymes in ABI topsoil and subsoil tended to be greater than that in the soil at the other elevations. The content of N-enzymes in the two soil layers was the maximum at ME. The content of P-enzymes in the ME soil was significantly higher than that at the other elevations ($p < 0.05$). Although the C-enzyme content was higher in ABI soil, lower CUE values were detected in rhizosphere soil, and the ME rhizosphere soil had a higher CUE value.

3.4. α-Diversity and Community Composition of Bacteria and Fungus in Soil in ABI, HE, ME and LE

The higher the Chao1 and Ace values, the higher the number of OTUs contained in the community and the greater the community richness. The richness of the bacterial and fungal communities in the topsoil of ABI, HE, ME, and LE were similar, but the richness of the ME community was slightly higher (Table 2). The richness of the topsoil community was higher than that of the subsoils. A higher Simpson index indicated low community diversity, which was negatively correlated with other diversity indices. A small difference in fungal community diversity was detected in the topsoil and subsoil. The higher the Shannon value, the richer the community diversity. The community diversity of the ABI fungus was lower than that of the HE, ME, and LE. The results of whole_tree PD_ exhibited

higher bacterial and fungal community diversity in topsoil than that in the subsoils. The coverage values in the soil layers and the four elevations were approximate. Overall, the bacterial and fungal community diversity in the ME soil was higher than that in the ABI and other elevations, and there was richer community diversity in the topsoil.

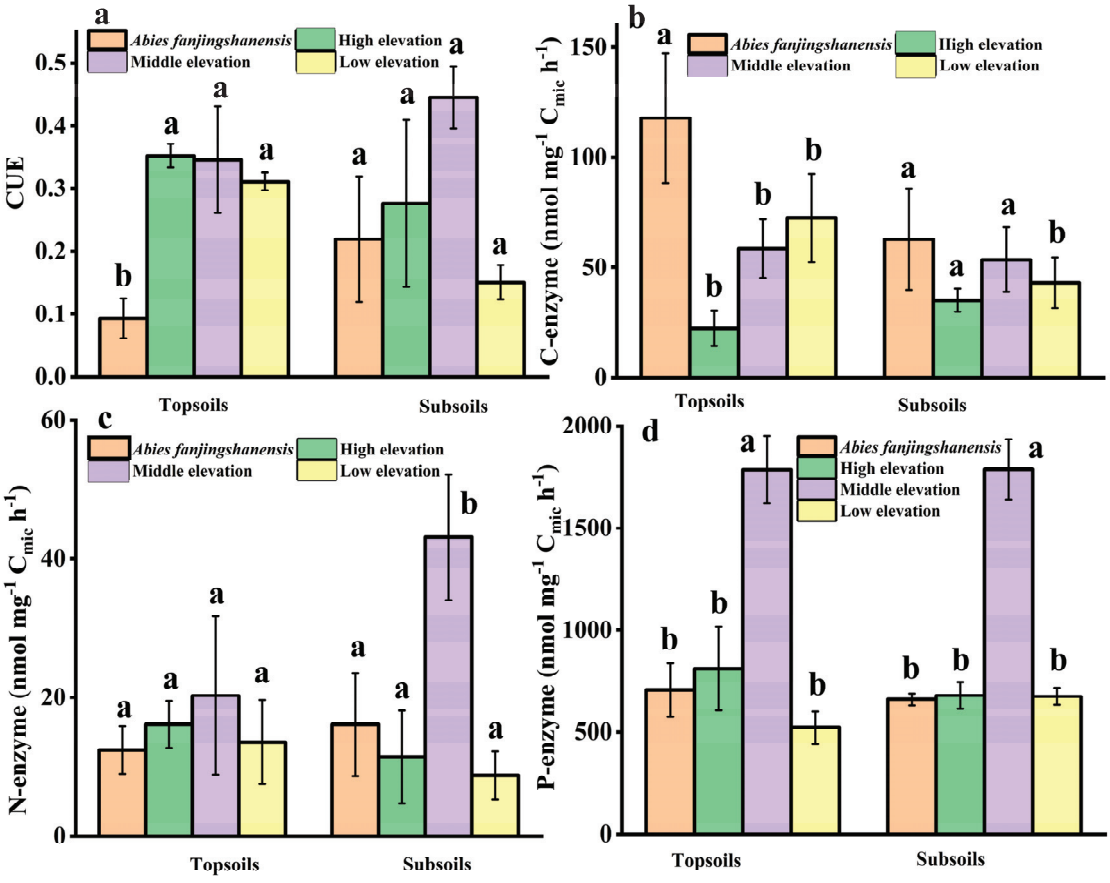

Figure 2. The CUE (**a**), C−enzymes (**b**), N−enzymes (**c**) and P−enzymes (**d**) contents in topsoil and subsoil in ABI, HE, ME and LE. Note: Mean ± SD, n = 3. Different superscript letters in each row represent significant differences between different treatments (ANOVA, $p < 0.05$).

Table 2. The α-diversity of microbia and fungi in topsoil and subsoil of ABI, HE, ME and LE.

		ABI		HE		ME		LE	
		Bacterials	**Fungus**	**Bacterials**	**Fungus**	**Bacterials**	**Fungus**	**Bacterials**	**Fungus**
ACE	Topsoil	1309 ± 98 ^{a}	603 ± 25 ^{a}	1257 ± 35 ^{b}	661 ± 83 ^{b}	1319 ± 24 ^{a}	639 ± 36 ^{a}	1289 ± 29 ^{b}	553 ± 53 ^{b}
	Subsoil	1286 ± 107 ^{a}	597 ± 23 ^{a}	1150 ± 131^{a}	577 ± 87 ^{b}	1346 ± 28 ^{b}	598± 31 ^{a}	1252 ± 58 ^{a}	534 ± 96 ^{c}
Chao1	Topsoil	1325 ± 101 ^{a}	625 ± 12 ^{a}	1287 ± 43 ^{a}	638 ± 27 ^{a}	1340 ± 41 ^{a}	647 ± 37 ^{b}	1310 ± 37 ^{a}	556 ± 59 ^{c}
	Subsoil	1296 ± 111 ^{a}	620 ± 27 ^{a}	1085 ± 251 ^{b}	562 ± 39 ^{b}	1367 ± 37 ^{a}	625 ± 43 ^{a}	1280 ± 40 ^{a}	555 ± 109 ^{b}
Simpson	Topsoil	0.99 ± 0.00 ^{a}	0.83 ± 0.06 ^{a}	0.98 ± 0.01 ^{a}	0.93 ± 0.03	0.99 ± 0.00 ^{a}	0.93 ± 0.03 ^{a}	0.99 ± 0.00 ^{a}	0.89 ± 0.08 ^{a}
	Subsoil	0.99 ± 0.00 ^{a}	0.83 ± 0.05 ^{a}	0.98 ± 0.00 ^{a}	0.95 ± 0.01 ^{a}	0.99 ± 0.00 ^{a}	0.88 ± 0.05 ^{a}	0.99 ± 0.00 ^{a}	0.83 ± 0.13 ^{a}
Shannon	Topsoil	8.29 ± 0.22 ^{a}	3.85 ± 0.64 ^{a}	7.89 ± 0.29 ^{a}	5.18 ± 1.00 ^{b}	8.44 ± 0.24 ^{a}	5.17 ± 0.73 ^{b}	8.62 ± 0.03 ^{b}	5.13 ± 0.79 ^{b}
	Subsoil	8.19 ± 0.22 ^{a}	3.83 ± 0.47a	7.43 ± 0.47 ^{b}	5.95 ± 0.61 ^{b}	8.24 ± 0.02 ^{a}	4.49 ± 0.51 ^{c}	8.19 ± 0.03 ^{a}	4.63 ± 1.53 ^{c}
PD_whole_tree	Topsoil	63 ± 4 ^{a}	86 ± 7 ^{a}	60 ± 2 ^{a}	90 ± 1 ^{a}	62 ± 1 ^{a}	91 ± 7 ^{a}	61 ± 2 ^{a}	83 ± 3 ^{a}
	Subsoil	61 ± 5 ^{a}	82 ± 4 ^{a}	52 ± 10 ^{a}	77 ± 5 ^{a}	63 ± 0 ^{a}	85± 1 ^{a}	60 ± 2 ^{a}	82 ± 10 ^{a}
Coverage	Topsoil	0.99 ± 0.00 ^{a}	0.99 ± 0.00 ^{a}	0.99 ± 0.00 ^{a}	0.99 ± 0.00 ^{a}	0.99 ± 0.00 ^{a}	0.99 ± 0.00 ^{a}	0.99 ± 0.00 ^{a}	0.99 ± 0.00 ^{a}
	Subsoil	0.99 ± 0.00 ^{a}	0.99 ± 0.00 ^{a}	0.99 ± 0.00 ^{a}	0.99 ± 0.00 ^{a}	0.99 ± 0.00 ^{a}	0.99 ± 0.00 ^{a}	0.99 ± 0.00 ^{a}	0.99 ± 0.00 ^{a}

Mean ± SD, n = 3. Different superscript letters in each row represent significant differences between different treatments (ANOVA, $p < 0.05$).

In this study, 23 bacterial phyla and 10 fungal phyla were detected in the topsoil and subsoil, respectively (Figure 3). Among them, Acidobacteria, Proteobacteria, Planctomycetes, and Actinobacteria were the dominant phyla in the two soil layers; the proportion of Acidobacteria and Proteobacteria gradually increased in topsoil, except for the ABI, and decreased with increasing elevation. There was a larger discrepancy in the fungal proportions. Although Basidiomycota and Ascomycota were the dominant phyla in the two soil layers, the proportion of Basidiomycota decreased slowly with increasing soil depth and elevation, respectively. The top 50 bacterial genera with the highest relative abundance were selected for the linear discriminant analysis effect size analysis, and only species with scores >3.5 were displayed (Table 3). Acidobacteria, Acidobacteriia, Acidobacteriales, Candidatus_Koribacter and Koribacteraceae were the indicator species in topsoil compared with the soils at the other elevations. Candidatus_Koribacter, Koribacter, Roseiarcus, Beijerinckiaceae, and Roseiarcus were the indicator species in the subsoil. Clavulinaceae, Tuber, Tuberaceae, and Tuber_zhongdianense were the fungal indicator species in the topsoil. Agaricales, Archaeorhizomycetales, Archaeorhizomycates, Archaeorhizomyces and Archaeorhizomycetaceae were the indicator species in the subsoil.

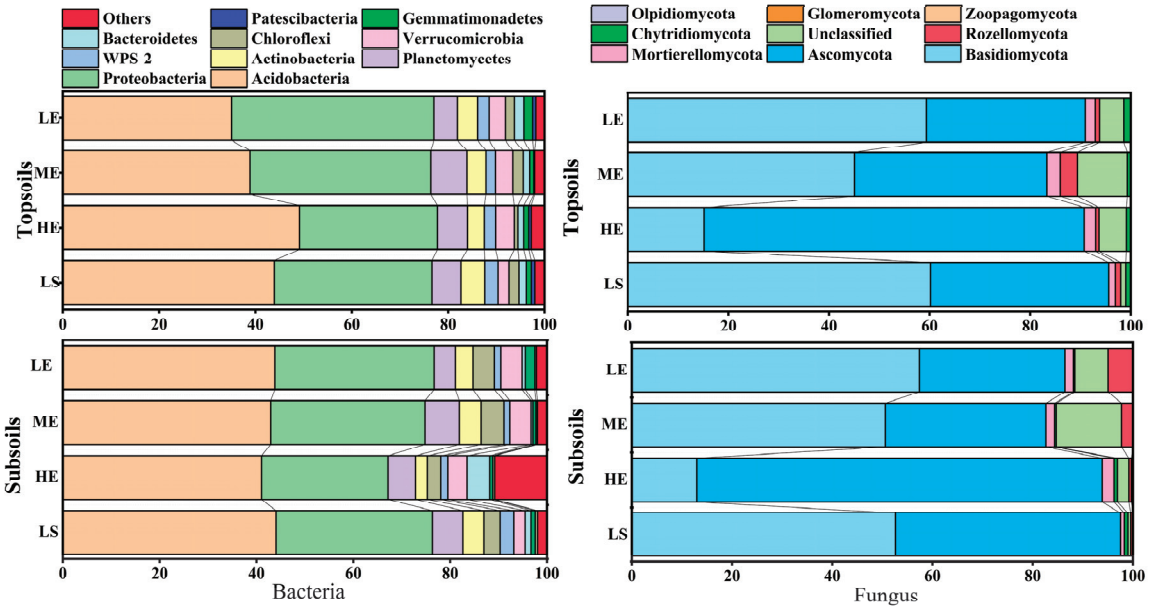

Figure 3. The proportion of relative abundance of bacteria and fungus under phylum level.

3.5. Factors Driving the Seasonal Variation in Soil Microbial Community Composition

Figure 4 shows the relationship between microorganisms and the soil physicochemical parameters. A significant positive correlation was observed between bacteria/fungus and the K content in the soil. Additionally, TP and MC contents were positively correlated with bacteria and fungus in the topsoil, respectively. TN in the topsoil was strongly positively correlated with microbial C:N and MC. Bacteria in the subsoil were positively correlated with the microbial C:N ratio. Fungi were positively correlated with Cu, TP, SOC, AK, MC, TP, and the microbial C:N ratio. SOC content was strongly positively correlated with AK, MC, TN, and the C:N ratio. Overall, the relationships between microorganisms and the subsoil physicochemical parameters were closer than those in the topsoil. Similarly, stronger correlations with the physicochemical parameters were found in the subsoil.

Figure 5 shows the relationships between bacteria (phylum level) and the soil physicochemical parameters. pH had a positive effect on Chloroflexi and a negative effect on

Bacteroidetes and Patescibacteria. The C:N ratio was positively and negatively correlated with Patescibacteria and Bacteroidetes, respectively. The physicochemical parameters mainly affected Ascomycota, Zoopagomycota, Mortierellomycota, Rozellomycota, and Basidiomycota. pH was positively correlated with Rozellomycota and Basidiomycota but negatively correlated with Ascomycota. Fe, TP, AP, Zn, and K affected fungi (phylum level).

Figure 6a–d displays the co-occurrence networks of bacteria in the ABI, HE, ME, and LE soils. The modularity indexes were 0.51, 0.56, 0.50, and 0.46 in ABI, HE, ME, and LE, reaching a degree of modularity, as their values were >0.44. Both the number of nodes and the edges of the microbial networks were slightly different in the bacteria and fungi in the ABI, HE, ME, and LE soils. A positive correlation in the microbial network reflected a cooperative relationship between species, while a negative correlation was competitive. The cooperative microbial network was dominant for bacteria and fungi. A tiny difference in the degree and complexity of the co-occurrence networks was found in the four rhizosphere soil samples (Figure 7a). The centrality of LE was higher in rhizosphere soil than that in the other soil elevations. The importance of a node depended on the number of neighboring nodes and the importance of the neighboring nodes (Figure 7b). A connected neighboring node was more important. This was evidence that the important nodes of the microbial co-occurrence network in the rhizosphere soil were richer in LE, enhancing network stability.

Table 3. LEfSe analysis of bacterial and fungus communities in topsoil and subsoil in ABI, HE, ME and LE (Scores > 3.5).

		ABI	HE	ME	LE
Bacterial	Topsoil	-	p_Acidobacteria c_Acidobacteriia o_Acidobacteriales g_Candidatus_Koribacter f_Koribacteraceae	f_Xanthobacteraceae	c_Gammaproteobacteria p_Proteobacteria o_Betaproteobacteriales
	Subsoil	-	g_Candidatus_Koribacter f_Koribacteraceae f_Beijerinckiaceae g_Roseiarcus	f_Burkholderiaceae	g_Candidatus_Solibacter o_Gammaproteobacteria_ Incertae_Sedis
Fungus	Topsoil	f_Clavulinaceae g_Tuber f_Tuberaceae s_Tuber zhongdianense	o_Archaeorhizomycetales c_Archaeorhizomycetes g_Archaeorhizomyces f_Archaeorhizomycetaceae g_Meliniomyces f_Helotiaceae	s_Lactarius salmonicolor s_Lactarius horakii f_Agaricaceae f_Entolomataceae	f_Cylindrosympodiaceae o_Venturiales s_Sympodiella_quercina g_Sympodiella o_Xylariales
	Subsoil	o_Agaricales o_Archaeorhizomycetales c_Archaeorhizomycetes g_Archaeorhizomyces f_Archaeorhizomycetaceae	O_Hypocreales f_Erysiphaceae s_Erysiphe paeoniae g_Erysiphe o_Erysiphales o_Eurotiales f_Nectriaceae f_Aspergillaceae f_Aspergillaceae s_Paecilomyces_penicillatus g_Paecilomyces g_Fusariumg Aspergillus s_Aspergillus_flavus f_Trichocomaceae g_Talaromyces	f_Entolomataceae	

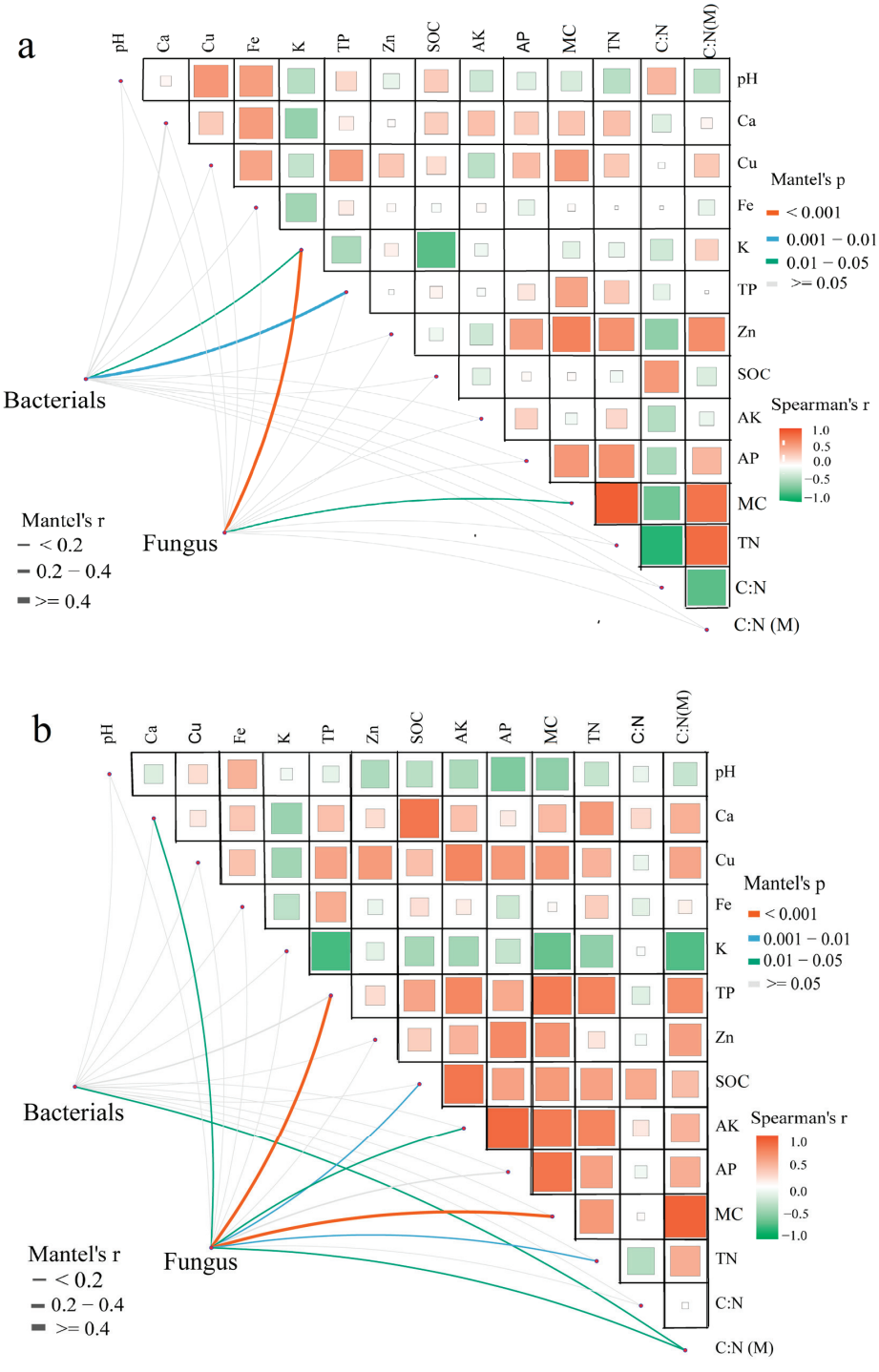

Figure 4. Relationship between bacteria/fungus and physicochemical indexes in topsoil (**a**) and subsoil (**b**).

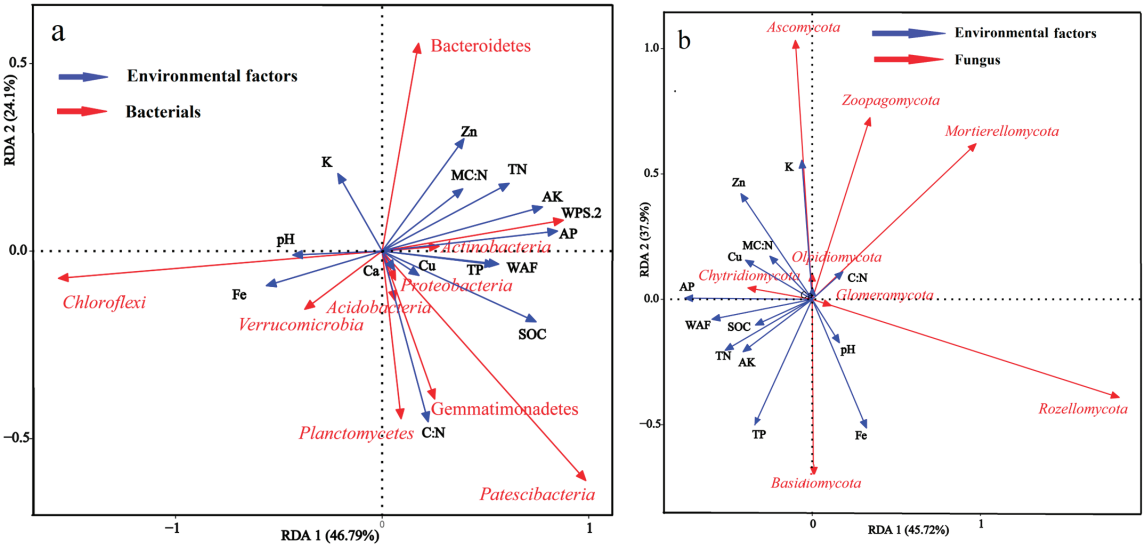

Figure 5. Relationship between bacteria (**a**) and fungus (**b**) (phylum level) and physicochemical parameters in soil using Redundancy analysis.

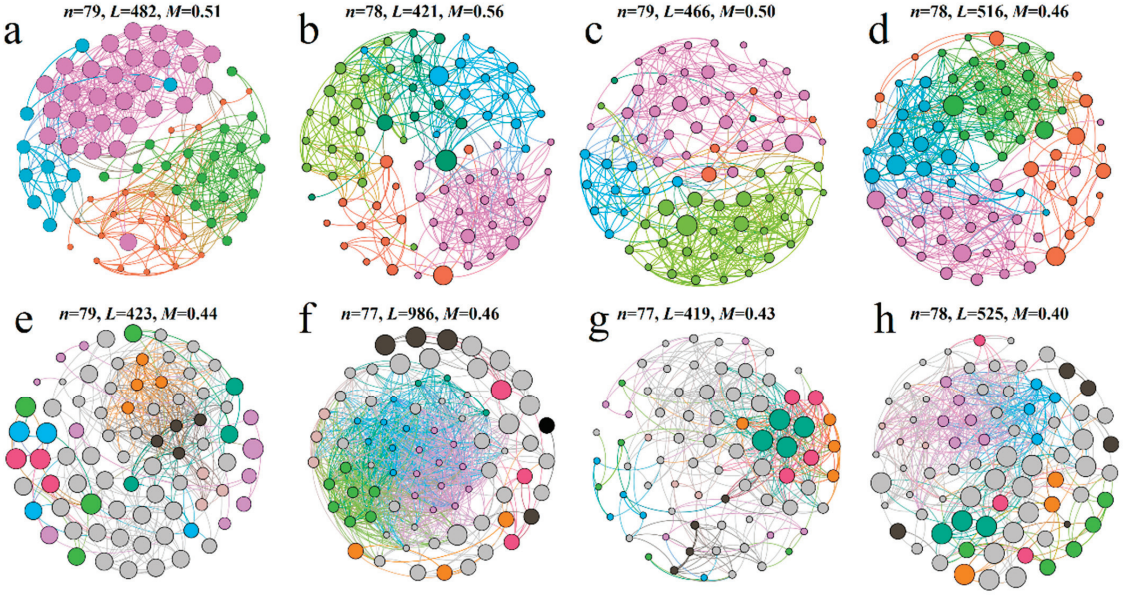

Figure 6. Co-occurrence networks of bacteria in ABI (**a**), HE (**b**), ME (**c**) and LE (**d**), and fungus in ABI (**e**), HE (**f**), ME (**g**) and LE (**h**) in soil. Small modules with <5 nodes were displayed in gray, and large modules with ≥5 nodes were in other colors.

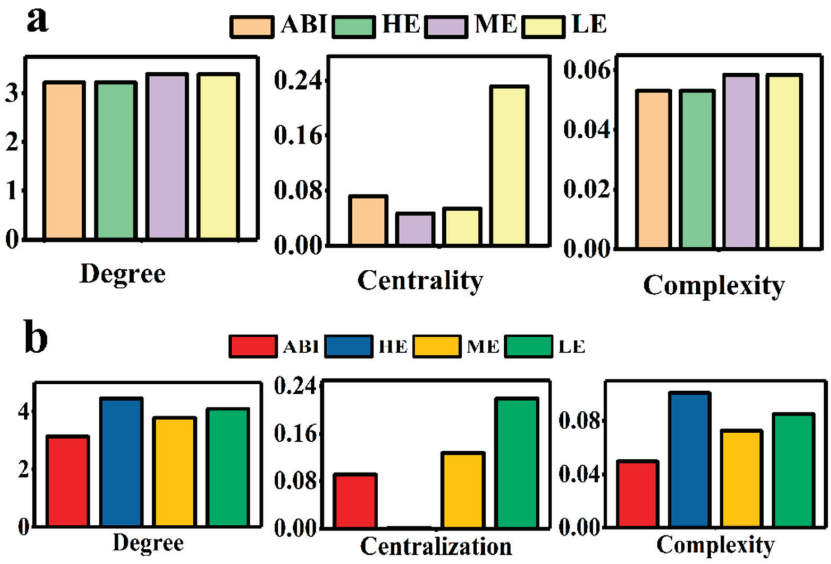

Figure 7. Degree, centrality, and complexity of co-occurrence networks of bacteria (**a**) and fungus (**b**) in ABI, HE, ME and LE.

4. Discussion

Overall, the physicochemical parameters in topsoil were of higher magnitude than those in the subsoil, and their contents in rhizospheric soil in ABI were greater than that in soils in HE, ME and LE. Although ABI grows in stone crevices, there are massive fallen leaves in surface soil. Fungi produce highly acidic humic acid when organic matter is decomposed, which lowers soil pH and reduces fertility [27], which explains the lower pH in the soil of ABI. However, soil pH is higher at mid-altitude due to natural (low temperature and a slower mineralization rate) and anthropogenic factors (mainly tourism activities) [28]. Although the temperature gradually decreases as the altitude increases, the plant species that make up the vegetation at high altitudes are relatively isolated, and most grow in stone crevices, causing the soil pH to gradually decrease [29]. Our result found that the contents of most of the soil physicochemical parameters, particularly SOC, increased first at LE and ME and then decreased in the HE. Many studies have shown that the carbon and nitrogen contents in soil increase with the increase in altitude, and simultaneously, soil microbial activity weakens. The weakened soil microbial activity will make the decomposition of litter slow down and deposit in the soil, significantly increasing the soil carbon and nitrogen content with altitude [30]; our studies also found this phenomenon. There was an annual average temperature of 7.3 °C, and the lowest temperature was −2.3 °C in the ABI growing environment. The lower soil temperature retarded the rate of chemical reactions and microbial activities, which was beneficial for the accumulation of organic matter. The higher moisture content probably restrained the ABI root system from absorbing soil nutrients [31]. Therefore, NO_3-N, MBC, MBP, and MBN contents in ABI topsoil and subsoil were significantly greater than those of the other elevation soils. Generally, with increasing soil pH value, the variable negative charge of soil colloid increased, and the cation exchange capacity increased [31]. This coincided with our result that pH values and CEC contents in the soil in ME were higher than that in the other elevation soils. The space between the particles of clay soil was small, the ventilation was poor, the soil temperature rose slowly, the water content was high, and the organic matter was easy to accumulate [32]. These peculiarities also resulted in lower microbial activity.

Microbial α-diversity in the soil tended to vary at different elevations. In the ABI rhizosphere soil, Acidobacteria, Proteobacteria, and Planctomycetes were the dominant phyla of

bacteria in the two soil layers, while the dominant fungal phyla were Basidiomycota and Ascomycota. Chen et al. [33] reported that Basidiomycota and Ascomycota are the dominant groups in a study of soil fungal communities in different forest types in the Xiaoxing'an Mountains, which was consistent with our results. Basidiomycetes and Ascomycetes are important soil decomposers, among which Ascomycota are mostly saprophytes, which play a key role in the degradation of complex organic matter [34], while basidiomycetes have an enhanced ability to decompose lignocellulose in plant residues [35]. Candidatus_Koribacter is the main indicator species in the rhizospheric topsoil and subsoil, which is a methanotroph in phylum Acidobacteria [36]. Tuberaceae is commonly found in coniferous and broad-leaved mixed forests, forming specialized mycorrhizal symbioses with various host plants. TP and MC contents were positively correlated with bacteria and fungi in the topsoil, respectively. Topsoil TN was strongly positively correlated with the microbial C:N ratio and MC. The relationships between microorganisms and the physicochemical parameters in the subsoil were more highly correlated than those in the topsoil. The amount of soil moisture has a significant impact on the growth and activity of soil microorganisms. Fungi are more sensitive than bacteria, indicating that under different soil moisture conditions, different communities of soil microorganisms have different adaptations and regulatory mechanisms [37]. It is generally believed that fungi have an advantage over bacteria in soil lacking water because bacteria are more adaptable to the environment and have a higher tolerance [38], whereas fungi have a single-celled structure, which is more flexible and not limited by water [39]. The important nodes in the microbial co-occurrence network of the rhizosphere soil at LE were richer, which enhanced network stability. The positive correlation in microbial networks is dominant. Chen et al. [40] suggested that the diversity of the microbial communities, the complexity of the co-occurrence networks, and the multifunctionality of ecosystems significantly decrease with increasing altitude. Positive correlations in these studies suggest cooperative behaviors, i.e., mutualistic interactions, syntrophic interactions, cross-feeding, and commensalism between co-existing members as well as taxa occupying similar guilds or niches [41].

pH was the most important factor affecting carbon use efficiency in topsoil (Figure 8). The pH values in topsoil and subsoil in ABI were relatively lower than those in the soils of the other elevations. In this study, there are two possible mechanisms resulting in the lower microbial CUE in soil in ABI. Firstly, an acidic environment forces microorganisms to consume more energy to maintain cell pH while less energy is used for growth. Secondly, under a low soil pH, the solubility of toxic metals such as Al^{3+} increases, and cells are subjected to stress [42], resulting in a decrease in soil CUE. In addition, the SOC contents in the topsoil were higher than that in the subsoil. Higher CUE values accelerated the decomposition of SOC, leading to the loss of SOC [43], while a lower CUE reduced the decomposition of soil carbon by microorganisms, which was beneficial for the accumulation of soil carbon. Fungal communities facilitate the decomposition of complex compounds and decompose litter, thereby promoting the stability of soil microbial biomass carbon and organic matter accumulation mediated by fungi [44]. The diversity of the fungus in the ABI rhizosphere soil and at LE was relatively lower, which is probably another reason leading to the lower CUE value. The turnover time of forest soil microbial biomass increases with increased soil depth. The lower microbial carbon uptake rate in deep soil may be partially compensated for by the longer microbial biomass carbon turnover time [45]. Soil microbial CUE affects ecosystem processes, such as soil carbon fixation, turnover, mineralization, and greenhouse gas emissions, as well as biogeochemistry feedback to climate change. Soil microbial CUE plays an important role in regulating soil microbial-mediated carbon and nutrient transformation and is also a key regulatory factor for soil microbial biomass turnover and soil carbon sequestration [46]. However, some still limitations of the current study should be discussed. It will be necessary to strengthen studies of soil microbial CUE in forest ecosystems, particularly in different forest vegetation types and different growth and development stages [44].

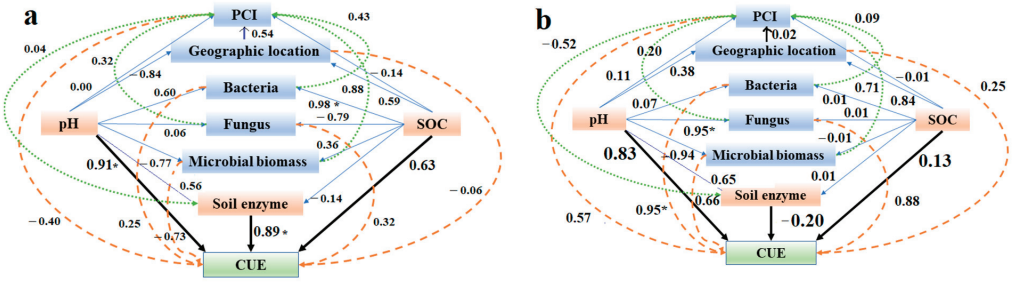

Figure 8. Structural equation model of microbial CUE in topsoil (**a**) (x^2 = 7.05, df = 7, p = 0.29, CFI = 0.92 and RMSEA= 0.00) and subsoil (**b**) (x^2 = 9.15, df = 8, p = 0.33, CFI = 0.94 and RMSEA = 0.00) ("*" represents that p value is lower than 0.05).

5. Conclusions

In this study, cooperation of the bacterial and fungal microbial networks was dominant, and there is a lower difference in the degree and complexity of the co-occurrence network in the four rhizosphere soil types. The structural equation model demonstrated that pH was the most important factor for carbon use efficiency in topsoil and subsoil. We inferred that the microorganisms in acidic soil environments were forced to consume more energy to maintain pH, while less energy was used for growth. Nevertheless, increasing the solubility of some toxic metals in acidic soil also coerced the microbial cells, resulting in a lower microbial CUE in ABI rhizospheric soil. Previous studies suggested that the massive death of ABI was mainly caused by the unbalanced chemometrics and nutrients in the soil. However, our results highlight that pH values in soil mainly affected microbial CUE, and a lower microbial carbon use efficiency may be another important factor as to why the ABI died in large numbers. Our suggestion is that, in the rhizospheric soil of ABI, the suitable application of biochar can enhance the pH value, and appropriately adding the exogenous nitrogenous fertilizer will increase the microbial CUE. The change in microbial CUE in soil is a long-term process which is affected by multiple factors. Therefore, future work will incorporate more influencing factors and conduct short-term and long-term studies to reveal the impact of different influencing factors on microbial CUE at multiple time scales and their interaction mechanism.

Author Contributions: Conceptualization, X.W. and Z.Z.; methodology, X.W. and Z.Z.; software, J.Z.; validation, Y.L., W.L., G.M. and X.H.; formal analysis, J.Z.; investigation, Y.L.; resources, W.L.; data curation, G.M.; writing—original draft preparation, X.W. and Z.Z.; writing—review and editing, X.W.; visualization, Z.Z.; supervision, Z.Z.; project administration, X.W. and Y.L.; funding acquisition, X.W. and Y.L. All authors have read and agreed to the published version of the manuscript.

Funding: This work was financially supported by the Youth Fund of Guizhou Academy of Sciences (No. Qiankeyuan [2021]13), Doctoral Research of Guizhou Academy of Sciences [Grant No. QKY-R-2021-03]. Provincial special fund for scientific research of Guizhou Academy of Sciences [Grant No. QKY-KZH-2022-03], Guizhou Academy of Sciences Innovation Plate Scientific Research Start-up Fund [Grant No. QKY-C-2021], Science-technology Support Plan Projects of Guizhou Institute of Biology [Grant No. QSS-2021-01], Guizhou province science and technology basic research Project [Grant No. QKHJC-ZK-2022-282], and Planing Project of Guiyang City (no. 629 Zhukehe [2021]3-30, no. Zhukehe [2021]3-27 and no. Zhukehe [2023]3-11).

Institutional Review Board Statement: Not applicable.

Informed Consent Statement: Not applicable.

Data Availability Statement: The data presented in this study are available on request from the corresponding author.

Conflicts of Interest: The authors declare no conflict of interest.

References

1. Wu, C.; Ma, Y.; Wang, D. Microbiology combined with metabonomics revealing the response of soil microorganisms and their metabolic functions exposed to phthalic acid esters. *Ecotoxicol. Environ. Saf.* **2022**, *233*, 113338. [CrossRef] [PubMed]
2. Zhang, K.; Maltais-Landry, G.; Liao, H.L. How soil biota regulate C cycling and soil C pools in diversified crop rotations. *Soil Biol. Biochem.* **2021**, *156*, 108219. [CrossRef]
3. Wang, Y.F.; Chen, P.; Wang, F.H. The ecological clusters of soil organisms drive the ecosystem multifunctionality under long-term fertilization. *Environ. Int.* **2022**, *161*, 107133. [CrossRef] [PubMed]
4. Lozowicka, B.; Wolejko, E.; Kaczynski, P. Effect of microorganism on behaviour of two commonly used herbicides in wheat/soil system. *Appl. Soil Ecol.* **2021**, *162*, 103879. [CrossRef]
5. Karhu, K.; Alaei, S.; Li, J. Microbial carbon use efficiency and priming of soil organic matter mineralization by glucose additions in boreal forest soils with different C:N ratios. *Soil Biol. Biochem.* **2022**, *167*, 108615. [CrossRef]
6. Zhu, Y.; Shao, T.; Zhou, Y. Periphyton improves soil conditions and offers a suitable environment for rice growth in coastal saline alkali soil. *Land Degrad. Dev.* **2021**, *32*, 2775–2788. [CrossRef]
7. Chen, W.Q.; Wang, J.Y.; Chen, X. Soil microbial network complexity predicts ecosystem function along elevation gradients on the Tibetan Plateau. *Soil Biol. Biochem.* **2022**, *172*, 108766. [CrossRef]
8. Geyer, K.M.; Dijkstra, P.; Sinsabaugh, R.; Frey, S.D. Clarifying the interpretation of carbon use efficiency in soil through methods comparison. *Soil Biol. Biochem.* **2019**, *128*, 79–88. [CrossRef]
9. Geyer, K.M.; Kyker-Snowman, E.; Grandy, A.S. Microbial carbon use efficiency: Accounting for population, community, and ecosystem-scale controls over the fate of metabolized organic matter. *Biogeochemistry* **2016**, *127*, 173–188. [CrossRef]
10. Fisk, M.; Santangelo, S.; Minick, K. Carbon mineralization is promoted by phosphorus and reduced by nitrogen addition in the organic horizon of northern hardwood forests. *Soil Biol. Biochem.* **2015**, *81*, 212–218. [CrossRef]
11. Xiong, X.; Lyu, M.; Deng, C.; Li, X.; Lu, Y.; Lin, W.; Jiang, Y.; Xie, J. Carbon and Nitrogen Availability Drives Seasonal Variation in Soil Microbial Communities along an Elevation Gradient. *Forests* **2022**, *13*, 1657. [CrossRef]
12. Lv, K.; Wang, J.J.; Wu, G.P. Elevational Pattern and Control Factors of Soil Microbial Carbon Use Efficiency in the Daiyun Mountain. *Environ. Sci.* **2022**, *43*, 4364–4371. (In Chinese)
13. Zhang, Y.; Chen, L.; Wang, J.Y.; Li, Y.; Wang, J.; Guo, Y.X.; Ren, C.J.; Bai, H.Y.; Sun, H.T.; Zhao, F.Z. Differences and influencing factors of microbial carbon use efficiency in forest rhizosphere soils at different altitudes in Taibai Mountain, China. *Chin. J. Plant Ecol.* **2023**, *47*, 275–288. (In Chinese) [CrossRef]
14. Liu, Y.Y.; Luo, W.M.; Mou, G.T.; Wu, X.L. C:N:P stoichiometric characteristics of the soil–vegetation system of three rare tree species growing on Mount Fanjing in Southwest China. *Glob. Ecol. Conserv.* **2021**, *32*, e01893. [CrossRef]
15. Wang, Z.X.; Liu, F.Z.; Li, H.B.; Du, J.H.; Li, W.D.; Wang, W. Assessment of Conservation Effectiveness of Protected Areas Based on Target Control Samples: A Case Study of Abies fanjingshanensis Communities. *Res. Environ. Sci.* **2022**, *35*, 519–529. (In Chinese)
16. Yao, L.M.; Shi, L.; Li, H.B.; Shang, K.; Zhu, Q.Q.; Zhou, G.R.; Jiang, L. A New Chinese Record Species of Glomeromycota through Morphology and Molecular Phylogeny Identification. *J. Guizhou Univ.* **2020**, *48*, 117–119. (In Chinese)
17. Li, X.Y.; Zhang, W.Y.; Liu, F. The Distribution Characteristics of Soil Carbon, Nitrogen and Phosphorus at Different Altitudes in Fanjingshan Mountain. *Res. Soil Water Conserv.* **2016**, *23*, 19–24. (In Chinese)
18. Hedley, M.J.; Stewart, J.W.B.; Chauhan, B.S.C. Changes in inorganic and organic soil phosphorus fractions induced by cultivation practices and by laboratory incubations. *Soil Sci. Soc. Am. J.* **1982**, *46*, 970–976. [CrossRef]
19. Van Laak, M.; Klingenberg, U.; Peiter, E.; Reitz, T.; Zimmer, D.; Buczko, U. The equivalence of the Calcium-Acetate-Lactate and Double-Lactate extraction methods to assess soil phosphorus fertility. *J. Plant Nutr. Soil Sci.* **2018**, *181*, 795–801. [CrossRef]
20. Eva-Maria, P.; Vesterdal, L.; Beer, C. Do tree species affect decadal changes in soil organic carbon and total nitrogen stocks in Danish common garden experiments? *Eur. J. Soil Sci.* **2022**, *73*, e13206.
21. Zhang, Z.M.; Wu, X.L.; Zhang, J.C.; Huang, X.F. Distribution and migration characteristics of microplastics in farmland soils, surface water and sediments in Caohai Lake, southwestern plateau of China. *J. Clean. Prod.* **2022**, *366*, 132912. [CrossRef]
22. Sinsabaugh, R.L.; Turner, B.L.; Talbot, J.M.; Waring, B.G.; Powers, J.S.; Kuske, C.R.; Moorhead, D.L.; Follstad Shah, J.J. Stoichiometry of microbial carbon use efficiency in soils. *Ecol. Monogr.* **2016**, *8*, 172–189. [CrossRef]
23. Chen, S.F.; Zhou, Y.Q.; Chen, Y.R. Fastp: An ulra-fast all-in-one FASTQ prepocessor. *Bioinformatics* **2018**, *34*, 884–890. [CrossRef] [PubMed]
24. Magoč, T.; Salzberg, S.L. LASH: Fast length adjustment of short reads to improve genome assemlies. *Bioinformatics* **2011**, *27*, 2957–2963. [CrossRef] [PubMed]
25. Edgar, R.C. UPARSE: Highly accurate OTU sequences from microbial amplicon reads. *Nat. Methods* **2013**, *10*, 996–998. [CrossRef] [PubMed]
26. Stackebrand, E.; Coebel, B.M. Taxonomic note: A place for DNA-DNA reassociation and 16S rRNA sequence analysis in the present species defimition in Bacteriology. *Int. J. Syst. Evol. Microbol.* **1994**, *44*, 846–849. [CrossRef]
27. Srensen, P. Carbon mineralization, nitrogen immobilization and pH change in soil after adding volatile fatty acids. *Eur. J. Soil Sci.* **2010**, *49*, 457–462. [CrossRef]
28. Thakur, S.; Negi, V.S.; Dhyani, R. Influence of environmental factors on tree species diversity and composition in the Indian western Himalaya. *For. Ecol. Manag.* **2022**, *503*, 119746. [CrossRef]

29. Lv, S.H.; Li, X.Q.; Bai, K.D. Microtopographic differentiation characteristics of soil physicochemical properties and leaf traits of Litsea glutinosa in karst rocky desertification mountain of southwestern Guangxi. *J. Plant Resour. Environ.* **2022**, *31*, 11–17. (In Chinese)
30. Wang, Q.C.; Zheng, Y.; Song, C.G. Impacts of simulated nitrogen and phosphorus depositions on soil microbial biomass and soil nutrients along two secondary succession stages in a subtropical forest. *Acta Ecol. Sin.* **2021**, *41*, 6245–6256.
31. Peng, S.; Liu, W.; Xu, G.A. meta-analysis of soil microbial and physicochemical properties following native forest conversion. *Catena* **2021**, *204*, 105447. [CrossRef]
32. Wang, Y.G.; Wang, N.; Li, Y.Y.; Zhou, Y.C.; Bao, N.S.; Zhao, X. Dump reclamation in jalai nur open-pit coal mine and feedback response of soil microbiome. *Environ. Eng.* **2022**, *7*, 45–51. (In Chinese)
33. Chen, X.B.; Zhu, D.Q.; Zhao, C.C.; Zhang, L.L.; Chen, L.X.; Duan, W.B. Community composition and diversity of fungi in soil sunder different types of Pinus koraiensis forests. *Acta Pedol. Sin.* **2019**, *56*, 1221–1234. (In Chinese)
34. Beimforde, C.; Feldberg, K.; Nylinder, S.; Rikkinen, J.; Tuovila, H.; Dorfelt, H. Estimating the Phanerozoic history of the Ascomycotalineages: Combining fossil and molecular data. *Mol. Phylogenet. Evol.* **2014**, *78*, 386–398. [CrossRef] [PubMed]
35. Frey, S.D.; Knorr, M.; Parrent, J.L.; Simpson, R.T. Chronicnitrogen enrichment affects the structure and function of thesoil microbial community in temperate hardwood and pineforests. *For. Ecol. Manag.* **2004**, *196*, 159–171. [CrossRef]
36. Bernardes, F.S.; Herrera, G.; Gabriel, M.C. Relationship between microbial community and environmental conditions in a constructed wetland system treating greywater. *Ecol. Eng.* **2019**, *139*, 105581. [CrossRef]
37. Ren, C.; Liu, K.; Dou, P. The Changes in Soil Microorganisms and Soil Chemical Properties Affect the Heterogeneity and Stability of Soil Aggregates before and after Grassland Conversion. *Agriculture* **2022**, *12*, 307. [CrossRef]
38. Jiao, S.; Lu, Y. Abundant fungi adapt to broader environmental gradients than rare fungi in agricultural fields. *Glob. Chang. Biol.* **2020**, *26*, 4506–4520. [CrossRef]
39. Noor, N.F.M.; Yusoff, M.E.; Rahman, M.A.A. The Disinfectant Effect of Modified Hydrothermal Nanotitania Extract on Candida albicans. *Bio. Med. Res. Int.* **2021**, *2021*, 6617645. [CrossRef]
40. Chen, M.; Zhu, X.; Zhao, C. Rapid microbial community evolution in initial Carex litter decomposition stages in Bayinbuluk alpine wetland during the freeze–thaw period. *Ecol. Indic.* **2021**, *121*, 107180. [CrossRef]
41. Byrnes, J.E.K.; Gamfeldt, L.; Isbell, F.; Lefcheck, J.S.; Griffin, J.N.; Hector, A.; Cardinale, B.J.; Hooper, D.U.; Dee, L.E.; Duffy, J.E. Investigating the relationship between biodiversity and ecosystem multifunctionality: Challenges andsolutions. *Methods Ecol. Evol.* **2014**, *5*, 111–124. [CrossRef]
42. Li, J.W.; Wang, G.S.; Allison, S.D. Soil carbon sensitivity to temperature and carbon use efficiency compared across microbial-ecosystem models of varying complexity. *Biogeochemistry* **2014**, *119*, 67–84. [CrossRef]
43. Kivlin, S.N.; Waring, B.G.; Averill, C. Tradeoffs inmicrobial carbon allocation may mediate soil carbon storage in future climates. *Front. Microbiol.* **2013**, *4*, 261–269. [CrossRef] [PubMed]
44. Zhu, W.Z.; Ma, S.G.; Wang, W.W.; Li, X. Reseaveh advances in sil micmobial carbon use efficiency. *Mount. Res.* **2023**, *41*, 1–18. (In Chinese)
45. Spohn, M.; Klaus, K.; Wanek, W. Microbial carbon use efficiency and biomass turnover times depending on soil depth-implications for carbon cycling. *Soil Biol. Biochem.* **2016**, *96*, 74–81. [CrossRef]
46. Zhran, M.; Ge, T.D.; Tong, Y.Y. Assessment of depth-dependent microbial carbon use efficiency in long-term fertilized paddy soil using an ^{18}O-H_2O approach. *Land Degrad. Dev.* **2021**, *32*, 199–207. [CrossRef]

MDPI
St. Alban-Anlage 66
4052 Basel
Switzerland
www.mdpi.com

Forests Editorial Office
E-mail: forests@mdpi.com
www.mdpi.com/journal/forests

Academic Open
Access Publishing

mdpi.com

ISBN 978-3-0365-9187-2